A Study on Fresh Properties, Strength, Microstructure and Chloride Induced Corrosion of Steel Reinforcement in Self-Compacting Concrete

A thesis submitted in partial fulfillment of the requirements

for the award of

DOCTOR OF PHILOSOPHY

In

Civil Engineering

By

Smrati Jain

(126104036)

Under the supervision of

Dr. Bulu Pradhan

(Professor)

Department of Civil Engineering

Indian Institute of Technology Guwahati

January 2019

Dedicated to

My Grandmother (Amma)

If tears could build a stairway,
and memories a lane,
I'd walk right up to heaven
and bring you home again.

DEPARTMENT OF CIVIL ENGINEERING

INDIAN INSTITUTE OF TECHNOLOGY GUWAHATI

GUWAHATI-781039, ASSAM, INDIA

Dr. Bulu Pradhan

Professor

Email: bulu@iitg.ac.in

Phone: +91-361-258-2425

CERTIFICATE

It is certified that the work contained in the thesis entitled "**A Study on Fresh Properties, Strength, Microstructure and Chloride Induced Corrosion of Steel Reinforcement in Self-Compacting Concrete**" submitted by **Ms. Smrati Jain (Roll No. 126104036)** to the Indian Institute of Technology Guwahati for the award of the degree of Doctor of Philosophy has been carried out under my supervision in the Department of Civil Engineering, Indian Institute of Technology Guwahati. This work has not been submitted elsewhere for the award of any other degree or diploma.

Place: IIT Guwahati

(Dr. Bulu Pradhan)

ACKNOWLEDGEMENT

"Starting something can be easy; it is finishing that is the highest hurdle"

This thesis is a results of combination of efforts of so many people who have helped me directly or indirectly during my exciting journey of PhD. Throughout this long journey, I have gained a lot by learning to persevere despite hardship. I would never have successfully completed this thesis without the assistance of numerous people who I am indebted to. Their direction, advice, support and contributions have proved invariable along the way.

First and foremost, I would like to profusely thank my supervisor, Prof. Bulu Pradhan for his constant valuable guidance, enthusiastic involvement and kind help throughout my research work. I appreciate all his contributions of time, ideas and funding to make my PhD experience productive and stimulating. A very special gratitude goes to him for encouraging my research. Thank you very much, sir, for your advice on my research, my career, as well as my personal life, has always been priceless.

It is an extreme delight to have Prof. Subashisa Dutta (Chairman), Prof. Vaibhav V. Goud (Dept. of Chemical Engineering IIT Guwahati) and Dr. Kaustubh Dasgupta the honourable members of my doctoral thesis committee. I would like to express my earnest gratitude to all of them for their invaluable time in evaluating the work progress, encouragement and fruitful advices towards improving the work quality from various perspectives. I also express my sincere thanks to the Head of the Department, Prof. Chandan Mahanta and to all respected faculties of the Department of Civil Engineering. I am also thankful to the scientific officers of the Dept. of Civil Engineering: Dr. Arun Borsaikia and Ms. Jonali Saikia ma'am for their support. I appreciate the staff members of various laboratories of the Dept. of Civil Engineering: Mr. Pranab Hazarika and Mr. P. Pathak for the help they provided whenever it was required.

Next, I would like to express my special sense of gratitude to the Department of Physics and specially Dr. Sidananda Sarma, Technical Officer for extending their help in XRD analysis. I also wish to express my gratitude to the Central Instruments Facility, IIT Guwahati for providing technical support. I would also like to take this opportunity to thanks all the other departments of IIT Guwahati, who have supported me directly or indirectly in various aspects.

I cordially thank Arya Anuj Jee for all his supports in a very special way and fruitful discussions at various stages of my work. I wish to express my appreciation to Om Prakash Prasad for being there to help me since I stepped into the study. I express sincere gratitude to Lalrosiama Zote for the hard work he put to carrying out experiments for this study with me. In my daily work, I have been blessed with a friendly and cheerful group of follow members like Fouzia Shaheen, Sathishraj Mani, Jyotish Kumar Das, Jnyanendra Kumar Prusty, Suresh Sarangi and Kunal Pradhan. I am very thankful to Chandrabhanu Gupt, Mayur Jain, Rashmi Ranjan Behera, Abhishek Singh, Srinivas Pattipaka, Susmita Rabha, Ila Verma, Radhakrishna Gattu and M. Prudhvi Raj for their unconditional help and support.

It is often said good friends are rare to get. In this context I find myself very lucky to have friends like Vishal Deshpande, Mayank Agrawal, Mahesh Patel, Isha Vishan, Needhi Kotoki, Jayshree Hazarika and Kishor Gajrani. Their friendly affection, timely help and encouragements never let me feel away from home during this long journey. Thank you all for your support and encouragement. For Vishal sir I would like to say that I am so fortunate to have him as a first person meet in IIT Guwahati. I must admit that during my initial phase I used to fear of survival in the IIT system. His tips and motivation helped me out to overcome this fear. He indeed helped me in developing my personality, attitude and morals. Thank you Vishal sir for your unwavering support and friendship.

In this precious moment of my life, I would like to express my deep sense of gratitude to my parents, Mr. K. C. Jain and Mrs. C. M. Jain for their love, blessings and constant encouragement throughout my life. I would like to thanks my brother, sisters and all extended members of my family for their love and best wishes. You have always been inspiring, supporting and teaching me to understand the true value of human life.

Smrati Jain

ABSTRACT

The placement and adequate compaction of concrete in heavily reinforced sections are the challenges faced during the construction of reinforced concrete structures. However, to obtain good quality concrete in all the structures in general and in heavily reinforced sections in particular, there is a need to ensure proper placement and adequate compaction of concrete. In heavily reinforced section, there may be segregation and blockage of concrete during its flow through the narrow openings, which will affect the internal structure of concrete leading to inadequate strength and durability properties. To avoid the problems related to the flow of concrete into every corner in the formwork of the structural elements especially in heavily reinforced sections and subsequent compaction, the self-compacting concrete (SCC) has been used in the construction of structures worldwide. Over the years, the SCC has become an attractive option in the area of construction as compared to normal vibrating concrete. The SCC is designed specially to provide excellent deformability in heavily congested reinforced sections and also it has the ability to flow into every corner of formwork under its self-weight during the placement process, without requirement of vibration for compaction. The SCC contains cement, aggregates, water and admixtures similar to normal vibrated concrete, but in different proportions. The proportioning of SCC is considered as a complex process due to its dependence on various factors such as quantity and particle size distribution of aggregates, quantities of cement and mineral admixtures, grain size distribution of powder, and dosages of superplasticizer and/or viscosity modifying admixture. Moreover, apart from selection of optimum raw materials for mix proportioning of SCC, its mixing procedure and duration of mixing are also important.

The reinforced concrete structures are subjected to several durability problems during their service life. Among the durability problems, chloride induced corrosion of steel reinforcement is the most significant one that occurs in the reinforced concrete structures. The aggressive agents such as chloride and sulfate ions can enter the concrete through its ingredients during the time of preparation or can penetrate the hardened concrete from the surrounding environment during the service life of concrete structures.

In this research work, an experimental investigation has been carried out to evaluate the effect of admixed chloride at different concentrations on the behaviour of self-compacting concrete (SCC) through fresh properties, strength development assessed through variations in hydration products with curing age, chloride binding, changes in

microstructure and thermal behaviour, and chloride induced corrosion of steel reinforcement. In addition, the performance of SCC mixes has been evaluated against external chloride and combined chloride-sulfate exposure conditions. For this purpose, the SCC mixes were prepared with different types of binder, and several water-to-binder (w/b) ratios, and admixed with different concentrations of chloride ions. Moreover, the SCC mixes (without admixed chloride) were exposed to external chloride and combined chloride-sulfate solutions. Various tests for fresh properties, compressive strength, chloride concentration, pH, thermal behaviour, microstructural analyses and corrosion of steel reinforcement in SCC were conducted.

In this research work, ordinary Portland cement (OPC), Portland pozzolana cement (PPC), and OPC+20% fly ash (OPC+20% FA) were used as binders. Locally available river sand as fine aggregate, and coarse aggregates of size 20 mm MSA (maximum size of aggregate) and 10 mm MSA were used in the preparation of SCC mixes. To enhance the fresh properties, polycarboxylic ether based high-range water reducing admixture (HRWRA) i.e. superplasticizer was used in the production of SCC mixes. Tempcore TMT (Thermomechanically treated) steel bar of 12 mm diameter was used as the steel reinforcement. Sodium chloride was used as the source of chloride ions, whereas sodium sulfate and magnesium sulfate were used as the sources of sulfate ions.

The mix proportioning of SCC mixes in the present research work was based on the results of trial tests carried out in the study. The mix parameters such as water content, binder content, w/b ratio, fine aggregate and coarse aggregate contents for the trial mixes were selected as per EFNARC and ACI guidelines. After complying with the fresh properties, the mix parameters for the final mixes were selected, where the SCC mixes were prepared at a constant water content of 195 kg/m^3. The w/b ratios of 0.37, 0.40 and 0.43 were used in the preparation of SCC mixes. The proportion of coarse aggregate and fine aggregate by weight was kept as 49% and 51%, respectively of the total aggregate content. The coarse aggregate content was taken corresponding to 28.5% of its total absolute volume. The proportion of 10 mm MSA and 20 mm MSA coarse aggregates was kept at 50% each of total weight of coarse aggregate. The dosages of superplasticizer used in the preparation of SCC mixes were 0.8%, 0.7%, and 0.6% by weight of binder for OPC, PPC, and OPC+20% FA, respectively. Sodium chloride (NaCl) was added in the mixing water at concentrations of 1%, 3%, and 5% (by weight of mixing water) during the preparation of SCC mixes for internal chloride exposure.

Just after the preparation of fresh SCC mixes, various tests were conducted to determine the parameters related to fresh properties of SCC such as slump flow spread, T_{50cm} and V-funnel flow times, L-box passing ratio, and segregation index. All the prepared SCC mixes satisfied the required criteria of fresh properties as per EFNARC guidelines. The cube specimens of size 150 mm and the prismatic specimens of size 72 mm × 72 mm × 300 mm with a centrally embedded steel bar were prepared from each SCC mix. The cube specimens were used for obtaining the compressive strength as well as concrete powder samples required for determining chloride concentration, pH, and for analyzing the microstructure of concrete. The prismatic reinforced concrete specimens were used for determining the corrosion parameters of the embedded steel reinforcement.

After completion of 28 days of moist curing, the prismatic reinforced concrete specimens from each SCC mix were kept in the ambient laboratory condition for 14 days. Two types of exposure condition i.e. laboratory drying (air curing) and water curing were adopted to study the effect of exposure condition on corrosion parameters. For laboratory drying (air curing), the specimens were kept further in the ambient laboratory condition for a period of 540 days. For water curing, the specimens were exposed to normal water with alternate wetting-drying cycles. One cycle consists of three days of wetting followed by drying in ambient laboratory condition for seven days. During wetting, the prismatic specimens were partially immersed in water up to a height of 255 mm from its bottom in plastic tanks. After 450 days of exposure to normal water with alternate wetting-drying cycles, the same specimens were further exposed to 5% NaCl solution with alternate wetting-drying cycles for another 240 days. In addition, separate cube and prismatic specimens were prepared from SCC mixes using the w/b ratio of 0.40 but with three types of binder. These specimens were admixed with higher concentration of NaCl, i.e. 7.5% and 12.5% by weight of mixing water during the time of preparation. After completion of 28 days of moist curing, the prismatic specimens were kept in the ambient laboratory condition for 14 days and were further exposed to laboratory drying for a period of 540 days. For external exposure, chloride solutions were prepared by dissolving sodium chloride in water at concentrations of 1%, 3% and 5% by weight of water. Similarly, combined chloride-sulfate solutions were prepared by dissolving sodium chloride with sodium sulfate, and sodium chloride with magnesium sulfate in water. The concentrations of sodium chloride in the combined solution were 1%, 3%, and 5% and those of sodium sulfate and magnesium sulfate were 3% each by weight of water. Similar to the internal

exposure condition, the prismatic reinforced concrete specimens were kept in the ambient laboratory condition for 14 days after the completion of 28 days of moist curing. After that, the specimens were exposed to chloride and combined chloride-sulfate solutions with alternate wetting-drying cycles for a period of 690 days. Three replicate cube specimens from each SCC mix were tested in a compression testing machine at the curing ages of 28, 90 and 360 days to investigate the effect of binder type, w/b ratio, admixed NaCl concentration, and curing age on the compressive strength of SCC mixes. After completion of compressive strength test, the concrete powder samples were collected from broken cube specimens. The concrete powder samples obtained from various SCC mixes were used for analyzing the microstructure (through EDX, XRD, TGA, FESEM, and FTIR analyses), and for determining the chloride concentration, and pH of SCC mixes. In this study, the electrochemical techniques used to evaluate the corrosion performance of steel reinforcement in SCC were corrosion potential and corrosion current density by linear polarization resistance (LPR) measurements.

From the obtained results, it is observed that all the SCC mixes satisfied the acceptance criteria with respect to filling ability, passing ability and segregation resistance as per EFNARC guidelines. The SCC mixes made with PPC exhibited higher filling ability, passing ability and segregation resistance as compared to those made with OPC+20% FA followed by OPC based SCC mixes. The analysis of variance (ANOVA) calculations indicated that binder type has significant effect on the fresh properties of SCC mixes followed by w/b ratio whereas admixed NaCl concentration has very less effect on the fresh properties of SCC. The results of analysis of variance of compressive strength showed that curing age has more significant effect on the compressive strength of SCC mixes followed by w/b ratio, binder type and admixed NaCl concentration. The Ca/Si ratio of C-S-H obtained from EDX analysis in OPC based SCC mixes increased whereas it decreased in PPC and OPC+20% FA based SCC mixes with curing age, which is consistent with the compressive strength development of SCC with curing age in OPC, PPC, and OPC+20% FA based SCC mixes. The results of XRD, TGA, FESEM and FTIR analyses indicated that NaCl admixed at various concentrations influenced the microstructure and thermal behaviour of SCC mixes. The peak intensity and wt. % (estimated using RIR method) of calcium chloroaluminate (CCA), calcium hydroxide (CH), ettringite (E) and gypsum (G) obtained from the XRD patterns indicated the variations in their formations in the SCC mixes with respect to binder type, w/b ratio and admixed NaCl concentration at different cuing ages. The variations in formation of

calcium hydroxide (CH) with binder type, curing age, admixed NaCl and w/b ratio as indicated by the XRD results are well explained by the CH content calculated from the mass loss in TGA as a result of its dehydration. The formation of C-S-H (calcium silicate hydrate), calcium hydroxide, calcium chloroaluminate and ettringite in the SCC mixes was indicated by the FESEM images, which further corroborates the results of XRD analysis. The obtained FTIR spectra of SCC mixes indicated the functional groups such as -OH, CO_3^{2-} , Si-O and Al-O, which are associated with the formation of various compounds in SCC mixes. The chloride binding as indicated by bound chloride concentration was higher in OPC based SCC mixes as compared to that in OPC+20% FA and PPC based SCC mixes. A strong linear relationship exists between free chloride and total chloride concentrations in the SCC mixes.

From the results of corrosion monitoring of steel reinforcement in SCC mixes admixed with internal chloride, it is observed that there is no systematic variation in the corrosion potential of steel reinforcement in SCC mixes between two exposure conditions i.e. air curing condition (laboratory drying), and normal water curing with alternate wetting-drying cycles. The corrosion current density of steel reinforcement was lower in OPC based SCC specimens as compared to that in OPC+20% FA and PPC based specimens when exposed to normal water; however, the corrosion current density of steel reinforcement increased significantly in OPC based SCC mixes as compared to OPC+20% FA and PPC based SCC mixes when exposed to 5% NaCl solution. Further, the SCC specimens exposed to normal water curing with alternate wetting-drying cycles mostly exhibited lower corrosion current density as compared to those exposed to air curing condition. For external exposure condition, the results obtained from corrosion potential measurement indicated lower probability of the occurrence of steel reinforcement corrosion in the SCC mixes exposed to combined chloride-sulfate exposure solutions (NaCl + Na_2SO_4 and NaCl + $MgSO_4$) as compared to that exposed to only chloride solutions (NaCl). Furthermore, it is observed that the corrosion potential was more negative in the SCC mixes exposed to NaCl + Na_2SO_4 solutions as compared to those exposed to NaCl + $MgSO_4$ solutions. The corrosion current density in the SCC specimens exposed to only NaCl exposure solution was higher than that exposed to both types of combined chloride-sulfate solutions (NaCl + Na_2SO_4 and NaCl + $MgSO_4$). Moreover, it is observed that the corrosion current density was lower in SCC specimens exposed to combined NaCl + $MgSO_4$ solutions as compared to those exposed to combined NaCl + Na_2SO_4 solutions.

TABLE OF CONTENTS

CHAPTER 3: EXPERIMENTAL WORK

CHAPTER 7: CORROSION PERFORMANCE OF STEEL REINFORCEMENT IN SCC EXPOSED TO EXTERNAL CHLORIDE AND COMBINED CHLORIDE-SULFATE SOLUTIONS

CHAPTER 8: CONCLUSIONS AND SUGGESTIONS FOR FURTHER WORK

LIST OF FIGURES

LIST OF TABLES

LIST OF SYMBOLS AND ABBREVIATIONS

θ	Diffraction angle of X-rays
λ	Wave length of X-ray
E_0	Corrosion potential
I_{corr}	Corrosion current density
BET	Brunauer-Emmett-Teller
Ca/Si	Calcium-to-silicon
CC	Calcium carbonate
CCA	Calcium chloroaluminate or Friedel's salt
CH	Calcium hydroxide or Portlandite
C-S-H	Calcium silicate hydrate
C_3A	Tricalcium aluminate
C_4AF	Tetracalcium aluminoferrite
C_2S	Dicalcium silicate
C_3S	Tricalcium silicate
DTG	Derivative thermo-gravimetry
E	Ettringite
EDX	Energy-dispersive X-ray
FA	Fly ash
FTIR	Fourier Transform Infrared
FESEM	Field Emission Scanning Electron Microscopy
G	Gypsum
HRWRA	High-range water reducing admixture
ICDD	International centre for diffraction data
LPR	Linear polarization resistance
MH	Magnesium hydroxide or Brucite
MS	Magnesium sulfate
M-S-H	Magnesium silicate hydrate
MSA	Maximum size aggregate
NC	Sodium chloride
NS	Sodium sulfate
OPC	Ordinary Portland cement
PDF	Powder diffraction file

PPC	Portland pozzolana cement
Q	Quartz
RIR	Reference intensity ratio
SCC	Self-compacting concrete
SCE	Saturated calomel electrode
SI	Segregation index
TGA	Thermo-gravimetry analysis
TMT	Thermomechanically treated
w/b	Water-to-binder
wt. %	Weight percentage
XRD	X-ray diffraction
XRF	X-ray fluorescence

CHAPTER 1

INTRODUCTION

1.1 General

Concrete is a composite material, which is widely used in the construction industry due to its versatile and extensive applications. Concrete must be of good quality and must exhibit excellent durability properties to reduce the deterioration in aggregative environmental conditions. For producing dense and good quality concrete, the compaction of freshly placed concrete is essential. Usually, a freshly placed concrete requires vibration for removing the entrapped air, which makes the concrete dense and homogeneous. Compaction strongly influences the internal structure of concrete and the bond between steel reinforcement and the surrounding concrete. The inadequate homogeneity in concrete because of poor compaction or segregation may significantly bring down the performance of mature concrete in situ [1]. In the early 1980s, the durability of concrete structures was a prominent issue in Japan's construction industry due to reduction in quality of construction work because of the inadequate compaction resulting from the gradual decrease in the number of skilled workers [2]. Okamura and his project team analyzed that the lack of adequate compaction was the real reason for the failure of concrete structures and had proposed a solution by increasing the workability of the fresh mix to an extent that the compaction was no longer necessary, i.e. the mix would become 'self-compacting' [3].

1.2 Self-compacting concrete

The first prototype of self-compacting concrete (SCC) was established in the year 1988 at the University of Tokyo [2]. The fundamental purpose behind the use of SCC was to reduce the construction time, to avoid the vibration in reinforced confined zones and to reduce the noise produced by vibration. The concept of SCC did not gain the expected appreciation in those days. A few large Japanese construction companies exploited the principle of self-compaction and developed their own specific mix designs and practical test methods. There were no practical guidelines available for the industry, on how to make concrete mixes, and then how to handle, transport and place such mixes efficiently and economically. Thus, Bartos [3] formed an international technical committee RLLEMTC145-WSM on Workability of Special Concrete Mixes in 1992 to overcome the practical complications. After that, there was widespread use of SCC technology in Japan, Europe and rest of the

world. NCC Sweden, GTM-Vinci France, and six other industry partners started a research project in the year 1997, which was financially supported by the European Commission [3]. The working group on SCC set up under RILEM TC145-WSM was converted to a new RILEM (TC174-SCC) committee who published its guidelines on SCC in the year 2000 [3]. After that, RILEM has played a key role in the subsequent progress of SCC for its acceptance worldwide. To define the specific requirements of material, composition and application of SCC, EFNARC published the guidelines in the year 2002 and then with some modifications in the year 2005. Also, the American Concrete Institute (ACI) committee published similar guidelines on SCC in the year 2007.

For recent decades, self-compacting concrete (SCC) is one of the outstanding innovations in concrete technology as a special type of concrete. According to the European guidelines [4], SCC does not require vibration for placing and compaction. It can flow under its own weight, completely fill the formwork and achieve full compaction even in the presence of congested reinforcement. The hardened concrete is dense, homogeneous and has the same engineering properties and durability as the conventional vibrated concrete. SCC offers many benefits as compared to conventional vibrated concrete in terms of productivity, working conditions and quality, which are discussed below.

- *Working and environmental benefits:* The placing and compaction of fresh concrete are generally recognized as the physically most demanding but unpleasant activities in the concrete construction process [3]. For normal vibrated concrete, full compaction is achieved by the vibrators, which cause noise, and increase the construction cost and duration. The major advantages of using SCC are in terms of reducing the number of workers and equipment required for its placing and compaction. The use of SCC ensures proper compaction by its own weight that reduces the need of skilled workers and equipment, which in turn decreases the total cost of construction. Since, SCC can be placed at faster rate with no vibration and less screeding, it decreases the number of workers and saves construction time. The heavy vibrating equipment induces noise pollution in construction site, which is harmful to the workers as well as to the surrounding population. Thus, SCC improves the working environment condition by reducing noise pollution and excluding health problems such as white fingers and deafness, which is related to the use of vibration equipment [3].

- *Design and quality benefits:* Although, there is some guidelines from certain technical organizations, there is no well-established standard method and procedure for mix design

of SCC, thus there is greater freedom in mix proportioning of the ingredients. SCC has excellent filling ability and passing ability characteristics that result in greater ease of placement even in more complex shaped structures, heavily congested reinforcement and very long formwork, and also eliminates honeycombing, blow holes as well as grout loss. Further, SCC provides good surface finishing without any pores and improves the aesthetical appearance of the concrete.

1.3 Difference between SCC and normal vibrated concrete

Self-compacting concrete basically consists of the same ingredients as the normal vibrated concrete (cement, water, aggregates, chemical and mineral admixtures) but the final composition of the mixture and its characteristics in the fresh state are different because SCC contains more powder content, less coarse aggregate content, comparatively a large dosage of high range water reducing admixture i.e. superplasticizer and frequently a viscosity modifying admixture (VMA) [2, 5]. Due to the high powder content (cement or cement plus mineral admixture) and chemical admixtures, the production cost of SCC is higher than that of normal vibrated concrete, which can be reduced by use of various mineral admixtures such as fly ash, slag, silica fume, metakaolin, and rice husk ash etc. as partial replacement of Portland cement. A general comparison between the mix proportions of SCC and normal vibrated concrete is shown in Fig. 1.1.

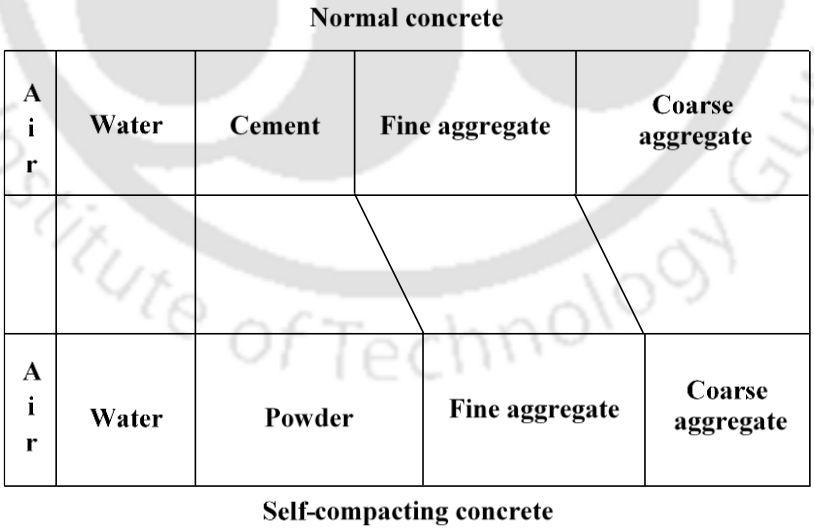

Fig. 1.1 Comparison of mix proportioning between SCC and normal concrete mixes [2]

1.4 Mix proportioning of self-compacting concrete

The mix proportioning of SCC is considered as a complex process due to its dependence on various factors such as quantity and particle size distribution of aggregates, quantities of cement and mineral admixtures, grain size distribution of powder, and dosages of superplasticizer and/or viscosity modifying admixture [6]. Many researchers [6-19] have carried out studies on the mix design of SCC and proposed a variety of mix design methods based on different principles and control parameters. However, very few studies have been carried out to develop a uniform criteria comprising of various factors for the mix proportioning of SCC. The first well-known SCC mix design method was proposed by Okamura et al. [10] at the University of Tokyo, which afterwards was known as the general method for the mix design of SCC. In this method, the authors have suggested fixing coarse and fine aggregate contents and then adjusting the water-to-powder ratio and superplasticizer dosage to ensure self-compatibility of the mix. The general method considered some of the mix design parameters as almost constant that allowed little flexibility in optimizing the granular skeleton, thus resulting in higher amount of paste in the mix when compared to an optimized granular structure [5]. Afterwards, the research works [7, 11] were focused on optimizing the mixture proportions with an aim to reduce the paste volume mainly by increasing the volume of aggregates in the mix.

In the year 1996, a new method for mix design of SCC was developed by Billberg and Petersson [12], known as CBI method. In this method, the concrete was considered as a solid aggregate phase in a liquid paste phase. The paste fills the voids in the aggregate matrix and provides a lubricating layer around each aggregate particle. This method was based on the void content and the blocking criteria. Van and Montgomety [13] have proposed additional criteria for the calculation of the minimum volume of cement paste to the solid blocking criteria of the CBI method. This method is ultimately based on the liquid phase criteria. It ensures that there is sufficient paste volume to provide a required minimum spacing between the aggregate particles. Sedran and Larrard [14] had developed a mathematical model to design the SCC at Laboratoire Central des Ponts et Chausses (LCPC), France in 1999. It is based on the compressible packing model (CPM) for optimization of the solid skeleton of the SCC. Many other approaches were developed using statistical factorial model [15, 16] and rheology of paste model [17, 18]. One of the limitations of SCC is that there is no well-established mix proportioning method yet, only guidelines are available.

All these approaches have contributed to mix design methods of SCC from different perspectives. Each methodology has its own advantages and drawbacks to reach the optimum design. Moreover, apart from the selection of raw materials in optimum proportions for mix design of SCC, the mixing procedure and the duration of mixing are also important. Various mixing durations have been reported in previous research works and the researchers have concluded that the mixing duration of SCC is more than that of normal vibrating concrete because of the additional time required for complete reaction of the superplasticizer with concrete ingredients [19, 20]. The fundamental principle of SCC is to satisfy the filling ability, passing ability and to exhibit good segregation resistance as well as better compressive strength as compared to normal vibrating concrete.

1.5 Key fresh properties of self-compacting concrete

SCC is characterized by its filling ability, passing ability and segregation resistance.

- *Filling ability* is the capability of the concrete mix in fresh state to flow under its self-weight and completely fill all the spaces in the formwork. To achieve high filling ability, the inter-particle friction between solid particles (powder, sand and coarse aggregate) can be reduced by using lower coarse aggregate content and higher dosage of superplasticizer in concrete mixes [21]. The more amount of water could enhance filling ability of concrete by reducing inter-particle friction, although it decreases the viscosity, thus leading to segregation. Also, excessive amount of water affects the strength and durability of concrete. The filling ability is determined by slump flow spread, T_{50cm} and V-funnel flow times (flow rate), O-funnel and Orimet tests.

- *Passing ability* is the ability of fresh concrete to flow through confined spaces, narrow openings and congested spaces between reinforcement bars in the formwork without blockage. It may be noted that the passing ability is significantly related to filling ability [3]. Thus, passing ability depends on the shape, size and amount of coarse aggregate. A reduced amount, as well as the size of coarse aggregate and proper selection of powder content, can overcome the blocking process effectively. Passing ability is determined by using J-ring test in field application, while, L-box and U-box test methods are mainly used in laboratory investigations.

- *Segregation resistance* is the ability of fresh concrete to maintain homogeneous distribution of its constituents during transport, placing and compaction. It is sometimes called as ‘stability’ of the fresh concrete. SCC is made of various ingredients with different

sizes and specific gravity, which leads to segregation of the mix easily. Segregation can occur in both stationary and flowing states between coarse aggregate and mortar. When the concrete is flowing, and the coarse aggregate lags behind the mortar, it is called as dynamic segregation. However, static segregation occurs when the concrete is at rest and the coarse aggregate settle down in the mortar. Segregation may bring down filling ability, passing ability, and non-uniform compressive strength [22]. Enhancement of segregation resistance can be achieved by using lower water-to-powder ratio and viscosity modifying admixture (VMA) or a high volume of powder, thus providing adequate viscosity to ensure homogenous flow. Limiting the size and content of coarse aggregate can also be effective in inhibiting the segregation. Sieve segregation test, settlement column segregation test, and penetration test for segregation are used to determine the segregation resistance of the fresh concrete mix.

All the three fresh properties of SCC are correlated as well as dependent on each other. An adjustment in one property will usually affect the other properties. SCC is a trade-off between filling ability and segregation resistance, which means that lower filling ability and higher segregation can lead to lower passing ability [23]. In addition, consistence retention and robustness are also necessary properties for SCC applications. Consistence retention relates to the period of duration of fresh properties. Robustness of SCC relates to maintaining its fresh properties when the quality and quantity of ingredients and the environmental conditions vary.

1.6 Hydration and microstructure of SCC

The hydration of cement affects the mechanical and durability properties of concrete. The formation of hydration products influences the microstructural characteristics of concrete that can change over time due to interaction with aggressive agents like chloride and sulfate ions. The mechanical properties of concrete depend on two basic hydration products such as calcium silicate hydrate (C-S-H) and calcium hydroxide (CH). The quantification of calcium hydroxide (CH) in concrete is of significant interest since it provides an indication of the progress of pozzolanic reaction as well as it is associated with the mechanical and durability related aspects of concrete. In addition, the lower availability of calcium hydroxide in concrete as a result of its consumption in the pozzolanic reaction may cause depassivation of the steel reinforcement because of the reduction in alkalinity of concrete pore solution [24]. The amount of calcium hydroxide in cementitious materials can be

determined by several methods such as traditional chemical methods, X-ray diffraction method and thermal analysis techniques. The chemical extraction methods, which have been proposed for the extraction of calcium hydroxide by titration involve various solvents such as ethylene glycol and alcohol-glycerol [25]. However, a well-known procedure is the Franke method, in which calcium oxide (CaO) or calcium hydroxide ($Ca(OH)_2$) is dissolved by using acetoacetic ester and isobutyl alcohol as solvents [24]. One of the major limitations of the chemical extraction methods is that their acid solvents may attack other hydrated products of ferrite and C-S-H phases. Further to some extent, these methods are also time-consuming. The X-ray diffraction method usually gives lower values of calcium hydroxide content because this method can only determine its crystallized form [25]. The thermal methods, which are widely used for the determination of calcium hydroxide content include thermo-gravimetry analysis (TGA), differential thermal analysis (DTA) and differential scanning calorimetry (DSC) [26].

The morphology and elemental composition of concrete are examined through field emission scanning electron microscope (FESEM), and energy dispersive X-ray (EDX) spectroscopy analyses, respectively. The Ca/Si ratio of C-S-H calculated from EDX analysis is related to the mechanical properties of concrete [27, 28, 29]. The Ca/Si ratio depends on various parameters such as curing period, water-to-binder ratio and binder type [27]. With the use of silica-rich mineral admixtures, the Ca/Si ratio of C-S-H decreases due to the consumption of $Ca(OH)_2$ in the pozzolanic reaction. To identify the functional groups associated with different products formed in concrete, Fourier transform infrared (FTIR) spectroscopy is generally performed.

1.7 Durability aspects of SCC

The durability problems encountered in reinforced concrete structures pose a serious threat to the concrete infrastructure around the world. Durable concrete means it maintains its original form and quality during its service life even exposed to aggressive environment. The deterioration of concrete structures can be due to physical or chemical actions [30]. The physical action refers to the surface wear, cracking because of crystallization of salts in the pores, and exposure to temperature extremes like frost action or fire. The chemical action includes leaching of the cement paste by acidic solutions, expansive reactions involving sulfate attack, alkali-aggregate reaction, and corrosion of the embedded steel reinforcement in concrete. Corrosion of steel reinforcement is a serious durability problem

encountered in reinforced concrete structures around the world. Steel bars embedded in concrete are protected from corrosion by a passive layer (thin layer of γ-Fe_2O_3) that is formed and maintained on their surfaces because of the highly alkaline environment of concrete pore solution (pH >13.5) [31]. This passive film is destroyed either by reduction in pH of concrete pore solution to a non-protection level (pH of about 9) or by the ingress of chloride ions to steel-concrete interface [32]. Out of these two causes, the presence of chloride is considered as the main cause of corrosion.

1.7.1 Corrosion of steel reinforcement in concrete

Corrosion of steel reinforcement in concrete is an electrochemical process. This process takes place when two dissimilar metals are in electrical contact with each other in the presence of oxygen and moisture. Similarly, this process also takes place on steel alone due to the difference in electrochemical potential on the steel surface thereby forming anodic and cathodic regions, which are connected by the electrolyte in the form of concrete pore solution [33]. At anode, the ferrous ions (Fe^{++} ions) pass into the electrolyte whereas the free electrons (e^-) move from anode towards the cathode along the steel. At cathode, the electrons combine with oxygen and water to form hydroxyl ions $(OH)^-$, which react with Fe^{++} ions in the electrolyte to form ferrous hydroxide ($Fe(OH)_2$). The ferrous hydroxide thus formed undergoes further oxidation and is converted to ferric hydroxide ($Fe(OH)_3$), which is rust [33]. The schematic diagram of electrochemical process of corrosion of steel reinforcement in concrete is shown in Fig. 1.2 [33].

The anodic and cathodic reactions of the corrosion process are as follows [33]:

$Fe \rightarrow Fe^{++} + 2e^-$ (anodic reaction) (1.1)

$2e^- + O_2 + 2H_2O \rightarrow 4(OH)^-$ (cathodic reaction) (1.2)

$Fe^{++} + 2(OH)^- \rightarrow Fe(OH)_2$ (Ferrous hydroxide) (1.3)

$4Fe(OH)_2 + 2H_2O + O_2 \rightarrow 4\ Fe(OH)_3$ (Ferric hydroxide) (1.4)

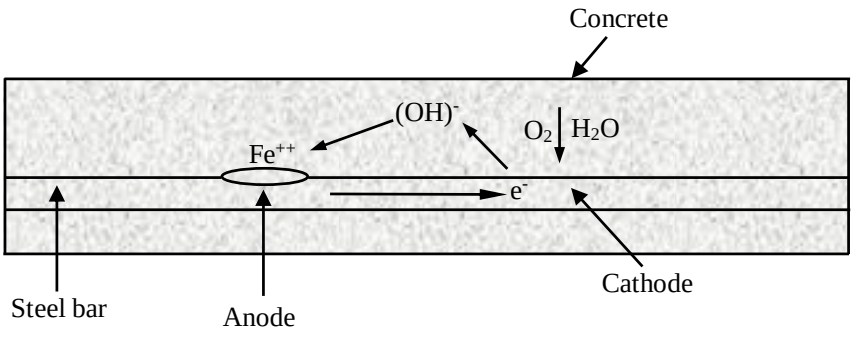

Fig. 1.2 Electrochemical process of corrosion of steel reinforcement in concrete [33]

1.7.1.1 Carbonation induced corrosion of steel reinforcement

In this process, CO_2 from the surrounding environment enters the concrete, which reacts with moisture in concrete to form carbonic acid (H_2CO_3). The carbonic acid reacts with calcium hydroxide ($Ca(OH)_2$) to form insoluble calcium carbonate. The reactions are as follows [33]:

$$CO_2 + H_2O \rightarrow H_2CO_3 \text{ (Carbonic acid)} \quad (1.5)$$

$$H_2CO_3 + Ca(OH)_2 \rightarrow CaCO_3 + 2H_2O \quad (1.6)$$

The consumption of calcium hydroxide results in reduction of pH of concrete and carbonation lowers the pH to about 9. At this low pH value, the passive layer on the steel surface is destroyed that results in initiation of corrosion of steel reinforcement. The rate of carbonation depends on various parameters such as permeability of concrete and its moisture content; and on CO_2 content and relative humidity of the ambient medium [33].

1.7.1.2 Chloride induced corrosion of steel reinforcement

Chloride induced corrosion of steel reinforcement is one of the major causes of durability failure of reinforced concrete structures [34]. The chloride ions can enter the concrete through the ingredients during its preparation (internal chloride) or can penetrate from the surrounding environment during the service life (external chloride) [33]. The sources of internal chloride are contaminated aggregates, mixing water and chloride containing chemical admixtures, which are added during the preparation of concrete whereas, the external chloride enters from the surrounding environment such as by the application of deicing salts on bridge decks and parking structures, from seawater in marine structures, and from soil and groundwater contaminated with chloride salts [35].

Chloride ions exist in concrete in two forms namely free chloride and bound chloride. The chloride ions soluble in the pore solution of concrete are known as free chlorides or water-soluble chlorides. Only free chloride ions are primarily responsible for the initiation of corrosion of steel reinforcement [35, 36]. It is irrespective of whether the chloride is added during the preparation of concrete or that penetrates into concrete during the hardened state, it binds with the hydration products. This process of binding of chloride ions with hydration products is known as the chloride binding-ability of concrete [37]. According to the binding mechanism, chloride ions can bind with the hydration products either chemically or by physical adsorption. Chemical binding in concrete occurs as a result of the reaction of chloride ions with the hydrated C_3A, which forms Friedel's salt or its analogue by the

reaction with C_4AF at early age [38, 39]. In the later ages, when the cement hydrate system is matured, the chemical binding is possibly caused by the anion exchange between chloride ions and AFm (Al_2O_3-Fe_2O_3-mono) phases [38]. The adsorption of chloride ions to the calcium-silicate-hydrates (C-S-H) surface is known as physical binding. Ramachandran [40] has reported that three types of adsorption of chloride ions to the C-S-H surfaces can be existed: i) in a chemisorbed layer on the surface of C-S-H, ii) present in the C-S-H interlayer spaces, and iii) intimately bound in the lattice of C-S-H. Because of the various binding mechanisms, the chloride binding is a complex process due to the interactions between chloride ions and cement hydrates, which can be affected by various factors such as composition of cement, supplementary cementitious materials, chloride concentration, cation type associated with chloride salts, temperature, carbonation and sulfate ions etc. [39]. The study of chloride binding-ability of concrete is essential as it reduces the porosity of concrete due to formation of Friedel's salt [38]. This may also slow down the transport of chloride ions to the surface of steel reinforcement.

The presence of chloride ions near the steel reinforcement in concrete activates the steel surface locally at the anode whereas the passive surface becomes cathode. The chloride ions react at the anode and form hydrochloric acid in the presence of water that destroys the passive film resulting in localized pitting corrosion of the steel reinforcement. The electrochemical reactions in the presence of chloride ions [33] are mentioned below. The other reactions including the cathodic reaction are same as that in the absence of chloride ions.

$$Fe^{++} + 2Cl^{-} \rightarrow FeCl_2 \quad (1.7)$$

$$FeCl_2 + 2H_2O \rightarrow Fe(OH)_2 + 2HCl \quad (1.8)$$

1.8 Durability performance of concrete in conjoint chloride-sulfate environment

The presence of both chloride and sulfate salts in seawater and groundwater poses a serious threat to the durability of reinforced concrete structures. When both chloride and sulfate ions are present in concrete, the mechanism of deterioration of concrete becomes complex due to the simultaneous interaction of these ions with hydrated cement phases. The chloride ions react with hydrated C_3A (tricalcium aluminate) to form calcium chloroaluminate (Friedel's salt) whereas the sulfate ions react with calcium hydroxide and hydrated C_3A to form gypsum and ettringite (calcium sulphoaluminate), respectively [33]. These products formed as a result of sulfate attack occupy a greater volume that results in expansion and

disruption of the hardened concrete. It is obvious that a higher proportion of C_3A would reduce the level of reinforcement corrosion by lowering the free chlorides from the electrolyte pore solution, however it would pose a serious threat to the concrete durability in terms of sulfate attack [41].

In case of exposure to both chloride and sulfate exposure environment, the mechanism of deterioration of concrete due to steel reinforcement corrosion and sulfate attack may become more complex because of simultaneous ingress of both chloride and sulfate ions. The presence of sulfate ions may influence the chloride attack, and similarly, the presence of chloride ions may affect the sulfate attack in concrete. These conditions are particularly significant, because in case of seawater the presence of very high concentrations of chloride ions can influence the effect of sulfate ions [42]. Similarly, the groundwater containing sulfate solutions has less concentration of chloride ions as compared to seawater, where the mechanism of attack could be different from seawater.

1.9 Novelty of the research work

Self-compacting concrete (SCC) has now been established as one of the special types of concrete that shows excellent fresh, mechanical and durability properties. In this line, several research works have been carried out by various researchers. However, the durability aspects of SCC form the view point of corrosion of steel reinforcement due to the action of aggressive ions such as chloride ions and combined chloride-sulfate ions has not been studied comprehensively in the literature. Keeping this in view, the objectives of the present research work have been formulated to study the microstructure and durability aspects of SCC in the presence of chloride and composite chloride-sulfate ions. For fulfilling the objectives, the present investigation focused on evaluating the effect of admixed chloride ions (internal chloride) on fresh, mechanical, microstructure, and durability properties of SCC. In addition, the behaviour of SCC mixes has also been evaluated against external chloride and combined chloride-sulfate exposure conditions.

1.10 Outline of the thesis

The research work carried out in the present work has been organized in eight chapters, which are outlined below.

- **Chapter 1** presents the introduction about the research area. In addition, the organization of the thesis is presented in this chapter.

- **Chapter 2** presents the review of literature of the research work on constituent materials, mix proportioning, fresh and hardened properties of SCC. This chapter also presents, literature review on microstructure and durability aspects of SCC. In addition, the research gap in the literature, the need and objectives of the present research work are presented in this chapter.
- **Chapter 3** describes the detailed experimental investigation carried out in the present study. The details about the materials used in preparation of SCC mixes, preparation of test specimens, and different tests conducted on SCC mixes are presented in this chapter.
- **Chapter 4** presents and discusses about the results obtained for the fresh properties of SCC mixes made with different binder types, w/b ratios and admixed with different concentrations of sodium chloride (NaCl). Further, the effects of binder type, w/b ratio, admixed NaCl concentration, and curing age on the compressive strength of SCC mixes are analyzed and discussed in this chapter. In addition, the variations in the Ca/Si ratio of C-S-H obtained from EDX analysis were evaluated and compared with the compressive strength development of SCC with curing age.
- **Chapter 5** discusses the results of the microstructural characterization of SCC mixes obtained using various techniques such as XRD, TGA, FESEM, and FTIR analyses. Further, the variations in chloride binding (as indicated by free and total chloride concentrations) in SCC mixes made with different binder types, w/b ratios, and NaCl concentrations are analyzed and discussed. In addition, the variations in the pH of chloride admixed SCC mixes are discussed in this chapter.
- **Chapter 6** presents and discusses the results obtained from the corrosion monitoring of steel reinforcement in NaCl admixed SCC mixes through the measurement of corrosion potential and corrosion current density. From the obtained results, the effects of binder type, w/b ratio, admixed NaCl concentration, exposure condition and exposure duration on the corrosion potential and corrosion current density of steel reinforcement in SCC mixes are analyzed and discussed in this chapter.
- **Chapter 7** discusses the corrosion performance of steel reinforcement in SCC mixes exposed to external chloride and combined chloride-sulfate solutions. In addition, the results of free chloride and total chloride concentrations of concrete in the vicinity of steel reinforcement in the SCC mixes are presented and discussed in this chapter. Further, the changes in microstructure of concrete near the rebar level in the SCC mixes analyzed through XRD, EDX and FESEM techniques are discussed.

- **Chapter 8** presents the conclusions obtained from the present research work. The recommendations for future research work are also provided in this chapter.

CHAPTER 2

LITERATURE REVIEW

2.1 General

In this chapter, the research work carried out by various researchers on fresh and hardened properties of self-compacting concrete (SCC) including the effects of various parameters such as binder type, replacement percentages of mineral admixtures, aggregate type, water to binder ratio, as well as type and dosage of chemical admixtures are discussed. Further, the literature review on durability and microstructure of SCC has been presented. Finally, the research gaps in the literature and objectives of the present research work are presented in this chapter.

2.2 Fresh and hardened properties of SCC

A key factor for successful mix proportioning and production of SCC is the understanding of the various constituents in the mix and their effects on the fresh and hardened properties. The research works carried out by various researchers on the fresh and hardened properties of SCC are presented in this section.

Kim et al. [43] carried out an experimental study on the fresh and hardened properties of self-flowing concrete containing fly ash and compared with ordinary concrete. Materials used in this experimental work were ASTM Type I Portland cement, Class F fly ash as mineral admixture, sea sand as fine aggregate, crushed stone as coarse aggregate and sulphonate naphthalene formaldehyde condensate as superplasticizer. Five mixes of SCC were prepared, out of them four mixes were made with fly ash replacement level of 30% by weight of binder content at water-binder (w/b) ratio of 35% and remaining one mix was made with fly ash replacement equivalent to 40% by weight of binder content at w/b ratio of 38%. For the control mix, three ordinary concrete mixes with target compressive strength values of 20 MPa, 40 MPa and 60 MPa were prepared. Fresh SCC mixes were tested for slump flow test, O-funnel test, fill-box test and L-box test. The hardened properties such as compressive strength, splitting tensile strength, modulus of elasticity, stress-strain relation, creep and drying shrinkage were obtained for different SCC mixes. Cylindrical specimens of size 100 mm (diameter) × 200 mm (height) were used for determining compressive strength, splitting tensile strength, modulus of elasticity and stress-strain relation. The authors have also prepared cylinders of size 150 mm (diameter) × 300 mm (height) and

prismatic specimens of size 100 × 100 × 400 mm for creep and drying shrinkage test, respectively. All mixes were tested for compressive strength and splitting tensile strength of concrete at 3, 7, 28, and 90 days, modulus of elasticity at 28 and 90 days, and stress-strain relation at 3, 7, and 28 days. The specimens were cured in moist condition or in air condition until the testing age. The results showed that SCC has sufficient flowability and workability when critical volume ratios of coarse aggregate-to-concrete exist in the range of 0.31 to 0.35. The increasing rate of compressive strength of SCC was lower at an early age but higher at later age as compared to ordinary concrete. Further, the effect of curing condition on compressive strength of SCC was less than that of ordinary concrete. The splitting tensile strength and stress-strain relation of SCC and ordinary concrete at same compressive strength were almost similar. However, creep rate of SCC was greater at early age and decreased with age. Further, the drying shrinkage of SCC was about 30 to 50% greater than that of ordinary concrete.

Bouzoubaa and Lachemi [44] carried out an experimental study to evaluate the performance of SCC made with high volume of fly ash (HVFA). The authors have used ASTM Type I ordinary Portland cement, Class F fly ash, sulphonated naphthalene formaldehyde as superplasticizer, synthetic resin type air-entraining admixture, crushed limestone and local natural sand in this experimental study. Ten concrete mixes were prepared, which included one control concrete and nine SCC mixes. The control mix was made with ASTM type I cement with powder content 336 kg/m^3 and water-cement ratio of 0.50 with 28 days compressive strength of 35 MPa. For nine SCC mixes, cementitious material content (400 kg/m^3) was kept constant, and cement was replaced by Class F fly ash (40%, 50% and 60% by weight of binder) with water to cementitious (w/ (C+FA)) ratios of 0.35, 0.40 and 0.45. The fresh properties of concrete were evaluated by slump, air content, bleeding, setting time, slump flow, V- funnel, and segregation resistance test. The hardened properties of concrete were determined by compressive strength test and drying shrinkage test on cylindrical specimens of size 102 mm diameter and 203 mm height, and prism specimens of size 76×102×390 mm, respectively. The results indicated that the slump flow of HVFA SCCs (except one) was in the range of 500 to 700 mm, flow time ranging from 3 to 7 s, segregation index ranging from 1.9 to 14% and bleeding water ranging from 0.025 to 0.129 ml/cm^2. It was also observed that the SCC mixes showed lower temperature rise and more setting times as compared to the control concrete. The SCC exhibited compressive strength ranging from 15 to 31 MPa at 7 days and from 26 to 48 MPa at 28

days. The authors observed that economical SCC can be achieved at 28-day compressive strength of approximately 35 MPa with 50% replacement of cement by fly ash with W/(C+FA) ratio of 0.45. Further regarding drying shrinkage, no difference was observed between control concrete and SCC.

Felekoglu et al. [45] carried out an experimental investigation to propose a mix design method of SCC by adjustment of the water-cement (w/c) ratio and superplasticizer dosage in optimum proportioning. In this study, ordinary Type-I Portland cement, limestone powder, crushed limestone of maximum size 15 mm as coarse aggregate, mix of crushed 0-5 mm limestone with natural river sand as fine aggregate and polycarboxylic based superplasticizer were used for the preparation of SCC mixes. The authors have prepared five different mixes of SCC with fixed cement content of approximately 377 kg/m^3 as well as with reduced free water content from 227 l/m^3 to 140 l/m^3 and at the same time with increased superplasticizer dosage from 3.7 l/m^3 to 13 l/m^3. The fresh properties of SCC were evaluated by slump flow, T_{50cm} time, V-flow time, L-box test and air content. To determine the hardened properties of SCC, cylindrical specimens of size100 mm diameter × 200 mm height were tested for compressive strength. In addition, cylindrical specimens of size150 mm diameter × 300 mm height were tested for splitting tensile strength and modulus of elasticity. The results indicated that the slump flow values were almost same with the reduction of free water content along with increase in the superplasticizer dosage but V-funnel times and L-box passing ratio results were quite different. It was observed that the effect of water reduction on V-funnel time seems to be more dominant than effect of superplasticizer dosage, and the SCC mixes with a w/c ratio of greater than 0.48 had a passing ratio greater than 0.8. It was also observed that the compressive strength of SCC increased by reducing free water content and w/c ratio. The SCC mixes had lower elastic modulus and higher splitting tensile strength as compared to normal vibrated concrete.

Khatib [46] has investigated the properties of SCC containing fly ash (FA: 0 – 80% by weight of binder) at a constant water to binder (w/b) ratio of 0.36. Modified synthetic carboxylated polymer was used as an admixture. Eight mixes were designed to examine the properties of SCC with and without fly ash (FA). The dosage of water-reducing admixture was constant at 0.7% (by weight of binder) for all FA mixes and it was varied (0.6%, 0.7% and 1.0%) for the mixes prepared without fly ash. The properties of SCC such as workability, density, water absorption, compressive strength, ultrasonic pulse velocity (UPV) and drying shrinkage were evaluated. The results indicated that at 56 days,

compressive strength was more than 65 N/mm^2 in SCC mixes replaced with 40% of FA. The variation of UPV was also similar to that of compressive strength results. Using medium dosage of admixture resulted in an increase in UPV as compared to low and high dosages of admixture. High absorption values were found in SCC mixes made with increasing amount of FA while, at 56 days all FA concrete showed absorption values of less than 2%. Drying shrinkage linearly decreased with increase in the amount of FA content in SCC. The correlation between strength and absorption values indicated that the compressive strength reduced when absorption was increased from 1 to 2%. Further, after 2% of absorption, the rate of reduction in compressive strength was much slower with increase in the water absorption value.

Sukumar et al. [47] carried out a study to assess the early age strength of SCC made with high volume fly ash. In this study, ordinary Portland cement, Class C fly ash, quarry dust, fine aggregate (river sand), crushed granite coarse aggregate (12 mm down), polycarboxylic ether based superplasticizer and polysaccharide based VMA were used in the preparation of SCC mixes. Two different series of SCC mixes such as fly ash as mineral admixture and fly ash with quarry dust as inert filler were designed for compressive of 30 – 70 MPa. Cement content, fly ash content and quarry dust content varied from 25% to 89%, 8% to 52% and 3% to 22% respectively by weight of total powder content for different grades of SCC. The dosage of superplasticizer of 0.40 to 0.70, water to powder ratio of 0.34 to 0.31 and VMA of 0.1% by weight of binder were used in the SCC mixes. The fresh properties of SCC were determined by slump flow, V-funnel, L-box and GTM screen stability tests and the obtained results were within the prescribed limits as per EFNARC guidelines. Compressive strength test was performed on cubes of size 150 mm at the ages of 12 hours, 18 hours, 1 day, 3 days, 7 days, 21 days and 28 days of curing. The split tensile strength test was conducted on cylindrical specimens (150 mm diameter × 300 mm height) after curing period of 1 day, 3 days, 7 days, 21 days and 28 days. The obtained results indicated that the rate of gain in compressive strength for different grades of SCC was slightly higher than the expected strength as per IS: SP: 23 1982 for conventional concrete at the same grades. The SCC mixes containing only fly ash provided higher compressive strength than the mixes containing quarry dust with fly ash.

Turkel and Kandemir [48] carried out an experimental study to determine the effect of different types of aggregate and mineral admixture on the fresh and hardened properties of SCC. Ordinary Portland cement, two types of mineral admixtures: Class C type fly ash and

limestone powder, two different types of aggregate: limestone and olivine basalt in saturated surface dry condition and polycarboxylate polymer based superplasticizer were used in the study. Total four SCC mixes were prepared, first two mixes contained small amount of limestone powder with fly ash and remaining two mixes contained only limestone powder as the mineral admixture. In this study, the cement and water content were almost kept constant for all the mixes with water to cement ratio of 0.55. Fresh properties such as, slump flow, T_{50cm} time and V-funnel time were measured as per EFNARC guidelines. For determining the hardened properties of SCC, compressive strength test at the ages of 3, 7 and 28 days and flexural strength test at the age of 28 days were conducted on cube specimens (150 mm) and prism specimens (100 × 100 × 600 mm), respectively. The results of fresh properties indicated highest self-compatibility in terms of slump flow and V-funnel time from the combination of limestone powder and limestone aggregate. However, SCC made with combination of limestone aggregate and fly ash gave superior results in terms of compressive strength as well as flexural strength. Basalt aggregate combination showed negative effect on the fresh properties as well as lowest flexural strength at 28 days. The authors concluded that effect of mineral admixture on fresh properties was more dominant than that of aggregate type.

Wang and Huang [49] carried out a study on fresh properties of self-consolidating glass concrete (SCGC) by using recycle waste LCD as fine aggregate. For experimentation, sand was replaced by glass sand (0%, 10%, 20%, and 30%) and cement was partially replaced by fly ash (20%) and slag (10%) with different W/B ratios of 0.28, 0.32, and 0.36. Type 1000 superplasticizer was used as per ASTM C494 type G admixture. Slump flow, V-funnel test, U-test, unit weight, air content test and setting time test were performed on all the SCGC mixes. Due to hydrophobic nature of waste LCD glass sand, the slump flow values increased with increase in replacement up to 30% by LCD glass sand. It was observed from U-test and V-funnel tests that, with increasing replacement of general sand by waste LCD glass sand, the time to fall into and pass through the space between steel bars also increased. The unit weight and air content of concrete were reduced with increase in waste LCD glass sand replacement and with decrease in W/B ratio, but the setting time was increased.

Girish et al. [50] have conducted an experimental investigation to determine the effect of increasing volume of paste (V_p) on workability of SCC. In this experimental study, materials such as ordinary Portland cement (C 53 grade), Class F fly ash as filler, natural

river sand as fine aggregate, crushed granite stone as coarse aggregate and poly-carboxylic ether based superplasticizer (Glenium B233) as chemical admixture were used in the preparation of SCC. Total 63 mixes were prepared with water content varying from 175 l/m^3 to 210 l/m^3 with three different paste contents of 0.38, 0.41 and 0.43. The workability of SCC was determined by slump flow, T_{50cm}, V funnel and J-ring tests. The authors reported that, when volume of paste, water and SP contents were same, the slump flow increased with increase in powder content; however, when paste content was greater than optimal value, the slump flow value was decreased. It was also observed that, at constant cement and water content, yield strength of the mix decreased and shear deformability increased with increase in fly ash content in the powder. V-funnel test results indicated that, plastic viscosity of fresh SCC mix decreased with increase in paste content. Similarly, the passing ability also improved with increase in the paste content.

Liu [20] carried out an experimental investigation to develop SCC with replacement of cement by fly ash up to 80% maintaining constant fresh properties for all mixes and also studied their corresponding hardened properties. The materials used were Portland cement, fly ash, fine aggregate, coarse aggregate (20 mm maximum size) and polycaoboxylate based superplasticizer. In the mix design proportions, powder content of 439 to 539 kg/m^3, sand to mortar volume ratio of 0.45 and coarse aggregate to concrete volume ratio of 0.35 were selected. SCCs were made with constant fresh concrete properties with a slump flow of 700 ± 50 mm, V-funnel time of 8.0 ± 3.0 s, J-ring step of less than 25 mm and segregation index in sieve stability test of less than 15%. The hardened properties such as compressive strength, ultrasonic pulse velocity (UPV), splitting tensile strength and dynamic elastic modulus (Ed) along with water absorption were determined using test specimens such as cube specimens of size 100 mm, cylindrical specimens of size 100 mm (diameter) × 200 mm (height) and prisms of size 100 mm × 100 mm × 505 mm. From the results, it was observed that when slump flow and V-funnel time were kept constant, the replacement of cement with fly ash required an increase in water to powder ratio and reduction in superplasticizer dosage. However, fly ash showed negative effects on passing ability, consistence retention and hardened concrete properties such as compressive strength, UPV, splitting tensile strength and dynamic elastic modulus. The sorptivity values of SCCs made up to 40% fly ash replacement were similar however, it was higher than the mixes made with 60-80% fly ash replacement. Further, it was observed that the replacement of cement with 20% fly ash showed no significant effects on the hardened concrete properties;

however, it showed good correlation between compressive strength and splitting tensile strength. Dynamic modulus and UPV were also in the range of normally vibrated concrete. The author concluded that the optimum dosage of fly ash content was 40% of cement replacement.

Safiuddin et al. [51] carried out an investigation to evaluate the hardened properties of self-consolidating high performance concrete (SCHPC) with different water-binder (w/b) ratios (0.30, 0.35, 0.40 and 0.50), rice husk ash contents (RHA: 0% to 30% by weight of cement) and air contents. Blended crushed and round aggregates were used with 50% each of total aggregate content. Optimum sand/aggregate ratio of 0.50 was used. A total 6% of air content for the air-entrained SCHPCs and 2% of entrapped air content for the non-air-entrained SCHPC were considered. Filling ability and air content of the fresh SCC were determined. The hardened properties of SCHPCs were measured by compressive strength, ultrasonic pulse velocity, water absorption, total porosity and true electrical resistivity tests. From the obtained results, the authors observed that filling ability and air content were satisfied for all SCHPCs. The test results revealed that compressive strength, ultrasonic pulse velocity and electrical resistivity increased, whereas the water absorption and total porosity decreased with decrease in W/B ratio and with increase in RHA content. In addition, the air content decreased the compressive strength, ultrasonic pulse velocity, water absorption, and total porosity but increased the electrical resistivity. The optimum RHA content for SCHPC was found to be 15% by weight of cement.

Melo and Carneiro [52] evaluated the effect of content and finesses of metakaolin on fresh and hardened properties of SCC made with different paste volumes. Three different finesses of metakaolin characterized as fine, normal and coarse were used at 5% and 35% replacement by weight of cement. In this study, slump flow and V-funnel for fresh properties and compressive strength test at the ages of 7 days and 56 days for hardened properties were conducted. The authors reported that higher finesses and content of metakaolin increased the demand of superplasticizer however, with increase in paste volume the demand of superplasticizer reduced. The compressive strength of SCC mixes reduced with the increase in content and reduction in fineness of metakaolin as well as with the increase of paste volume at the ages of 7 days and 56 days.

Uysal and Yilmaz [53] carried out a study to determine the effect of mineral admixtures such as limestone powder (LP), basalt powder (BP) and marble powder (MP) on the fresh and hardened properties of SCC. Ten mixes were prepared, one control mix and reaming

nine mixes were prepared with replacement levels of 10% to 30% by weight of cement with MP, LP, and BP. The water-to-powder (w/p) ratio of 0.33 was selected, and the total powder content was kept fixed. A polycarboxylate-based high range water reducing admixture was used. Fresh concrete properties were evaluated by slump-flow, T_{50cm} flow time, L-box passing ratio, unit weight, and air content. The hardened concrete properties such as compressive strength, ultrasonic pulse velocity, and static and dynamic elastic moduli were determined to evaluate the performance of SCCs. The authors observed that the incorporation of LP, BP and MP showed positive effects on the workability of SCC. Among them, the best mineral admixture was MP, which satisfied all the fresh properties of mixes. All the mineral admixtures showed different compressive strength performance and the MP mixes exhibited the highest compressive strength. The 20% MP and 10% MP mixes exhibited highest static and dynamic elastic modulus, respectively. However, in general, both static and dynamic elastic modulus depend upon compressive strength of concrete. For all mineral admixtures, it was observed that with increase in replacement level of mineral admixture, the unit strength cost of SCCs decreased. In this study, 30% replacement level of MP was the most economical mix as suggested by the authors.

Madandoust and Mousavi [54] carried out a study to characterize the fresh and hardened properties of SCC containing metakaolin (MK: 0 – 20% by weight of cement). The mix proportions of SCC were divided into three groups according to three water-to-binder (w/b) ratios (0.32, 0.38 and 0.45) and partial replacement of MK (5%, 10%, 15% and 20% by weight of cement). Polycarboxylic ether based high range water reducer (HRWR) namely Glenium 51 and a polysaccharide-based VMA were used. The fresh and hardened properties were evaluated by slump flow, T_{50cm}, visual segregation index (VSI), V-funnel, L-box test, and by compressive strength, splitting tensile strength, UPV, initial (30 min) and final water absorption and electrical resistivity tests. The slump flow values were also measured at different hauling times of 8, 30 and 60 min. From the results, it was observed that SCC containing MK showed good performance in terms of slump flow values and visual stability index by adjusting the high range water reducer dosage. The passing ability of SCC containing MK was reduced, and no blockage in the L-box test was observed. The authors observed that the workability of SCC containing MK (up to 15%) was maintained up to 60 min of hauling time. Further, the SCC made with MK showed proper stability without the use of viscosity modifying agent at different W/B ratios. It was also observed that the early age compressive strength (3-14 days) as well as long-term strength (28-56

days) increased by addition of MK in the SCC, while the rate of strength development was more significant in the first 14 days. Similar to the compressive strength, the UPV values and splitting tensile strength were also influenced by addition of MK. Water absorption of SCC containing MK decreased with decrease in W/B ratio, whereas the electrical resistivity increased.

Dehwah [55] studied the use of quarry dust powder (QDP) in SCC. Materials were used in this study were Portland cement, quarry dust powder, silica fume (SF), fly ash (FA), crushed coarse aggregate, dune sand, polycarboxylic ether based superplasticizer and water-soluble copolymers as a stabilizer. Fifteen concrete mixes were prepared out of them five mixes satisfied flow criteria evaluated by slump flow test, V-flow test, U-box flow test and L-box flow test. The selected five SCC mixes were as follows; M1: 8% QDP with water-to-cementitious material (w/cm) ratio of 0.40, M2: 8% QDP with w/cm ratio of 0.38, M3: 10% QDP with w/cm ratio of 0.40, M4: 8% QDP plus 5% SF with w/cm ratio of 0.40, and M5: 30% fly ash with w/cm ratio of 0.40. Mechanical properties were evaluated by compressive strength (using cube specimen of size 100 mm), pulse velocity and splitting tensile strength (using cylindrical specimen of size 75 mm diameter × 150 mm height), and flexural strength (prismatic specimen of size 100 mm × 100 mm × 500 mm). The obtained results indicated that compressive strength and pulse velocity in all SCC specimens increased with age. The compressive strength, pulse velocity, splitting tensile strength and flexural strength of SCC specimens made with only QDP were higher than those incorporating SF plus QDP or fly ash alone. The maximum compressive strength, pulse velocity, splitting tensile strength and maximum flexural strength were observed in M2 mix specimens, whereas the minimum was noted in M5 mix specimens.

Naik et al. [56] carried out a study to develop high-strength SCC by using high volume of Class C fly ash. In addition, the authors had focused on economy, advantages, and disadvantages of the developed concrete. In this study, Portland cement was replaced by Class C fly ash with 35%, 45% and 55% by the weight of cement. Two chemical admixtures such as a HRWRA (Glenium 3200 HES) and a VMA (Rheomac VMA 362) were used in the preparation of the mix. The fresh properties were evaluated by slump flow and U-flow tests. In addition, the air content and fresh density of SCC mixes were also determined. The compressive strength of developed SCC was obtained at the ages of 3, 7, and 28 days using 4″ × 8″ cylindrical specimens. The obtained results indicated that, high volume of fly ash in SCC not only reduces the cement content but also reduces the demand of superplasticizer

and viscosity modifying agents significantly. The desired compressive strength was about 48 MPa at the age of 28 days for SCC mix containing 55% of fly ash. The authors suggested that high-strength, economical self-consolidating concrete can be produced by replacing at least 35% of cement by Class C fly ash.

Siddique et al. [57] carried out a study to determine the influence of water to powder ratio on the fresh and strength properties of SCC containing Class F fly ash and coal bottom ash. For this experiment, twenty SCC mixes were prepared with bottom ash as partial replacement of fine aggregate (10%, 20% and 30%) and fly ash as replacement of cement with 15 – 35% along with the different water-to-powder (w/p) ratios and polycarboxylic ether based superplasticizer. Coarse aggregate and fine aggregate content were maintained at 39% by volume of concrete and 45% by volume of mortar in concrete, respectively, with assumed air content of 2%. The fresh properties such as slump flow, T_{50cm} flow time, V-funnel flow time, L-box, U-box difference in height at the time of preparation and strength properties like compressive strength and splitting tensile strength at the ages of 28 days, 90 days and 365 days were measured. The obtained results showed that SCC mixes made with fly ash, and bottom ash satisfied all fresh properties within the range as per EFNARC guidelines. Further, compressive strength and splitting tensile strength of SCC mixes increased with decrease in w/p ratio, fly ash and bottom ash contents. The authors suggested that the optimum percentages of replacement of fly ash and bottom ash were 25 – 35% and 20%, respectively.

Belaidi et al. [58] conducted a study to examine the effect of natural pozzolana and marble powder on the fresh and hardened properties of self-compacting mortar (SCM) and self-compacting concrete (SCC). Materials used in this study were ordinary Portland cement (CEMI 42.5), natural pozzolana (PZ) and marble powder (MP), continuously graded aggregates and polycarboxylic ether based superplasticizer. Initially, six SCM mixes were prepared with different dosages of superplasticizer (0.8, 0.9, 1, 1.1, 1.2 and 1.4%) at a water-to-powder (w/p) ratio of 0.40. Out of them, the dosage of 0.9% SP was used for further binary and ternary mortar mixes by using 5 – 40% of PZ and MP by weight of cement. The workability of fresh SCM was evaluated by slump test and V-funnel flow time test. From the results, it was observed that the slump flow values of binary SCM mixes with more than 15% of PZ was not within the limit of 250 – 300 mm whereas, V-funnel flow time increased with increase in PZ. The ternary SCM mix made with PZ + MP showed remarkable increase in slump flow values except for the mix made with 10%PZ + 30%MP

and decrease in flow time with increase the amount of MP. The SCC mixes were prepared same as SCM mixes using constant w/p ratio of 0.40 and powder content of 475 kg/m^3. The workability of binary and ternary mixes was determined by using slump flow spread (diameter) with flow time (T_{50cm}), V-funnel flow time, J-Ring, L-Box and sieve stability tests. Compressive strength was determined at the ages of 7, 28, 56 and 90 days. The results indicated that the workability of SCC mixes was enhanced for binary mixes made with 15% PZ and ternary mixes up to 30% MP. Compressive strength of binary and ternary SCC mixes decreased with increase in PZ and MP content. At 28 days, binary mix made with 5% PZ and ternary mix made with 5% PZ + 5% MP gained maximum compressive strength.

Uysal [59] carried out an investigation to evaluate the effect of type of coarse aggregate on fresh and hardened properties of SCC. For this purpose, eleven different mixes were prepared by using CEM I 42.5N cement with Class C fly ash, polycarboxylate-based HRWRA, five different types of crushed coarse aggregate such as basalt, marble, dolomite, limestone, and sandstone with maximum size of 16 mm and river sand. Fresh concrete properties such as slump-flow, T_{50cm} time, V-funnel time, and hardened concrete properties such as abrasion resistance, compressive strength, ultrasonic pulse velocity (UPV), and static and dynamic elasticity moduli were obtained for all mixes. From the results, it was concluded that all the mixes with various types of coarse aggregate satisfied the fresh properties of SCC. The abrasion depths and mass losses were within the range of 0.98 – 3.02 mm and 0.71 – 3.24% respectively, after exposure to abrasion. At the age of 28 days, 56 days, and 90 days, SCC mixes made with basalt aggregate exhibited highest compressive strength as well as UPV values whereas, SCC mixes made with limestone aggregate showed lowest compressive strength and UPV values. Further, static and dynamic elastic moduli were higher in basalt aggregate mix, while the SCC mix made with limestone aggregate showed an opposite trend. The author concluded that SCC mixes made with basalt aggregate showed the best performance in hardened state.

Jawahar et al. [60] carried out a study to determine the effect of blending and percentage content of different coarse aggregates on mechanical properties of SCC. Ordinary Portland cement of 53 grade, Class F fly ash with 35% replacement of cement, crushed granite stones of size 20 mm and 10 mm, sand, SikaViscocrete 10R as superplasticizer and Sika Stabilizer 4R as VMA were used at water-cementitious ratio of 0.36 in the preparation of SCC mixes. Coarse aggregates of size 20 mm and 10 mm size were blended in 60:40 and 40:60

proportions in percentage by weight of total coarse aggregate. In this investigation, fresh properties such as filling ability, passing ability and retention were measured. Hardened properties such as unit weight, compressive strength, modulus of elasticity (MOE) and splitting tensile strength (STS) of SCC mixes were obtained at 7 days, 28 days and 56 days. These properties were compared to a conventional M25 grade concrete. From the obtained results, it was found that the unit weight, modulus of elasticity, and splitting tensile strength of SCC mixes for a given coarse aggregate content and concrete strength were higher in higher volume of maximum size of coarse aggregate. The authors introduced a new parameter called coarse aggregate points (CAPs) and the CAPs were calculated based on coarse aggregate content, size, and blending. The authors concluded that for a given concrete strength, higher the CAP value, higher is the value of unit weight, modulus of elasticity, and splitting tensile strength of SCC mixes.

Ashtiani et al. [61] conducted an experimental study to determine the fresh and mechanical properties of high-strength self-compacting concrete (HSSCC) prepared with 30% of Class C fly ash. For comparison with HSSCC, conventionally vibrated high-strength concrete (CVHSC) was designed with similar water-to-binder (w/b) ratio (0.30) and similar compressive strength. One more mix was designed with lower w/b ratio (0.27) but adjusting the coarse and fine aggregates contents in such a way to obtain similar compressive strength as HSSCC. A polycarboxylic ether polymer based superplasticizer was used in all mixes. Tests for fresh properties such as slump value, slump flow, J-ring, L-box and V-funnel, and mechanical properties such compressive strength, splitting tensile strength and flexural strength as well as modulus of elasticity and drying shrinkage were measured at 3, 7, 28 and 90 days. The microstructure of the mixes was evaluated by means of resistivity, porosity and SEM imaging. From the obtained results, it was found that with similar w/b ratio, HSSCC showed higher compressive strength (by 15 MPa or more) as compared to that of CVHSC whereas, at lower w/b ratio CVHSC exhibited almost similar compressive strength as compared to that of HSSCC (with w/b ratio of 0.30). Before 28 days, the splitting tensile strength of both CVHSC mixes showed to be slightly higher than HSSCC mix, but HSSCC developed higher splitting tensile strength at 90 days as compared to CVHSC with lower w/b ratio. The flexural strength of all three concrete mixes showed almost similar variation as splitting tensile strength. At a given compressive strength, HSSCC showed lower modulus of elasticity and slightly higher drying shrinkage as compared to CVHSC mixes.

Ranjbar et al. [62] carried out a study to evaluate the effects of natural zeolite on the fresh and hardened properties of self-compacting concrete (SCC). A poly-carboxylic ether based HRWR admixture, polysaccharide-based viscosity modified admixture (VMA), cement partially replaced at 5%, 10%, 15% and 20% by natural zeolite were used for the preparation of SCC mixes. A total ten SCC mixes were prepared, in which five SCC mixes prepared with w/b ratio of 0.45 and remaining five SCC mixes with w/b ratio of 0.38. The fresh properties were evaluated by slump flow, visual stability index (VSI), T_{50cm} flow time, V-funnel flow time and L-box tests. Changes in slump flow, VSI and compressive strength with hauling time were also measured. The hardened properties such as compressive strength, splitting tensile strength, ultrasonic pulse velocity (UPV), initial (30 mints) and final absorption were determined. It was observed that mixtures with higher content of natural zeolite required higher HRWR admixture dosage to maintain its flowability. The results obtained from L-box passing ratio, T_{50cm} and V-funnel flow times satisfied the range as per the EFNARC recommendation. The flowability reduced with hauling time at 8, 30 and 60 min, while the higher amount of natural zeolite indicated less loss of slump flow in all mixes. SCC with natural zeolite showed better performance in terms of long-term compressive strength as compared to the reference SCC (without natural zeolite) at lower w/b ratio. The splitting tensile strength showed relatively similar variation like compressive strength of SCC with natural zeolite. After 30 or 60 min hauling time, the strength was lower than the reference mix when its slump flow was lower than 550 mm. The authors concluded that 10% natural zeolite in SCC fulfilled all the requirements for fresh and hardened properties at both w/b ratios.

Safiuddin et al. [63] carried out a study to investigate the effects of different water- binder (w/b) ratios and palm oil fuel ash (POFA) on filling ability, passing ability, segregation resistance and compressive strength of self-consolidating high-strength concrete (SCHSC). The concrete mixes were prepared, using POFA replacement of 0 – 30% by weight of cement with constant water content at four w/b ratios from 0.25 to 0.40 and polycarboxylate based HRWR chemical admixture. Based on the maximum bulk density of aggregate, the fine aggregate to total aggregate ratio of 0.50 was selected for preparation of concrete mixes. Fresh property tests such as slump flow, T_{50cm} slump flow time, inverted slump cone flow spread and time, V-funnel flow time, J-ring flow, L-box flow, sieve and column segregation tests were performed. Compressive strength test was performed on cylindrical specimens of size 100 mm diameter × 200 mm height. From the obtained results, the

authors concluded that lower w/b ratio and higher POFA content increased the filling ability and passing ability of SCHSC at appropriate dosages of HRWR. Higher dosage of HRWR resulted in lower segregation resistance of concrete. Further, compressive strength increased with decrease in w/b ratio up to 20% replacement of POFA in SCHSC mixes. The authors suggested that 20% POFA content was appropriate for filling ability, passing ability, segregation resistance and maximum compressive strength.

Sfikas et al. [64] investigated the effect of metakaolin on the fresh and mechanical properties of SCC mixes. In this study, metakaolin (MK) was used at different replacement levels either with cement (C) or limestone powder (LP) (up to MK/C = 20% and MK/LP = 40% by weight). Total nine SCC mixes were prepared, i.e. one reference mix and other eight mixes divided into two groups. In the first group of mixes, the water-to-binder ratio (w/b) was kept constant at 0.60, whereas in the second group of mixes the water-to-cement ratio (w/c) was kept constant at 0.60. For the reference mix, both w/b ratio and w/c ratio were equal to 0.60. In all the mixes, polycarboxylic ether based superplasticizer was used. Slump flow test, visual stability index, V-Funnel, and L-box tests were conducted for rheological behaviour of fresh concrete mixes. The compressive strength was determined at 28 and 360 days using cube specimens, and splitting tensile strength was determined at 28 days using cylindrical specimens. From the obtained results, at similar or higher dosage of superplasticizer in SCC mixes incorporating MK, lower slump-flow values, higher V-funnel flow times and lower L-box ratios were observed as compared to the reference mix. Minor blocking issues were observed for higher replacement levels of MK for both groups of mixes however, no bleeding or segregation was observed from the test. Compressive strength and tensile splitting strength were higher for higher replacement levels of MK irrespective of the replaced material (cement or limestone powder). Strong linear correlations with similar slopes between the different replacement cases (MK/C or MK/LP) were evident at each examined age (28 and 360 days). A good correlation was evident between tensile splitting strength and compressive strength for MK/LP replacement case, in contrast to the unclear effect for MK/C replacement case. From the obtained results, the authors did not find the optimum replacement level of MK/C or MK/LP.

2.3 Durability properties of SCC

Various durability problems are encountered in reinforced concrete structures during their service life. The research works carried out by various researchers on durability aspects of

SCC in terms of water permeability, electrical resistivity, rapid chloride permeability, freezing and thawing, sulfate attack, chloride diffusion, and others are presented in this section.

Persson [65] compared the performance of SCC with the corresponding properties of vibrated concrete (VC) under the influence of sodium sulphate. The materials used were Portland cement, limestone powder, polycarboxylic ether based superplasticizer and air-entrainment agent. In this study, seven different concretes were studied, six SCC and one VC. Two types of mixing orders of concrete were used: ordinary mixing order and new reversed mixing order. Out of the total number of specimens, one-third of specimens were placed in a solution made with 18 g/l of sodium sulphate in distilled water, other one-third placed in 1% sodium chloride seawater, and the remaining specimens were placed in distilled water. All the specimens were immersed in a particular exposure solution up to 900 days. The author observed that SCC made with ordinary mixing order, the weight and internal fundamental frequency (IFF) were continuously increased over 900 days. Further, the author found that the increase of the weight and IFF were independent from the type of compaction, air content, limestone filler as well as pouring pressure. However, it was observed that for SCC made with new mixing order, their weight was decreased when exposed to sodium sulphate solution, but there was no decrease in IFF of these SCC mixes. The author concluded that it is not suitable to use SCC with large amounts of limestone powder together with the new reversed mixing order when the contents of sulphates in the groundwater is not known.

Nehdi et al. [66] studied the long-term performance of self-consolidating concrete and established its potential life-cycle cost savings. For this purpose, supplementary cementitious materials such as Class F fly ash, ground granulated blast furnace slag, and silica fume or rice husk ash were used. Total seven mixes were prepared, which included one reference, two binaries, two ternaries, and two quaternary mixes at a constant water-binder ratio of 0.38. A naphthalene-sulfonated superplasticizer, polysaccharide welan gum powder VMA and a commercial synthetic detergent-based air-entraining admixture were used in the preparation of SCC mixes. The fresh properties such as slump flow, L-box flow, segregation index and visual inspection, and hardened property such as compressive strength were measured at the ages of 1, 7, 28 and 91 days. To measure the durability aspects, sulfate expansion after 9 months of immersion in 5% Na_2SO_4 solution, resistance to deicing salt surface scaling under 50 freezing-thawing cycles and rapid chloride ion

penetrability at 28 and 91 days were examined in the SCC specimens. From the obtained experimental results, the authors have reported that the workability criteria were found to be satisfactory for SCC made with 50% replacement of Portland cement, and corresponding compressive strength of those mixes were higher than the reference mix at 28 and 91 days. Further, SCC made with ternary, and quaternary mixes showed lower chloride ion penetrability as compared to the reference SCC mix. The resistance to deicing salt surface scaling was enhanced by using VMA in high-volume replacement SCC mixes. Sulfate expansion was observed very low in SCC mixes made with high-volume replacement binary, ternary and quaternary mixes as compared to the reference SCC mix. The authors concluded that SCC can be made with high-volume replacement of composite cementitious materials with good workability, high long-term strength, good deicing salt surface scaling resistance, low sulfate expansion, and very low chloride ion penetrability.

Assie et al. [67] evaluated the durability of SCC and compared it with reference vibrated concrete (VC) having similar compressive strength. In this study, the durability of SCC was evaluated by various tests such as water porosity, chloride diffusion, oxygen permeability, mercury porosity, water absorption by capillarity, carbonation and ammonium nitrate leaching. For the SCC and VC mixes, two types of cement (CEM II/A-LL 32.5 R and CEM I 52.5 N), siliceous round aggregates of grade 0/4 mm for sand, and 4/12 mm or 4/20 mm for gravel, and a polycarboxylate modified superplasticizer were used for preparation of different grades of concrete (20MPa, 40MPa and 60MPa). The differences in mix proportions between SCC and VC were the use of limestone filler, quantity of superplasticizer and volume of higher paste content in SCC mixes. The obtained results indicated that the compressive strength of SCC was equivalent or better than that of VC even at higher water-cement ratio for each grade of concrete. The chloride diffusion and water absorption were equivalent for both types of concrete mixes. The results obtained from oxygen permeability test showed more resistant to gas ingress in SCC mixes as compared to VC. Form the results obtained from carbonation accelerated test, more degradation of SCC was observed as compared to corresponding VC; however, in case of ammonium nitrate leaching, the observed degradation of SCC and VC was equal. The more resistance to gas ingress in SCC may be attributed to lower permeability whereas more carbonation degradation in SCC may be due to the dominant effect of absorption process in concrete carbonation (under accelerated condition) than permeability and diffusion process.

Yazıcı [68] has investigated the mechanical and durability properties of SCC made with replacement of cement by fly ash (FA) and silica fume (SF). In this study, two types of mixes were prepared. In the first mix, cement was replaced with 30% to 60% fly ash and in the second mix, cement was replaced with same amount of FA along with 10% SF. The SCC mixes were prepared using total cementitious material content of 600 kg/m^3, water content of 168 kg/m^3 and different dosages of polycarboxylate based superplasticizer. Fresh concrete tests, compressive strength at 90 days, splitting tensile strength and modulus of elasticity at 28 days, compressive strength and splitting tensile strength after 90 freeze-thaw cycles, and chloride penetration depths were evaluated for the SCC mixes. From the obtained results of fresh properties, it was observed that the superplasticizer demand increased with incorporation of FA and FA+SF. Both, early and ultimate compressive strength were decreased with the incorporation of FA. However, incorporation of FA+SF showed positive effects on compressive strength at all ages. Incorporation of 10% SF along with up to 50% FA did not affect the modulus of elasticity, while the modulus of elasticity was decreased by increasing the FA content only. The chloride penetration resistance was good with the incorporation of FA and FA+SF in SCC i.e. chloride penetration depth was less as compared to the Portland cement SCC mix. After freezing and thawing, SCC incorporated with FA and FA+SF showed better residual compressive strength than the control SCC mix. The residual splitting tensile strength reduced with increase in FA content after 90 freeze-thaw cycles; however, at the same time, all SCC mixes incorporated with FA+SF showed greater residual splitting tensile strength than the control mix.

Dinakar et al. [19] carried out an experimental study on strength and durability performance of SCC made with varying amounts of fly ash content (0, 10, 30, 50, 70 and 85%). Eight SCC mixes were prepared using sulphonated naphthalene formaldehyde condensate based high range water reducer and five normal vibrated concrete mixes were also prepared for comparison at equivalent strength. The durability properties were evaluated by permeable voids, water absorption, acid attack and chloride permeation. The obtained results indicated that the compressive strength of SCC mixes were inversely proportional to the fly ash replacement; however, 60-90 MPa strength was achieved using 30-50% fly ash replacement. It was also observed that SCC mixes indicated higher permeable voids and water absorption as compared to normal vibrated concretes of the same strength grades. The higher permeable voids and water absorption in SCC (made with OPC plus different replacement levels of fly ash) as compared to that in normal vibrated

concrete (made with OPC) of same strength grade may be attributed to higher paste volume of SCC due to lower specific gravity of fly ash. Acid attack due to 3% H_2SO_4 solution showed significant decrease in weight loss with increase in fly ash replacement in SCC. Further, high volume fly ash based SCC mixes exhibited very low chloride permeability. The very low chloride permeability of high volume fly ash based SCC mixes may be attributed to higher chloride binding in these mixes.

Gesoglu et al. [69] carried out a study to find out the optimal mix proportioning of SCC by using different types of mineral admixtures. The materials used for preparation of binary, ternary and quaternary cementitious mixes were Portland cement (PC), fly ash (FA), ground granulated blast furnace slag (GGBS), silica fume (SF), coarse aggregate (maximum size 16 mm), fine aggregate and polycarboxylic-ether based superplasticizer. Total 22 concrete mixes were prepared with a water-binder ratio of 0.44 and total binder content of 450 kg/m^3. The replacement levels of FA and GGBS were 20%, 40%, and 60%, whereas that of SF were 5%, 10% and 15% by weight of cement. The fresh properties of mixes were determined by slump flow, T_{50cm} slump flow time, L-box, and V- funnel flow time. Furthermore, hardened properties were determined from compressive strength, ultrasonic pulse velocity, water permeability, sorptivity index, electrical resistivity, drying shrinkage and chloride ion permeability tests. From the obtained results, it was observed that the incorporation of mineral admixtures improved the filling and passing abilities of SCCs. Further, FA based binary and ternary mixes showed lower compressive strength as compared to GGBS and SF based binary and ternary mixes. Water permeability, sorptivity, and chloride ion permeability were decreased as compared to control mixes when mineral admixtures were used in SCCs. Further, it was observed that an increased amount of mineral admixtures improved the electrical resistivity of SCCs. In binary mixes, FA and GGBS caused a reduction in the free shrinkage of the SCC mixes, while SF increased the drying shrinkage. At the end of the multi-objective optimization process, the authors obtained thirty-six different mixes that satisfied the specified constraints and limits, and the desirability function values of these mixes were in the range from 0.348 to 0.823. Based on the results of the multi-objective optimization, the authors proposed the following mix proportioning for an optimum design value of 0.823: cement of 183.4 kg/m^3, fly ash of 5.2 kg/m^3, ground granulated blast furnace slag of 196.2 kg/m^3, silica fume of 64.1 kg/m^3 and the amount of superplasticizer of 5.2 kg/m^3.

Sahmaran et al. [70] carried out an experimental study to investigate the fresh, mechanical and transport properties of self-consolidating concrete (SCC) containing high percentages of low-lime and high-lime fly ash (FA). In this experimental work, 11 concrete mixes were prepared. The control mix included only Portland cement (PC) as a binder, and remaining mixes included high-lime fly ash and low-lime fly ash with replacement levels of 30%, 40%, 50%, 60% and 70% by weight of Portland cement. The total amount of cementitious material (cement + fly ash) and the amount of polycarboxylic-ether type high range water reducer admixture for all the mixes were kept constant and only water-cementitious material (w/cm) ratios were changed with the change in water content. In all mixes, limestone powder (LP) was used as a fine material. The workability properties of SCCwere measured with respect to slump flow time and diameter, V-funnel flow time, L-box height ratio, and segregation ratio. The hardened properties such as compressive strength at 28, 90, 180 and 365 days, splitting tensile strength at 28, 90 and 180 days and drying shrinkage at 365 days were determined. The transport properties such as absorption, sorptivity, and rapid chloride permeability tests were evaluated at 28, 90, 180 and 365 days. Form the obtained results, it was obseeved that all workability test results were in the range according to EFNARC norms except for V-funnel flow time in some cases. After 28 days, the compressive strength of SCC mixes containing fly ash was lower than the control mix. At the testing ages of 90, 180 and 365 days, the compressive strength was higher for low-lime fly ash as compared to the high-lime fly ash SCC mixes. It was observed that the splitting tensile strength of all SCC mixes increased with age, while at early ages the splitting tensile strength of the SCC decreased with increase in FA content. Both low-lime fly ash and high-lime fly ash reduced the drying shrinkage in comparison with the control SCC mix. At the same w/cm ratio, the chloride ion penetration for SCC mixes containing both high-lime and low lime fly ash was lower than the control mix. It was also observed that the volume of penetrable pores measured with the absorption test was in good linear correlation with the sorptivity test measured within the first two hours of immersion.

Hossain and Lachemi [71] studied the cost effectiveness of SCC by incorporating volcanic ash (VA) with varying water-to-binder (w/b) ratios and varying dosages of superplasticizer. For this purpose, twelve VA based SCC mixes were prepared with a constant binder content, w/b ratios of 0.35, 0.40 and 0.45, superplasticizer dosages of 3.4, 2.4, and 1.5 l /m^3 and replacement of cement by VA with 0%, 20%, 30%, 40% and 50% by weight. The fresh concrete properties were evaluated by slump flow, V-funnel flow time, bleeding, air

content, and segregation tests. The mechanical and durability properties such as compressive strength, freezing-thawing resistance, rapid chloride permeability, surface scaling resistance and drying shrinkage were measured. The authors have reported that all the VA based SCC mixes showed good workable performance. Both the initial and final setting time increased with increase in VA content and w/b ratio. The compressive strength of SCC decreased with addition of VA. The drying shrinkage increased with age and at combination of lower w/b ratio and higher percentage of VA, the drying shrinkage value decreased. Chloride ion resistance of VA based SCC mixes increased with increase in addition of VA. Entrainment of air can improve the freezing and thawing resistance of the concrete mixes but in this study, non-air-entrained nature of concrete mixes were used and low values of durability factor were estimated. According to ASTM C672, the surface scaling resistance ratings of concrete mixes is on a scale of 0 – 5. With a rating of 5, VA based SCC mix with addition of more than 20% VA showed poor scaling resistance.

Leemann et al. [72] determined the porosity in the interfacial transition zone (ITZ) of SCC mixes produced with four different binders (ordinary Portland cement, Portland limestone cement, slag cement and ordinary Portland cement combined with fly ash)and determined the chloride resistance and compressive strength of those SCC mixes. Further, the bleeding of self-compacting mortars (SCM) made with the same binders as the SCC mixes were measured. From the obtained results, there was no significant difference in bleeding behaviour of different types of cements and no relation between bleeding and ITZ porosity obtained. It was observed that the porosity in the ITZ of all four SCC mixes was more than the porosity of the bulk paste however, all SCC mixes showed a similar width of the ITZ. It was also seen that the pores in the ITZ and in the bulk paste were distributed non-uniformly. The ITZ porosity at the top of aggregates was always significantly lower than the side and bottom of the aggregates. The substantial differences in the chloride migration coefficients showed that the binder type had a stronger influence on permeability than the pore volume in the ITZ.

Wang and Huang [73] studied the durability properties of self-consolidating concrete using waste LCD glass as a fine aggregate. For experimentation, sand was replaced by glass sand (0%, 10%, 20%, and 30%) and cement was partially replaced by fly ash and slag at a water-binder (w/b) ratio of 0.28. Type G water-reducing retarder was used as per ASTM C494 guidelines. Compressive strength, flexural strength, ultrasonic pulse velocity, shrinkage, electric resistivity, sulfate attack and chloride ion penetration resistance tests

were performed on all the concrete mixes. From the obtained results, highest compressive strength and flexural strength were observed in the SCC mixes made with 20% glass sand followed by a decrease with an increase in LCD glass content. Self-compacting glass concrete showed increase in ultrasonic pulse velocity as well as electric resistivity with respect to replacement LCD glass content and time. Further, shrinkage increased with increase in amount of LCD glass replacement. It was observed that weight loss due to sulfate attack reduced with increase in glass sand content after eight cycles and chloride ion penetration was less than 100 C at aged for 180 days. The authors concluded that the durability properties of SCC were improved by using waste LCD glass up to 30% replacement of fine aggregate.

Siddique [74] carried out a study to evaluate the properties of self-compacting concrete (SCC) made with Class F fly ash (15% to 35%). Five concrete mixes were prepared with different w-b ratios (0.41–0.44 by weight) and total powder content of 550 kg/m^3 by assuming air-content of 2%. Coarse aggregate content was 39% by volume of concrete and fine aggregate content was 45% by volume of mortar. A polycarboxylic ether based superplasticizer was in the preparation of the mixes. The fresh, mechanical and durability properties were evaluated by slump flow, J-ring, V-funnel, L-box, U-box; compressive strength and splitting tensile strength; deicing salt surface scaling, carbonation and rapid chloride penetration resistance tests. The SCC mixes made with fly ash content up to 35% satisfied all the fresh properties as per the criteria given by EFNARC. The compressive strength and splitting tensile strength (at 7, 28, 90 and 365 days) increased with decrease in w/b ratio and fly ash content. The carbonation depth increased with increase in age from 90 to 365 days for all SCC mixes. Deicing salt surface scaling resistance test showed that the weight loss increased with increase in fly ash content (except SCC with 15% fly ash). At the ages of 90 and 365 days, the SCC mixes with fly ash reduced the rapid chloride ion penetrability.

Hassan et al. [75] studied the effect of incorporating metakaolin (MK) and silica fume (SF) on the durability of self-consolidating concrete. In SCC, the replacement of cement by MK were 0%, 3%, 5%, 8%, 11%, 15%, 20% and 25%, and that by SF were 0%, 3%, 5%, 8% and 11%. HRWR (high range water reducer) admixture, and a constant water-binder ratio of 0.4 were used in the preparation of SCC mixes. The fresh properties such as slump flow, L-box, V-funnel and HRWR admixture demand; the hardened properties such as compressive strength and air void characteristics; and durability performance such as

drying shrinkage, freezing and thawing, salt scaling and rapid chloride permeability were evaluated. The results indicated that the viscosity of SCC mixes increased with incorporation of MK; however, the incorporation of silica fume showed no effect on viscosity. The passing ability was enhanced with increase in percentage of MK. The HRWR admixture demand decreased by using MK as compared to replacement of cement with the same amount of silica fume. The compressive strength of SCC increased by addition of MK from 0% to 25% and it was also observed that at 8% replacement, MK and SF exhibited same compressive strength. For the scaling resistance of SCC, the use of MK was more effective than SF at the same level of cement replacement. It was also observed that the effects of drying shrinkage, and freezing and thawing resistance were higher in SCC made with addition of MK as compared to SF at the same level of replacement. The chloride permeability decreased with the addition of SF as compared to MK at the same level of cement replacement.

Kanellopoulos et al. [76] carried out a study on the durability performance of SCC, and compared with conventional concrete. Total eight mixes were prepared with varying water-binder ratios. Out of eight mixes, six of them were self-compacting concretes (three with silica fume and three without silica fume) and remaining two were normal vibrated concrete mixes (NVC). In the production of all SCC mixes, cement and silica fume (7%, 15%, and 20%) as binder, limestone powder as filler, coarse and fine aggregate and polycarboxylate water reducing agent (PCWRA) were used. All the ingredients in NVC were same as SCC except limestone powder, silica fume, and PCWRA. In NVC, a poly-naphthalene based superplasticizer was used for preparation of concrete mix. The mechanical and durability properties of SCC were evaluated by compressive strength, modulus of elasticity, sorptivity, porosity, and chloride ion permeability tests. From the obtained results, it was observed that the mechanical performance of SCC made without silica fume were better than NVCs. The SCC mixes enhanced the durability properties as compared to NVCs including even the SCC made with more water content and without silica fume. Silica fume reduced the chloride ion permeability and also reduced the open porosity and capillary absorption as compared to other SCC and NVC mixes. The correlation between sorptivity and open porosity for all SCC mixes showed perfect linear correlation and similar correlation was also observed between sorptivity and chloride permeability.

Pathak and Siddique [77] carried out a study to determine the properties of SCC containing fly ash and subjected to different temperatures such as 20°C, 100°C, 200°C, and

300°C. For this experimental work, one control mix was prepared with ordinary Portland cement, and the other three concrete mixes were prepared by replacing cement with 30%, 40%, and 50% of Class F fly ash by weight of total powder content (500 kg/m^3). Polycarboxylic ether based superplasticizer was used at dosage of less than 2% of total powder content for all the mixes. The water-to-binder ratio varied from 0.38 to 0.42 by weight and 2% air content was assumed. Self-compatibility of concrete was determined by slump flow test and U-box (difference in height) test. Compressive strength at 28 days and 91 days, splitting tensile strength, rapid chloride permeability, porosity and mass loss tests were also performed on all the SCC mixes. To determine the compressive strength, cubes of size 150 mm were prepared. While cylinders of size 150 mm (diameter) × 300 mm (height) and 100 mm (diameter) × 50 mm (height) were prepared for splitting tensile strength and rapid chloride permeability test, respectively. From the obtained results, it was observed that all high volume fly ash concretes exhibited fresh properties in good agreement with European guidelines. Without heating, the compressive strength increased with decrease in percentage of fly ash replacement. However, a small loss of strength was observed in the temperature range between 20 to 200ºC while, in the temperature range of 200 to 300ºC, a little improvement in compressive strength was observed in all concrete specimens as compared to the strength at 100ºC. The little improvement in compressive strength in the temperature range of 200 to 300ºC is attributed to the hydration of anhydrous cement particles that leads to the formation of hydrates having better bonding properties. It was also observed that the rate of loss of splitting tensile strength was more than the rate of loss of compressive strength at elevated temperatures. For both before and after heating, the high volume fly ash SCC mixes showed significantly lower chloride ion permeability than the SCC mix made without fly ash.

Uysal et al. [78] studied to evaluate the effect of mineral admixtures on mechanical properties, chloride ion permeability and impermeability of SCC. In this experiment, fly ash (FA: 15%, 25%, 35%), granulated blast furnace slag (GGBS: 20%, 40%, 60%), limestone powder (LP: 10%, 20% and 30%), basalt powder (BP: 10%, 20% and 30%) and marble powder (MP: 10%, 20% and 30%) were used as part replacement of cement. Workability of SCC was evaluated by slump flow, T_{50cm} time, L-box, and V-funnel tests. The hardened properties such as ultrasonic pulse velocity and compressive strength were determined at 7 and 28 days. Durability properties of SCC mixes were evaluated by chloride ion permeability and water impermeability tests. From the results, it was observed

that the workability was increased in SCC made with FA and GBSF as compared to all others mineral admixtures. At 28 days, SCC with 20% GGBS showed highest compressive strength, which was more than 78 MPa as compared to all others mixes. Chloride ion permeability decreased considerably when mineral admixtures were used in the production of SCC. Further, SCC with 60% GGBS showed best resistance to chloride ion permeability. Impermeability depth test results showed that the water impermeability depth increased with increase in amount of mineral admixtures in SCC.

Ramezanianpour et al. [79] carried out a study to determine the effect of natural zeolite on properties of SCC mixes. For this purpose, two methods were adopted: dense aggregate grading and partially replacement of Portland cement by natural zeolite (NZ:10%, 15%, 20%, 25% and 30%). Total seven concrete mixes were prepared. Out of seven mixes, one of them was control SCC (CTRL), another was conventional concrete mix with a slump value of 150 mm (NC-CTRL), and remaining mixes were cement replaced with NZ. Constant water-cementitious materials ratio of 0.45 and total cementitious materials of 350 kg/m^3 were used for all the mixes. Polycarboxylate ether type HRWRA (high range water reducing admixture) was used in the preparation of mixes. Slump flow, T_{50cm} time, J-ring, and GTM screen stability on fresh concrete, and compressive strength, electrical resistivity and rapid chloride penetration tests (RCPTs) at the ages of 28, 90, 180, and 270 days were carried out to on hardened concrete to evaluate the properties of SCC mixes. From the obtained results, the criteria as per EFNARC for fresh properties was satisfied with the incorporation of 10% to 25% NZ while control SCC mix did not satisfy fresh properties because of significant bleeding. It was also observed that to maintain the required flowability, HRWRA demand was increased in case of higher levels of cement replacement by NZ, and also NZ led to high viscosity. The compressive strength increased with incorporating NZ at the age of greater than 28 days. However, NZ with 10% mix showed higher strength values as compared to NC-CTRL mix at 270 days of curing. At hardened state, using higher replacement levels of NZ resulted in lower RCPT values and higher surface resistivity.

El-Chabib and Syed [80] carried out an experimental investigation to determine the properties of self-consolidating concrete (SCC) mixes prepared with binary, ternary and quaternary blends. The authors have used high content of supplementary cementitious materials (SCM) such as fly ash (Class C and Class F), silica fume, and granulated blast furnace slag, for replacement of Portland cement up to 70%. For all SCC mixes,

polycarboxylate-based HRWRA (high range water reducing admixture) was used and for air-entrained concrete mixes, sodium dodecylbenzenesulfanate air-entraining admixture (AEA) was used. The fresh properties of SCC mixes were determined by slump-flow, T_{50cm} test, J-ring test, and segregation index test. The mechanical and durability properties of concrete mixes were evaluated by compressive strength (1, 7, 28, and 90 days), splitting tensile strength (28 days), free shrinkage (up to 90 days) and resistance to chloride ingress by rapid-chloride-permeability test (56 days). The obtained results indicated that the addition of fly ash and slag as partial replacement of cement increased the workability as well as the long-term compressive strength of concrete, but silica fume reduced the workability and increased the compressive strength of SCC mixes when added up to 10% in ternary and quaternary blends. The binary SCC mixes incorporating 60% Class F fly ash exhibited low early-age compressive strength. The permeability as well as free shrinkage of SCC mixes with high contents of SCM were lower than that of control mix.

Sabet et al. [81] carried out a study on mechanical and durability properties of self-consolidating high-performance concrete (SCHPC) incorporating natural zeolite (NZ), silica fume (SF) and fly ash (FA) with each of 0%, 10% and 20% replacement by weight of cement. The water-to-cementitious materials ratio of 0.33 and total cementitious materials content of 500 kg/m^3 were used. For all mixes, fine aggregate to coarse aggregate ratio (by weight) was considered at about 1.5:1. Poly-carboxylic acid-based superplasticizer was used with a specific gravity of 1.07 and solids content of 36%. The properties of concrete were evaluated by slump flow, compressive strength, electrical resistivity, water absorption and chloride permeability tests. From the obtained results of fresh properties, it was observed that the superplasticizer demand of the SCHPCs increased by incorporation of NZ and SF while the use of FA decreased the demand. The effect of SF was more in enhancing the compressive strength as compared to NZ. The replacement of cement by FA in SCHPCs decreased the compressive strength that was more than 30%. Electrical resistivity of SCHPC mixes increased by addition of all mineral admixtures at later ages. Among all SCHPC mixes, SF mixes were most effective in reduction of final water absorption. Although, final water absorption was reduced with the addition of NZ and FA; however, these mineral admixtures were not as effective as compared to that of SF. Among three mineral admixtures, silica fume was the most effective one in decreasing the chloride penetration and chloride diffusion into concrete. Use of 10% silica fume decreased effective diffusion coefficient and further increase in silica fume content did not

improve chloride diffusivity significantly. Addition of NZ and FA decreased the effective diffusion coefficient and fly ash was found to be less effective than that of NZ. Incorporation of NZ in SCHPC decreased the effective diffusion coefficient by more than two times as compared to the control mix. The final results indicated that in the SCHPC mixes, silica fume was slightly more effective than natural zeolite or fly ash, while natural zeolite was much more cost-effective.

Sideris and Anagnostopoulos [82] studied the durability properties of normal strength SCC and compared them with same properties measured on normally vibrated concretes (VC) of the same strength class, and also calculated the service life of reinforced concrete structures. Eight different SCC and VC mixes were made using cement, limestone as a filler, coarse aggregate and different types of sands (limestone and siliceous river sand), but limestone was not used in VC. Carboxylic ether polymer admixture was used as a high range water reducing admixture. The durability properties were evaluated by water absorption, carbonation depth and chloride diffusion coefficient. From the obtained results, it was observed that the water capillary absorption (sorptivity), carbonation depth and chloride penetration values of SCCs were lower as compared to that of VCs i.e., durability characteristics of SCC was better than those of VC at same strength class. Further, the use of SCC prolonged the service life of reinforced concrete structures against carbonation and chloride induced corrosion, which was used for calculating the total life-cycle cost of concrete structures. The initial production cost of SCC was greater than that of VC for the same strength class however, the difference in the production cost was decreased with increase in strength of the concrete mixes. It was also observed that, in case of SCC mixes the cost per year of service life of the structures was further decreased and became close to or smaller than VC for equivalent strength class.

Dinakar et al. [83] carried out an experimental investigation to determine the behaviour of self-compacting concrete using Portland pozzolana cement (PPC) replaced with 10 – 70% fly ash. For the preparation of all mixes, polycarboxylate ether based superplasticizer and a constant w/b of 0.30 were used. Blending of aggregates with 20 mm - 21%, 12.5 mm - 30% and 4.75 mm - 49% of the total aggregate content were used in all the mixes. Fresh properties such as slump flow, V-funnel time and L-box; mechanical properties such as compressive strength, splitting tensile strength and elastic modulus; and durability properties such as water absorption, water penetration depth and chloride permeability were evaluated to determine the behaviour of self-compacting concrete. It was observed that the

optimum dosage of fly ash is 30% when PPC is used and it exhibited highest compressive strength, splitting tensile strength and elastic modulus and also exhibited less chloride permeation. However, the water absorption of SCCs increased with increase in fly ash content. The initial absorption values of all SCCs were below 3% and SCC with 70% replacement of fly ash showed highest water absorption.

Wang and Lin [84] evaluated the variations in fresh and engineering properties of self-compacting high slag concrete (SCHSC). In this study, type G admixture (superplasticizer) with a constant water-binder ratio of 0.37 was used in the preparation of the concrete mixes with 0%, 15% and 30% furnace slag as replacement of cement by weight. The tests for slump, slump flow, unit weight, air content and chloride ion concentration were carried out. In addition, compressive strength, ultrasonic-pulse velocity and volume change of the concrete mixes were also evaluated. From the obtained results, 15% furnace slag based SCC showed with 25 cm slump, 55 – 70 cm slump flow, air content of less than 3% and chloride ion concentration of less than 0.3 kg/m^3. The compressive strength results indicated that the concrete mix made with 15% furnace slag replacement showed higher compressive strength than the control group (higher with 13%). For MOCK-UP model, the cores were drilled from upper, middle and lower layers of the field specimen. According to the compression test on the drilled core from the MOCK-UP model, the compressive strength of the 15% furnace slag group was apparently higher than that of the control group (higher with 5.1%). The shrinkage increased as the amount of slag added increased. The ultrasonic pulse velocity was higher in the SCHSC containing 15% and 30% furnace slag as compared to control group.

Nikbin et al. [85] carried out a comprehensive investigation to evaluate the mechanical behaviour of SCC in terms of water-cement (w/c) ratio and powder content. In this study, sixteen SCC mixes were prepared and divided into two series. In the first series, eight mixes were considered to determine the effect of w/c ratio (varying from 0.35 to 0.70). In the second series, other eight mixes were considered with different amounts of limestone powder (25%, 50%, 75% and 100%) at two w/c ratios of 0.47 and 0.60. All these mixes were prepared with 12.5 mm maximum size of coarse aggregate and third generation (Gelenium 110) based superplasticizer. The flowability, passing ability, and segregation resistance were evaluated by slump flow, L-box and sieve segregation tests. For each mix, cube specimens of size 100 mm were prepared to determine the compressive strength and cylindrical specimens of size 150 mm (diameter) × 300 mm (height) were prepared to

determine the modulus of elasticity and splitting tensile strength. Additionally, this study presented an extensive evaluation and comparison between mechanical properties of SCC using current international codes and predictive equations proposed by other researchers. The comprehensive data reported by many researchers for SCC and NVC (normal vibrated concrete) were used to compare and validate the obtained results. From the obtained results, with increase in w/c ratio from 0.35 to 0.70 the mechanical properties of SCC were decreased by 66%, 51%, and 44% for compressive strength, tensile strength, and modulus of elasticity, respectively. With increase in limestone powder content from 25% to 100% in SCC mixes for two w/c ratios of 0.60 and 0.47, the compressive strength increased by 20% and 38%, respectively, similarly tensile strength increased by 17% and 12%, and modulus of elasticity increased roughly by 9% for both w/c ratios. The obtained mechanical properties were in good agreement with the results reported by other researchers. The authors observed that the effect of w/c ratio on variations in compressive strength and tensile strength was more than that of modulus of elasticity.

Celik et al. [86] carried out a study to evaluate the effects of natural pozzolan (NP) and Class-F fly ash (FA) on compressive strength and durability properties such as non-steady state chloride migration and gas permeability of self-consolidating concretes (SCC). For the preparation of concrete mixes, the water-to-total binder ratio and the total aggregate to fines ratio were kept constant at 0.35 and 4:1, respectively. For the binary mixes, cement was replaced with NP and FAF by 30 to 65 % by weight, while for the ternary blend mixes, limestone filler (LF) was fixed at 15% by weight of cement and replacement of NP or FAF varied from 30 to 50 % by weight. From the obtained results, it was observed that the supplementary cementitious material replacement contents did not have explicit influence on the flowability of SCC. Further, at the ages of 7, 28 and 91 days, the binary mix made with 70% OPC-30% NP showed higher compressive strength as compared to 70% OPC-30% FA mix while, 50% OPC-50% NP showed lower compressive strength than 50% OPC-50% FA mix. All the binary and ternary mixes confirmed that the chloride migration was lower as compared to the control mixes. Further, gas permeability of binary mixes made with NP indicated lower resistance as compared to the mixes made with FA, while the ternary mixes made with NP-LF showed higher resistance to gas permeability as compared to the mixes made with FA-LF. The authors suggested that the low-cost and environmental friendly SCC can be produced by using natural pozzolan and Class-F fly ash.

Ryan and O'Connor [87] have studied the durability performance concerning to chloride resistance of SCC and compared with normal vibrated concrete (VC). Total six concrete mixes of SCC and VC were prepared with OPC and OPC plus pulverised fuel ash (PFA), and ground granulated blast furnace slag (GGBS) at w/b ratio of 0.44. Cube specimens of size 100 mm were prepared for different tests including compressive strength and salt fog chamber tests. For salt fog test, the cubes specimens were wet cured for 28 days, afterward epoxy coating was applied on five faces except one face for salt exposure. The salt exposure chamber filled with 5% NaCl solution fog. To accelerate the ingress of chloride ions, the wetting-drying cycle was carried out for 12 hours wetting followed by 12 hours drying. The chloride transport properties were determined in terms of chloride diffusion coefficient using Fick's second law of diffusion followed by prediction of service life for both types of concrete. From the obtained results, it was observed that, both types of concrete (SCC and VC) made with OPC+GGBS showed similar mean compressive strength. However, for OPC and OPC+PFA, VC mixes showed higher mean compressive strength as compared to SCC mixes. Further, the VC mixes made with OPC and OPC+PFA showed greater resistance against chloride ingress than the equivalent SCC mixes. For OPC and OPC+PFA, the greater resistance of VC mixes against chloride ingress as compared to SCC mixes may be attributed to lower volume of cement paste per unit volume of concrete in VC mix that contains less voids. For concrete mix made with OPC+GGBS, the durability was similar for both SCC and VC mixes.

Vivek and Dhinakaran [88] studied the durability properties of binary SCC made with three different supplementary cementitious materials. For binary mixes, ground granulated blast furnace slag (GGBS: 25%, 50% and 75%), metakaolin (MK: 10%, 20% and 30%) and silica fume (SF: 5%, 10% and 15%) were used as supplementary cementitious materials as replacement of cement. To assess the suitability of mineral admixtures concerning durability of SCC mixes, resistance against acid attack, sulphate attack, water absorption and sorptivity tests were carried out. The cube specimens were immersed in dilute 5% of H_2SO_4 solution and 5% of Na_2SO_4 solution for weight loss due to acid attack and sulphate attack respectively till the age of 28 days and 56 days. All 11 mixes showed higher resistance to sulphate attack after 28 and 56 days immersion in 5% Na_2SO_4 solution. The higher replacement of SCC with 75% GGBS, 15% SF and 30% MK showed lower weight loss after immersion in 5% H_2SO_4 solution at 28 and 56 days. The SCC mixes made with 50% GGBS, 20% MK and 10% SF and exposed to sulphuric acid, and sodium sulphate

solution showed better strength among all the nine different mixes. The authors also calculated the economic feasibility by economy index, and concluded that SCC mixes with 50% GGBS, 20% MK and 5 to 10% of SF were optimum mixes.

Benli et al. [89] investigated the mechanical and durability properties of SCC containing binary and ternary mixes of silica fume (SF) and fly ash (FA). In this experimental study, 14 series of mortar specimens were prepared including control mix with Portland cement, Portland cement replaced with 10%, 20% and 30% by weight of Class C fly ash and 6%, 9%, 12% and 15% by weight of silica fume. Further, ternary mixes were produced using 10% of FA with 6%, 9%, 12%, and 15% of SF and 20% of FA with 6%, and 9% of SF. Both binary and ternary mixes were prepared at w/b ratios in the range of 0.42 to 0.52. The fresh properties were determined using mini-slump flow test and V-funnel flow test. The mechanical properties were determined using compressive and flexural strength tests on 40 × 40 × 160 mm prim specimens at different ages and exposed to different exposure solutions such as: 3, 28, 56 and 180 days cured in water; 28, 56, 90 and 180 days immersed in sea water and 10% $MgSO_4$ solution. Sorptivity and porosity tests were also performed on cube specimens of size 50 mm. From the obtained results, the self-compacting mortars exhibited satisfactory fresh self-compacting properties. Further, FA series mixes showed better workability properties as compared to SF series mixes. All the specimens showed increasing compressive strength up to 90 days when exposed to $MgSO_4$ solution as compared to water and seawater solution followed by decrease at the age of 180 days. Addition of FA showed decrease in compressive strength and tensile strength with increase in FA replacement ratio. The best resistance concerning tensile strength was observed in control specimens exposed to seawater. The SF binary blended self-compacting mortars cured in water for 28 days showed higher porosity than ternary blended self-compacting mortars however, the control specimens cured in water for 28 days showed lowest porosity. Deterioration such as crack formation due to surface softening was observed in self-compacting mortar exposed to magnesium sulphate solution.

2.4 Durability properties of SCC with respect to steel reinforcement corrosion

Corrosion of steel reinforcement is one of the most serious durability problems encountered in reinforced concrete structures. Several studies have been carried out by various researchers on corrosion performance of steel reinforcement in normal vibrated concrete. However, few studies have been carried out by the researchers on corrosion performance

of steel reinforcement in SCC. The reported research work in the literature on corrosion performance of steel reinforcement in SCC are presented in this section.

Hassan et al. [90] investigated the long-term performance of self-consolidating concrete (SCC) and compared it with normal concrete (NC) in terms of corrosion resistance of steel reinforcement. The authors have studied the corrosion performance in full-scale beams and small cylindrical specimens. The corrosion performance of NC/SCC beams was measured by current measurement, half-cell potential tests, chloride ion content, rebar mass loss and rebar diameter degradation. The effect of admixture type and size of the specimen on corrosion performance of NC/SCC beams were also studies. An accelerated corrosion test was continued until beam specimens containing epoxy-coated stirrup**s** reached a moderate corrosion level while specimens containing non-epoxy-coated stirrup**s** reached a severe corrosion level. The results reported that SCC beams showed less cracking as compared to NC beams for both moderate and severe corrosion levels, and also the average crack width of SCC beams was less than average crack width of NC beams. NC beams indicated earlier corrosion initiation and a higher corrosion rate as compared to SCC beams. The results of half-cell potential measurement showed higher probability of corrosion in NC beams than that of SCC beams. It was also observed that there was strong correlation between the predicted rebar mass loss obtained by Faraday's equation and the experiment, which can be used to examine the effect of corrosion over time. It was observed that types of admixture used in SCC mixes have no effect on corrosion performance in terms of corrosion initiation, corrosion rate, and crack patterns and widths. In terms of corrosion performance, the difference between SCC and NC mixes was only evident in large-scale concrete beams and no such difference was observed in small-scale cylindrical specimens.

Dinakar et al. [91] evaluated the corrosion performance of SCC made with high-volume replacements of fly ash. In this study, eight self-compacting fly-ash concretes were prepared with various strength grades. The replacement levels of fly ash were 0%, 10%, 30%, 50%, 70% and 85% by weight of cement. For comparison, five different mixes of normal vibrated concrete at equivalent strength grades were also prepared. For evaluating the fresh properties of SCC, slump flow, V-funnel and J-ring tests were conducted. The compressive strength test was also carried out at the ages of 28, 90, and 180 days. The corrosion behaviour of developed concretes was studied through the measurement of resistivity, pH, carbonation depth, half-cell potential and corrosion rate. The cube specimens of size 100 mm were used for determining the compressive strength and

resistivity of concrete. After compressive strength test, middle portion of the cube was crushed and concrete powder was obtained by sieving though 300 µm mesh. The carbonation depth was measured on split cylinder specimens after 90 days of water curing till 12 months of outdoor exposure of CO_2. The half-cell potential and electrochemical potentiodynamic polarization measurements were carried out on 100 × 200 mm cylinders with a centrally embedded 8 mm diameter and 100 mm long rebar. For half-cell potential measurement, the specimens were immersed in normal water and for corrosion rate, the specimens were immersed in 3% NaCl solution for 4 days before the testing age of 90 days. From the results, it was observed that fly ash based SCC showed higher resistivity and carbonation depth than the corresponding normal vibrated concrete. Increase in replacement level of fly ash increased the resistivity of SCC mixes. The measured pH values of fly ash based SCC showed higher alkalinity (pH of 12 or above) at 70% and 85% replacement levels of fly ash. The fly ash based SCC mixes showed less negative potential with time and with increasing strength at 90 days. The corrosion rate was also less in fly ash based SCC as compared to corresponding normal vibrated concrete. Further, the corrosion rate decreased with increase in fly ash replacement level. The authors concluded that SCC at all levels of fly ash replacement exhibited significantly better performance than the corresponding normal vibrated concrete.

Dehwah [92] carried out an experimental study on the corrosion resistance of self-compacting concrete produced by incorporating quarry dust powder (8 and 10% of total aggregate) as a filler material, silica fume (5% replacement of cement) and fly ash (30% replacement of cement) as mineral admixtures. ASTM C 150 Type I Portland cement, crushed limestone coarse aggregate, dune sand, polycarboxylic ether based superplasticizer and stabilizer, which consists of a mix of water-soluble copolymers were used in this study. Five different concrete mixes were prepared at w/c ratios of 0.38 and 0.40. Different tests such as corrosion potential using saturated calomel reference electrode, corrosion current density, chloride diffusion test, and chloride permeability test were performed on cylindrical concrete specimens of size 75 mm diameter and 150 mm height. For corrosion tests, cylindrical concrete specimens were prepared with a centrally embedded steel bar of 12 mm diameter. After 28 days of curing, the cylindrical specimens were exposed to 5% NaCl solution up to a height of 100 mm from the bottom of specimens for two years. For chloride diffusion test, the cylindrical concrete specimens were immersed in 5% sodium chloride solution for four months and to ensure unidirectional diffusion of chloride ions,

all the faces except one were coated with epoxy coating. After the end of exposure period, 5 mm thick slices were cut from various depths and after that the slices were crushed to obtain the powder. The powder was soaked in deionized water for 24 hours and then the filtrate was analyzed for determining chloride concentration by spectrophotometric method. From the obtained results of the experimental study, it was observed that SCC made with quarry dust powder or along with silica fume did not show corrosion activation till the exposure duration of two years and the time to initiation of corrosion was also long. Further, SCC made with incorporating quarry dust powder, and silica fume showed lower chloride permeability as well as lower chloride concentration. The highest diffusion coefficient was observed in fly ash incorporated SCC. From the study, it was concluded that SCC incorporated with quarry dust powder or along with silica fume are suitable for structures exposed to the chloride-bearing environment.

Ahmad et al. [93] carried out a study on high-performance SCC using different combinations of filler materials such as silica fume (SF), natural pozzolana (NP) and metakaolin (MK) in conjunction with limestone powder (LPS) to evaluate its various properties. Crushed limestone coarse aggregate of size 20 mm and dune sand were used in all the mixes with sand to total aggregate ratio of 0.50 by weight. Constant water-to-powder ratio of 0.30 was selected for the mixes. New generation polycarboxylic-based ether hyperplasticiser and high-molecular weight synthetic copolymer (stabilizer/viscosity modifying admixture) were used in the preparation of SCC mixes. The self-compactability tests such as slump flow, V-funnel and U-box tests, and segregation resistance (by visual judgment) were carried out on all SCC mixes in the fresh state. For corrosion resistance, 75 mm (diameter) × 150 mm (height) cylinders were prepared with a centrally embedded 12 mm diameter rebar. All the cylinders were exposed to 5% NaCl solution until 450 days after 28 days of curing. In the hardened state, compressive strength, splitting tensile strength, bond strength, modulus of elasticity, drying shrinkage, water permeability, rapid chloride permeability, electrical resistivity, corrosion potential and corrosion current density were evaluated. From the obtained results, it was concluded that the SCC made with LSP-SF blend showed best performance as compared to blends of other fillers in terms of mechanical and durability performance. In the durability performance, all the mixes showed water penetration depths with average of below 30 mm. Further, the results of rapid chloride permeability indicated that all the mixes have very low chloride permeability in addition to their very high electrical resistivity indicating low to negligible probability of

corrosion. The SCC made with LSP-MK blend showed the time to initiation of corrosion of around 300 days of exposure to 5% NaCl however, steel reinforcement in all other SCC mixes remained in a passive state even after 450 days of exposure.

Adekunle et al. [94] developed high strength SCC mixes using low-cost mineral fillers, which included limestone powder, cement kiln dust, bag house dust, pulverized steel slag, and metakaolin and evaluated their mechanical and durability properties. For ternary mixes, each mineral filler blend with natural pozzolana as the base filler. A new generation polycarboxylic-based ether hyperplasticizer and an aqueous solution of a high-molecular weight synthetic copolymer were used as superplasticizer and viscosity modifying admixture respectively. The mix design of SCC mixes was done based on trial test results, in which all the parameters were fixed, except the dosages of superplasticizer and viscosity modifying admixture. The filling-ability (slump flow and V-funnel), passing-ability (U-box), and segregation resistance (visual examination based on a set of mortar bandwidth criteria) of SCC were evaluated as per EFNARC guidelines. The mechanical properties of SCC mixes were determined by compressive strength, splitting tensile strength, bond (pull-out) strength and static modulus of elasticity. The drying shrinkage of the SCC mixes was also evaluated. The durability properties of SCC mixes were evaluated by water permeability, rapid chloride permeability, and electrical resistivity. In addition, corrosion resistance performance of SCC mixes was evaluated by corrosion potential and linear polarization measurement on 75 mm diameter × 150 mm height cylinders with a centrally embedded rebar of 12 mm diameter. For corrosion resistance performance, all the cylindrical specimens were exposed to 5% NaCl solution until 450 days after 28 days of curing. From the obtained results, it was observed that all the developed SCC mixes showed high compressive strength in the ranges of 36 – 49 MPa, 47 – 56 MPa, 65 – 68 MPa and 70 – 83 MPa at the ages of 3, 7, 28 and 90 days, respectively. The average elastic modulus of developed SCC mixes varied from 40 to 42 GPa while, the splitting tensile strength and pull-out bond strength varied from 5.3 to 6.1 MPa and 21 to 36 MPa respectively. The SCC mix made with blend of bag house dust and natural pozzolana showed about 40% more shrinkage strain than other mixes. The results of the indirect assessment of corrosion resistance such as chloride permeability and electrical resistivity showed lower probability of reinforcement corrosion, which was also confirmed by direct assessment using corrosion current density measurement. The authors concluded that the developed SCC mixes using

industrial wastes such as mineral fillers showed high performance as well as excellent corrosion resistance except the SCC mix incorporating bag house dust.

Ghanooni-Bagha et al. [95] studied the corrosion resistance self-compacting concrete and examined the correlation between the corrosion and concrete compressive strength reduction. Concrete mixes were prepared using ordinary Portland cement type II and with addition of mineral admixtures such as limestone powder (LP), silica fume (SF), metakaolin (MK), fly ash (FA), and a low activity ground and granulated blast-furnace slag (SL) with a w/cm ratio of 0.40. Polycarboxylate based high-range water reducing admixture was used in the preparation of SCC mixes. Two types of test specimen such as square cube and rectangular block specimens were prepared by placing 1 and 2 rebars, respectively. The specimens were exposed to 5% salt water for 3 days and after that accelerated corrosion test was conducted. The corroded and non-corroded samples were tested for compressive strength after 28 and 90 days. From the obtained results, the authors found a direct relationship between the magnitude of reduced compressive strength and the degree of corrosion along with corrosion crack width. The authors found that the concrete mix with lower compressive strength and mineral admixtures showed highest corrosion resistance. Further, it can be concluded that it is possible to increase the time-to-corrosion by 2–4 times by protecting the structures against aggressive factors and chloride environments or by increasing the curing duration from 1 to 3 months.

2.5 Microstructure of concrete

The hydration and microstructure characteristics of concrete can affect its transport and durability properties. The use of mineral admixtures and fillers as partial replacement of Portland cement as well as the absence of vibration in self-compacting concrete may influence its microstructure. The studies carried out by various researchers to evaluate the microstructure of SCC are presented in this section.

Ye et al. [96] carried out an experimental investigation to study the hydration and microstructure of cement paste in SCC made with limestone as a filler. The SCC paste (SCCP) was prepared with two w/c ratios of 0.41 and 0.48. For comparison, high-performance cement paste (HPCP) with w/c ratio of 0.33 and traditional cement paste (TCP) with w/c ratio of 0.48 were also prepared. The rate of heat evolution of all the pastes was measured in a thermometric isothermal conduction calorimeter. The pore size distribution of pastes was determined by mercury intrusion porosimetry (MIP), and the

phase distribution was evaluated by scanning electron microscopy (SEM) with the help of backscattered electron (BSE) image analysis. The thermogravimetric analysis (TGA) and the derivative thermogravimetric analysis (DTG) were carried out to evaluate the phase constituents of cement pasts. From the results of heat evolution test, it was observed that hydration was influenced by limestone filler in the SCC pastes and it also act as an accelerator during early cement hydration. The pore structure (total pore volume, pore size distribution, and critical pore diameter) of the SCC paste (SCCP) was similar to that of high-performance cement paste (HPCP) mix, which was confirmed from both MIP and BSE image analysis. The relative calcium hydroxide (CH) phases in SCC paste were different from high-performance cement paste and traditional cement paste.

Fares et al. [97] have carried out an experimental study on the performance of self-consolidating concrete (SCC) subjected to high temperature. Three mixes were developed: two different SCC mixes and one vibrated concrete (VC). The mechanical behavior was investigated on cylindrical specimens of size 16 cm diameter with 32 cm height, and prismatic specimens of size 10 cm × 10 cm × 40 cm. Each specimen was heated from 20 °C to 150, 300, 450 and 600 °C at a heating rate of 1°C/ min, afterward the temperature was kept constant at the target temperature for one hour before cooling. Thermogravimetric analysis (TGA) and differential thermal analysis (DTA), X-ray diffraction and SEM analyses were performed on the specimens at ambient temperature as well as after heating to examine the physical, chemical and microstructural properties. For these tests, samples of 3 or 4 cm were drilled out from concrete without considering coarse aggregate. The SEM images were taken on polished mortar samples however, for TGA the mortar samples were crushed and kept in a hermetic flask for analysis. From the SEM images, it was observed that up to 150 °C no visible cracks were appeared but the cracks were more noticeable when heated up to 600 °C. From the results of TGA, it was observed that there was departure of bound water as well as free water in the concrete between the temperature range from 20 to 150 °C, which resulted in slight modification in the porosity of concrete. Further, the porosity of concrete increased due to departure of water from different hydrates within the paste at the temperature range from 150 to 300 °C. Beyond 300 °C, the porosity increased by about 7%, due to some chemical transformations (solid solution Fe_2O_3 or brucite), decomposition of the portlandite and transformation of quartz-α into quartz-β. The fraction of anhydrous phases reduced for both SCC mixes as determined by SEM image analysis, which showed additional hydration of anhydrous cement grains. Different crystal phases

such as portlandite, calcite, and quartz-α were present in both unheated as well as heated at 150 and 300 °C samples as observed from the XRD analysis.

Mohammed et al. [98] carried out an investigation to study the microstructure and hydration of sustainable SCC produced by using fly ash and limestone powder as a filler. Both mixes were designed for the compressive strength of 50 – 60 MPa by considering total amount of binder replaced with about 33% of filler. Different microstructure techniques such as X-ray diffraction, scanning electron microscopy (SEM) with energy-dispersive X-ray (EDX) analysis, image analysis, mercury intrusion porosimetry (MIP) and thermo-gravimetric analysis were performed to study the microstructure and hydration effect of these two fillers. The results obtained from the microstructural investigation indicated that the fly ash based SCC mix exhibited relatively dense concrete matrix as compared to the limestone powder based SCC mix. The Ca/Si ratio determined from EDX analysis was distributed approximately constant across the ITZ interface in fly ash based SCC mix, whereas it varied across the thickness of ITZ in limestone powder based SCC mix. From the results of MIP test, it was observed that the nature of porosity of SCC was not influenced by the type of filler used, whereas it influenced the critical pore diameter notably at 28-days. The limestone powder performed like a relatively active mineral as confirmed by the presence of higher amounts of $Ca(OH)_2$ and $CaCO_3$ in limestone powder based SCC mix in both ITZ and bulk cement paste as compared to fly ash based SCC mix. Both $Ca(OH)_2$ and $CaCO_3$ determined by, thermo-gravimetric analysis and XRD analysis were corroborated with each other.

Jawahar et al. [28] evaluated the micro and macrolevel properties of Class F fly ash based SCC after 28, 56 and 112 days of curing. For this purpose, ordinary Portland cement of 53 grade was replaced by 35% of Class F fly ash at water-cementitious (w/cm) ratio of 0.36 by weight. Coarse aggregates of size 20 mm and 10 mm size were blended in proportion of 60%: 40% by weight of total coarse aggregate. Polycarboxylate ether based superplasticizer and viscosity modifying agent were used in the preparation of SCC mixes. The fresh properties of SCC were determined by slump flow, T_{50cm} flow time at initial and after 60 min, V-funnel time at initial and after 5 min, and L-box test. The macrolevel properties such as compressive strength, modulus of elasticity and splitting tensile strength were determined. To examine the microcracks width and atomic Ca/Si ratio of the paste matrix near the ITZ, scanning electron microscope (SEM) and energy dispersive X-ray analysis (EDAX) were performed. For comparison, conventional concrete was also prepared as

equivalent to 28 day SCC compressive strength and all the properties were examined. Form the obtained results, it was observed that Class F fly ash based SCC reduced the microcracking width and Ca/Si ratio significantly due to pozzolanic action of fly ash at later ages, which was contributed to enhancing the macrolevel properties of SCC. In case of conventional concrete, the improvement of microlevel properties was less due to reduced microcracking width and increased Ca/Si ratio. Thus, the improvement in mechanical properties of conventional concrete was less as compared to fly ash based SCC mixes at later ages.

Said et al. [99] carried out a study to determine the effects of three different mineral admixtures and three strength classes on the behavior of SCCs in sodium sulfate environment. For this purpose, limestone filler (LF), fly ash (FA) and natural pozzolan (PZ) were used to prepare 30 MPa, 50 MPa and 70 MPa strength class SCC mixes as well as vibrated concrete (VC) mixes. Fresh properties of SCC were determined as per Association Française de Génie Civil (AFGC) recommendations. In hardened state, concrete specimens were put into 5% sodium sulfate solution for 720 days to determine the resistance against sodium sulfate attack by measuring the mass change, shrinkage or expansion (dimensional variation) and change in compressive strength. The SEM and XRD analyses were conducted on several layers of degraded samples to examine the microstructure of SCC mixes. Penetration depth and mechanism of damage were studied using a graphical treatment of microanalyses carried with backscattered electron imaging of polished surfaces. Visual inspection test was also carried out on the immersed samples in sodium sulfate and freshwater solutions. While comparing the effect of solution types, samples immersed in sulfate solution showed a higher mass gain as compared to samples immersed in fresh water. It was noted that, VC mixes showed higher expansion, mass loss and strength loss as compared to SCC mixes. Natural pozzolan and fly ash based SCC showed better physical and mechanical performances as compared to vibrated concrete and limestone filler mixes. From the results of microstructure analysis, the formation of ettringite was noticeable in all the mixes in the degraded zone while, more amount of gypsum was found in vibrated concrete and limestone filler mixes as compared to other mixes. The penetration depth of sulfate in different concrete samples determined using SEM-EDS, and the obtained results from XRD analysis were consistent with each other. The authors concluded that the natural pozzolan as a mineral admixture in SCC is beneficial for resistance against sodium sulfate attack.

Kannan and Ganesan [100] investigated the durability performance of binary and ternary blend SCC mixes containing rice husk ash (RHA), metakaolin (MK) and the combination of RHA and MK. Total seventeen mixes were prepared. OPC was replaced with 5%, 10%, 15%, 20%, 25%, and 30% RHA and MK in binary mixes and, combination of RHA and MK with 10%, 20%, 30%, and 40% replacement in ternary mixes at same proportion. In this study, for the preparation of SCC mixes, the ratio of fine and coarse aggregates was fixed at 1.1 and a constant w/b ratio of 0.55 was used along with 2% sulphonated naphthalene polymers based superplasticizer. All the mixes were designed to satisfy the target mean compressive strength of M 30 grade in normal vibrated concrete. Fresh property tests such as slump flow, V-funnel, and L-box tests were performed on all SCC mixes. Compressive strength test, permeability related tests (water absorption, sorptivity, and chloride penetration) and acid attack (in 5% sulfuric or 5% hydrochloric acid solutions with immersion up to 12 weeks) were performed after 28 days of water curing. In addition, the relationship between the silica ratio (SR) of the binder and the resistance to acid attack on SCC were assessed. To determine the morphological behaviour of SCC, scanning electron microscopy (SEM) with energy dispersive X-ray analysis (EDAX) was carried out. As observed from the results, the compressive strength was improved in the SCC mixes replaced with different admixtures up to 15% with RHA, up to 20% with MK, and up to 30% with RHA + MK. Among all mixes, RHA based SCC, and combination of RHA and MK based SCC showed a significant improvement in durability properties as compared to SCC with 100% OPC (unblended). The SEM images showed that the formation of ettringite was reduced in blended SCC mixes due to the pozzolanic reaction. From the EDAX spectrum analysis, it was noted that the silica content of blended SCC with RHA and MK was higher than that of unblended SCC. From the regression analysis, a perfect correlation between water absorption and other durability parameters was observed for ternary blended SCC whereas, poor correlation was found for binary blended SCC. The authors concluded that the most durable and optimum level of replacement for OPC as supplementary cementitious materials was SCC mix with 15% rice husk ash, and 15% metakaolin.

Jalal et al. [101] investigated the rheological, mechanical, thermal, transport and microstructural properties of high performance self-compacting concrete (HPSCC). Total fourteen concrete mixes were prepared with a constant water-binder ratio of 0.38 and total binder contents of 400 and 500 kg/m^3. Concrete mixes were prepared with replacement of Portland cement by Class F fly ash (5%, 10% and 15%), silica fume (10%), nano silica

(2%), and silica fume + nanosilica (10% + 2%) by weight. The fresh rheological properties of HPSCC were evaluated by slump flow time and diameter, and V-funnel flow time. The mechanical properties such as compressive, splitting tensile and flexural strengths and transport properties such as water absorption, capillary absorption and chloride ion penetration were also evaluated. Thermal and microstructure properties were investigated through thermogravimetric and scanning electron microscopy (SEM) micrographs, respectively. The authors reported that the rheological properties of HPSCC improved with increase in fly ash content. The mechanical and transport properties were improved with silica fume + nano silica admixed concrete mixes. After 28 days of curing, the thermogravimetric analysis was performed in the temperature range of 110 – 650 °C and it was observed that the weight loss of the HPSCC specimens increased with decrease in cement content in the concrete. From the SEM micrographs, it was observed that the nano silica particles act as filler, which leads to enhance the density as well as reduce the porosity of concrete.

Kavitha et al. [29] investigated the fresh, micro and macrolevel properties of SCC made with metakaolin. In this investigation, cement was replaced with metakaolin at 5, 10 and 15% by weight. PCE based superplasticizer was used in the preparation of SCC with low w/p ratio. The fresh properties of concrete were assessed by slump flow, T_{50cm} time, V-funnel flow time, L-box. The macrolevel properties such as compressive strength and splitting tensile strength were performed on 150 mm cube, and 150 mm diameter with 300 mm height cylinder specimens, respectively. The micro-level changes were observed using scanning electron microscope (SEM), X-ray diffraction analysis (XRD), and energy dispersive X-ray (EDX) analysis. From the results of fresh property tests, all the SCC mixes satisfied the rheological properties as per EFNARC guidelines. The authors concluded that based on compressive strength as well as splitting tensile strength results, the optimum replacement of meakaolin was 10% to improve the micro- and macrolevel properties of SCC. Also, additional formation of C-S-H, and reduction of Ca/Si ratio and microcrack width enhanced the microlevel properties by the pozzolanic action of metakaolin.

Siad et al. [102] assessed the performance of self-compacting concrete (SCC) made with different mineral admixtures and exposed to magnesium sulphate environment for 4 years. Twelve concrete mixes with three mineral admixtures (fly ash, natural pozzolan and limestone filler) and three strength classes (30, 50 and 70 MPa) were prepared for this study. For comparison purpose, ordinary concrete mixes (OC) with similar strength grades

were also prepared. The effect of magnesium sulphate attack was measured through visual inspection and dimensional variation. The cubes of size of 10 cm were prepared for measurement of compressive strength and mass changes, before and after immersion in the magnesium sulphate solution. The visual inspection and dimensional variation measurement were carried out on prismatic specimens of size 7 cm × 7 cm × 28 cm after immersion. These specimens were immersed in the fresh water and in 5% magnesium sulphate solution for 1440 days (4 years). The microstructural changes on degraded samples were examined using scanning electron microscopy (SEM) and X-ray diffraction (XRD) analysis. The sulphate profile was measured through backscattered electron imaging from the surface towards the core of the concrete samples by avoiding aggregates. The mechanisms of damage were studied using a microanalysis graphical treatment of the infected and uninfected zones. Form the obtained results, it was observed that the physical damage, expansion and compressive strength loss were more from higher to lower strength classes of concretes due to magnesium sulphate attack. The lower strength (30MPa) of SCC with limestone showed higher expansion as compared to the ordinary concrete mixes after exposure of 4 years to magnesium sulphate solution. All concrete specimens showed a decrease in compressive strength due to sulphate attack, but the highest loss was observed in limestone based SCC specimens. The SEM-EDS and XRD analysis showed that the formation of gypsum and ettringite were found in different amounts in all concrete mixes. The formation of thaumasite was noticeable in ordinary concrete mixes and in higher amounts in limestone based SCC mixes. Form the obtained results, the authors concluded that the durability performance of SCC under magnesium sulphate exposure depends on the type of mineral admixture. Among all three mineral admixtures, the natural pozzolan showed better long-term durability performance in magnesium sulphate environment.

Kavitha et al. [103] carried out a microstructural studied to determine the eco-friendly aspect as well as durability properties of SCC blended with metakaolin (MK). For this purpose, 0%, 5%, 10%, and 15% of MK as partial replacement of ordinary Portland cement were used. The test of water absorption and weight loss due to sulphate attack on 100 mm size cube specimens and rapid chloride permeation test on 100 mm diameter by 200 mm height cylindrical specimens were performed to evaluated the durability properties of SCC. For sulphate attack, the cube specimens were immersed in 5% by volume of magnesium sulphate solutions for 12 weeks. The microstructural analysis was examined by scanning electron microscope (SEM), X-ray diffraction analysis (XRD) and energy dispersive X-ray

analysis (EDX). In this study, energy saved and CO_2 emission were also calculated. The obtained results indicated that 10% of MK by weight of cement was optimum in terms of durability performance. The SCC made with 10% MK showed higher resistance against magnesium sulphate attack, less chloride diffusion, and less water absorption. Due to sulphate attack, expansion and cracking of concrete occurred, which was reduced by using 10% MK, and this was confirmed from the intensity of gypsum, ettringite, and brucite in the XRD analysis. Further, MK exhibited positive environmental effect due to less CO_2 emission with less thermal energy consumption and chemical reaction. The authors suggested that the service life of structures can be improved by use of SCC blended with metakaolin due to increase in durability.

Ghoddousi and Saadabadi [104] investigated the hydration products formation of self-compacting concrete made with the binary and ternary mixes. The self-compacting mixes and pastes were prepared using type II ordinary Portland cement (PC) along with partial replacement of OPC with silica fume (SF) and metakaolin (MK) at a w/b ratio of 0.45. The binary and ternary mixes were prepared with 92% PC+8% SF, 80% PC+20% MK, and 72% PC+8% SF+20% MK, respectively. For determination of hydration products of cement paste, X-ray diffraction (XRD) and thermogravimetric analyses (TGA) were performed on powdered cementitious samples. The electrical resistivity test was also performed on cube specimens of size 100 mm to determine the electrical properties of SCC mix. TGA and electrical resistivity tests were performed at different ages up to 365 days and XRD analysis was performed at different ages up to 28 days. From the obtained results, it was observed that the electrical resistivity improved over time in all SCC mix. The mix containing pozzolanic materials showed lower calcium hydroxide (CH) content as compared to control mix at the ages of 3, 7, 28, and 365 days. In the ternary mix, all the CH content consumed throughout the period of 365 days as indicated by TGA. From the results of XRD analysis and TGA, it was observed that the pozzolanic reaction of MK starts earlier than SF. The relationship between CH content and electrical resistivity showed negative slope for samples containing pozzolans with a correlation coefficient of 0.97 and showed positive slope for reference SCC with a correlation coefficient of 0.96. The authors suggested that electrical resistivity is a simple method to estimate the CH content in cement paste.

2.6 Summary of literature review and research needs

From the review of literature, it is observed that several investigations have been carried out on the fresh and mechanical properties of self-compacting concrete prepared with Portland cement and different types of mineral admixture as a partial replacement of cement. Further, some studies have been carried out to study the microstructure, and to evaluate the durability properties of SCC by rapid chloride permeability test, chloride diffusion coefficient, carbonation depth, acid attack, freezing-thawing effect, and sulfate attack, etc. In addition, very few studies have been carried out on the corrosion behaviour of steel reinforcement in SCC exposed to external chloride environment. In these limited studies, the authors have carried out investigations to evaluate the corrosion performance of steel reinforcement in self-compacting concrete exposed to chloride solutions by measuring various corrosion parameters. However, the reported research work in literature on fresh and mechanical properties, chloride binding, changes in microstructure and thermal behaviour, and corrosion behavior of steel reinforcement in SCC in the presence of internal chloride is scanty. Further, the research work on the corrosion behaviour of steel reinforcement in SCC subjected to combined chloride-sulfate exposure environment is very little.

Keeping in view the research gap in literature, in the present research work, an experimental investigation has been carried out to evaluate the effect of admixed chloride at different concentrations on the behaviour of SCC through fresh properties, strength development assessed through variations in hydration products with curing age, chloride binding, changes in microstructure and thermal behaviour, and chloride induced corrosion of steel reinforcement. In addition, the performance of SCC exposed to external chloride and combined chloride-sulfate solutions has also been assessed. For this purpose, the SCC mixes were prepared with different types of binder and water-to-binder (w/b) ratio, and admixed with different concentrations of chloride ions. In addition, the SCC mixes (without admixed chloride) were exposed to external chloride and combined chloride-sulfate solutions. Tests for fresh properties, compressive strength, chloride concentration, pH, thermal behaviour, microstructural analyses and corrosion of steel reinforcement in SCC were conducted.

2.7 Objectives of the present research work

Keeping in view the research needs identified from the review of literature, the objectives of the present research work have been formulated as follows:

1. To determine the effect of binder type, w/b ratio, and admixed chloride on the fresh properties and compressive strength of self-compacting concrete (SCC).
2. To study the microstructural changes in SCC mixes admixed with and without chloride ions by performing EDX, XRD, FESEM, and FTIR analyses.
3. To analyze the thermal behaviour of SCC mixes by conducting thermo-gravimetry analysis (TGA).
4. To study the chloride binding in SCC mixes by determining free and total chloride concentrations.
5. To evaluate the effect of binder type, w/b ratio, admixed chloride and exposure condition on the corrosion of steel reinforcement in SCC by performing corrosion potential and corrosion current density measurements.
6. To assess the corrosion performance of steel reinforcement in SCC subjected to external chloride and combined chloride-sulfate exposure solutions.

CHAPTER 3

EXPERIMENTAL WORK

3.1 General

This chapter presents the details about the experimental work that includes materials used for the preparation of self-compacting concrete (SCC), preparation of test specimens and the procedure for carrying out various tests.

3.2 Materials

In this section, the details about different constituents of the concrete mix such as cement, mineral admixture, chemical admixture, fine aggregate, coarse aggregate, chloride salt, and steel reinforcement used in the preparation of specimens are described.

3.2.1 Binder

Ordinary Portland cement (OPC) conforming to IS: 8112-2013 [105] and ASTM Type I [106]; Portland pozzolana cement (PPC) conforming to IS: 1489-1991 (part-1) [107] and ASTM Type IP [108]; and mineral admixture such as fly ash (FA) conforming to ASTM: C618 [109] were used as binders to produce the SCC mixes. In this study, OPC was replaced by 20% fly ash by weight of binder in the SCC mixes prepared with OPC plus fly ash. The chemical composition of OPC, PPC and fly ash was determined by XRF (X-ray fluorescence) analysis, whereas the physical properties such as specific gravity and specific surface area of the binder were determined as per the guidelines of IS: 4031 (Part 11)-1988 [110] and BET method by nitrogen adsorption, respectively. The chemical composition of the binders is presented in Table 3.1. The measured values of specific gravity of OPC, PPC and fly ash were 3.12, 2.78, and 2.10, respectively. The obtaiened values of specific surface area (BET) of OPC, PPC and fly ash were 926 m^2/kg, 1629 m^2/kg, and 795 m^2/kg, respectively. The phase composition of OPC, PPC and fly ash obtained by X-ray diffraction (XRD) analysis are shown in Fig. 3.1 (a - c). From the XRD patterns shown in Fig. 3.1 (a, b), the major compounds of cement (OPC and PPC) identified were calcium silicates (C_3S, and C_2S), calcium aluminum oxide phase (C_3A) and anhydrite ($CaSO_4$) form of gypsum, which is interground with the clinker during the manufacturing process to control the early setting and hardening behaviour of cement. On the other hand, the fly ash consists of three main crystalline phases: Quartz (SiO_2), Mullite ($Al_6Si_2O_{13}$) and Hematite (Fe_2O_3), as observed from the XRD pattern shown in Fig. 3.1 (c). Further, the elemental composition

of binders was determined by energy dispersive X-ray (EDX) spectroscopy and the results are shown in Fig. 3.2 (a - c). These plots provide the information about the comparative difference in wt. % of various elements among the binder type. In order to analyze the surface morphology of binders, field emission scanning electron microscopy (FESEM) was performed, and the typical in-lens images are presented in Fig. 3.3 (a - c). As observed from these images, OPC has irregular shape particles, whereas PPC and fly ash have mostly spherical particles with smooth surface texture.

Table 3.1 Oxide composition of OPC, PPC and fly ash obtained by XRF analysis

Compound (wt.%)	CaO	SiO_2	Al_2O_3	Fe_2O_3	MgO	SO_3	K_2O	Na_2O
OPC	65.26	21.46	4.98	1.46	2.83	2.09	0.41	0.83
PPC	63.10	23.11	3.14	1.94	2.41	1.9	1.12	2.53
Fly ash	1.47	53.23	22.48	4.95	0.73	--	1.00	0.78

CaO: Calcium oxide, SiO_2: Silicon dioxide, Al_2O_3: Aluminium oxide, Fe_2O_3: Ferric oxide, MgO: Magnesium oxide, SO_3: Sulphur trioxide, K_2O: Potassium oxide, Na_2O: Sodium oxide

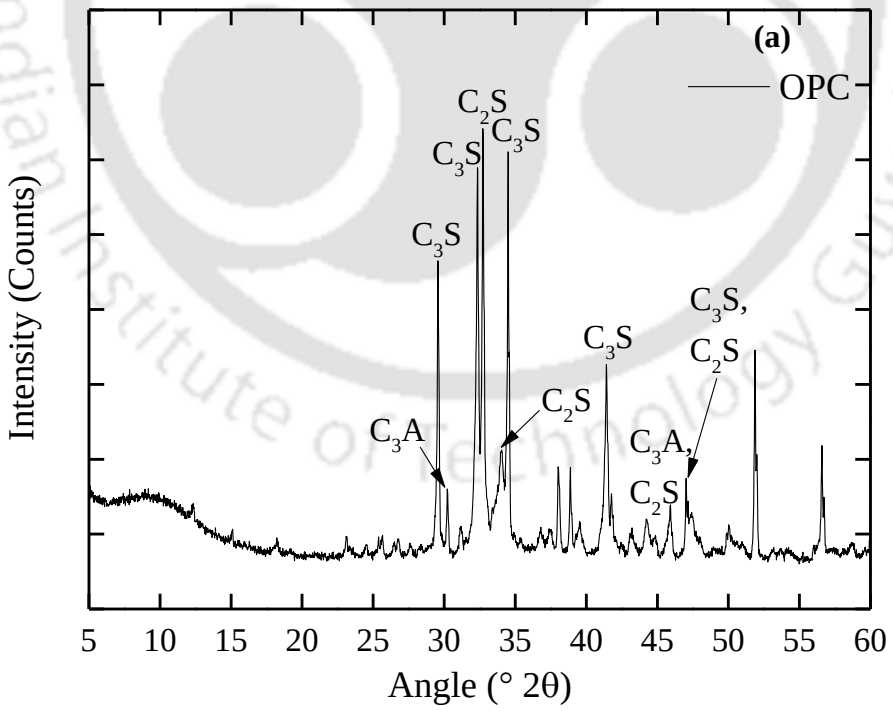

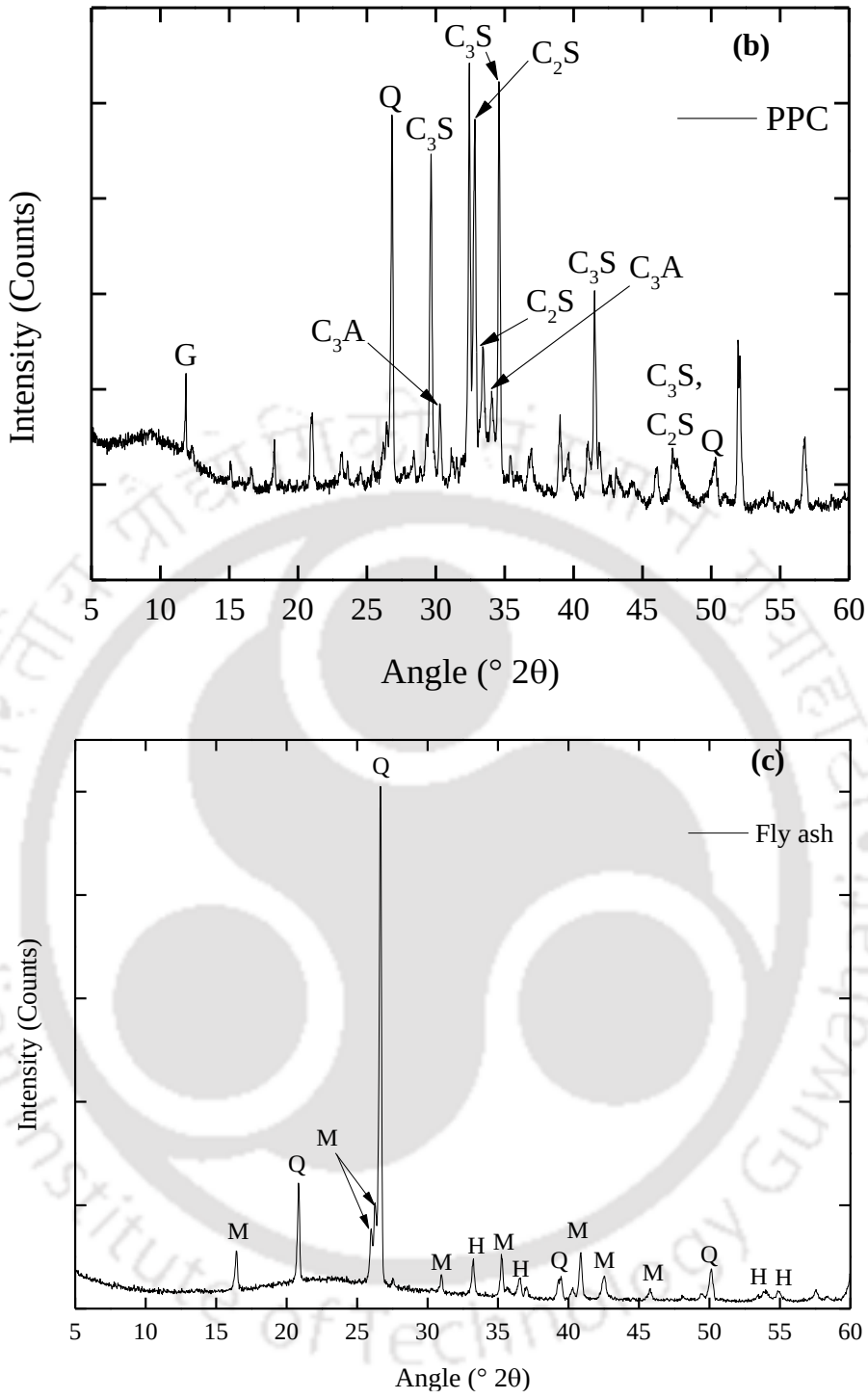

Fig. 3.1 Phase composition of binders obtained by XRD analysis: (a) OPC, (b) PPC, and (c) Fly ash

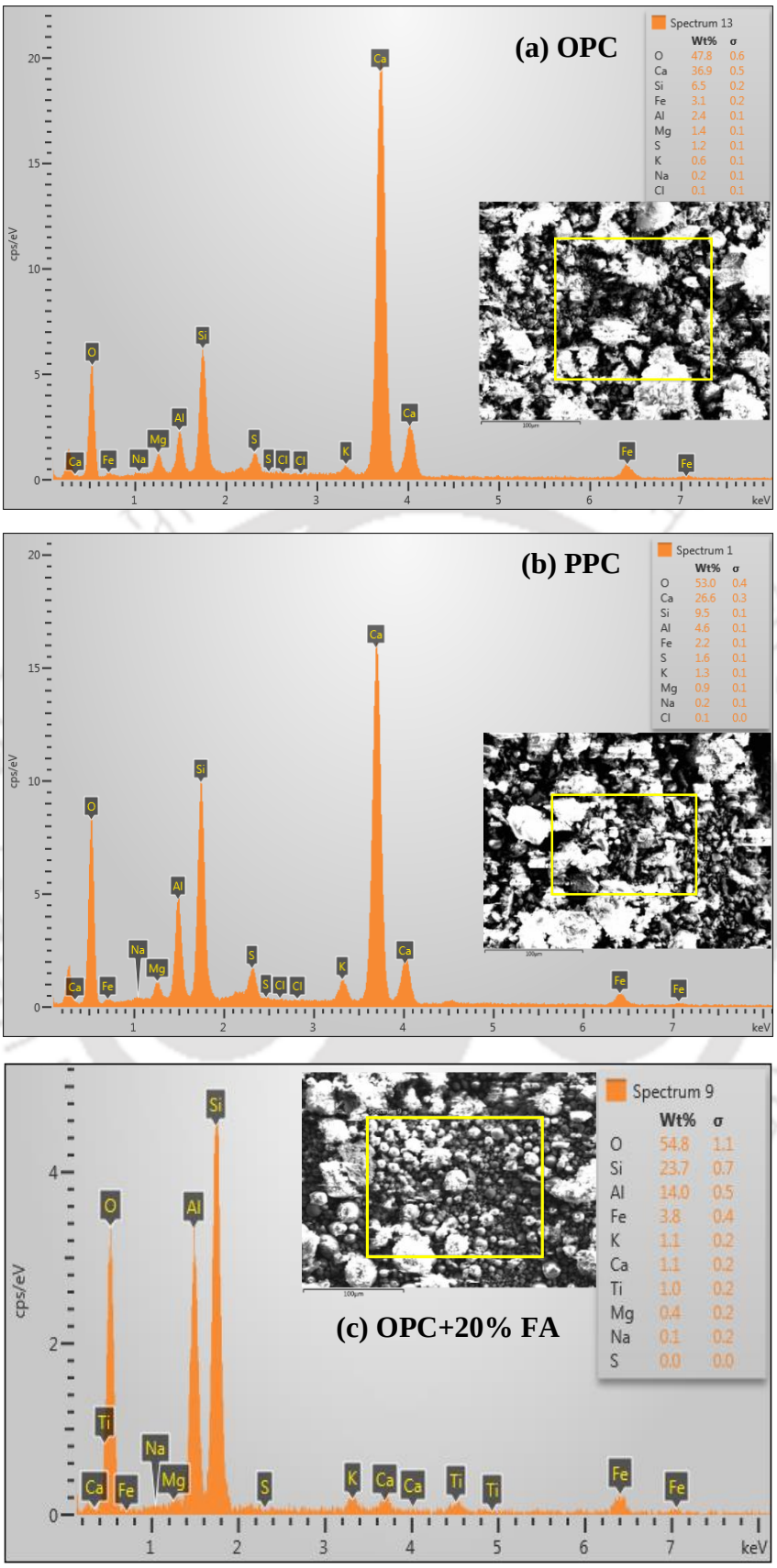

Fig. 3.2 Chemical elements of binders obtained by EDX analysis: (a) OPC, (b) PPC, and (c) Fly ash

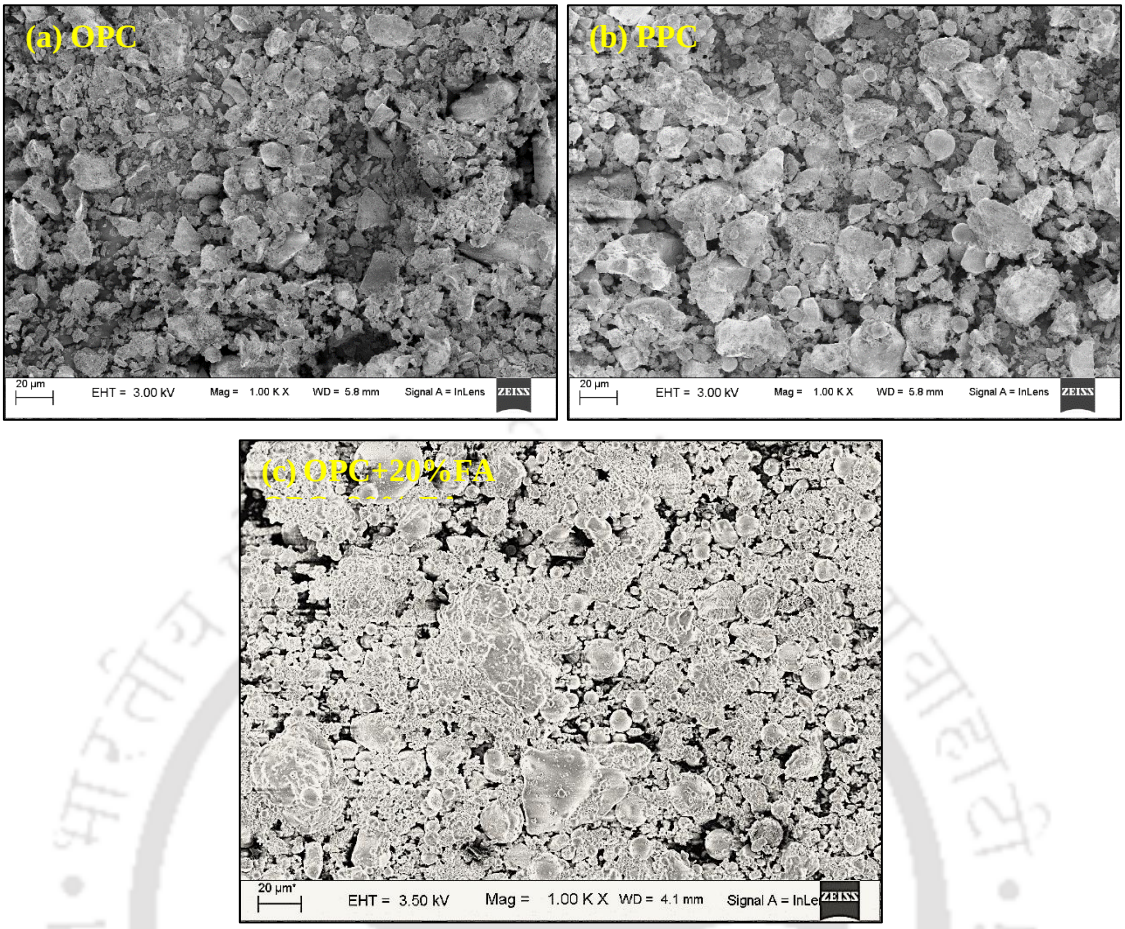

Fig. 3.3 Surface morphology of binders obtained by FESEM analysis: (a) OPC, (b) PPC, and (c) Fly ash

3.2.2 Chemical admixture

To enhance the fresh properties of concrete mix, polycarboxylic ether based high-range water reducing admixture (HRWRA), i.e., superplasticizer (SP) was used in the preparation of SCC mixes. The physical properties of the superplasticizer (STRUCTURO 201, manufactured by FOSROC) are presented in Table 3.2.

Table 3.2 Physical properties of superplasticizer: STRUCTURO 201, FOSROC

Properties	STRUCTURO 201
Physical state	Liquid
Colour	Light brown
Specific gravity	1.06
Solids content	30.18% by mass
Chloride content	0.027% by mass

3.2.3 Aggregates

Locally available sand was used as fine aggregate and coarse aggregates of 20 mm MSA (maximum size of aggregate) and 10 mm MSA were used in the preparation of SCC mixes. The specific gravity of fine aggregate and 10 mm MSA coarse aggregate were determined using pycnometer method, whereas the specific gravity of 20 mm MSA coarse aggregate was determined by using wire basket method as per guidelines mentioned in IS: 2386-1963 (Part III) [111]. The measured values of specific gravity of fine aggregate, 10 mm MSA and 20 mm MSA coarse aggregates were 2.62, 2.65 and 2.65, respectively. The water absorption of aggregates was calculated according to IS: 2386-1963 (Part III) [111] guidelines and the obtained values of water absorption for fine aggregate, 10 mm MSA and 20 mm MSA coarse aggregates were 0.30%, 0.20%, and 0.10%, respectively. The sieve analysis of fine aggregate, 10 mm MSA, and 20 mm MSA coarse aggregates were carried out as per the guidelines mentioned in IS: 2386-1963 (Part I) [112]. From the cumulative percentage passing values, it was observed that the fine aggregate is conforming to grading zone III as per IS: 383-1970 [113]. Fineness moduli of fine aggregate, 10 mm MSA and 20 mm MSA coarse aggregates were 2.55, 6.00, and 7.73, respectively. The grading curves of fine aggregate,10 mm MSA and 20 mm MSA coarse aggregates are shown in Fig. 3.4 (a - c).

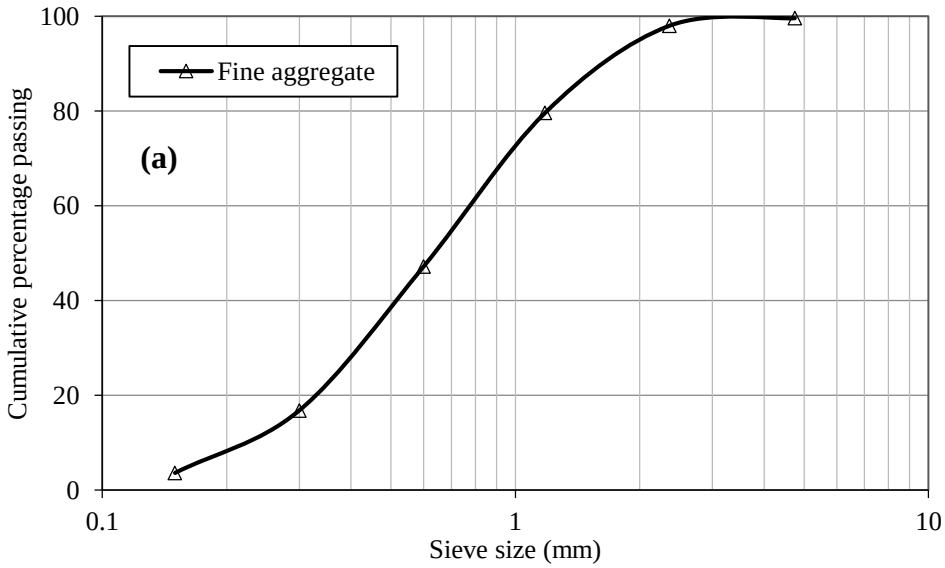

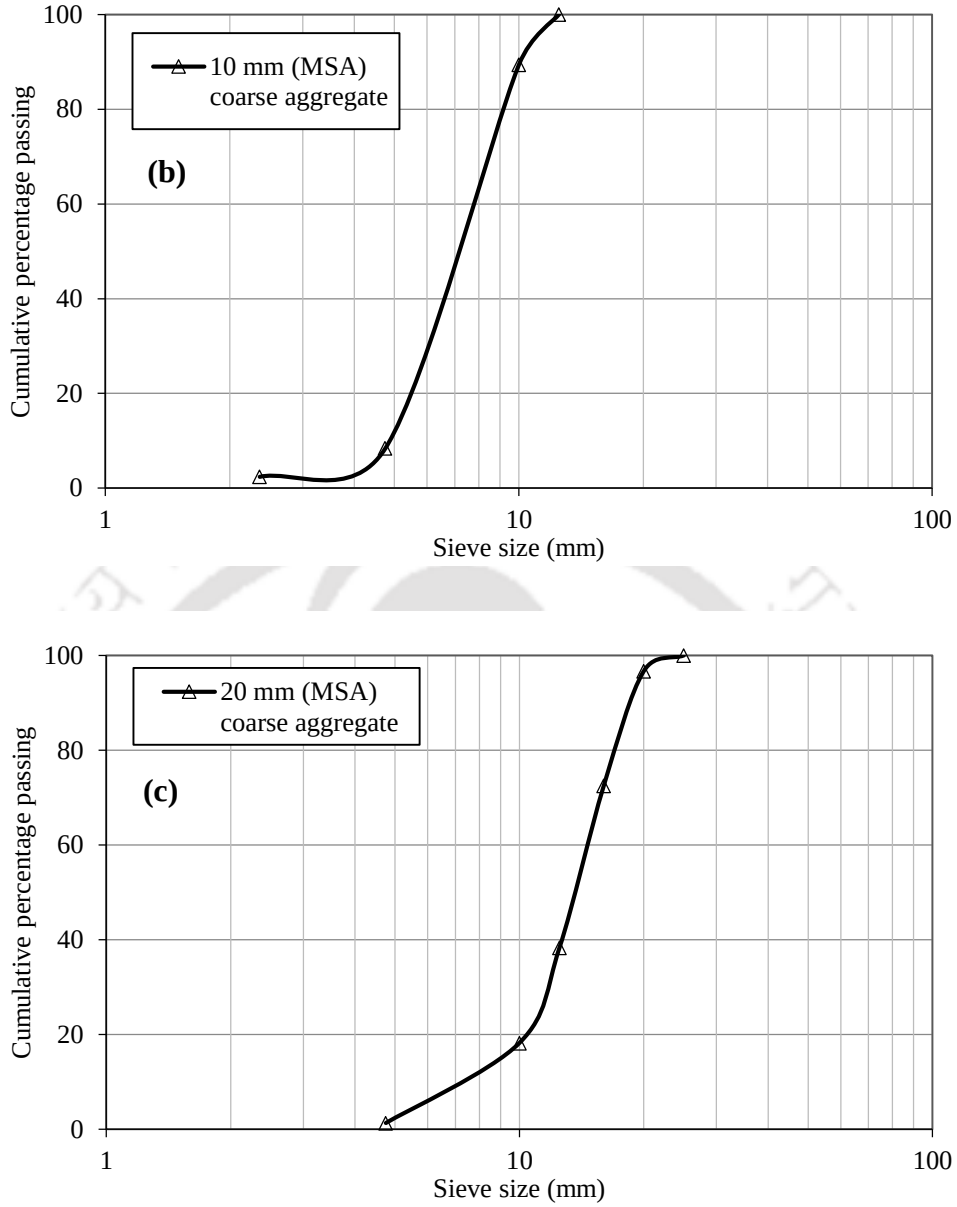

Fig. 3.4 Grading curve of aggregates: (a) fine aggregate (sand), (b) 10 mm MSA coarse aggregate, and (c) 20 mm MSA coarse aggregate

3.2.4 Admixed chloride salt

From the review of literature, it is observed that various researchers have used sodium chloride as the source of chloride ions for chloride exposure conditions. Further, seawater contains about 35000 ppm of dissolved salts of sodium, calcium, magnesium, and potassium. Out of these salts, sodium chloride is the most dominant, which is about 88% by weight of salts [114]. By keeping in view these information, in this study, sodium chloride was used as the source of chloride ions for internal chloride as well as for external chloride exposure conditions.

3.2.5 Steel type

Tempcore TMT (Thermomechanically treated) steel bars of diameter 12 mm were used as the steel reinforcement. The wt. % of chemical elements of steel reinforcement determined by energy dispersive X-ray (EDX) analysis are presented in Table 3.3.

Table 3.3 Chemical elements of steel reinforcement obtained by EDX analysis

Chemical elements	Mn	Si	Ni	Cr	Cu	S	P	C	Fe
wt. %	1.2	0.6	0.2	0.2	0.1	0.2	0.1	< 0.1	Balance

3.3 Trial mixes

Various researchers have carried out studies on mix proportioning of SCC and proposed a variety of mix design methods based on different principles and control parameters [7,10,15,16,18,115]. The mix proportioning of SCC mixes in the present research work was based on the trial tests following the EFNARC [4] and ACI [116] guidelines. The typical range of mix parameters of SCC mixes as per EFNARC and ACI guidelines are presented in Table 3.4 and Table 3.5, respectively. The tests for fresh properties were carried out on the trial mixes till the mix satisfied the filling ability, passing ability, and segregation resistance criteria as per EFNARC [4] guidelines.

Table 3.4 Typical range of mix parameters of SCC by EFNARC guidelines [4]

Parameters	Typical range
Volume of paste	300 - 380 (litres/m^3)
Water-to-powder ratio	0.85 - 1.10 (litres/m^3)
Powder content	380 - 600 (kg/m^3)
Water content	150 - 210 (kg/m^3)
Fine aggregate in total aggregate	48 - 55% (by weight)
Coarse aggregate content	750 - 1000 (kg/m^3)

Table 3.5 Typical range of mix parameters of SCC by ACI guidelines [116]

Parameters	Typical range
Volume of paste	34 - 40%
Water-to-cementitious ratio	0.32 - 0.45
Powder content	355 – 458 (+) (kg/m^3)
Volume of mortar	68 to 72% (total mixture volume)
Absolute coarse aggregate content	28 - 32%

As per ACI guidelines, the SCC mixes prepared with water-cementitious ratio (w/cm ratio) of 0.32 to 0.40 are typically used for the production of precast units and those prepared with w/cm ratio greater than 0.40 are sometimes used for cast-in-place concrete and repair applications [116]. These SCC mixes prepared with comparatively higher w/cm ratio have strength characteristics similar to the conventional concrete. By keeping in view these guidelines, in the present study, the trial mixes were prepared with water-to-binder (w/b) ratios of 0.37, 0.40 and 0.43. Initially, the mix proportioning of the concrete was carried out at a mixing water content of 180 kg/m^3 and w/b ratio of 0.40. The binder content was calculated by dividing the water content by w/b ratio. As per ACI guidelines [116], as an initial starting point, the coarse aggregate content (by weight) was considered as 50% of its bulk dry density. The bulk dry density of coarse aggregate was determined as per IS: 2386 (Part III) 1963 [111] guidelines with blending of 10 mm and 20 mm MSA coarse aggregates in different proportions. The blending of 10 mm and 20 mm MSA coarse aggregates in the proportion of 36%: 64% (by weight) exhibited highest bulk dry density and thus considered for the initial stage of mix proportioning (Table 3.6: Series I-A). The dosage of superplasticizer (SP) was initially kept at 2.5% by weight of total binder content. The fine aggregate content was calculated by absolute volume method (i.e., by subtracting sum of the volumes of other constituents from 1 m^3 volume of concrete). Hand mixing was adopted to prepare the fresh concrete mix. However, as visually observed, these mixes were not flowable and hence the required parameters related to fresh properties of SCC mixes were not measured. Further, the trial mixes were prepared by considering the coarse aggregate content (by weight) corresponding to its absolute volume with respect to the total volume of concrete mix as per ACI guidelines [116] and the mix details are shown under Series I-B in Table 3.6. The different types of binder used in this series were OPC+20% fly ash, OPC and PPC. The w/b ratio was varied from 0.37 to 0.43 and the water content was almost kept at 205 kg/m^3 with varying dosages of superplasticizer. Different proportions (by weight) of 10 mm MSA and 20 mm MSA coarse aggregates were used in these trial mixes as shown in Table 3.6. Further, the fine aggregate content was calculated by absolute volume method and the concrete mixes were prepared by hand mixing. The parameters such as V-funnel flow time (for filling ability) and L-box passing ratio (passing ability) of the concrete mixes were measured as per EFNARC guidelines [4]. As observed from the obtained results, only few mixes satisfied the acceptance criteria of these two parameters for SCC. From these trial mixes, it was observed that mostly the mixes prepared with coarse aggregate content corresponding its absolute volume equal to 28.5% of total volume of

concrete, and proportion of 10 mm MSA and 20 mm MSA coarse aggregates as 50%:50% by weight satisfied acceptance criteria for SCC. In these mixes, the proportions of coarse aggregate (by weight) with respect to total aggregate content were 49.2% and 48%, and that of fine aggregate were 50.8% and 52%. By keeping in view these observations, further trial mixes were prepared by keeping the absolute volume of coarse aggregate as 28.5% of total volume of concrete, proportion of coarse aggregate and fine aggregate by weight as 49% and 51%, and proportion of 10 mm MSA and 20 mm MSA coarse aggregates as 50%:50% by weight, as shown in Series II (Table 3.7). In these mixes, the water content was kept at 205 kg/m^3 and different dosages of superplasticizer were used. These trial mixes were also prepared with hand mixing. From the obtained results, it was observed that mostly all the mixes satisfied the acceptance criteria for V-funnel flow time and L-box passing ratio. After that, further trial mixes were prepared by machine (concrete mixer) mixing (Series III), since the final SCC mixes had to be prepared using the concrete mixer. The proportions of coarse and fine aggregates, absolute volume of coarse aggregate as percentage of total volume of concrete, and proportion of 10 mm MSA and 20 mm MSA coarse aggregates in Series III were kept same as those used in the trial mixes of Series II. Initially, the dosage of superplasticizer was used as 2% by weight of binder in the preparation of SCC mixes using the concrete mixer, however, at this dosage, bleeding was observed in these mixes. Thus, the trial mixes were prepared at lower dosages of superplasticizer, using the concrete mixer, as shown in Table 3.8 for Series III. The water contents used in the preparation of trial mixes were 195 kg/m^3 and 205 kg/m^3. The tests such as slump flow spread for filling ability, T_{50cm} and V- funnel flow times for flow-rate, L-box test (passing ratio) for passing ability, and sieve segregation test (segregation index) for segregation resistance were conducted on the trial mixes and the results are presented in Table 3.8. From these results, it was observed that all the trial mixes satisfied the fresh properties of SCC as per the acceptance criteria [4]. After that, the final mix proportions for SCC mixes were selected from the trial mixes of Series III.

Table 3.6 Series I: details of trial mixes of SCC by hand mixing

Binder type	w/b ratio	Binder (kg/m^3)	Water (kg/m^3)	Cement (kg/m^3)	Fly ash (kg/m^3)	Proportion of 10 mm and 20 mm MSA (%)	Coarse aggregate (kg/m^3)	Fine aggregate (kg/m^3)	Proportion of coarse and fine aggregates (%)	SP* (%)		
OPC + 20% FA	Coarse aggregate content (by weight) corresponding to 50% of its bulk dry density (Series I-A)											
	0.40	450.00	180.00	360.00	90.00	64/36	756.00	943.20	44.5/55.5	2.5%		
	0.40	475.00	190.00	380.00	95.00	64/36	756.00	892.23	45.9/54.1	2.5%		
	0.40	487.50	195.00	390.00	97.50	64/36	756.00	867.46	46.6/53.4	2.5%		
	0.40	500.00	200.00	400.00	100.00	64/36	756.00	841.10	47.3/52.7	2.0%		
	Coarse aggregate content (by weight) corresponding to its absolute volume with respect to the total volume of concrete (Series I-B)											
	w/b ratio	Binder (kg/m^3)	Water (kg/m^3)	Cement (kg/m^3)	Fly ash (kg/m^3)	Proportion of 10 mm and 20 mm MSA (%)	Absolute volume of coarse aggregate (%)	Coarse aggregate (kg/m^3)	Fine aggregate (kg/m^3)	Proportion of coarse and fine aggregates (%)	SP (%)	V-funnel flow time (s)	L-box Passing ratio
	0.40	500.00	200.00	400.00	100.00	62/38	30.0%	795.00	804.14	49.7/50.3	1.5%	-	-
	0.40	512.50	205.00	410.00	102.50	60/40	30.0%	795.00	780.20	50.5/49.5	1.3%	-	-
	0.40	512.50	205.00	410.00	102.50	50/50	30.0%	795.00	779.38	50.5/49.5	1.5%	30.34	0.35
	0.40	512.50	205.00	410.00	102.50	45/55	29.0%	768.50	803.93	48.9/51.1	2.0%	-	0.50
	0.40	525.00	210.00	420.00	105.00	45/55	29.0%	768.50	779.13	49.7/50.3	2.0%	10.79	0.86
	0.40	512.50	205.00	410.00	102.50	45/55	28.5%	755.25	817.03	48/52	2.0%	8.94	0.70
	0.40	512.50	205.00	410.00	102.50	**50/50**	**28.5%**	**755.25**	**817.03**	**48/52**	**2.0%**	**5.34**	**0.79**
	0.43	476.74	205.00	381.39	95.35	50/50	29.0%	768.50	836.43	47.9/52.1	2.0%	6.50	0.72
	0.43	476.74	205.00	381.39	95.35	45/55	29.0%	768.50	836.43	47.9/52.1	2.0%	6.50	0.79
	0.43	476.74	205.00	381.39	95.35	45/55	29.5%	781.75	821.25	48.8/51.2	3.0%	-	0.37
	0.43	476.74	205.00	381.39	95.35	40/60	29.5%	781.75	823.55	48.7/51.3	2.3%	-	-
	0.37	554.05	205.00	443.24	110.81	50/50	28.0%	742.00	791.24	48.4/51.6	2.0%	8.62	0.85
	0.37	554.05	205.00	443.24	110.81	**50/50**	**28.5%**	**755.25**	**779.91**	**49.2/50.8**	2.0%	**7.75**	**0.87**

OPC	0.40	512.50	205.00	512.50	-	50/50	28.0%	755.25	860.21	46.8/53.2	1.5%	18.10	0.46
	0.40	512.50	205.00	512.50	-	50/50	28.5%	755.25	858.56	46.8/53.2	2.0%	17.58	0.64
	0.40	512.50	205.00	512.50	-	50/50	28.0%	755.25	855.01	46.9/53.1	2.5%	8.15	0.77
	0.40	512.50	205.00	512.50	-	45/55	28.5%	755.25	857.79	46.8/53.2	2.3%	22.47	0.48
	0.37	554.05	205.00	554.05	-	50/50	28.0%	742.00	836.13	47/53	2.0%	9.47	0.74
	0.40	512.50	205.00	512.50	-	50/50	28.5%	755.25	856.92	46.8/53.2	2.8%	7.10	0.78
	0.37	554.05	205.00	554.05	-	50/50	28.0%	755.25	822.14	47.9/52.1	2.5%	12.38	0.78
PPC	0.40	512.50	205.00	512.50	-	50/50	28.5%	755.25	804.51	48.4/51.6	1.3%	9.78	0.92
	0.37	554.05	205.00	554.05	-	50/50	28.0%	755.25	765.48	49.7/50.3	1.0%	11.79	0.97
	0.37	554.05	205.00	554.05	-	50/50	28.5%	755.25	766.19	48.4/51.6	0.8%	11.56	0.91

** SP: Superplasticizer, "-": parameter not measured.*

Recommended criteria: V-funnel flow time ≤ 8 s and L-box passing ratio: 0.80 to 1.0

Table 3.7 Series II: details of trial mixes of SCC by hand mixing

Binder type	w/b ratio	Binder (kg/m^3)	Water (kg/m^3)	Cement (kg/m^3)	Fly ash (kg/m^3)	Proportion of 10 mm and 20 mm MSA (%)	% of absolute volume of coarse aggregate	Coarse aggregate (kg/m^3)	Fine aggregate (kg/m^3)	Proportion of coarse and fine aggregates (%)	SP (%)	V-funnel flow time (s)	L-box Passing ratio
OPC+20% FA	0.40	512.50	205.00	410.00	102.50	50/50	28.5%	755.25	786.08	49/51	2.0%	**7.91**	**0.86**
	0.43	476.74	205.00	381.39	95.35	50/50	28.5%	755.25	786.08	49/51	2.0%	8.21	**0.80**
OPC	0.37	554.05	205.00	554.05	-	50/50	28.5%	755.25	786.08	49/51	2.3%	**7.53**	**0.90**
	0.40	512.50	205.00	512.50	-	50/50	28.5%	755.25	786.08	49/51	2.5%	**8.00**	**0.82**
	0.43	476.74	205.00	476.74	-	50/50	28.5%	755.25	786.08	49/51	2.5%	**7.16**	**0.85**
PPC	0.43	476.74	205.00	476.74	-	50/50	28.5%	755.25	786.08	49/51	0.8%	**6.56**	**0.79**

Recommended criteria: V-funnel flow time ≤ 8 s and L-box passing ratio: 0.80 to 1.0

Table 3.8 Series III: details of trial mixes of SCC by machine mixing (concrete mixer)

Binder type	w/b ratio	Water (kg/m^3)	Binder (kg/m^3)	Coarse aggregate (kg/m^3)	Fine aggregate (kg/m^3)	SP (%)	Slump flow spread (mm)	T_{50cm} flow time (s)	V-funnel flow time (s)	L-box passing ratio	SI (%)
OPC+ 20% FA	0.40	205.00	512.50	755.25	786.08	0.50%	**725.0**	**1.47**	**4.94**	**0.86**	**11.31%**
	0.40	205.00	512.50	755.25	786.08	0.40%	**732.5**	**1.85**	**4.13**	**0.89**	**7.11%**
	0.40	205.00	512.50	755.25	786.08	0.30%	**655.0**	3.22	**6.00**	**0.81**	**3.87%**
	0.43	205.00	476.74	775.25	786.08	0.50%	-	-	**4.22**	**0.90**	**7.36%**
	0.43	195.00	453.49	755.25	786.08	0.70%	**705.0**	**0.98**	**3.65**	**0.85**	**9.36%**
	0.43	195.00	453.49	755.25	786.08	0.60%	**660.0**	**1.03**	**3.00**	**0.81**	**7.03%**
	0.43	195.00	453.49	755.25	786.08	0.50%	620.0	**0.83**	**3.36**	0.73	**5.16%**
OPC	0.37	205.00	554.05	755.25	786.08	1.00%	-	-	-	-	21.03%
	0.37	205.00	554.05	755.25	786.08	0.60%	-	-	**5.86**	**0.90**	**5.02%**
	0.40	205.00	512.50	755.25	786.08	0.60%	-	-	**4.72**	**0.82**	**4.39%**
	0.43	205.00	476.74	775.25	786.08	0.60%	-	-	**5.05**	**0.80**	**4.68%**
	0.37	195.00	527.03	755.25	786.08	0.80%	**675.0**	**1.11**	**3.85**	**0.88**	**0.91%**
	0.40	195.00	487.50	755.25	786.08	0.80%	**650.0**	**1.15**	**3.61**	**0.80**	**0.99%**
	0.43	195.00	453.49	755.25	786.08	0.80%	**655.0**	**1.29**	**3.63**	**0.80**	**2.03%**
PPC	0.37	205.00	554.05	755.25	786.08	1.00%	-	-	**6.40**	**0.89**	20.55%
	0.37	205.00	554.05	755.25	786.08	0.70%	**735.0**	2.22	**6.47**	**0.91**	**8.50%**
	0.40	205.00	512.50	755.25	786.08	0.60%	**710.0**	**1.86**	**4.12**	**0.87**	**8.69%**
	0.43	205.00	476.74	755.25	786.08	0.60%	**717.5**	**1.12**	**3.54**	**0.90**	**10.11%**
	0.43	205.00	476.74	755.25	786.08	0.50%	610.0	3.05	**3.84**	**0.81**	**2.34%**
	0.37	195.00	527.03	755.25	786.08	0.70%	**720.0**	**1.75**	**7.08**	**0.95**	**0.94%**
	0.40	195.00	487.50	755.25	786.08	0.70%	**710.0**	**1.37**	**6.20**	**0.97**	**6.09%**
	0.43	195.00	453.49	755.25	786.08	0.70%	**725.0**	**0.92**	**3.89**	**0.91**	**2.98%**

Recommended criteria: Slum flow spread: 650 - 850 mm, T_{50cm} flow time ≤ 2 s, V-funnel flow time ≤ 8 s, L-box passing ratio: 0.80 to 1.0 and Segregation index: <15%

3.4 Final mix proportion of SCC

By analyzing the obtained results of fresh properties of the trial mixes of Series III (Table 3.8), the mix parameters adopted for the preparation of final SCC mixes at w/b ratios of 0.37, 0.40 and 0.43 are: i) water content of 195 kg/m^3, ii) coarse aggregate content corresponding its absolute volume equal to 28.5% of total volume of concrete, iii) proportion of 10 mm MSA and 20 mm MSA coarse aggregates as 50% : 50% by weight, and iv) proportion of coarse aggregate and fine aggregate by weight as 49% and 51% of total aggregate content. The dosages of superplasticizer adopted for the SCC mixes were 0.8%, 0.7% and 0.6% by weight of binder for OPC, PPC and OPC plus 20% fly ash, respectively. In addition to the control SCC mixes, the chloride admixed mixes were also prepared in the present investigation to study the corrosion beahviour of steel reinforcement in SCC. From the literature [117-119], it is observed that several studies have been carried out to determine the effect of internal chloride (admixed during preparation) on steel reinforcement corrosion in normal vibrated concrete and in these studies the authors have used sodium chloride (NaCl) in different concentrations as the source of internal chloride. However, there is no reported research work on corrosion beahviour of steel reinforcement in SCC in the presence of internal chloride (admixed chloride). Since, sodium chloride is present in varying concentrations in seawater and groundwater and also keeping in view the concentrations of sodium chloride used by various researchers as the source of internal chloride in case of normal vibrated concrete, in the present study, the concentrations of sodium chloride admixed during preparation of SCC mixes were 1%, 3%, and 5% by weight of mixing water content for all the three w/b ratios. The corresponding admixed sodium chloride concentrations by weight of binder were 0.37%, 1.11%, and 1.8% at w/b ratio of 0.37; 0.40%, 1.2% and 2% at w/b ratio of 0.40; and 0.43%, 1.29%, and 2.15% at w/b ratio of 0.43, respectively. In addition, the SCC mixes were also prepared with higher concentrations of admixed sodium chloride i.e. 7.5% and 12.5% by weight of mixing water at w/b ratio of 0.40 from three types of binder. The corresponding admixed sodium chloride concentrations by weight of binder were 3%, and 5%, respectively. The final mix quantities of SCC mixes are presented in Table 3.9.

Table 3.9 Mix quantities of SCC mixes (machine mixing)

Binder type	w/b ratio	Cement (kg/m^3)	Fly ash (kg/m^3)	Water (kg/m^3)	Coarse aggregate (kg/m^3)	Fine aggregate (kg/m^3)	SP* (%)	NaCl** (%)
OPC	0.37	527.03	-	195.00	755.25	786.08	0.80	0.0
								1.0
								3.0
								5.0
	0.40	487.50	-	195.00	755.25	786.08	0.80	0.0
								1.0
								3.0
								5.0
								7.5
								12.5
	0.43	453.49	-	195.00	755.25	786.08	0.80	0.0
								1.0
								3.0
								5.0
PPC	0.37	527.03	-	195.00	755.25	786.08	0.70	0.0
								1.0
								3.0
								5.0
	0.40	487.50	-	195.00	755.25	786.08	0.70	0.0
								1.0
								3.0
								5.0
								7.5
								12.5
	0.43	453.49	-	195.00	755.25	786.08	0.70	0.0
								1.0
								3.0
								5.0
OPC + 20% FA	0.37	421.62	105.41	195.00	755.25	786.08	0.60	0.0
								1.0
								3.0
								5.0
	0.40	390.00	97.5	195.00	755.25	786.08	0.60	0.0
								1.0
								3.0
								5.0
								7.5
								12.5
	0.43	362.79	90.70	195.00	755.25	786.08	0.60	0.0
								1.0
								3.0
								5.0

* SP: Superplasticizer added as % by weight of binder

** NaCl admixed as % by weight of mixing water

3.5 Preparation of SCC mixes

To obtain homogeneity in SCC mixes, the mixing procedure and duration of mixing are also important. All the SCC mixes were prepared in a laboratory concrete drum mixer. The ingredients of SCC mixes were batched by weight. First the binder and aggregates were mixed in the concrete mixer for 3 minutes. Then, the entire amount of mixing water containing the whole amount of superplasticizer and the amount of sodium chloride corresponding to its concentration was added in the mixer and the mixing was continued for another 5 minutes. After that the mix was kept for a rest period of 1 minute to allow for the effective dispersing effect of the superplasticizer, and finally the mixing was continued for another 1 minute before discharging the fresh concrete from the concrete mixer. Thus, the total duration of mixing was 10 minutes. The outline of the mixing procedure of SCC mixes is shown in Fig. 3.5. Immediately after the preparation of fresh mix, a variety of tests were conducted as per EFNARC guidelines [4] to determine fresh properties of SCC, i.e., slump flow spread, T_{50cm} flow time, V-funnel flow time, L-box passing ratio, and segregation index.

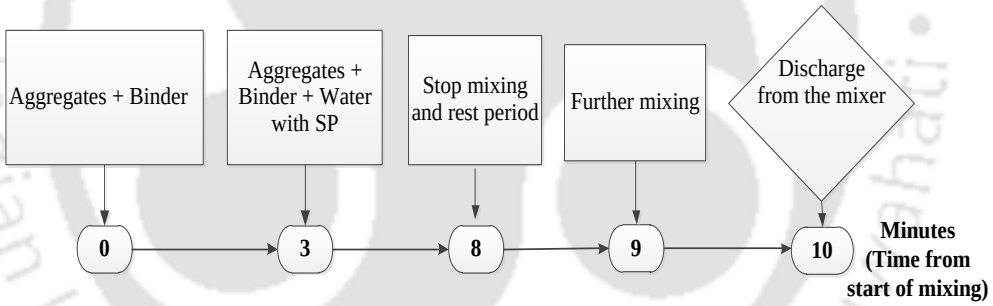

SP: superplasticizer

Fig. 3.5 Mixing procedure with duration for SCC mixes

3.6 Measurement techniques for fresh properties of SCC

The evaluation of fresh properties of SCC includes determining its filling ability, passing ability, and segregation resistance. The tests such as slump flow spread for filling ability, T_{50cm} and V- funnel flow times for flow-rate, L-box test (passing ratio) for passing ability, and sieve segregation test (segregation index) for segregation resistance were carried out as per the EFNARC guidelines.

3.6.1 Test for slump flow spread and T_{50cm} flow time

For slump flow spread test, first inside of standard slump cone mould, and the top surface of the base plate were moistened. The slump cone was filled with the fresh concrete sample

and it was then lifted within 30 s of filling it with the fresh mix. The concrete was then allowed to flow freely on the base plate. When the flow had stopped, the diameter of the flow spread was measured in two perpendicular directions (largest diameter and its perpendicular direction) and the average value was reported as the slump flow spread of the SCC mix [4]. The T_{50cm} flow time was measured in seconds between the instant the slump cone leaves base plate till the spreading concrete mix first reaches the circle of 50 cm diameter mark on the base plate [4]. The test set-up for measurement slum flow spread and T_{50cm} flow time is shown in Fig. 3.6 (a). The photograph of the flow spread is shown in Fig. 3.6 (b). The expression for slump flow spread is as follows;

$$SF = \frac{d_{\max} + d_{perp}}{2} \tag{3.1}$$

Where, SF = Slump flow spread

d_{max} = largest diameter of the flow spread

d_{perp} = diameter perpendicular to the largest flow spread

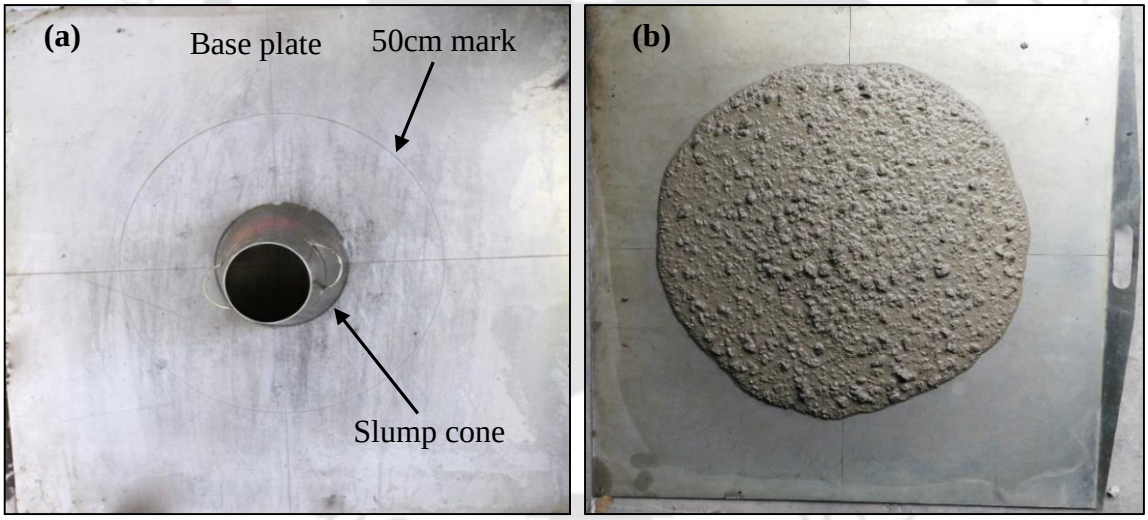

Fig. 3.6 Test for slump flow spread and T_{50cm} flow time: (a) test set-up, and (b) photograph of flow spread

3.6.2 V-funnel flow time test

V-funnel flow time test is suitable for the SCC mixes where the maximum size of aggregate does not exceed 20 mm. In the V-funnel flow time test, the inside of the V-shaped metal container (open at the top and with a sliding gate at the bottom) was first moistened and a container was placed underneath the funnel. It was then filled completely with the fresh concrete sample with the bottom sliding gate in closed position. After a wait of

approximately 10 s, the bottom gate was opened, thereby allowing the concrete to flow out of the V-funnel. The time taken from when the bottom gate was opened till the light was seen from above through the funnel was measured as V-funnel flow time in seconds. The test set-up and the photograph during the test are shown in Fig. 3.7 (a, b).

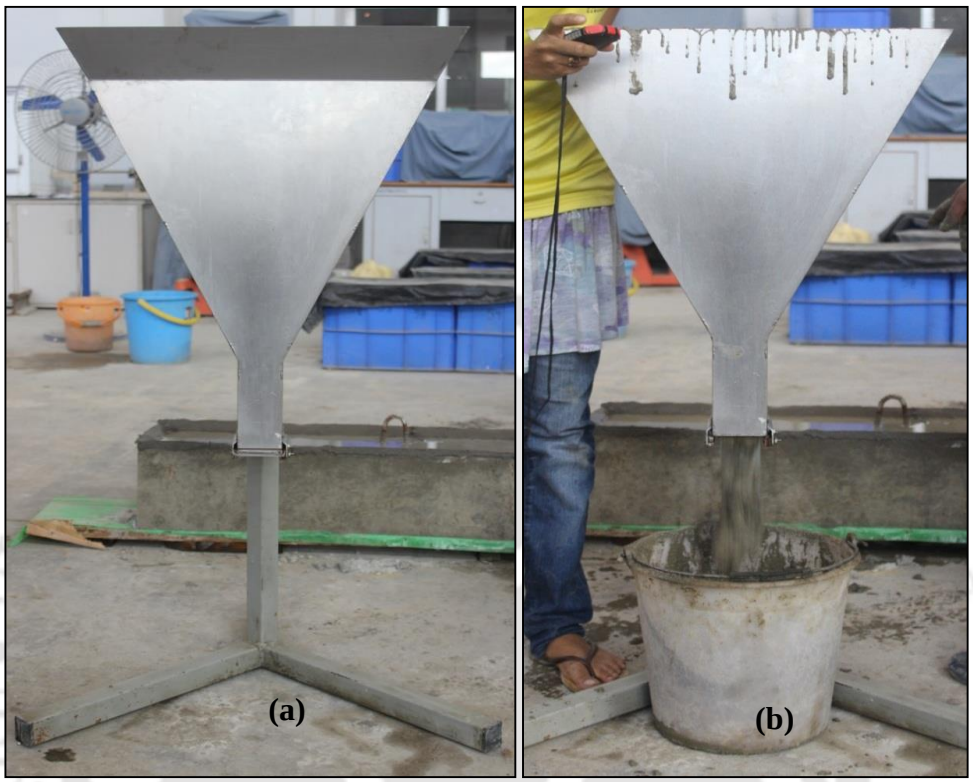

Fig. 3.7 Test for V-funnel flow time: (a) test set-up, and (b) photograph during the test

3.6.3 L-box test

L-box consists of vertical and horizontal rectangular sections in the shape of 'L', which are separated by a movable gate, in front of which vertical plain steel bars are fitted. The L-box with 3-bar set-up was used to determine the passing ratio of the SCC mixes. The test set-up and the photograph during the L-box test are shown in Fig. 3.8 (a, b). First, the inside surface of the L-box was moistened and it was then placed on a horizontal surface. The vertical section of the box was then filled with the fresh concrete sample. After the surplus concrete sample was struck off, the concrete sample was allowed to stand inside the vertical section for 1 minute, to observe any segregation. After that, the gate was lifted to allow the concrete to flow into the horizontal section. When the concrete had stopped flowing, the height difference between the top surface of concrete and the top edge of the vertical section was measured at three locations equally spaced along the wider side of the vertical section, to calculate the mean height (H_1) of concrete behind the gate. Similarly, the height

difference between the top surface of concrete and the top edge of the horizontal section was measured at three locations equally spaced along the width of the horizontal section at the end, to calculate the mean height (H_2) of concrete. The passing ratio was calculated as follows;

$$Passing\ Ratio = \frac{H_2}{H_1}$$

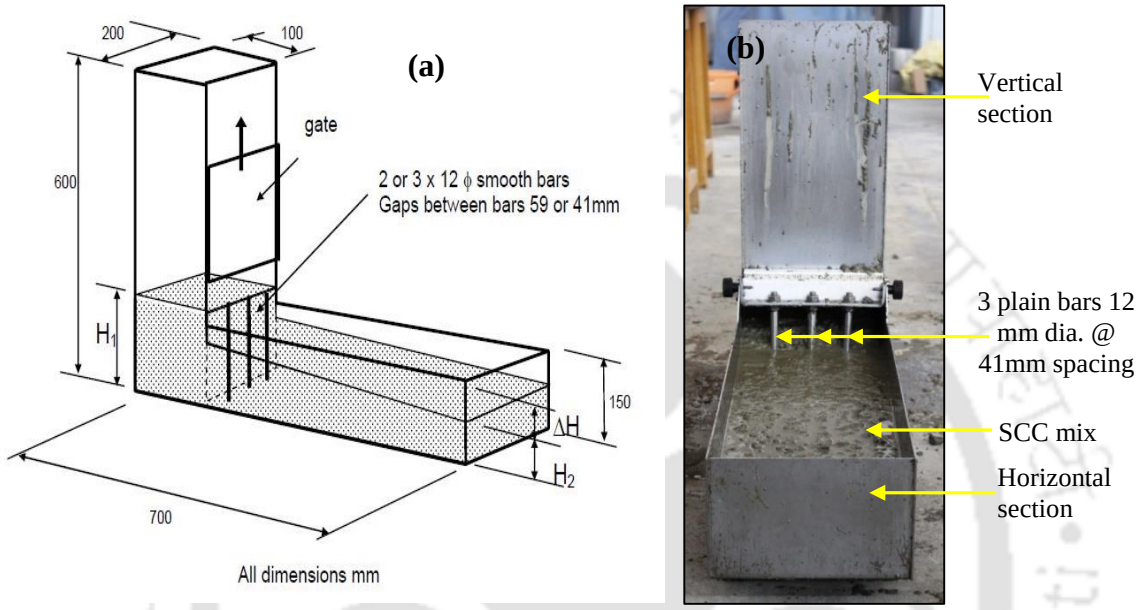

Fig. 3.8 L-box test: (a) Schematic diagram [4], and (b) photograph during the test

3.6.4 Sieve segregation test

In this test, 10 l of the freshly prepared concrete sample was placed in a bucket, which was then covered with a lid. The concrete sample in the bucket was allowed to stand for a rest period of 15 minutes without any disturbance. A sieve (300 mm diameter and 40 mm height) having 5 mm square openings along with a pan were placed on a weighing balance as shown in Fig. 3.9. After the rest period of 15 minutes, a sample of about 5 kg of concrete was poured from a height of 50 cm onto the sieve. The poured concrete was then allowed to stand in the sieve undisturbed for 2 minutes and after that the sieve was lifted vertically without any agitation. The segregation index was then calculated in percentage as mass of sieved material (passed through the sieve) with respect to the mass of concrete poured onto the sieve using the following equation:

$$Segregation\ Index\ (SI) = \frac{W_{ps} - W_p}{W_c} \times 100 \qquad (3.3)$$

Where, W_{ps} = mass of pan with the sieved material

W_p = mass of pan

W_c = mass of concrete sample poured onto the sieve

Fig. 3.9 Photograph of sieve segregation test

3.7 Preparation of SCC test specimens

All the prepared SCC mixes satisfied the required criteria of fresh properties as per EFNARC guidelines [4]. Cubes of size 150 mm and prismatic specimens of size 72 mm × 72 mm × 300 mm with a centrally embedded steel bar of diameter 12 mm were prepared from each SCC mix. The cube specimens were used for obtaining the compressive strength as well as the concrete powder samples required for determining chloride concentration, pH and for analyzing the microstructure of concrete. Prismatic reinforced concrete specimens were used for determining the corrosion parameters of the embedded steel reinforcement. As mentioned earlier, Tempcore TMT steel bars of diameter 12 mm were used as steel reinforcement. The steel bars were cut to a length of 335 mm and were cleaned with a wire brush to remove any surface scale before embedding into the prismatic specimen. In order to prevent crevice corrosion, insulating tape was applied followed by epoxy coating over the steel bar at the locations of discontinuity of steel bar with the surrounding concrete. The exposure length of steel bar inside the prismatic specimen was 170 mm. The concrete cover to the steel bar at the bottom and on all longitudinal sides of the prismatic specimen was 30 mm. The schematic diagrams of the steel bar and prismatic specimen are shown in Fig. 3.10 and Fig. 3.11, respectively. The cubes and prismatic

specimens were removed from the moulds after 24 hours of preparation and were then moist cured in a water curing tank.

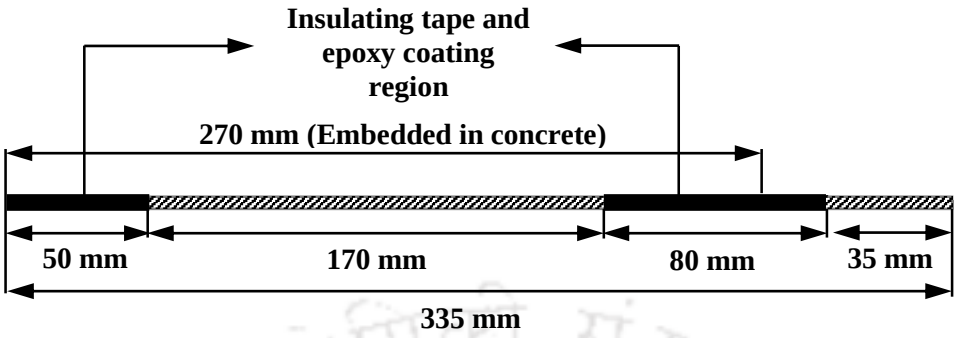

Fig. 3.10 Schematic diagram of the steel bar

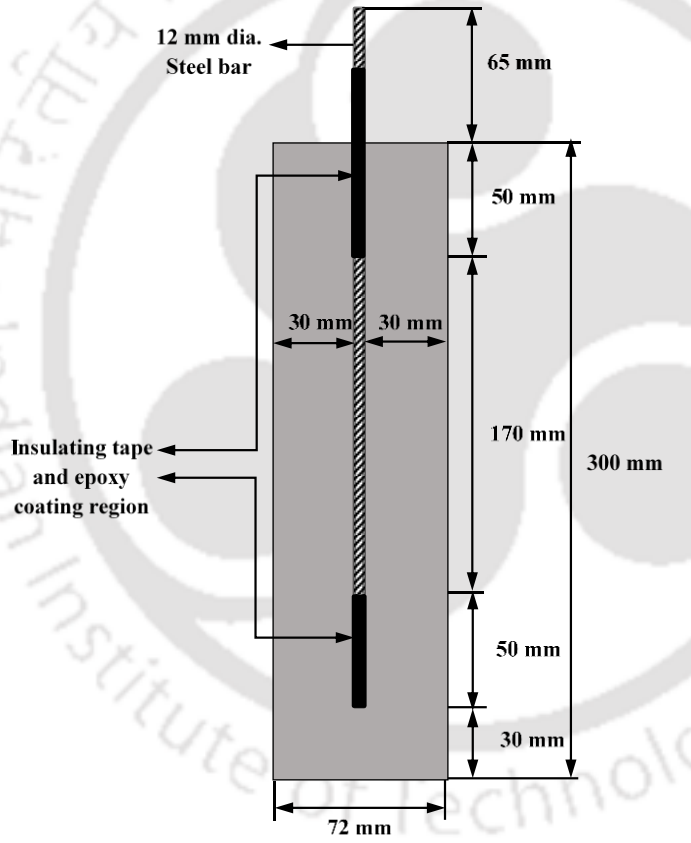

Fig. 3.11 Schematic diagram of the prismatic reinforced SCC specimen

3.8 Exposure conditions

In this research work, the following exposure conditions were adopted for the SCC mixes.

- Internal exposure
- External exposure

3.8.1 Internal exposure

As mentioned earlier in Section 3.4, sodium chloride (NaCl) was admixed in the SCC mixes at different concentrations during the time of preparation. After the completion of 28 days of moist curing, the prismatic reinforced concrete specimens from each SCC mix were kept in the ambient laboratory condition for 14 days. Two types of exposure condition were adopted i.e. laboratory drying (air curing) and water curing. For laboratory drying (air curing), the prismatic specimens were kept further in the ambient laboratory condition for a period of 540 days. For water curing, the specimens were exposed to normal water with alternate wetting-drying cycles. One cycle consists of three days of wetting followed by drying in ambient laboratory condition for seven days. During wetting, the prismatic specimens were partially immersed in water up to a height of 255 mm from its bottom in plastic tanks. After 450 days of exposure to normal water with alternate wetting-drying cycles, the same specimens were further exposed to 5% NaCl solution with alternate wetting-drying cycles for another 240 days. As already mentioned in Section 3.4, SCC mixes were also prepared with higher concentrations of admixed sodium chloride i.e. 7.5% and 12.5% by weight of mixing water at w/b ratio of 0.40 and from these SCC mixes, cube and prismatic specimens were also prepared from three types of binder. After completion of 28 days of moist curing, the prismatic specimens were kept in the ambient laboratory condition for 14 days and were further exposed to laboratory drying (air curing) for a period of 540 days.

3.8.2 External exposure

In addition to chloride salts, sulfate salts are also present in seawater and groundwater. When both chloride and sulfate ions enter into concrete, the mechanism of deterioration may become more complex because of interaction of these ions with cement hydration products. From the literature, it is observed that several studies have been carried out to evaluate the durability of normal vibrated concrete exposed to chloride, sulfate, and combined chloride-sulfate exposure solutions of different concentrations [32,35,120-122]. In the present research work, for external exposure conditions, sodium chloride (NaCl) was used as the source of chloride ions, whereas sodium sulfate (Na_2SO_4) and magnesium sulfate ($MgSO_4$) were used as the sources of sulfate ions. The chloride solutions were prepared by dissolving sodium chloride in water at concentrations of 1%, 3% and 5% by weight of water. Similarly, the combined chloride-sulfate solutions were prepared by dissolving sodium chloride with sodium sulfate, and sodium chloride with magnesium

sulfate in water. The concentrations of sodium chloride in the combined solution were 1%, 3%, and 5%, and those of sodium sulfate and magnesium sulfate were 3% each by weight of water. Thus, total nine solutions i.e. 3 numbers of chloride solutions and 6 numbers of combined chloride-sulfate solutions were used for external exposure conditions. Similar to the internal exposure condition, the prismatic reinforced concrete specimens were kept in the ambient laboratory condition for 14 days after the completion of 28 days of moist curing. After that, the specimens were exposed to chloride and combined chloride-sulfate solutions with alternate wetting-drying cycles for a period of 690 days. One cycle consists of three days of partial immersion of the prismatic specimen in the exposure solution up to a height of 255 mm from its bottom in plastic tanks during wetting followed by drying in ambient laboratory condition for seven days. The details about the internal and external exposure conditions used in the present experimental study are presented in Fig. 3.12. A photograph of laboratory wetting-drying exposure of prismatic specimens is shown in Fig. 3.13.

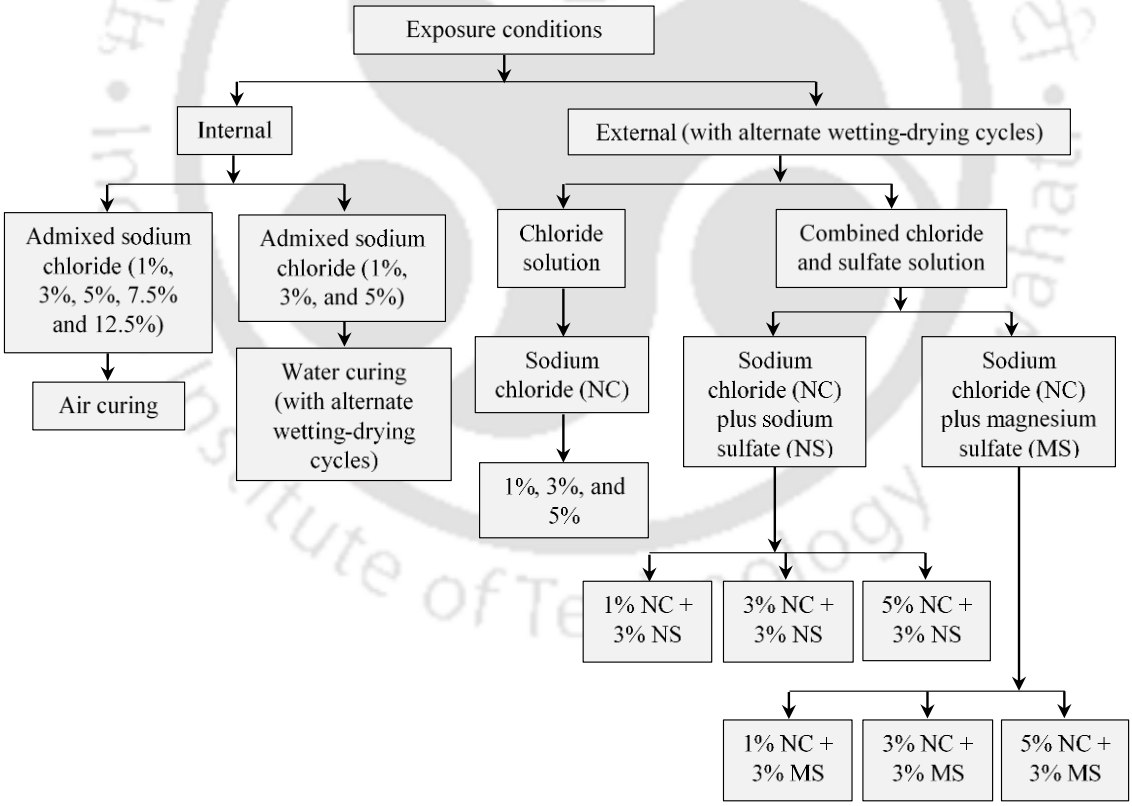

Fig. 3.12 Exposure condition of the prismatic reinforced SCC specimens

It is to be noted that three replicate cube specimens were prepared from each SCC mix for a given curing age. Similarly, four replicate prismatic specimens were prepared from each SCC mix. The details about the number of specimens prepared from the SCC mixes for different exposure conditions are provided in Table 3.10. Further, the number of specimens prepared from the SCC mixes admixed with higher concentrations of NaCl (7.5% and 12.5%) are mentioned in Table 3.11.

Table 3.10 Details about the number of prismatic specimens and cubes of SCC mixes

Binder type	w/b ratio	Number of prismatic reinforced concrete specimens					Number of cube specimens		
		Internal exposure		External exposure			Curing age		
		Admixed NaCl (0%, 1%, 3% and 5%)		NaCl (1%, 3% and 5%)	NaCl (1%, 3% and 5%) + Na_2SO_4 (3%)	NaCl (1%, 3% and 5%) + $MgSO_4$ (3%)	28 days	90 days	360 days
		Water curing	Air curing				Admixed NaCl (0%, 1%, 3% and 5%)		
OPC	0.37	16	16	12	12	12	12	12	12
	0.40	16	16	12	12	12	12	12	12
	0.43	16	16	12	12	12	12	12	12
PPC	0.37	16	16	12	12	12	12	12	12
	0.40	16	16	12	12	12	12	12	12
	0.43	16	16	12	12	12	12	12	12
OPC+ 20% FA	0.37	16	16	12	12	12	12	12	12
	0.40	16	16	12	12	12	12	12	12
	0.43	16	16	12	12	12	12	12	12

Table 3.11 Details about the number of prismatic specimens and cubes of SCC mixes admixed with NaCl concentrations of 7.5% and 12.5% at w/b ratio of 0.40

w/b ratio	Binder type	Number of prismatic reinforced concrete specimens		Number of cube specimens	
		Air curing		Curing age	
				28 days	360 days
		7.5% NaCl	12.5% NaCl	Admixed NaCl (7.5% and 12.5%)	
0.40	OPC	4	4	6	6
	PPC	4	4	6	6
	OPC+20% FA	4	4	6	6

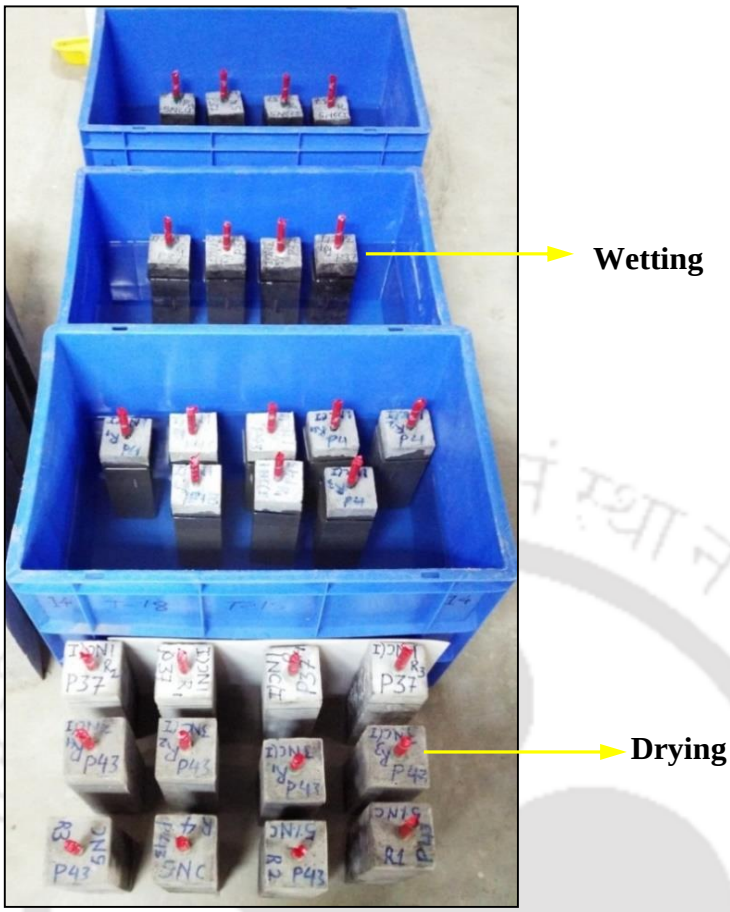

Fig. 3.13 Photograph of some of the prismatic specimens used during wetting-drying cycles

3.9 Compressive strength test

Three replicate cube specimens from each SCC mix were tested in a compression testing machine at the curing ages of 28, 90 and 360 days to investigate the effect of binder type, w/b ratio, admixed chloride concentration and curing age on compressive strength of SCC mixes. The average value of three replicate cube specimens was reported as the compressive strength of a given SCC mix at the respective curing ages.

3.10 Preparation of concrete powder from cube specimens

After completion of compressive strength test, the broken cube specimens were further crushed in a pulverizer. The crushed concrete samples were then passed through a sieve having 75 µm square openings. The sieved concrete powder was then stored in air tight plastic containers, which was further used for analyzing the microstructure (through EDX, XRD, TGA, FESEM, and FTIR analyses), and for determining chloride concentration and

pH of SCC mixes. The procedure for preparation of concrete powder sample is shown in Fig. 3.14.

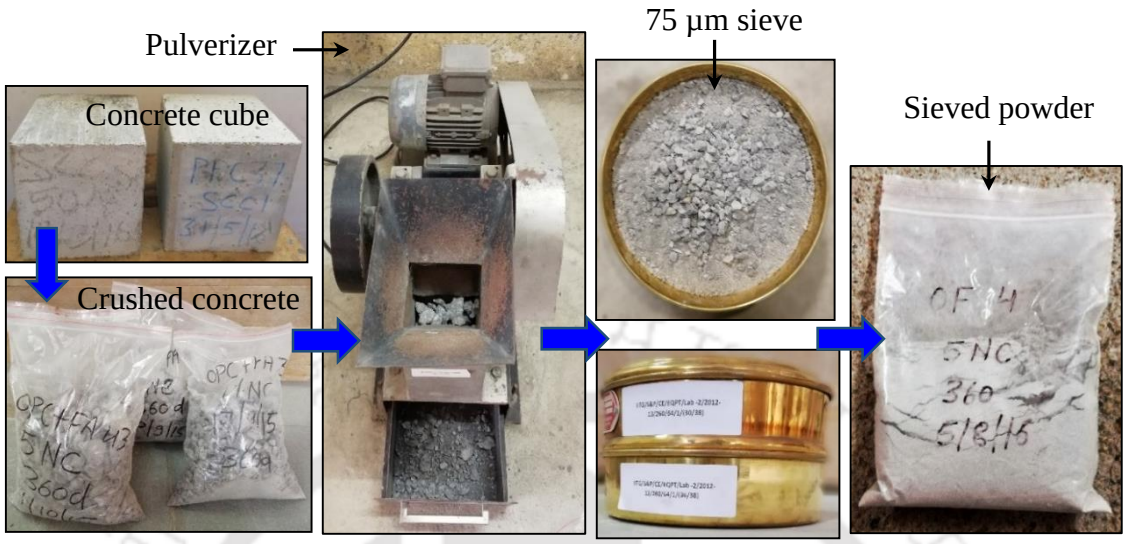

Fig. 3.14 Procedure for preparation of concrete powder sample

3.11 Microstructures of SCC mixes

Following analyses were carried out to exmine the microstructure of SCC mixes:

- Energy dispersive X-ray (EDX) analysis
- X-ray diffraction (XRD) analysis
- Thermo-gravimetry analysis (TGA)
- Field emission scanning electron microscope (FESEM) analysis
- Fourier transform infrared (FTIR) spectroscopy

3.11.1 Energy dispersive X-ray spectroscopy (EDX) analysis

Energy dispersive X-ray spectroscopy was used to determine the elemental composition of SCC mixes. FESEM (Sigma Zeiss) coupled with Oxford EDX instrument was used with an accelerating voltage of 20 kV at magnification of 1000 X over the area of the concrete powder sample in secondary electron (SE) mode. The elements chosen for analysis were based on the chemical elements of the binders used in the preparation of SCC mixes.

3.11.2 X-ray diffraction (XRD) analysis

X-ray diffraction analysis was conducted on concrete powder samples using Rigaku high power X-ray diffractometer (TTRAX III model) with CuKα radiation (λ=1.5405 Å) and operating at voltage 50 kV and current 100 mA. All the concrete powder samples were

scanned over a range of 8.0° to 60.0° (2θ) at a scan speed of 3° 2θ per minute. From the obtained XRD patterns, the phase compositions were identified using the PDF2 reference library (ICDD: International Centre for Diffraction Data) and PANalytical X'Pert HighScore Plus software. The weight percentage (wt. %) of identified compounds were estimated semi-quantitatively using the normalized reference intensity ratio (RIR) matrix-flushing method [123-125]. For consistency, the same reference phase was employed for each compound in all the samples so that RIR concentrations were used consistently between the samples. The following equation was used to calculate the weight percentage (wt. %) of the compounds [126].

$$W_i = \frac{I_i / RIR_i}{\sum_{i=1}^{N} (I_i / RIR_i)} \tag{3.4}$$

$$W_1 + W_2 + \cdots + W_N = 1$$

Where, W_i represents the relative mass of compound *i*, RIR_i denotes the reference intensity ratio of compound *i*, which is mentioned in the PDF reference library of ICDD, I_i is the integral intensity of the highest peak of compound *i*, which is calculated using X'Pert HighScore Plus software, and N is the number of compounds in the sample.

3.11.3 Thermo-gravimetry analysis (TGA)

For evaluating the thermal behaviour of SCC mixes, thermo-gravimetry analysis (TGA) was carried out on the powdered SCC samples. TGA measures the mass loss of a concrete sample in a heated environment as a result of decomposition of the phases present in it. In concrete investigations, TGA is commonly used with the first derivative of the change of mass to determine the sharp yield peaks. TGA with derivative thermo-gravimetry (DTG) test was performed on the powdered SCC samples using the instrument NETZSCH STA 449F3. During the experiment, the powdered sample was heated in an aluminum crucible from ambient temperature to 950 ºC at 10 ºC/min in argon environment flowing at 60 ml per minute. The obtained mass loss from TGA was used to estimate the calcium hydroxide (CH) content in the SCC mixes. The calcium hydroxide content was estimated using Taylor's formula [127] as follows:

$$CH\ (\%) = W_{CH} \times \frac{M_{CH}}{M_{H_2O}} \tag{3.5}$$

Where, W_{CH} = mass loss during dehydration of calcium hydroxide as percentage of the ignited mass (%), M_{CH} = molar mass of calcium hydroxide, and M_{H_2O} = molar mass of water.

3.11.4 Field emission scanning electron microscope (FESEM) analysis

The morphology of SCC mixes was analyzed using Zeiss Sigma field emission scanning electron microscope. The concrete powder sample was placed on a stub above the carbon tape. Before loading into the FESEM chamber, the concrete powder sample was coated with a thin gold layer by sputtering method. The surface morphology of the powder sample was observed with in-lens mode. In the analysis, the maximum accelerating voltage of 4 kV was used, and the images were captured at the magnification level of 20 KX.

3.11.5 Fourier transform infrared (FTIR) spectroscopy

Fourier transform infrared (FTIR) spectroscopy was performed on the concrete powder sample to study the functional groups associated with the products formed in concrete. The FTIR spectra of powdered SCC samples were recorded in the transmission mode on a PerkinElmer Spectrum Two FTIR spectrometer, using potassium bromide (KBr) pellets method. For the preparation of sample pellets, 3 mg of concrete powder was mixed with 250 mg of KBr and was then compressed using a hydraulic compressor to obtain the pellets. Five scans were recorded over a range of 4000 cm^{-1} to 400 cm^{-1}. First, the background spectrum was collected at the ambient atmosphere and after that the spectra of the samples were collected.

3.12 Chloride concentration of SCC mixes

The free and total chloride concentrations of SCC mixes were determined through potentiometric titration using an automatic titrator; make: Meterohm, and model: 848 Titrino Plus. For determining free chloride or total chloride concentration, 3 g of concrete powder sample was put into a 100 ml beaker and 50 ml of the respective solvent (distilled water for free chloride and concentrated nitric acid (3N) for total chloride) was added [117, 128,129]. For free chloride, the sample was heated gently and thoroughly mixed by a stirrer. After that, the solution was cooled to the room temperature and was then titrated against 0.1 M $AgNO_3$ solution. For total chloride, concentrated nitric acid (3N) was added to the concrete powder sample and then thoroughly mixed by the stirrer without heating followed by titrating against 0.1 M $AgNO_3$ solution. The resulting free or total chloride concentration

was expressed as percentage by mass of concrete. It should be noted that the free and total chloride concentrations of a given concrete powder sample were determined separately. The photograph during the measurement of chloride concentrations of SCC mixes is shown in Fig. 3.15.

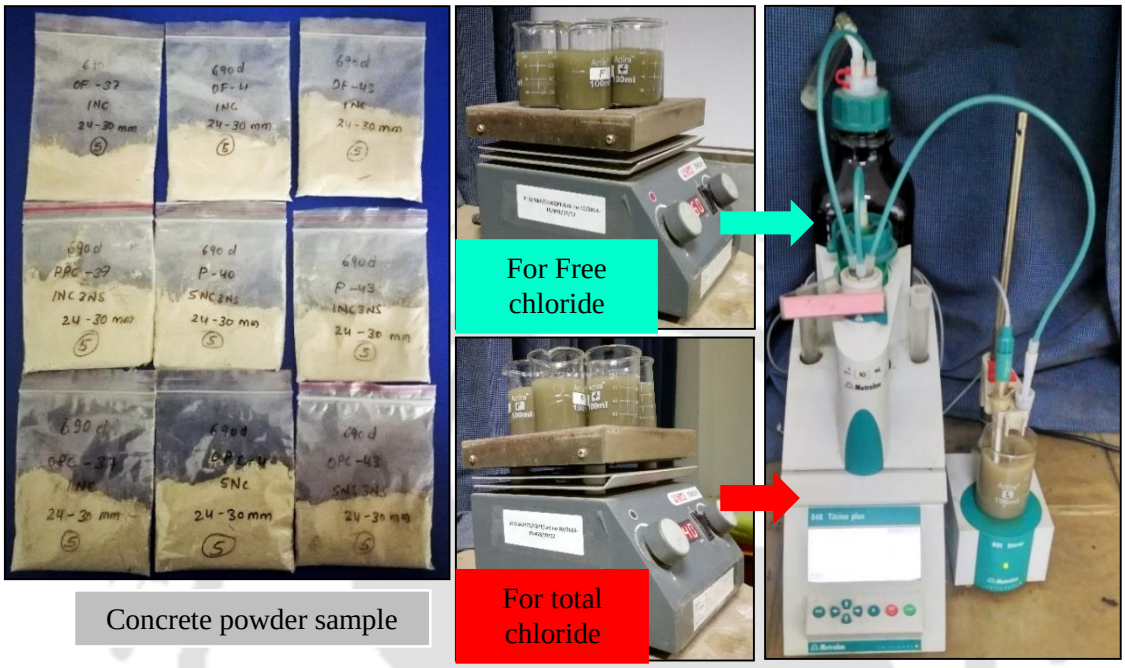

Fig. 3.15 Photograph during measurement of chloride concentration of SCC mixes

3.13 Measurement of pH of SCC mixes

A digital pH meter was used for determining the pH of concrete powder solution. For this test, the aqueous solution of concrete powder was prepared in the same manner as that was used for determining the free chloride concentration. After that, the solution was filtered through Whatman no. 1 filter paper and was then used for measuring pH of the SCC mixes. The photograph during the measurement of pH of the concrete powder aqueous solution is shown in Fig. 3.16.

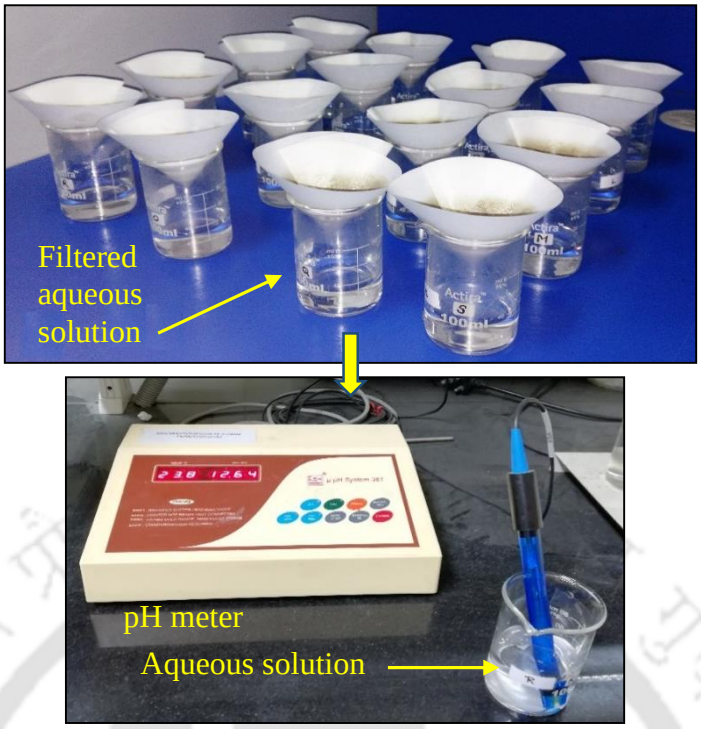

Fig. 3.16 Photograph during the measurement of pH of concrete powder aqueous solution of SCC mixes

3.14 Measurement of corrosion parameters

In this study, the electrochemical techniques used to evaluate the corrosion performance of steel reinforcement in SCC were corrosion potential and linear polarization resistance (LPR) measurements. The corrosion potential value is used to estimate the probability of occurrence of steel reinforcement corrosion, whereas the corrosion current density (obtained from LPR technique) provides information about the corrosion rate of steel reinforcement. The schematic diagram of the experimental set-up for corrosion potential and linear polarization resistance (LPR) measurements is shown in Fig. 3.17. The corrosion potential of the embedded steel bar (working electrode) in the prismatic specimen was measured with reference to saturated calomel electrode (SCE). A pair of stainless steel plates were used as auxiliary electrode. The working electrode, reference electrode, and auxiliary electrode were connected to the corrosion monitoring instrument (Make: ACM, Model: Gill AC serial no. 1542 sequencer). The photograph of the experimental set-up is shown in Fig. 3.18. During testing, the prismatic specimen was partially immersed in the test solution in a container. For prismatic specimens admixed with internal chloride, the concentration of NaCl in the test solution was the same as that admixed during the preparation of SCC mixes. For prismatic specimens exposed to external solutions, the

concentrations of NaCl, Na_2SO_4 and $MgSO_4$ in the test solution were same as that in the exposure solutions. For determining the corrosion current density by linear polarization resistance (LPR) technique, the steel bar embedded in the prismatic specimen was polarized to ± 20 mV from the equilibrium potential at a scan rate of 0.1 mV per second. The corrosion current density (I_{corr}) of steel reinforcement was determined by using the Stern-Geary equation [35,121]:

$$I_{corr} = \frac{B}{R_p} \tag{3.6}$$

Where, B = Stern-Geray constant, and R_p = polarization resistance of steel reinforcement.

The Stern-Geray constant B is given by;

$$B = \frac{[\beta_a \times \beta_c]}{2.3[\beta_a + \beta_c]} \tag{3.7}$$

Where β_a and β_c are anodic and cathodic Tafel constants, respectively. In this work, the value of B was taken as 26 mV considering the steel bar in active condition [35,121]. The corrosion potential and linear polarization resistance (LPR) measurements were performed on the prismatic SCC specimens at different periods up to the completion of exposure duration.

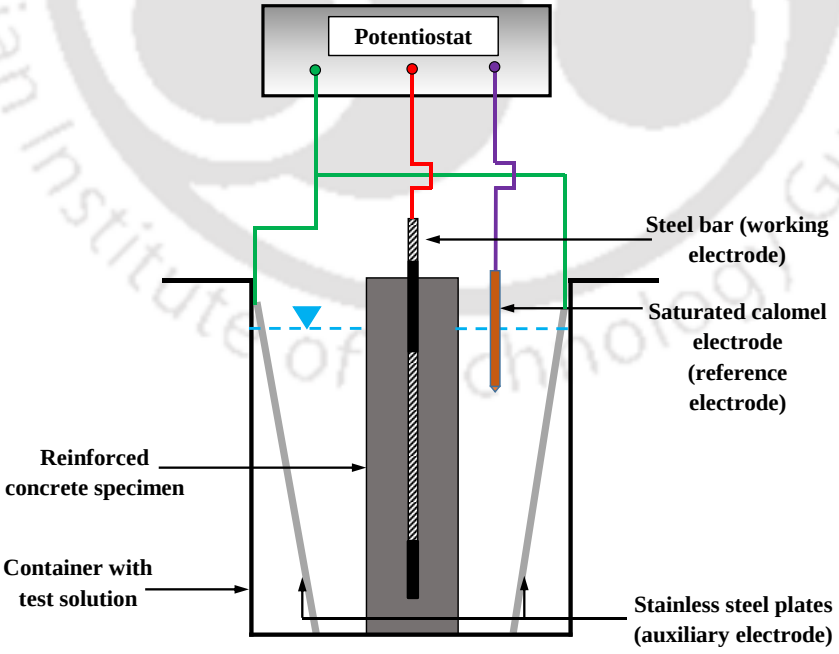

Fig. 3.17 Schematic diagram of experimental set-up for corrosion potential and LPR measurements

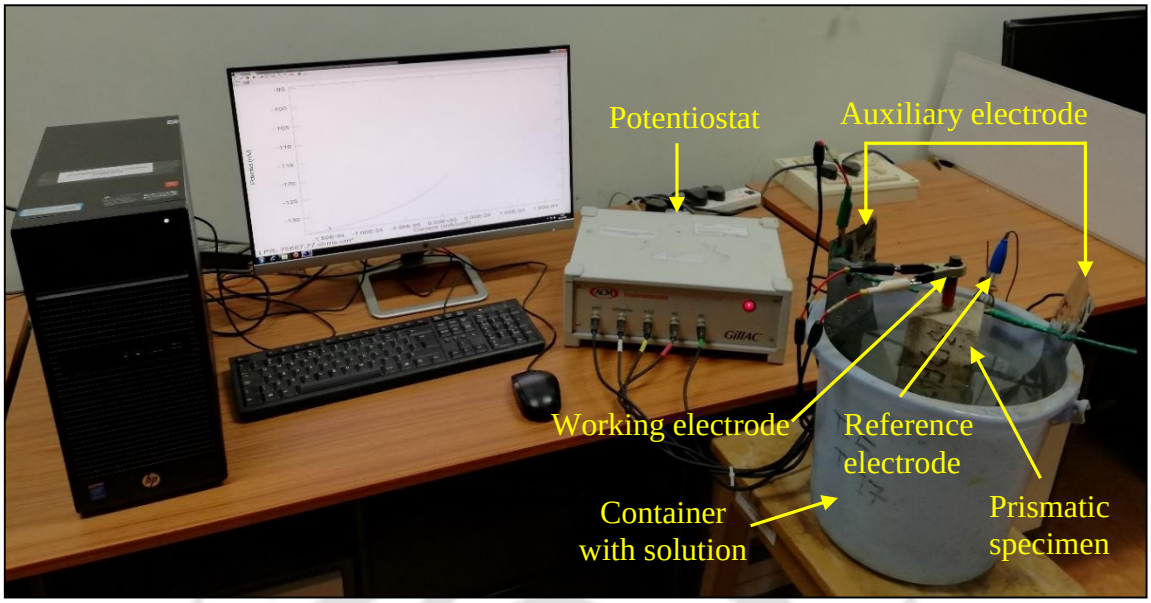

Fig. 3.18 Photograph of experimental set-up for corrosion potential and LPR measurements

3.15 Preparation of concrete powder from prismatic reinforced specimens

After completion of the exposure period, the prismatic specimens subjected to external exposure solutions were drilled at depth intervals of 0 - 6 mm, 6 - 12 mm, 12 - 18 mm, 18 - 24 mm and 24 - 30 mm from the surface of all the four longitudinal sides of the prismatic specimen to collect the concrete powder samples. Subsequently, the drilled concrete powder samples collected from respective depth intervals from all the four sides were mixed to obtain the concrete powder sample at a given depth interval. The concrete powder samples collected from the depth interval of 24 - 30 mm from the surface of prismatic specimen represent the concrete near the rebar level. It may be noted that the concrete cover to the rebar in the prismatic specimen was 30 mm. The drilled concrete powder samples collected from the depth interval of 24 - 30 mm were passed through a sieve having square openings of size 75 µm and the sieved concrete powder samples were stored in air tight containers. To determine the chloride concnetrtaion and to investigate the microstructure of concrete near the steel bar level, the concrete powder samples were used for chloride, XRD, EDX, and FESEM analyses. The photographs of drilled prismatic specimens and sieved concrete powder samples are shown in Fig. 3.19.

Fig. 3.19 Drilled prismatic specimens and sieved concrete powder samples

3.16 Summary

The experimental investigation carried out in the present research work on self-compacting concrete (SCC) comprised of characterizing the materials used in its preparation, carrying out various trial tests to arrive at the final mix proportion, and preparation of different test specimens followed by conducting various tests on these specimens. The SCC mixes were prepared from three types of binder and three w/b ratios. For different exposure conditions, sodium chloride was used as the source of chloride ions (for both internal and external exposures), whereas sodium sulfate and magnesium sulfate were used as the sources of sulfate ions (for external exposure). The tests for fresh properties of SCC such as slump flow spread for filling ability, T_{50cm} and V- funnel flow times for flow-rate, L-box test (passing ratio) for passing ability, and sieve segregation test for segregation resistance were carried out as per the EFNARC guidelines. The compressive strength of SCC mixes were determined at different curing ages. Further, the concrete powder samples obtained from various SCC mixes were analyzed (through EDX, XRD, TGA, FESEM, and FTIR analyses) to study the microstructure of SCC. In addition, chloride concentration, and pH of SCC mixes were also determined. In this research work, the electrochemical techniques such as corrosion potential and corrosion current density by linear polarization resistance (LPR) measurement were used to evaluate the corrosion performance of steel reinforcement in SCC.

CHAPTER 4

FRESH AND HARDENED PROPERTIES OF SCC

4.1 General

This chapter presents and discusses the obtained results for the fresh properties and compressive strength of self-compacting concrete (SCC) made with different types of binder, w/b ratio and varying concentrations of admixed sodium chloride. For evaluating the self-compactibility characteristics, various tests were conducted on fresh SCC mixes to determine slump flow spread, T_{50cm} flow time, V-funnel flow time, passing ratio (from L-box test) and sieve segregation resistance (presented in Chapter 3). In addition, compressive strength and EDX analysis were performed on SCC mixes at the curing ages of 28 days, 90 days and 360 days. The effects of binder type, w/b ratio and admixed chloride concentration on fresh properties and compressive strength of SCC were evaluated. In addition, the variations in Ca/Si ratio of C-S-H determined from EDX analysis performed on SCC mixes are discussed in this chapter.

4.2 Fresh properties

The filling ability, passing ability, and segregation resistance are the key properties of SCC, which were examined by various tests as described in Chapter 3. The measured slump flow spread values of SCC mixes admixed with different concentrations of NaCl at the w/b ratios of 0.37, 0.40, and 0.43 are shown in Fig. 4.1 (a - c). From this figure, it is inferred that the slump values of SCC mixes varied from 655 mm to 685 mm for OPC, 660 mm to 750 mm for PPC and 655 mm to 695 mm for OPC+20% FA irrespective of w/b ratio and admixed NaCl concentration. The observed values lie in the specified range of 650 mm - 850 mm as per EFNARC guidelines [4], which indicate good filling ability of all the SCC mixes. The results of T_{50cm} and V-funnel flow times of all the SCC mixes admixed with different concentrations of NaCl at w/b ratios of 0.37, 0.40, and 0.43 are shown in Fig. 4.2 (a - c) and Fig. 4.3 (a - c), respectively. The flow times (T_{50cm} and V-funnel) are closely related to viscosity of the SCC mix. The T_{50cm} and V-funnel flow times of SCC mixes varied from 1.06 s to 1.70 s, and 3.40 s to 4.09 s for OPC;1.31 s to 1.95 s, and 4.10 s to 5.56 s for PPC; and 1.36 to 1.78 s, and 3.68 to 4.43 s for OPC+20% FA, respectively irrespective of the w/b ratio and admixed concentration of NaCl, which satisfied the criteria as per EFNARC guidelines (recommended criteria for moderate to high flow-rate: T_{50cm} flow time $\leq$ 2 s and

V-funnel flow time ≤ 8 s) [4]. Thus, the obtained values of T_{50cm} and V-funnel flow times indicate moderate to high flow-rate, which exhibited good filling ability of SCC mixes.

The measured values of the passing ratio (from L-box test) of SCC mixes admixed with different concentrations of NaCl at the w/b ratios of 0.37, 0.40, and 0.43 are shown in Fig. 4.4 (a - c). The passing ratios of SCC mixes varied from 0.80 to 0.86 for OPC, 0.82 to 0.94 for PPC, and 0.81 to 0.87 for OPC+20% FA. According to EFNARC guidelines [4], the acceptable range of passing ratio varies from 0.80 to 1.0. Thus, the obtained values of passing ratio indicate higher passing ability with lower risk of blocking for all the SCC mixes.

The obtained results of sieve segregation test are shown in Fig. 4.5 (a - c). The segregation index of SCC mixes varied from 3.42% to 10.2% for OPC, 0.79% to 4.96% for PPC, and 1.49% to 5.47% for OPC+20% FA, which indicates that all the SCC mixes have higher resistance against segregation as per EFNARC guidelines (limiting value of segregation index: <15%) [4].

The results of fresh properties of SCC mixes made with the w/b ratio of 0.40 and admixed with higher concentrations of NaCl (7.5% and 12.5%) are shown in Table 4.1. From this table, it is observed that the SCC mixes made with OPC, PPC and OPC+20% FA are satisfying the acceptance criteria with respect to filling ability, passing ability and segregation resistance as per EFNARC guidelines, in the presence of higher concentrations of chloride ions.

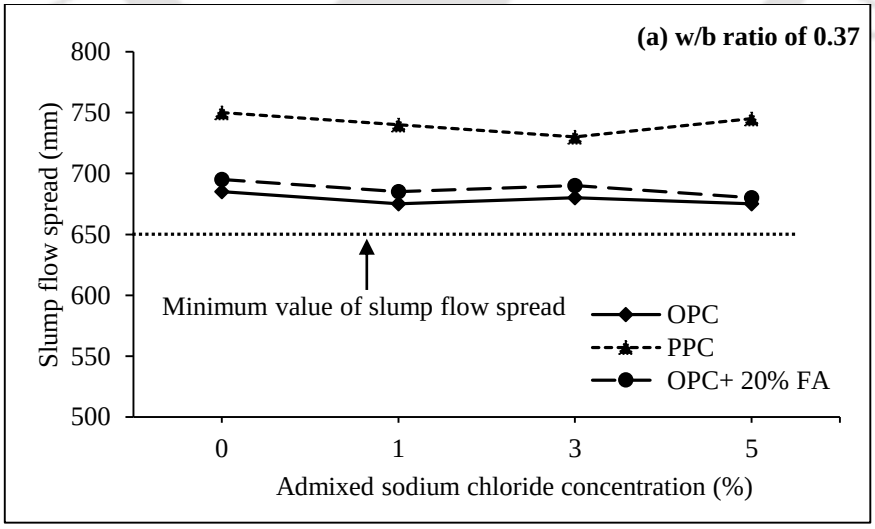

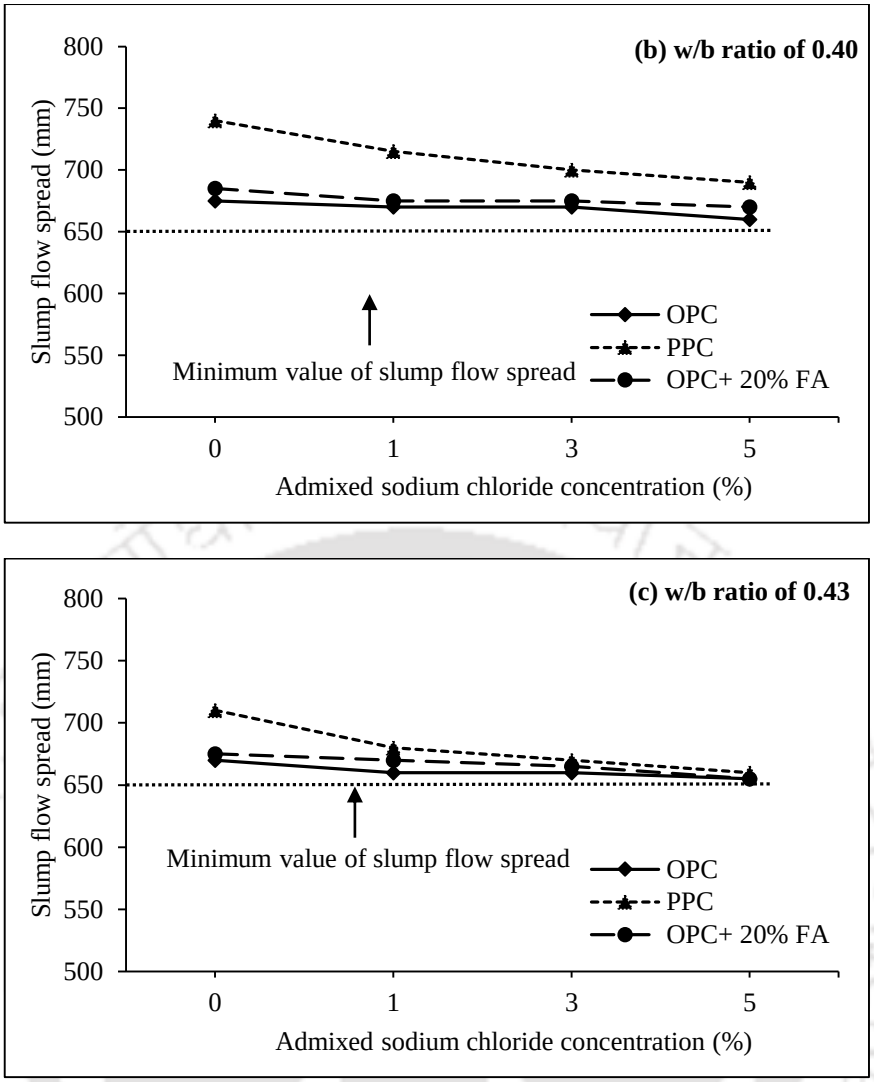

Fig. 4.1 Slump flow spread values of SCC mixes admixed with different concentrations of NaCl at w/b ratios of: (a) 0.37, (b) 0.40, and (c) 0.43

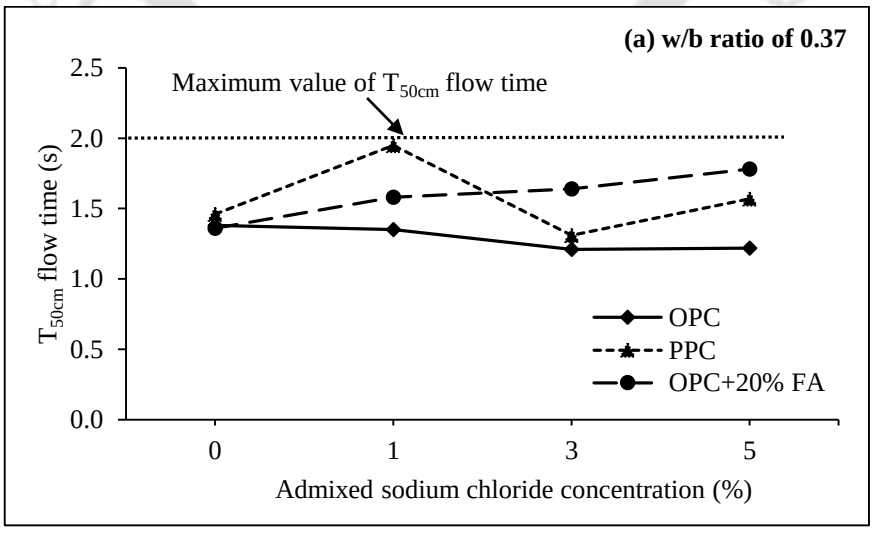

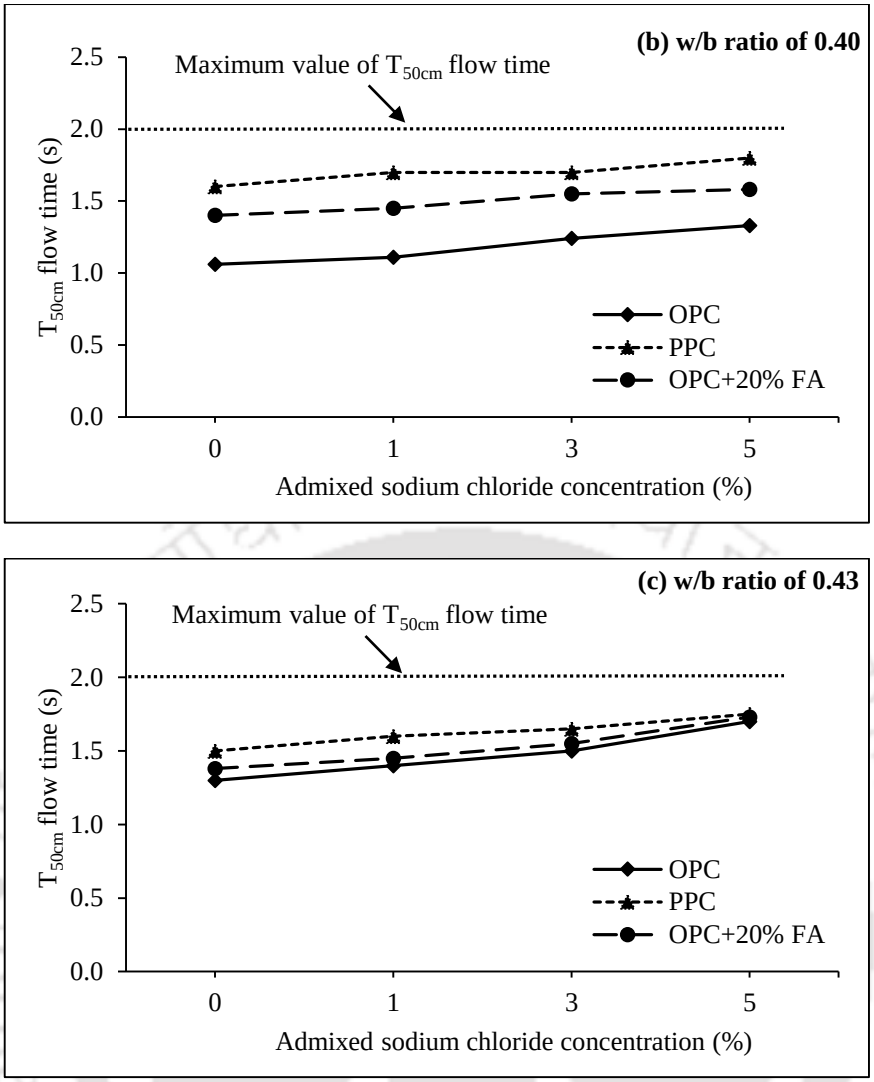

Fig. 4.2 T_{50cm} flow time of SCC mixes admixed with different concentrations of NaCl at w/b ratios of: (a) 0.37, (b) 0.40, and (c) 0.43

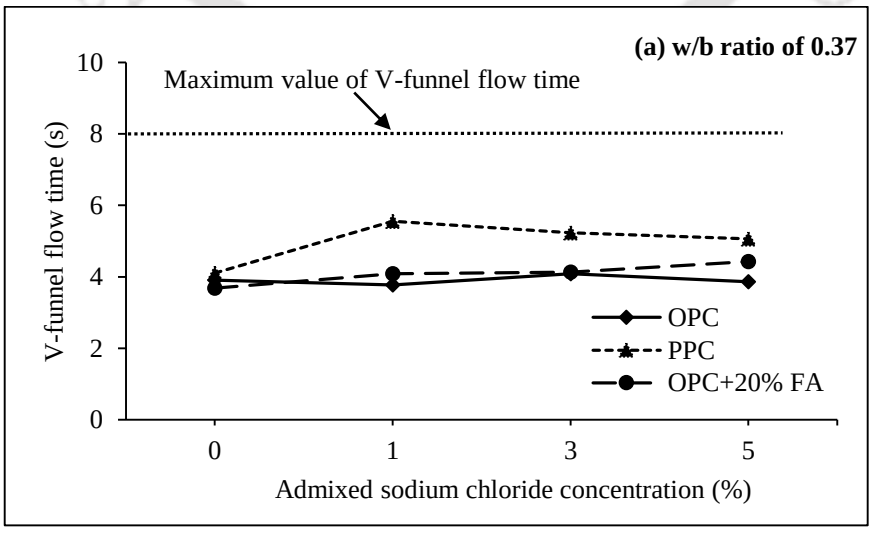

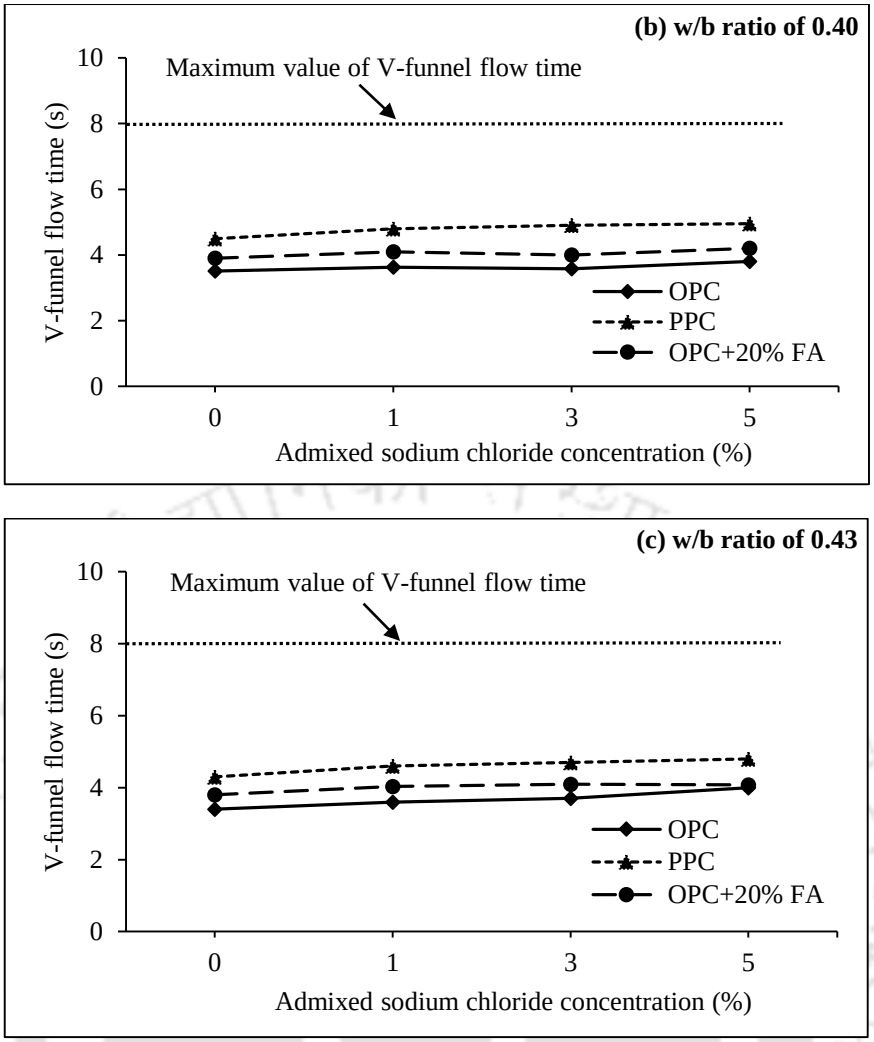

Fig. 4.3 V-funnel flow time of SCC mixes admixed with different concentrations of NaCl at w/b ratios of: (a) 0.37, (b) 0.40, and (c) 0.43

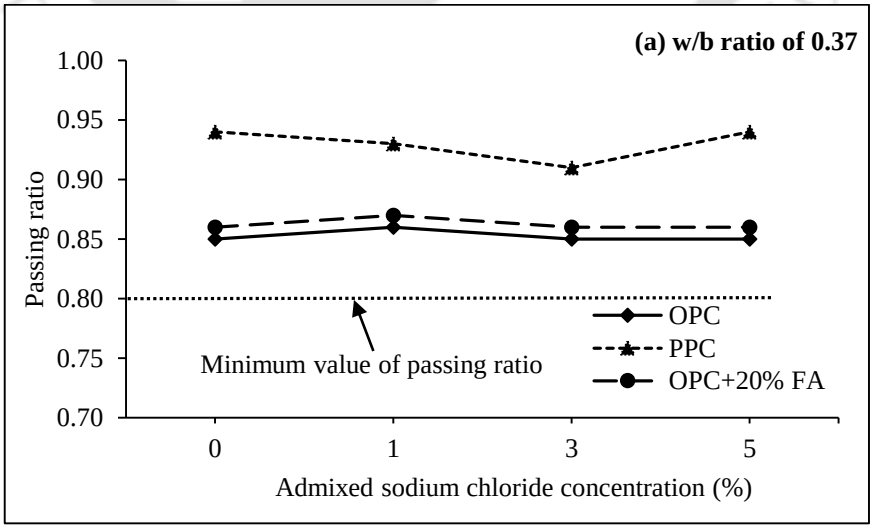

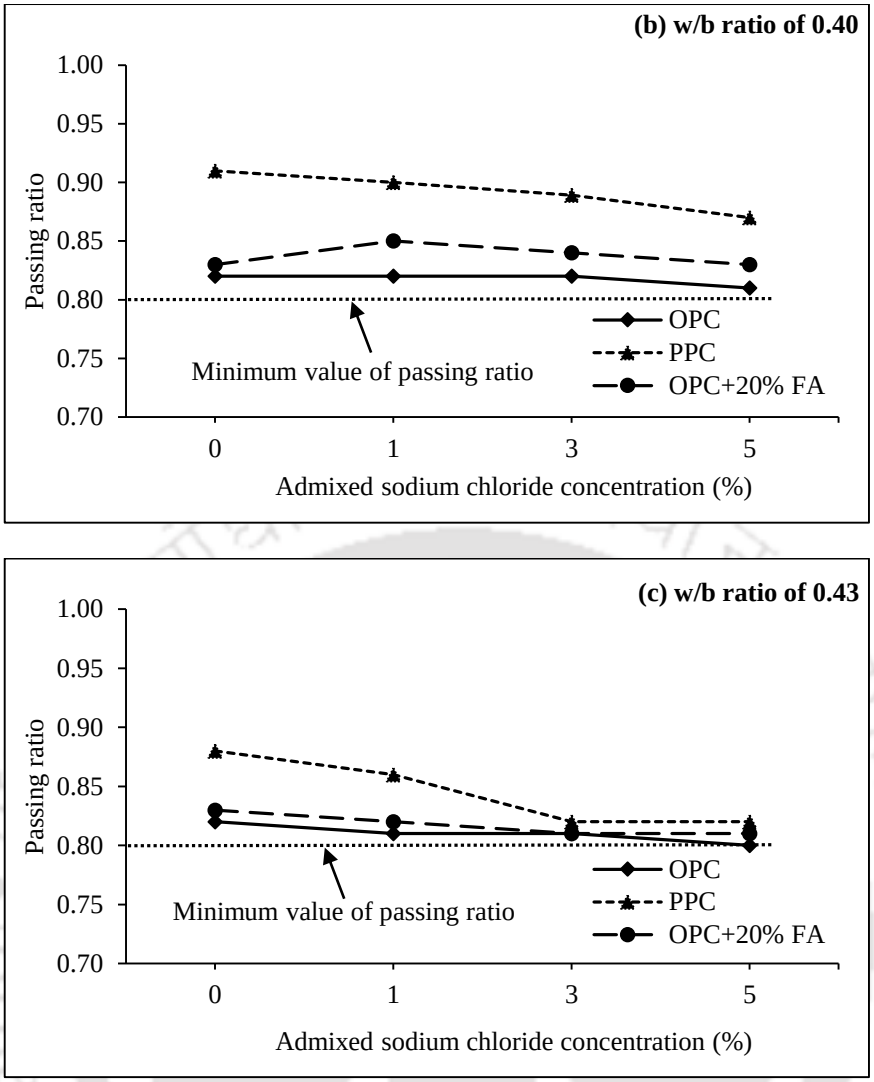

Fig. 4.4 L-box passing ratio of SCC mixes admixed with different concentrations of NaCl at w/b ratios of: (a) 0.37, (b) 0.40, and (c) 0.43

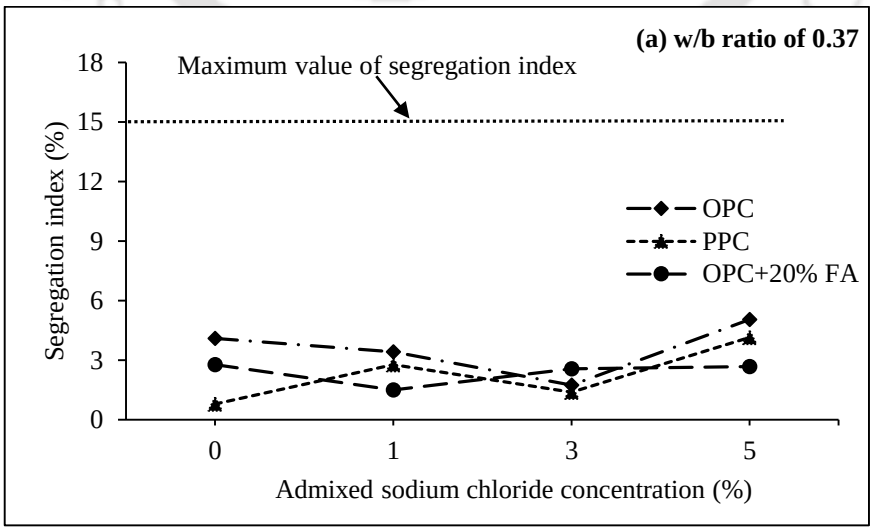

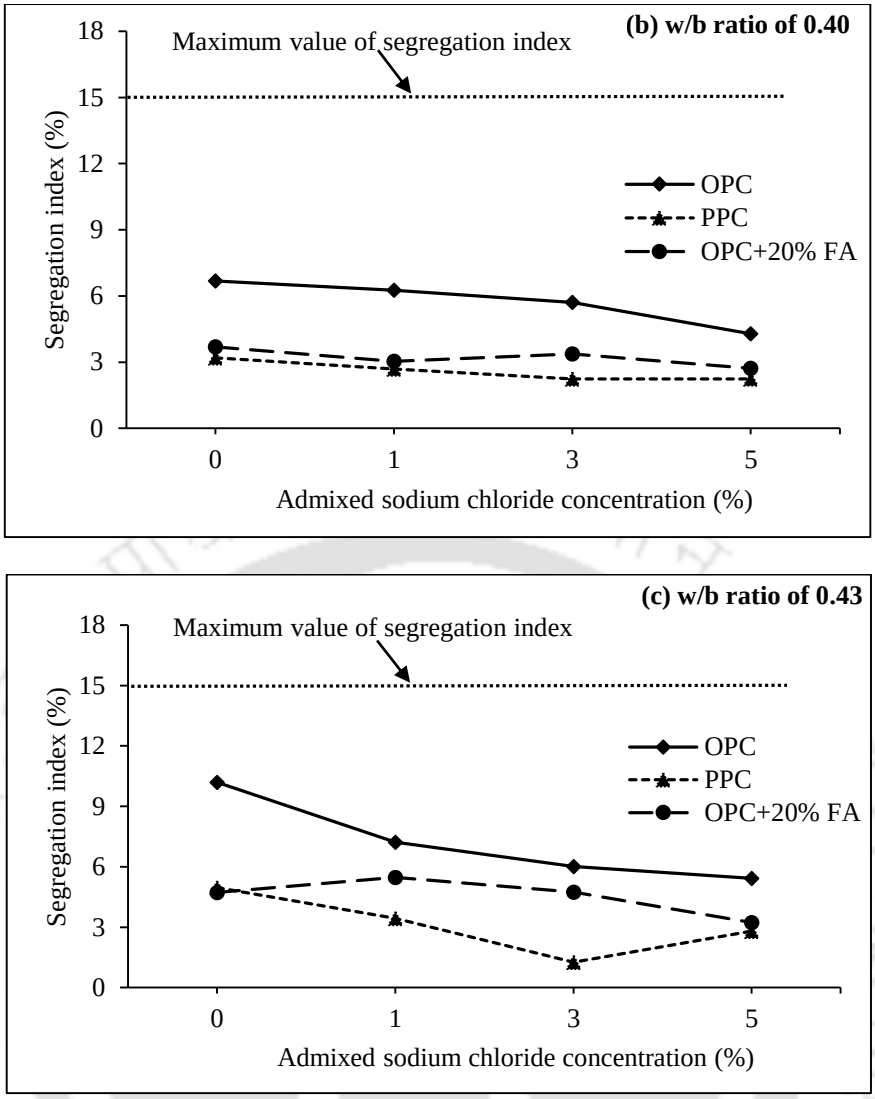

Fig. 4.5 Segregation index of SCC mixes admixed with different concentrations of NaCl at w/b ratios of: (a) 0.37, (b) 0.40, and (c) 0.43

Table 4.1 Fresh properties of SCC mixes admixed 7.5% and 12.5% NaCl concentrations at w/b ratio of 0.40

Tests	OPC		PPC		OPC+20% FA	
	7.5% NaCl	12.5% NaCl	7.5% NaCl	12.5% NaCl	7.5% NaCl	12.5% NaCl
Slump flow spread (mm)	660	655	685	690	670	660
T_{50cm} flow time (s)	1.38	1.45	1.88	1.80	1.67	1.68
V-funnel flow time (s)	4.02	4.15	5.10	5.40	4.40	4.50
Passing ratio	0.81	0.80	0.85	0.83	0.82	0.81
Segregation index (%)	3.74	3.35	2.58	2.20	2.95	2.65

4.2.1 Effect of binder type on fresh properties of SCC

While evaluating the effect of binder type on fresh properties of SCC, it is inferred that the SCC mixes made with PPC showed higher slump flow spread, T_{50cm} flow time and V-funnel flow time as compared to those made with OPC+20% FA followed by OPC at all concentrations of admixed NaCl (0%, 1%, 3% and 5%) and at all w/b ratios (0.37, 0.40 and 0.43), as evident from Fig. 4.1 (a - c) to Fig. 4.3 (a - c), respectively. The similar variations in slump flow spread, T_{50cm} flow time and V-funnel flow time with respect to binder type are also observed at higher concentrations of admixed NaCl i.e. 7.5% and 12.5% as evident from Table 4.1. The higher slump spread of SCC mixes made with PPC and OPC+20% FA may be attributed to the dispersing effect of the spherical fly ash particles present in these binders. Due to spherical shape, the fly ash particles easily roll over one another and also result in dispersion of the agglomeration of cement particles [78, 81]. Further, the spherical shape of fly ash particles reduces the friction at the aggregate-paste interface that produce a ball-bearing effect at the point of contact. Further, in case of PPC based SCC mixes, the higher T_{50cm} and V-funnel flow times are attributed to more viscous nature of the mix due to higher fineness of PPC.

From Fig. 4.4 (a - c), it is observed that the SCC mixes prepared with PPC showed higher passing ratio as compared to OPC+20% FA followed by OPC for admixed NaCl concentrations (0%, 1%, 3% and 5%). The same variation in passing ratio with respect to binder type is also observed at NaCl concentrations of 7.5% and 12.5% as evident from Table 4.1. The higher passing ratio of PPC and OPC+20% FA based SCC mixes as compared to those made with OPC is attributed to the increase in flowability of the concrete mix due to the presence of fly ash particles in PPC and OPC+20% FA. The passing ability is significantly related to filling ability [3] and as mentioned earlier, PPC based SCC mixes exhibited higher filling ability as compared to OPC+20% FA followed by OPC based SCC mixes.

Further, the SCC mixes made with PPC exhibited higher segregation resistance as indicated by lower segregation index as compared to OPC+20% FA followed by OPC for all concentrations of admixed NaCl, as evident from Fig. 4.5 (a - c) and Table 4.1. The higher segregation resistance in case of PPC and OPC+20% FA as compared to OPC is attributed to the more viscous nature of PPC and OPC+20% FA based SCC mixes that resulted in a more cohesive mix. The higher segregation resistance of PPC and OPC+20% FA based SCC mixes as indicated by lower segregation index corroborates with their lower flow-rate

of PPC and OPC+20% FA based SCC mixes as evident from higher T_{50cm} and V-funnel flow times.

Overall, the SCC mixes made with PPC showed an average increase of 6.12%, 25.53%, 28.35%, and 7.51% in the values of slump flow spread, T_{50cm} flow time, V-funnel flow time and passing ratio, respectively as compared to those made with OPC, irrespective of w/b ratio and admixed NaCl concentration. Further, the PPC based SCC mixes showed an average decrease of 48.91% in the value of segregation index as compared to OPC based SCC mixes, irrespective of w/b ratio and admixed NaCl concentration. Similarly, the SCC mixes made with OPC+20% FA showed an average increase of 1.06%, 18.20%, 8.43%, and 1.52% in the values of slump flow spread, T_{50cm} flow time, V-funnel flow time, and passing ratio, respectively as compared to those made with OPC, irrespective of w/b ratio and admixed NaCl concentration. Further, the OPC+20% FA based SCC mixes showed an average decrease of 33.47% in the value of segregation index as compared to OPC based SCC mixes. Thus, from the viewpoint of fresh properties, the SCC mixes made with PPC showed better performance as compared to those made with OPC+20% FA followed by OPC. Thus, between PPC and OPC+20% FA, fly ash blended with cement clinker during the manufacturing of PPC showed improved effect on the fresh properties of SCC as compared to that mixed with OPC during the preparation of SCC mixes.

4.2.2 Effect of water-to-binder (w/b) ratio on fresh properties of SCC

From the slump flow spread, T_{50cm} flow time, V-funnel flow time, passing ratio and segregation index values shown in Fig. 4.1 (a - c) to Fig. 4.5 (a - c), respectively, it is observed that the slump flow spread and passing ratio increased with decrease in the w/b ratio of SCC mixes irrespective of binder type and admixed NaCl concentration. This may be attributed to higher amount of paste in SCC mixes made with lower w/b ratio as compared to that made with higher w/b ratio. Further, the segregation index of SCC mixes decreased with decrease in w/b ratio i.e. the segregation resistance increased with the decrease in w/b ratio, which may be attributed to higher cohesive SCC mix made with lower w/b ratio as compared to that made with higher w/b ratio. Overall, the SCC mixes made with w/b ratio of 0.37 showed an average increase of 4.97%, and 6.97% in the values of slump flow spread, and passing ratio, respectively as compared to those made with the w/b ratio of 0.40, irrespective of binder type and admixed NaCl concentration. Further, the SCC mixes made with w/b ratio of 0.37 showed an average decrease of 34.49% in the values of segregation index as compared to the w/b ratio of 0.40, irrespective of binder type

and admixed NaCl concentration. Similarly, the SCC mixes made with w/b ratio of 0.40 showed an average increase of 2.41%, and 3.01% in the values of slump flow spread, and passing ratio, respectively as compared to those made with the w/b ratio of 0.43. Further, the SCC mixes made with the w/b ratio of 0.40 showed an average decrease of 15.40% in segregation index as compared to w/b ratio of 0.43, irrespective of binder type and admixed NaCl concentration. From Fig. 4.1 (a - c) to Fig. 4.5 (a - c), it is inferred that there is no systematic variation in T_{50cm} and V-funnel flow times with w/b ratio of the SCC mixes for different concentrations of admixed NaCl. This may be attributed to the dominant effect of the presence of chloride ions in the mix that altered the viscosity of the paste, thus affecting the flow rate. Overall from the viewpoint of fresh properties, the SCC mixes made with lower w/b ratio showed better performance as compared to those made with higher w/b ratio.

4.2.3 Effect of admixed NaCl concentration on fresh properties of SCC

While analyzing the effect of admixed NaCl on fresh properties, it is observed that there is no systematic variation in slump flow spread with concentration of admixed NaCl (1%, 3% and 5%) irrespective of binder type and w/b ratio as observed from Fig. 4.1 (a - c). Also, the difference in slump flow spread values among the admixed NaCl concentrations was very less. The similar variation in slump flow spread with respect to admixed NaCl was also observed at higher concentrations i.e. 7.5% and 12.5%. However, the slump flow spread was slightly higher in the SCC mix without NaCl as compared to that admixed with NaCl as observed from Fig. 4.1 (a - c). The unsystematic variation in slump flow spread with admixed NaCl concentration may be attributed to the variations in the interaction of chloride ions with the paste at different concentrations of NaCl that altered its viscosity.

From Fig. 4.2 (a), it is observed that there is no systematic variation in T_{50cm} flow time with increase in concentration of NaCl at w/b ratio of 0.37. At w/b ratios of 0.40 and 0.43, the T_{50cm} flow time mostly increased with increase in concentration of NaCl as observed from Fig. 4.2 (b, c) and Table 4.1, however the increase was very small. The less increase in T_{50cm} flow time may be attributed to slight improvement in the viscosity of the mix with increase in NaCl concentration. The similar variation was observed in case of V-funnel flow time i.e. V-funnel flow time mostly increased with increase in NaCl concentration at w/b ratios of 0.40 and 0.43, however the increase was small, as observed from Fig. 4.3 (b - c) and Table 4.1. At w/b ratio of 0.37, there is no systematic variation in V-funnel flow time with increase in concentration of admixed NaCl as observed from Fig. 4.3 (a).

From Fig. 4.4 (a), it is observed that, there is no systematic variation in passing ratio with concentration of admixed NaCl at w/b ratio of 0.37. At w/b ratios of 0.40 and 0.43, the passing ratio mostly decreased with increase in NaCl concentration, however, in most of the cases the decrease was very less as observed from Fig. 4.4 (b, c) and Table 4.1. The small decrease in passing ratio with increase in admixed NaCl concentration at higher w/b ratio may be attributed to a decrease in flowability of the SCC mix due to slight improvement in the viscosity of the mix. From Fig. 4.5 (a), it is observed that there is no systematic variation in segregation index with increase in NaCl concentration at w/b ratio of 0.37. However, the segregation index decreased slightly with increase in NaCl concentration at w/b ratios of 0.40 and 0.43 in most of the cases as observed from 4.5 (b, c) and Table 4.1. From the aforementioned discussion, it can be summarized that the presence of chloride ions in the SCC mix did not affect its fresh properties significantly, although, the NaCl admixed SCC mixes satisfied all the criteria with respect to fresh properties as per EFNARC guidelines.

4.2.4 Analysis of variance (ANOVA) for fresh properties of SCC

For the purpose of evaluating the effect of different parameters on fresh properties of SCC prepared with different binder types, w/b ratios and admixed with different concentrations of NaCl, the analysis of variance (ANOVA) calculation was carried out as per the guidelines presented by Hicks [130]. First, the fresh properties (slump flow spread, T_{50cm} flow time, V-funnel flow time, L-box passing ratio, and sieve segregation index) for three binders (OPC, PPC and OPC+20% FA) were considered as replicates. These replicate values of a given fresh property for three w/b ratios (0.37, 0.40 and 0.43) and four levels of admixed NaCl concentration (0%, 1%, 3% and 5%) were tabulated. The total sum of squares was then calculated, which is divided into the sum of squares (SS) of individual parameters (w/b ratio and admixed NaCl concentration) and that of the residual random error. After that, the mean squares (MS) of the parameters (w/b ratio and admixed NaCl concentration) were calculated by dividing their sum of squares by the corresponding associated degrees of freedom (df). The effect of individual parameters (w/b ratio and admixed NaCl concentration) on a given fresh property was then evaluated by testing the hypothesis of equality of variances, which is the test of null hypothesis or simply the significance test at a particular probability level. For determining this, the F-statistic, which is the ratio of mean squares of a parameter to the mean squares of the residual error was calculated and then compared with the tabulated F-values related to Fisher distribution. The

F-values related to Fisher distribution at a given probability level depend on the degrees of freedom of individual parameters and that of the residual error and are readily available in the relevant texts [130]. Subsequently, the obtained values of a given fresh property at three w/b ratios (0.37, 0.40 and 0.43) were considered as the replicates and the same procedure was followed to evaluate the effects of admixed NaCl concentration and binder type on that fresh property. Similarly, the obtained values of a given fresh property at four levels of admixed NaCl concentration (0%, 1%, 3% and 5%) were considered as the replicates and the same procedure was followed to evaluate the effects of binder type and w/b ratio on that fresh property. The aforementioned procedure was then used for all the obtained fresh properties of SCC mixes and the results of analysis of variance for slump flow spread, T_{50cm} flow time, V-funnel flow time, passing ratio and sieve segregation index are presented in Table 4.2 to Table 4.6, respectively.

Table 4.2 Results of analysis of variance (ANOVA) for slump flow spread of SCC mixes

Source	Level	Degree of freedom (df)	Sum of squares (SS)	Mean squares (MS)	F-ratio	'F' from Fisher's distribution at 99% probability
With binder type as replicates						
w/b ratio	3	2	6668.06	3334.03	6.43	5.39
Admixed NaCl concentration	4	3	2279.86	759.95	1.47	4.51
Error		30	15559.72	518.66		
Total		35	24507.64			
With w/b ratio as replicates						
Admixed NaCl concentration	4	3	2279.86	759.95	2.16	4.51
Binder type	3	2	11676.39	5838.19	16.60	5.39
Error		30	10551.39	351.71		
Total		35	24507.64			
With admixed NaCl concentration as replicates						
Binder type	3	2	11676.39	5838.19	29.37	5.36
w/b ratio	3	2	6668.06	3334.03	16.77	5.36
Error		31	6163.19	198.81		
Total		35	24507.64			

Table 4.3 Results of analysis of variance for T_{50cm} flow time of SCC mixes

Source	Level	Degree of freedom (df)	Sum of squares (SS)	Mean squares (MS)	F-ratio	'F' from Fisher's distribution at 99% probability
With binder type as replicates						
w/b ratio	3	2	0.043	0.022	0.54	5.39
Admixed NaCl concentration	4	3	0.230	0.077	1.92	4.51
Error		30	1.196	0.040		
Total		35	1.469			
With w/b ratio as replicates						
Admixed NaCl concentration	4	3	0.230	0.077	3.78	4.51
Binder type	3	2	0.630	0.315	15.53	5.39
Error		30	0.609	0.020		
Total		35	1.469			
With admixed NaCl concentration as replicates						
Binder type	3	2	0.630	0.315	12.28	5.36
w/b ratio	3	2	0.043	0.022	0.84	5.36
Error		31	0.795	0.026		
Total		35	1.47			

Table 4.4 Results of analysis of variance for V-funnel flow time of SCC mixes

Source	Level	Degree of freedom (df)	Sum of squares (SS)	Mean squares (MS)	F-ratio	'F' from Fisher's distribution at 99% probability
With binder type as replicates						
w/b ratio	3	2	0.35	0.17	0.64	5.39
Admixed NaCl concentration	4	3	1.08	0.36	1.31	4.51
Error		30	8.24	0.27		
Total			35	9.67		
With w/b ratio as replicates						
Admixed NaCl concentration	4	3	1.08	0.36	7.04	4.51
Binder type	3	2	7.05	3.53	69.01	5.39
Error		30	1.53	0.05		
Total		35	9.67			
With admixed NaCl concentration as replicates						
Binder type	3	2	7.05	3.53	48.31	5.36
w/b ratio	3	2	0.35	0.17	2.39	5.36
Error		31	2.26	0.07		
Total		35	9.67			

Table 4.5 Results of analysis of variance for L-box passing ratio of SCC mixes

Source	Level	Degree of freedom (df)	Sum of squares (SS)	Mean squares (MS)	F-ratio	'F' from Fisher's distribution at 99% probability
With binder type as replicates						
w/b ratio	3	2	0.01996	0.00998	9.31	5.39
Admixed NaCl concentration	4	3	0.00193	0.00064	0.60	4.51
Error		30	0.03213	0.00107		
Total		35	0.0540			
With w/b ratio as replicates						
Admixed NaCl concentration	4	3	0.00193	0.00064	0.75	4.51
Binder type	3	2	0.03	0.01	15.15	5.39
Error		30	0.02591	0.00086		
Total		35	0.0540			
With admixed NaCl concentration as replicates						
Binder type	3	2	0.02618	0.01309	51.39	5.36
w/b ratio	3	2	0.01996	0.00998	39.18	5.36
Error		31	0.00789	0.00025		
Total		35	0.0540			

Table 4.6 Results of analysis of variance for sieve segregation index of SCC mixes

Source	Level	Degree of freedom (df)	Sum of squares (SS)	Mean squares (MS)	F-ratio	'F' from Fisher's distribution at 99% probability
With binder type as replicates						
w/b ratio	3	2	29.50	14.75	4.73	5.39
Admixed NaCl concentration	4	3	8.80	2.93	0.94	4.51
Error		30	93.58	3.12		
Total		35	131.89			
With w/b ratio as replicates						
Admixed NaCl concentration	4	3	8.80	2.93	1.25	4.51
Binder type	3	2	52.73	26.37	11.24	5.39
Error		30	70.35	2.35		
Total		35	131.89			
With admixed NaCl concentration as replicates						
Binder type	3	2	52.73	26.37	16.46	5.36
w/b ratio	3	2	29.50	14.75	9.21	5.36
Error		31	49.66	1.60		
Total		35	131.89			

From Table 4.2, it is observed that both binder type and w/b ratio are affecting the slump flow spread of the SCC mixes as the estimated F-values are higher than the corresponding tabulated F-values at 99% confidence level. However, the binder type has significant effect on slump flow spread than w/b ratio as the estimated F-value for binder type is significantly higher than the tabulated F-value as evident from Table 4.2. Further, the admixed NaCl concentration has very less effect on slump flow spread of the SCC mixes as the estimated F-value for admixed NaCl concentration is less than the tabulated F-value at 99% confidence level.

From Tables 4.3 and 4.4, it is inferred that among all parameters binder type has greater effect on T_{50cm} and V-funnel flow times as the estimated F-values for binder type are significantly higher than the tabulated F-values at 99% confidence level. Further, w/b ratio and admixed NaCl concentration mostly have less effect on T_{50cm} and V-funnel flow times of the SCC mixes as the estimated F-values are less than the tabulated F-values at the same confidence level except in the case of w/b ratio as replicates for V-funnel flow time where the estimated F-value for admixed NaCl concentration is higher than the tabulated F-value at 99% confidence level as observed from Table 4.4.

From Tables 4.5 and 4.6, it is observed that that binder type has significant effect on passing ratio and segregation index of the SCC mixes followed by w/b ratio as the estimated F-values for binder type and w/b ratio are higher than the tabulated F-values (99% confidence level). However, admixed NaCl concentration has very less effect on passing ratio and segregation index as the estimated F-values were less than tabulated F-values at the same confidence level as evident from Tables 4.5 and 4.6. Overall among the three parameters, the binder type has more effect on the fresh properties of SCC mixes followed by w/b ratio. However, admixed NaCl concentration has very less effect on the fresh properties of SCC.

4.3 Compressive strength of SCC

The average compressive strength along with standard deviation of SCC mixes made with OPC, PPC and OPC+20% FA and admixed with different concentrations of NaCl (0%, 1%, 3% and 5%) for curing ages of 28 days, 90 days and 360 days are shown in Fig. 4.6 (a - c), Fig. 4.7 (a - c) and Fig. 4.8 (a - c) for w/b ratios of 0.37, 0.40 and 0.43, respectively. Similarly, the average compressive strength along with standard deviation of SCC mixes made with w/b ratio of 0.40 and admixed with NaCl concentrations of 7.5% and 12.5% are shown in Fig. 4.9 (a, b) for curing ages of 28 days and 360 days. Each value of compressive

strength shown in these figures is the average value of three replicate cube specimens. The standard deviation values of compressive strength are shown as error bars in these figures. From these figures, it is observed that the compressive strength of SCC mixes at the curing age of 28 days varied from 32.89 N/mm^2 to 50.81 N/mm^2 for OPC, 33.04 N/mm^2 to 41.04 N/mm^2 for PPC, and 31.56 N/mm^2 to 42.22 N/mm^2 for OPC+20% FA based SCC mixes irrespective of w/b ratio and admixed NaCl concentration. At the curing age of 90 days, the compressive strength of SCC mixes varied from 40 N/mm^2 to 54.52 N/mm^2, 44.74 N/mm^2 to 56.15 N/mm^2, and 37.93 N/mm^2 to 59.85 N/mm^2 for OPC, PPC, OPC+20% FA based SCC mixes respectively, irrespective of w/b ratio and admixed NaCl concentration. Similarly, at the curing age of 360 days, the compressive strength of SCC mixes varied from 46.52 N/mm^2 to 59.26 N/mm^2 for OPC, 45.78 N/mm^2 to 69.19 N/mm^2 for PPC, and 42.37 N/mm^2 to 62.89 N/mm^2 for OPC+20% FA based SCC mixes.

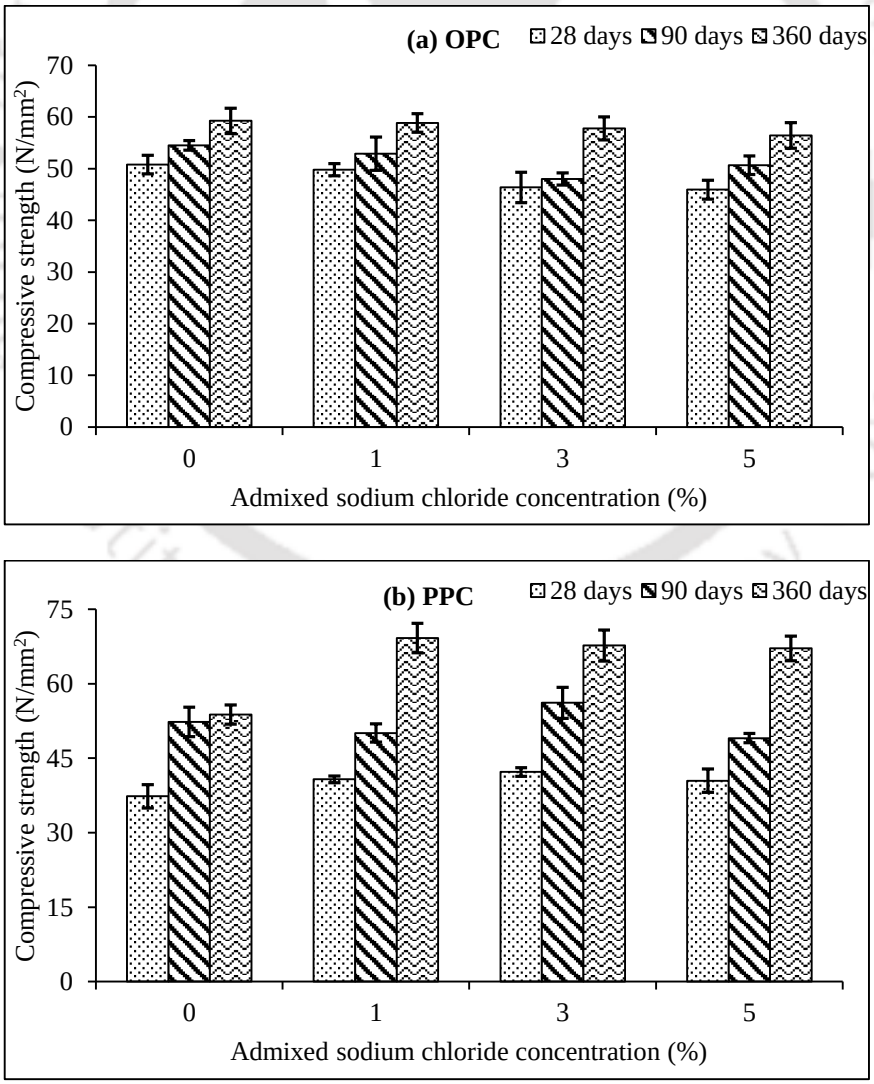

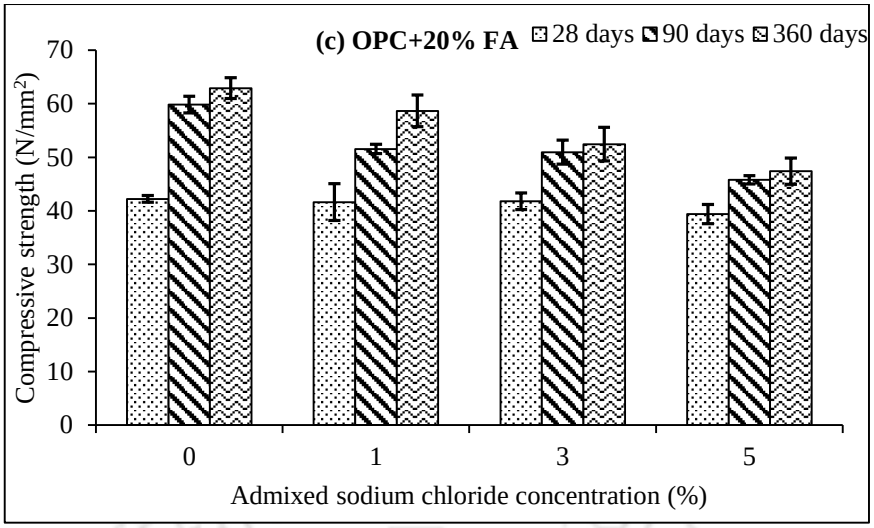

Fig. 4.6 Compressive strength of SCC mixes admixed with different concentrations of NaCl at w/b ratio of 0.37 for (a) OPC, (b) PPC, and (c) OPC+20% FA

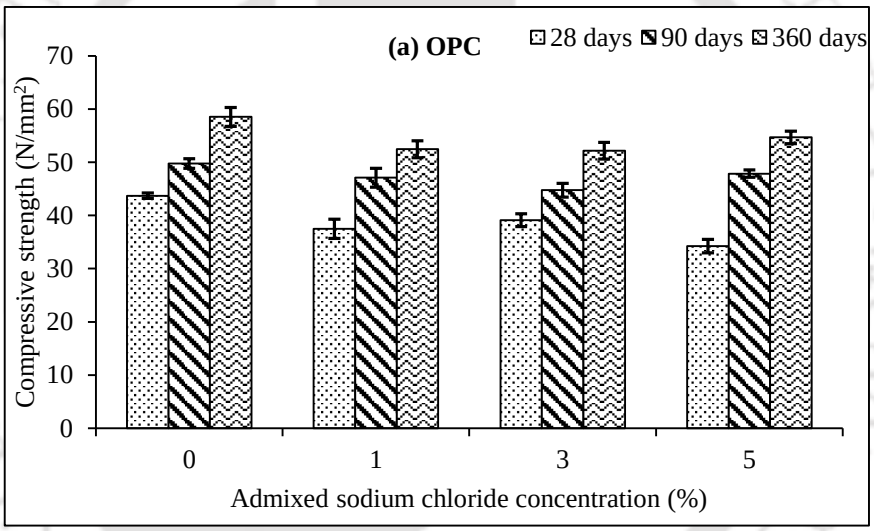

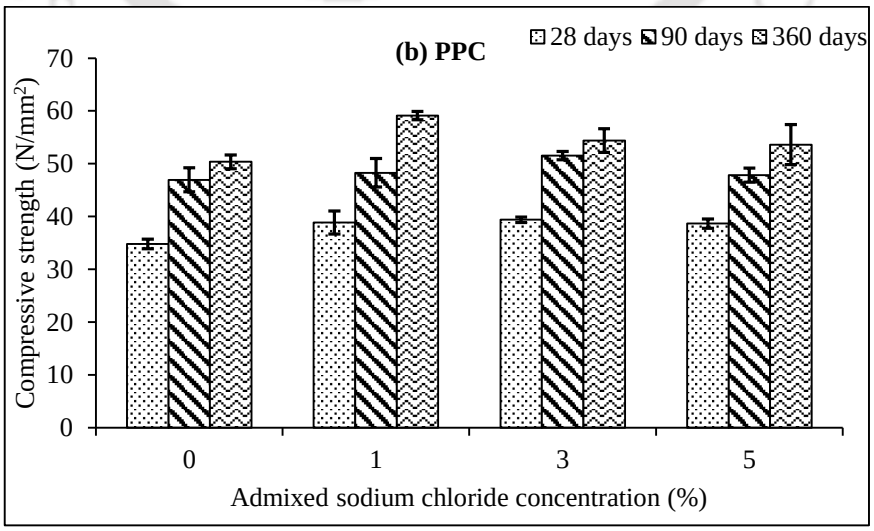

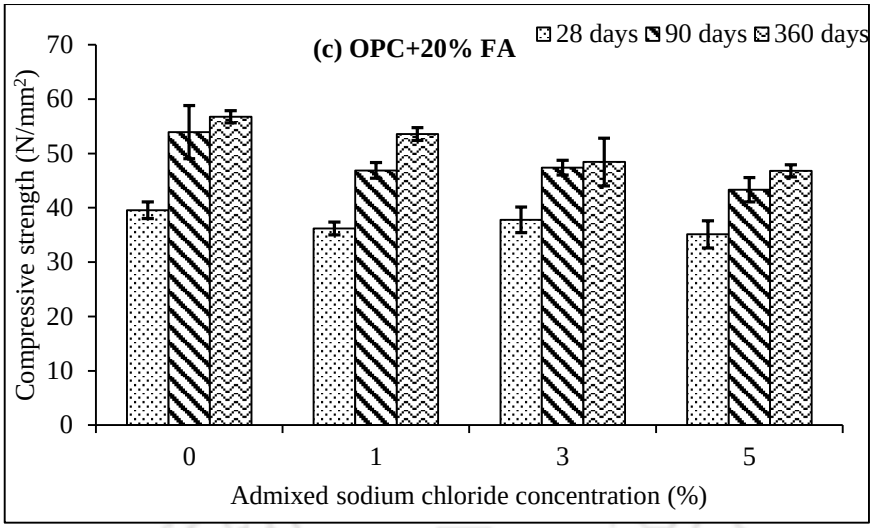

Fig. 4.7 Compressive strength of SCC mixes admixed with different concentrations of NaCl at w/b ratio of 0.40 for (a) OPC, (b) PPC, and (c) OPC+20% FA

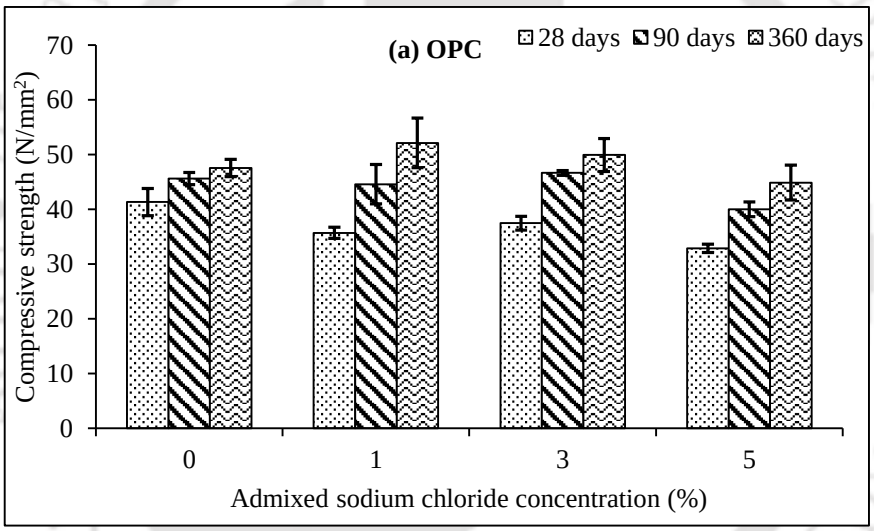

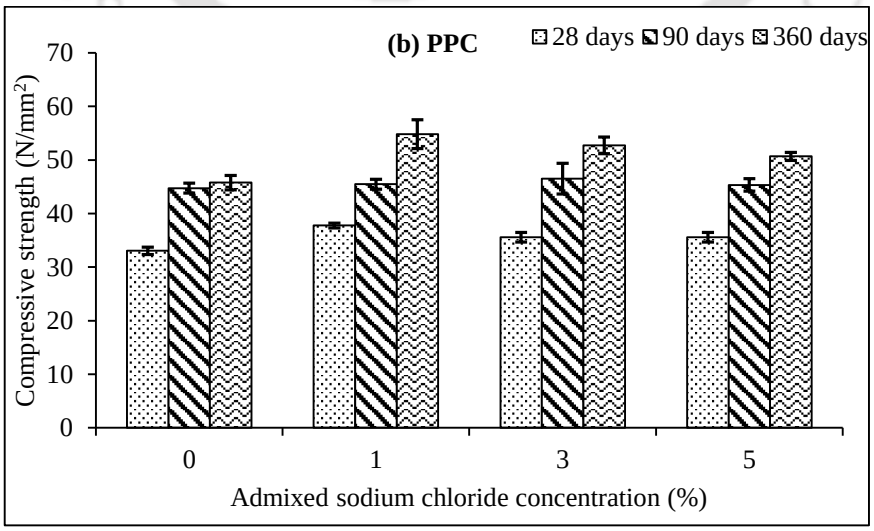

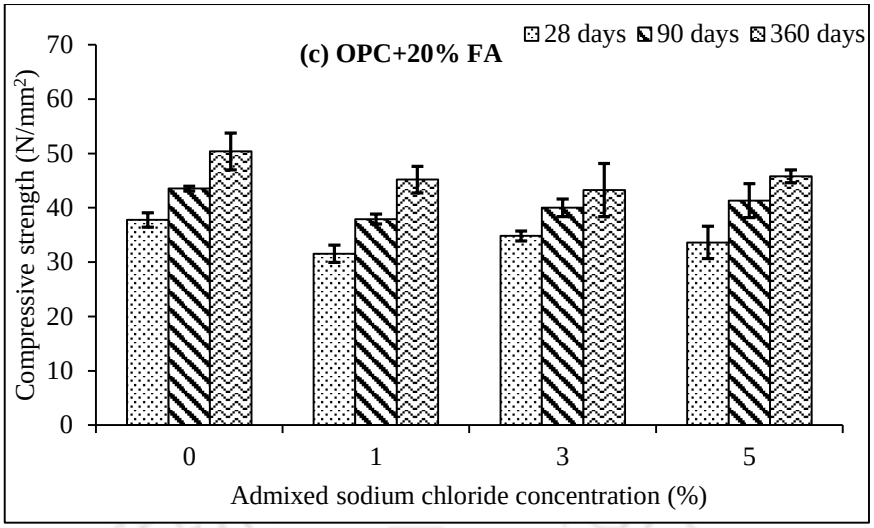

Fig. 4.8 Compressive strength of SCC mixes admixed with different concentrations of NaCl at w/b ratio of 0.43 for (a) OPC, (b) PPC, and (c) OPC+20% FA

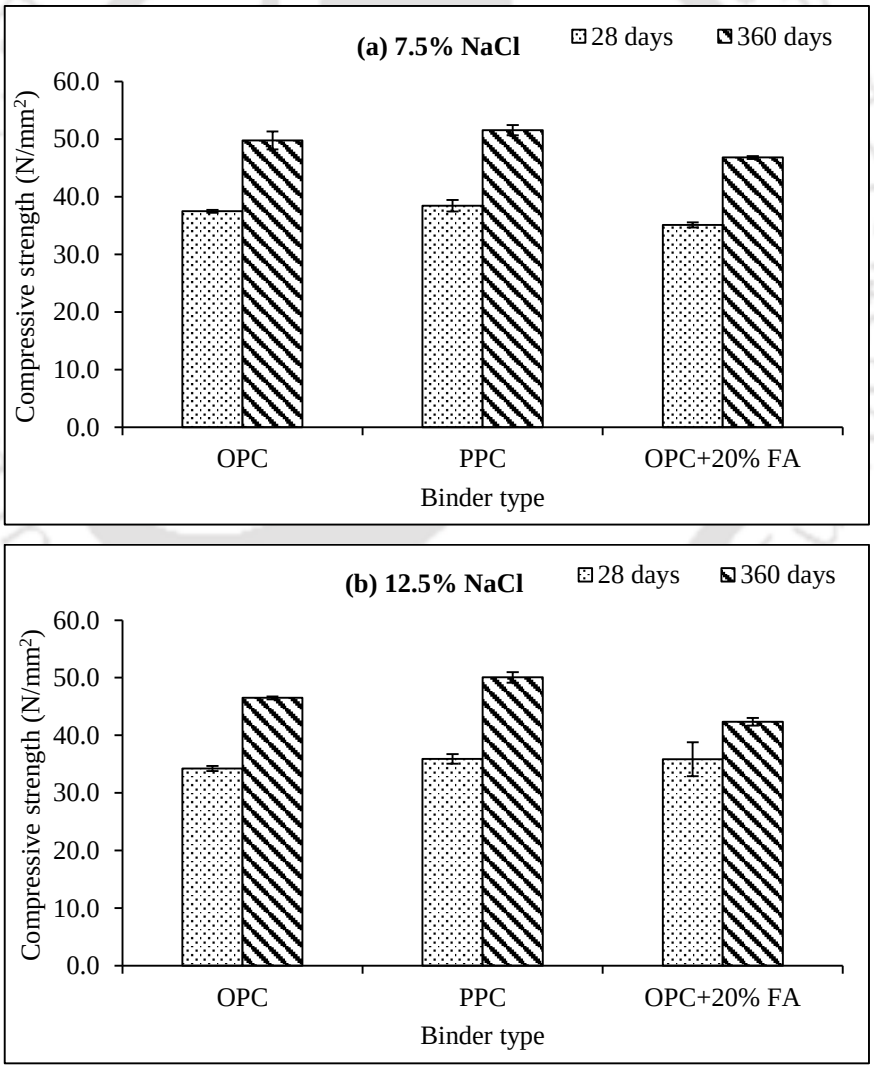

Fig. 4.9 Compressive strength of SCC mixes admixed with NaCl concentrations of (a) 7.5%, and (b) 12.5%, at w/b ratio of 0.40

4.3.1 Effect of binder type and admixed NaCl concentration on compressive strength of SCC

While evaluating the effect of binder type, it is observed that the SCC mixes made with OPC mostly exhibited higher compressive strength as compared to those made with OPC+20% FA followed by PPC at 0% admixed NaCl concentration at all w/b ratios (0.37, 0.40 and 0.43), and curing ages (28 days, 90 days and 360 days). However, in the case of SCC mixes admixed with NaCl (1%, 3%, and 5%), PPC mixes mostly showed higher compressive strength as compared to OPC followed by OPC+20% FA mixes at all curing ages and w/b ratios as observed from Fig. 4.6 (a - c) to Fig. 4.8 (a - c). The higher compressive strength of the SCC mixes made with OPC at 0% NaCl concentration may be attributed to the dominant effect of hydration reaction in OPC mixes as compared to the pozzolanic reaction in PPC and OPC+20% FA mixes.

The higher compressive strength of PPC based SCC mixes in the presence of NaCl may be attributed to the dominant effect of filling of pores in concrete with sufficient amount of primary ettringite and lower amount of calcium chloroaluminate (CCA) as compared to that in OPC and OPC+20% FA based SCC mixes. The primary ettringite is formed as a result of the reaction of gypsum with hydrated C_3A, whereas calcium chloroaluminate is formed by the reaction of chloride ions with hydrated C_3A in concrete. The lower compressive strength of OPC and OPC+20% FA based SCC mixes in the presence of chloride ions is attributed to the dominant effect of crystallization of CCA in the pores of concrete to a greater extent [129] than the pore filling effect of ettringite. The formation of ettringite (E) and calcium chloroaluminate in the SCC mixes is evident from the XRD patterns and FESEM images shown in Chapter 5. Further, the formation of lower amount of calcium chloroaluminate in PPC based SCC mixes as compared to that in OPC and OPC+20% FA based SCC mixes is substantiated with XRD results wherein the peak intensity and weight % of CCA were lower in PPC as compared to those of in OPC and OPC+20% FA based SCC mixes and there was no systematic variation in formation of ettringite with binder type in the SCC mixes (detailed discussion presented in Chapter 5).

From Fig. 4.6 to Fig. 4.8, it is observed that there is no systematic variation in compressive strength of SCC mixes with NaCl concentration (1%, 3% and 5%) for all binders, w/b ratios and curing ages except at the curing age of 360 days where SCC mix admixed with 5% NaCl showed lower compressive strength as compared to those admixed with 1% and 3% NaCl concentrations. The unsystematic variation in the compressive strength of SCC mixes

with admixed NaCl concentration may be attributed to the fact that the presence of chloride ions in different concentrations might have altered the extent of hydration and pozzolanic reactions in the SCC mixes. Also the variations in filling of pores in concrete with ettringite and calcium chloroaluminate at different concentrations of admixed NaCl might have affected the compressive strength of SCC mixes at different curing ages. At the curing age of 360 days, the lower compressive strength of SCC mixes admixed with 5% NaCl concentration may be attributed to the dominant effect of crystallization of calcium chloroaluminate in the pores of concrete to a greater extent. Similarly, the compressive strength of SCC mixes admixed with NaCl concentrations of 7.5% and 12.5% showed lower compressive strength as compared to that admixed with 5% NaCl concentration for all binders as observed from Fig. 4.9.

4.3.2 Effect of curing age on compressive strength of SCC

While analyzing the effect of curing age, it is observed that compressive strength of all the SCC mixes increased with increase in curing age irrespective of binder type, w/b ratio and admixed NaCl concentration, as evident from Fig. 4.6 to Fig. 4.9. This is attributed to the formation of denser microstructure in the concrete due to the production of more amount of C-S-H gel with curing age as a result of continued hydration reaction in OPC based SCC mixes and due to the dominant effect of pozzolanic reaction in PPC and OPC+20% FA based SCC mixes. The average increase in compressive strength at the longer curing ages of 90 days and 360 days with respect to 28 days are in the range of 15.84% to 32.71% for the SCC mixes prepared with OPC, 29.67% to 49.54% for SCC mixes prepared with PPC, and 23.39% to 35.74% for the SCC mixes prepared with OPC+20% FA, irrespective of w/b ratio and admixed NaCl concentration. The higher rate of increase in compressive strength with curing age in PPC and OPC+20% FA based SCC mixes than that in OPC based SCC mixes is attributed to the dominant effect of pozzolanic reaction in PPC and OPC+20% FA concrete mixes.

4.3.3 Effect of water-to-binder (w/b) ratio on compressive strength of SCC

From the compressive strength values shown in Fig. 4.6 to Fig. 4.8, it is observed that SCC specimens made with the w/b ratio of 0.37 exhibited higher compressive strength as compared to those made with the w/b ratio of 0.40 followed by 0.43 for all binders, admixed NaCl concentrations and curing ages. The higher compressive strength of the SCC mixes made with lower w/b ratio is attributed to the formation of denser microstructure due to the

production of more amount of C-S-H gel in concrete. Overall, the SCC mixes made with w/b ratios of 0.37 and 0.40 showed an average increase of 20.50% and 10.14%, respectively in the compressive strength as compared to those made with w/b ratio of 0.43, irrespective of binder type, admixed NaCl concentration and curing age.

4.3.4 Analysis of variance (ANOVA) for compressive strength of SCC

For evaluating the effect of different parameters on compressive strength of SCC, the analysis of variance (ANOVA) calculation was carried out as per the guidelines presented by Hicks [130]. The compressive strength values of three replicate cubes from each SCC mix for three types of binder (OPC, PPC, and OPC+20% FA), three w/b ratios (0.37, 0.40 and 0.43), four levels of admixed NaCl concentration (0%, 1%, 3% and 5%) and three curing ages (28 days, 90 days and 365 days) were arranged in a tabular form. The sum of squares (SS), mean squares (MS) and F-statistic of individual parameters were calculated in the same manner as calculated in case of fresh properties of SCC (Section 4.2.4). The estimated F-value of individual parameters was compared with the tabulated F-values related to Fisher distribution at a given probability level. The results of analysis of variance for compressive strength of SCC mixes are presented in Table 4.7.

From Table 4.7, it is observed that all the parameters i.e. binder type, w/b ratio, admixed NaCl concentration and curing age are affecting the compressive strength of SCC mixes as the estimated F-values corresponding to these parameters are higher than the tabulated F-values at 99% confidence level. Further, among these parameters, curing age has more significant effect on compressive strength of SCC mixes as compared to other parameters as estimated F-value for curing age is significantly higher than the tabulated F-value at 99% confidence level as evident from Table 4.7. After curing age, w/b ratio has significant effect on compressive strength of SCC mixes followed by binder type. Further, admixed NaCl concentrations has comparatively less effect on compressive strength of SCC mixes as compared to other parameters, as the estimated F-value is slightly higher than the tabulated F-value as evident from Table 4.7.

Table 4.7 Results of analysis of variance for compressive strength of SCC mixes

Source	Level	Degree of freedom (df)	Sum of squares (SS)	Mean squares (MS)	F-ratio	'F' from Fisher's distribution at 99% probability
Binder type	3	2	737.75	368.88	13.06	4.67
w/b ratio	3	2	4078.42	2039.21	72.19	4.67
Admixed NaCl concentration	4	3	636.46	212.15	7.51	3.84
Curing age	3	2	13909.45	6954.72	246.20	4.67
Error		314	8870.02	28.25		
Total		323	28232.10			

4.4 Variation in Ca/Si ratio with calcium hydroxide content in SCC

Typical plots of EDX analysis of SCC mixes made with OPC, PPC and OPC+20% FA at w/b ratio of 0.40 are shown in Fig. 4.10 and Fig. 4.11 for 0% and 3% admixed NaCl concentrations respectively, at the curing age of 28 days. The remaining plots of EDX analysis of SCC mixes are presented in Appendix A. The weight % of different elements such as O, Ca, Si, Al, Fe, Na, Mg, K, S, and Cl present in the SCC mixes are shown in these figures. The Ca/Si ratio of C-S-H calculated from EDX analysis and the compressive strength of SCC mixes are plotted against the curing age and are shown in Fig. 4.12 to Fig. 4.14. From these figures, it is inferred that both the Ca/Si ratio and compressive strength increased with curing age for OPC based SCC mixes at different concentrations of admixed NaCl. However, in the the case of PPC and OPC+20% FA based SCC mixes, the compressive strength increased whereas the Ca/Si ratio decreased with increase in curing age. In OPC based SCC mixes, the increase in Ca/Si ratio with curing age is attributed to the availability of the higher amount of calcium hydroxide due to its production as a result of continued hydration reaction in OPC concrete. In case of PPC and OPC+20% FA based SCC mixes, the decrease in Ca/Si ratio with curing age is attributed to the consumption of calcium hydroxide in the pozzolanic reaction that continued with the curing age of concrete.

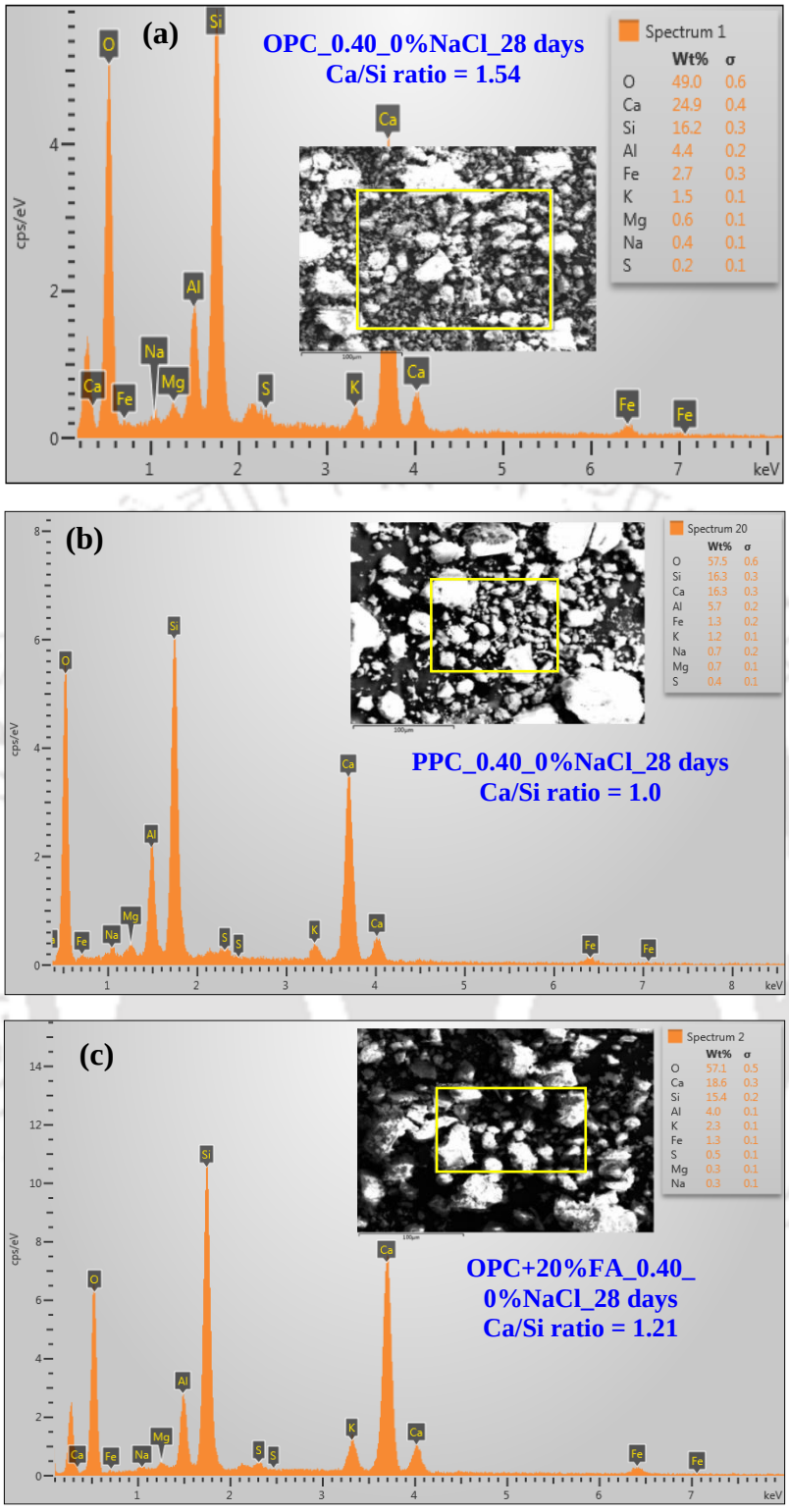

Fig. 4.10 EDX analysis of SCC mixes admixed with 0% NaCl concentration at w/b ratio of 0.40 and curing age of 28 days: (a) OPC, (b) PPC, and (c) OPC+20% FA

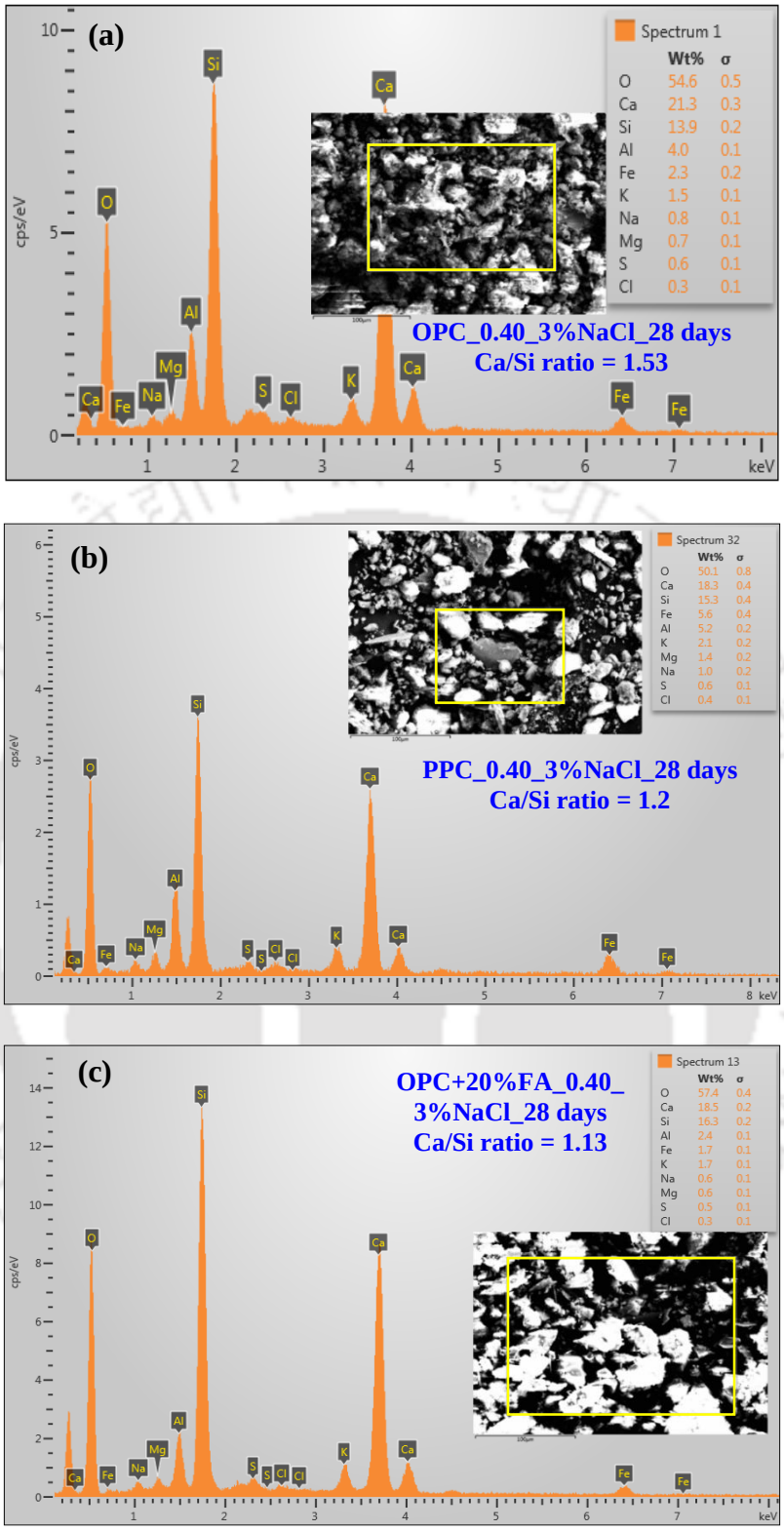

Fig. 4.11 EDX analysis of SCC mixes admixed with 3% NaCl concentration at w/b ratio of 0.40 and curing age of 28 days: (a) OPC, (b) PPC, and (c) OPC+20% FA

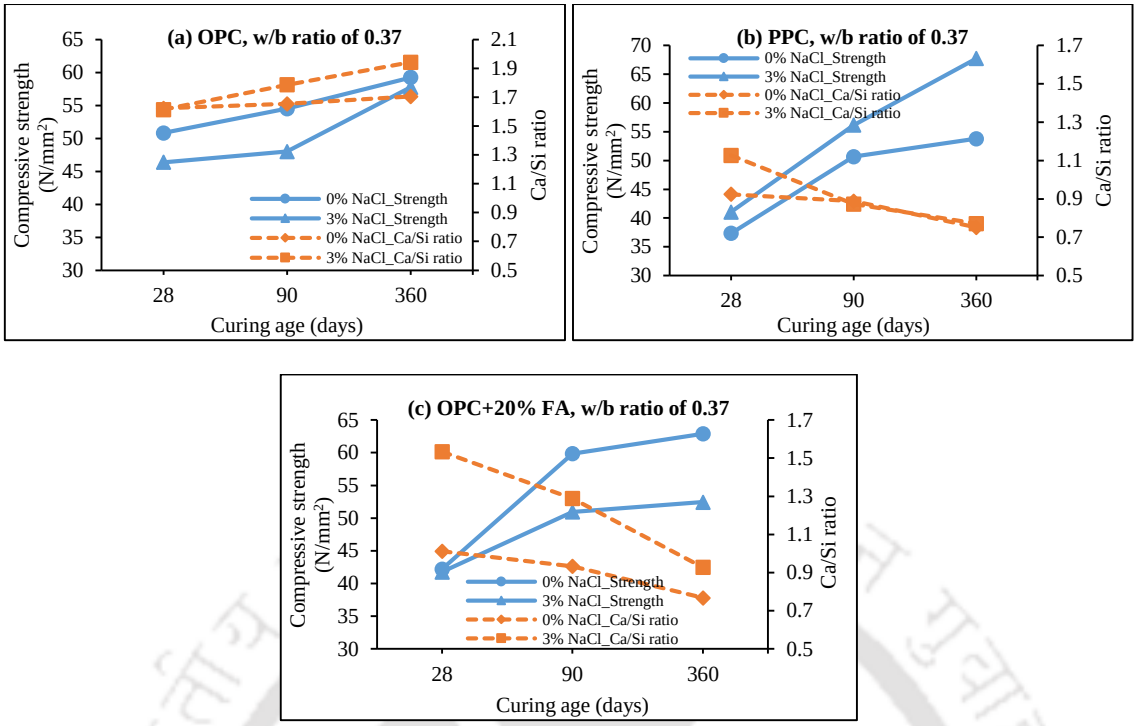

Fig. 4.12 Variations in compressive strength and Ca/Si ratio with curing age for SCC mixes admixed with different concentrations of NaCl at w/b ratio of 0.37: (a) OPC, (b) PPC, and (c) OPC+20% FA

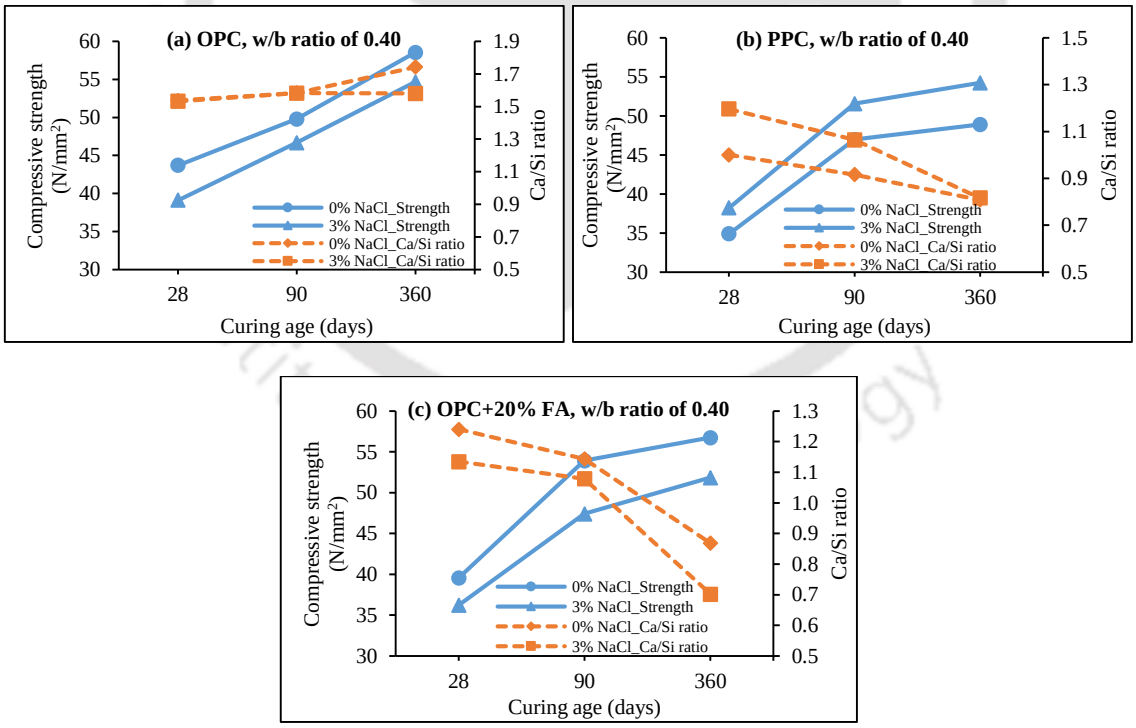

Fig. 4.13 Variations in compressive strength and Ca/Si ratio with curing age for SCC mixes admixed with different concentrations of NaCl at w/b ratio of 0.40: (a) OPC, (b) PPC, and (c) OPC+20% FA

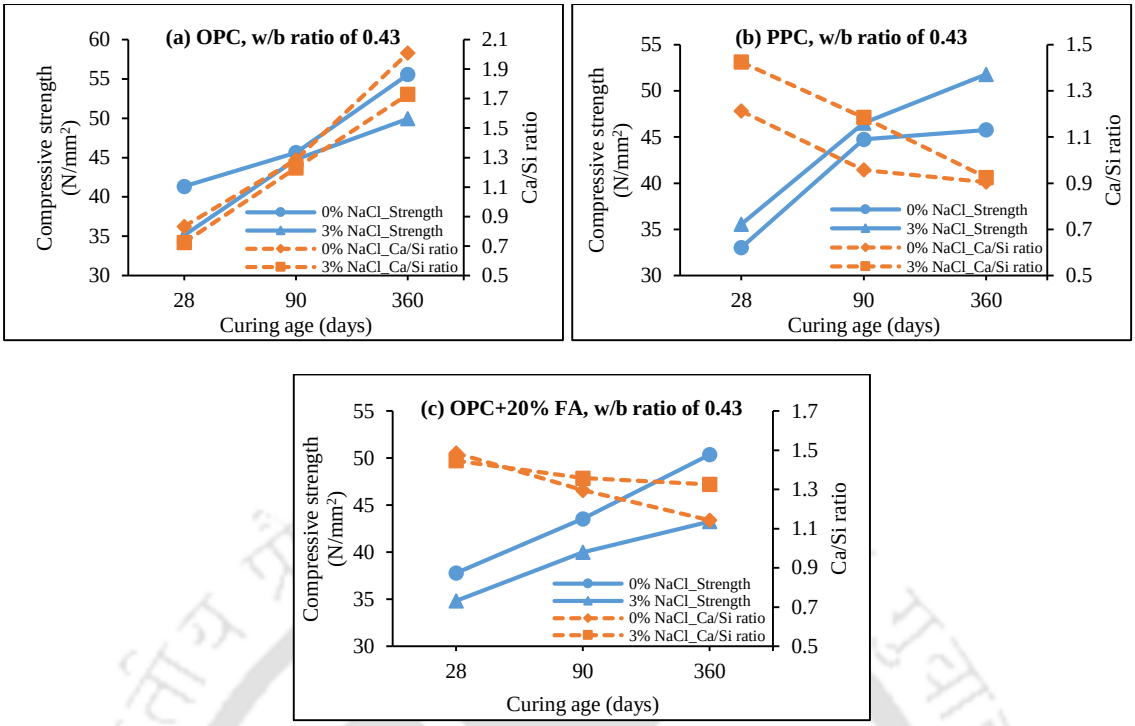

Fig. 4.14 Variations in compressive strength and Ca/Si ratio with curing age for SCC mixes admixed with different concentrations of NaCl at w/b ratio of 0.43: (a) OPC, (b) PPC, and (c) OPC+20% FA

4.5 Cost analysis

In the present study, the cost analysis was carried out to compare the cost of producing 1 m^3 of SCC mix from OPC, PPC and OPC+20% FA at w/b ratios of 0.37, 0.40 and 0.43. In the calculations, the cost of handling, transportation and placement were not considered. Similarly, the cost of water and fly ash were considered as zero as these materials were available free of cost. Further, sodium chloride was also not considered in the calculation of cost. By using the prices of materials as per the local market, the materials cost of producing 1 m^3 of SCC mix for different types of binder and w/b ratio are presented in Table 4.8. From this table, it is observed that the materials cost of producing 1 m^3 of SCC mix is lower for OPC+20% FA as compared to OPC followed by PPC. Further, the materials cost of producing 1 m^3 of SCC mix increased with decrease in w/b ratio, which is due to the use of higher quantities of binder and superplasticizer at lower w/b ratio.

Table 4.8 Materials cost of producing 1 m^3 of SCC mix from OPC, PPC and OPC+20% FA

Mix parameters		**OPC**						
		Quantity (kg/m^3)			Unit cost	Amount in Rs.		
w/b ratio		0.37	0.40	0.43	(Rs./kg)	0.37	0.40	0.43
Cement		527.03	487.50	453.49	7.70	4058	3754	3492
Fly ash		0.00	0.00	0.00	0.00	0	0	0
Water		195.00	195.00	195.00	0.00	0	0	0
Fine aggregate		786.08	786.08	786.08	0.99	776	776	776
Coarse aggregate	10 mm MSA	377.63	377.63	377.63	1.26	475	475	475
	20 mm MSA	377.63	377.63	377.63	1.70	642	642	642
Superplasticizer		4.22	3.90	3.63	132.08	557	515	479
Mix parameters		**Total amount (Rs.)**				6508	6162	5864
		PPC						
Cement		527.03	487.50	453.49	8.10	4269	3949	3673
Fly ash		0.00	0.00	0.00	0.00	0	0	0
Water		195.00	195.00	195.00	0.00	0	0	0
Fine aggregate		786.08	786.08	786.08	0.99	776	776	776
Coarse aggregate	10 mm MSA	377.63	377.63	377.63	1.26	475	475	475
	20 mm MSA	377.63	377.63	377.63	1.70	642	642	642
Superplasticizer		3.69	3.41	3.17	132.08	487	451	419
Mix parameters		**Total amount (Rs.)**				6649	6293	5986
		OPC+20% FA						
Cement		421.62	390.00	362.79	7.70	3246	3003	2793
Fly ash		105.41	97.50	90.70	0.00	0	0	0
Water		195.00	195.00	195.00	0.00	0	0	0
Fine aggregate		786.08	786.08	786.08	0.99	776	776	776
Coarse aggregate	10 mm MSA	377.63	377.63	377.63	1.26	475	475	475
	20 mm MSA	377.63	377.63	377.63	1.70	642	642	642
Superplasticizer		3.16	2.93	2.72	132.08	418	386	359
		Total amount (Rs.)				5557	5282	5046

Keeping in view the different values of compressive strength of SCC obtained at the curing age of 28 days for different types of binder and w/b ratio, the materials cost alone for producing 1 m^3 of SCC mix may not provide a comprehensive cost comparison of the mixes. Thus, the materials cost of producing 1 m^3 of SCC mix per unit 28 days compressive

strength was calculated [53] for different types of binder and w/b ratio and the calculated values are shown in Fig. 4.15. From this figure, it is observed that materials cost of 1 m^3 of SCC mix per unit 28 days compressive strength is again lower for OPC+20% FA as compared to OPC followed by PPC. This indicates that the variation in compressive strength of SCC with binder type did not have any effect on materials cost of SCC. However, the materials cost of 1 m^3 of SCC mix per unit 28 days compressive strength decreased slightly with decrease in w/b ratio as evident from Fig. 4.15. This is attributed to the effect of increase in compressive strength of SCC due to decrease in w/b ratio.

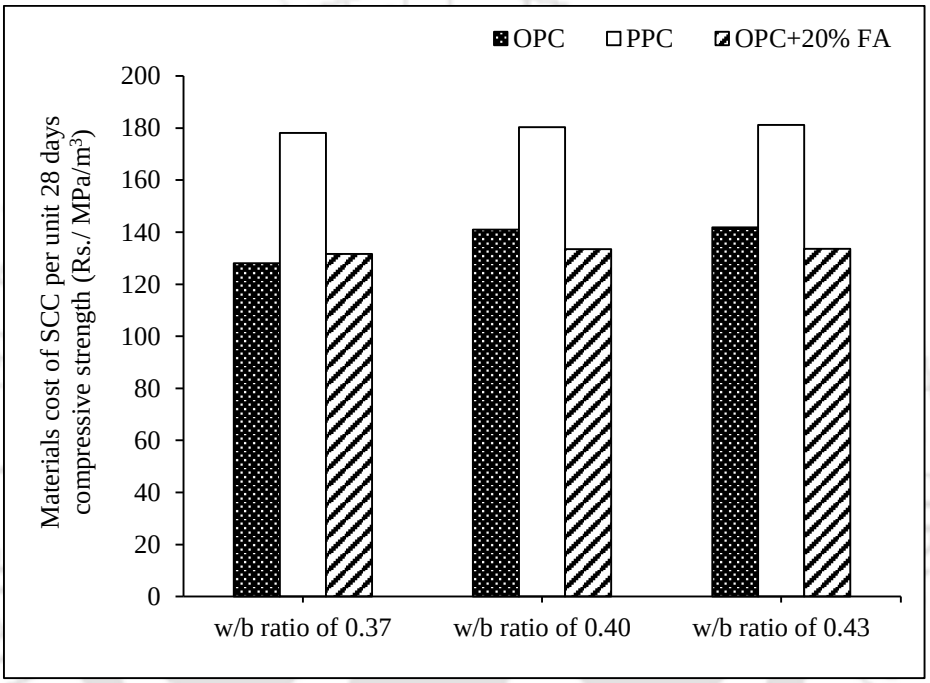

Fig. 4.15 Materials cost of SCC per unit 28 days compressive strength for OPC, PPC, and OPC+20% FA

4.6 Summary

The obtained results of fresh properties indicate that all the SCC mixes (all binders, w/b ratios and admixed NaCl concentrations) satisfied the acceptance criteria with respect to filling ability, passing ability and segregation resistance as per EFNARC guidelines. The SCC mixes made with PPC exhibited higher slump flow spread, T_{50cm} flow time, V-funnel flow time, L-box passing ratio, and lower segregation index as compared to those made with OPC+20% FA followed by OPC based SCC mixes. Further, slump flow spread, and passing ratio increased whereas segregation index decreased with decrease in the w/b ratio of SCC mixes. However, there was no systematic variation in T_{50cm} and V-funnel flow times

with w/b ratio at different concentrations of admixed NaCl. In addition, the variations in slump flow spread, T_{50cm} flow time, V-funnel flow time, passing ratio, and segregation index of SCC mixes were not systematic with NaCl concentration at lower w/b ratio. However, at higher w/b ratio, the variations in these parameters with admixed NaCl concentration were systematic, although the difference in the values of these parameters among different concentrations of admixed NaCl was very less. From analysis of variance (ANOVA) calculations, it is observed that binder type has significant effect on the fresh properties of SCC mixes followed by w/b ratio whereas admixed NaCl concentration has very less effect on the fresh properties of SCC.

From the obtained results of compressive strength, it is observed that at 0% admixed NaCl concentration the SCC mixes made with OPC exhibited higher compressive strength as compared to those made with OPC+20% FA and PPC at all w/b ratios and curing ages. However, in case of SCC mixes admixed with NaCl, PPC based SCC mixes showed higher compressive strength as compared to OPC and OPC+20% FA based SCC mixes at all curing ages and w/b ratios. While analyzing the rate of increase of compressive strength with curing age, it is observed that SCC mixes made with PPC and OPC+20% FA showed higher increase in compressive strength as compared to those made with OPC. From analysis of variance calculations, it is observed that curing age has more significant effect on compressive strength of SCC mixes followed by w/b ratio and binder type. Further, admixed NaCl concentrations has comparatively less effect on compressive strength of SCC mixes as compared to other parameters. The Ca/Si ratio of C-S-H obtained from EDX analysis in OPC based SCC mixes increased whereas it decreased in PPC and OPC+20% FA based SCC mixes with curing age, which is consistent with the compressive strength development of SCC with curing age in OPC, PPC, and OPC+20% FA based SCC mixes. From the cost analysis, it is observed that both the materials cost of producing 1 m^3 of SCC mix and that of producing 1 m^3 of SCC mix per unit 28 days compressive strength were lower for OPC+20% FA as compared to OPC followed by PPC. Similarly, the materials cost of producing 1 m^3 of SCC mix increased with decrease in w/b ratio, whereas the materials cost of 1 m^3 of SCC mix per unit 28 days compressive strength decreased slightly with decrease in w/b ratio.

CHAPTER 5

MICROSTRUCTURE CHARACTERIZATION AND CHLORIDE ANALYSIS OF SCC

5.1 General

This chapter presents the results of microstructure study, thermal behaviour, and chloride analysis of self-compacting concrete (SCC) made with different types of binder, w/b ratio and admixed with chloride ions. After the completion of compressive strength test at the curing ages of 28 days, 90 days and 360 days, the collected concrete powder samples were used for analyzing the microstructure of concrete by various techniques such as X-ray diffraction (XRD) analysis, field emission scanning electron microscopy (FESEM) and Fourier transform infrared (FTIR) spectroscopy. In addition, the thermo-gravimetry analysis (TGA) with derivative thermo-gravimetry (DTG) was conducted on the concrete powder samples to evaluate the thermal behaviour of SCC as well as to quantify the amount of calcium hydroxide. Further, from the XRD patterns, the semi-quantification analysis using RIR (reference intensity ratio) method was used to quantify the compounds formed in concrete. The variations in chloride binding in SCC as indicated by free and total chloride concentrations as well as the obtained results of pH of SCC mixes are analyzed and discussed.

5.2 X-ray diffraction (XRD) analysis

The XRD analysis was performed on all the SCC mixes made with and without admixed NaCl to identify the phase composition of hardened concrete at the curing ages of 28 days, 90 days and 360 days. The XRD patterns of OPC based SCC mixes admixed with 0% NaCl (control mix) at the curing ages of 28 days, 90 days and 360 days are shown in Fig. 5.1 (a), Fig. 5.1 (b), and Fig. 5.1 (c) for w/b ratios of 0.37, 0.40 and 0.43, respectively. Similarly, the XRD patterns of the SCC mixes prepared from PPC and OPC+20% FA for 0% NaCl are shown in Fig. 5.2 (a - c) and Fig. 5.3 (a - c), respectively. Further, the XRD patterns of OPC, PPC and OPC+20% FA based SCC mixes admixed with 3% NaCl at curing ages of 28, 90 and 360 days are shown in Fig. 5.4 (a - c), Fig. 5.5 (a - c), and Fig. 5.6 (a - c), respectively. The XRD patterns of SCC admixed with 7.5% and 12.5% NaCl are shown in Fig. 5.7 (a), Fig. 5.7 (b) and Fig. 5.7 (c) for OPC, PPC and OPC+20% FA, respectively at the w/b ratio of 0.40. The XRD patterns of OPC, PPC and OPC+20% FA based SCC mixes

admixed with 1% NaCl and 5% NaCl at the w/b ratio of 0.37, 0.40 and 0.43 are shown in Fig. B1 to Fig. B3 (in Appendix B) for the curing ages of 28, 90 and 360 days.

As mentioned in Chapter 3, the phase compositions of SCC mixes were identified using the PDF2 reference library (ICDD) and PANalytical X'Pert HighScore Plus software. From ICDD reference library, six compounds were identified for the SCC mixes, which are shown in Table 5.1.

Table 5.1 Information of compounds from the PDF2 reference library of ICDD

Ref. Code	Compound Name	Chemical Formula	RIR
00-046-1045	Quartz (Q)	SiO_2	3.41
00-004-0733	Portlandite (CH)	$Ca(OH)_2$	1.40
01-072-0646	Ettringite (E)	$Ca_6(Al(OH)_6)_2(SO_4)_3(H_2O)_{26}$	1.61
00-021-0816	Gypsum (G)	$CaSO_4.2H_2O$	1.70
00-005-0586	Calcite (CC)	$CaCO_3$	2.00
01-078-1219	Calcium aluminum chloride hydroxide hydrate (Friedel's salt: CCA)	$Ca_2Al(OH)_6Cl(H_2O)_2$	1.36

As stated in Chapter 3, the weight percentage (wt. %) of each compound was calculated semi-quantitatively using the normalized reference intensity ratio (RIR) matrix-flushing method. The value of different compounds calculated by RIR method is near to unit weight percentage and the sum of the values of compounds is equal to 100% ± 1%. The results of wt. % of different compounds obtained by semi-quantification analysis using the RIR method for OPC, PPC and OPC+20% FA based SCC mixes admixed with 0% NaCl at the curing ages of 28 days, 90 days and 360 days are shown in Fig. 5.8 (a), Fig. 5.8 (b) and Fig. 5.8 (c) for w/b ratio of 0.37, 0.40 and 0.43, respectively. Similarly, the results of wt. % of different compounds of SCC mixes admixed with NaCl concentrations of 1%, 3% and 5% are shown in Fig. 5.9 (a - c), Fig. 5.10 (a - c) and Fig. 5.11 (a - c), respectively. Further, the wt. % of compounds from the XRD patterns using RIR method for OPC, PPC and OPC+20% FA based SCC mixes at the w/b ratio of 0.40 and admixed with 7.5% and 12.5% NaCl concentrations are shown in Fig. 5.12 (a) and Fig. 5.12 (b), respectively.

In the XRD patterns shown in Fig. 5.4 (a - c) to Fig. 5.7 (a - c), the calcium chloroaluminate (CCA) peaks in SCC mixes were found at 11.2° 2θ and 23.2° 2θ. The calcium chloroaluminate (Friedel's salt) is formed in concrete due to the reaction of chloride ions

with the hydrated C_3A. The XRD patterns of control SCC mixes (0% NaCl) did not show any peak of CCA for all types of binder as observed from Fig. 5.1 (a - c) to Fig. 5.3 (a - c). The peak intensity of CCA was more in the SCC mixes made with OPC+20% FA as compared to those made from OPC and PPC at all concentrations of admixed NaCl and w/b ratios for all the curing ages as observed from Fig. 5.4 to Fig. 5.7. The same variation is also obtained from the semi-quantitative results (wt. %) shown in Fig. 5.9 to Fig. 5.12 for NaCl admixed SCC mixes for all the binders. The CCA content (wt. %) varied from 2% to 19% in OPC+20% FA, 2% to 16% in OPC, and 1% to 13% in PPC based SCC mixes irrespective of w/b ratio, admixed NaCl concentration and curing age. The formation of higher amount of CCA in OPC+20% FA based SCC mixes as compared to that in OPC followed by PPC based SCC mixes may be attributed to the reaction of chloride ions with Al_2O_3 to a greater extent in OPC+20% FA mix as compared to that in OPC and PPC mixes [126,131]. It may be noted that the wt. % of Al_2O_3 in fly ash was higher as compared to that in OPC followed by PPC as observed from Table 3.1 (Chapter 3).

In all types of binder, the SCC mixes admixed with 5% NaCl showed higher peak intensity of CCA as compared to 3% NaCl followed by 1% NaCl at all w/b ratios and curing ages as observed from Fig. 5.4 to Fig. 5.6 and Fig. B1 to Fig. B3 (in Appendix B). In addition, the SCC mixes admixed with 12.5% NaCl showed higher peak intensity of CCA as compared to 7.5% NaCl concentration as observed from Fig. 5.7. The same variation in CCA content with the increase in NaCl concentration is also obtained from the results of semi-quantification analysis using RIR method shown in Fig. 5.9 to Fig. 5.12. This may be attributed to the binding of chloride ions with hydrated C_3A to a greater extent in the case of SCC mixes admixed with higher concentration of NaCl. While analyzing the effect of w/b ratio on formation of CCA, it is observed that the peak intensity of CCA increased with increase in w/b ratio (Fig. 5.4 to Fig. 5.6). The same variation was also observed from the results of semi-quantification analysis using RIR method shown in Fig. 5.9 to Fig. 5.12. Although the C_3A content in the concrete made with higher w/b ratio is less (because of lower binder content) as compared to that made with lower w/b ratio, the increase in CCA content with increase in w/b ratio may be attributed to the complexity of the chloroaluminate formation mechanism, which is not only the function C_3A content but may also be affected by the pore structure of concrete, which varies with w/b ratio, and also by the pore solution chemistry that may influence the chloroaluminate solubility [132]. From the XRD patterns, it is observed that there is no systematic variation in peak intensity and

wt. % of CCA with curing age in all the SCC mixes as observed from Fig. 5.4 (a - c) to Fig. 5.7 (a - c) and Fig. 5.9 (a - c) to Fig. 5.12 (a - c).

The peaks of calcium hydroxide (portlandite, CH) in the XRD patterns were found at 18.1° 2θ, 34.1° 2θ, 36.55° 2θ, and 47.2° 2θ. From the XRD patterns (Fig. 5.1 to Fig. 5.7), it is observed that the peak intensity of CH was less in PPC and OPC+20% FA based SCC mixes as compared to that in OPC based SCC mixes at all w/b ratios, curing cuing ages and for all concentrations of admixed NaCl including the control mix. The same variation is also obtained from the semi-quantitative results (wt. %) shown in Fig. 5.8 to Fig. 5.12. The wt. % of CH varied from 19% to 46% in OPC, from 1% to 17% in PPC, and from 6% to 25% in OPC+20% FA based SCC mixes irrespective of w/b ratio, admixed NaCl concentration and curing age. The lower CH content in PPC and OPC+20% FA based SCC mixes is attributed to the consumption of calcium hydroxide in the pozzolanic reaction. Further from XRD patterns and semi-quantitative results (wt. %), it is observed that the SCC mixes made with 0% NaCl (control mix) showed higher CH content as compared to NaCl admixed SCC mixes for all binders, w/b ratios and curing ages. The lower CH content in NaCl admixed SCC mixes may be attributed to its leaching in the presence of chloride ions.

While comparing the effect of w/b ratio, it is observed that the wt. % of CH was mostly higher in the SCC mixes made with lower w/b ratio (0.37) as compared to those made with higher w/b ratio (0.40 and 0.43) in control mix (0% NaCl), which may be attributed to the formation of higher amount of CH in the hydration reaction at lower w/b ratio due to higher binder content. However, there was no systematic variation in wt. % of CH in the SCC mixes admixed with different concentrations of NaCl, which may be attributed to the effect of chloride ions affecting the hydration and pozzolanic reactions and also due to the variations in the leaching of CH at different w/b ratios in the presence of chloride ions.

From the XRD patterns, it can be clearly seen that the peak intensity of CH increased with curing age in the SCC mixes made with OPC, whereas that deceased with curing age in the SCC mixes made with PPC and OPC+20% FA. This is due to the release of CH from hydration reaction with curing age in the OPC based SCC mixes and consumption of CH in the pozzolanic reaction with curing age in the PPC and OPC+20% FA based SCC mixes. These variations in calcium hydroxide content of SCC mixes with curing age are consistent with the variation in Ca/Si ratio of C-S-H estimated from EDX analysis (presented in Section 4.4, Chapter 4) wherein the Ca/Si ratio the increase in curing age for OPC based

SCC mixes whereas it decreased with increase in curing age for PPC and OPC+20% FA based SCC mixes.

From the obtained results of semi-quantification analysis using RIR method, it is also observed that CH content (wt. %) increased from 27% to 46% in OPC based SCC mixes, whereas in PPC and OPC+20% FA based SCC mixes it decreased from 17% to 4% and 25% to 6%, respectively with increase in curing age from 28 days to 360 days for control mixes irrespective of w/b ratio as shown in Fig. 5.8 (a - c). The similar variation in CH content with curing age was also observed for all NaCl admixed SCC mixes (Fig. 5.9 to Fig. 5.12). The CH content (wt. %) in OPC based SCC mixes increased from 21% to 37%, 22% to 44%, and 22% to 39% at admixed NaCl concentrations 1%, 3% and 5%, respectively with increase in curing age from 28 days to 360 days irrespective of w/b ratio. Further, the CH content (wt. %) in PPC based SCC mixes decreased from 17% to 7%, 15% to 3%, and 9% to 2%, and that in OPC+20% FA based SCC mixes decreased from 17% to 8%, 20% to 7%, and 20% to 8% at the admixed NaCl concentrations of 1%, 3% and 5%, respectively with increase in curing age from 28 days to 360 days irrespective of w/b ratio. Similarly, in case of SCC mixes admixed with higher concentrations of NaCl at w/b ratio of 0.40, the CH content (wt. %) in OPC based SCC mixes increased from 29% to 32% and 19% to 30%, whereas the CH content (wt. %) deceased from 4% to 1%, and 5% to 3% in PPC and from 16% to 13%, and 14% to 13% in OPC+20% FA based SCC mixes at the admixed NaCl concentrations of 7.5%, and 12.5%, respectively with increase in curing age from 28 days to 360 days.

The peaks of gypsum in the SCC mixes were identified at 32.1° 2θ and 50.5° 2θ as observed from Fig. 5.1 to Fig. 5.7. The presence of gypsum in concrete mixes may be due to its addition during the manufacturing process of Portland cement to control its early setting and hardening behaviour. From the XRD patterns as well as from the results of semi-quantification analysis using RIR method, it is observed that the peak intensity of gypsum was lower in OPC mixes as compared to that in PPC and OPC +20% FA at 0% NaCl concentration. However, there is no systematic variation in the peak intensity and wt. % of gypsum with binder type in NaCl admixed SCC mixes. Similarly, there is no systematic variation in the peak intensity and wt. % of gypsum with w/b ratio, admixed NaCl concentration and curing age as observed from Fig. 5.1 to Fig. 5.7, and Fig. 5.8 to Fig. 5.12. The ettringite (E) peaks were found at 8.8° 2θ, 15.75° 2θ, 25.6° 2θ, and 27.5° 2θ as observed from the XRD patterns shown in Fig. 5.1 to Fig. 5.7. The formation of ettringite is due to

the reaction of gypsum with hydrated C_3A. From the XRD patterns (Fig. 5.1 to Fig. 5.3), it is inferred that the ettringite peaks were mostly more intense in OPC+20% FA and PPC based SCC mixes as compared to that in OPC based SCC mixes at all w/b ratios and curing ages at 0% NaCl. This may be attributed to the reaction of gypsum with hydrated C_3A to a greater extent in OPC+20% FA and PPC mixes as compared to that in OPC mixes. In the case of NaCl admixed SCC mixes, there is no systematic variation in peak intensity and wt. % of ettringite with binder type, w/b ratio and curing age as observed from Fig. 5.4 to Fig. 5.7, and Fig. 5.9 to Fig. 5.12. This may be attributed to the effect of chloride ions altering the extent of reaction of gypsum with hydrated C_3A in different types of binder at different w/b ratios and curing ages.

The peaks of quartz (Q) were identified at 20.78° 2θ, 26.65° 2θ, 39.45° 2θ, 42.45° 2θ and 50.2° 2θ in all the SCC mixes at all curing ages as observed from Fig. 5.1 to Fig. 5.7. The availability of quartz is mainly due to the presence aggregates in concrete. From the peak intensity and wt. % of quartz, it is observed that the quartz content is higher in PPC and OPC+20% FA based SCC mixes as compared to that in OPC based SCC mixes. This may be attributed to the effect of the unreacted silica (SiO_2) content in PPC and OPC+20% FA mixes as compared to that in OPC mixes. It may be noted that the wt. % of SiO_2 was higher in fly ash and PPC as compared to that in OPC as observed from Table 3.1 (Chapter 3). Further, it is observed that the peak intensity and wt. % of quartz mostly decreased with curing age in OPC based SCC mixes whereas these parameters mostly increased with curing age in PPC and OPC+20% FA based SCC mixes. These variations in quartz content with curing age may be attributed to the variations in availability of unreacted silica as a result of alteration in the extent of hydration and pozzolanic reactions with curing age. The calcite (CC) peak was found at 29.45º 2θ in the SCC mixes as observed from XRD patterns shown in Fig. 5.1 to Fig. 5.7.

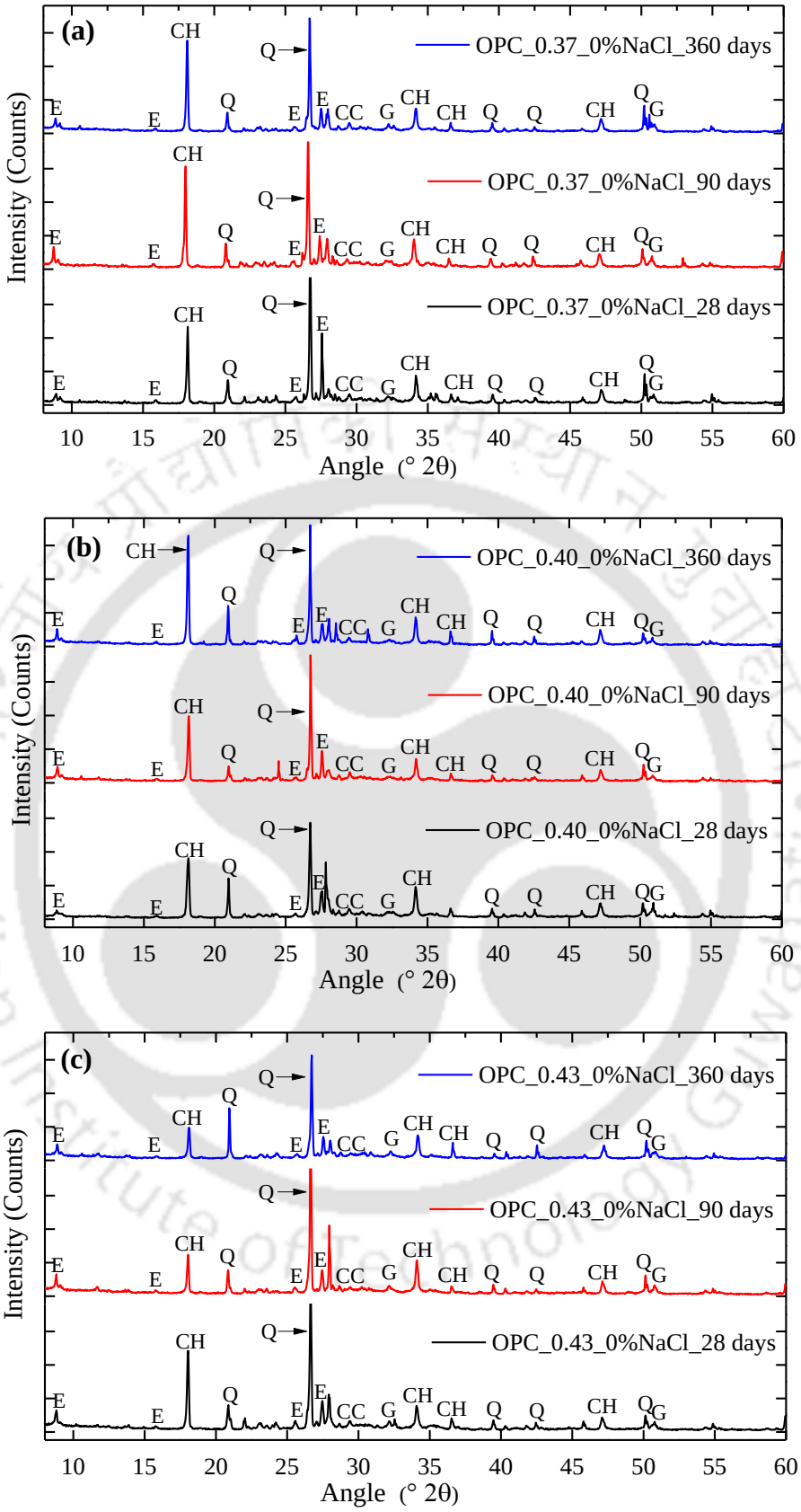

Fig. 5.1 XRD patterns of OPC based SCC mixes admixed with 0% NaCl for curing ages of 28, 90 and 360 days: (a) w/b ratio = 0.37, (b) w/b ratio = 0.40, and (c) w/b ratio = 0.43

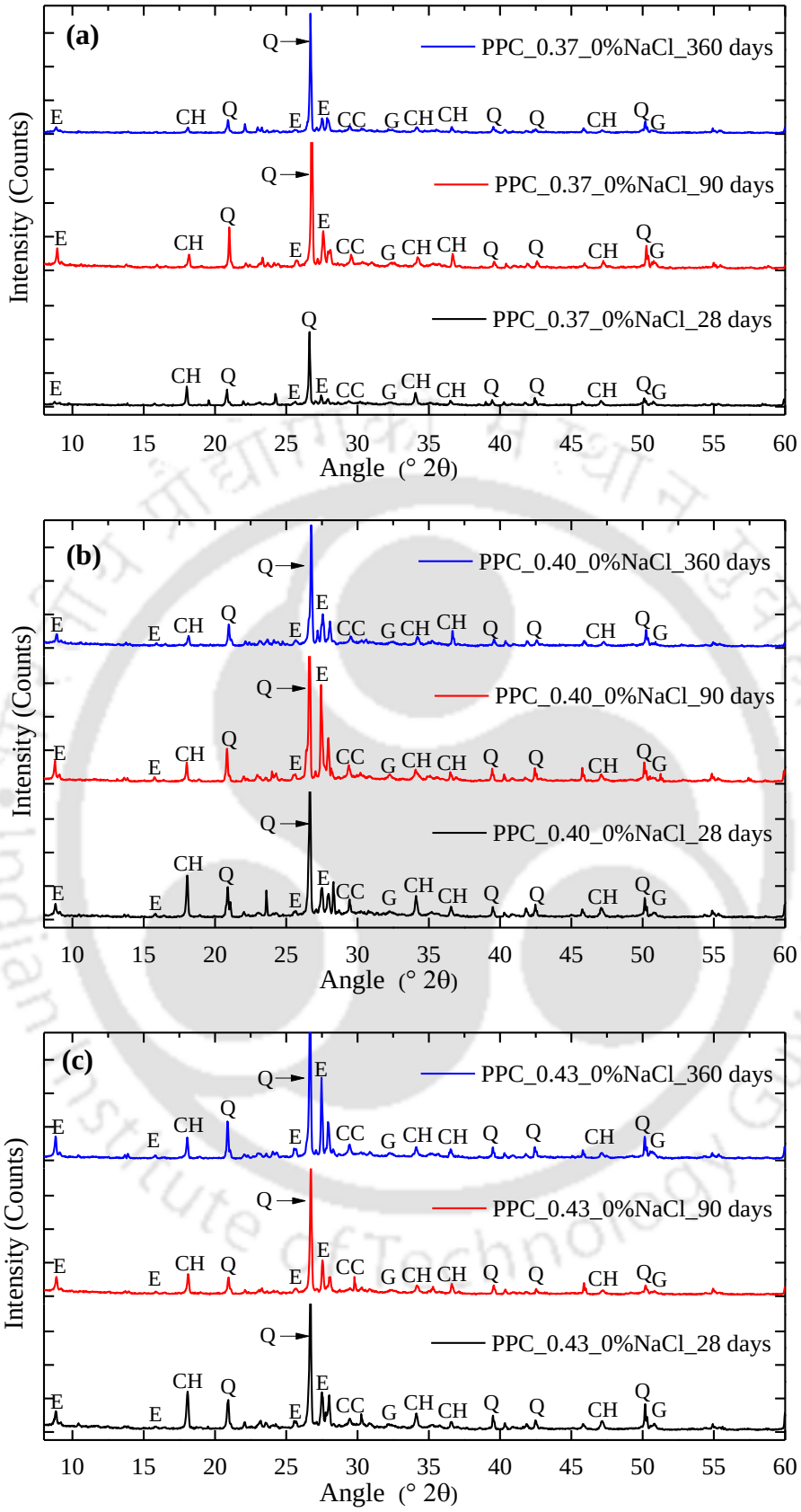

Fig. 5.2 XRD patterns of PPC based SCC mixes admixed with 0% NaCl for curing ages of 28, 90 and 360 days: (a) w/b ratio = 0.37, (b) w/b ratio = 0.40, and (c) w/b ratio = 0.43

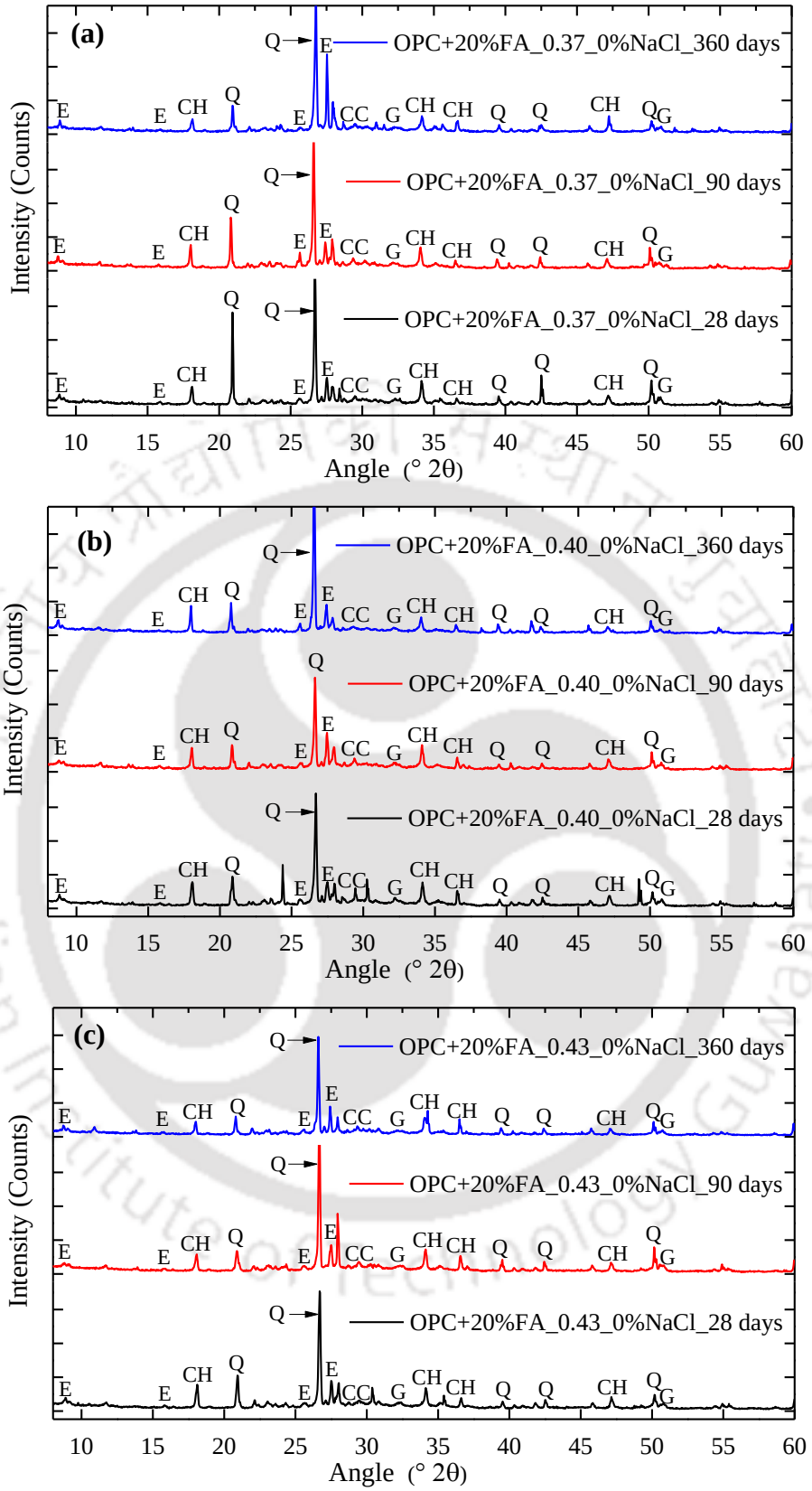

Fig. 5.3 XRD patterns of OPC+20% FA based SCC mixes admixed with 0% NaCl for curing ages of 28, 90 and 360 days: (a) w/b ratio = 0.37, (b) w/b ratio = 0.40, and (c) w/b = 0.43

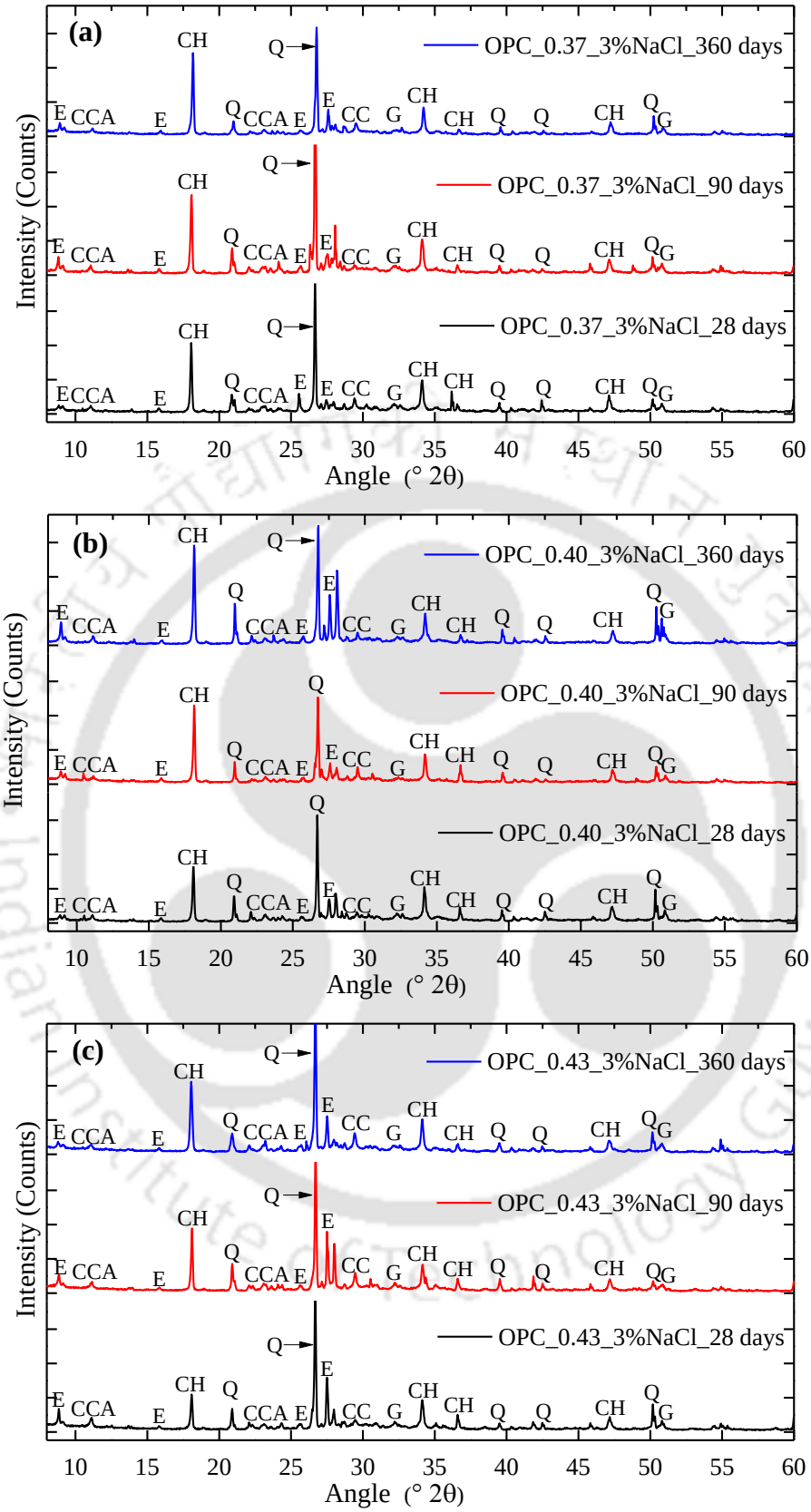

Fig. 5.4 XRD patterns of OPC based SCC mixes admixed with 3% NaCl for curing ages of 28, 90 and 360 days: (a) w/b ratio = 0.37, (b) w/b ratio = 0.40, and (c) w/b ratio = 0.43

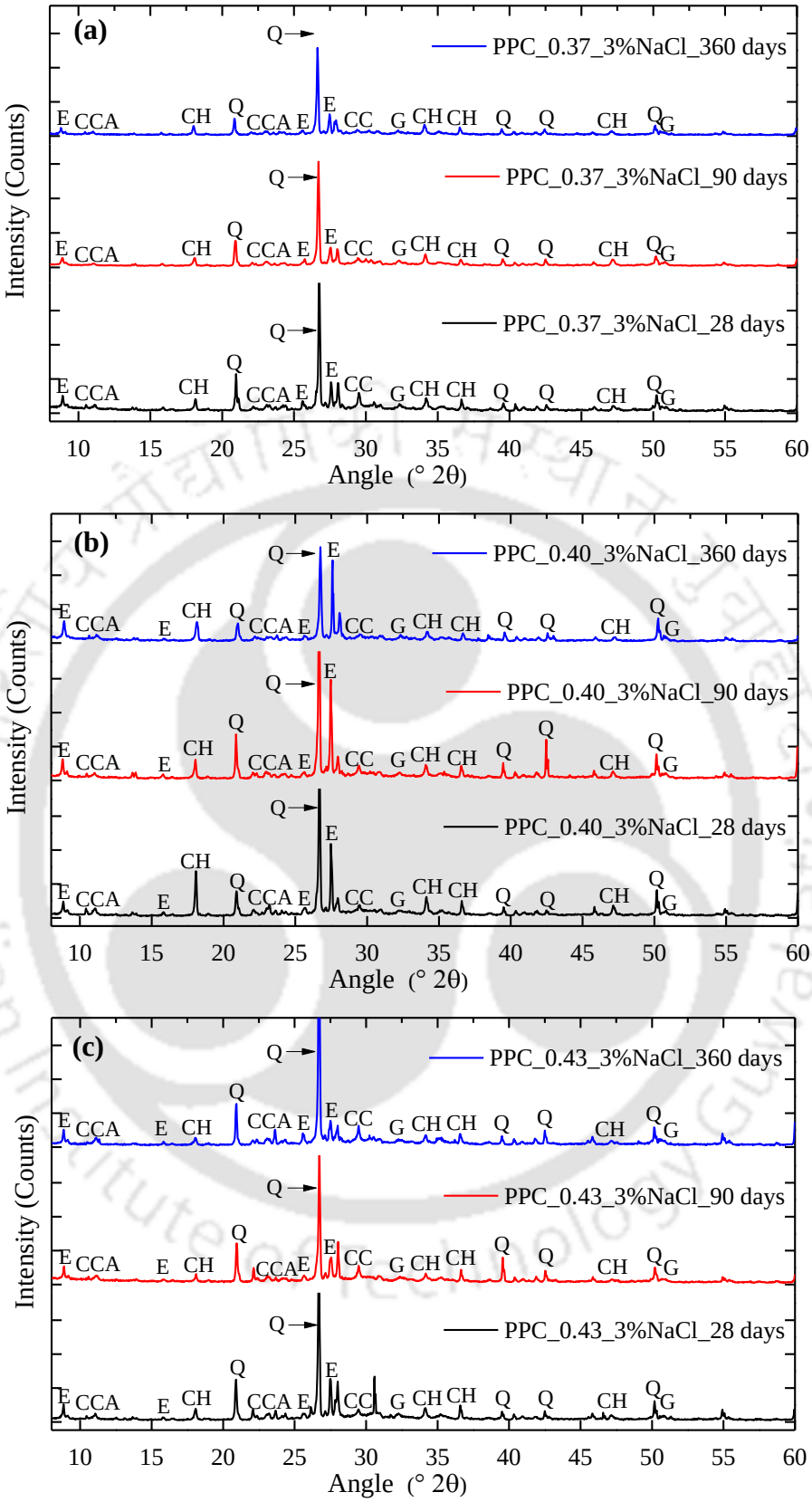

Fig. 5.5 XRD patterns of PPC based SCC mixes admixed with 3% NaCl for curing ages of 28, 90 and 360 days: (a) w/b ratio = 0.37, (b) w/b ratio = 0.40, and (c) w/b ratio = 0.43

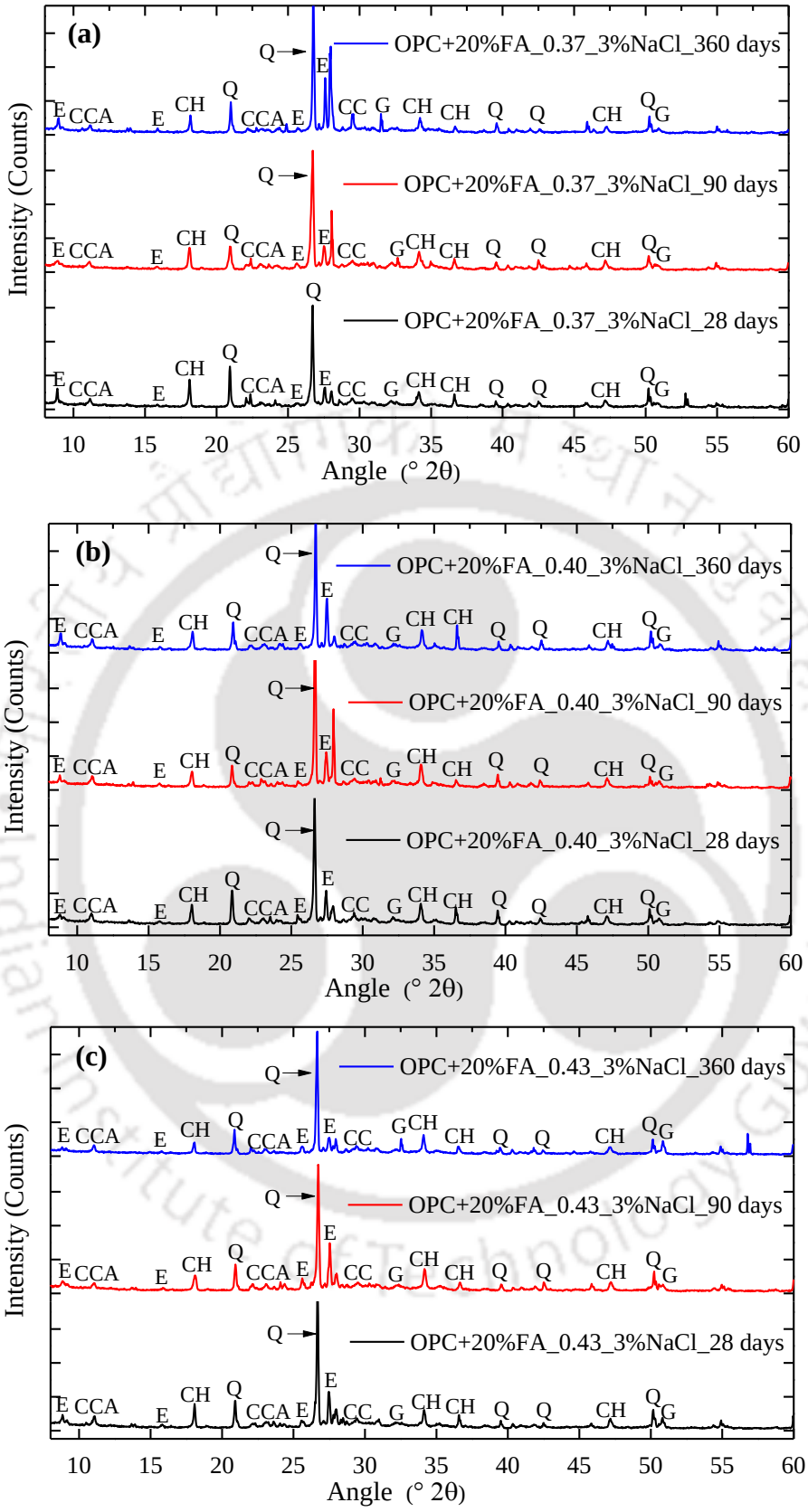

Fig. 5.6 XRD patterns of OPC+20% FA based SCC mixes admixed with 3% NaCl for curing ages of 28, 90 and 360 days: (a) w/b ratio = 0.37, (b) w/b ratio = 0.40, and (c) w/b ratio = 0.43

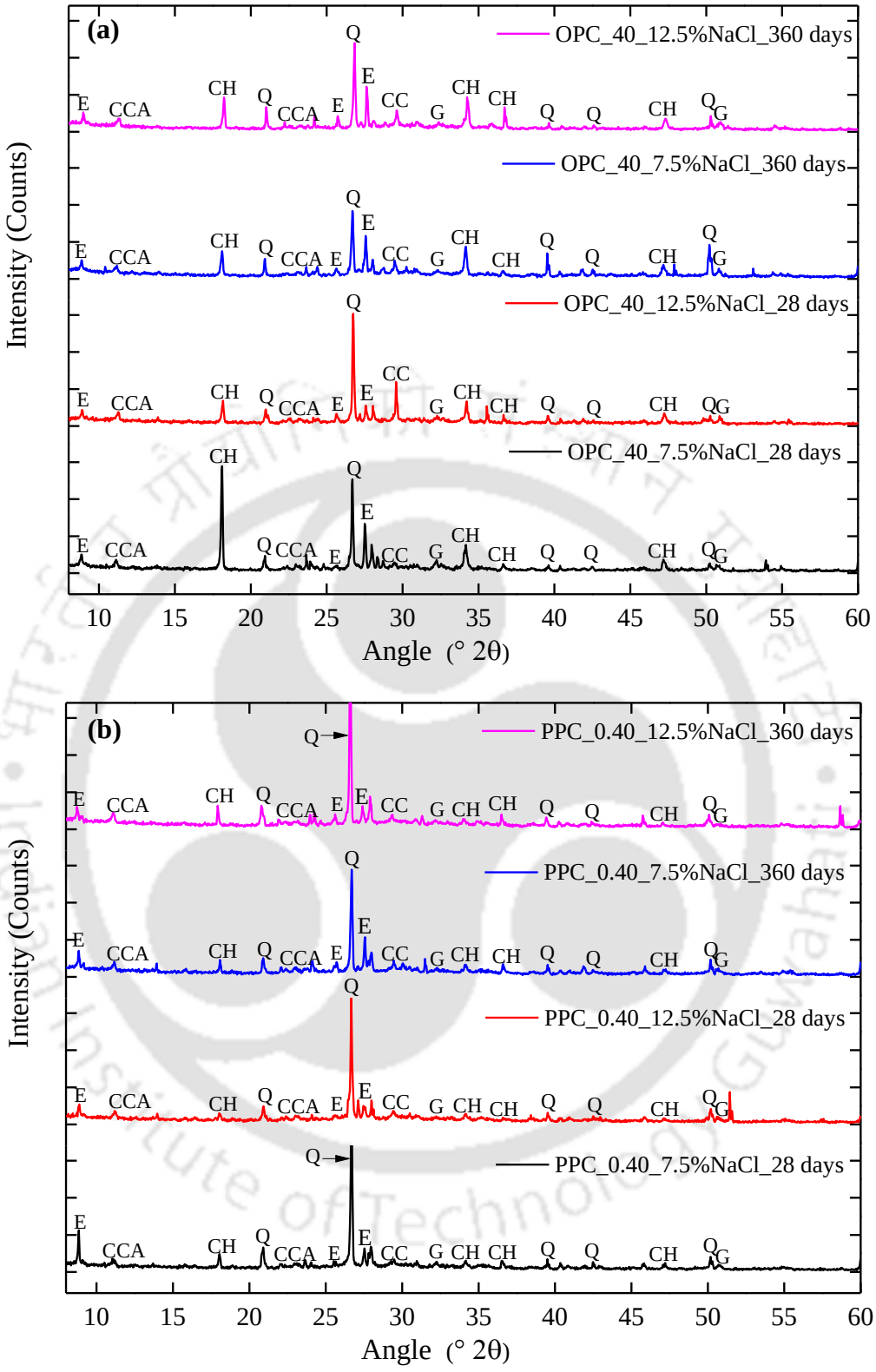

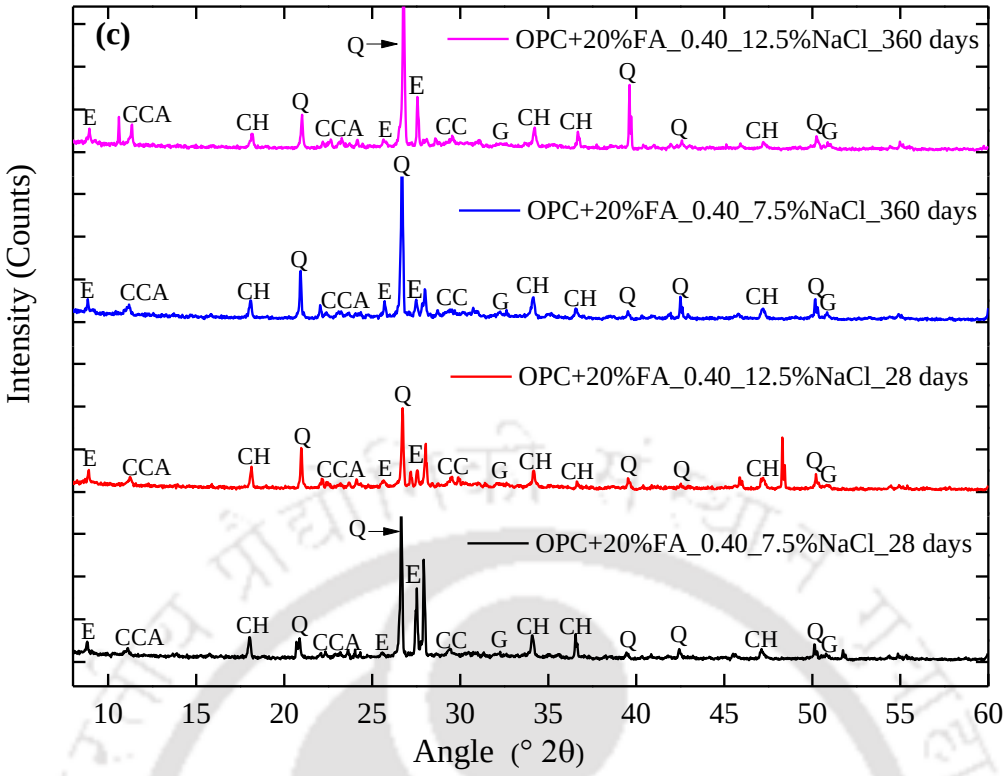

Fig. 5.7 XRD patterns of SCC mixes admixed with NaCl concentrations of 7.5% and 12.5% for curing ages of 28 and 360 days at w/b ratio of 0.40: (a) OPC, (b) PPC, and (c) OPC+20% FA

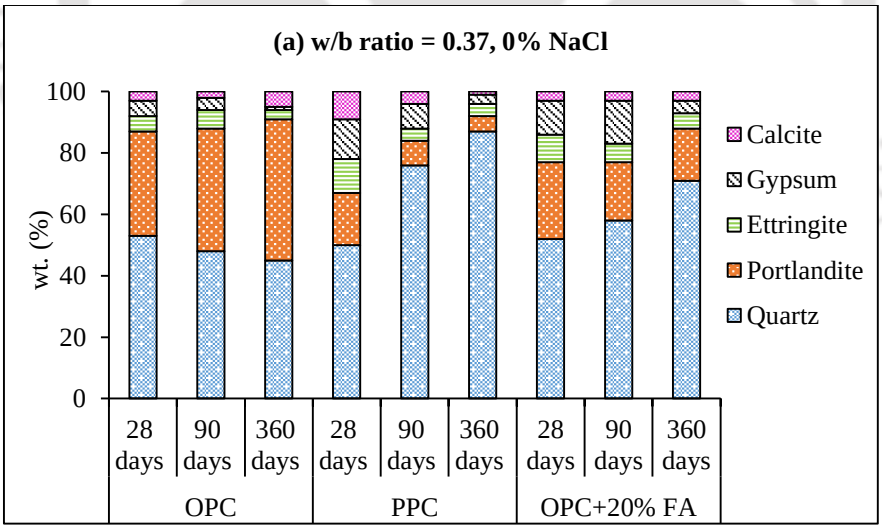

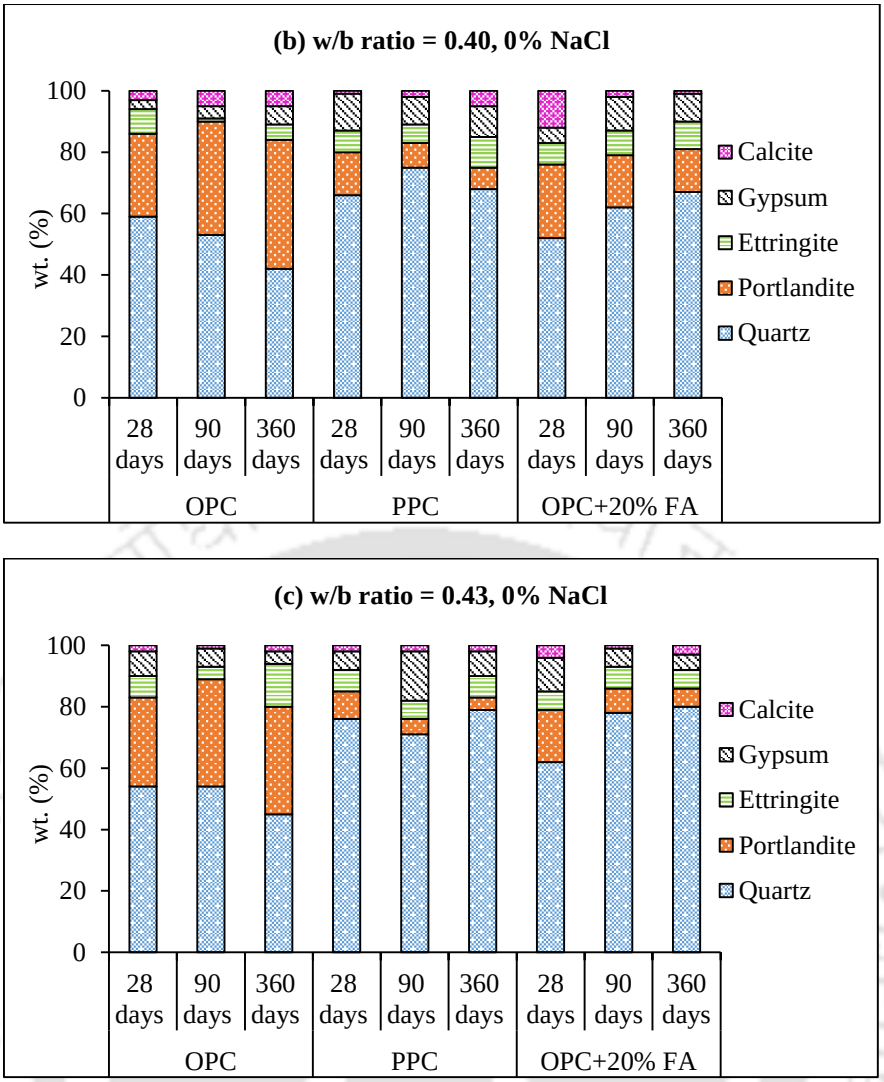

Fig. 5.8 Weight % of various compounds from the XRD patterns using RIR method for OPC, PPC and OPC+20% FA based SCC mixes admixed with 0% NaCl: (a) w/b ratio = 0.37, (b) w/b ratio = 0.40, and (c) w/b ratio = 0.43

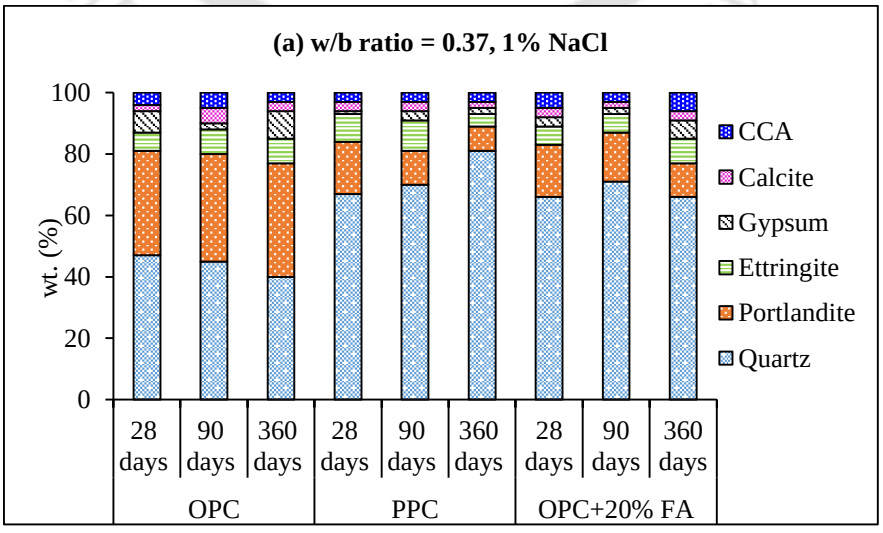

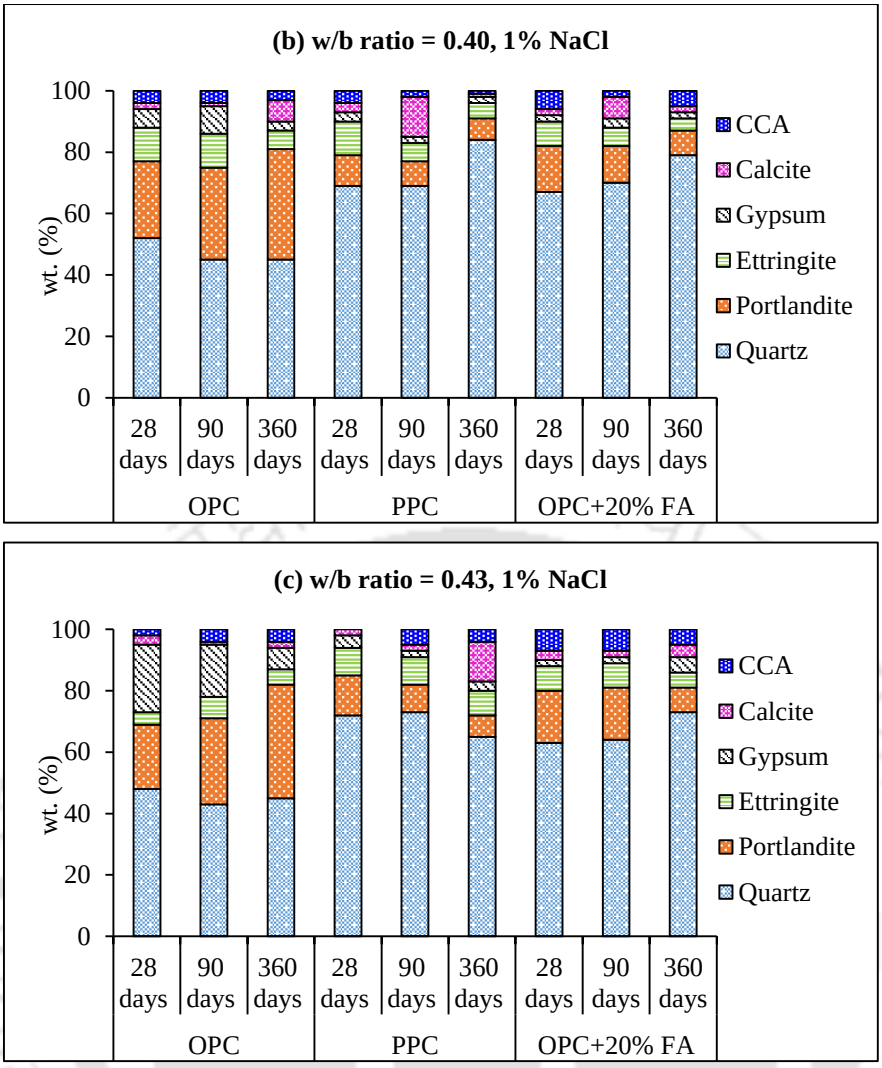

Fig. 5.9 Weight % of various compounds from the XRD patterns using RIR method for OPC, PPC and OPC+20% FA based SCC mixes admixed with 1% NaCl: (a) w/b ratio = 0.37, (b) w/b ratio = 0.40, and (c) w/b ratio = 0.43

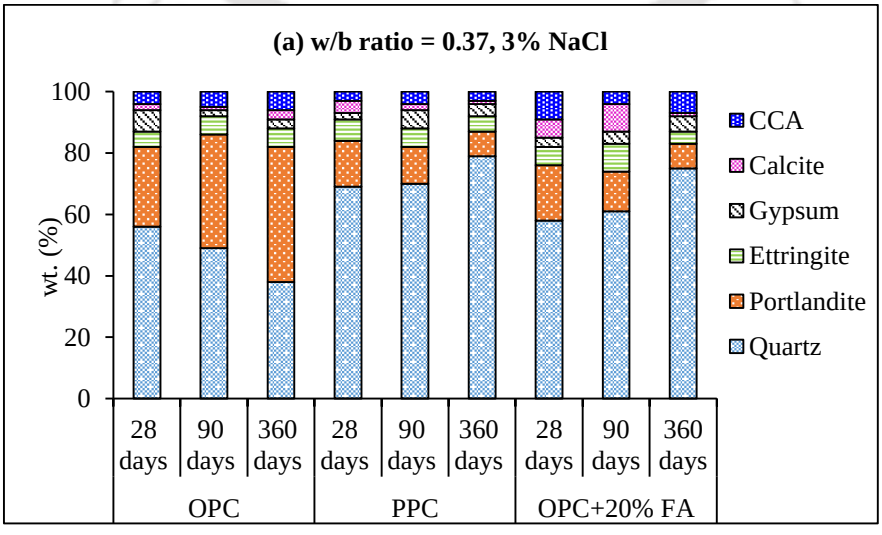

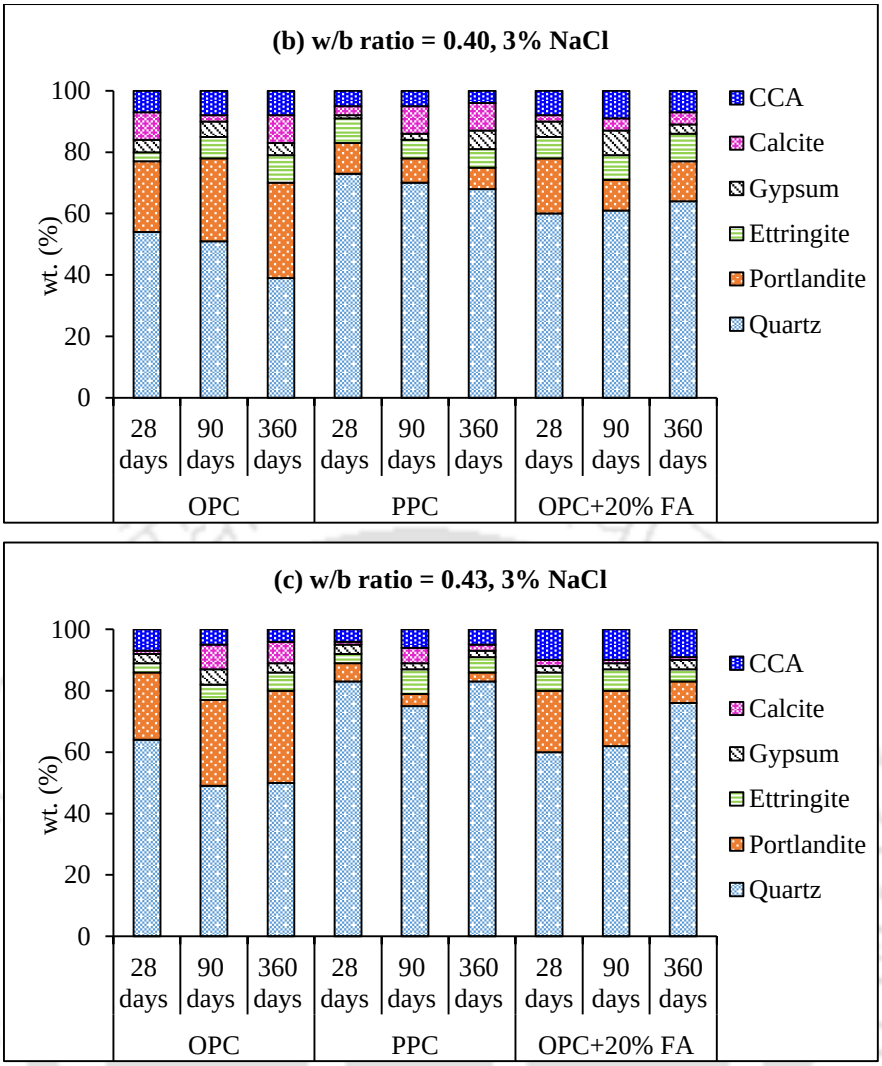

Fig. 5.10 Weight % of various compounds from the XRD patterns using RIR method for OPC, PPC and OPC+20% FA based SCC mixes admixed with 3% NaCl: (a) w/b ratio = 0.37, (b) w/b ratio = 0.40, and (c) w/b ratio = 0.43

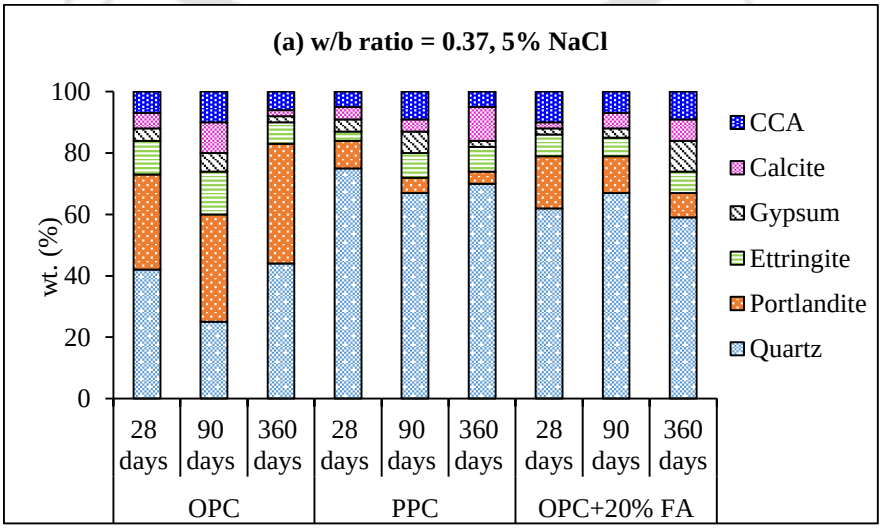

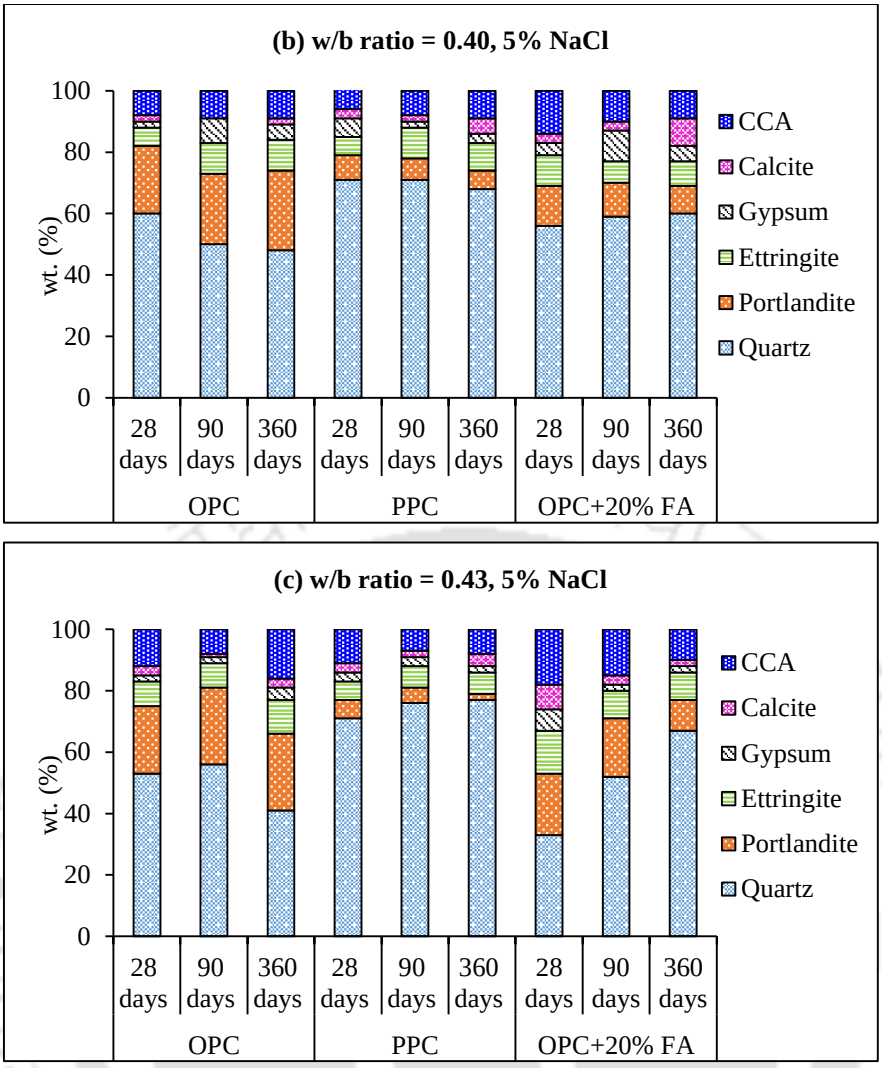

Fig. 5.11 Weight % of various compounds from the XRD patterns using RIR method for OPC, PPC and OPC+20% FA based SCC mixes admixed with 5% NaCl: (a) w/b ratio = 0.37, (b) w/b ratio = 0.40, and (c) w/b ratio = 0.43

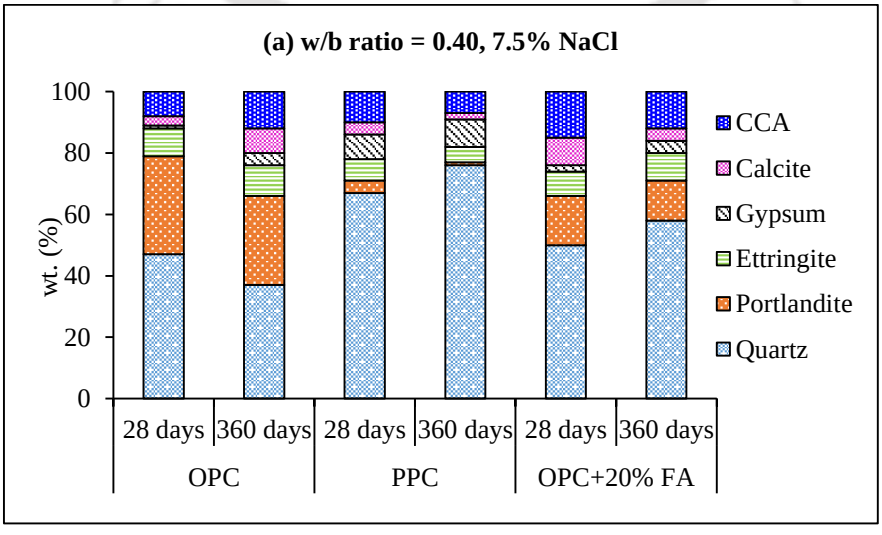

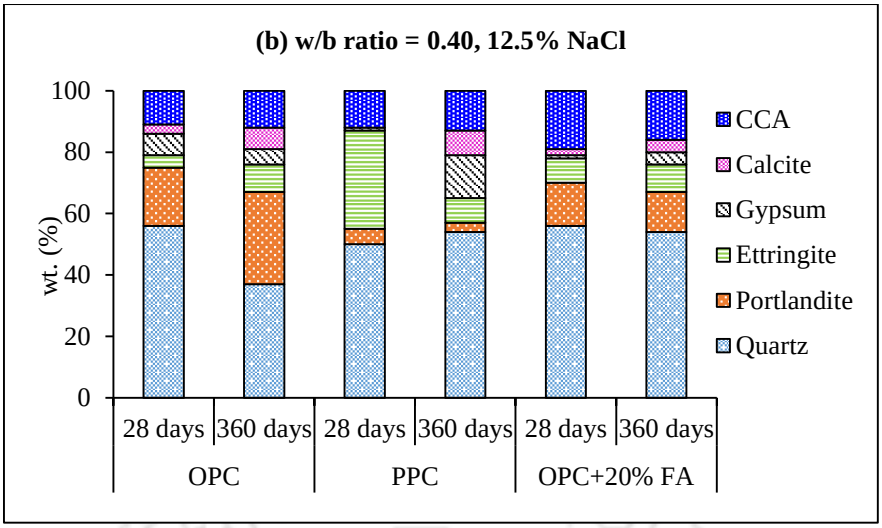

Fig. 5.12 Weight % of various compounds from the XRD patterns using RIR method for OPC, PPC and OPC+20% FA based SCC at w/b ratio of 0.40 admixed with: (a) 7.5% NaCl and (b) 12.5% NaCl

5.3 Thermo-gravimetry analysis (TGA)

Thermo-gravimetry analysis (TGA) was performed on OPC, PPC and OPC+20% FA based SCC mixes admixed with 0% NaCl (control mix) and 3% NaCl at w/b ratios of 0.37, 0.40 and 0.43 and for curing ages of 28, 90 and 360 days. In addition, TGA was performed on the SCC mixes made with w/b ratio 0.40 and admixed with higher concentrations of NaCl i.e. 7.5% and 12.5%, at the curing ages of 28 days and 360 days. As stated in Chapter 3, in the present research work, TGA was used with first derivative (derivative thermo-gravimetry: DTG) of the change of mass to determine the sharp yield peaks.

The TGA-DTG curves of SCC mixes admixed with 0% NaCl (control mix), at curing ages of 28 days, 90 days and 360 days are shown in Fig. 5.13 (a), Fig. 5.13 (b) and Fig. 5.13 (c) for OPC, PPC and OPC+20% FA based SCC mixes, respectively for w/b ratio of 0.40. Similarly, the TGA-DTG curves of SCC mixes admixed with 3% NaCl, at curing ages of 28 days, 90 days and 360 days are shown in Fig. 5.14 (a), Fig. 5.14 (b) and Fig. 5.14 (c) for OPC, PPC and OPC+20% FA based SCC mixes, respectively for w/b ratio of 0.40. Further, the TGA-DTG curves of SCC mixes admixed with 7.5% and 12.5% NaCl concentrations at w/b ratio of 0.40 are shown in Fig. 5.15 (a, b) and Fig. 5.16 (a, b) for curing ages of 28 days and 360 days, respectively. The remaining TGA-DTG curves of OPC, PPC and OPC+20% FA based SCC mixes admixed with 0% NaCl and 3% NaCl at the w/b ratio of

0.37, and 0.43 are shown in Fig. B4 to Fig. B5 (in Appendix B) for curing ages of 28, 90 and 360 days.

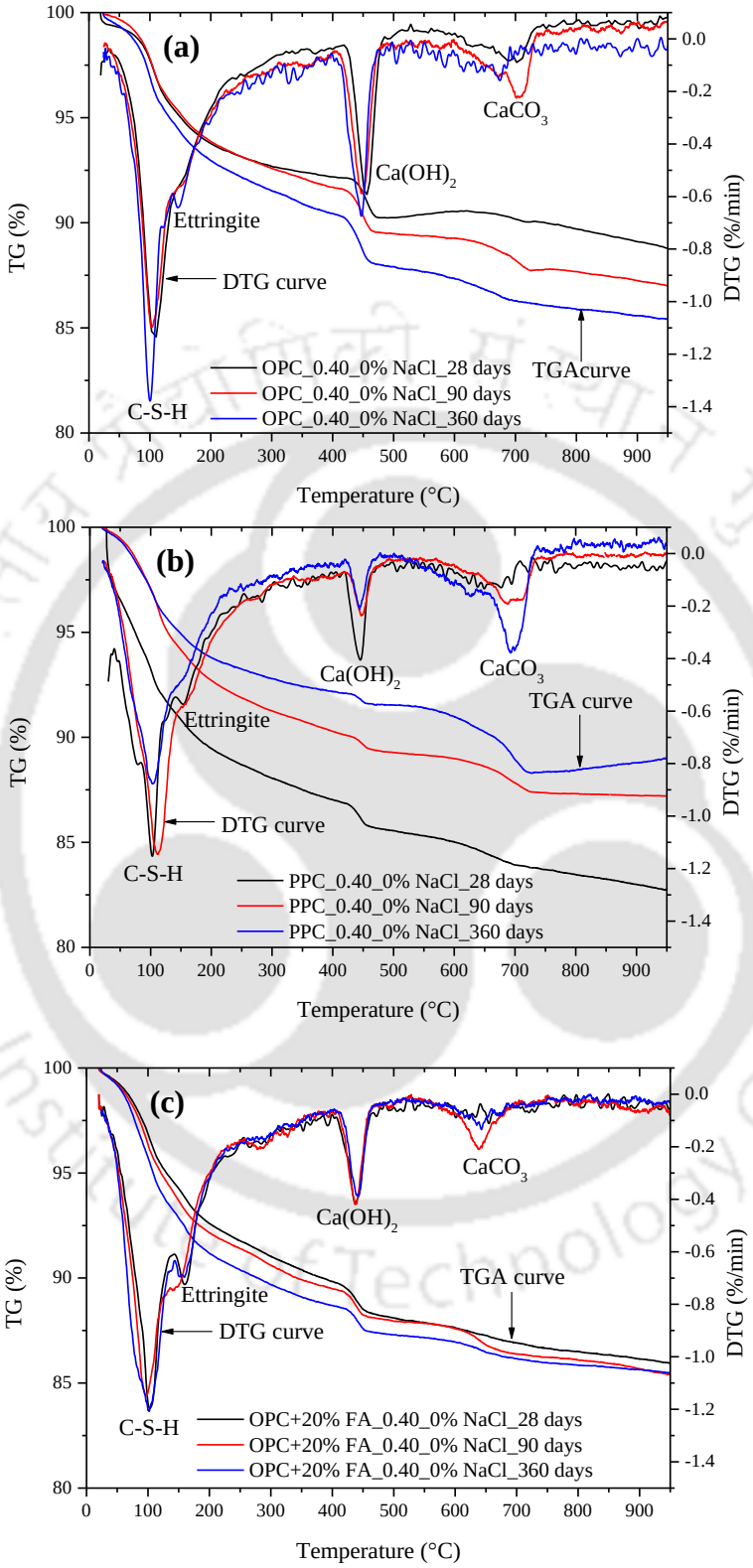

Fig. 5.13 TGA-DTG curves of SCC mixes admixed with 0% NaCl concentration for curing ages of 28, 90 and 360 days at w/b ratio of 0.40: (a) OPC, (b) PPC, and (c) OPC+20% FA

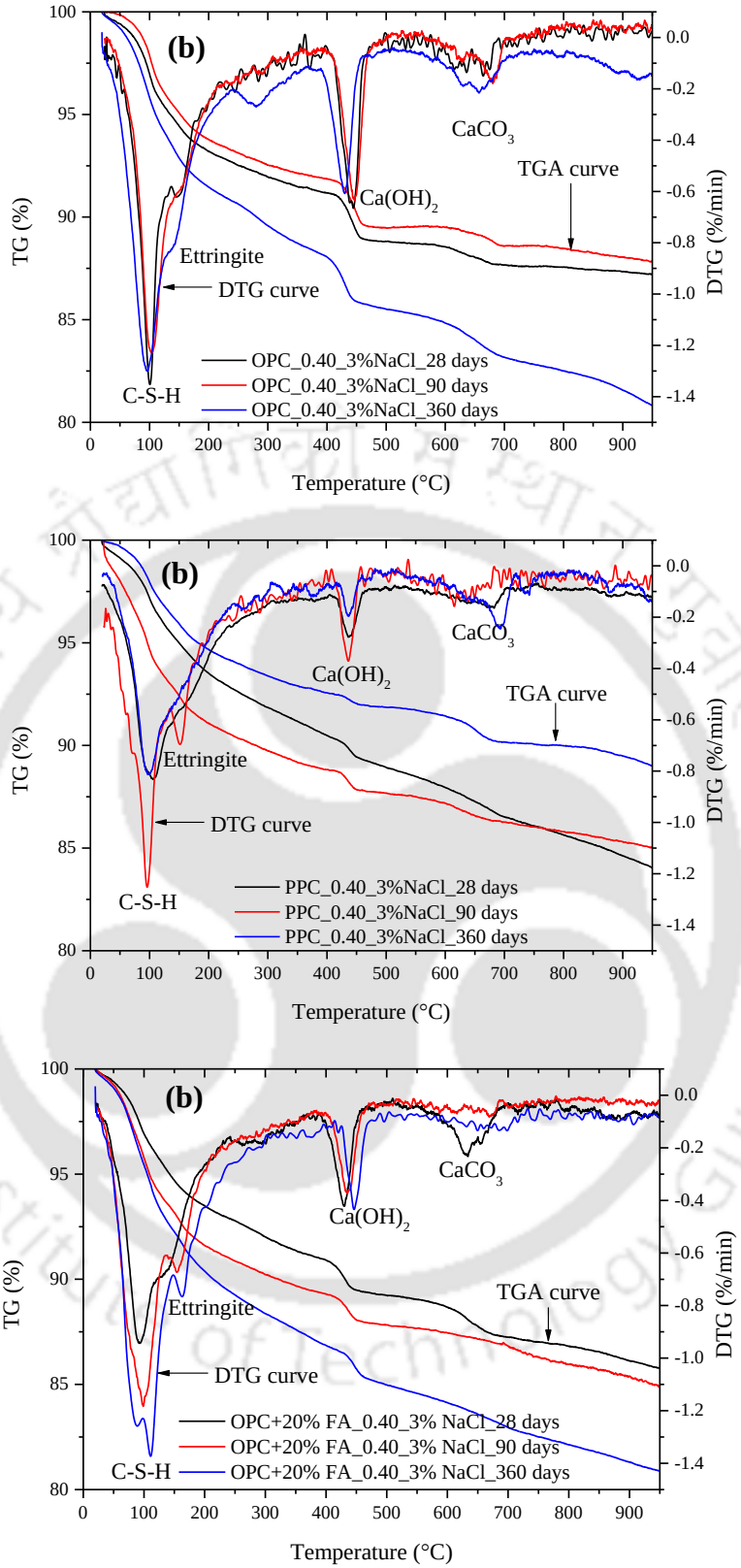

Fig. 5.14 TGA-DTG curves of SCC mixes admixed with 3% NaCl concentration for curing ages of 28, 90 and 360 days at w/b ratio of 0.40: (a) OPC, (b) PPC, and (c) OPC+20% FA

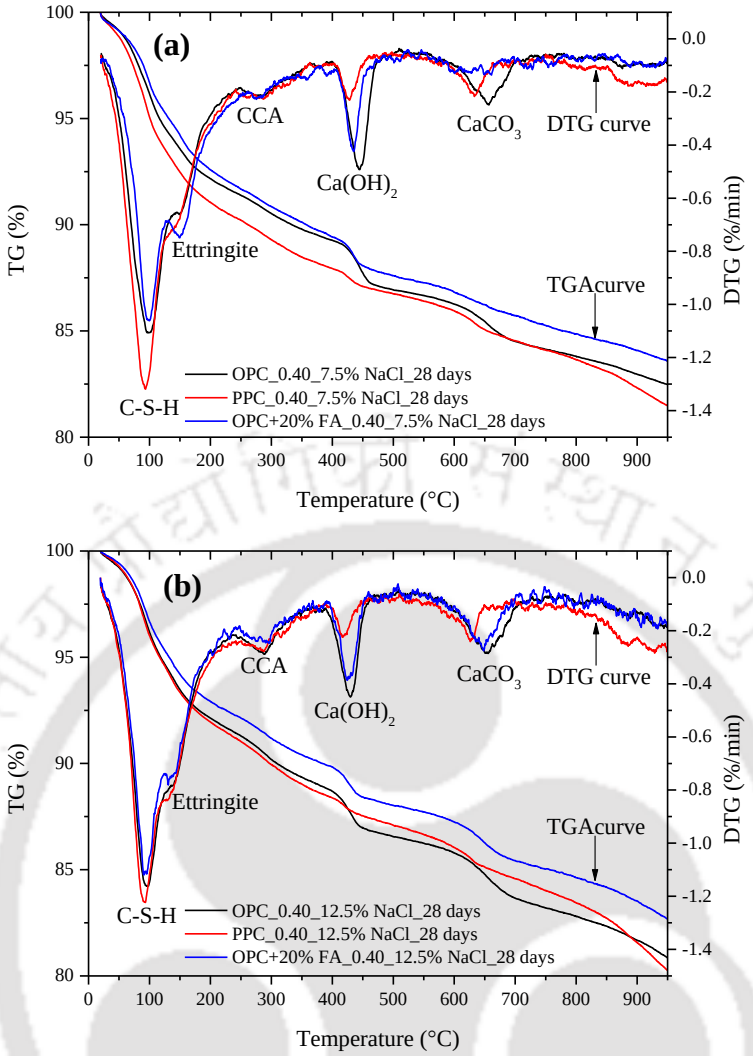

Fig. 5.15 TGA-DTG curves of SCC mixes made at w/b ratio of 0.40 for curing age of 28 days and admixed with: (a) 7.5% NaCl and (b) 12.5% NaCl

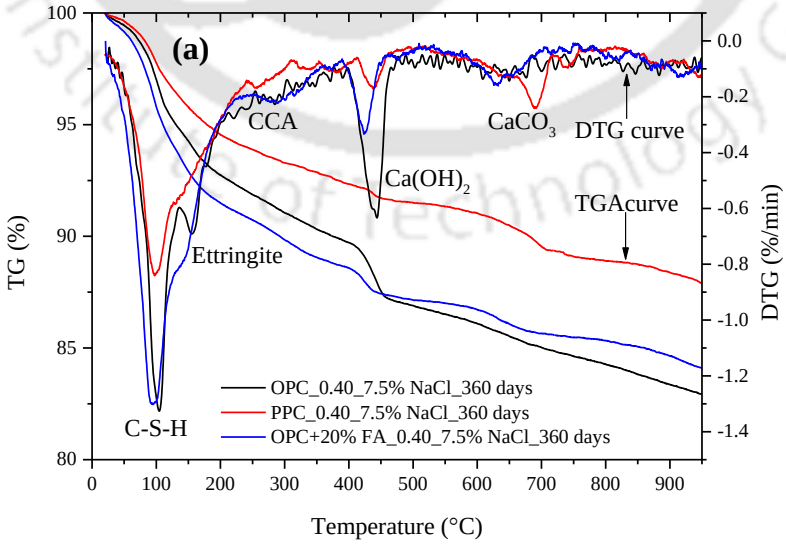

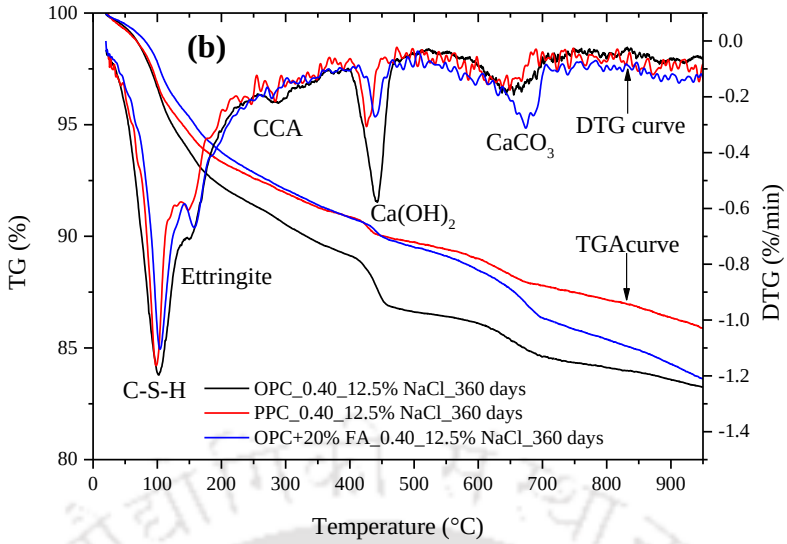

Fig. 5.16 TGA-DTG curves of SCC mixes made at w/b ratio of 0.40 for curing age of 360 days and admixed with: (a) 7.5% NaCl and (b) 12.5% NaCl

The mass loss between ambient temperature and 105°C as shown in TGA curves (Fig. 5.13 to Fig. 5.16) is due to the departure of free water in concrete. The mass loss between temperature of 105°C and 400°C as indicated in TGA curve is attributed to the loss of combined water due to dehydration of C-S-H, aluminate hydrates and ferroaluminate hydrates [133,134]. The DTG curve showed a more intense endothermic peak at temperature of about 105°C, which is due to the loss of combined water in the C-S-H gel. Another less intense endothermic peak observed in DTG curve at temperature of about 150°C is attributed to the departure of combined water in the ettringite. A steep change in the slope of TGA curve (Fig. 5.13 to Fig. 5.16) observed in the temperature range of 400°C to 480°C indicates the mass loss due to dehydration of calcium hydroxide [133,134]. The same is also indicated by a strong intense endothermic peak in the DTG curve in this temperature range. The mass loss in the temperature range of 480°C to 950°C as indicated in TGA curve is associated with decarbonation of calcium carbonate that results in CO_2 escape from concrete [133,134].

From Fig. 5.13 to Fig. 5.16, it is observed that, the extent of dehydration of calcium hydroxide (CH) in the temperature range of 400°C to 480°C is lower in all the SCC mixes made from PPC and OPC+20% FA than those made from OPC at all curing ages as indicated by less intense endothermic peak for PPC and OPC+20% FA in the DTG curve than that for OPC. The same trend is also observed from the change in slope of TGA curves. This is attributed to the availability of calcium hydroxide in lesser amount as result of its

consumption in the pozzolanic reaction in PPC and OPC+20% FA based SCC mixes than that in OPC based SCC mixes.

As stated earlier (Section 3.11.3), the obtained results of TGA were used for estimating the calcium hydroxide (CH) content in the SCC mixes using Taylor's formula (Equation 3.5). The calculated quantities of calcium hydroxide are presented in Table 5.2.

Table 5.2 Calcium hydroxide content (%) of SCC mixes

w/b ratio	Admixed chloride	Calcium hydroxide content (%)								
		OPC			PPC			OPC+20% FA		
		28 days	90 days	360 days	28 days	90 days	360 days	28 days	90 days	360 days
0.37	0% NaCl	8.48	8.87	10.84	6.01	3.71	3.32	6.96	6.22	5.38
	3% NaCl	8.75	10.45	10.51	5.37	4.76	3.14	6.99	6.14	5.31
0.40	0% NaCl	8.0	8.94	10.08	5.70	3.88	2.52	6.68	5.89	5.49
	3% NaCl	9.59	9.65	9.93	5.58	4.46	2.70	6.53	5.75	5.05
	7.5% NaCl	9.02	-	10.99	4.32	-	3.18	6.82	-	5.46
	12.5% NaCl	8.12	-	9.82	4.55	-	4.22	6.86	-	4.73
0.43	0% NaCl	6.83	6.99	9.46	5.39	3.74	1.60	6.22	5.57	4.43
	3% NaCl	8.23	9.05	9.30	3.82	2.06	0.70	5.92	5.71	4.08

Note: "-": not measured.

From Table 5.2, it is observed that the CH content is less in the SCC mixes made with PPC as compared to those made with OPC+20% FA followed by OPC at all curing ages. Further, the CH content reduced with curing age from 28 days to 360 days in the SCC mixes made with PPC and OPC+20% FA, whereas it increased with curing age in the SCC mixes made with OPC as observed from Table 5.2. This variation in CH content is attributed to the consumption of CH in the pozzolanic reaction with curing age in PPC and OPC+20% FA based SCC mixes, whereas the release of CH from hydration reaction with curing age in the OPC based SCC mixes. This is in line with the results of XRD analysis discussed earlier (Section 5.2), wherein the variations in peak intensity and wt. % of CH with binder type are the same as those in the CH content calculated from TGA. While analyzing the effect of w/b ratio on the estimated CH content from TGA, it is observed that the CH content was mostly higher in the SCC mixes made with lower w/b ratio (0.37) as compared to those made with higher w/b ratio (0.40 and 0.43) for 0% NaCl (control) as well as 3% NaCl admixed SCC mixes. This may be attributed to the availability of higher amount of CH at

lower w/b ratio than that at higher w/b ratio. This variation in CH content with w/b ratio obtained from TGA is consistent with the variations in peak intensity and wt. % of CH with w/b ratio obtained from XRD results for 0% and 3% admixed NaCl concentration (Fig. 5.1 to 5.6, and Fig. 5.8 and Fig. 5.10).

While evaluating the effect of admixed NaCl on the mass loss obtained from TGA curves (Fig. 5.13 to Fig. 5.16), it is inferred that mostly higher mass loss was observed in the NaCl admixed SCC mixes as compared to that in control mix (0% NaCl) for OPC, PPC and OPC+20% FA, and at all w/b ratios and curing ages. This may be attributed to the dehydration of Friedel's salt (aluminate hydrate) that is formed in the presence of chloride ions in the SCC mixes admixed with NaCl. The SCC mixes admixed with NaCl showed a less intense endothermic peak at about 300°C in the DTG curves (Fig. 5.14 to Fig. 5.16), whereas the control SCC mixes did not show any endothermic peak at the same temperature (Fig. 5.13). It may be noted that, the formation of calcium chloroalumiate (CCA) was confirmed through the peaks found at 11.2° 2θ and 23.2° 2θ in the XRD patterns of NaCl admixed SCC mixes, as discussed earlier (Section 5.2). Further, it is also observed that the mass loss mostly increased in SCC mixes with the increase in admixed NaCl concentration as observed from Fig. 5.14 to Fig. 5.16.

The obtained mass loss (%) in different temperature ranges and also the total mass loss (%) are presented in Table 5.3, 5.4 and 5.5 for the SCC mixes made with the w/b ratios of 0.37, 0.40 and 0.43, respectively. From Table 5.3 to Table 5.5, it is observed that the mass loss due to departure of combined water (temperature of 105°C to 480°C) constitutes a significant portion of total mass loss in OPC, PPC and OPC+20% FA based SCC mixes at all w/b ratios, admixed NaCl concentrations and curing ages. The percentage mass loss (with respect to total mass loss) due to departure of combined water varied from 47.39% to 65.24%, 41.44% to 55.02%, and 47.12% to 59.97% in OPC, PPC and OPC+20% FA based SCC mixes respectively at the curing ages of 28 days for different concentrations of admixed NaCl and w/b ratio. Similarly, at curing age of 90 days, the percentage mass loss due to departure of combined water varied from 60.33% to 67.04%, 43.50% to 60.02%, and 49.04% to 58.20% in OPC, PPC and OPC+20% FA based SCC mixes respectively and that at curing age of 360 days, varied from 50.83% to 66.02%, 44.68% to 52.27%, and 46.97% to 71.19% in OPC, PPC and OPC+20% FA based SCC mixes respectively. From these values, it is observed that the mass loss due to departure of combined water was mostly lower in PPC based SCC mixes as compared to that in OPC+20% FA and OPC

based SCC mixes at all w/b ratios and curing ages for different concentrations of admixed NaCl. The lower mass loss due to departure of combined water in PPC based SCC mixes may be attributed to the dominant effect of the formation of lower amount of calcium chloroaluminate (CCA) and calcium hydroxide (CH) in PPC as compared to that in OPC+20% FA and OPC based mixes, which is also corroborated from the XRD results wherein less intense peaks and lower wt. % of CCA and CH were found in case of PPC based SCC mixes. The higher mass loss due to departure of combined water in OPC based SCC mixes may be due to the dominant effect of the formation of higher amount of C-S-H and calcium hydroxide, whereas in OPC+20% FA based SCC mixes, the higher mass loss may be attributed to the dominant effect of formation of higher amount of calcium chloroaluminate and calcium hydroxide as compared to PPC based SCC mixes. While comparing between OPC and OPC+20% FA, it is observed that the mass loss due to departure of combined water was mostly higher in OPC as compared to that in OPC+20% FA based SCC mixes, which may be attributed to the effect of formation of higher amount of C-S-H and CH in OPC as compared to that in OPC+20% FA based SCC mixes. These variations in mass loss due to departure of combined water in OPC and OPC+20% FA based SCC mixes as a result of variations in formations of C-S-H and CH in are also substantiated with the results of compressive strength (higher in OPC than that in OPC +20% FA), and peak intensity and wt. % of CH (higher in OPC than that in OPC +20% FA) obtained from the XRD patterns. Further, the total mass loss mostly increased with curing age in OPC whereas it decreased with curing age in PPC and OPC+20% FA based SCC mixes for all control and NaCl admixed SCC mixes, as observed from Table 5.3 to Table 5.5. These variations in total mass loss of OPC, PPC and OPC+20% FA based SCC mixes may be attributed to the dominant effect of the variations in the formation of calcium hydroxide with increase in curing age.

Table 5.3 Thermo-gravimetry analysis of SCC mixes at w/b ratio of 0.37

Binder type	Admixed chloride	Curing age	Mass loss (%)				Total mass loss (%) (Ambient - 950°C)
			Ambient -105°C	105 - 400°C	400 - 480°C	480 - 950°C	
OPC	0% NaCl	28 days	2.55	4.98	2.06	2.55	12.15
		90 days	2.76	6.07	2.16	2.65	13.64
		360 days	2.54	6.16	2.64	2.38	13.71
	3% NaCl	28 days	3.89	4.62	2.13	1.34	11.98
		90 days	2.80	6.49	2.54	2.43	14.26
		360 days	1.96	6.57	2.56	2.74	13.82
PPC	0% NaCl	28 days	3.75	5.59	1.46	3.49	14.29
		90 days	2.11	5.20	0.90	1.96	10.17
		360 days	4.72	6.90	0.81	2.77	15.19
	3% NaCl	28 days	5.03	5.97	1.31	5.15	17.45
		90 days	5.22	6.30	1.16	4.20	16.87
		360 days	4.15	7.10	0.76	3.02	15.04
OPC+20% FA	0% NaCl	28 days	3.78	7.13	1.69	4.18	16.78
		90 days	4.36	6.20	1.51	2.22	14.29
		360 days	2.86	6.11	1.31	0.14	10.42
	3% NaCl	28 days	4.99	8.16	1.70	4.28	19.13
		90 days	2.58	7.11	1.49	4.32	15.50
		360 days	3.10	6.74	1.29	2.44	13.57

Table 5.4 Thermo-gravimetry analysis of SCC mixes at w/b ratio of 0.40

Binder type	Admixed chloride	Curing age	Mass loss (%)				Total mass loss (%) (Ambient-950°C)
			Ambient -105°C	105 - 400°C	400 - 480°C	480 - 950°C	
OPC	0% NaCl	28 days	2.45	5.37	1.94	1.45	11.21
		90 days	2.63	5.68	2.17	2.53	13.01
		360 days	3.59	5.98	2.45	2.58	14.60
	3% NaCl	28 days	3.54	5.29	2.33	1.62	12.78
		90 days	2.66	5.49	2.35	1.65	12.15
		360 days	4.61	7.34	2.41	4.83	19.18
	7.5% NaCl	28 days	4.28	6.45	2.19	4.60	17.53
		360 days	3.48	6.80	2.67	4.12	17.07
	12.5% NaCl	28 days	4.21	7.10	1.97	5.87	19.16
		360 days	3.77	7.10	2.39	3.49	16.75
PPC	0% NaCl	28 days	7.21	5.77	1.39	2.90	17.27
		90 days	3.26	6.46	0.94	2.13	12.79
		360 days	3.28	4.54	0.61	2.58	11.01
	3% NaCl	28 days	3.17	6.35	1.36	5.08	15.96
		90 days	5.74	5.43	1.09	2.73	14.98
		360 days	2.36	5.08	0.66	2.93	11.02
	7.5% NaCl	28 days	5.37	6.69	1.05	5.41	18.53
		360 days	2.54	5.12	0.77	3.69	12.12
	12.5% NaCl	28 days	4.33	7.29	1.11	7.03	19.76
		360 days	3.56	5.57	1.03	3.95	14.11
OPC+ 20% FA	0% NaCl	28 days	3.57	6.60	1.63	2.27	14.06
		90 days	4.07	6.44	1.43	2.66	14.60
		360 days	4.70	6.60	1.33	1.88	14.52
	3% NaCl	28 days	3.36	5.73	1.59	3.56	14.24
		90 days	4.67	6.04	1.40	3.05	15.16
		360 days	2.84	5.81	1.23	0.18	10.07
	7.5% NaCl	28 days	3.71	6.87	1.66	4.16	16.41
		360 days	4.61	6.80	1.33	3.15	15.89
	12.5% NaCl	28 days	3.67	6.50	1.67	5.49	17.33
		360 days	2.62	6.55	1.15	6.07	16.39

Table 5.5 Thermo-gravimetry analysis of SCC mixes at w/b ratio of 0.43

Binder type	Admixed chloride	Curing age	Mass loss (%)				Total mass loss (%) (Ambient-950°C)
			Ambient-105°C	105 - 400°C	400 - 480°C	480 - 950°C	
OPC	0% NaCl	28 days	2.28	4.44	1.66	1.25	9.63
		90 days	2.93	6.13	1.70	0.92	11.68
		360 days	3.11	7.48	2.30	2.76	15.65
	3% NaCl	28 days	2.93	5.77	2.00	2.61	13.31
		90 days	2.30	7.55	2.20	2.63	14.68
		360 days	4.01	7.11	2.26	1.41	14.79
PPC	0% NaCl	28 days	2.71	5.69	1.31	3.09	12.80
		90 days	3.45	6.16	0.91	4.36	14.88
		360 days	2.43	4.12	0.39	2.98	9.92
	3% NaCl	28 days	3.21	5.48	0.93	2.03	11.65
		90 days	2.75	4.65	0.50	2.95	10.85
		360 days	2.92	3.61	0.17	1.76	8.46
OPC+20% FA	0% NaCl	28 days	2.81	5.84	1.51	2.09	12.26
		90 days	3.25	5.35	1.35	1.57	11.52
		360 days	1.67	5.47	1.08	0.99	9.21
	3% NaCl	28 days	3.57	6.44	1.44	2.34	13.79
		90 days	4.23	6.20	1.39	2.33	14.15
		360 days	2.29	5.15	0.99	1.11	9.55

5.4 Field emission scanning electron microscope (FESEM) analysis

The FESEM analysis was carried out to analyze the morphology of SCC mixes. The typical FESEM images of OPC based SCC mixes admixed with 0%, 7.5% and 12.5% NaCl concentrations at w/b ratio of 0.40 for curing ages of 28 days and 360 days are shown in Fig. 5.17 (a - f). Similarly, the typical FESEM images of SCC mixes made with PPC and OPC+20% FA are shown in Fig. 5.18 (a - f) and Fig. 5.19 (a - f), respectively. The remaining FESEM images of OPC, PPC and OPC+20% FA based SCC mixes admixed with 0% and 3% NaCl concentrations at the w/b ratios of 0.37, 0.40, and 0.43 are shown in Fig. B6 to B15 (in Appendix B) for different curing ages.

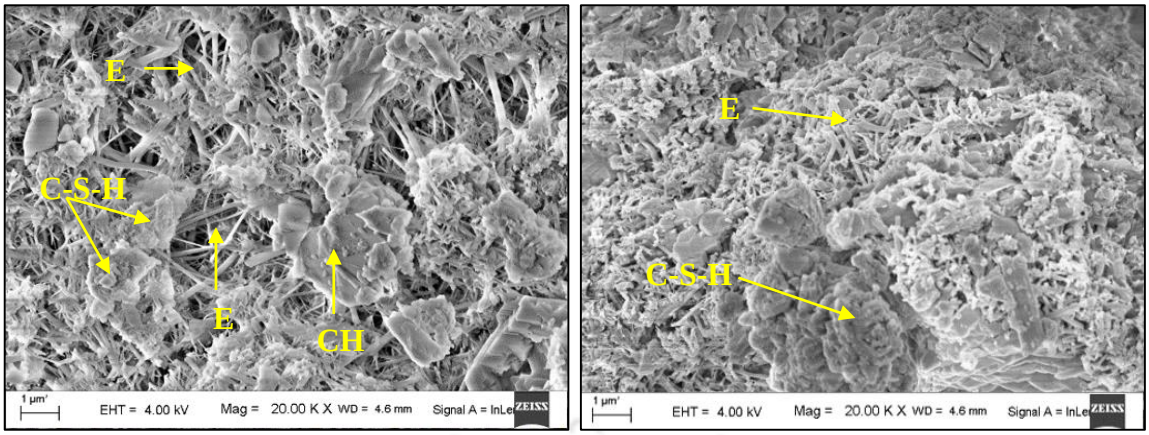

(a) 0% NaCl (28 days) (b) 0% NaCl (360 days)

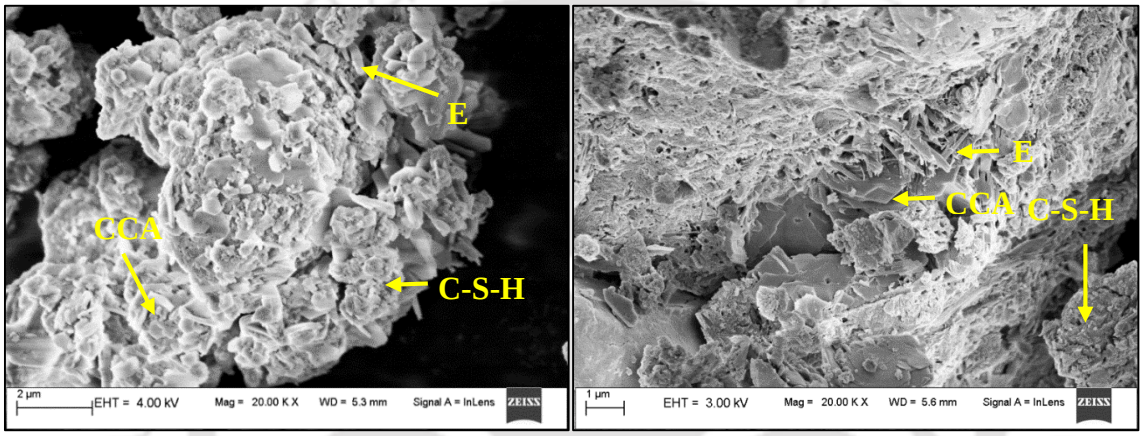

(c) 7.5% NaCl (28 days) (d) 7.5% NaCl (360 days)

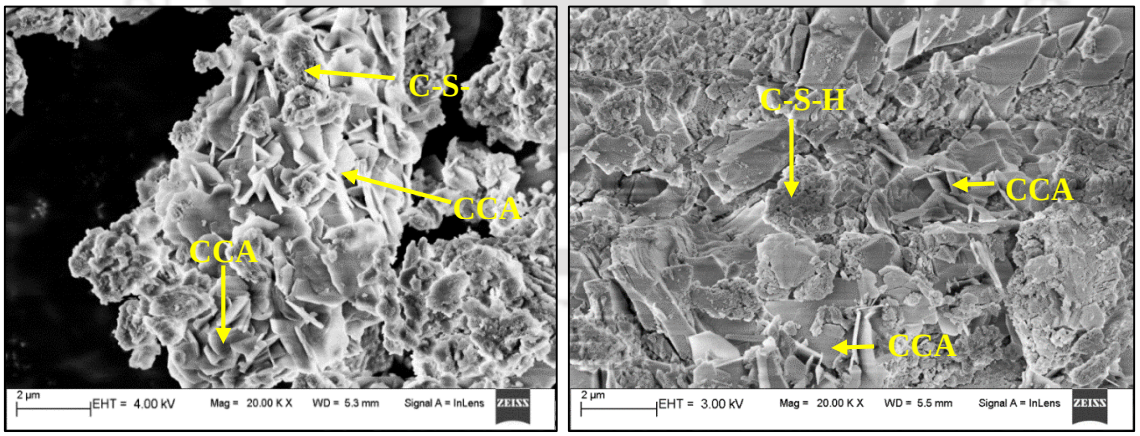

(e) 12.5% NaCl (28 days) (f) 12.5% NaCl (360 days)

Fig. 5.17 FESEM images of OPC based SCC mixes admixed with different concentrations of NaCl at w/b ratio of 0.40 for curing ages of 28 days and 360 days

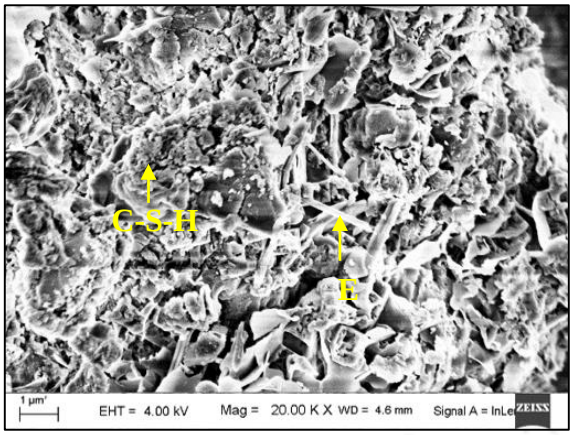

(a) 0% NaCl (28 days)

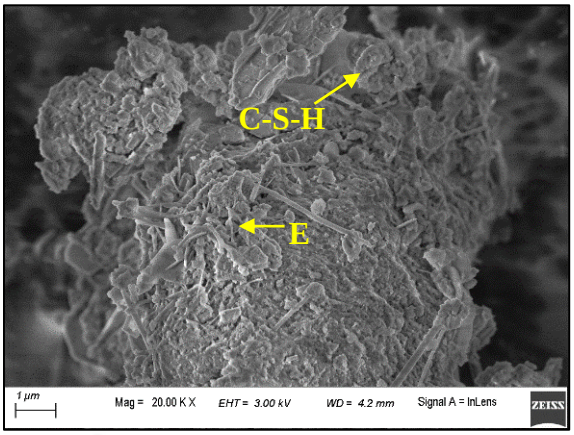

(b) 0% NaCl (360 days))

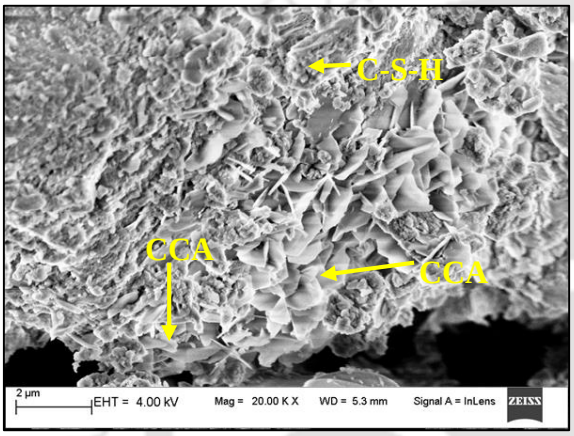

(c) 7.5% NaCl (28 days)

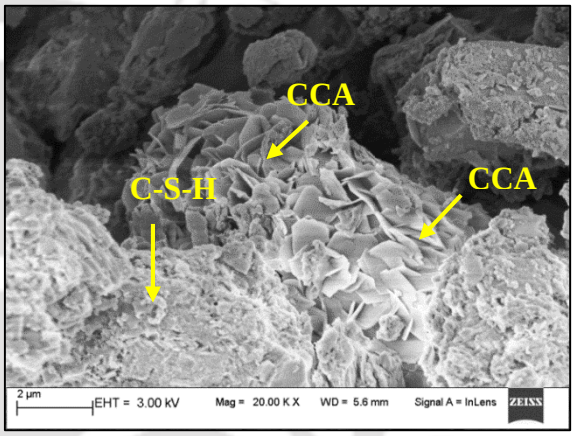

(d) 7.5% NaCl (360 days)

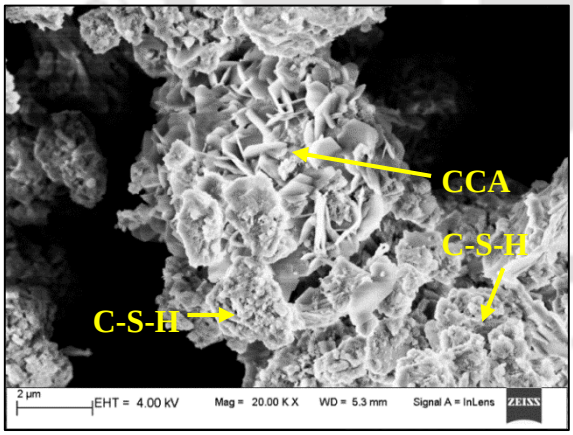

(e) 12.5% NaCl (28 days)

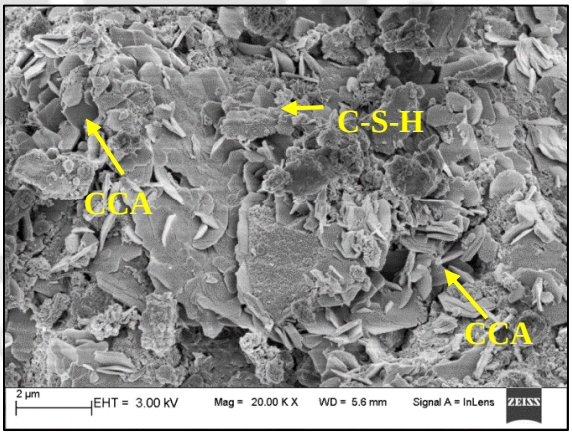

(f) 12.5% NaCl (360 days)

Fig. 5.18 FESEM images of PPC based SCC mixes admixed with different concentrations of NaCl at w/b ratio of 0.40 for curing ages of 28 days and 360 days

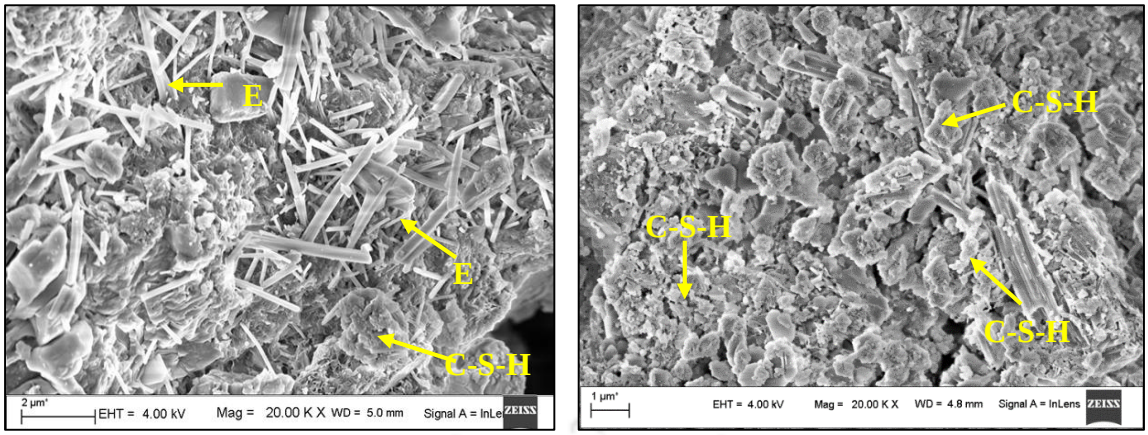

(a) 0% NaCl (28 days) (b) 0% NaCl (360 days)

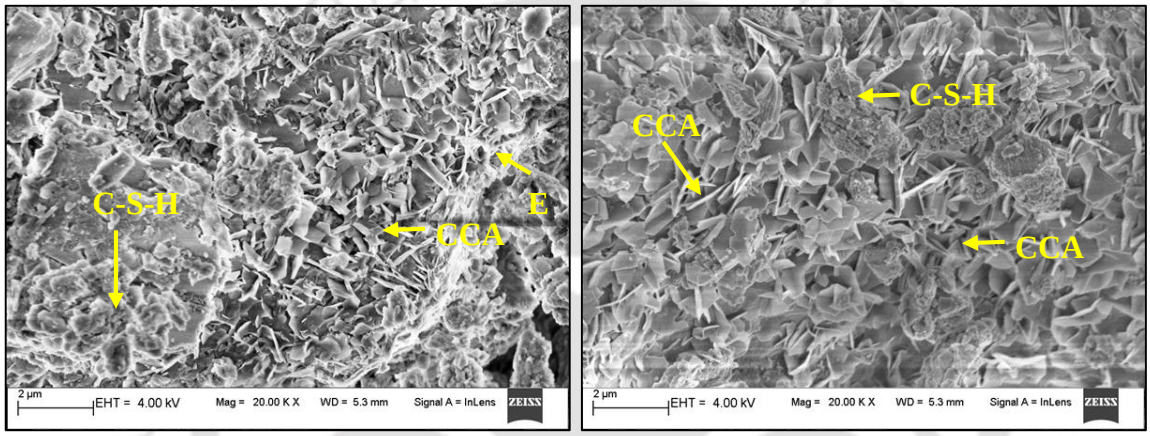

(c) 7.5% NaCl (28 days) (d) 7.5% NaCl (360 days)

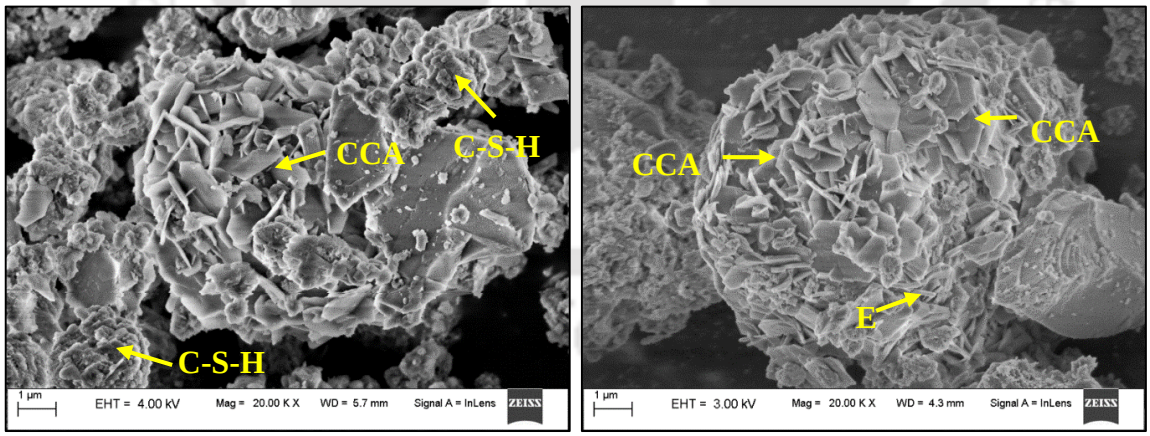

(e) 12.5% NaCl (28 days) (f) 12.5% NaCl (360 days)

Fig. 5.19 FESEM images of OPC+20% FA based SCC mixes admixed with different concentrations of NaCl at w/b ratio of 0.40 for curing ages of 28 days and 360 days

The formation of calcium silicate hydrate (C-S-H), calcium hydroxide (CH), calcium chloroaluminate (CCA) and ettringite (E) in the SCC mixes can be seen from these images (Fig. 5.17 to Fig. 5.19), which further confirms the results of XRD analysis. The structure of C-S-H gel in FESEM images is generally observed in the form of reticular network [135]. The FESEM images shown in Fig. 5.17 to Fig. 5.19 indicate the formation of C-S-H in all the SCC mixes irrespective of binder type, w/b ratio, admixed NaCl concentration and curing age, as the reticular network structure was observed in these images. Further, denser microstructure was observed at the longer curing age 360 days as compared to that at the curing age of 28 days as observed from Fig. 5.17 to Fig. 5.19, which is attributed to the formation of more amount of C-S-H in the concrete mixes at the longer curing age. The calcium hydroxide crystals appeared in hexagonal shape as observed from the FESEM images. Further, the ettringite phase was observed in the shape of needle like crystals in both control as well as in NaCl admixed SCC mixes, which was also indicated by the XRD patterns. As already stated earlier, the ettringite is formed in concrete mixes due to the reaction of gypsum with hydrated C_3A. The calcium chloroaluminate crystals were appeared in hexagonal-slice shape only in NaCl admixed OPC, PPC and OPC+20% FA based SCC mixes as observed from the FESEM images (Fig. 5.17 to Fig. 5.19), which corroborates the XRD results wherein the calcium chloroaluminate peaks were found in the XRD patterns of NaCl admixed SCC mixes.

5.5 Fourier transform infrared (FTIR) spectroscopy

The FTIR spectroscopy was performed to identify the functional groups associated with different compounds formed in SCC mixes prepared from different types of binder, w/b ratio and admixed NaCl concentration. The typical FTIR spectra of SCC mixes made with OPC, PPC and OPC+20% FA at w/b ratios of 0.40 are shown in Fig. 5.20 for 0% NaCl (control mix) and in Fig. 5.21 for 3% NaCl, at curing ages of 28 days, 90 days and 360 days. Similarly, the FTIR spectra of SCC mixes made at w/b ratio of 0.40 and admixed with the NaCl concentrations of 7.5% and 12.5% are shown in Fig. 5.22 (a), Fig. 5.22 (b) and Fig. 5.22 (c) for OPC, PPC and OPC+20% FA, respectively. The FTIR spectra of OPC, PPC and OPC+20% FA based SCC mixes admixed with 0% NaCl and 3% NaCl at w/b ratios of 0.37, and 0.43 are shown in Fig. B16 to Fig. B21 (in Appendix B) for the curing ages of 28, 90 and 360 days.

From Fig. 5.20 to Fig. 5.22, it is observed that the bands ranging from 3640 cm^{-1} to 3643 cm^{-1} for OPC, 3639 cm^{-1} to 3646 cm^{-1} for PPC and 3639 cm^{-1} to 3643 cm^{-1} for OPC+20% FA are attributed to the stretching vibration of the –OH band in calcium hydroxide [120,126], irrespective of w/b ratio and curing age in control (0% NaCl) and NaCl admixed SCC mixes. This band appeared more intense in OPC based SCC mixes as compared to that in PPC and OPC+20% FA based SCC mixes, which is attributed to the availability of more amount of calcium hydroxide in OPC mixes. Further, the bands ranging from 3436 cm-^{1} to 3486 cm^{-1} and 1622 cm^{-1} to 1638 cm^{-1} for OPC, from 3436 cm^{-1} to 3469 cm^{-1} and 1628 cm^{-1} to 1642 cm^{-1} for PPC, and those ranging from 3436 cm^{-1} to 3482 cm^{-1} and 1637 cm^{-1} to 1644 cm^{-1} for OPC+20% FA irrespective of w/b ratio and curing age in control and NaCl admixed SCC mixes are caused by the stretching vibration of -OH band in the structural water of hydration products and the bending vibration of -OH band in the interlayer water of hydration products [126,136].

The presence of calcium carbonate in SCC mixes was indicated by CO_3^{2-} bands ranging from 1419 cm^{-1} to 1428 cm^{-1} for OPC, 1416 cm^{-1} to 1428 cm^{-1} for PPC, and 1414 cm^{-1} to 1428 cm^{-1} for OPC+20% FA (Fig. 5.20 - 5.22), which substantiates the XRD peaks of calcium carbonate found at 29.45° 2θ (shown in Fig. 5.1 to Fig. 5.7). Similarly, the bands ranging from 873 cm^{-1} to 875 cm^{-1} for OPC, from 874 cm^{-1} to 876 cm^{-1} for PPC, and that ranging from 873 cm^{-1} to 875 cm^{-1} for OPC+20% FA based SCC mixes are due to the out-of-plane bending of CO_3^{2-} bands [136,137].

In control as well as NaCl admixed SCC mixes, the bands varying from 995 cm^{-1} to 1008 cm^{-1}, 991 cm^{-1} to 1015 cm^{-1}, and 986 cm^{-1} to 1012 cm^{-1} for OPC, PPC and OPC+20% FA respectively are due to the asymmetric stretching vibration of Si-O band in C-S-H gel [126]. The bands ranging from 533 cm^{-1} to 535 cm^{-1} for OPC, from 531 cm^{-1} to 536 cm^{-1} for PPC, and from 532 cm^{-1} to 538 cm^{-1} for OPC+20% FA based SCC mixes are attributed to the out-of-plane Si-O bending due to the presence of anhydrous calcium silicates in concrete [137]. The bands ranging from 777 cm^{-1} to 779 cm^{-1} for OPC, from 776 cm^{-1} to 780 cm^{-1} for PPC, and that from 777 cm^{-1} to 780 cm^{-1} for OPC+20% FA are caused due to the stretching vibrations of Al-O bands [138], which may be attributed to the formation of ettringite in the concrete mixes. This substantiates the XRD results wherein the formation of ettringite was indicated by the peaks found at 8.8° 2θ, 15.75° 2θ, 25.6° 2θ, and 27.5° 2θ in the XRD patterns shown in Fig. 5.1 to Fig. 5.7.

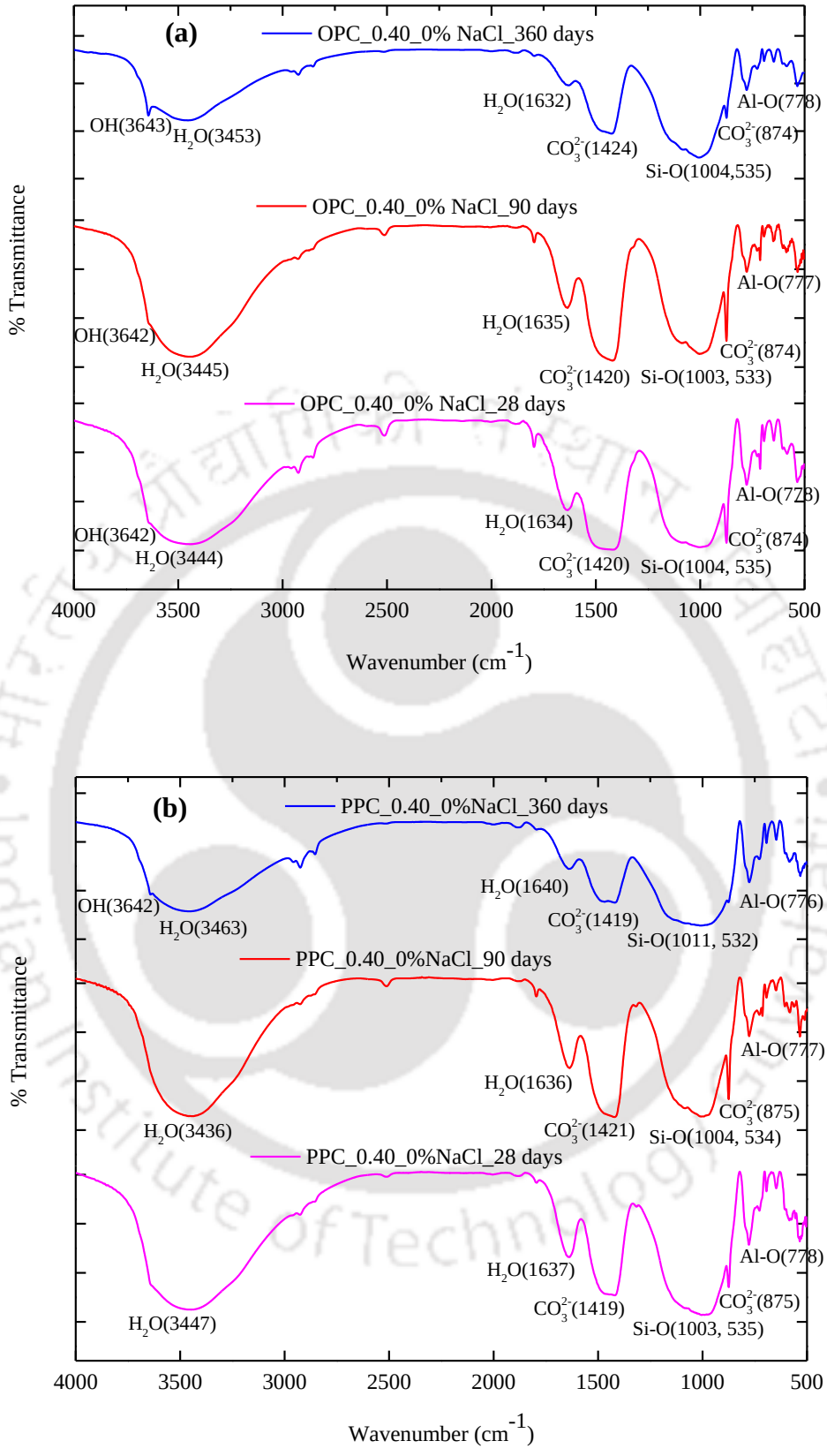

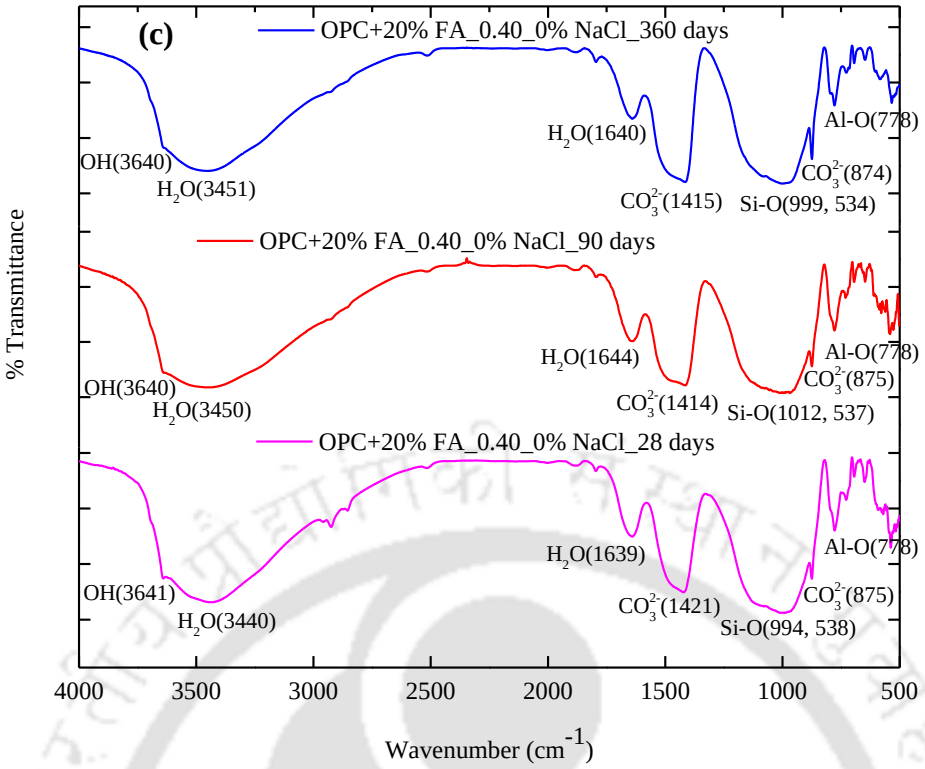

Fig. 5.20 FTIR spectra of SCC mixes admixed with 0% NaCl concentration for curing ages of 28, 90 and 360 days at w/b ratio of 0.40: (a) OPC, (b) PPC, and (c) OPC+20% FA

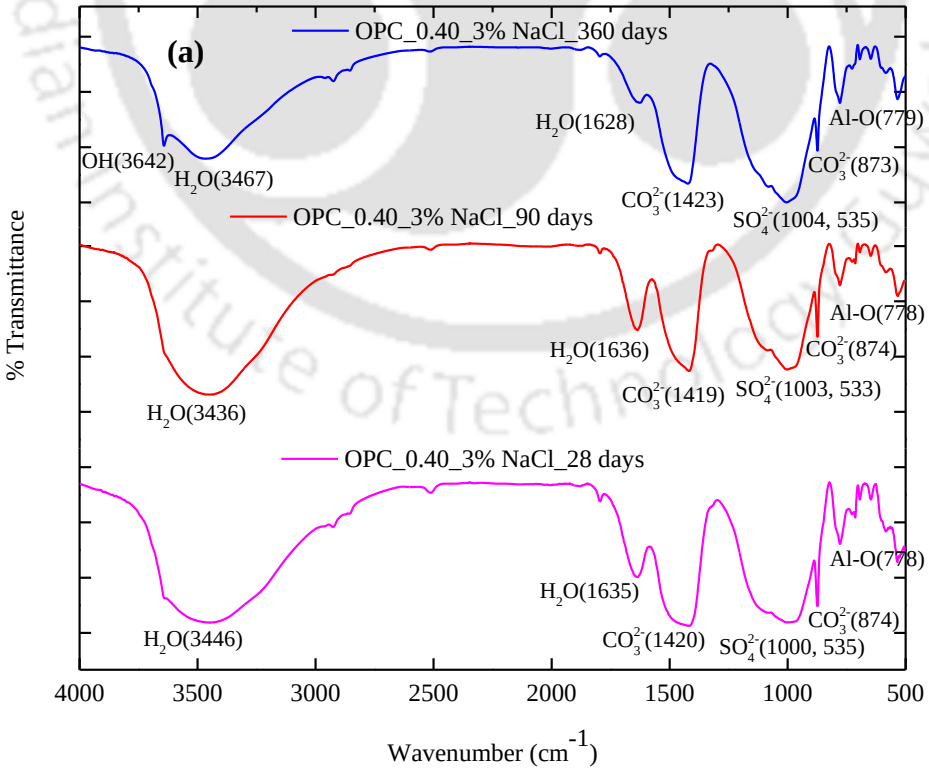

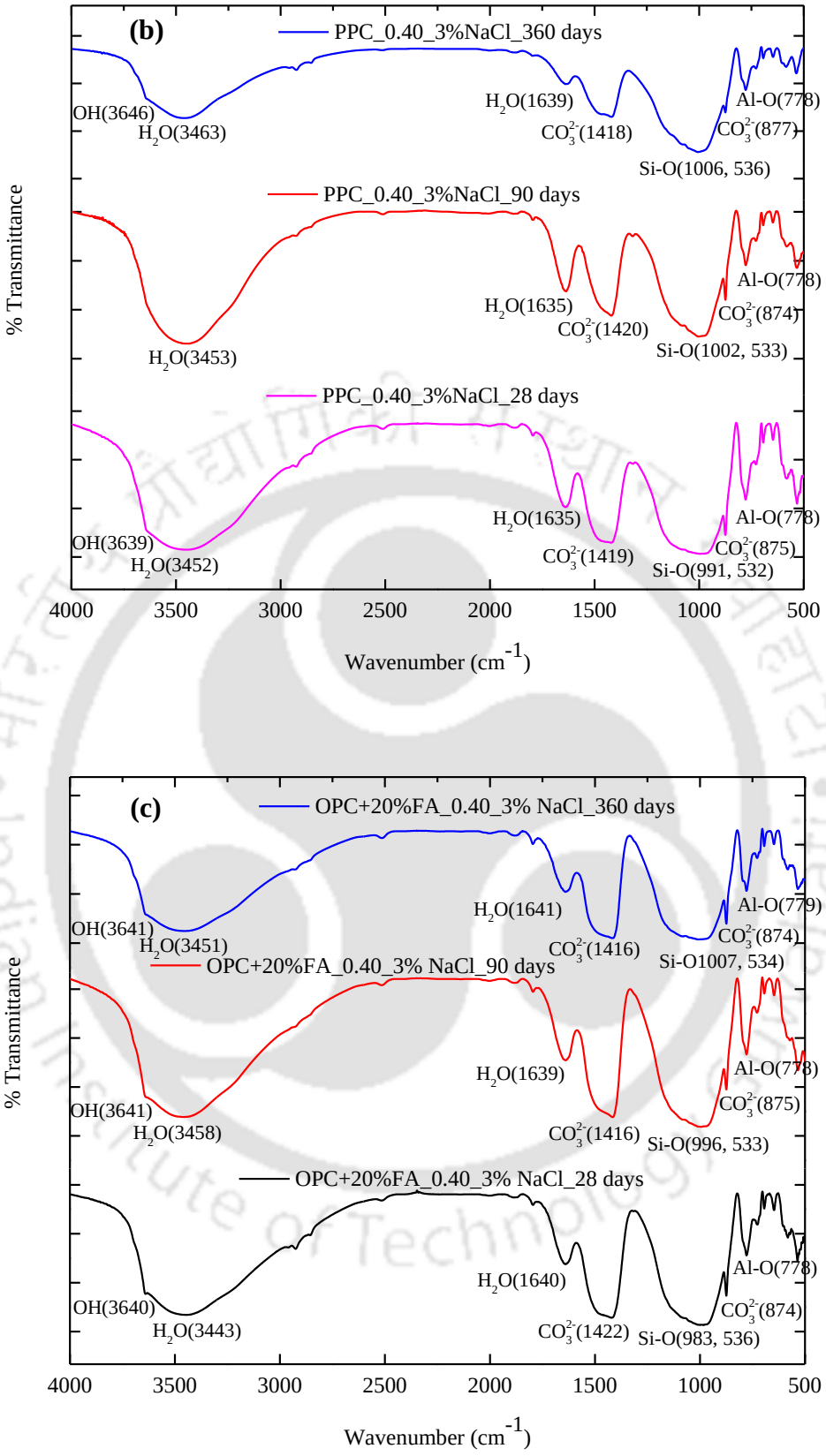

Fig. 5.21 FTIR spectra of SCC mixes admixed with 3% NaCl concentration for curing ages of 28, 90 and 360 days at w/b ratio of 0.40: (a) OPC, (b) PPC, and (c) OPC+20% FA

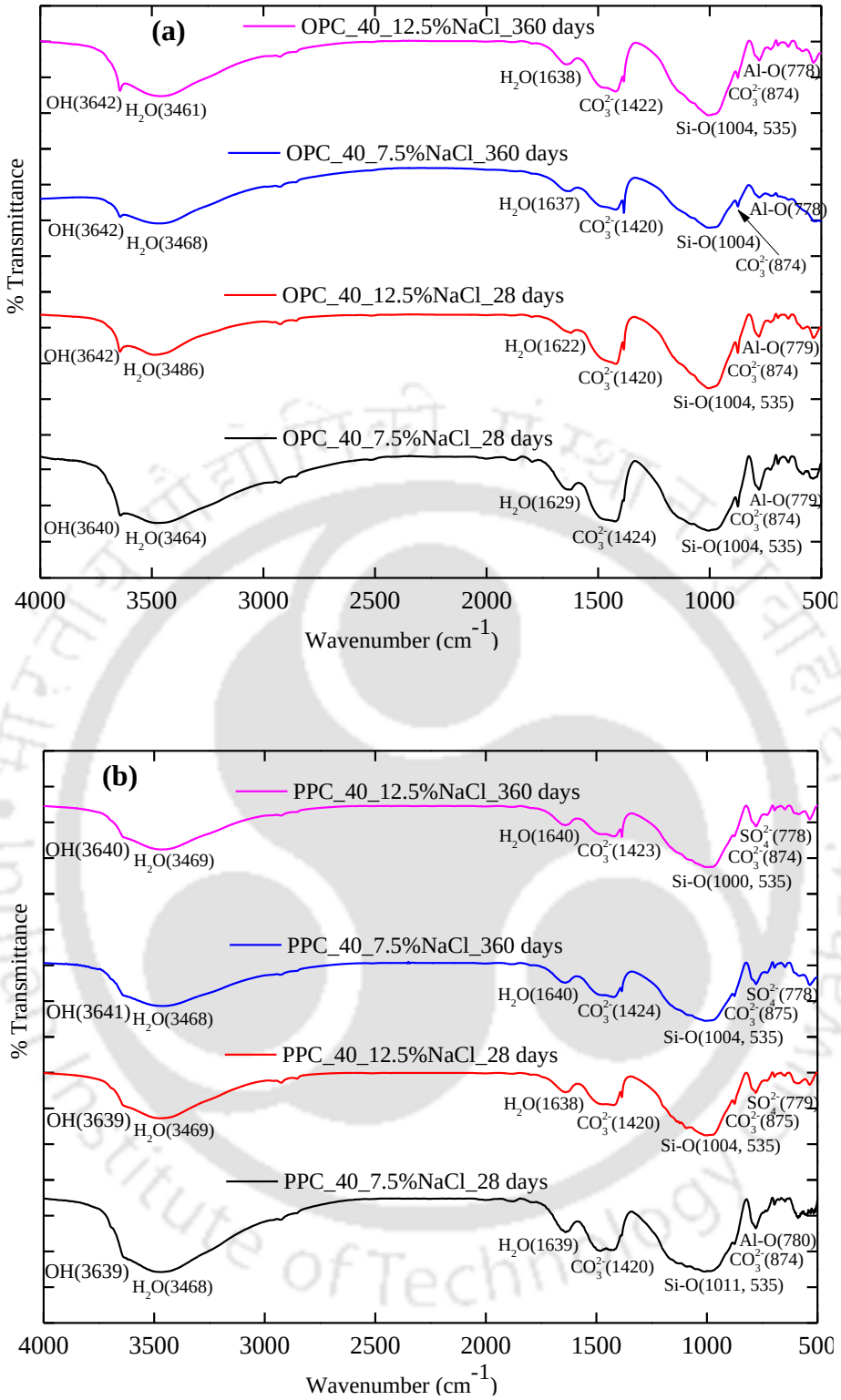

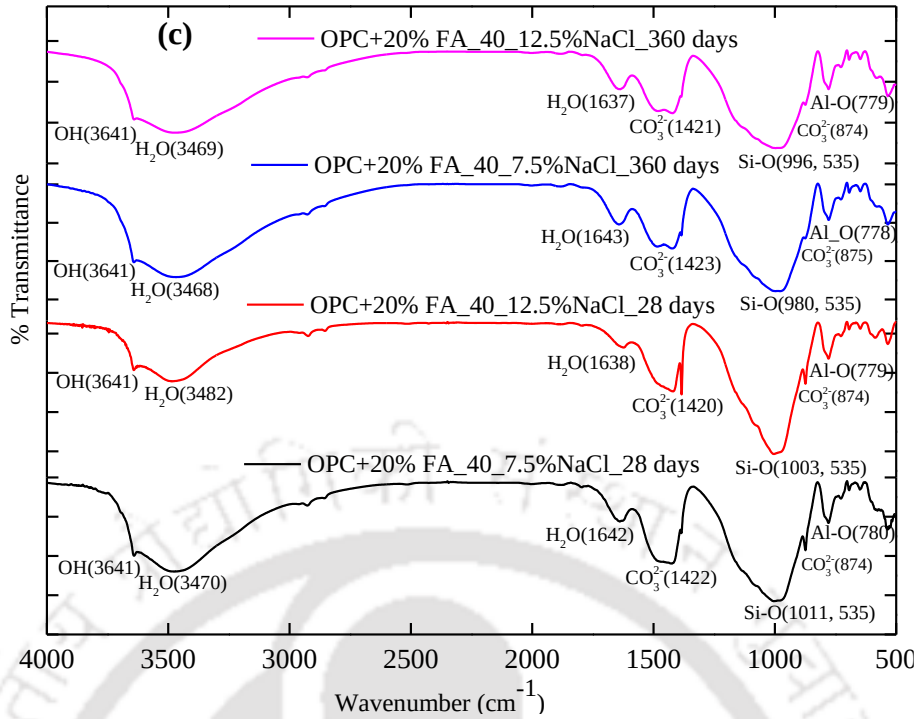

Fig. 5.22 FTIR spectra of SCC mixes admixed with NaCl concentrations of 7.5% and 12.5% for curing ages of 28 and 360 days at w/b ratio of 0.40: (a) OPC, (b) PPC, and (c) OPC+20% FA

5.6 Chloride analysis of SCC mixes

As stated earlier in Chapter 3, the free and total chloride concentrations of SCC mixes were determined using potentiometric titration. From the measured free and total chloride concentrations of SCC mixes, the bound chloride concentration was calculated as the difference between total chloride and free chloride concentrations. The free and bound chloride concentrations of OPC, PPC and OPC+20% FA based SCC mixes admixed with varying concentration of NaCl (1%, 3% and 5%) are shown in Fig. 5.23 (a - c), Fig. 5.24 (a - c), and Fig. 5.25 (a - c), respectively at the w/b ratio of 0.37, 0.40 and 0.43 for different curing ages. From these figures, it is observed that the SCC mixes made with PPC exhibited higher amount of free chloride as compared to those made with OPC at all concentrations of admixed NaCl, all w/b ratios and all curing ages. Between PPC and OPC+20% FA, the free chloride concentration was mostly higher in PPC based SCC mixes except few cases where there was higher free chloride concentration in OPC+20% FA as compared to that in PPC. Further from Fig. 5.23 to Fig. 5.25, it is inferred that the SCC mixes made with OPC showed higher bound chloride concentration as compared to those made from PPC. This indicates higher chloride binding in OPC than that in PPC mixes. The higher chloride

binding in SCC mixes made from OPC may be attributed to the dominant effect of formation of higher amount of CCA as compared to PPC based SCC mixes, which is confirmed form the XRD analysis (discussed earlier) wherein, the peak intensity and wt. % of calcium chloroaluminate (CCA) were higher in SCC mixes made from OPC as compared to that made from PPC at all concentrations of admixed NaCl, all w/b ratios and curing ages. In addition, from Fig. 5.23 to Fig. 5.25, it is inferred that the SCC mixes made from OPC showed higher bound chloride concentration as compared to those made from OPC+20% FA SCC mixes. The higher chloride binding in OPC mixes than that in OPC+20% FA mixes may be due to the dominant effect of physical binding of chloride ions with C-S-H to a greater extent than the chemical binding (binding of chloride ions with aluminate hydrates) in OPC based SCC mixes. It may be noted that there was formation of higher amount of C-S-H in OPC based SCC mixes than that in OPC+20% FA based SCC mixes as indicated by higher compressive strength of OPC mixes than that of OPC+20% FA mixes. Further, the peak intensity and wt. % of calcium chloroaluminate (CCA) were higher in SCC mixes made with OPC+20% FA as compared to that made with OPC (discussed earlier in Section 5.2).

From Fig. 5.23 to Fig. 5.25, it is inferred that the free chloride concentration increased and the bound chloride concentration decreased with increase in w/b ratio in all the SCC mixes. The higher bound chloride concentration at lower w/b ratio may be attributed to the dominant effect of physical binding of chloride ions with C-S-H to a greater extent because of the formation of higher amount of C-S-H due to higher binder content at lower w/b ratio. Further from Fig. 5.23 to Fig. 5.25, it is observed that the bound chloride concentration increased with increase in concentration of admixed NaCl. The increase in bound chloride concentration with increase in concentration of admixed NaCl is also confirmed from the XRD results wherein the peak intensity and wt. % of CCA were higher in the SCC mixes admixed with higher concentration of NaCl as compared to those admixed with lower concentration of NaCl.

Further, the bound chloride concentration increased and the free chloride concentration decreased with increase in curing age in all the SCC mixes as observed from Fig. 5.23 to Fig. 5.25. The increase in bound chloride concentration with increase in curing age may be due to the dominant effect of physical binding of chloride ions with C-S-H in the SCC mixes to a greater extent that resulted in lower free chloride concentration. It may be noted that the compressive strength of SCC mixes increased with the increase in curing age

irrespective of binder type, w/b ratio and admixed NaCl concentration, indicating the production of higher amount of C-S-H with increase in curing age.

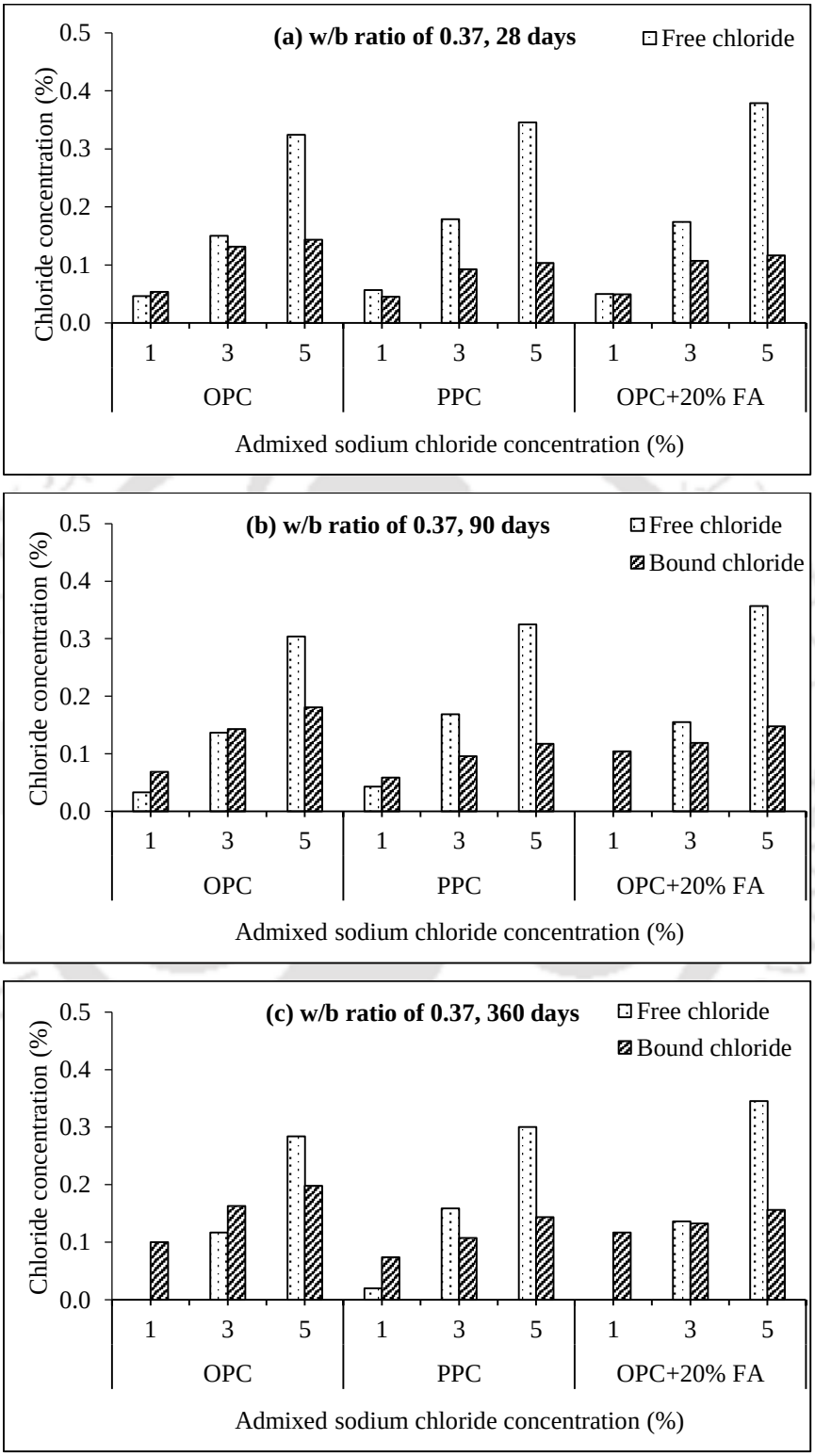

Fig. 5.23 Free and bound chloride concentrations of SCC mixes made with OPC, PPC and OPC+20% FA at w/b ratio of 0.37 and at curing ages of: (a) 28 days, (b) 90 days, and (c) 360 days

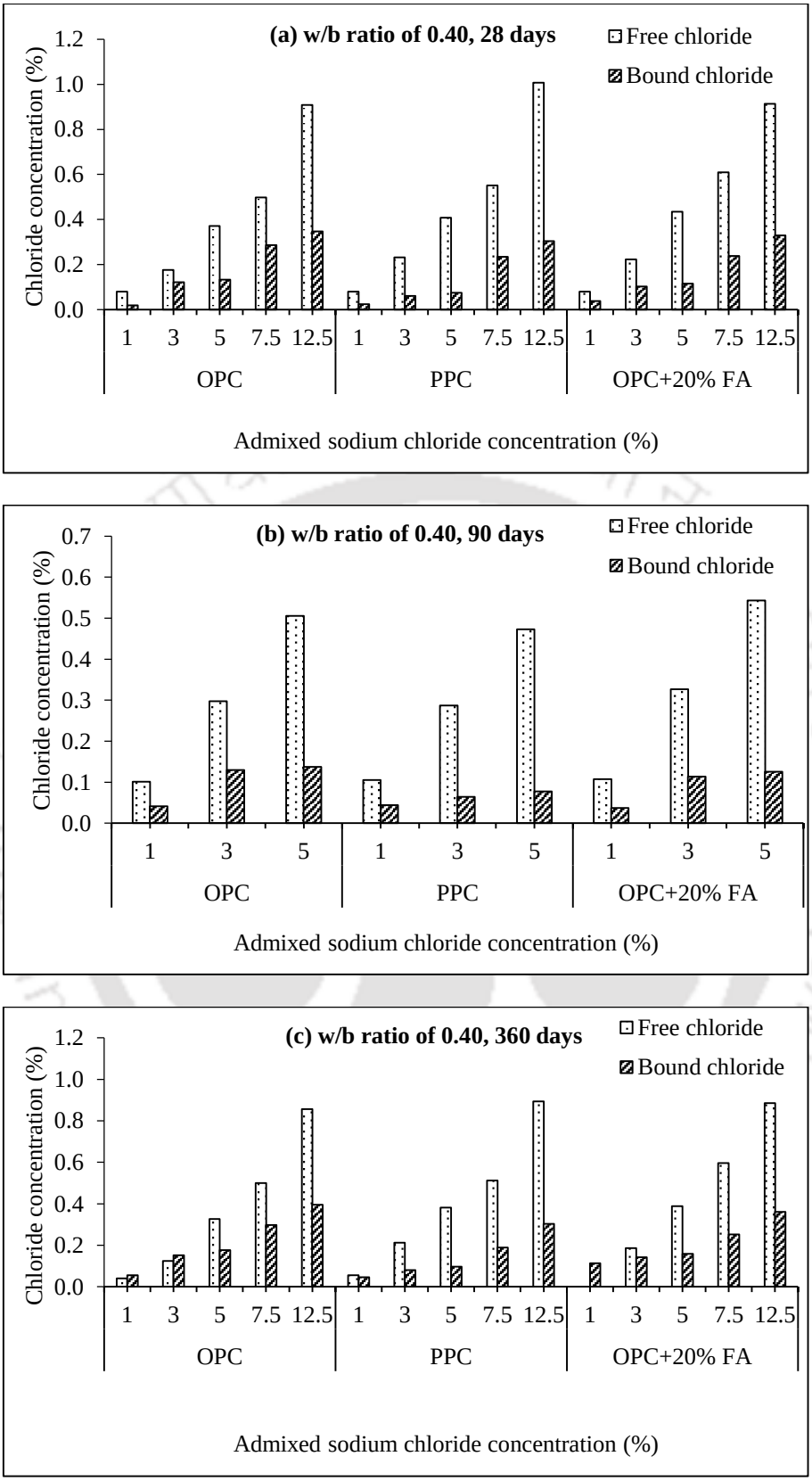

Fig. 5.24 Free and bound chloride concentrations of SCC mixes made with OPC, PPC and OPC+20% FA at w/b ratio of 0.40 and at curing ages of: (a) 28 days, (b) 90 days, and (c) 360 days

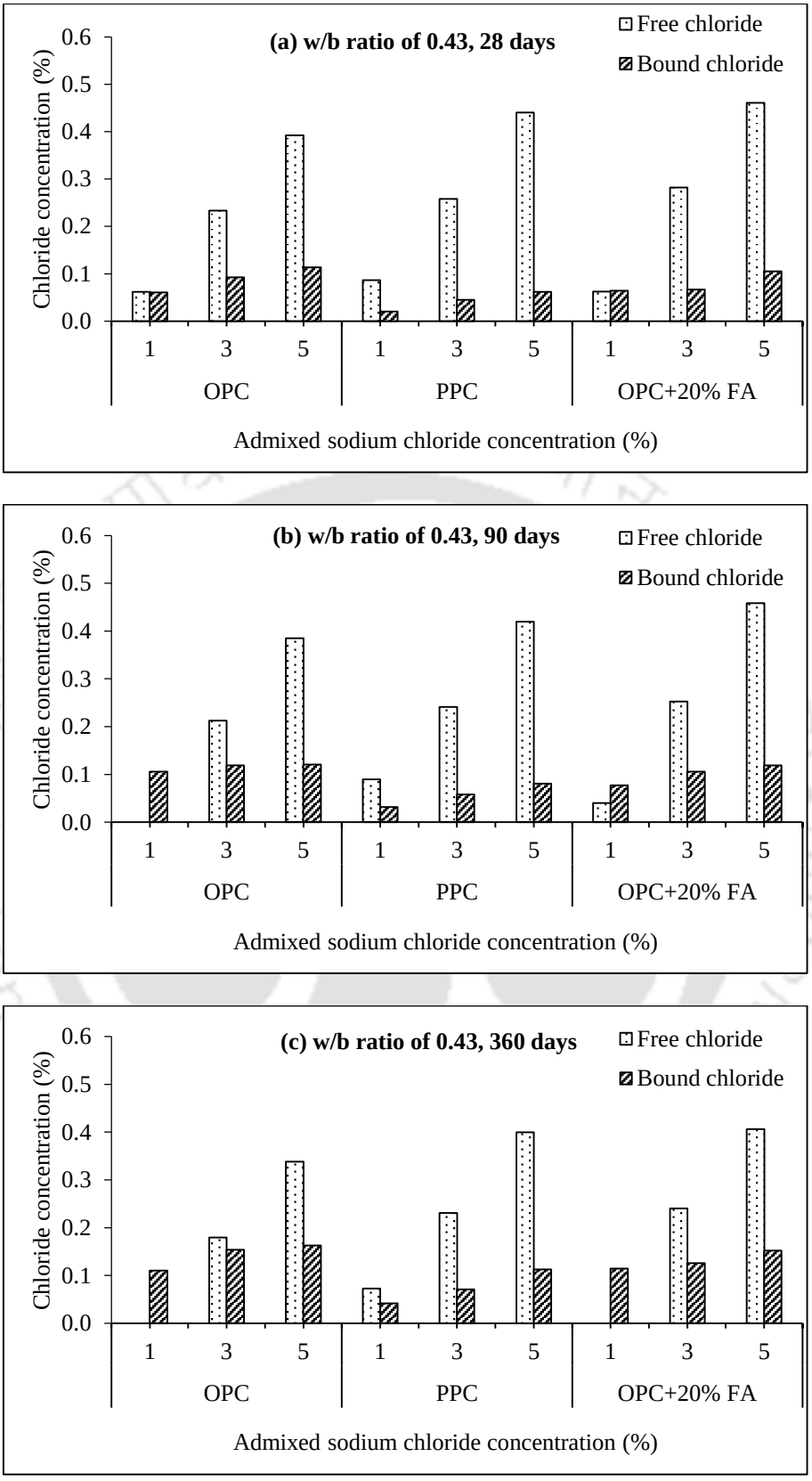

Fig. 5.25 Free and bound chloride concentrations of SCC mixes made with OPC, PPC and OPC+20% FA at w/b ratio of 0.43 and at curing ages of: (a) 28 days, (b) 90 days, and (c) 360 days

The obtained results of free and total chloride concentrations of OPC, PPC and OPC+20% FA based SCC mixes are shown in Fig. 5.26 (a) irrespective of w/b ratio, curing age and admixed NaCl concentration. Similarly, the results of free and total chloride concentrations of SCC mixes made with the w/b ratios of 0.37, 0.40 and 0.43 are shown in Fig. 5.26 (b) irrespective of binder type, curing age and admixed NaCl concentration, and that for curing ages of 28 days, 90 days and 360 days are shown and Fig. 5.26 (c) irrespective of binder type, w/b ratio and admixed NaCl concentration. The relationship between free chloride and total chloride concentrations is also shown in these figures. From Fig. 5.26, it is observed that there exists a strong linear relationship between free chloride and total chloride concentrations as indicated by higher value of regression coefficient (R^2). The obtained empirical relation between free and total chloride concentrations is as follows:

$$C_f = m \times C_t - n \tag{5.1}$$

Where C_f is the free chloride concentration, C_t is the total chloride concentration, and '*m*' and '*n*' are two constants. The term '*m*' represents the rate of increase of free chloride with total chloride concentration. From Fig. 5.26 (a), it is observed that the value of '*m*' is less for OPC (0.7215) as compared to that for OPC+20% FA (0.7835) followed by PPC (0.8293) based SCC mixes. The lower rate of increase in free chloride concentration with total chloride concentration in OPC based SCC mixes indicates higher chloride binding as compared to that in OPC+20% FA followed by PPC based SCC mixes. Further from Fig. 5.26 (b), it is observed that the slope of the linear relationship at w/b ratio of 0.37 (*m* = 0.7208) is less as compared to that at w/b ratio of 0.40 (*m* = 0.7668) followed by w/b ratio of 0.43 (*m* = 0.8165). This indicates higher chloride binding in SCC mixes at lower w/b ratio as compared that at higher w/b ratio. Fig. 5.26 (c) illustrates the effect of curing age on chloride binding of SCC mixes. As observed from this figure, the chloride binding in all the SCC mixes increased with curing age, as the rate of increase in free chloride concentration with total chloride concentration decreased with curing age as indicated by the slope (*m*) of the linear relationship.

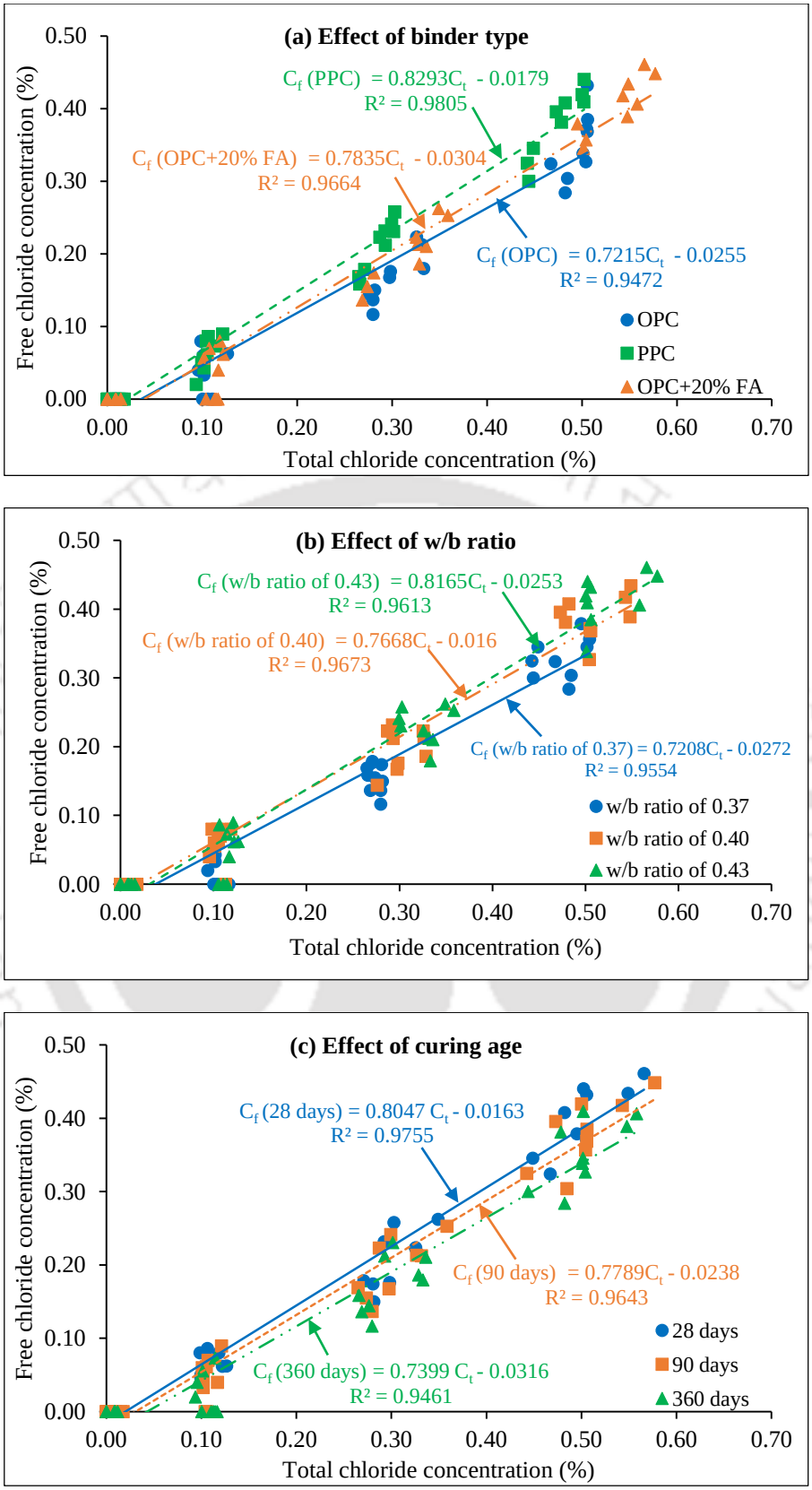

Fig. 5.26 Free chloride versus total chloride concentrations of SCC mixes: (a) Effect of binder type, (b) Effect of w/b ratio, and (c) Effect of curing age

5.7 pH value of SCC mixes

The obtained pH values of OPC, PPC and OPC+20% FA based SCC mixes admixed with varying concentrations of NaCl at w/b ratios of 0.37, 0.40 and 0.43 are presented in Table 5.6 for the curing ages of 28 days, 90 days and 360 days.

From Table 5.6, it is observed that the obtained pH values of aqueous solutions of OPC, PPC and OPC+20% FA based SCC mixes lie in the range of 12.05 - 12.74, 12.02 - 12.54 and 12.12 - 12.60, respectively, irrespective of w/b ratio, curing age and admixed NaCl concentration. From these values, it is inferred that the pH value of OPC based SCC mixes was higher as compared to that of PPC and OPC+20% FA based SCC mixes, which may attributed to dominat effect of availibility of higher amount of calicium hydroxide in OPC as compared to that in PPC and OPC+20% FA based SCC mixes. However in very few cases, i.e. in higher NaCl (7.5% and 12.5%) admixed SCC mixes at w/b ratio of 0.40, the pH value was higher in OPC+20% FA based SCC mixes as compared to that in OPC based SCC mixes. This indicates that in the presence of higher chloride concnetration, OPC+20% FA based SCC mixes showed relatively higher alkalinity as compared to OPC based SCC mixes.

Further from Table 5.6, it is observed that the SCC mixes admixed with NaCl showed lower pH value as compared to the control mix (i.e. the mix admixed with 0% NaCl). The lower pH of NaCl admixed SCC mixes may be attributed to the dominant effct of free chloride ions that might have affected the stable equilibrium of the alkali hydrates with the pore solution of concrete thus reducing its alkalinity. Further, the pH value of SCC mixes decreased with increase in admixed NaCl concentration as observed from Table 5.6.

From Table 5.6, it is inferred that the pH value of SCC mixes increased with decrease in w/b rtaio irrespective of binder type, admixed NaCl concnetrtaion and curing age. This may be due to the effect of formation of higher amount of alkali hydrates at higher binder content corresponding to lower w/b ratio and also due to the presence of lower amount of free chloride at lower w/b ratio in NaCl admixed SCC mixes. It may be noted that free chloride concentration was lower in the SCC mixes made with lower wb ratio as compared to that made with higher w/b ratio (already stated in Section 5.6). Further, it is noted that the pH value of all the SCC mixes increased with increase in curing age as evident from Table 5.6. The increase in pH value of NaCl admixed SCC mixes with increase in curing age is attributed to the dominant effect of the reduced free chloride cocentration at longer curing age as the chloirde binding increased with curing age that enhanced the alkalinity of

concrete. In case of control SCC mixes, the increase in pH value with curing age is ascribed to the effect of the formation of higher amount of alkali hydrates in concrete with the increase in curing age.

Table 5.6 pH value of SCC mixes made with OPC, PPC and OPC+20% FA at w/b ratios of 0.37, 0.40 and 0.43, for curing ages of 28 days, 90 days and 360 days

Binder type	w/b ratio	Curing age	0% NaCl	1% NaCl	3% NaCl	5% NaCl	7.5% NaCl	12.5% NaCl
OPC	w/b ratio of 0.37	28 days	12.49	12.46	12.44	12.43	-	-
		90 days	12.72	12.67	12.58	12.55	-	-
		360 days	12.74	12.72	12.69	12.63	-	-
	w/b ratio of 0.40	28 days	12.48	12.42	12.4	12.39	12.19	12.12
		90 days	12.66	12.62	12.57	12.51	-	-
		360 days	12.7	12.69	12.67	12.63	12.17	12.05
	w/b ratio of 0.43	28 days	12.44	12.4	12.39	12.35	-	-
		90 days	12.62	12.6	12.51	12.46	-	-
		360 days	12.69	12.67	12.63	12.6	-	-
PPC	w/b ratio of 0.37	28 days	12.35	12.32	12.26	12.21	-	-
		90 days	12.44	12.37	12.36	12.36	-	-
		360 days	12.54	12.48	12.47	12.42	-	-
	w/b ratio of 0.40	28 days	12.35	12.31	12.13	12.06	12.1	12.06
		90 days	12.37	12.32	12.27	12.36	-	-
		360 days	12.47	12.44	12.4	12.37	12.04	12.02
	w/b ratio of 0.43	28 days	12.29	12.21	12.21	12.03	-	-
		90 days	12.37	12.34	12.32	12.3	-	-
		360 days	12.39	12.38	12.36	12.34	-	-
OPC+20 % FA	w/b ratio of 0.37	28 days	12.47	12.46	12.41	12.39	-	-
		90 days	12.53	12.47	12.45	12.44	-	-
		360 days	12.62	12.6	12.57	12.53	-	-
	w/b ratio of 0.40	28 days	12.44	12.39	12.34	12.31	12.25	12.21
		90 days	12.5	12.43	12.37	12.33	-	-
		360 days	12.58	12.53	12.51	12.5	12.2	12.12
	w/b ratio of 0.43	28 days	12.39	12.34	12.3	12.15	-	-
		90 days	12.43	12.35	12.29	12.23	-	-
		360 days	12.48	12.38	12.33	12.28	-	-

Note: "-": not measured.

5.8 Summary

The results obtained from XRD, TGA, FESEM and FTIR analyses indicated that NaCl admixed at various concentrations influenced the microstructure and thermal behaviour of SCC mixes made with different types of binder and w/b ratios for all curing ages. The peak intensity and wt. % (estimated using RIR method) of calcium chloroaluminate (CCA), calcium hydroxide (CH), ettringite (E) and gypsum (G) obtained from the XRD patterns indicated the variations in their formations in the SCC mixes with respect to binder type, w/b ratio and admixed NaCl concentration at different curing ages. The formation of calcium chloroaluminate (CCA) was higher in SCC mixes made with OPC+20% FA as compared to those made with OPC and PPC at all concentrations of admixed NaCl and w/b ratios for all the curing ages as indicated by XRD analysis. Further, the XRD results indicated that there was formation of higher amount of CCA in the SCC mixes admixed with 5% NaCl as compared to that admixed with 3% NaCl followed by 1% NaCl for all binders, w/b ratios and curing ages. In addition, the formation of CCA in the SCC mixes increased with increase in w/b ratio. The XRD analysis showed that there was no systematic variation in the formation of gypsum and ettringite with binder type, w/b ratio and curing age in NaCl admixed SCC mixes.

From the XRD analysis, it is inferred that the peak intensity and wt. % of calcium hydroxide (CH) was lower in PPC and OPC+20% FA based SCC mixes as compared to that in OPC based SCC mixes. Further, the CH content (wt. %) was higher in the SCC mixes made with lower w/b ratio as compared to that made with higher w/b ratio in control (0% NaCl) SCC mixes, whereas there was no systematic variation in wt. % of CH in the SCC mixes admixed with different concentrations of NaCl. In addition, the CH content was higher in the SCC mixes made with 0% NaCl (control mix) as compared to that in NaCl admixed SCC mixes as observed from XRD patterns and results of semi-quantitative analysis (wt. %). From the XRD patterns and wt. %, it is inferred that the CH content increased with curing age in the SCC mixes made with OPC, whereas that deceased with curing age in the SCC mixes made with PPC and OPC+20% FA. The variations in formation of calcium hydroxide (CH) with binder type, curing age, admixed NaCl and w/b ratio as indicated by the XRD results are well explained by the CH content calculated from the mass loss in TGA as a result of its dehydration. While evaluating the effect of admixed NaCl, it is inferred that mass loss was higher in NaCl admixed SCC mixes as compared to that in control mix (0% NaCl) for all binders, w/b ratios and curing ages and the mass loss mostly increased in the SCC mixes

with increase in admixed NaCl concentration. Further, the total mass loss mostly increased with curing age in OPC based SCC mixes, whereas it decreased with curing age in PPC and OPC+20% FA based SCC mixes. The formation of C-S-H (calcium silicate hydrate), calcium hydroxide, calcium chloroaluminate and ettringite in the SCC mixes is evident from the FESEM images, which further corroborates the results of XRD analysis. The obtained FTIR spectra of SCC mixes indicated the functional groups such as -OH, CO_3^{2-} , Si-O and Al-O, which are associated with various compounds formed in SCC mixes.

The chloride binding as indicated by bound chloride concentration was higher in OPC based SCC mixes as compared to that in OPC+20% FA and PPC based SCC mixes. Further the bound chloride concentration increased with decrease in w/b ratio and with increase in curing age in all the SCC mixes. In addition, the bound chloride concentration increased with increase in concentration of admixed NaCl in the SCC mixes, which corroborates the variations in peak intensity and wt. % of CCA (XRD analysis) with admixed NaCl concentration. A strong linear relationship exists between free chloride and total chloride concentrations in the SCC mixes. The rate of increase in free chloride concentration with total chloride concentration as indicated by the slope of linear relationship was lower in OPC as compared to that in OPC+20% FA followed by PPC based SCC mixes. Similarly, the rate of increase in free chloride concentration with total chloride concentration decreased with decrease in w/b ratio and with increase in curing age in all the SCC mixes. From the results of pH, it is observed that the binder type, w/b ratio, admixed NaCl concentration and curing age affected the alkalinity of SCC mixes.

CHAPTER 6

CORROSION PERFORMANCE OF STEEL REINFORCEMENT IN SCC AGAINST INTERNAL CHLORIDE

6.1 General

This chapter discusses the results of the investigation carried out to evaluate the corrosion performance of steel reinforcement in self-compacting concrete against internal chloride. For internal chloride, the SCC mixes were admixed with different concentrations of NaCl during the time of preparation (discussed in Chapter 3). It may be noted that the prismatic specimens with a centrally embedded reinforcing steel bar were prepared from SCC mixes for determining the corrosion parameters. For evaluating the corrosion performance of steel reinforcement, the corrosion potential by half-cell potential measurement and corrosion current density by linear polarization resistance (LPR) measurement were determined. From the obtained results, the effects of binder type, w/b ratio, admixed chloride concentration and exposure duration as well as exposure condition on the corrosion performance of steel reinforcement in SCC were evaluated.

6.2 Corrosion potential of steel reinforcement in SCC

The half-cell potential measurement was carried out to determine the probability of occurrence of steel reinforcement corrosion in SCC mixes. The prismatic specimens were prepared from SCC mixes using OPC, PPC and OPC+20% FA at the w/b ratios of 0.37, 0.40 and 0.43 and admixed with different concentrations of NaCl (details already presented in Chapter 3). As mentioned in Chapter 3, two types of exposure condition were adopted for the specimens admixed with internal chloride i.e. laboratory drying (air curing) and water curing. For laboratory drying, the prismatic specimens were kept in the ambient laboratory condition for a period of 540 days and the corrosion potential was measured at regular intervals of 90 days up to 540 days. For water curing, the prismatic specimens were partially immersed in normal water with alternate wetting-drying cycles. After 450 days of exposure to normal water, the same specimens were further exposed to 5% NaCl solution with alternate wetting-drying cycles for another 240 days. For water curing condition, the corrosion potential was measured at regular intervals of 90 days up to 630 days followed by measuring at the end of exposure period i.e. at 690 days.

6.2.1 Effect of laboratory drying (air curing) on corrosion potential of SCC mixes

For laboratory drying (air curing) condition, the results of corrosion potential (E_0) of SCC specimens made with OPC, PPC and OPC+20% FA and admixed with different concentrations of NaCl (0%, 1%, 3% and 5%) at w/b ratios of 0.37, 0.40 and 0.43 are shown in Fig. 6.1, Fig. 6.2, and Fig. 6.3, respectively. Similarly, the corrosion potential values of the specimens made with w/b ratio of 0.40 and admixed with NaCl concentrations of 7.5% and 12.5% are shown in Fig. 6.4 for laboratory drying condition. Each value of corrosion potential shown in these figures is the average values of four replicate prismatic specimens.

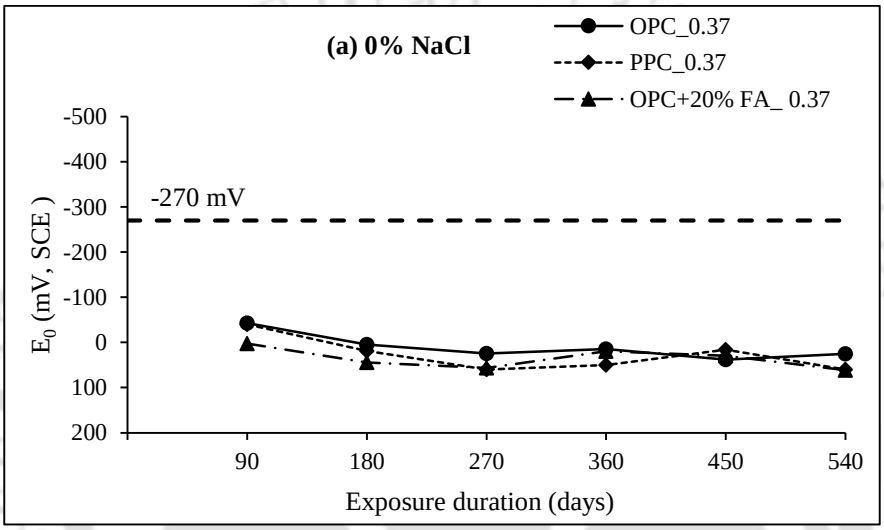

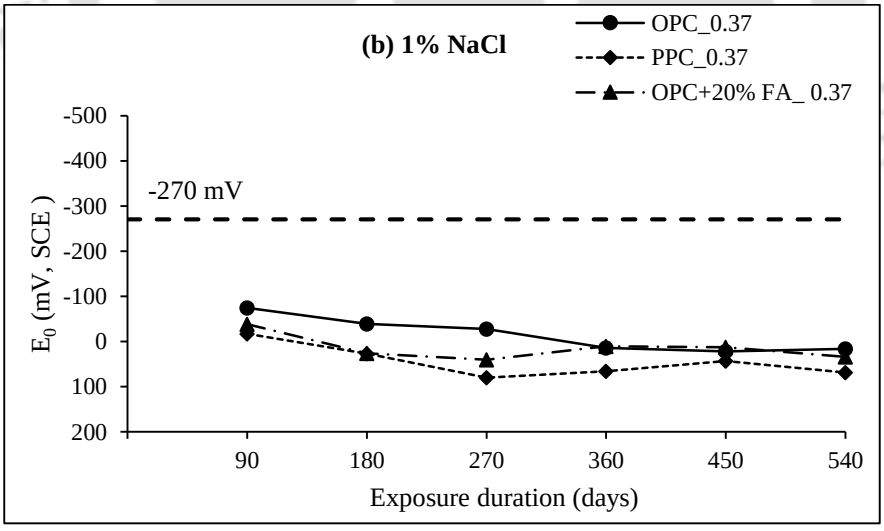

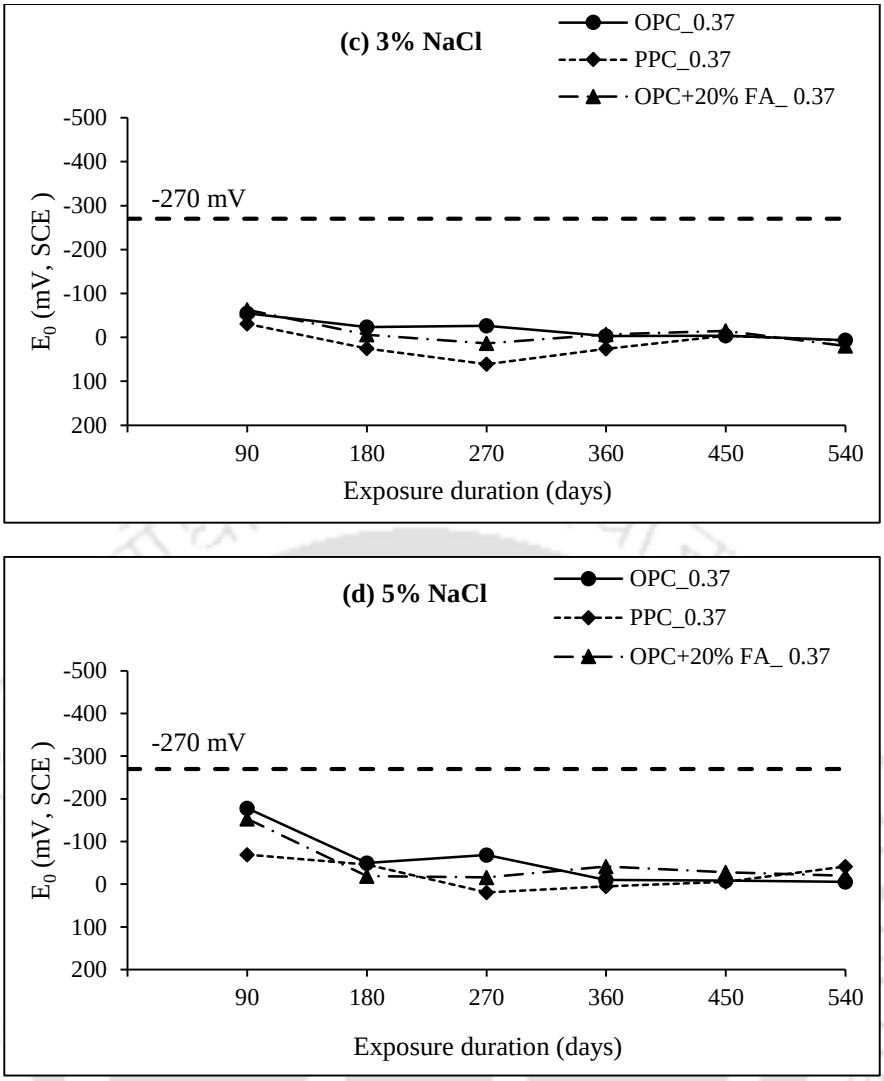

Fig. 6.1 Corrosion potential (E_0) of steel reinforcement in SCC mixes made with OPC, PPC and OPC+20% FA and w/b ratio of 0.37 for admixed NaCl concentrations of (a) 0% NaCl, (b) 1% NaCl, (c) 3% NaCl, and (d) 5 % NaCl, for air curing condition

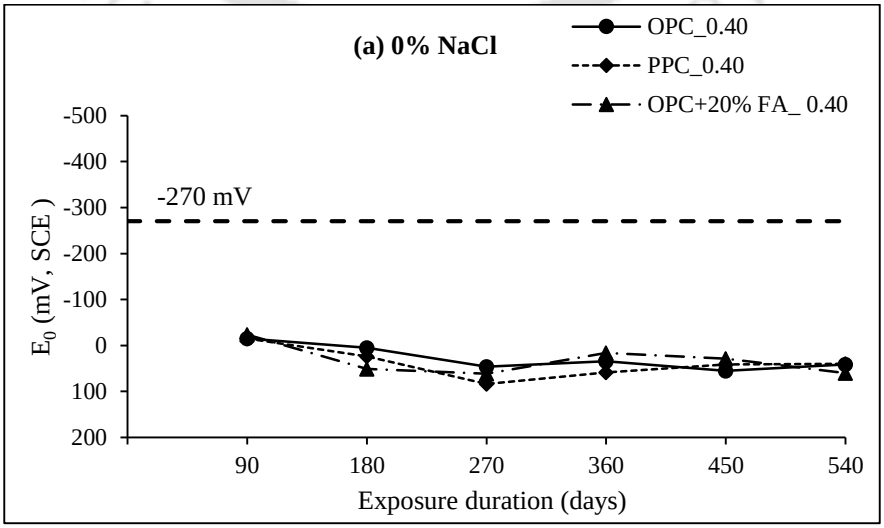

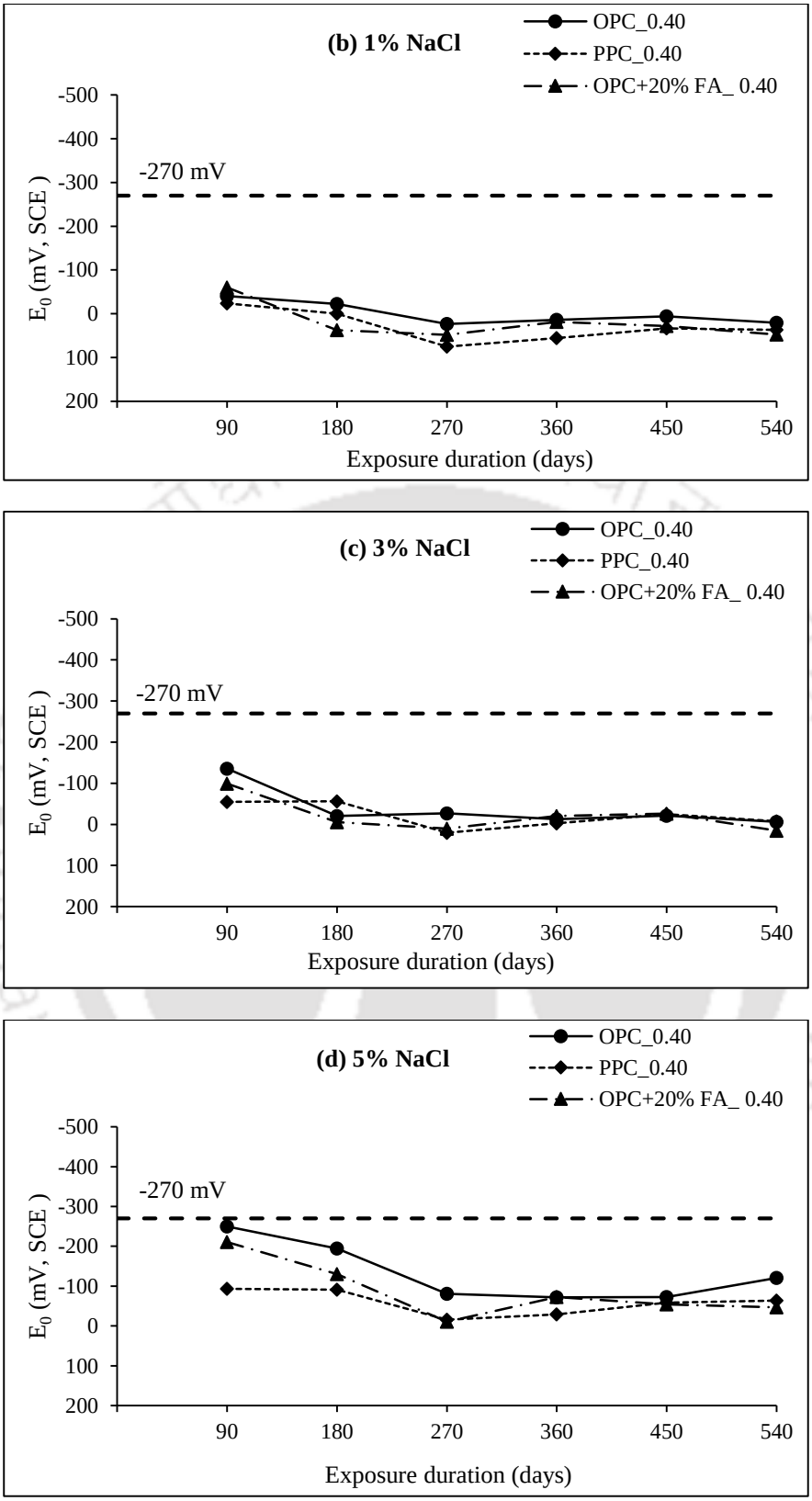

Fig. 6.2 Corrosion potential (E_0) of steel reinforcement in SCC mixes made with OPC, PPC and OPC+20% FA and w/b ratio of 0.40 for admixed NaCl concentrations of (a) 0% NaCl, (b) 1% NaCl, (c) 3% NaCl, and (d) 5 % NaCl, for air curing condition

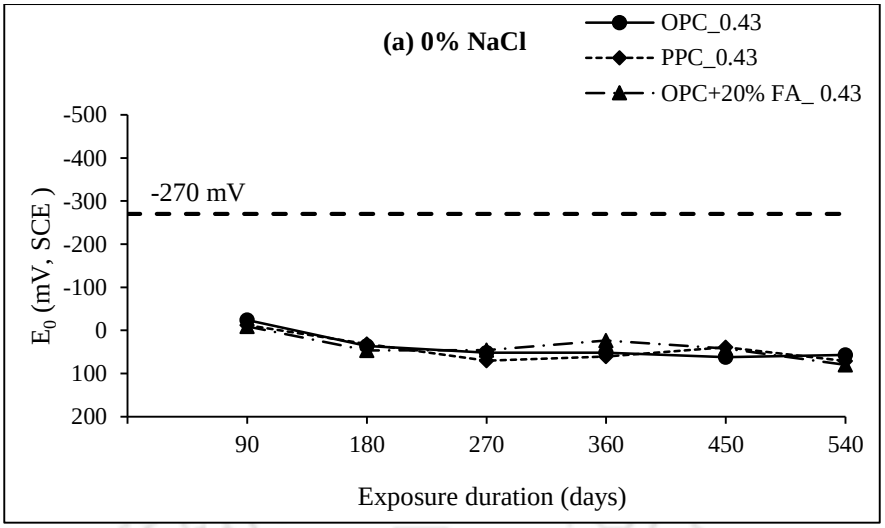
(a) 0% NaCl
OPC_0.43
PPC_0.43
OPC+20% FA_ 0.43
-270 mV
E0 (mV, SCE)
-500
-400
-300
-200
-100
0
100
200
90
180
270
360
450
540
Exposure duration (days)

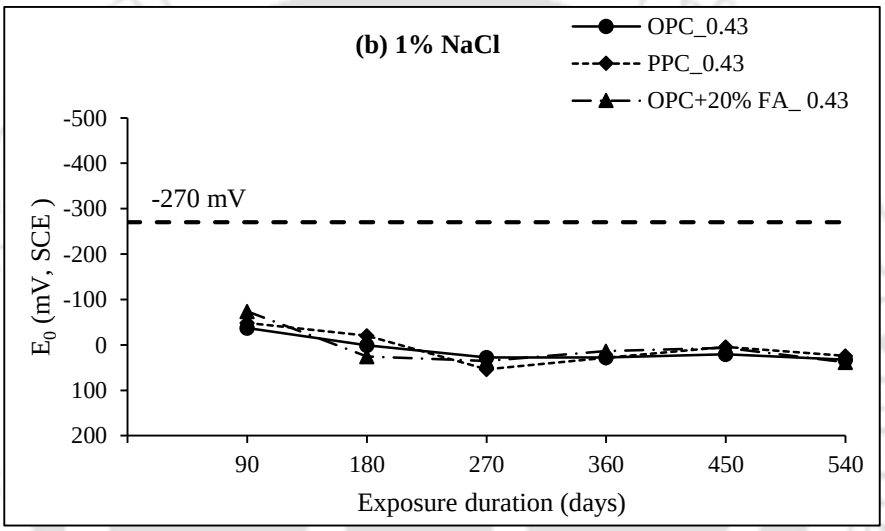
(b) 1% NaCl
OPC_0.43
PPC_0.43
OPC+20% FA_ 0.43
-270 mV
E0 (mV, SCE)
-500
-400
-300
-200
-100
0
100
200
90
180
270
360
450
540
Exposure duration (days)

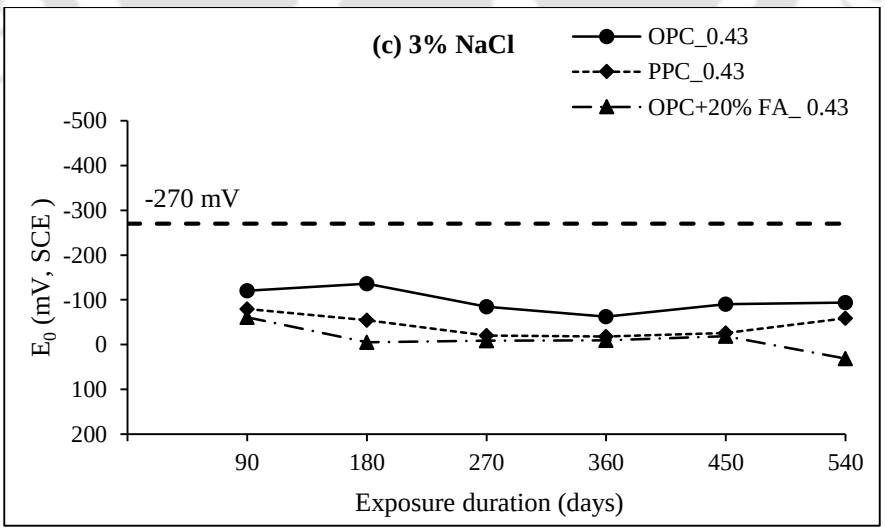
(c) 3% NaCl
OPC_0.43
PPC_0.43
OPC+20% FA_ 0.43
-270 mV
E0 (mV, SCE)
-500
-400
-300
-200
-100
0
100
200
90
180
270
360
450
540
Exposure duration (days)

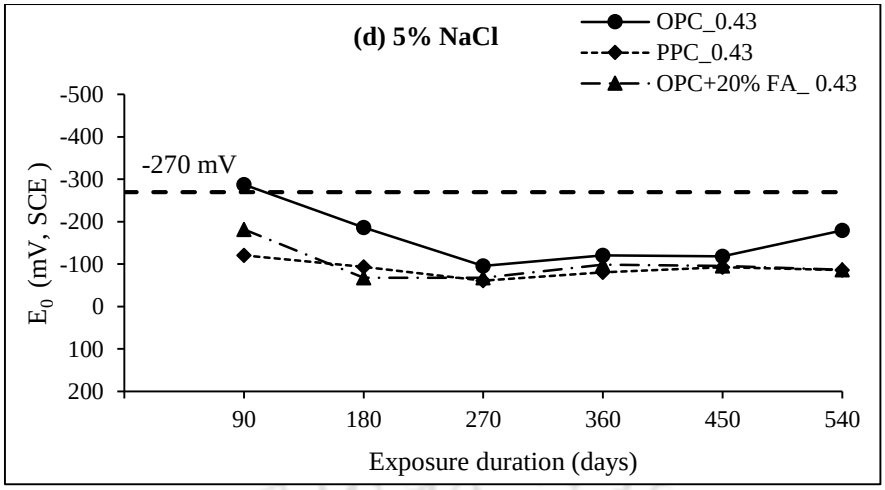

Fig. 6.3 Corrosion potential (E_0) of steel reinforcement in SCC mixes made with OPC, PPC and OPC+20% FA and w/b ratio of 0.43 for admixed NaCl concentrations of (a) 0% NaCl, (b) 1% NaCl, (c) 3% NaCl, and (d) 5 % NaCl, for air curing condition

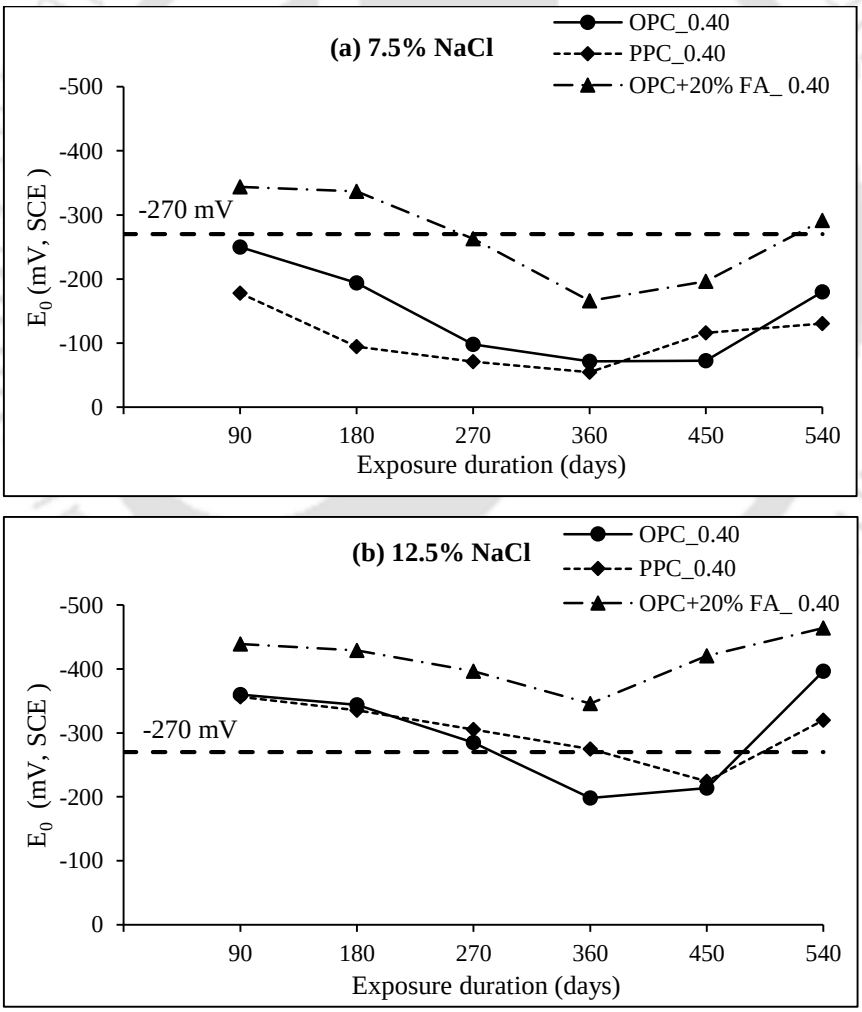

Fig. 6.4 Corrosion potential (E_0) of steel reinforcement in SCC mixes made with OPC, PPC and OPC+20% FA and w/b ratio of 0.40 for admixed NaCl concentrations of (a) 7.5% NaCl and (b) 12.5% NaCl, for air curing condition

As per ASTM C876-15 [139], the potential values more negative than -350 mV ($Cu/CuSO_4$ electrode)/-270 mV (SCE) correspond to greater than 90% probability of occurrence of steel reinforcement corrosion. From Fig. 6.1 to Fig. 6.3, it is inferred that the corrosion potential values were less negative than -270 mV (SCE) in all the SCC mixes irrespective of admixed NaCl concentration till the period of 540 days of laboratory drying exposure, which indicates lower probability of occurrence of steel reinforcement corrosion in all the SCC mixes. Further, in the SCC mixes admixed with 7.5% and 12.5% NaCl concentrations, the corrosion potential values were more negative than -270 mV (SCE) in few cases for 7.5% NaCl concentration, and in majority of the cases for 12.5% NaCl concentration as observed from Fig. 6.4. This indicates that the presence of higher amount of chloride ions increased probability of occurrence of steel reinforcement corrosion in SCC mixes.

While comparing the effect of binder type, it is observed that the variation in corrosion potential values among the binder type is not systematic as well as not significant for the admixed NaCl concentrations till 5% as observed from Fig. 6.1 to Fig. 6.3. However, in some cases the corrosion potential values were more negative in OPC based SCC mixes as compared to that in PPC and OPC+20% FA based SCC mixes. At higher concentrations of admixed NaCl (7.5% and 12.5%) for the w/b ratio of 0.40, the corrosion potential values of steel reinforcement were more negative in OPC+20% FA based SCC mixes as compared to that in OPC and PPC based SCC mixes as observed from Fig. 6.4. In addition, the corrosion potential values were more negative than -270 mV (SCE) in OPC +20% FA based SCC mixes in majority of the cases as compared to that in OPC and PPC based SCC mixes. This may be attributed to the higher concentration of iron ions in the electrolytic pore solution of the concrete [35,117] made with OPC+20% FA as compared to those made from OPC and PPC.

From Fig. 6.1 to Fig. 6.4, it is noted that the corrosion potential values became more negative with increase in admixed NaCl concentration in all the SCC mixes up to the exposure duration of 540 days. This indicates greater probability of occurrence of steel reinforcement corrosion, which may be attributed to the increase in free chloride concentration in the vicinity of steel reinforcement embedded in SCC specimens with increase in concentration of NaCl. Further, it is observed that the difference in corrosion potential values among w/b ratios was very less and not systematic as observed from Fig. 6.1 to Fig. 6.3. While analyzing the variation in corrosion potential with increase in exposure duration, it is observed that mostly there is no systematic variation in corrosion

potential with increase in exposure period although the corrosion potential was slightly more negative at the early exposure period for NaCl concentrations of 0%, 1%, 3% and 5% as evident from Fig 6.1 to Fig. 6.3. From Fig. 6.4, it is noted that the corrosion potential was more negative during the early exposure periods, however it became less negative afterwards followed by becoming more negative again with increase in exposure period for all the binders at w/b ratio of 0.40. This variation in corrosion potential with increase in exposure period may be attributed to the alteration in the free chloride concentration near the steel reinforcement level in concrete.

6.2.2 Effect of water curing on corrosion potential

As stated earlier for water curing, the prismatic specimens were partially immersed in normal water with alternate wetting-drying cycles for a period of 450 days followed by exposure to 5% NaCl solution with alternate wetting-drying cycles for another 240 days. For water curing condition, the corrosion potential values of steel reinforcement in SCC specimens made with the w/b ratios of 0.37, 0.40 and 0.43 are shown in Fig. 6.5, Fig. 6.6 and Fig. 6.7, respectively for all binders (OPC, PPC and OPC+20% FA) and admixed NaCl concentrations of 1%, 3% and 5%. Each potential value shown in these figures is the average values of four replicate prismatic specimens.

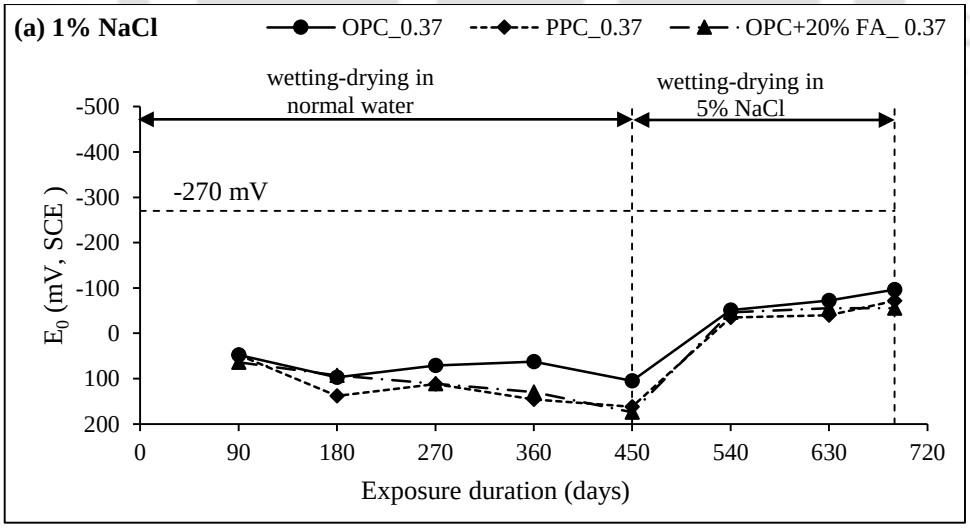

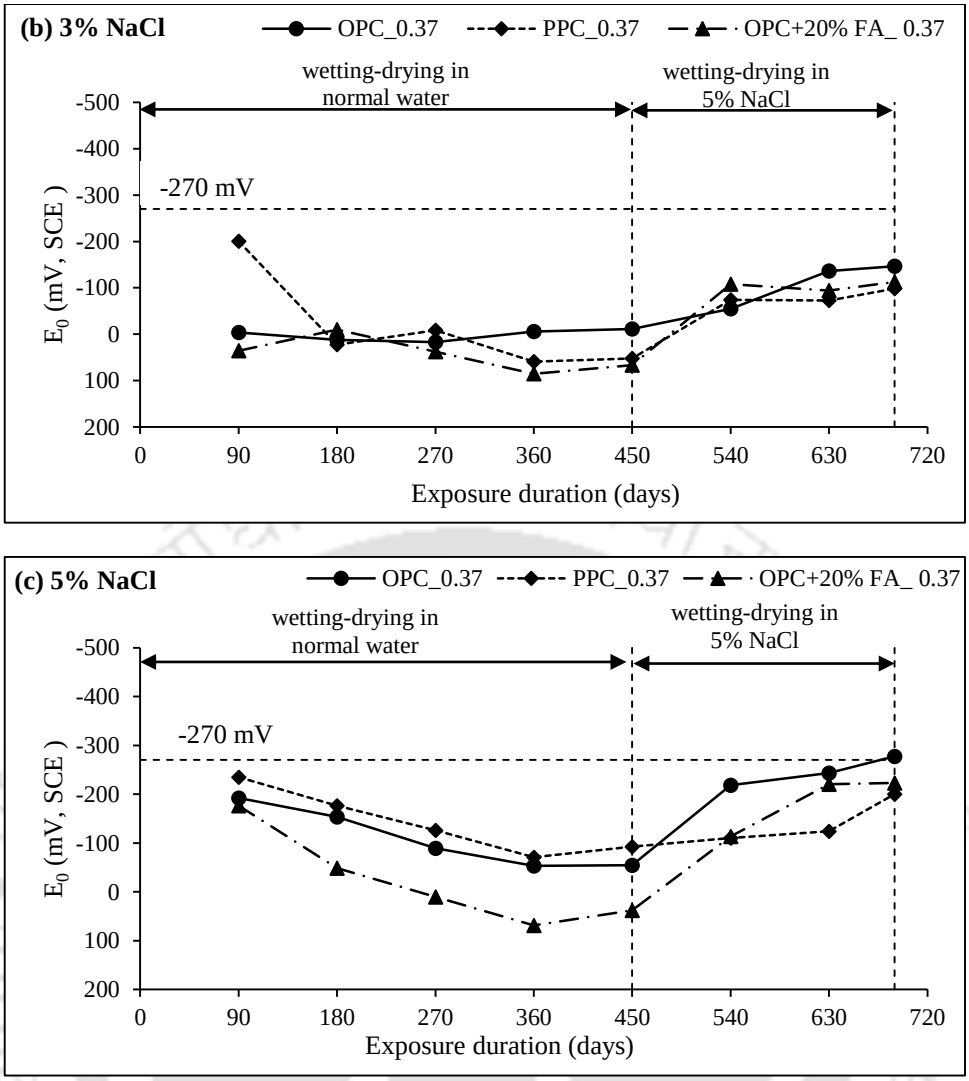

Fig. 6.5 Corrosion potential (E_0) of steel reinforcement in SCC mixes made with OPC, PPC and OPC+20% FA and w/b ratio of 0.37 for admixed NaCl concentrations of (a) 1% NaCl, (b) 3% NaCl, and (c) 5% NaCl, for water curing condition

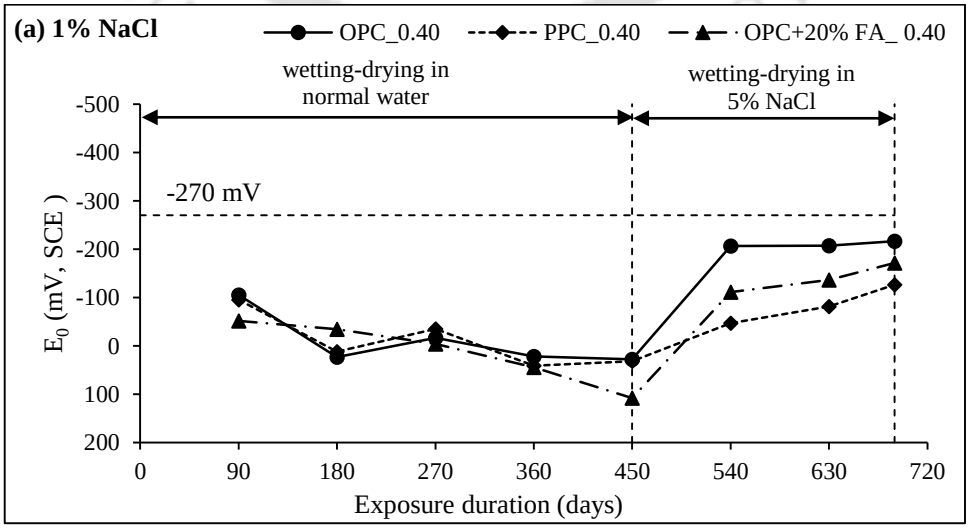

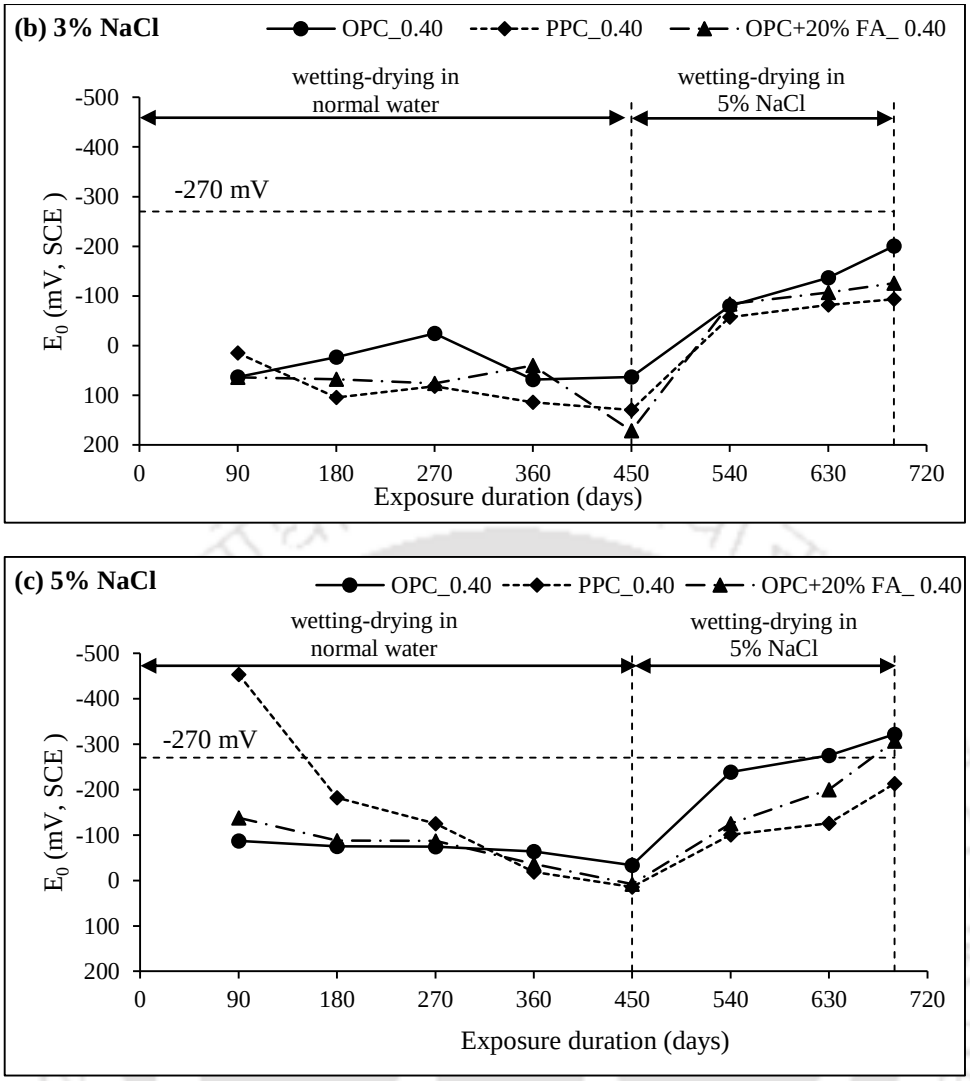

Fig. 6.6 Corrosion potential (E_0) of steel reinforcement in SCC mixes made with OPC, PPC and OPC+20% FA and w/b ratio of 0.40 for admixed NaCl concentrations of ((a) 1% NaCl, (b) 3% NaCl, and (c) 5% NaCl, for water curing condition

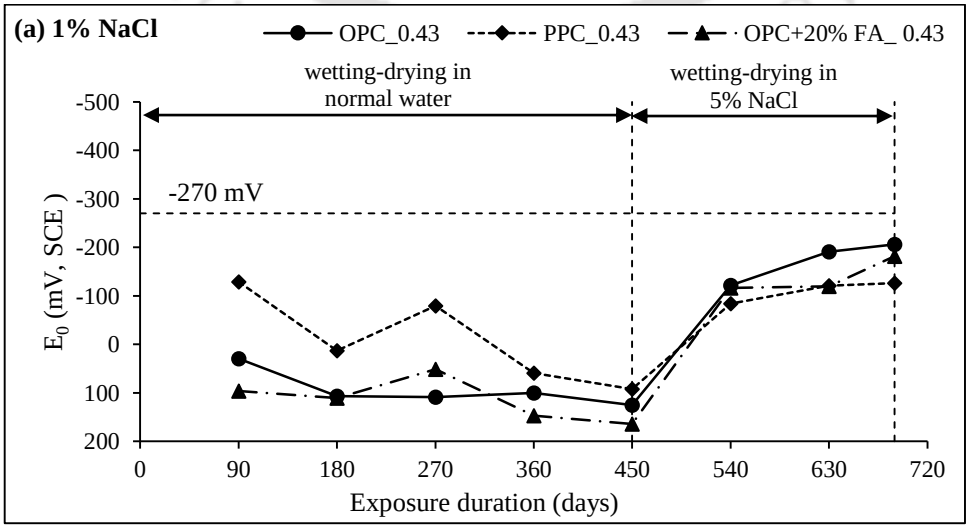

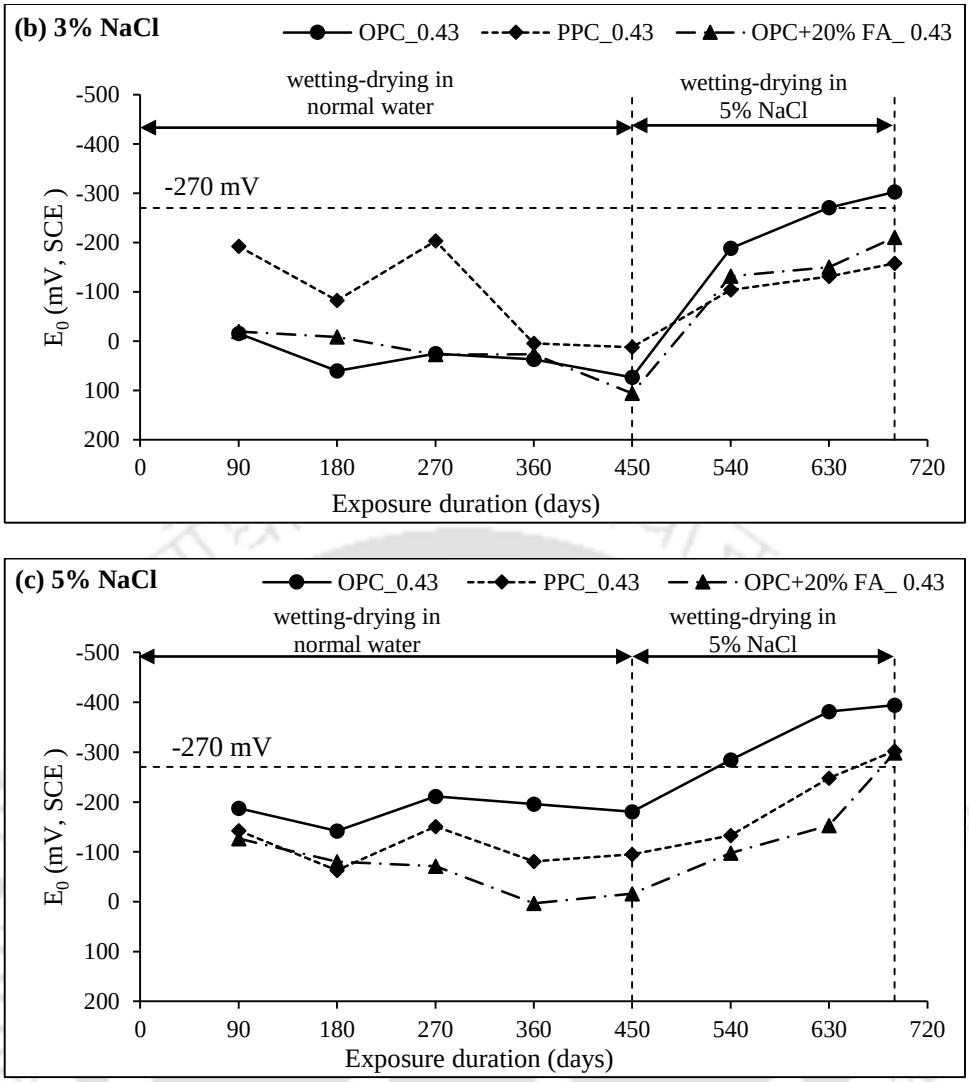

Fig. 6.7 Corrosion potential (E_0) of steel reinforcement in SCC mixes made with OPC, PPC and OPC+20% FA and w/b ratio of 0.43 for admixed NaCl concentrations of (a) 1% NaCl, (b) 3% NaCl, and (c) 5% NaCl, for water curing condition

From the obtained corrosion potential values shown in Fig. 6.5 to Fig. 6.7, it is observed that the potential values were less negative than -270 mV (SCE) when exposed to water curing (with alternate wetting-drying cycles) till 450 days for all binders, w/b ratios, and admixed NaCl concentrations, which indicates lower probability of occurrence of steel reinforcement corrosion. This may be attributed to the dominant effect of the variation in the availability of oxygen in the vicinity of the steel reinforcement. Further, there is no systematic variation in the corrosion potential with increase in exposure period till 450 days. However, the corrosion potential values became more negative with increase in exposure period when exposed to 5% NaCl solution (with alternate wetting-drying cycles) after 450 days of exposure to normal water, for all types of binder, w/b ratio and admixed

NaCl concentration. This may be attributed to dominant effect of the presence of comparatively higher concentrations chloride ions near the steel reinforcement due to ingress of chloride ions when exposed to NaCl solution as compared to the normal water. While comparing the binder type, it is observed that there was no systematic variation in corrosion potential among the binder type when exposed to normal water (till exposure period of 450 days). However, the corrosion potential was more negative in OPC based SCC mixes as compared to that in OPC+20% FA followed by PPC based SCC mixes when exposed to 5% NaCl solution (after 450 days) at all w/b ratios as observed from Fig. 6.5 to Fig. 6.7. The less negative potential value in OPC+20% FA and PPC as compared to that in OPC based SCC specimens may be attributed to lower concentration of free chloride near the steel reinforcement level due to ingress of lower amount of chloride ions as a result of formation of denser microstructure in PPC and OPC+20% FA based SCC mixes. Further, the SCC specimens admixed with 5% NaCl concentration showed more negative corrosion potential values as compared to those admixed with 3% and 1% NaCl concentrations for all binders, w/b ratios and both types of exposure condition (exposure to: normal water and 5% NaCl solution) as observed from Fig. 6.5 to Fig. 6.7. The more negative potential in 5% NaCl admixed specimens indicates greater probability of corrosion activity of the steel reinforcement in SCC mixes.

While comparing the effect of w/b ratio, it is inferred that there is no systematic variation in corrosion potential of steel reinforcement in SCC mixes when exposed to normal water with alternate wetting-drying cycles up to 450 days for all binders and admixed NaCl concentrations as observed from Fig. 6.5 to Fig. 6.7. However, the SCC specimens made with lower w/b ratio of 0.37 mostly showed less negative potential values as compared to those made with higher w/b ratios of 0.40 and 0.43 when exposed to 5% NaCl solution with alternate wetting-drying cycles after 450 days for all binders and admixed NaCl concentrations. The less negative potential value in SCC mixes made with lower w/b ratio may be attributed to the formation of denser microstructure that resulted in lower amount of free chloride in the vicinity of steel reinforcement.

Further, the corrosion potential values were more negative than -270 mV (SCE) in SCC specimens made with OPC (at all w/b ratios for admixed NaCl concentration of 5% and at w/b ratio of 0.43 for admixed NaCl concentration of 3%) and OPC+20% FA (at w/b ratios of 0.40 and 0.43 for admixed NaCl concentration of 5%) at the exposure period of 690 days for exposure to 5% NaCl solution as observed from Fig. 6.5 to Fig. 6.7. However, the SCC

specimens made with PPC mostly showed corrosion potential values less negative than -270 mV (SCE) for all w/b ratios and admixed NaCl concentrations when exposed to 5% NaCl solution, which indicates that the steel reinforcement in PPC based SCC mixes remained in a passive state as far as the corrosion activity is concerned.

While comparing the effect of exposure condition, it is observed that there is no systematic variation in corrosion potential of steel reinforcement between the two exposure conditions i.e. air curing and normal water curing with alternate wetting-drying cycles till the exposure duration of 450 days for different binders, w/b ratios and admixed NaCl concentrations as observed from Fig. 6.1 to 6.3 and Fig. 6.5 to Fig. 6.7. The unsystematic variation in corrosion potential of steel reinforcement with exposure condition may be attributed to the changes in the electrolytic pore solution of concrete due to the variations in the moisture content and chloride concentration as well as owing to the variations in the availability of oxygen near the rebar level that altered the initiation of corrosion activity of steel reinforcement. After 450 days of exposure, there was change in exposure environment for the SCC specimens exposed to normal water (with wetting-drying cycles) where the specimens were further exposed to 5% NaCl solution with alternate wetting-drying cycles, whereas the SCC specimens subjected to air curing (laboratory drying) were continued with the same exposure condition till the end of exposure.

6.3 Corrosion current density of steel reinforcement in SCC

For determining corrosion current density (I_{corr}) of steel reinforcement in SCC mixes, linear polarization resistance (LPR) measurement was performed on prismatic specimens for different exposure conditions same as that for the measurement of corrosion potential of steel reinforcement.

6.3.1 Effect of laboratory drying (air curing) on corrosion current density

For laboratory drying (air curing) condition, the corrosion current density (I_{corr}) values of steel reinforcement embedded in SCC specimens made with OPC, PPC and OPC+20% FA and admixed with NaCl concentrations of 0%, 1%, 3% and 5% are shown in Fig. 6.8, Fig. 6.9, and Fig. 6.10 for w/b ratios of 0.37, 0.40 and 0.43 respectively. Similarly, the corrosion current density values of steel reinforcement embedded in specimens made with w/b ratio of 0.40 and admixed with NaCl concentrations of 7.5% and 12.5% are shown in Fig. 6.11. Each value of corrosion current density shown in these figures is the average value of four replicate prismatic specimens.

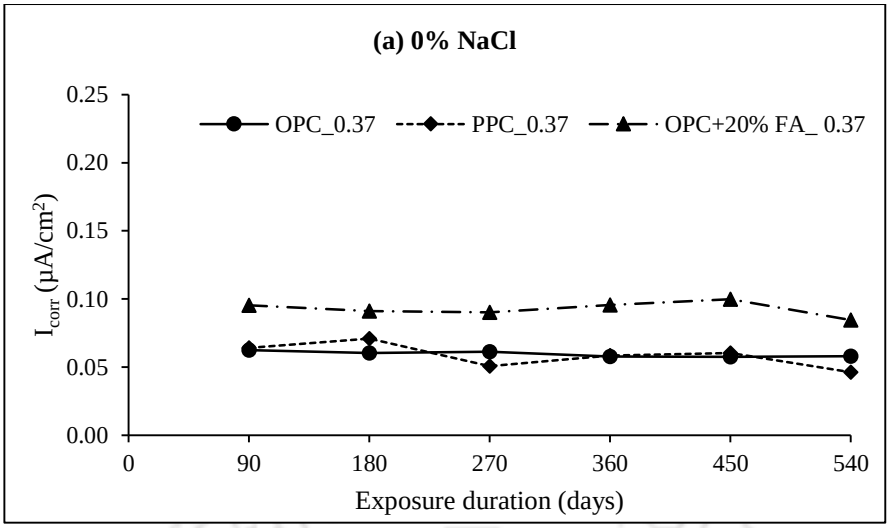

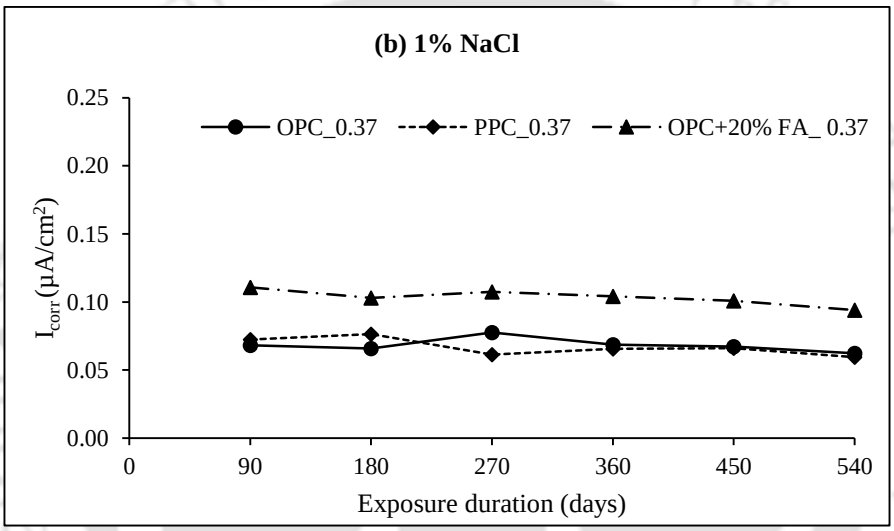

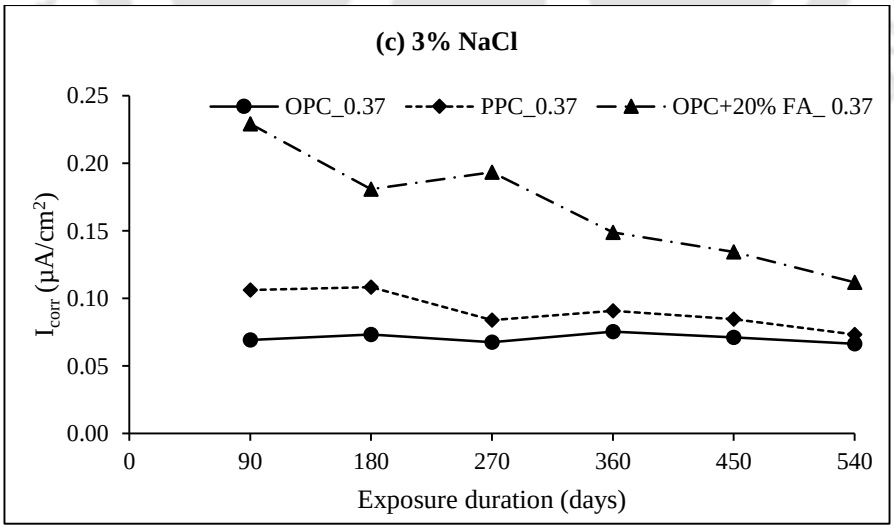

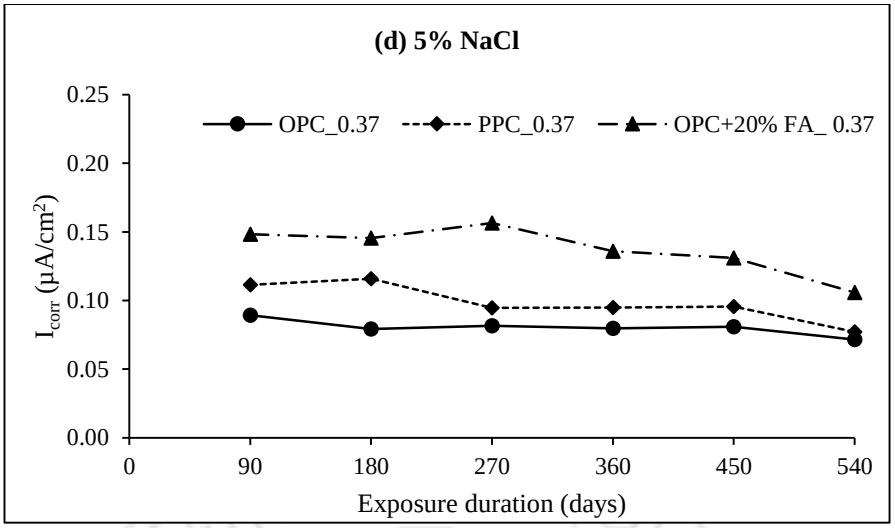

Fig. 6.8 Corrosion current density (I_{corr}) of steel reinforcement in SCC mixes made with OPC, PPC and OPC+20% FA and w/b ratio of 0.37 for admixed NaCl concentrations of (a) 0% NaCl, (b) 1% NaCl, (c) 3% NaCl, and (d) 5 % NaCl, for air curing condition

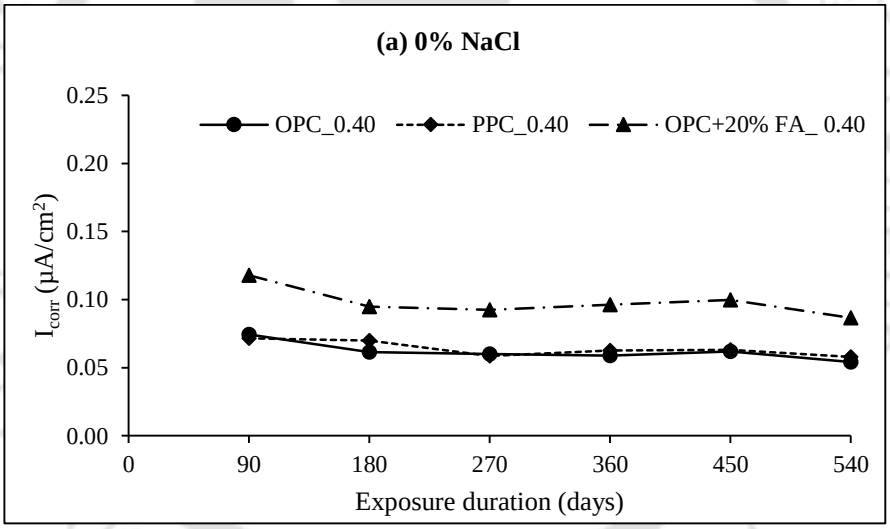

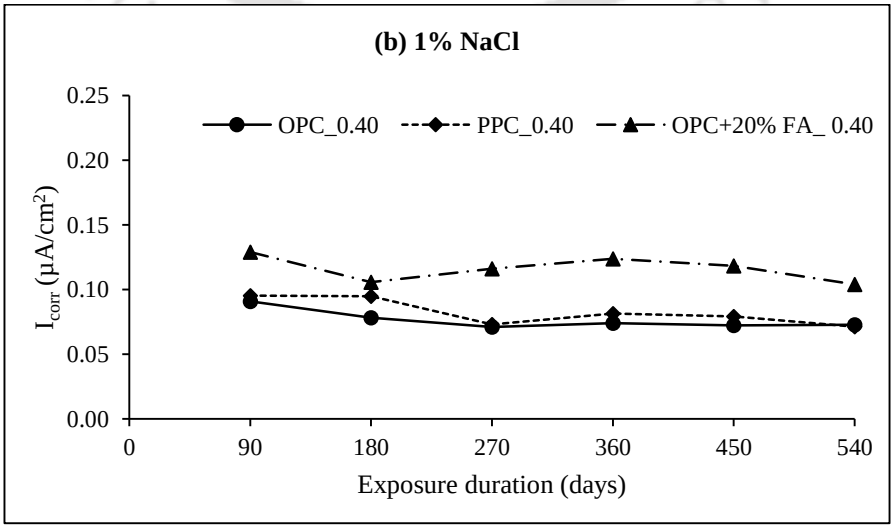

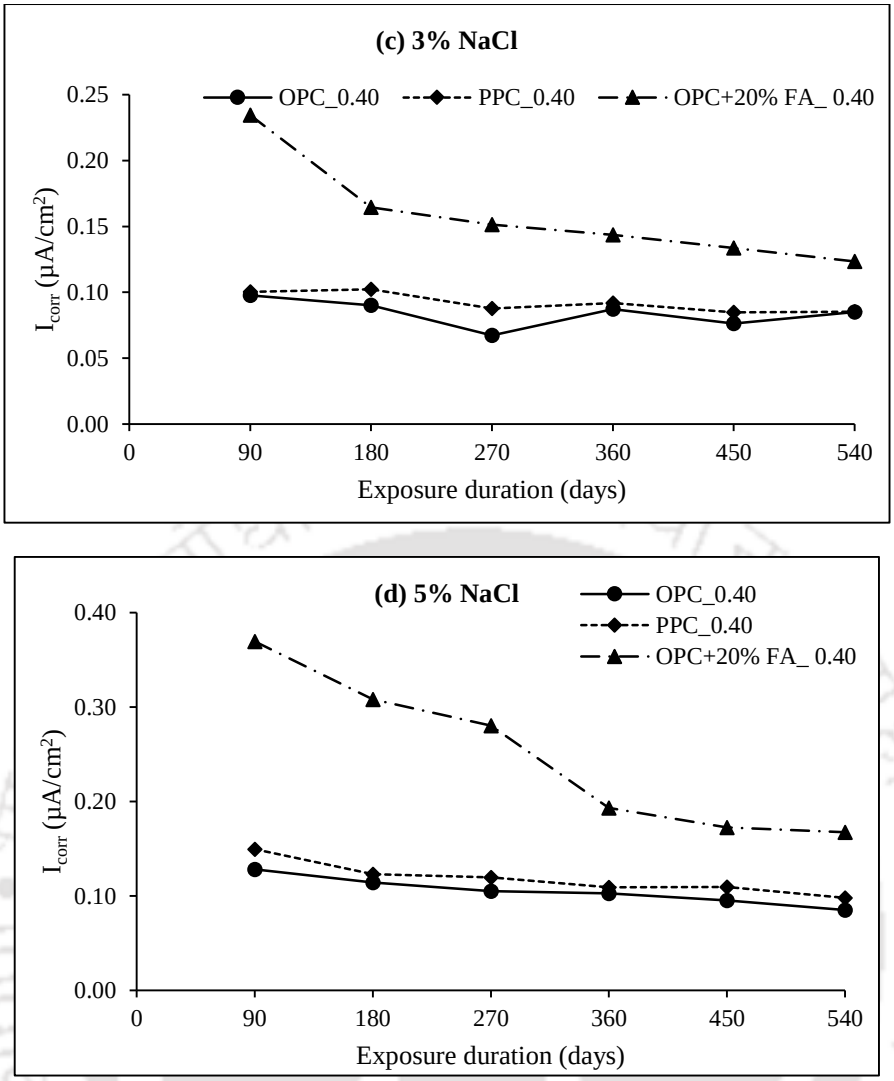

Fig. 6.9 Corrosion current density (I_{corr}) of steel reinforcement in SCC mixes made with OPC, PPC and OPC+20% FA and w/b ratio of 0.40 for admixed NaCl concentrations of (a) 0% NaCl, (b) 1% NaCl, (c) 3% NaCl, and (d) 5 % NaCl, for air curing condition

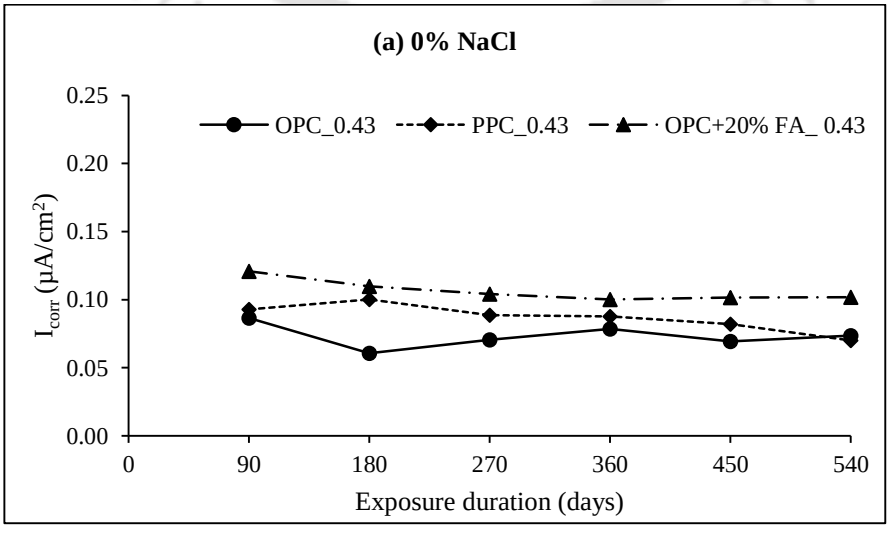

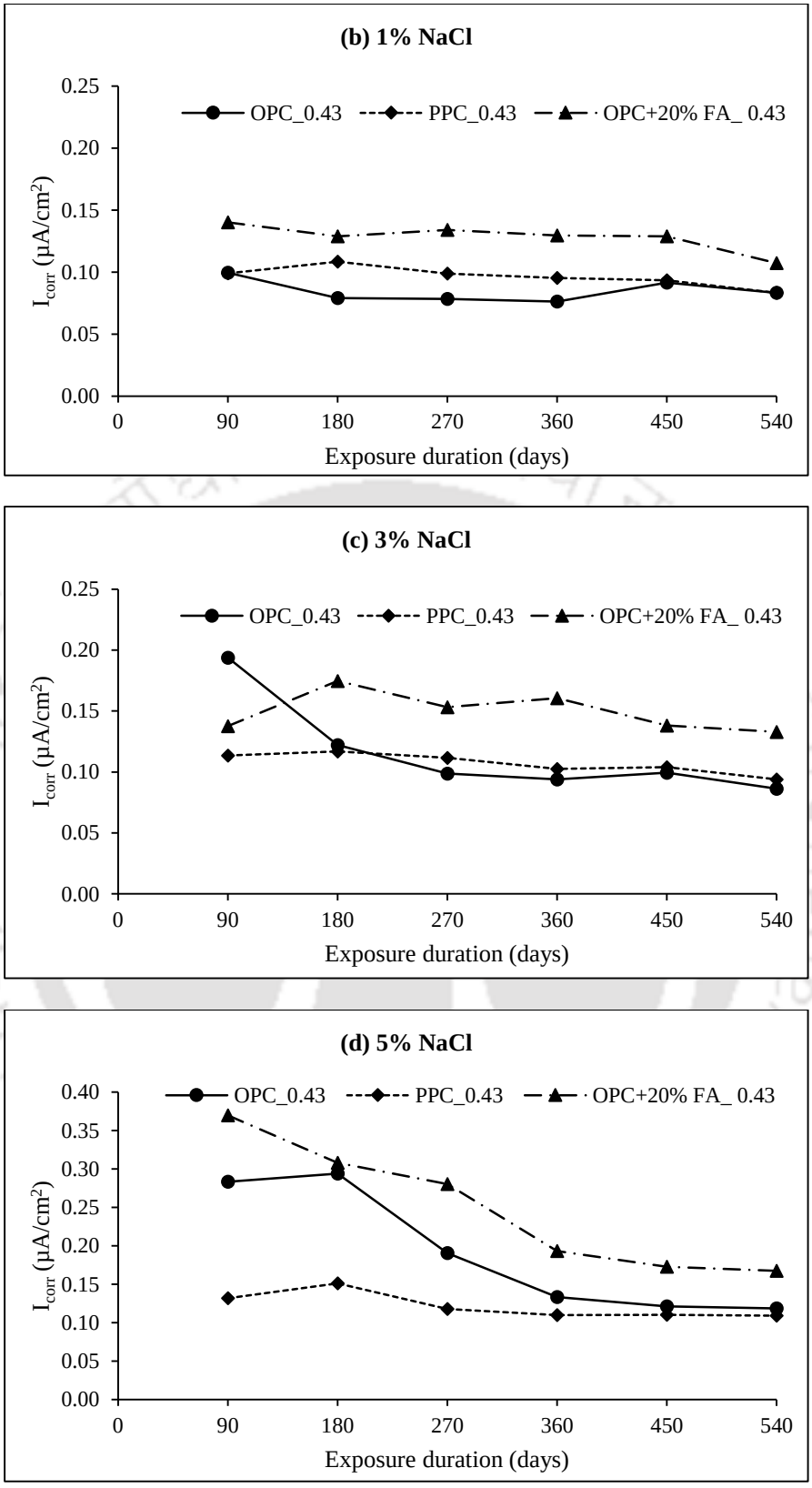

Fig. 6.10 Corrosion current density (I_{corr}) of steel reinforcement in SCC mixes made with OPC, PPC and OPC+20% FA and w/b ratio of 0.43 for admixed NaCl concentrations of (a) 0% NaCl, (b) 1% NaCl, (c) 3% NaCl, and (d) 5 % NaCl, for air curing condition

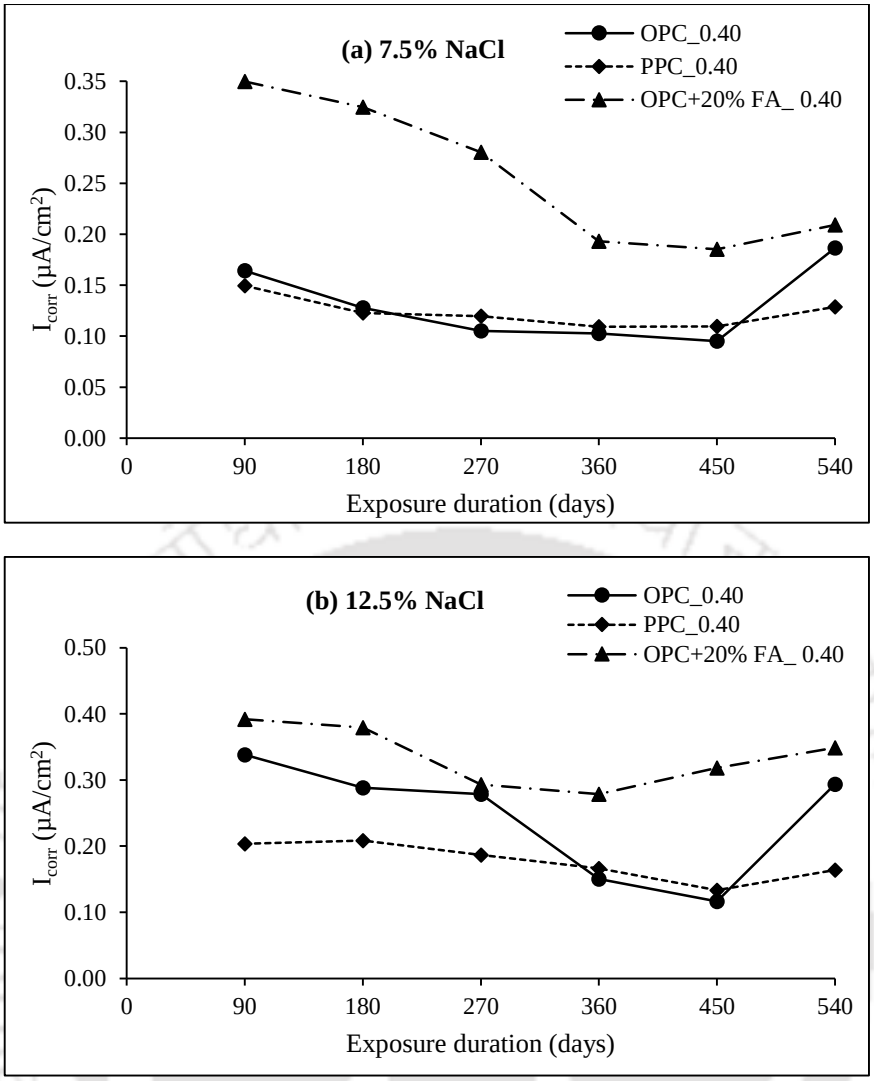

Fig. 6.11 Corrosion current density (I_{corr}) of steel reinforcement in SCC mixes made with OPC, PPC and OPC+20% FA and w/b ratio of 0.40 for admixed NaCl concentrations of (a) 7.% NaCl and (b) 12.5% NaCl, for air curing condition

From Fig. 6.8 to Fig. 6.11, it is observed that the corrosion current density of steel reinforcement was higher in OPC+20% FA based SCC specimens as compared to that in PPC and OPC based SCC mixes at all w/b ratios, admixed NaCl concentrations and exposure durations for laboratory dry (air curing) condition. The higher corrosion current density in OPC+20% FA based SCC mixes may be attributed to the increase in conductivity as a result of the higher free chloride concentration in concrete. Between OPC and PPC, the corrosion current density was mostly lower in OPC based SCC specimens as compared to that in PPC based specimens, although in some cases the difference was very less, as observed from Fig. 6.8 to Fig. 6.11. The lower corrosion current density in OPC based SCC mixes may be attributed to the fact that electrolytic pore solution of OPC mix might have

maintained the passivity of the steel reinforcement to a relatively greater degree in the presence of chloride ions as compared to that in PPC based SCC mixes.

The corrosion current density of steel reinforcement in control SCC mixes (0% NaCl) was lower as compared to that in chloride admixed SCC mixes for all concentrations of NaCl (1%, 3%, 5%, 7.5% and 12.5%) as observed from Fig. 6.8 to Fig. 6.11. Further from Fig. 6.8 to Fig. 6.11, it is noted that the corrosion current density of steel reinforcement increased with increase in admixed NaCl concentration for all binders, w/b ratios and exposure durations. This may be attributed to increase in conductivity of the SCC mixes with increase in chloride ion concentration thereby resulting in higher corrosion current density of steel reinforcement. While comparing the effect of w/b ratio on corrosion current density, it is inferred that the SCC specimens made with lower w/b ratio of 0.37 mostly showed lower corrosion current density as compared to those made with higher w/b ratios of 0.40 and 0.43 for all binders and admixed NaCl concentrations, as observed from Fig. 6.8 to Fig. 6.10. The lower corrosion current density at lower w/b ratio may be attributed to the effect of higher resistivity of the SCC mixes due to the formation of denser microstructure at lower w/b ratio that retarded the access of oxygen and chloride ions in the vicinity of steel reinforcement.

From Fig. 6.8 to Fig. 6.10, it is inferred that the variation in corrosion current density of steel reinforcement with exposure period was very less although in some cases the corrosion current density decreased with increase in exposure period for admixed NaCl concentrations up to 5% in OPC, PPC and OPC+20% FA for laboratory dry (air curing) condition. These variations in corrosion current density with exposure period may be attributed to the variations in the availability of chloride ions and oxygen in the vicinity of steel reinforcement in concrete. For higher concentrations of admixed NaCl (7.5% and 12.5%), the corrosion current density of steel reinforcement mostly decreased with increase in exposure period up to 450 days followed by an increase at the exposure period of 540 days for all the binders as observed from Fig. 6.11. This variation in corrosion current density with increase in exposure period in case of higher concentration of admixed NaCl may be attributed to the dominant effect of the variation in the free chloride concentration near the steel reinforcement as a result of the variation in chloride binding in concrete with increase in exposure period.

6.3.2 Effect of water curing on corrosion current density

For water curing condition, the corrosion current density of steel reinforcement in SCC specimens made with w/b ratios of 0.37, 0.40 and 0.43 are shown in Fig. 6.12, Fig. 6.13 and Fig. 6.14 respectively, for OPC, PPC and OPC+20% FA and admixed with NaCl concentrations of 1%, 3% and 5%. Each value of corrosion current density shown in these figures is the average values of four replicate specimens.

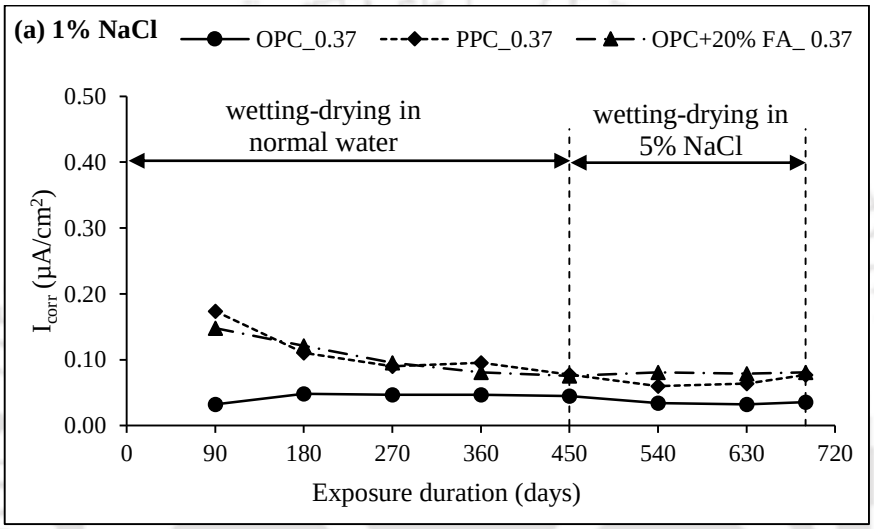

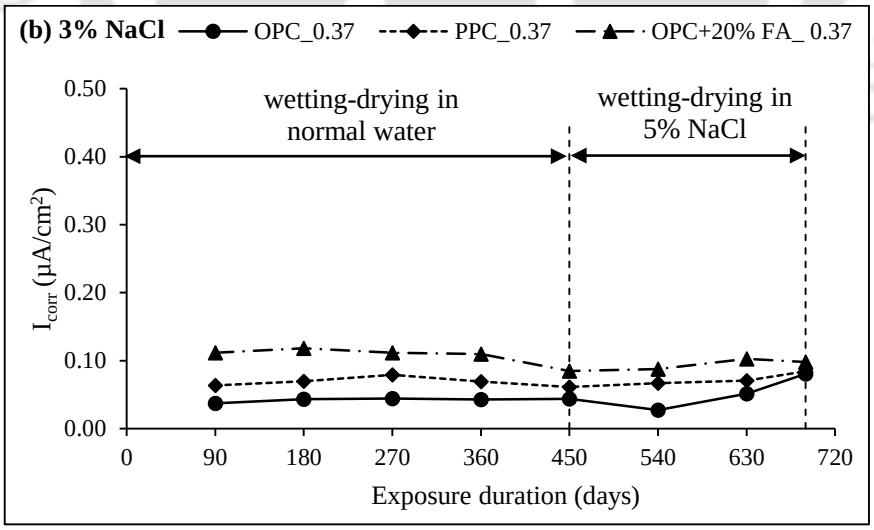

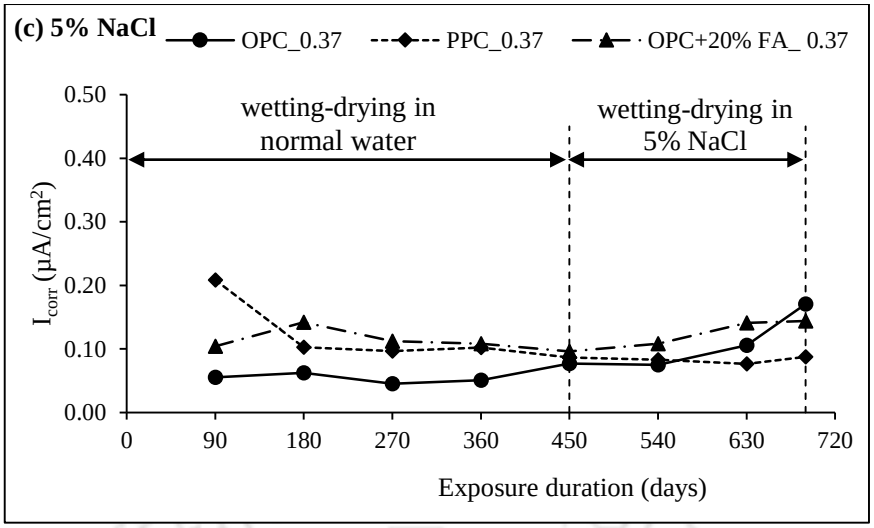

Fig. 6.12 Corrosion current density (I_{corr}) of steel reinforcement in SCC mixes made with OPC, PPC and OPC+20% FA and w/b ratio of 0.37 for admixed NaCl concentrations of (a) 1% NaCl, (b) 3% NaCl, and (c) 5% NaCl, for water curing condition

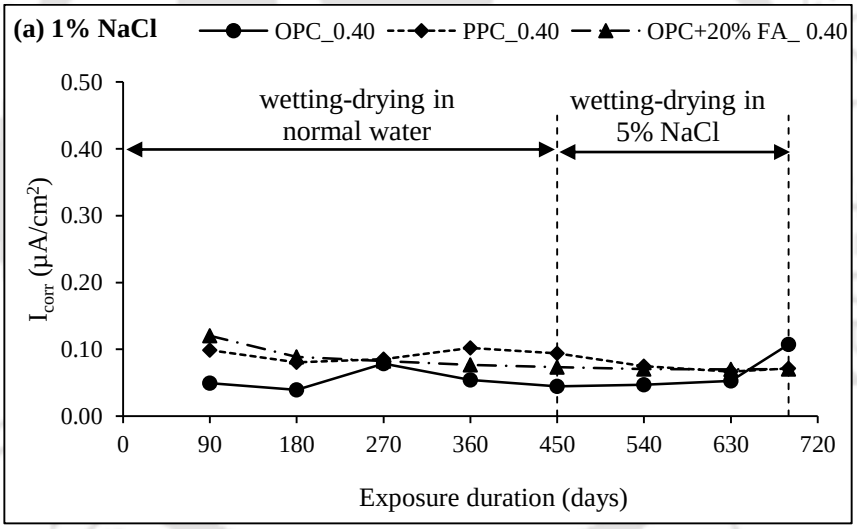

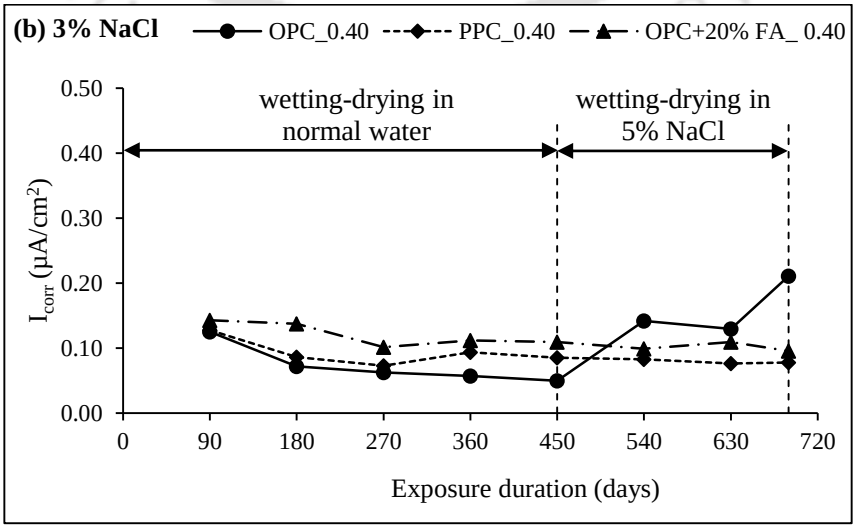

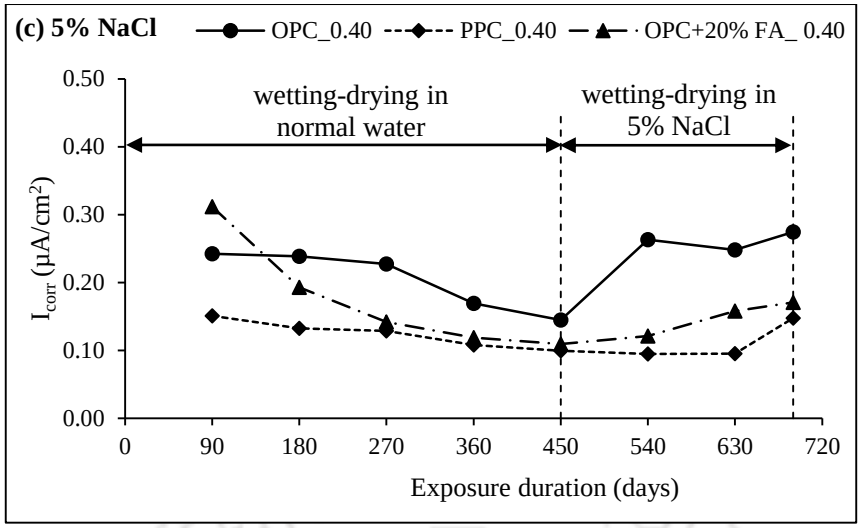

Fig. 6.13 Corrosion current density (I_{corr}) of steel reinforcement in SCC mixes made with OPC, PPC and OPC+20% FA and w/b ratio of 0.40 for admixed NaCl concentrations of (a) 1% NaCl, (b) 3% NaCl, and (c) 5% NaCl, for water curing condition

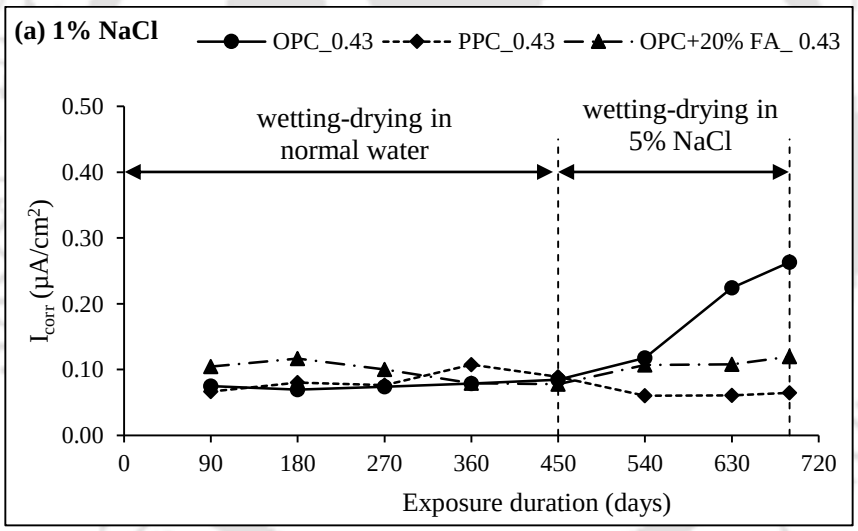

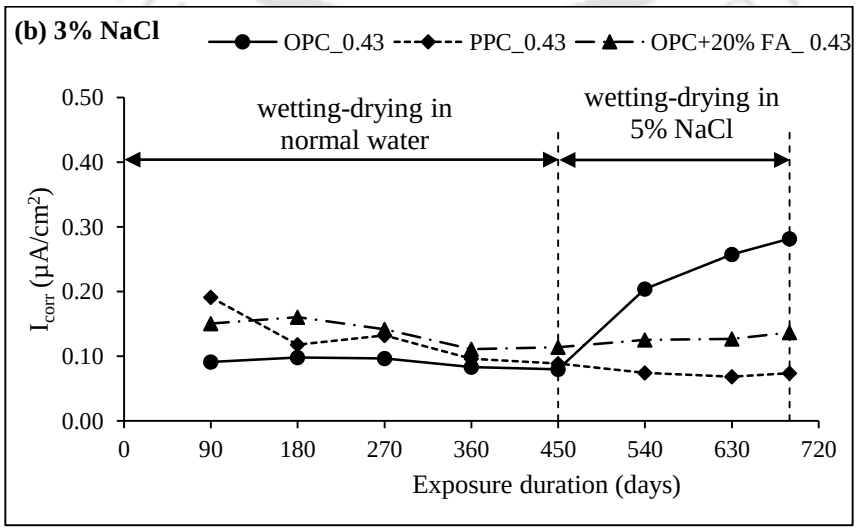

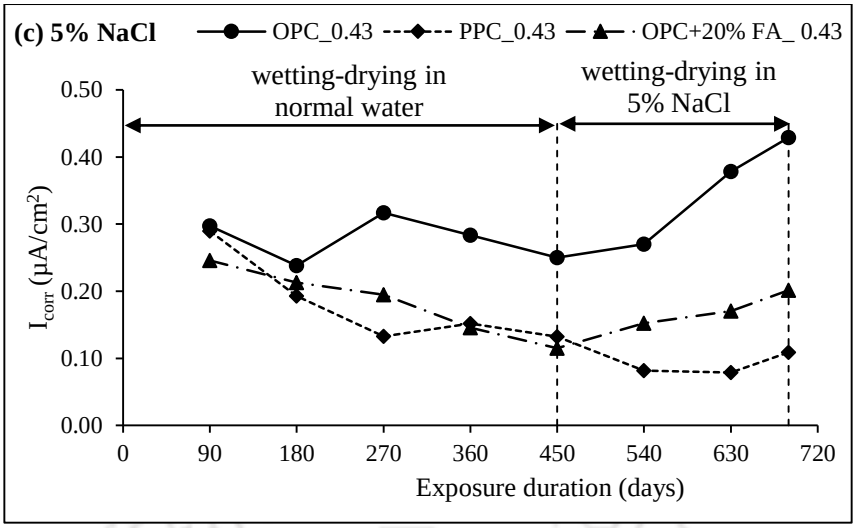

Fig. 6.14 Corrosion current density (I_{corr}) of steel reinforcement in SCC mixes made with OPC, PPC and OPC+20% FA and w/b ratio of 0.43 for admixed NaCl concentrations of (a) 1% NaCl, (b) 3% NaCl, and (c) 5% NaCl, for water curing condition

While evaluating the effect of exposure duration, it is observed that mostly there is no systematic variation in corrosion current density with exposure period in OPC based SCC mixes till the period of 450 days when exposed to normal water with alternate wetting-drying cycles as observed from Fig. 6.12 to Fig. 6.14 for all w/b ratios and admixed concentrations of NaCl. In addition, the difference in corrosion density with exposure period was also not significant in OPC based SCC mixes till the exposure period of 450 days. However, in PPC and OPC+20% FA based SCC mixes, the corrosion current density mostly decreased with exposure period till 450 days when exposed to normal water with alternate wetting-drying cycles for all w/b ratios and admixed concentrations of NaCl as observed from Fig. 6.12 to Fig. 6.14. These variations in corrosion current density for different binders may be attributed to the effect of the variations in the availability of oxygen and moisture near the rebar level in concrete mixes in the presence of internal chloride.

While comparing the effect of binder type, it is observed that the corrosion current density of steel reinforcement was mostly lower in OPC based SCC specimens as compared to that in OPC+20% FA and PPC based specimens when exposed to normal water till 450 days as observed from Fig. 6.12 to Fig. 6.14 for all concentrations of admixed NaCl. The lower corrosion current density in OPC based SCC mixes during the exposure to normal water may be attributed to the dominant effect of lower amount of chloride ions near the rebar level as a result of higher chloride binding in OPC mixes. The higher corrosion current

density in PPC and OPC+20% FA based SCC mixes during the exposure to normal water may be ascribed to the dominant effect of the variations in the availability of moisture and oxygen near the rebar level. Further, the corrosion current density of steel reinforcement in OPC based SCC mixes increased significantly after 450 days when exposed to 5% NaCl solution except in few cases as observed from Fig. 6.12 to Fig. 6.14. The increase in corrosion current density of steel reinforcement in OPC mixes after exposure to 5% NaCl solution may be attributed to ingress of higher amount of chloride ions thereby increasing the conductivity of concrete. However, in the cases of PPC and OPC+20% FA based SCC mixes, the increase in corrosion current density was very less as evident from Fig. 6.12 to Fig. 6.14, which may be due to the penetration of lower amount of chloride ions as a result of formation of denser microstructure in concrete. While comparing the effect of w/b ratio on corrosion current density, it is observed that there is no systematic variation in corrosion current density with w/b ratio in PPC and OPC+20% FA based SCC PPC mixes for all concentrations of admixed NaCl as observed from Fig. 6.12 to Fig. 6.14. In OPC based SCC specimens the corrosion current density was mostly lower at lower w/b ratio as compared to that at higher w/b ratio. Further, the SCC specimens admixed with higher concentration of NaCl exhibited higher corrosion current density as compared to those admixed with lower concentration of NaCl for all binders, w/b ratios and for both types of exposure condition (normal water and 5% NaCl solution).

While comparing the effect of exposure condition, it is observed that the SCC specimens exposed to normal water curing with alternate wetting-drying cycles mostly exhibited lower corrosion current density as compared to those exposed to air curing (laboratory drying) for different binders, w/b ratios and admixed NaCl concentrations till the exposure period of 450 days as observed from Fig. 6.1 to 6.3 and Fig. 6.5 to Fig. 6.7. The lower corrosion current density in the SCC specimens exposed to normal water curing with alternate wetting-drying cycles may be attributed to the dominant effect of the availability of a lower amount of oxygen near the rebar level that might have decreased the extent of corrosion process in the presence of chloride ions. It may be noted that all the specimens for both types of exposure condition were admixed with different concentrations of NaCl during the preparation of SCC mixes.

6.4 Summary

The results obtained from corrosion potential measurement indicated lower probability of occurrence of steel reinforcement corrosion in all the SCC mixes exposed to air curing (laboratory drying) for admixed NaCl concentrations 0%, 1%, 3% and 5%, however the corrosion potential was more negative than -270 mV (SCE) for higher concentrations of admixed NaCl i.e. 7.5% and 12.5%. Further the variation in corrosion potential with binder type was not systematic as well as not significant for the admixed NaCl concentrations till 5%, however at higher concentration of admixed NaCl (7.5% and 12.5%), the corrosion potential was more negative in OPC+20% FA based SCC mixes as compared to those in OPC and PPC based SCC mixes for air curing exposure condition. In the case of exposure to normal water curing with alternate wetting-drying cycles, the corrosion potential values in SCC specimens were less negative indicating lower probability of occurrence of corrosion, however after subsequent exposure to 5% NaCl solution the corrosion potential became more negative with increase in exposure period. Further, there was no systematic variation in the corrosion potential with binder type when exposed to normal water, however, the corrosion potential was more negative in OPC based SCC mixes as compared to that in OPC+20% FA followed by PPC based SCC mixes after exposure to 5% NaCl solution. For both exposure conditions (air curing and normal water curing with alternate wetting-drying cycles), the corrosion potential in SCC mixes became more negative with increase in admixed NaCl concentration. Further, there was no systematic variation in corrosion potential with w/b ratio for both exposure conditions. However, the SCC specimens made with lower w/b ratio mostly exhibited less negative potential as compared to those made with higher w/b ratio after exposure to 5% NaCl solution with alternate wetting-drying cycles. While comparing the effect of exposure condition, it is observed that there was no systematic variation in the corrosion potential of steel reinforcement in SCC mixes between two exposure conditions i.e. air curing condition (laboratory drying), and normal water curing with alternate wetting-drying cycles.

The results obtained from LPR measurement indicated the higher corrosion current density of steel reinforcement in OPC+20% FA based SCC specimens as compared to those in PPC and OPC based SCC mixes exposed to air curing condition. Further, the corrosion current density of steel reinforcement was lower at lower w/b ratio as compared to that at higher w/b ratio. For air curing condition, the variation in corrosion current density with exposure period was very less for admixed NaCl concentrations up to 5%, however for higher

concentrations of admixed NaCl (7.5% and 12.5%), the corrosion current density of steel reinforcement mostly decreased with increase in exposure period followed by an increase towards the end of exposure period. In the case of exposure to normal water curing with alternate wetting-drying cycles, there was no systematic variation in corrosion current density with exposure period in OPC based SCC mixes, however the corrosion current density mostly decreased with exposure period in PPC and OPC+20% FA based SCC mixes. Among the binder type, the corrosion current density of steel reinforcement was lower in OPC based SCC specimens as compared to that in OPC+20% FA and PPC based specimens when exposed to normal water however, the corrosion density of steel reinforcement increased significantly in OPC based SCC mixes when exposed to 5% NaCl solution with alternate wetting-drying cycles. The increase in corrosion current density in OPC mixes after exposure to 5% NaCl solution may be attributed to increase in conductivity of concrete due to ingress of higher amount of chloride ions. In case of PPC and OPC+20% FA based SCC mixes, the increase in corrosion current density was very less when exposed to 5% NaCl solution, which may be attributed to the formation of denser microstructure in PPC and OPC+20% FA based SCC mixes that resulted in penetration of lower amount of chloride ions into concrete nixes. While comparing the effect of w/b ratio, there was no systematic variation in corrosion current density with w/b ratio in PPC and OPC+20% FA based SCC PPC mixes, however the corrosion current density was mostly lower at lower w/b ratio as compared to that at higher w/b ratio in OPC based SCC specimens.

For both exposure conditions (air curing and normal water curing with alternate wetting-drying cycles), the corrosion current density of steel reinforcement increased with the increase in admixed NaCl concentration. While comparing the effect of exposure condition, it is inferred that the SCC specimens exposed to normal water curing with alternate wetting-drying cycles mostly exhibited lower corrosion current density as compared to those exposed to air curing condition (laboratory drying).

CHAPTER 7

CORROSION PERFORMANCE OF STEEL REINFORCEMENT IN SCC EXPOSED TO EXTERNAL CHLORIDE AND COMBINED CHLORIDE-SULFATE SOLUTIONS

7.1 General

This chapter presents and discusses the results obtained from the investigation carried out to determine the corrosion potential and corrosion current density of steel reinforcement embedded in prismatic specimens made from SCC mixes and subjected to external chloride and combined chloride-sulfate exposure solutions with alternate wetting-drying cycles. Sodium chloride (NaCl) of different concentrations were used for the preparation of chloride solutions. Similarly, combination of sodium chloride (NaCl) and sodium sulfate (Na_2SO_4) and that of sodium chloride (NaCl) and magnesium sulfate ($MgSO_4$) of different concentrations were used for the preparation of combined chloride-sulfate solutions. From the obtained results, the effects of binder type, w/b ratio and exposure solution on corrosion potential and corrosion current density of steel reinforcement in SCC mixes were evaluated for different exposure periods. In addition, the corrosion potential and corrosion current density of steel reinforcement were compared between sodium chloride plus sodium sulfate and sodium chloride plus magnesium sulfate exposure solutions. Further, the variations in free and total chloride concentrations of concrete near the vicinity of steel reinforcement in SCC mixes were analyzed for different types of binder, w/b ratio and exposure solutions. The changes in microstructure of concrete near the vicinity of steel reinforcement in SCC mixes examined through XRD, EDX and FESEM are also discussed.

7.2 Corrosion potential

The corrosion potential provides qualitative information about the corrosion initiation of steel reinforcement in concrete. As mentioned in Chapter 3, the prismatic specimens with a centrally embedded steel bar were prepared from OPC, PPC and OPC+20% FA based SCC mixes at the w/b ratios of 0.37, 0.40 and 0.43. After completion of 28 days of moist curing, the prismatic reinforced specimens from each SCC mix were kept in the laboratory dry condition for 14 days. After that, the specimens were exposed to chloride and combined chloride-sulfate solutions with alternate wetting-drying cycles for a period of 690 days. Total nine solutions i.e. three chloride solutions and six combined chloride-sulfate solutions

were used for external exposure conditions. The corrosion potential (E_0) was measured at the regular intervals of 90 days up to 630 days followed by measuring at the end of exposure period i.e. at 690 days. The corrosion potential of steel reinforcement was measured with reference to a saturated calomel electrode (SCE). As already stated in Chapter 6, the potential values more negative than -270 mV (SCE), correspond to greater probability (more than 90%) of occurrence of reinforcing steel corrosion in concrete (as per ASTM C876-15 [139]).

7.2.1 Corrosion potential of steel reinforcement in SCC exposed to NaCl solutions

The variations in corrosion potential of steel reinforcement in SCC specimens made with OPC and exposed to NaCl solutions of varying concentrations (0%, 1%, 3% and 5%) with exposure duration are shown in Fig. 7.1 (a), Fig. 7.1 (b), and Fig. 7.1 (c) for the w/b ratios of 0.37, 0.40 and 0.43, respectively. Similarly, the obtained corrosion potential values for PPC and OPC+20% FA based SCC mixes are shown in Fig. 7.2 (a - c) and Fig. 7.3 (a - c), respectively. Each value of corrosion potential shown in these figures is the average value of four replicate prismatic specimens.

From the corrosion potential values (E_0) shown in Fig. 7.1 (a - c) to Fig. 7.3 (a - c), it is observed that the corrosion potential values are less negative than -270 mV (SCE) for the SCC mixes exposed to normal water (0% NaCl solution) irrespective of binder type, w/b ratio and exposure duration. From Fig. 7.1 (a - c) to Fig. 7.3 (a - c), it is observed that the corrosion potential became more negative with increase in concentration of NaCl in the exposure solution i.e. the corrosion potential values were more negative for exposure to 5% NaCl solution as compared to 3% NaCl solution followed by 1% NaCl for all binders, w/b ratios and exposure durations. This indicates higher probability of occurrence of steel reinforcing corrosion in SCC specimens exposed to higher concentrations of NaCl solution. This may be attributed to the ingress of higher amount of chloride ions in the SCC specimens that might have affected the passivity of steel reinforcement.

From Fig. 7.1, it is observed that the corrosion potential values of steel reinforcement in OPC based SCC specimens were more negative than -270 mV (SCE) for exposure to NaCl solutions of 1%, 3% and 5% concentrations at w/b ratios of 0.40 and 0.43, particularly during the later stages of the exposure period. However, the corrosion potential values were mostly less negative than -270 mV (SCE) at w/b ratio of 0.37 in OPC specimens except for the exposure to 5% NaCl solution wherein the corrosion potential was more negative than

-270 mV (SCE) after the exposure period of 690 days. In PPC and OPC+20% FA based SCC specimens, the corrosion potential values were mostly less negative than -270 mV (SCE) for different concentrations of NaCl solution and w/b ratios as observed from Fig. 7.2 and Fig. 7.3. Further from Fig. 7.2, it is inferred that in PPC specimens, the corrosion potential values were more negative during the early periods of exposure than those at later exposure periods, which may be attributed to the dominant effect of the variation in oxygen availability near the steel reinforcement level. From Fig. 7.1 to Fig. 7.3, it is noted that the corrosion potential values of steel reinforcement in SCC specimens made from OPC, PPC and OPC+20% FA based SCC mixes were in the ranges of -73.11 mV to -442.40 mV, -18.54 mV to -275.31 mV and 38.51 mV to -240.10 mV, respectively at the exposure duration of 690 days irrespective of w/b ratio (0.37, 0.40 and 0.43) and exposure solution (1%, 3% and 5%). From these potential values, it is inferred that OPC based SCC mixes showed more negative potential values as compared to PPC and OPC+20% FA based SCC mixes, which indicates higher chance of occurrence of steel reinforcement corrosion in OPC based SCC mixes as compared to that in PPC and OPC+20% FA based SCC mixes. The less negative potential of steel reinforcement in PPC and OPC+20% FA based SCC mixes may be attributed to lower free chloride concentration near the steel reinforcement level due to ingress of less amount of chloride ions as a result of the formation of denser microstructure in PPC and OPC+20% FA based SCC mixes due to the production of additional C-S-H gel from the pozzolanic reaction. Thus, PPC and OPC+20% FA based SCC mixes performed better as compared to OPC based SCC mixes from the view point of occurrence of steel reinforcement corrosion, when exposed to external chloride solutions.

While analyzing the effect of w/b ratio on corrosion potential, it is noted that the SCC specimens made with w/b ratio of 0.37 mostly showed less negative potential values as compared to that made with w/b ratio of 0.40 followed by 0.43, as observed from Fig. 7.1 (a - c) to Fig. 7.3 (a - c), which indicates higher probability of occurrence of reinforcing steel corrosion at higher w/b ratio as compared to that at lower w/b ratio. The penetration of less amount of chloride ions into concrete as a result of formation of denser microstructure at lower w/b ratio might have resulted in less negative corrosion potential. Further from Fig. 7.1 (a - c), it is observed that the corrosion potential of steel reinforcement in OPC based SCC mixes became more negative with increase in exposure duration whereas in case of SCC specimens made with PPC, the corrosion potential became less

negative with increase in exposure period as observed from Fig. 7.2 (a - c). In the case of OPC+20% FA based SCC mixes, the variation in corrosion potential with increase in exposure period was not systematic as well as not significant as observed from Fig. 7.3 (a - c).

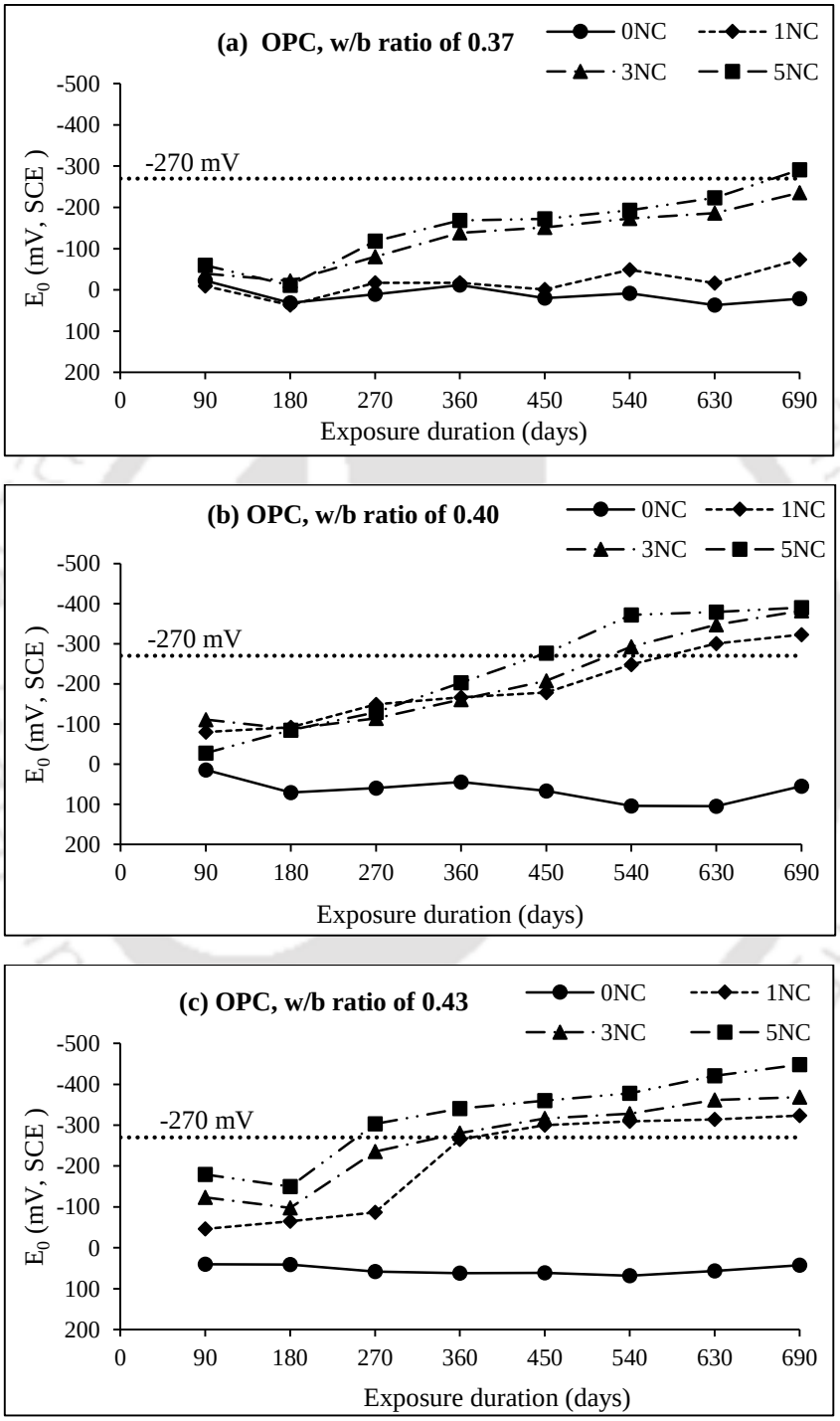

Fig. 7.1 Corrosion potential (E_0) of steel reinforcement in SCC mixes made with OPC and exposed to NaCl solutions, at w/b ratios of (a) 0.37, (b) 0.40, and (c) 0.43

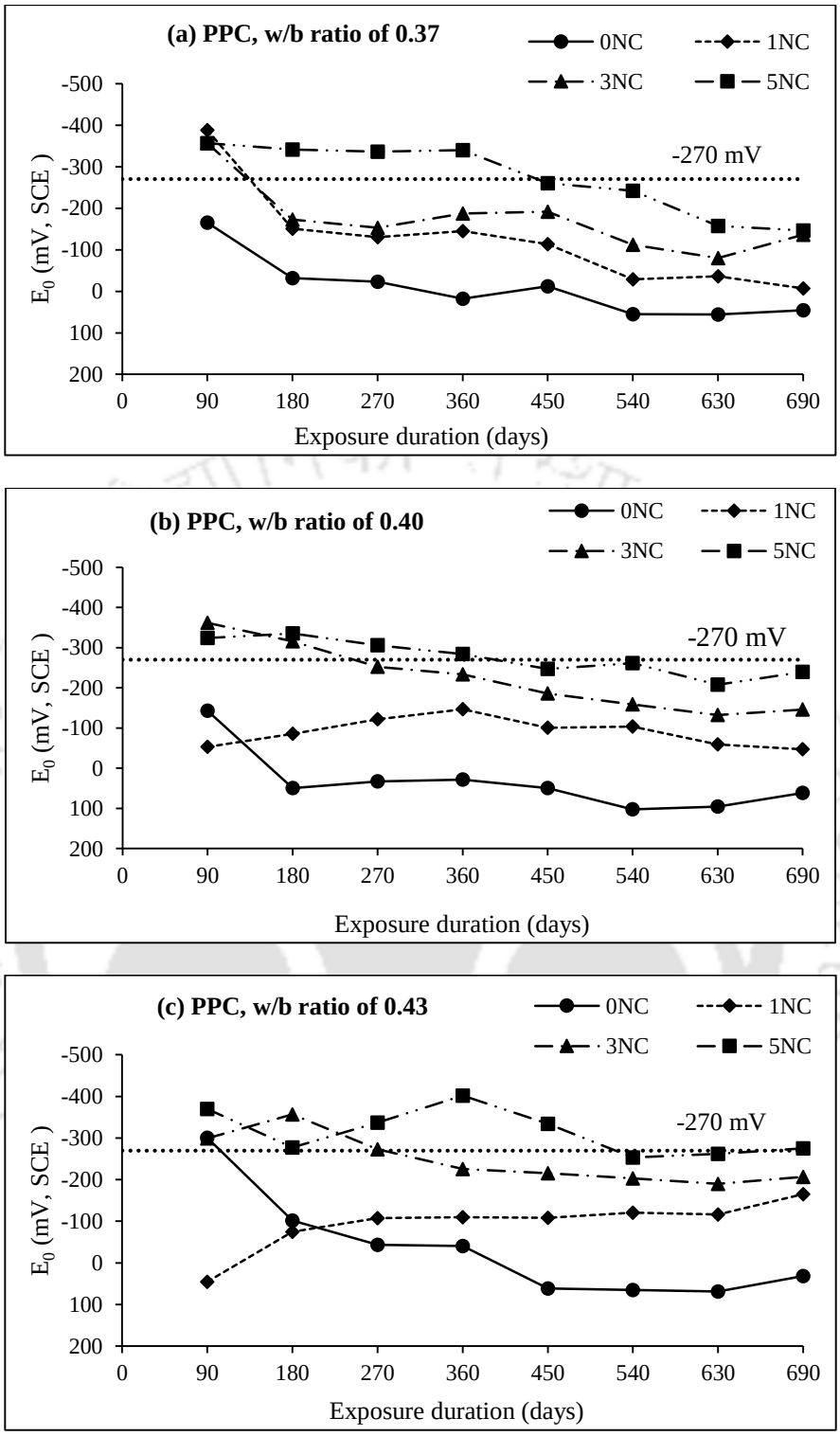

Fig. 7.2 Corrosion potential (E_0) of steel reinforcement in SCC mixes made with PPC and exposed to NaCl solutions, at w/b ratios of (a) 0.37, (b) 0.40, and (c) 0.43

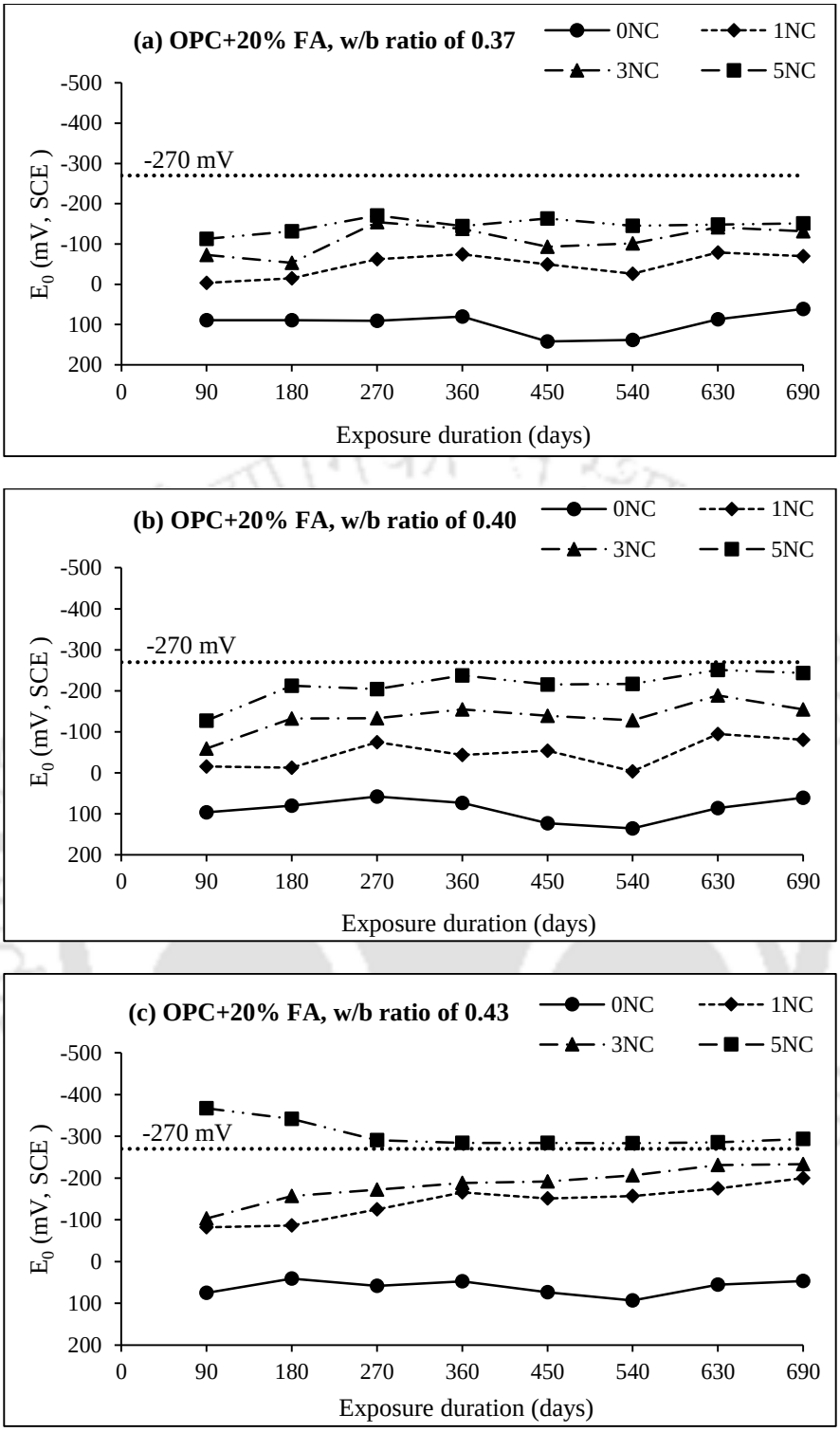

Fig. 7.3 Corrosion potential (E_0) of steel reinforcement in SCC mixes made with OPC+20% FA and exposed to NaCl solutions, at w/b ratios of (a) 0.37, (b) 0.40, and (c) 0.43

7.2.2 Corrosion potential of steel reinforcement in SCC exposed to NaCl + Na_2SO_4 and NaCl + $MgSO_4$ solutions

The corrosion potential values of steel reinforcement in OPC based SCC mixes exposed to varying concentrations of NaCl (1%, 3% and 5%) + Na_2SO_4 (3%) solutions are plotted against the exposure duration and are shown in Fig. 7.4 (a), Fig. 7.4 (b), and Fig. 7.4 (c) for w/b ratios of 0.37, 0.40 and 0.43, respectively. Similarly, the corrosion potential values of steel reinforcement in SCC mixes prepared with PPC and OPC+20% FA are shown in Fig. 7.5 (a - c) and Fig. 7.6 (a - c), respectively. Further, the corrosion potential values of steel reinforcement in SCC specimens exposed to varying concentrations of NaCl (1%, 3% and 5%) + $MgSO_4$ (3%) solutions are shown in Fig. 7.7 (a - c), Fig. 7.8 (a - c) and Fig. 7.9 (a - c) for OPC, PPC and OPC+20% FA, respectively. Each value of corrosion potential shown in these figures is the average value of four replicate prismatic specimens.

From Fig. 7.4 to Fig. 7.6, it is observed that the corrosion potential values of steel reinforcement became more negative with increase in NaCl concentration in combined NaCl + Na_2SO_4 exposure solutions for all SCC mixes. In other words, the SCC specimens exposed to 5% NaCl + 3% Na_2SO_4 solution showed more negative corrosion potential as compared to those exposed to 3% NaCl + 3% Na_2SO_4 solution followed by 1% NaCl + 3% Na_2SO_4 solution for all binders and w/b ratios. Similarly, the corrosion potential of steel reinforcement in SCC mixes became more negative with increase in NaCl concentration in the combined NaCl + $MgSO_4$ solutions as observed from Fig. 7.7 to Fig. 7.9. Further from 7.4, it is inferred that for combined NaCl + Na_2SO_4 exposure solutions, the corrosion potential became more negative with increase in exposure period in the case of OPC based SCC mixes. However, in case of PPC based SCC mixes, the corrosion potential became less negative with increase in exposure period and there was no significant variation in corrosion potential with exposure period in case of OPC+20% FA based SCC mixes, as observed from Fig. 7.5 and Fig. 7.6. These variations in corrosion potential with increase in exposure period for different binders in case of combined NaCl + Na_2SO_4 exposure solutions may be attributed to the variations in the concentrations of chloride ions and oxygen near the vicinity of steel reinforcement. For combined NaCl + $MgSO_4$ exposure solutions, the variation in corrosion potential with increase in exposure period is not systematic irrespective of binder type and w/b ratio as observed from Fig. 7.7 to Fig 7.9.

While comparing the effect of binder type, it is inferred that corrosion potential values were more negative than -270 mV (SCE) in the case of OPC based SCC mixes during the later

stages of the exposure period for combined NaCl + Na_2SO_4 exposure solutions with 3% and 5% NaCl concentrations and for higher w/b ratios (0.40 and 0.43) as observed from Fig. 7.4 (b, c), whereas at w/b ratio 0.37, the corrosion potential values were less negative than -270 mV (SCE) for all concentrations of NaCl (Fig. 7.4 (a)). In PPC and OPC+20% FA based SCC mixes, the corrosion potential values were mostly less negative than -270 mV (SCE) for all w/b ratios and all concentrations of NaCl + Na_2SO_4 exposure solution as observed from Fig. 7.5 and Fig. 7.6. This indicates higher chance of initiation of steel reinforcement corrosion in OPC based SCC mixes as compared to that in PPC and OPC+20% FA based SCC mixes when exposed to combined NaCl + Na_2SO_4 solutions. Further, the corrosion potential values were mostly less negative at lower w/b ratio as compared to that at higher w/b ratio for all binders as observed from Fig. 7.4 to Fig. 7.6 for combined NaCl + Na_2SO_4 exposure solutions. From Fig. 7.7 to Fig. 7.9, it is observed that for NaCl + $MgSO_4$ solutions, the corrosion potential values of steel reinforcement in all the SCC mixes were less negative than -270 mV (SCE) throughout the exposure period, thereby indicating lower probability of initiation of corrosion activity of steel reinforcement in SCC specimens exposed to combined NaCl + $MgSO_4$ solutions. Further, it is inferred that in the case of exposure to combined NaCl + $MgSO_4$ solutions, the variation in corrosion potential with binder type, and exposure period is not systematic as observed from Fig. 7.7 to Fig. 7.9. However, the corrosion potential values of steel reinforcement were less negative at lower w/b ratio as compared to those at higher w/b ratio in OPC and OPC+20% FA based SCC specimens, whereas there is no systematic variation in corrosion potential with w/b ratio in PPC based SCC specimens when exposed to NaCl + $MgSO_4$ solutions, as observed from Fig. 7.7 to Fig. 7.9.

On comparing the effect of chloride and combined chloride-sulfate exposure solutions, it is observed that the SCC specimens exposed to only NaCl solutions showed more negative corrosion potential as compared to those exposed to combined chloride-sulfate exposure solutions for all binders, w/b ratios and all concentrations of exposure solutions, as observed from Fig. 7.1 to Fig. 7.9. This may be attributed to the fact that the sulfate ions might have hindered the penetration of chloride ions into concrete when exposed to combined chloride-sulfate solutions thereby decreasing the concentration of chloride ions in concrete as compared to that exposed to only chloride solutions, thereby by altering the corrosion potential of steel reinforcement. Further, while comparing the effect of cation type (Na^+ and Mg^{++}) associated with sulfate ions, it is inferred that the corrosion potential values were more negative when exposed to NaCl + Na_2SO_4 solutions as compared to NaCl

+ $MgSO_4$ solutions for all binders and w/b ratios as observed from Fig. 7.4 to Fig. 7.9. This may be attributed to the effect of Na^+ ions in the electrolytic pore solution of SCC mixes exposed to NaCl + Na_2SO_4 solutions that might have altered the conductivity of concrete. This indicates that under combined chloride-sulfate exposure conditions, the cation type associated with sulfate ions affects the corrosion initiation of steel reinforcement.

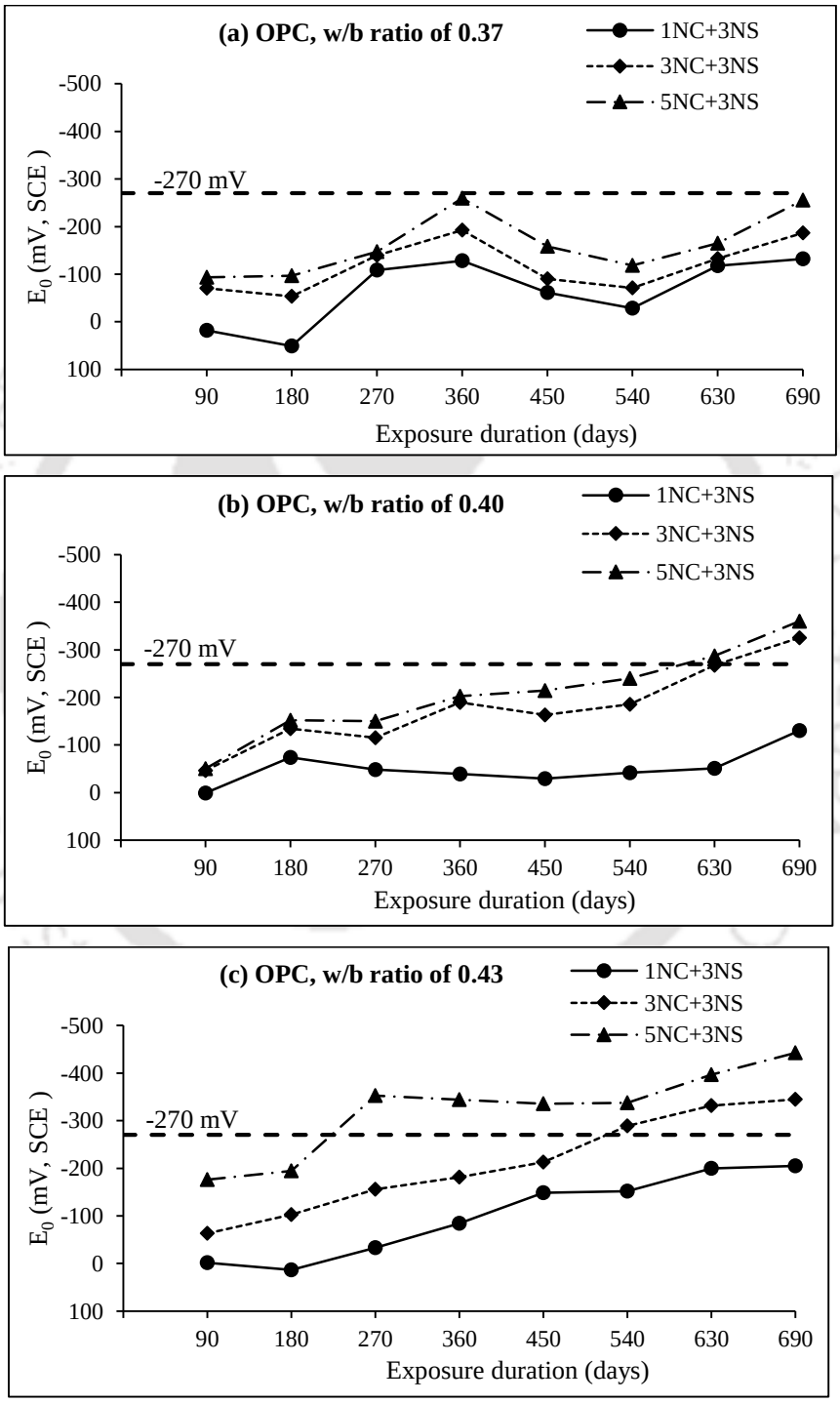

Fig. 7.4 Corrosion potential (E_0) of steel reinforcement in SCC mixes made with OPC and exposed to NaCl + Na_2SO_4 solutions, at w/b ratios of (a) 0.37, (b) 0.40, and (c) 0.43

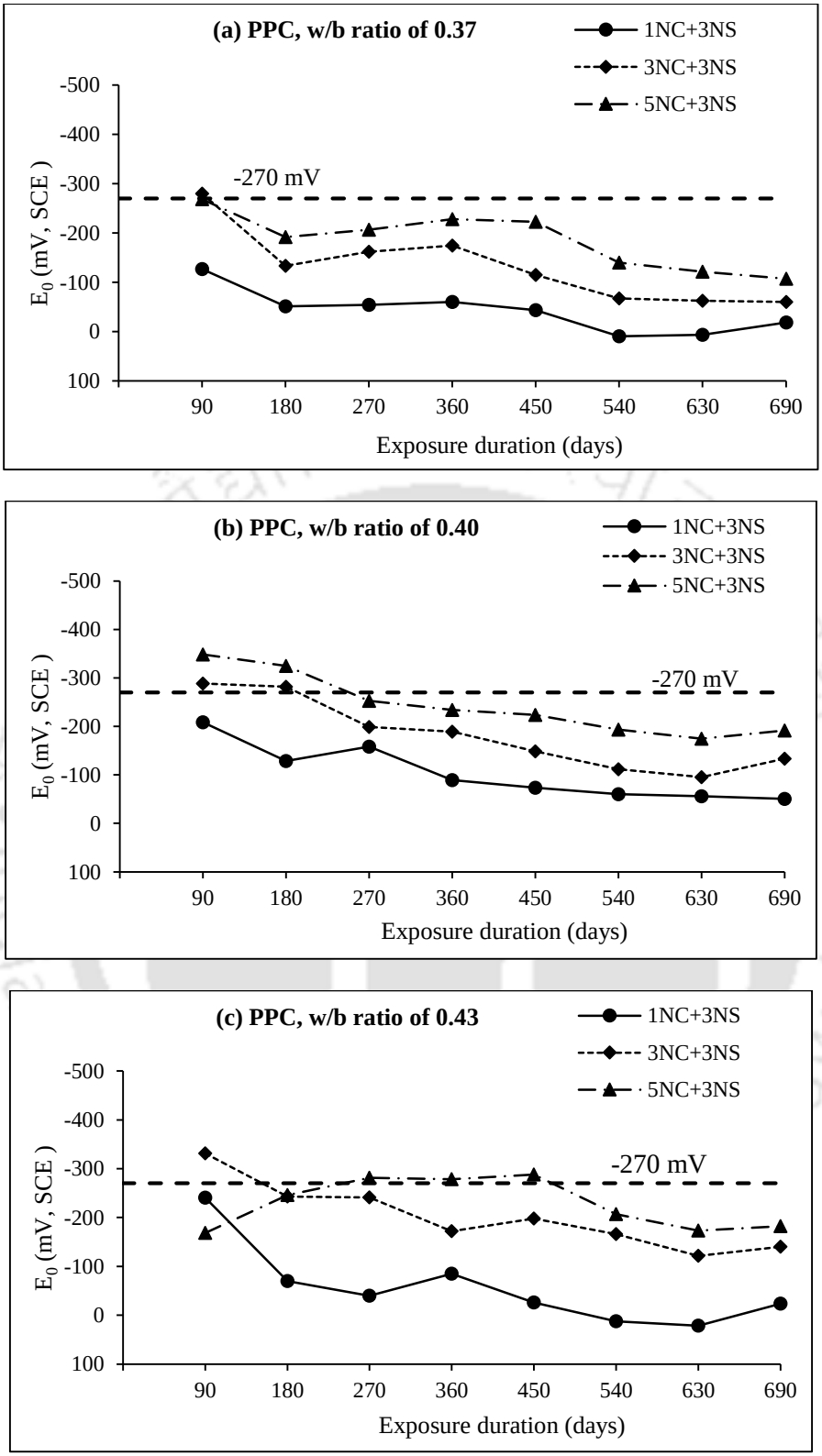

Fig. 7.5 Corrosion potential (E_0) of steel reinforcement in SCC mixes made with PPC and exposed to NaCl + Na_2SO_4 solutions, at w/b ratios of (a) 0.37, (b) 0.40, and (c) 0.43

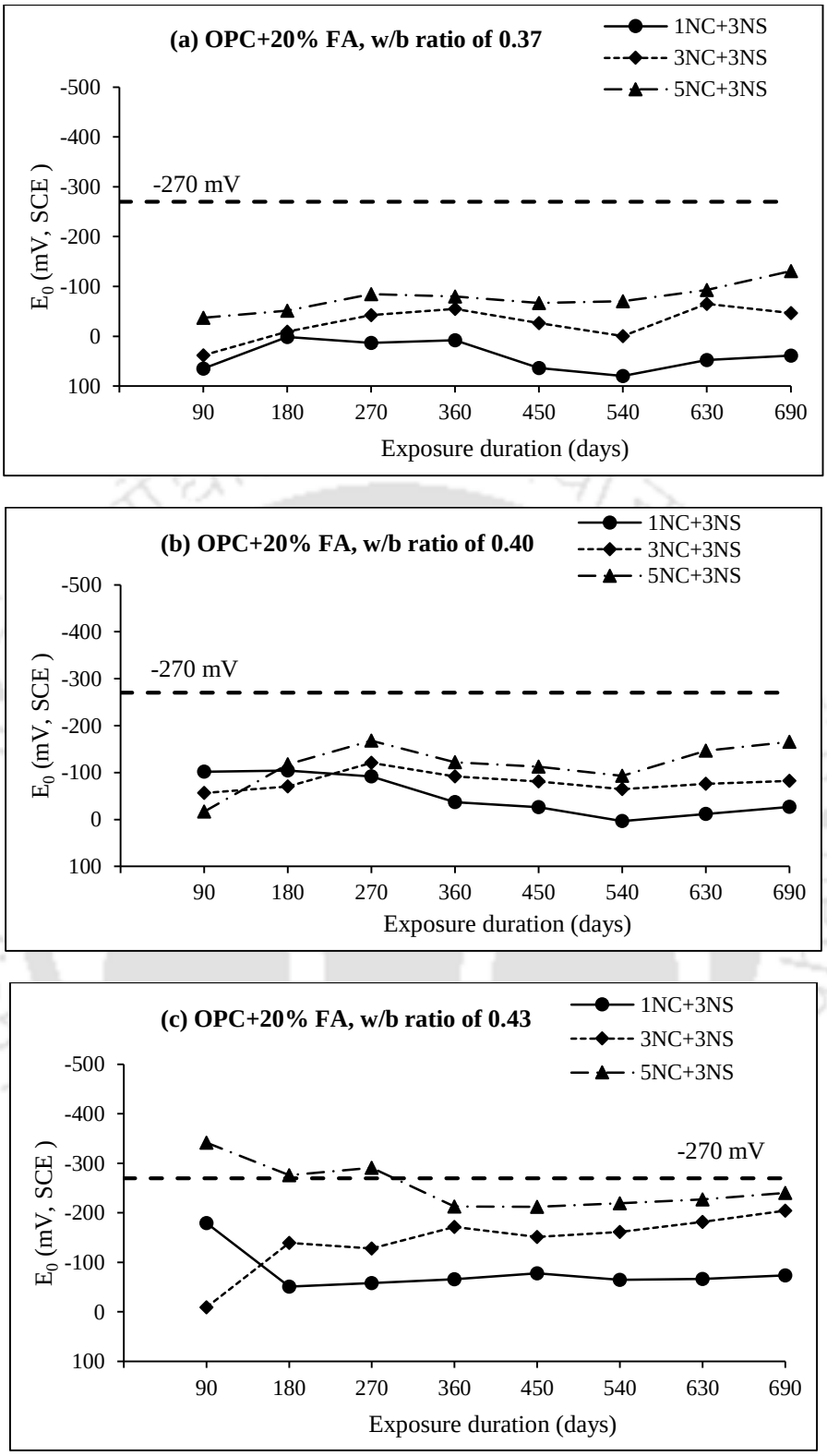

Fig. 7.6 Corrosion potential (E_0) of steel reinforcement in SCC mixes made with OPC+20% FA and exposed to NaCl + Na_2SO_4 solutions, at w/b ratios of (a) 0.37, (b) 0.40, and (c) 0.43

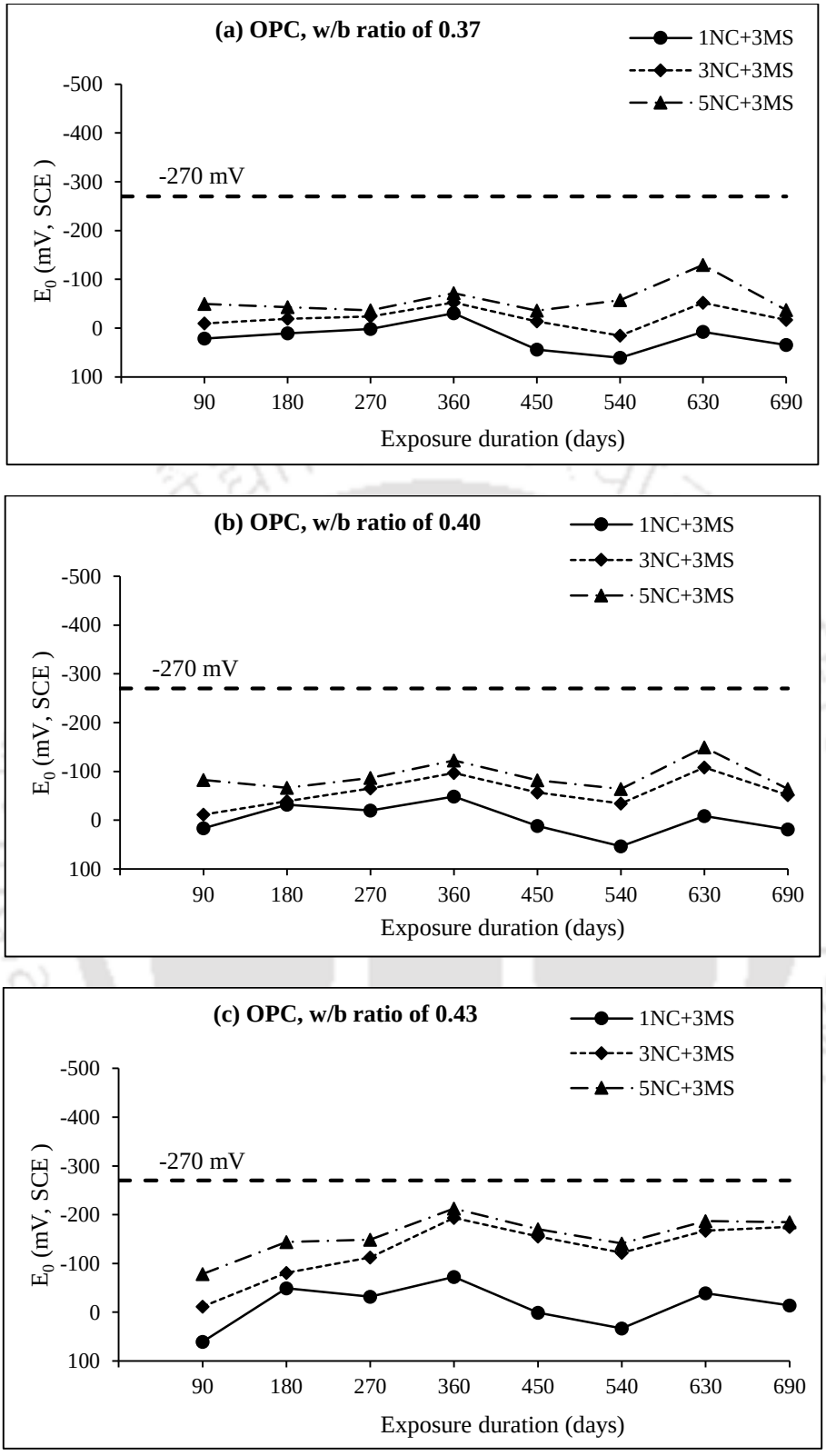

Fig. 7.7 Corrosion potential (E_0) of steel reinforcement in SCC mixes made with OPC and exposed to NaCl + $MgSO_4$ solutions, at w/b ratios of (a) 0.37, (b) 0.40, and (c) 0.43

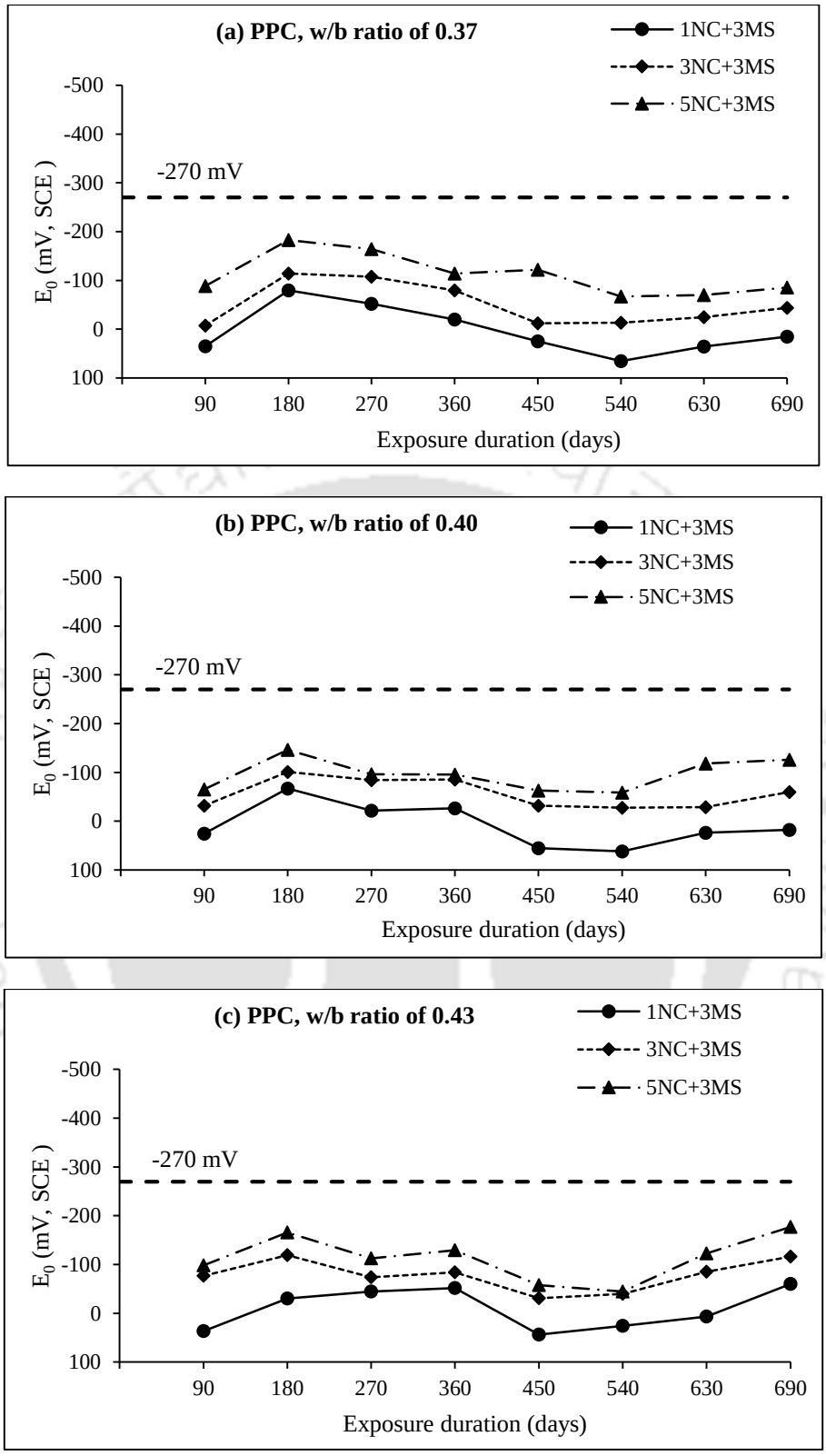

Fig. 7.8 Corrosion potential (E_0) of steel reinforcement in SCC mixes made with PPC and exposed to NaCl + $MgSO_4$ solutions, at w/b ratios of (a) 0.37, (b) 0.40, and (c) 0.43

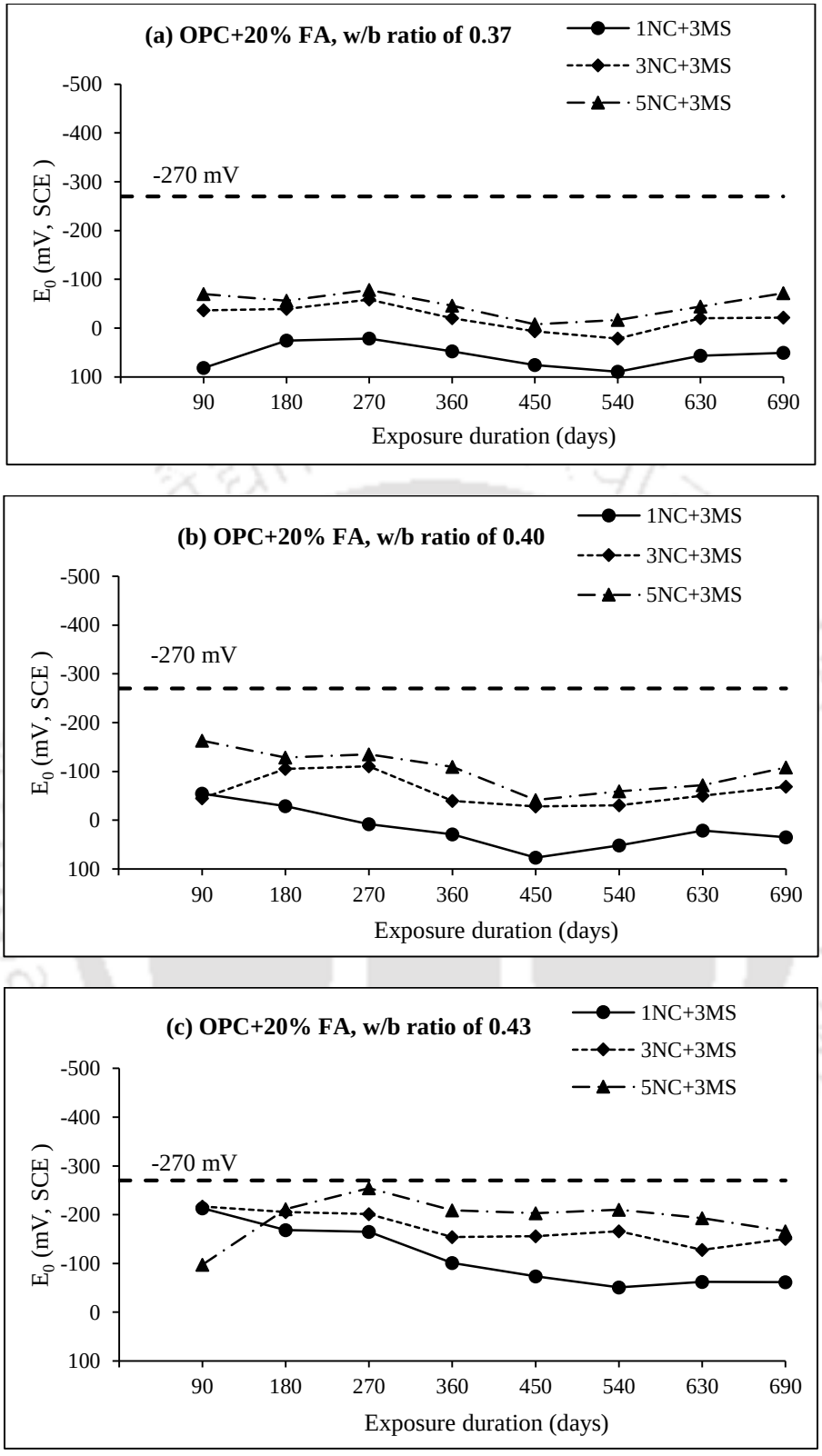

Fig. 7.9 Corrosion potential (E_0) of steel reinforcement in SCC mixes made with OPC+20% FA and exposed to NaCl + $MgSO_4$ solutions, at w/b ratios of (a) 0.37, (b) 0.40, and (c) 0.43

7.3 Corrosion current density

As stated in Chapter 3, the linear polarization resistance (LPR) measurement was carried out to determine the corrosion current density (I_{corr}) of steel reinforcement embedded in prismatic specimens made from SCC mixes and exposed to chloride and combined chloride-sulfate solutions with alternate wetting-drying cycles. The corrosion current density of steel reinforcement was measured at regular intervals of 90 days up to a period of 630 days followed by measuring at the end of exposure period i.e. at 690 days.

7.3.1 Corrosion current density of steel reinforcement in SCC exposed to NaCl solutions

The measured corrosion current density (I_{corr}) values of steel reinforcement in OPC based SCC specimens exposed to varying concentrations of NaCl are shown in Fig. 7.10 (a), Fig. 7.10 (b), and Fig. 7.10 (c) for the w/b ratios of 0.37, 0.40 and 0.43, respectively. Similarly, the corrosion current density of steel reinforcement in PPC and OPC+20% FA based SCC specimens are shown in Fig. 7.11 (a - c) and Fig. 7.12 (a - c), respectively. Each value of corrosion current density shown in these figures is the average value of four replicate prismatic specimens.

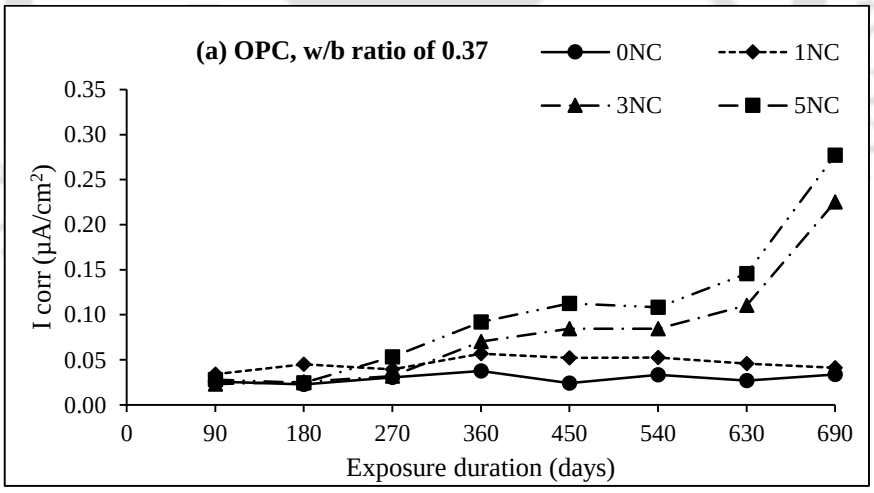

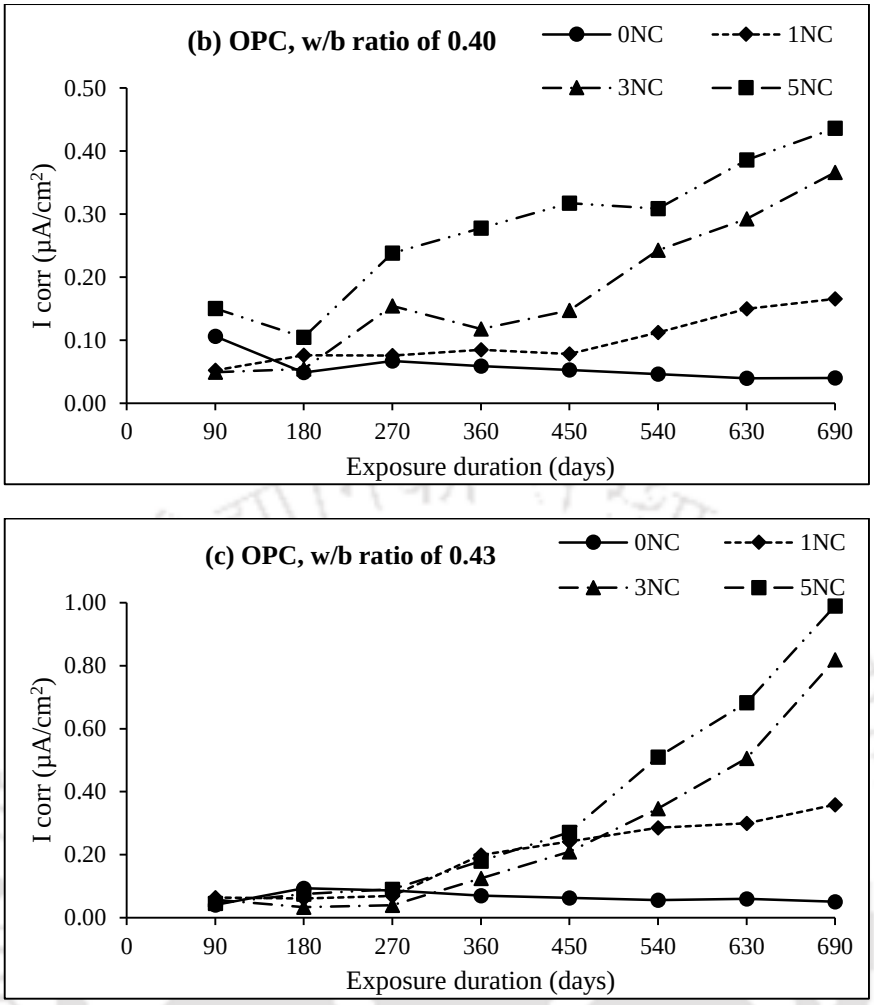

Fig. 7.10 Corrosion current density (I_{corr}) of steel reinforcement in SCC mixes made with OPC and exposed to NaCl solutions, at w/b ratios: (a) 0.37, (b) 0.40, and (c) 0.43

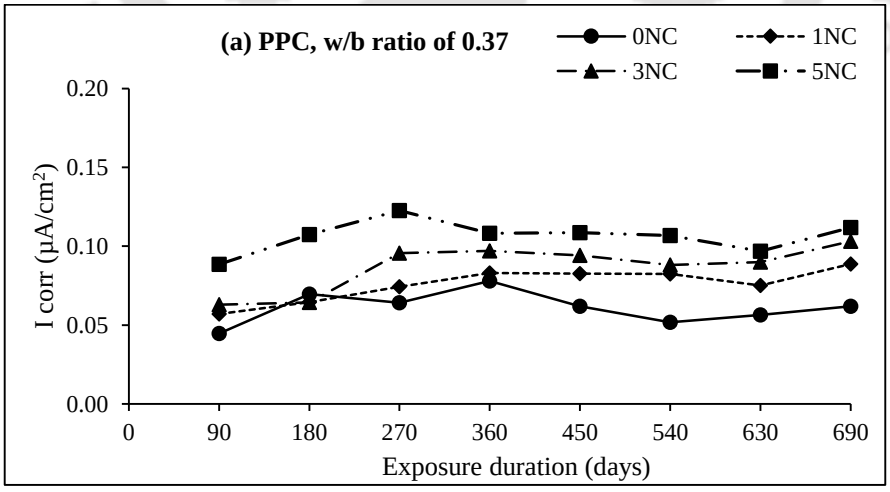

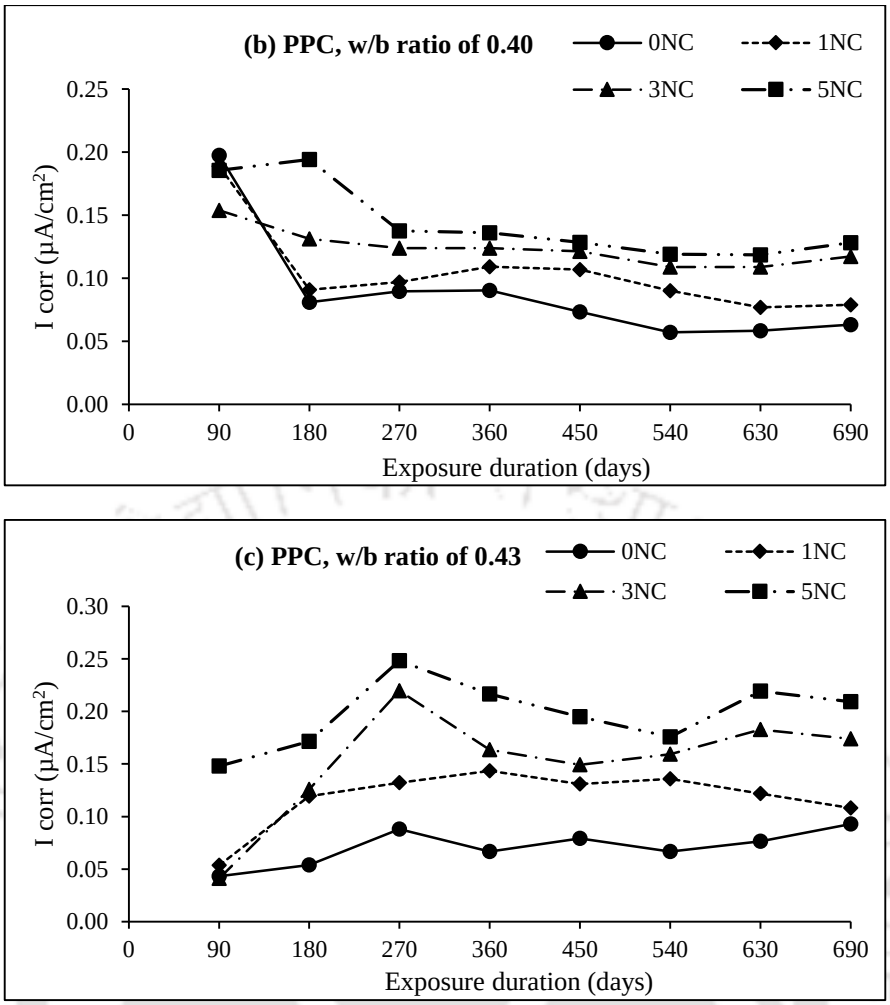

Fig. 7.11 Corrosion current density (I_{corr}) of steel reinforcement in SCC mixes made with PPC and exposed to NaCl solutions, at w/b ratios: (a) 0.37, (b) 0.40, and (c) 0.43

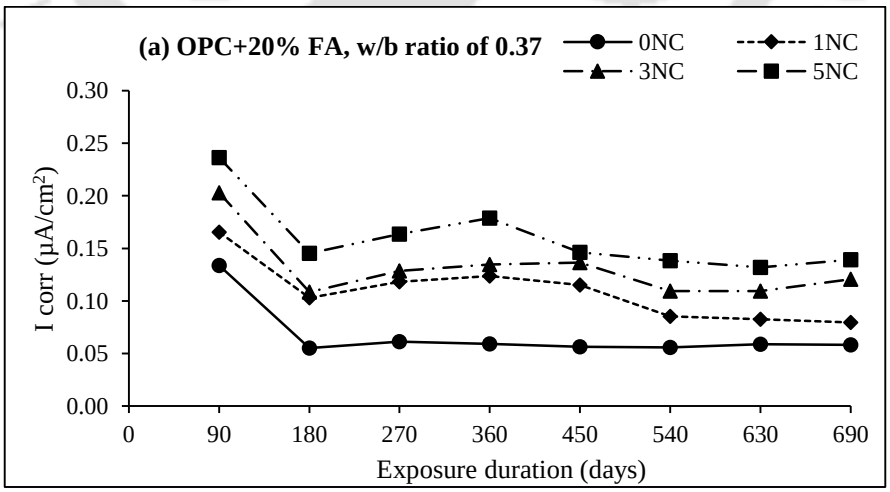

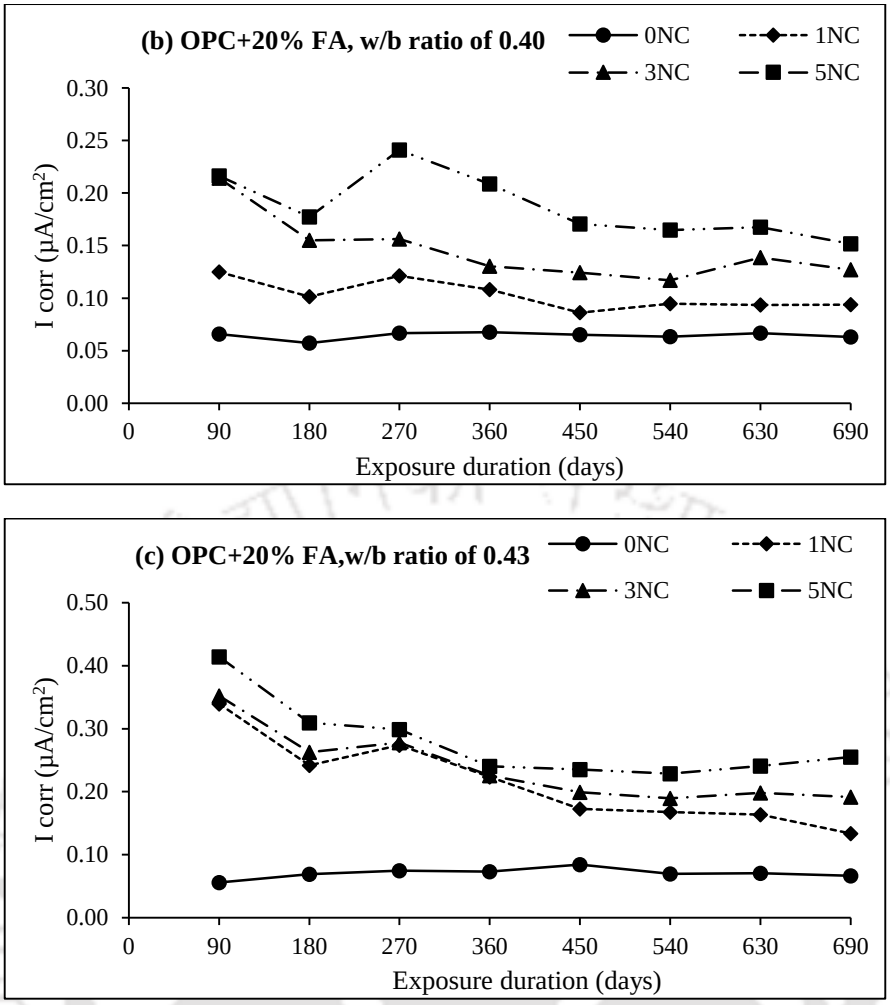

Fig. 7.12 Corrosion current density (I_{corr}) of steel reinforcement in SCC mixes made with OPC+20% FA and exposed to NaCl solutions, at w/b ratios: (a) 0.37, (b) 0.40, and (c) 0.43

From Fig. 7.10 (a - c) to Fig. 7.12 (a - c), it is observed that the corrosion current density of steel reinforcement in SCC specimens exposed to normal water was lower as compared to those exposed to NaCl solutions irrespective of binder type, w/b ratio and exposure duration. Further, the variation in corrosion current density with increase in exposure period was less in the case of exposure to normal water. From the results, it is observed that the corrosion current density increased with increase NaCl concentration in the exposure solution for all binders and w/b ratios, as evident from Fig. 7.10 (a - c) to Fig. 7.12 (a - c). This is attributed to higher chloride concentration in concrete exposed to NaCl solutions of higher concentration because of ingress of more amount of chloride ions that might have increased the conductivity of concrete. It has been mentioned in Chapter 3 that the free and total chloride concentrations of concrete powder collected at reinforcing steel bar level in the prismatic specimens at the end of exposure period (690 days) were determined using

potentiometric titration. The results of free and total chloride concentrations of concrete at rebar level in the SCC mixes at the end of exposure period are presented in Table 7.1. From this table, it is observed that the free chloride concentration at the rebar level was higher for 5% NaCl solution as compared to that for 3% followed by 1% NaCl solution at the end of exposure period. The total chloride concentration was also higher for exposure solutions of higher NaCl concentration as observed from Table 7.1. The higher chloride concentration near the rebar level resulted in an increase in the corrosion current density of steel reinforcement in SCC mixes.

Table 7.1 Total and free chloride concentrations (% by mass of concrete) at rebar level in SCC mixes at the end of exposure period for NaCl exposure solutions

Binder type	Concentration of exposure solution	w/b ratio of 0.37		w/b ratio of 0.40		w/b ratio of 0.43	
		Total chloride	Free chloride	Total chloride	Free chloride	Total chloride	Free chloride
OPC	1% NaCl	0.02	0.00	0.09	0.00	0.14	0.09
	3% NaCl	0.07	0.00	0.20	0.16	0.41	0.22
	5% NaCl	0.18	0.14	0.37	0.26	0.55	0.43
PPC	1% NaCl	0.00	0.00	0.01	0.00	0.04	0.00
	3% NaCl	0.02	0.00	0.05	0.00	0.09	0.06
	5% NaCl	0.03	0.00	0.05	0.00	0.09	0.05
OPC+20 % FA	1% NaCl	0.00	0.00	0.02	0.00	0.03	0.00
	3% NaCl	0.02	0.00	0.05	0.00	0.07	0.00
	5% NaCl	0.04	0.00	0.08	0.06	0.12	0.10

While analyzing the effect of binder type on the corrosion current density of steel reinforcement, it is observed that the corrosion current density was lower in OPC based SCC mixes as compared to that in PPC and OPC+20% FA based SCC mixes during the early exposure period, however during the later exposure period, the opposite variation was observed i.e. the corrosion current density was higher in OPC as compared to that in PPC and OPC+20% FA based SCC mixes, as observed from Fig. 7.10 to Fig. 7.12. The higher corrosion current density in PPC and OPC+20% FA based SCC mixes during the early exposure period may be attributed to the dominant effect of the alterations in the oxygen and moisture contents near the rebar level. The lower corrosion current density in OPC

based SCC mixes during the early period of exposure may be attributed to the dominant effect of the ingress of lower amount of chloride ions into the concrete. The lower corrosion current density in PPC and OPC+20% FA based SCC mixes during the later exposure period may be attributed to the formation denser microstructure due to the production of additional C-S-H gel in the pozzolanic reaction that reduced the penetration of chloride ions into the concrete thereby resulting in lower amount of chloride ions near the rebar level. The corrosion current density was mostly lower in PPC as compared to that in OPC+20% FA based SCC mixes for all w/b ratios and chloride exposure solutions. This may be attributed to uniform blending of fly ash with clinker during manufacturing of PPC that has resulted in formation of improved microstructure in PPC concrete as compared to that in OPC+20% FA concrete. The consumption of calcium hydroxide in the pozzolanic reaction in PPC and OPC+20% FA based SCC mixes is evident from the typical XRD patterns shown in Fig. 7.13 (a - c) for 3% NaCl exposure solution at the end of exposure period (690 days). From the XRD results, the peak intensity of calcium hydroxide (CH) and its weight percentage (shown in Table 7.2) estimated semi-quantitatively using the normalized RIR method (mentioned in Chapter 3) were lower in PPC and OPC+20% FA based SCC mixes as compared to that in OPC based SCC mixes. It may be noted that XRD analysis was conducted on the concrete powder samples collected from the rebar level in the prismatic specimens at the end of exposure period (690 days). The peaks of calcium hydroxide (CH) in SCC mixes were identified at 18.11° 2θ, 34.1° 2θ, and 36.55° 2θ as observed from Fig. 7.13. The variations in calcium hydroxide (CH) content estimated from RIR method using the XRD results for different types of binder are corroborated with the Ca/Si ratio of C-S-H estimated from EDX analysis. The typical plots of EDX analysis for SCC mixes made with OPC, PPC and OPC+20% FA and exposed to 3% NaCl solution are shown in Fig. 7.14 (a - c), Fig. 7.15 (a - c) and Fig. 7.16 (a - c), respectively. The Ca/Si ratio of C-S-H estimated from EDX analysis was lower in PPC and OPC+20% FA based SCC mixes as compared to that in OPC based SCC mixes, which is attributed to the consumption of calcium hydroxide during the pozzolanic reaction in PPC and OPC+20% FA concrete.

The higher corrosion density in OPC based SCC mixes during later exposure period may be attributed to penetration of higher concentration of chloride ions into concrete, thereby increasing the conductivity of concrete. The penetration of higher concentration of chloride ions in OPC based SCC mixes during later ages is substantiated with the measured free and

total chloride concentrations of concrete powder collected from the rebar level at the end of exposure period, which are presented in Table 7.1. From this table, it is observed that the free and total chloride concentrations were higher in OPC based SCC mixes as compared to those in PPC and OPC+20% FA based SCC mixes for all w/b ratios and NaCl solutions. In addition, in PPC and OPC+20% FA based SCC mixes, the measured free chloride concentration was zero in majority of the cases as observed from Table 7.1, thus resulting in lower corrosion current density at the age of 690 days. The bound chloride concentration values (difference of total and free chloride concentrations) were also higher in OPC based SCC mixes as compared to that in PPC and OPC+20% FA based SCC mixes. This indicates that higher concentrations of both free and bound chloride in OPC based SCC mixes are attributed to penetration of higher amount of chloride ions as compared to that in PPC and OPC+20% FA based SCC mixes. The higher chloride binding in OPC based SCC mixes is corroborated with the typical XRD patterns shown in Fig. 7.13 (a) wherein the peak of calcium chloroaluminate (CCA: formed due to reaction of chloride ions with hydrated C_3A) found only in OPC based SCC mix although at w/b ratio of 0.43 only. However, in PPC and OPC +20% FA based SCC mixes, the peaks of CCA were not found irrespective of w/b ratio as observed from the typical XRD patterns shown in Fig. 7.13 (b, c). The peaks of gypsum (G) were found at 32.1° 2θ and 50.5° 2θ and those of ettringite (E: formed due to the reaction of gypsum with hydrated C_3A) were found at 8.8° 2θ, 15.75° 2θ, 25.6° 2θ, and 27.5° 2θ as observed from the XRD patterns shown in Fig. 7.13. The peak intensity and wt. % of ettringite were higher in OPC based SCC mixes as compared to that in PPC and OPC+20% FA based SCC mixes, which may be attributed to the availability of comparatively more amount of C_3A in OPC as compared to that in PPC and OPC+20% FA based SCC mixes (Fig. 7.13 and Table 7.2). The peaks of quartz in the SCC mixes were found at 20.78° 2θ, 26.65° 2θ, 39.45° 2θ, 42.45° 2θ, and 50.2° 2θ as observed from the XRD patterns shown in Fig. 7.13. At the end of exposure period (i.e. 690 days), the corrosion current density of steel reinforcement in SCC mixes made with OPC was 3.29 times and 1.15 times higher than that in OPC+20% FA and PPC based SCC mixes, respectively irrespective of the w/b ratio of concrete and concentration of NaCl solution.

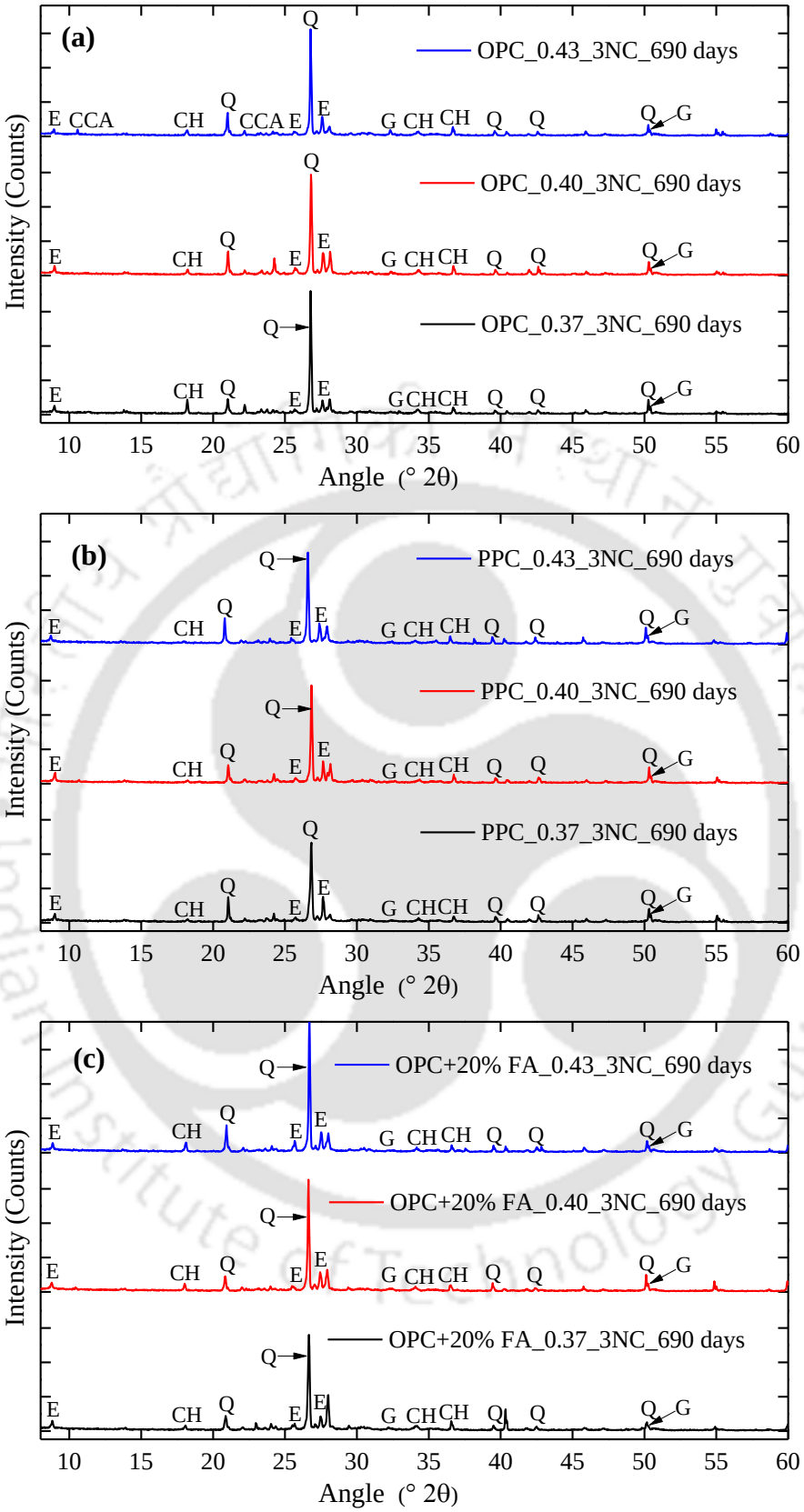

Fig. 7.13 XRD patterns of SCC mixes at exposure duration of 690 days in 3% NaCl exposure solution at w/b ratios of 0.37, 0.40 and 0.43: (a) OPC, (b) PPC and (c) OPC+20% FA

Table 7.2 Weight % of various compounds from the XRD patterns using RIR method for SCC mixes exposed to 3% NaCl solution

Compound name	Weight percentage (wt. %)								
	OPC			PPC			OPC+20% FA		
	w/b ratio of 0.37	w/b ratio of 0.40	w/b ratio of 0.43	w/b ratio of 0.37	w/b ratio of 0.40	w/b ratio of 0.43	w/b ratio of 0.37	w/b ratio of 0.40	w/b ratio of 0.43
Quartz	84	80	89	83	88	91	82	87	88
Portlandite	6	6	4	4	2	2	6	5	4
Ettringite	8	7	4	7	4	2	8	5	4
Gypsum	2	7	1	6	6	4	4	2	4
CCA	0	0	3	0	0	0	0	0	0

While comparing the effect of w/b ratio on corrosion current density of steel reinforcement, it is observed that the corrosion current density in SCC specimens mostly decreased with decrease in w/b ratio as observed from Fig. 7.10 to Fig. 7.12 for all binders and NaCl solutions. The lower corrosion current density of steel reinforcement at lower w/b ratio may be ascribed to the formation of denser microstructure thereby decreasing the penetration of chloride ions into concrete. The formation of denser microstructure at lower w/b ratio resulted in increase in resistivity of concrete thereby decreasing the corrosion current density of steel reinforcement. In addition, the free and total chloride concentrations shown in Table 7.1 indicate penetration of lower amount chloride ions into concrete at lower w/b ratio as compared to that at higher w/b ratio.

Further, the peak intensity (in XRD patterns) and the wt. % (estimated from semi-quantification analysis using RIR method) of calcium hydroxide (CH) in SCC mostly increased with decrease in w/b ratio for all binders as observed from Fig. 7.13 and Table 7.2. This may be attributed to availability of higher amount of calcium hydroxide in concrete at lower w/b ratio because of higher binder content. Further, the Ca/Si ratio of C-S-H increased with decrease in w/b ratio as observed from Fig. 7.14 to Fig. 7.16. From Fig. 7.13 and Table 7.2, it is observed that the peak intensity and wt. % of ettringite (E) increased with decrease in w/b ratio in the SCC mixes for all types of binder. This may be attributed to the reaction of gypsum with hydrated C_3A to a greater extent at lower w/b ratio due to the availability of higher amount of C_3A in concrete at lower w/b ratio.

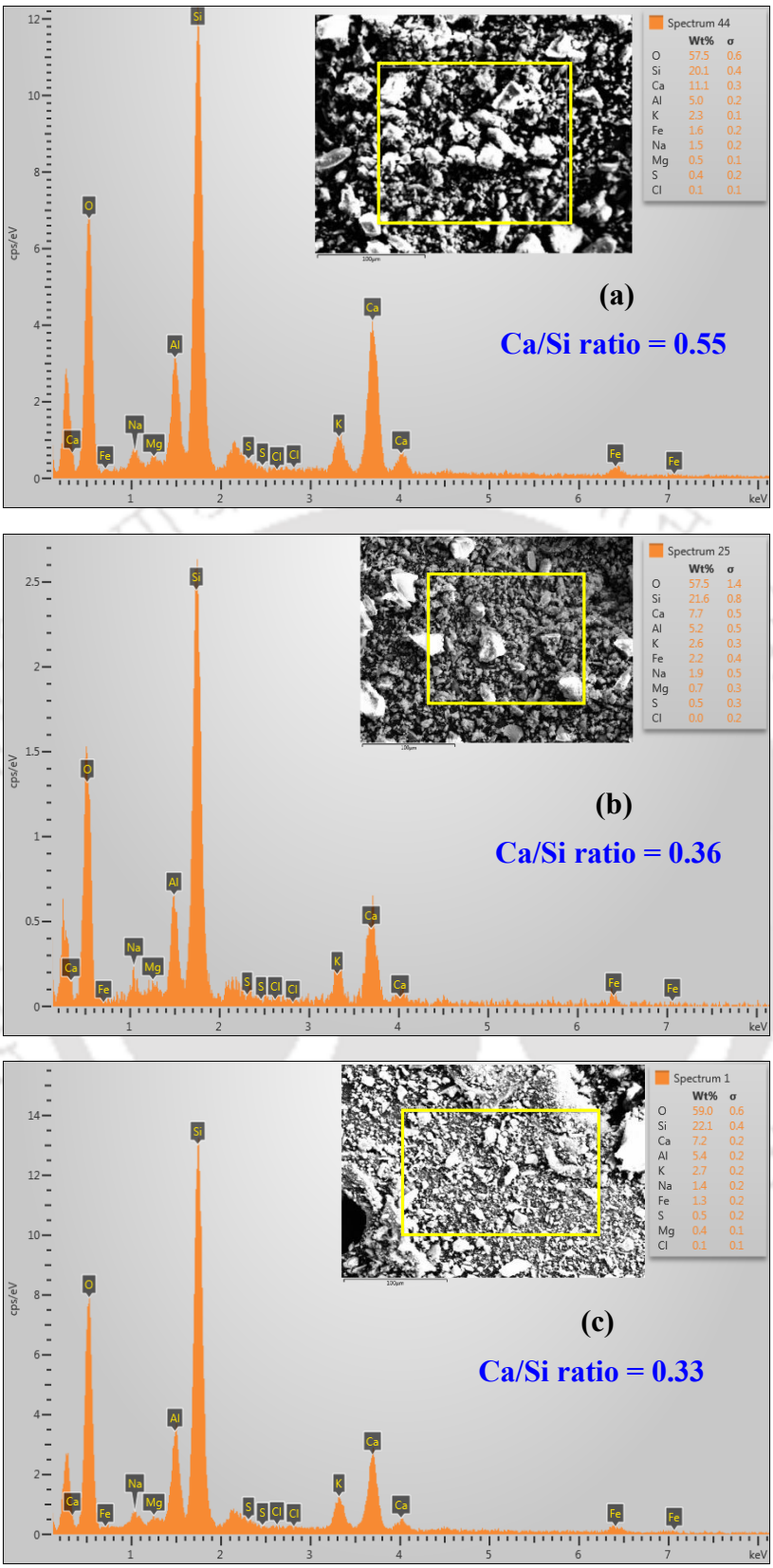

Fig. 7.14 EDX analysis of OPC based SCC mixes at exposure duration of 690 days in 3% NaCl solution: (a) w/b ratio of 0.37, (b) w/b ratio of 0.40, and (c) w/b ratio of 0.43

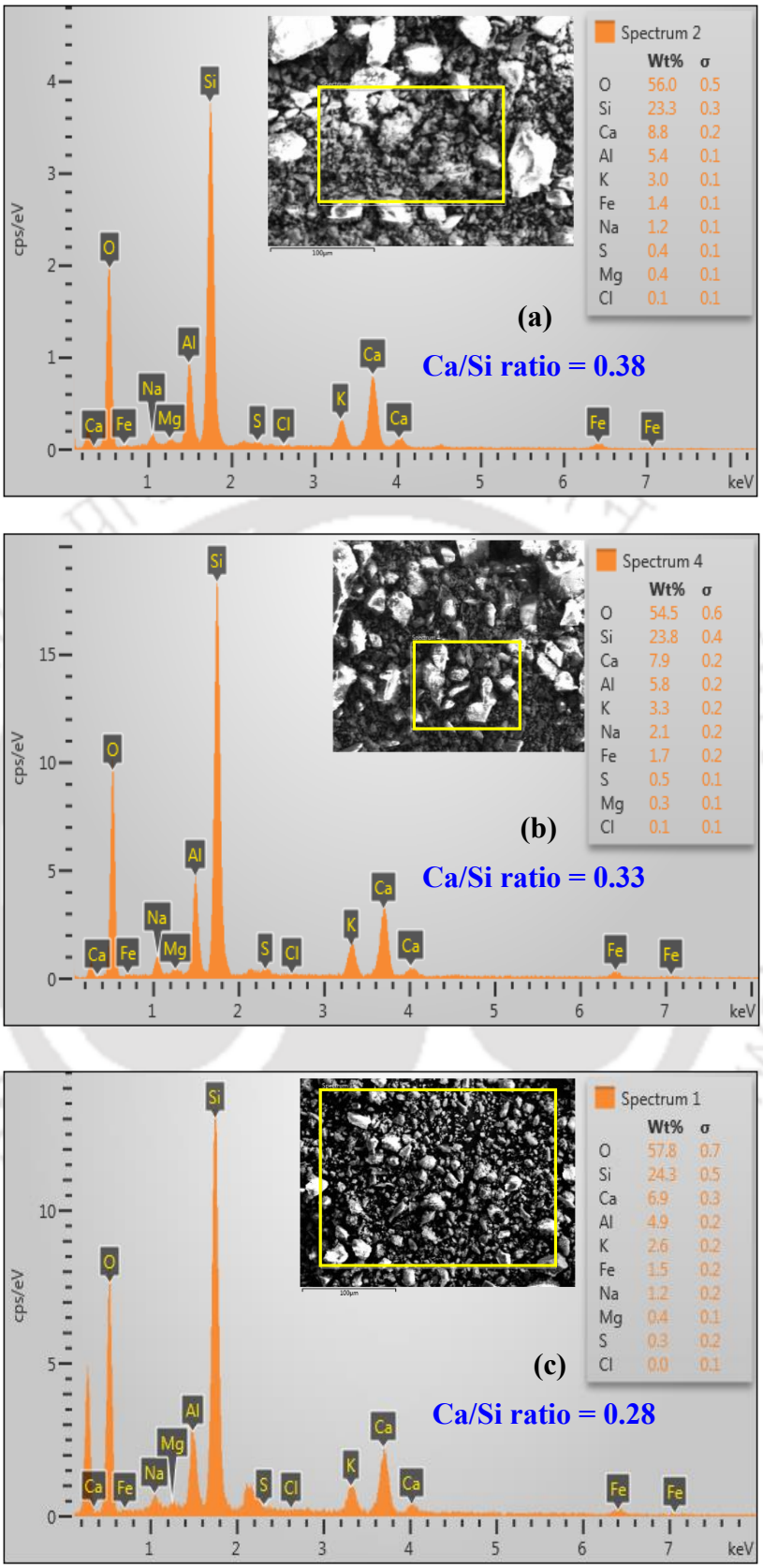

Fig. 7.15 EDX analysis of PPC based SCC mixes at exposure duration of 690 days in 3% NaCl solution: (a) w/b ratio of 0.37, (b) w/b ratio of 0.40, and (c) w/b ratio of 0.43

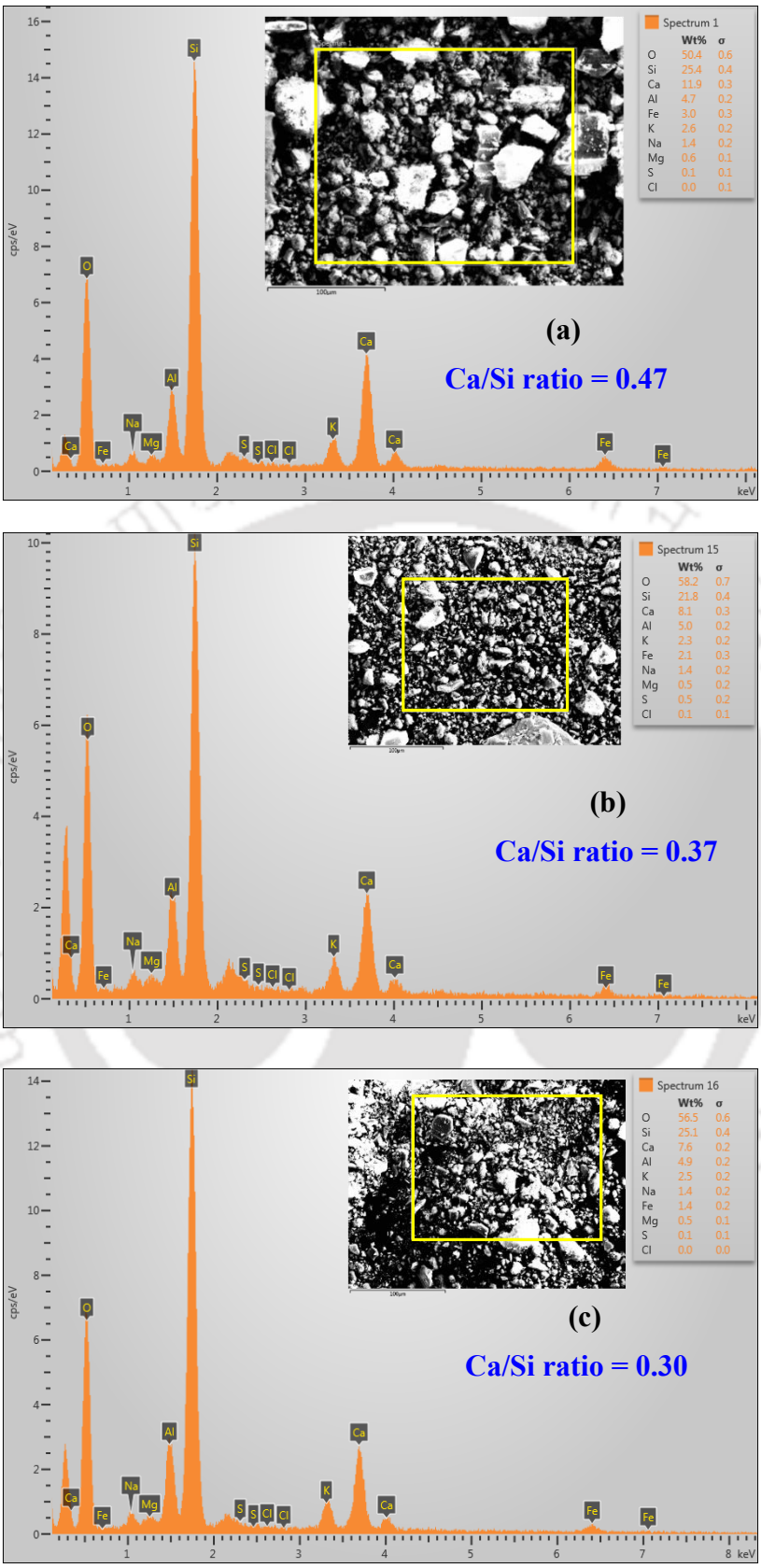

Fig. 7.16 EDX analysis of OPC+20% FA based SCC mixes at exposure duration of 690 days in 3% NaCl solution: (a) w/b ratio of 0.37, (b) w/b ratio of 0.40, and (c) w/b ratio of 0.43

The morphology of the SCC mixes was analyzed through FESEM analysis, which was carried out on the concrete powder samples collected from the rebar level in the prismatic specimens at the end of exposure period (690 days). The typical FESEM images are shown in Fig. 7.17, Fig. 7.18 and Fig. 7.19, respectively for OPC, PPC and OPC+20% FA based SCC mixes for 3% NaCl solution. The FESEM images shown in these figures indicate the formation of C-S-H in the form of reticular network structure in all the SCC mixes irrespective of binder type and w/b ratio. The formation of calcium chloroaluminate (CCA) in OPC based SCC mixes was confirmed as CCA crystals were appeared in hexagonal-slice shape, as observed from Fig. 7.17 (c). However, CCA crystals were not observed in the FESEM images shown in Fig. 7.18 and Fig. 7.19 for the SCC mixes made from PPC and OPC+20% FA, respectively. Further, ettringite (E) in the form of needle like crystals was observed in the SCC mixes for all binders as indicated by FESEM images shown in Fig. 7.17 to Fig. 7.19. In addition, the presence of calcium hydroxide (CH) was observed in the form of hexagonal shape crystals as observed from the FESEM image shown in Fig. 7.17 (a).

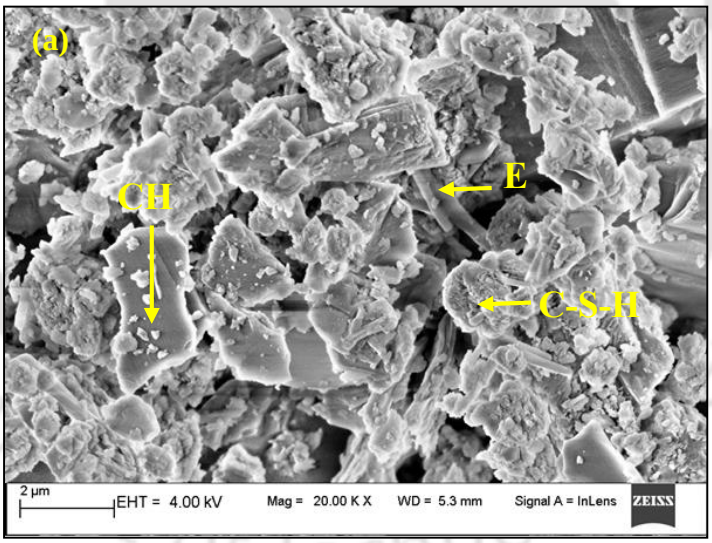

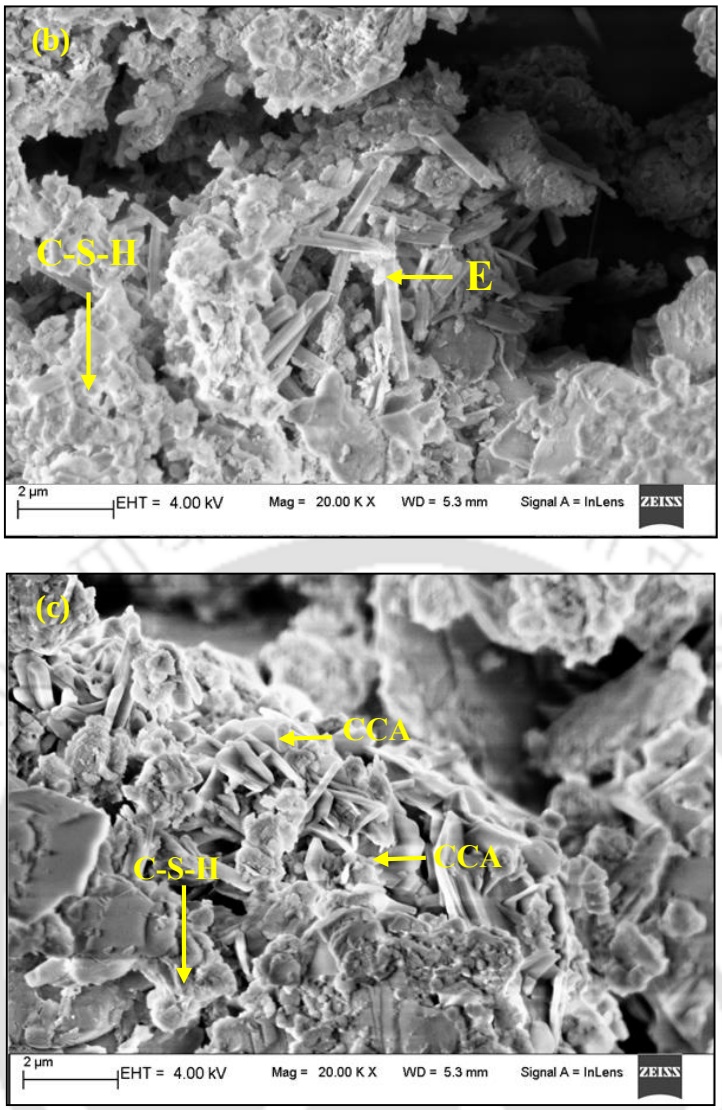

Fig. 7.17 FESEM images of OPC based SCC mixes at exposure duration of 690 days in 3% NaCl solution: (a) w/b ratio of 0.37, (b) w/b ratio of 0.40, and (c) w/b ratio of 0.43

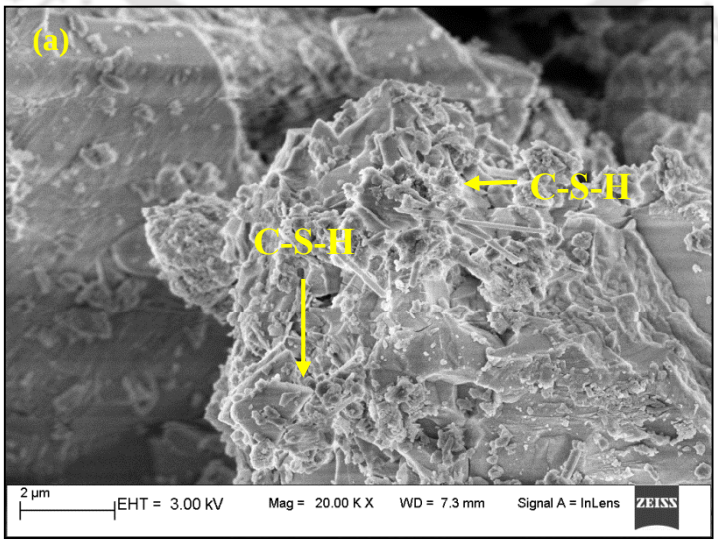

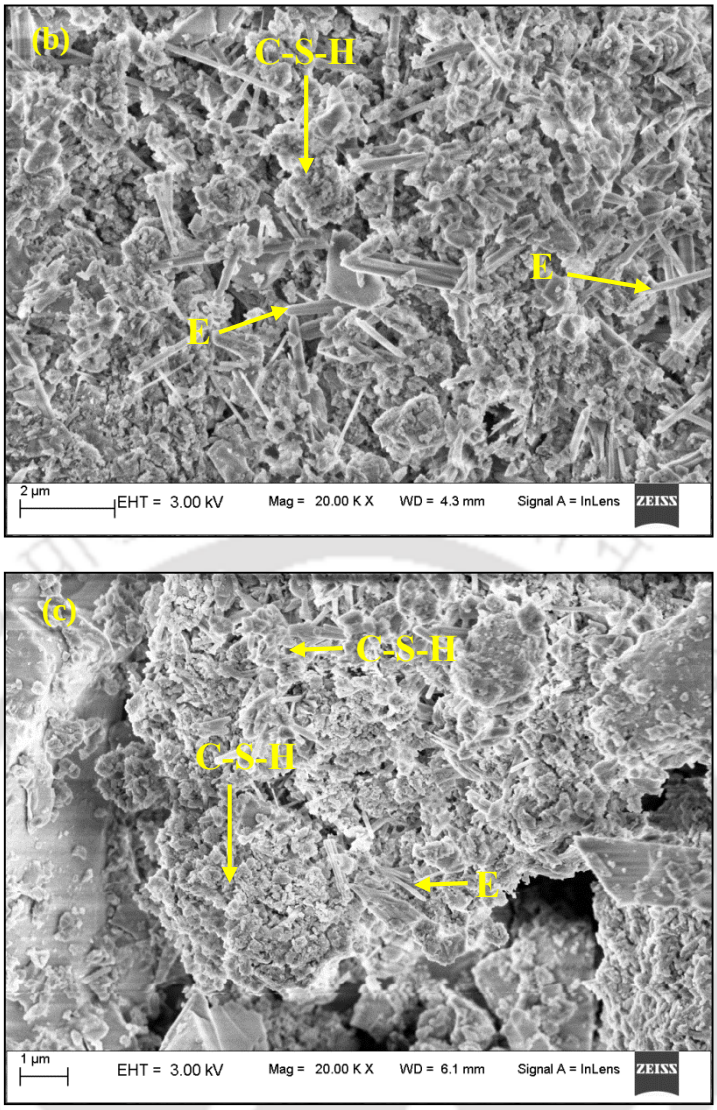

Fig. 7.18 FESEM images of PPC based SCC mixes at exposure duration of 690 days in 3% NaCl solution: (a) w/b ratio of 0.37, (b) w/b ratio of 0.40, and (c) w/b ratio of 0.43

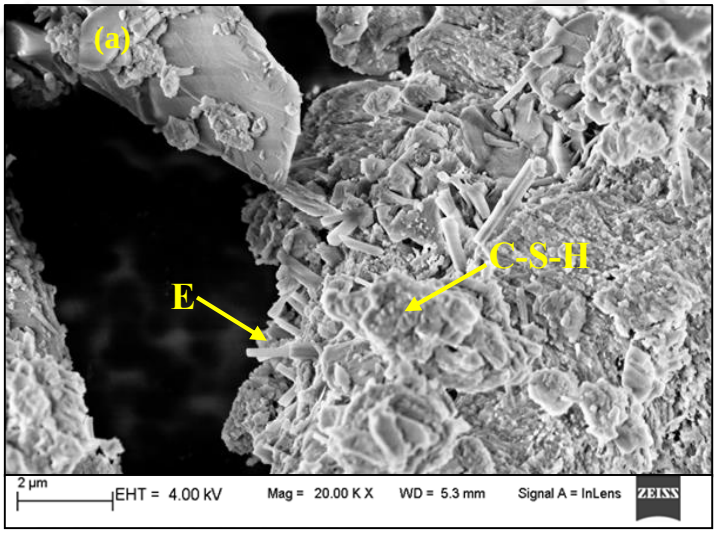

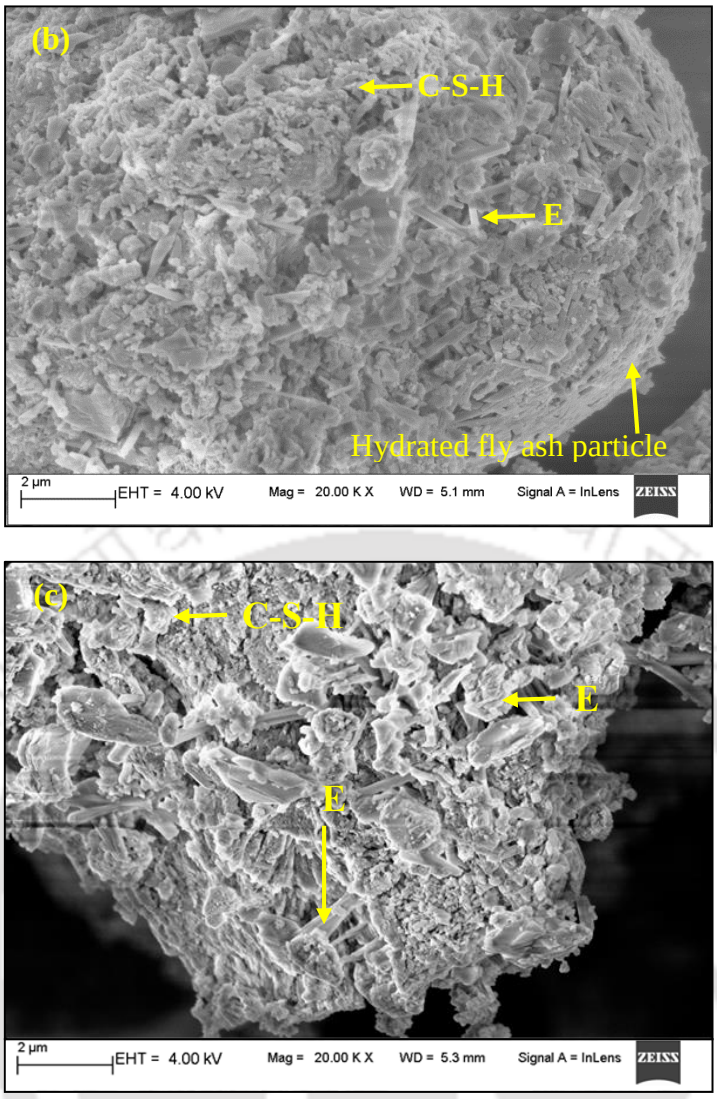

Fig. 7.19 FESEM images of OPC+20% FA based SCC mixes at exposure duration of 690 days in 3% NaCl solution: (a) w/b ratio of 0.37, (b) w/b ratio of 0.40, and (c) w/b ratio of 0.43

7.3.2 Corrosion current density of steel reinforcement in SCC exposed to NaCl + Na_2SO_4 and NaCl + $MgSO_4$ solutions

The measured corrosion current density (I_{corr}) of steel reinforcement in OPC based prismatic SCC specimens exposed to varying concentrations of combined NaCl + Na_2SO_4 solutions at w/b ratios of 0.37, 0.40 and 0.43 are shown in Fig. 7.20 (a), Fig. 7.20 (b), and Fig. 7.20 (c), respectively. Similarly, corrosion current density of steel reinforcement in prismatic SCC specimens made with PPC and OPC+20% FA are shown in Fig. 7.21 (a - c) and Fig. 7.22 (a - c), respectively. Further, the corrosion current density (I_{corr}) of steel reinforcement in OPC, PPC and OPC+20% FA based prismatic SCC specimens exposed

to varying concentrations of combined NaCl + $MgSO_4$ solutions are shown in Fig. 7.23 (a - c), Fig. 7.24 (a - c) and Fig. 7.25 (a - c), respectively. Each value of corrosion current density shown in these figures is the average value of four replicate prismatic specimens.

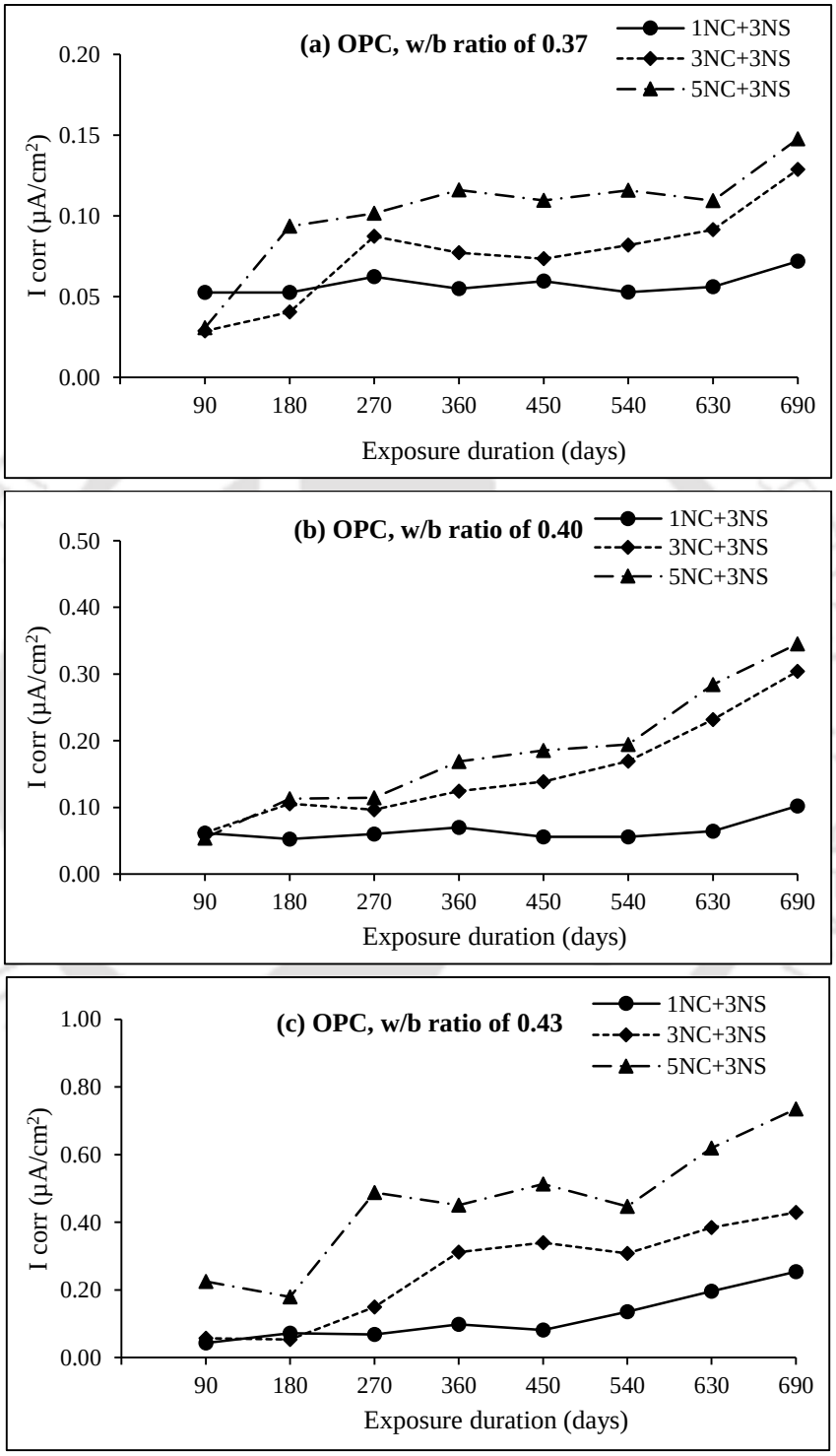

Fig. 7.20 Corrosion current density (I_{corr}) of steel reinforcement in SCC mixes made with OPC and exposed to NaCl + Na_2SO_4 solutions, at w/b ratios: (a) 0.37, (b) 0.40, and (c) 0.43

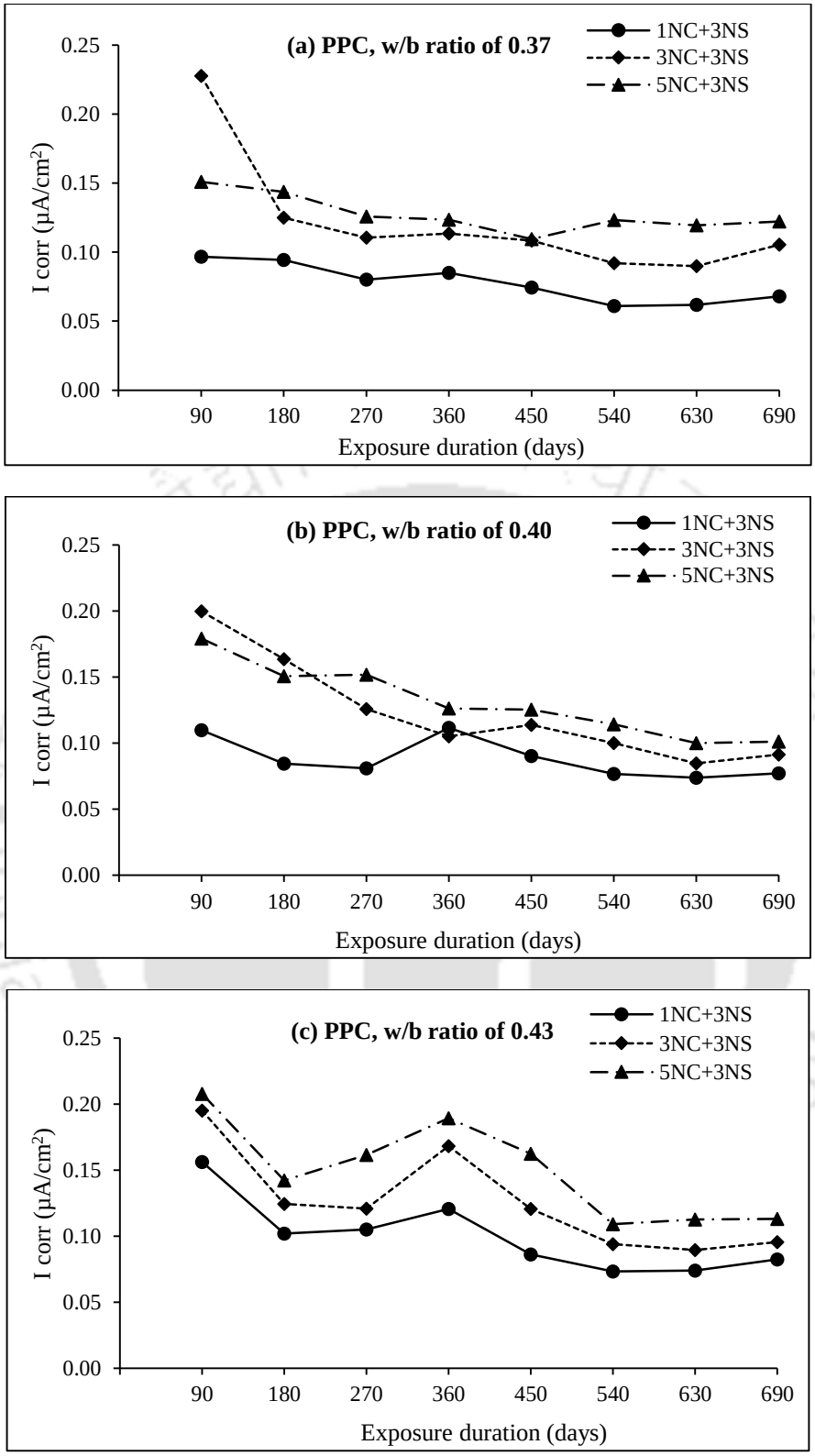

Fig. 7.21 Corrosion current density (I_{corr}) of steel reinforcement in SCC mixes made with PPC and exposed to NaCl + Na_2SO_4 solutions, at w/b ratios: (a) 0.37, (b) 0.40, and (c) 0.43

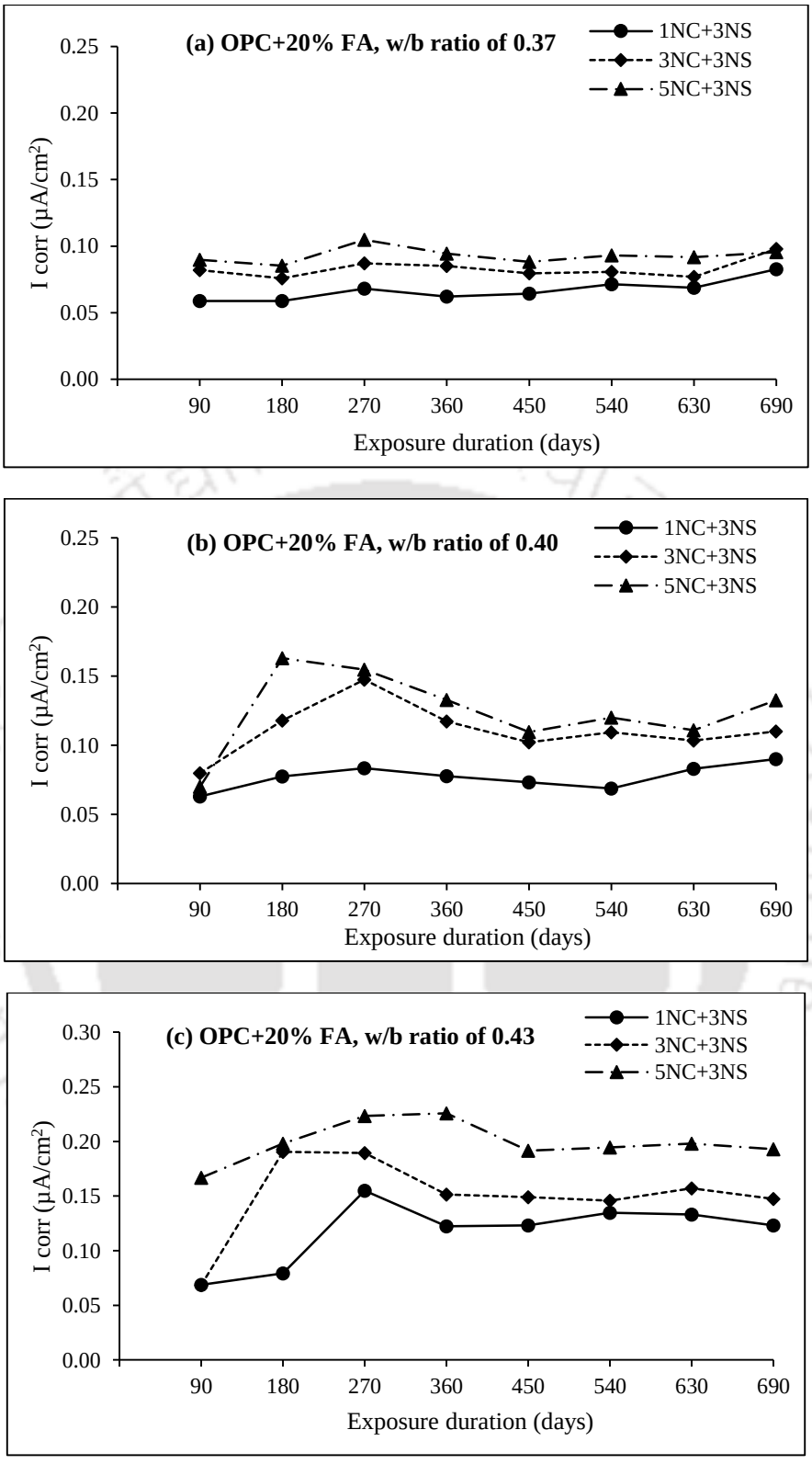

Fig. 7.22 Corrosion current density (I_{corr}) of steel reinforcement in SCC mixes made with OPC + 20% FA and exposed to NaCl + Na_2SO_4 solutions, at w/b ratios: (a) 0.37, (b) 0.40, and (c) 0.43

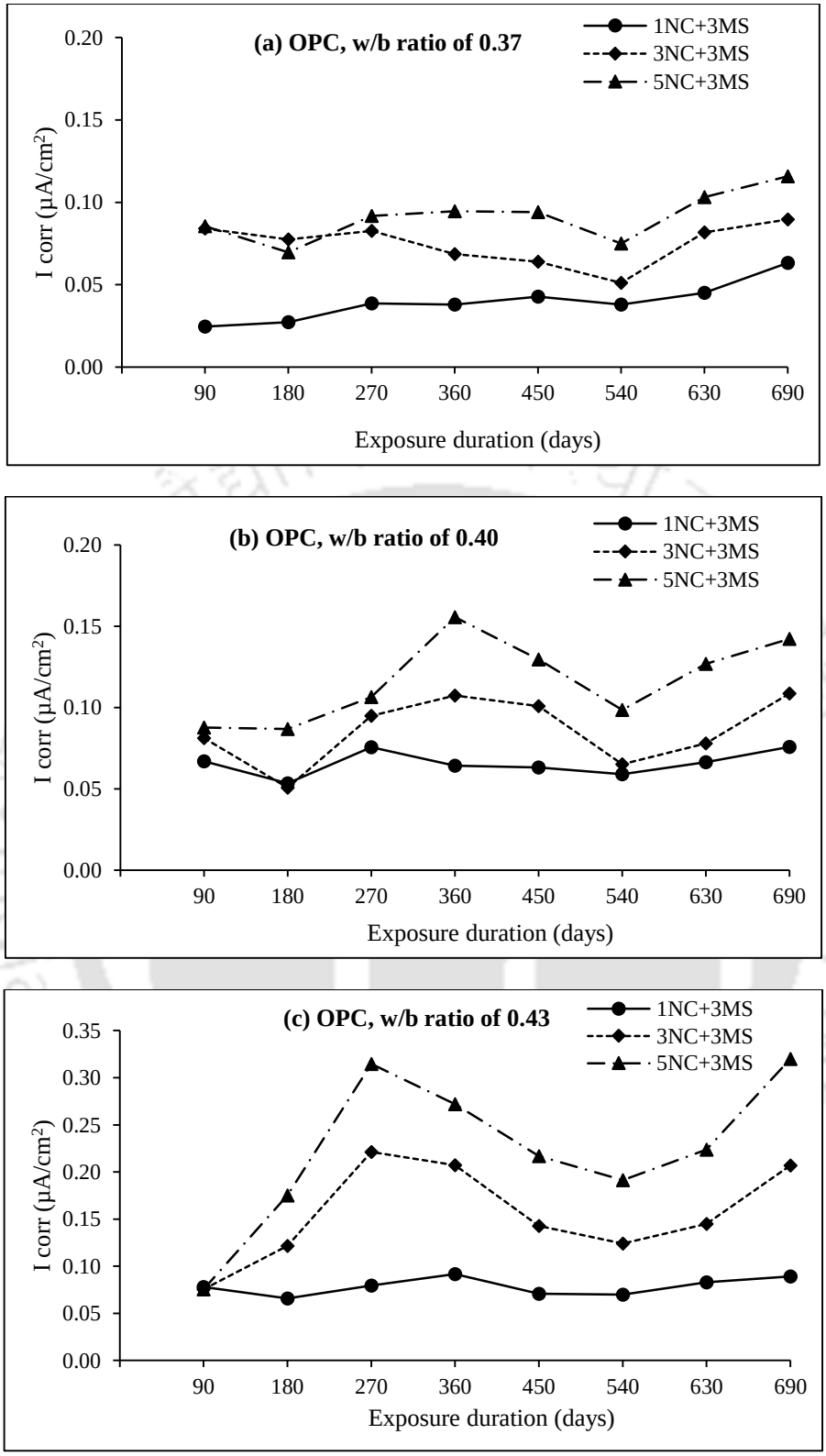

Fig. 7.23 Corrosion current density (I_{corr}) of steel reinforcement in SCC mixes made with OPC and exposed to NaCl + $MgSO_4$ solutions, at w/b ratios: (a) 0.37, (b) 0.40, and (c) 0.43

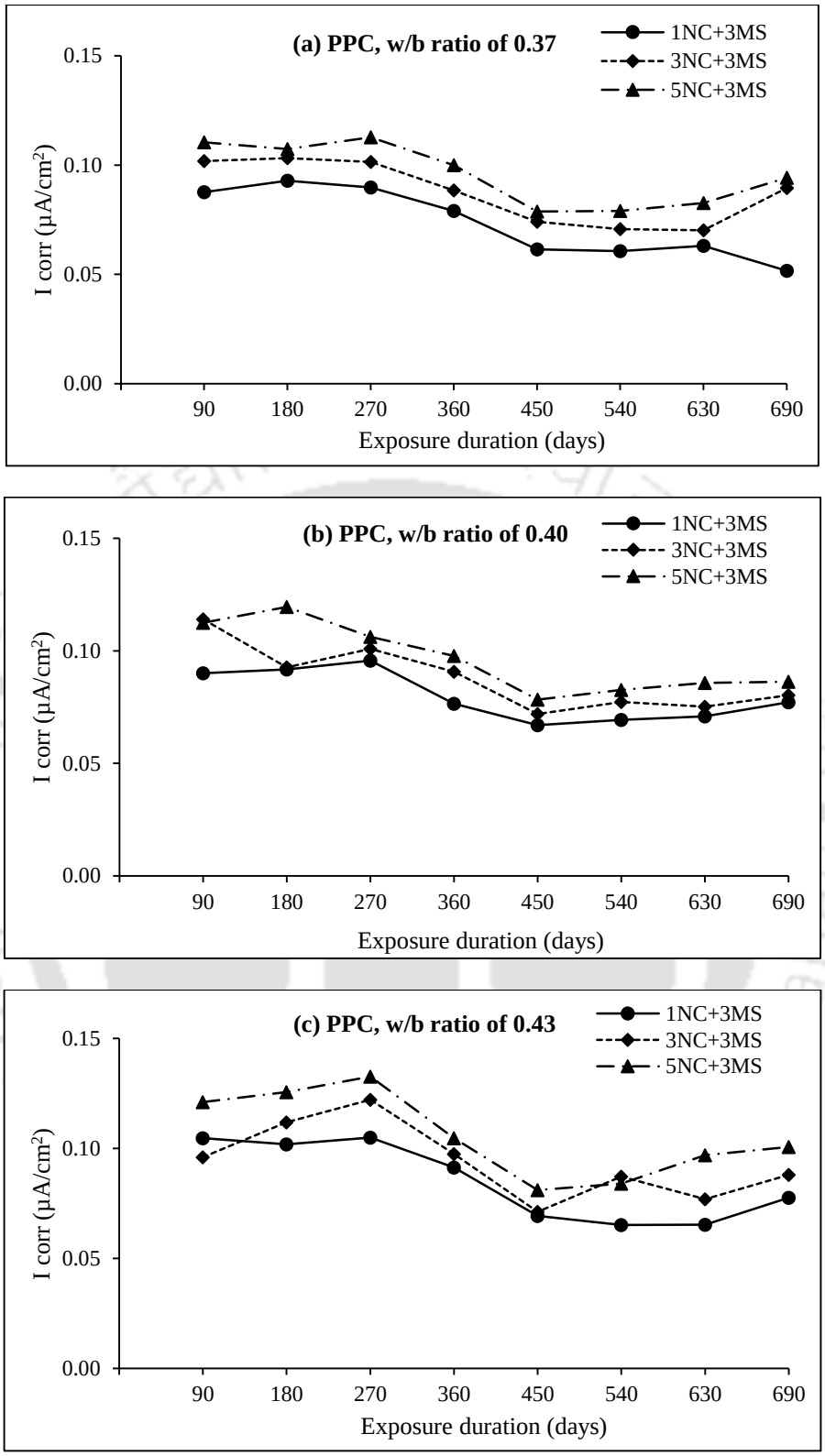

Fig. 7.24 Corrosion current density (I_{corr}) of steel reinforcement in SCC mixes made with PPC and exposed to NaCl + $MgSO_4$ solutions, at w/b ratios: (a) 0.37, (b) 0.40, and (c) 0.43

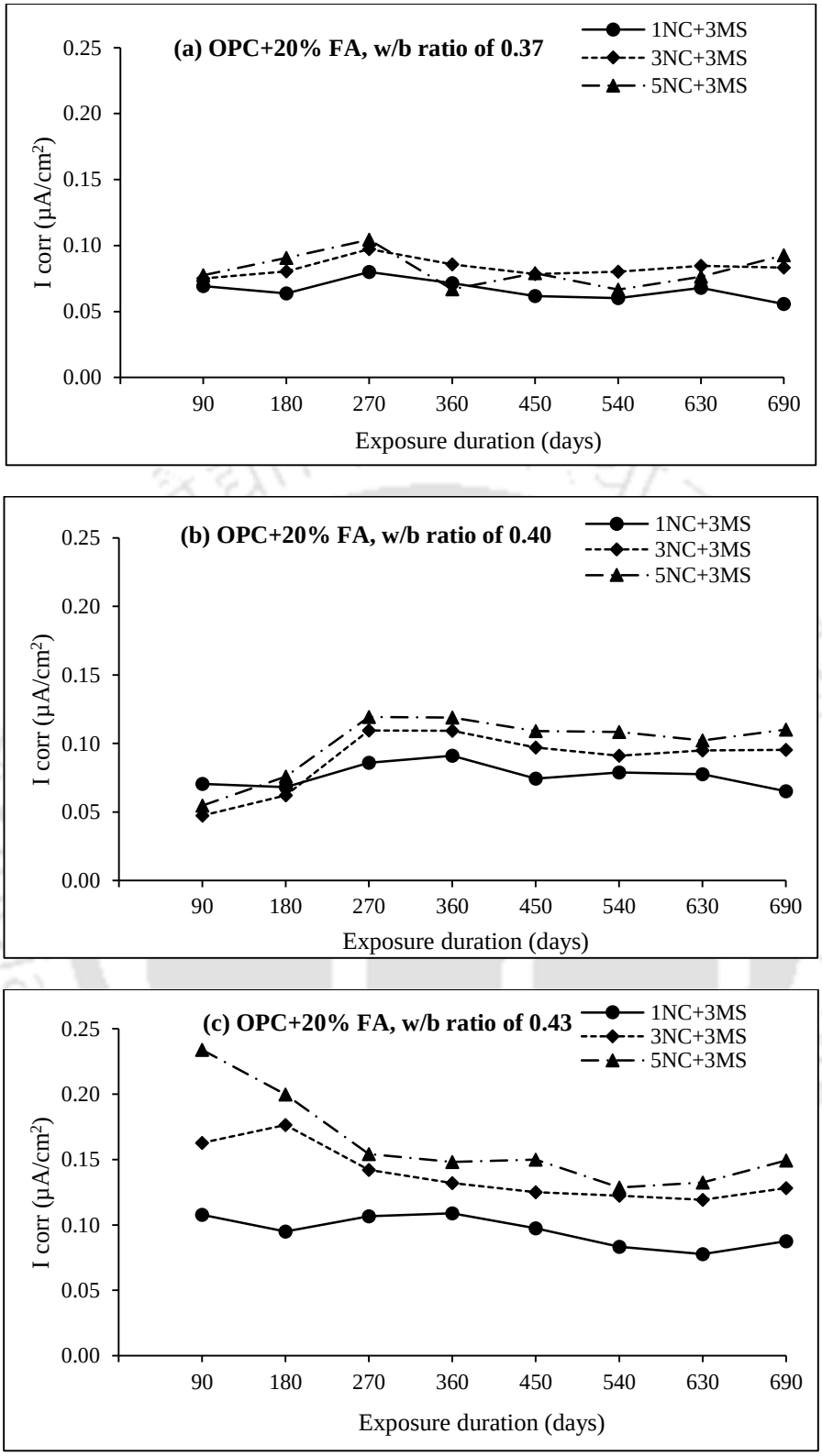

Fig. 7.25 Corrosion current density (I_{corr}) of steel reinforcement in SCC mixes made with OPC+20% FA and exposed to NaCl + $MgSO_4$ solutions, at w/b ratios: (a) 0.37, (b) 0.40, and (c) 0.43

From the corrosion current density values shown in Fig. 7.20 (a - c) to Fig. 7.22 (a - c), it is observed that the corrosion current density of steel reinforcement increased with increase in NaCl concentration in combined NaCl + Na_2SO_4 exposure solutions for all the SCC mixes irrespective of binder type, w/b ratio and exposure duration. Similarly, the corrosion current density of steel reinforcement increased with increase in NaCl concentration in combined NaCl + $MgSO_4$ exposure solutions, as observed from Fig. 7.23 to Fig. 7.25. This is attributed to the increase in conductivity of the SCC mixes due to the penetration of more chloride ions of higher concentration into the SCC mixes exposed to chloride-sulfate solutions containing higher concentration of NaCl. From the measured total and free chloride concentrations of the concrete powder samples collected from the rebar level in the prismatic specimens at the end of exposure period (i.e. 690 days), it is observed that the total and free chloride concentrations at the rebar level were higher for higher concentration of NaCl in the exposure solution as observed from Table 7.3, although in most of the cases the free chloride concentration of concrete at the rebar level was zero.

While comparing the binder type, it is inferred that the SCC specimens made with PPC and OPC+20% FA showed higher corrosion current density as compared to those made with OPC during the early exposure periods for both types of combined exposure solutions (NaCl + Na_2SO_4 and NaCl + $MgSO_4$) as observed from Fig. 7.20 to Fig. 7.25. However, during the later exposure periods, the corrosion current density was lower in PPC and OPC+20% FA based SCC specimens as compared to that in OPC based SCC specimens. The lower corrosion current density in OPC based SCC mixes during early exposure periods may be due to the dominant effect of the penetration of lower amount of chloride ions into the concrete, although the penetration of sulfate ions might have affected the conductivity of concrete. The higher corrosion current density in PPC and OPC+20% FA based SCC mixed during the early exposure periods may be attributed to the dominant effect of the alterations in the oxygen and moisture content near the rebar level that altered the conductivity of concrete in the presence of sulfate ions, which might have penetrated into the concrete from the exposure solution. During the later exposure periods, the higher corrosion current density in OPC based SCC mixes may be ascribed to the penetration of higher amount of chloride ions into the concrete along with the ingress of sulfate ions. The penetration of chloride ions of higher concentration increased amount of chloride ions near the rebar level thus increasing the corrosion current density of steel reinforcement in OPC based SCC mixes. The lower corrosion current density in PPC and OPC+20% FA based

SCC mixes during the later exposure periods is ascribed to the penetration of lower amount of chloride and sulfate ions due to the formation of denser microstructure that decreased in amount of chloride ions near the rebar level.

Table 7.3 Total and free chloride concentrations (% by mass of concrete) at rebar level in SCC mixes at the end of exposure period for combined chloride-sulfate exposure solutions

Binder type	w/b ratio	Chloride type	1% NaCl + 3% Na_2SO_4	3% NaCl + 3% Na_2SO_4	5% NaCl + 3% Na_2SO_4	1% NaCl + 3% $MgSO_4$	3% NaCl + 3% $MgSO_4$	5% NaCl + 3% $MgSO_4$
OPC	0.37	Total chloride	0.02	0.06	0.15	0.01	0.01	0.03
		Free chloride	0.00	0.00	0.11	0.00	0.00	0.00
	0.40	Total chloride	0.07	0.14	0.23	0.01	0.03	0.08
		Free chloride	0.00	0.10	0.19	0.00	0.00	0.00
	0.43	Total chloride	0.07	0.37	0.51	0.02	0.06	0.08
		Free chloride	0.00	0.26	0.36	0.00	0.00	0.04
PPC	0.37	Total chloride	0.01	0.02	0.03	0.01	0.01	0.02
		Free chloride	0.00	0.00	0.00	0.00	0.00	0.00
	0.40	Total chloride	0.01	0.02	0.03	0.01	0.01	0.03
		Free chloride	0.00	0.00	0.00	0.00	0.00	0.00
	0.43	Total chloride	0.01	0.02	0.03	0.01	0.02	0.02
		Free chloride	0.00	0.00	0.00	0.00	0.00	0.00
OPC+20% FA	0.37	Total chloride	0.00	0.01	0.02	0.00	0.01	0.02
		Free chloride	0.00	0.00	0.00	0.00	0.00	0.00
	0.40	Total chloride	0.01	0.02	0.02	0.01	0.02	0.02
		Free chloride	0.00	0.00	0.00	0.00	0.00	0.00
	0.43	Total chloride	0.01	0.02	0.03	0.01	0.02	0.02
		Free chloride	0.00	0.00	0.00	0.00	0.00	0.00

From Table 7.3, it is observed that the measured chloride concentrations of the concrete powder samples collected from the rebar level in the prismatic specimens at the end of exposure period (i.e. 690 days) were lower in PPC and OPC+20% FA based SCC mixes as compared to that in OPC based SCC mixes for all w/b ratios and combined chloride-sulfate solutions. The formation of denser microstructure during the later exposure period in PPC and OPC+20% FA based SCC mixes is attributed to the production of more amount of C-S-H gel as a result of pozzolanic reaction in these concrete mixes. The decrease in calcium hydroxide (CH) content as a result of its consumption in the pozzolanic reaction in PPC and OPC+20% FA based SCC mixes is evident from the typical XRD patterns (shown in Fig. 7.26 for 3% NaCl + 3% Na_2SO_4 and Fig. 7.27 for 3% NaCl + 3% $MgSO_4$ exposure solutions) and weight percentage (wt. %) estimated by RIR method (Table 7.4 for or 3%

NaCl + 3% Na_2SO_4, and Table 7.5 for 3% NaCl + 3% $MgSO_4$) wherein the peak intensity and wt. % of calcium hydroxide were lower in PPC and OPC+20% FA based SCC mixes as compared to those in OPC based SCC mixes. The typical XRD patterns shown in Fig. 7.26 and 7.27 and the wt. % of compounds (estimated using RIR method from the XRD patterns) presented in Table 7.4 and 7.5 correspond to the concrete powder samples collected from the rebar level of the prismatic specimens at the age of 690 days (end of exposure period). The variations in the peak intensity (in XRD patterns) and wt. % (estimated from RIR method) of calcium hydroxide (CH) are consistent with the variations in Ca/Si ratio of C-S-H calculated from EDX analysis for the SCC mixes at the end of the exposure period. The typical plots of EDX analysis for the SCC mixes made with OPC, PPC and OPC+20% FA are shown in Fig. 7.28 (a - c) to Fig. 7.30 (a - c), respectively for 3% NaCl + 3% Na_2SO_4 exposure solution and in Fig. 7.31 (a - c) to Fig. 7.33 (a - c) for 3% NaCl + 3% $MgSO_4$ exposure solution. The results of EDX analysis indicate that the Ca/Si ratio of C-S-H was lower in PPC and OPC+20% FA based SCC mixes than that in OPC based SCC mixes This is ascribed to the dominant effect of the consumption of calcium hydroxide during the pozzolanic reaction in PPC and OPC+20% FA based SCC mixes. The formation of C-S-H in the SCC mixes is observed from the typical FESEM images shown in Fig. 7.34 for OPC, PPC and OPC+20% FA based SCC mixes exposed to 3% NaCl + 3% Na_2SO_4 solution wherein the C-S-H gel appeared in the form of reticular network structure.

Between PPC and OPC+20% FA based SCC mixes, the corrosion current density was lower in PPC as compared to that in OPC+20% FA based SCC mixes for both NaCl + Na_2SO_4 and NaCl + $MgSO_4$ exposure solutions as observed from Fig. 7.20 to Fig. 7.25. The corrosion current density of steel reinforcement in the SCC mixes made with OPC were 2.85 times and 2.94 times higher than that in OPC+20% FA and PPC based SCC mixes, respectively for NaCl + Na_2SO_4 exposure solutions at the end of exposure period, irrespective of w/b ratio and concentration of NaCl + Na_2SO_4 solutions. Similarly, the corrosion current density of steel reinforcement in the SCC mixes made with OPC were 1.40 times and 1.63 times higher than that in OPC+20% FA and PPC based SCC mixes at the end of exposure period for NaCl + $MgSO_4$ exposure solutions.

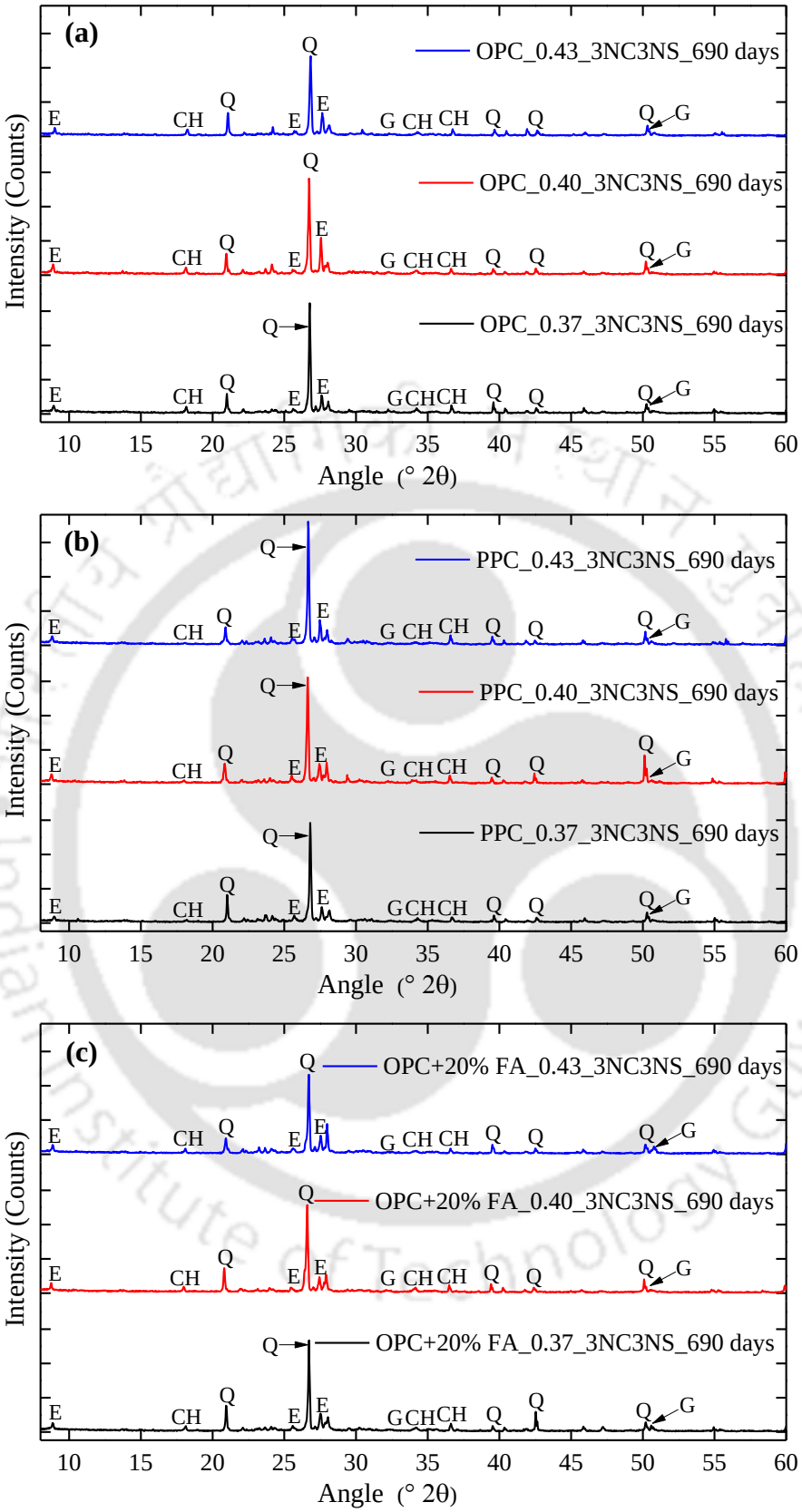

Fig. 7.26 XRD patterns of SCC mixes at exposure duration of 690 days for w/b ratios of 0.37, 0.40 and 0.43 and exposed to 3% NaCl + 3% Na_2SO_4 solution: (a) OPC, (b) PPC, and (c) OPC+20% FA

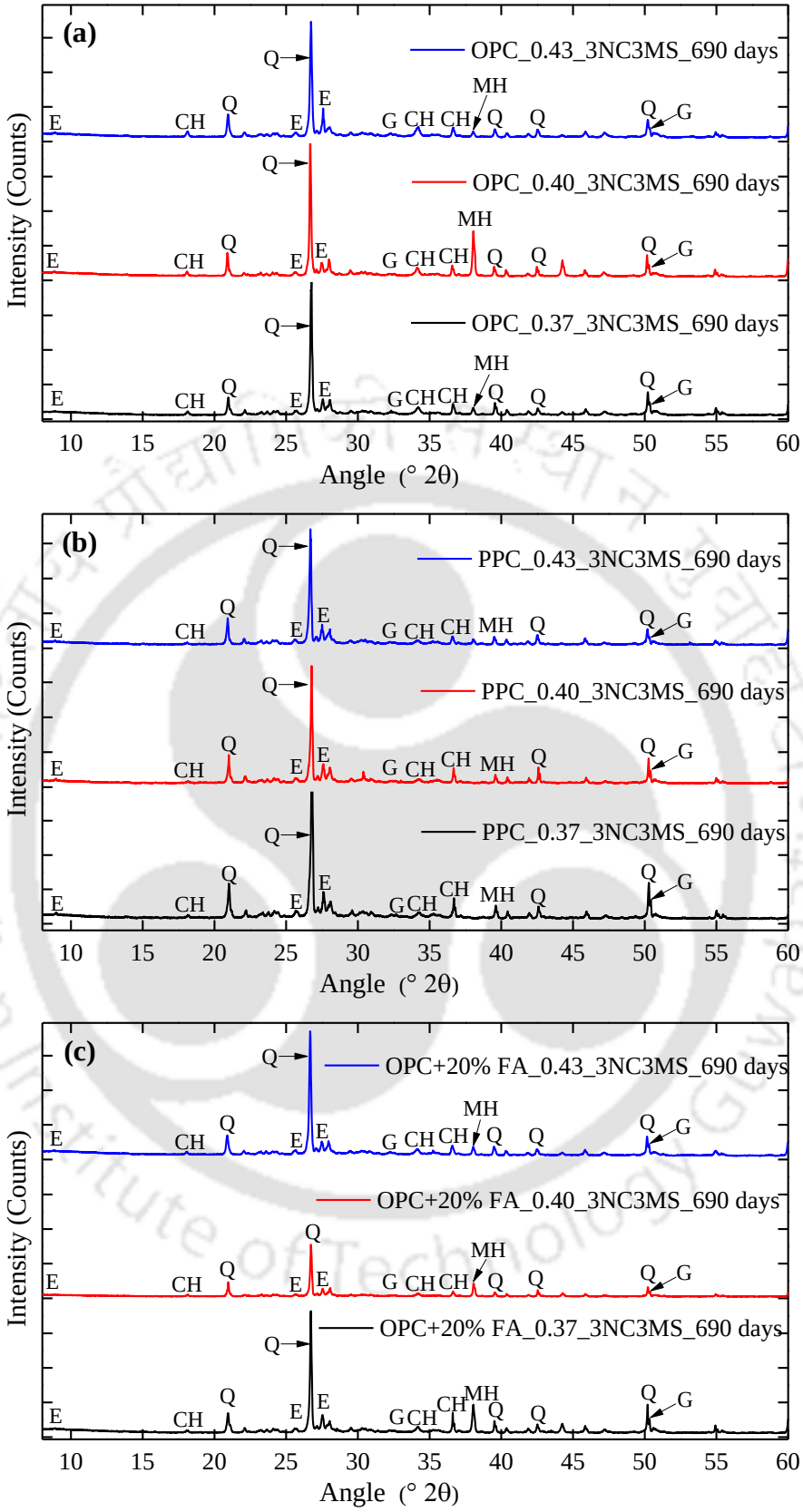

Fig. 7.27 XRD patterns of SCC mixes at exposure duration of 690 days for w/b ratios of 0.37, 0.40 and 0.43 and exposed to 3% NaCl + 3% $MgSO_4$ solution: (a) OPC, (b) PPC, and (c) OPC+20% FA

Table 7.4 Weight % of various compounds from the XRD patterns using RIR method for SCC mixes exposed to 3% NaCl + 3% Na_2SO_4 solution

Compound name	Weight percentage (wt. %)								
	OPC			PPC			OPC+20% FA		
	w/b ratio of 0.37	w/b ratio of 0.40	w/b ratio of 0.43	w/b ratio of 0.37	w/b ratio of 0.40	w/b ratio of 0.43	w/b ratio of 0.37	w/b ratio of 0.40	w/b ratio of 0.43
Quartz	65	73	81	74	78	79	75	79	81
Portlandite	18	11	8	2	3	5	9	6	6
Ettringite	10	9	6	21	14	12	13	7	3
Gypsum	7	7	5	3	5	3	3	7	10

Table 7.5 Weight % of various compounds from the XRD patterns using RIR method for SCC mixes exposed to 3% NaCl + 3% $MgSO_4$ solution

Compound name	Weight percentage (wt. %)								
	OPC			PPC			OPC+20% FA		
	w/b ratio of 0.37	w/b ratio of 0.40	w/b ratio of 0.43	w/b ratio of 0.37	w/b ratio of 0.40	w/b ratio of 0.43	w/b ratio of 0.37	w/b ratio of 0.40	w/b ratio of 0.43
Quartz	45	51	54	56	57	59	51	63	60
Portlandite	7	6	9	4	2	4	4	4	6
Brucite	8	4	3	3	3	2	10	2	2
Ettringite	38	36	32	35	35	31	31	30	22
Gypsum	2	3	2	1	3	5	3	2	10

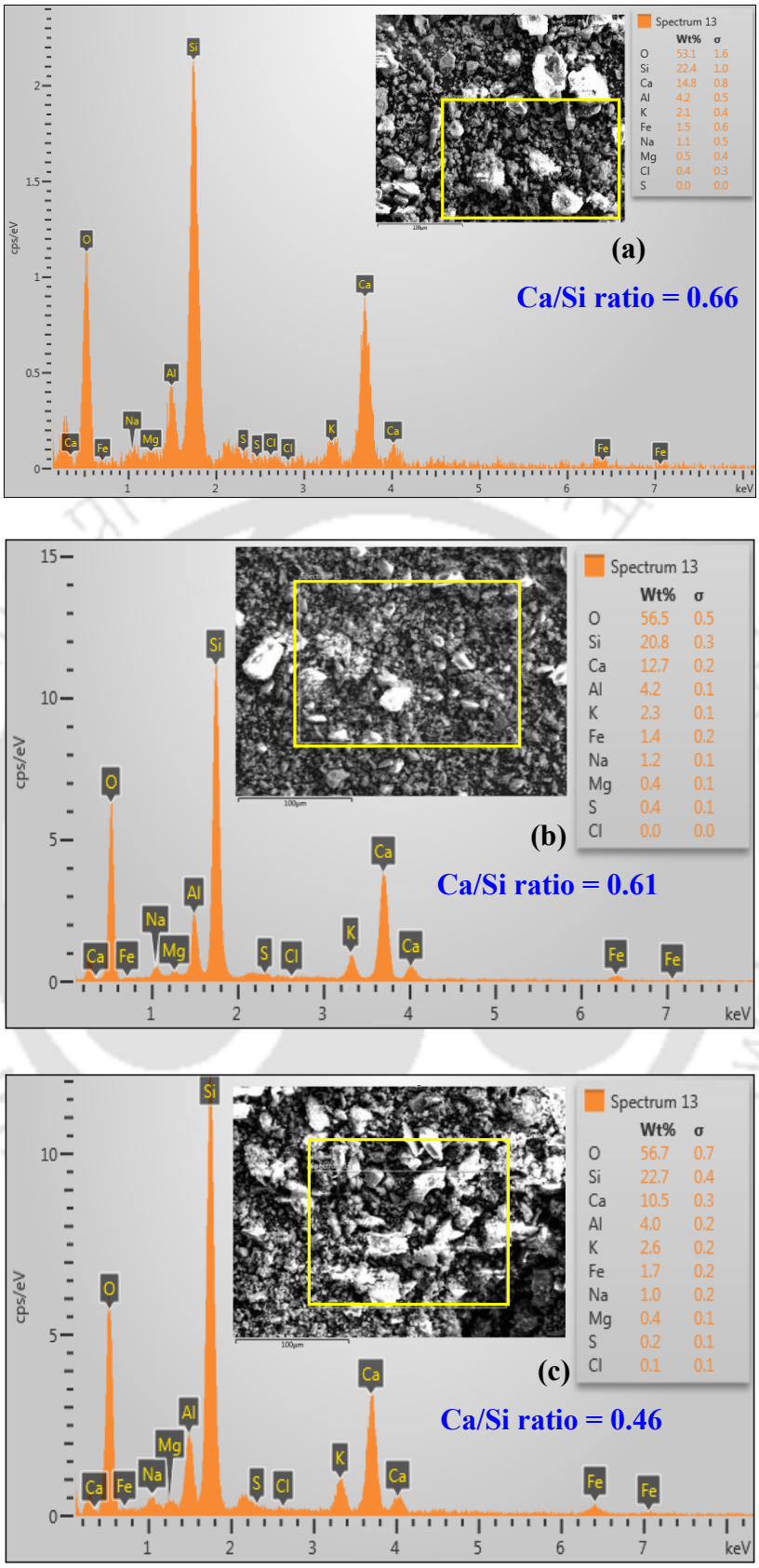

Fig. 7.28 EDX analysis of OPC based SCC mixes at exposure duration of 690 days for 3% NaCl + 3% Na_2SO_4 exposure solution: (a) w/b ratio of 0.37, (b) w/b ratio of 0.40, and (c) w/b ratio of 0.43

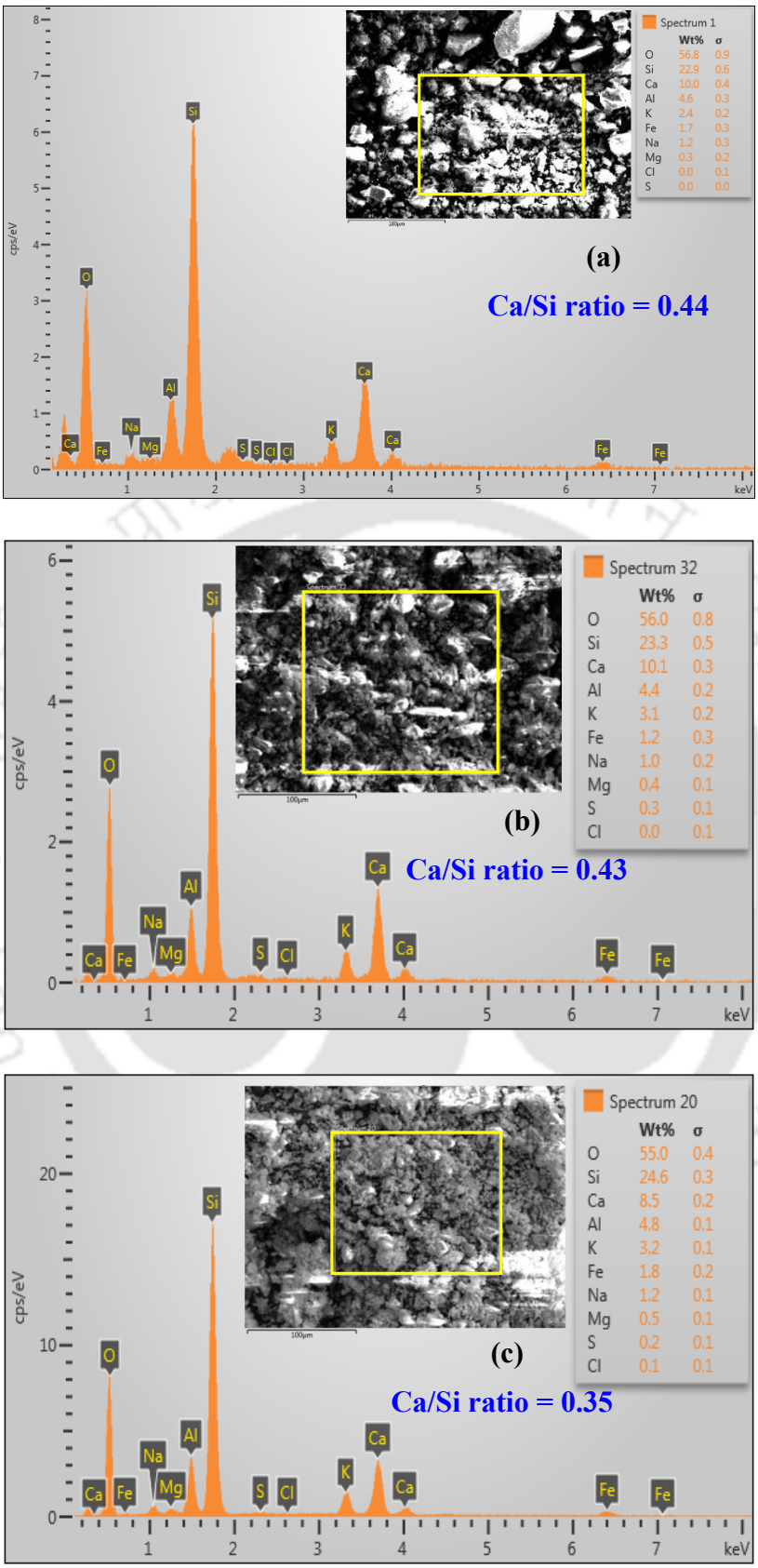

Fig. 7.29 EDX analysis of PPC based SCC mixes at exposure duration of 690 days for 3% NaCl + 3% Na_2SO_4 exposure solution: (a) w/b ratio of 0.37, (b) w/b ratio of 0.40, and (c) w/b ratio of 0.43

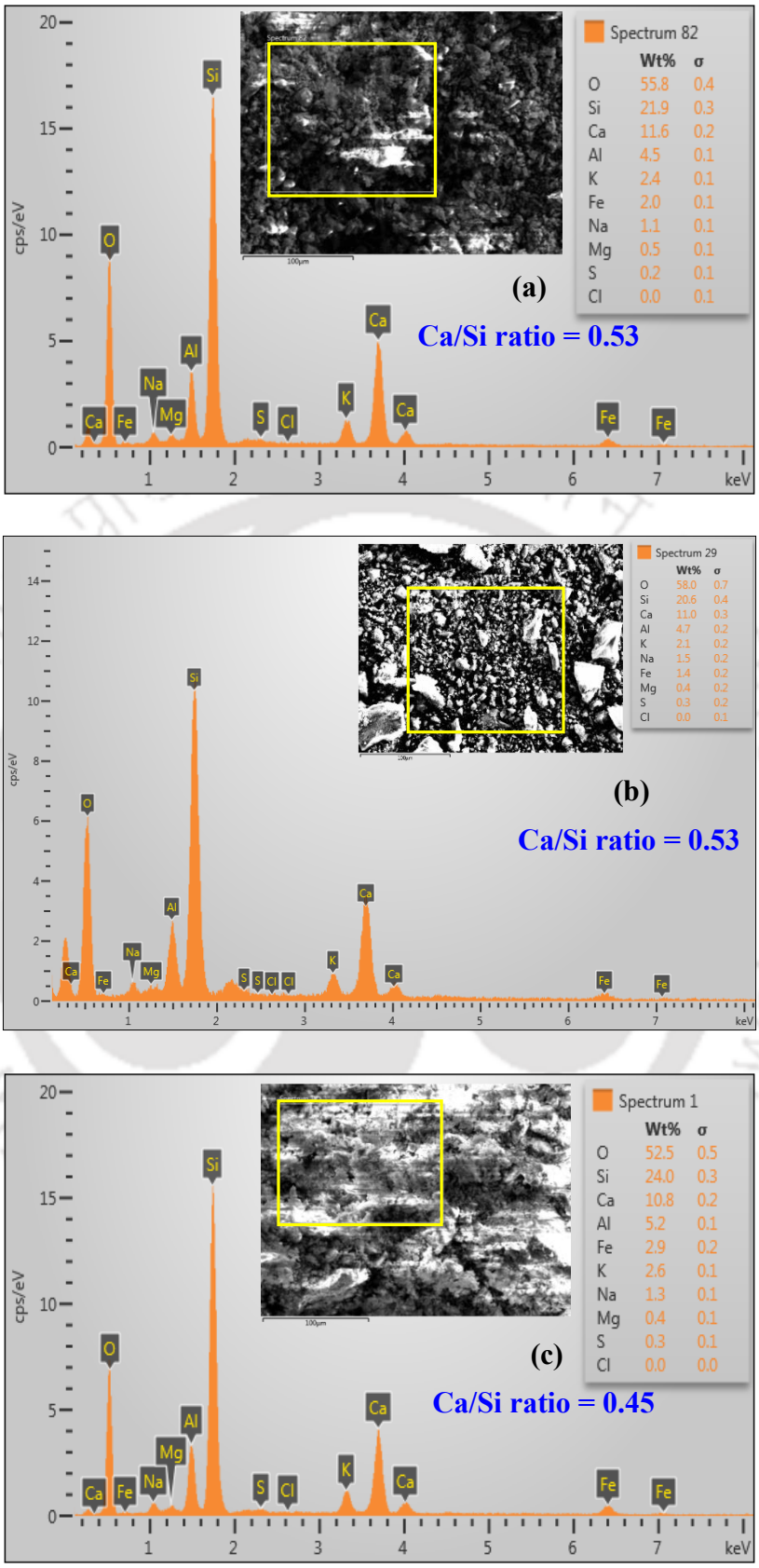

Fig. 7.30 EDX analysis of OPC+20% FA based SCC mixes at exposure duration of 690 days for 3% NaCl + 3% Na_2SO_4 exposure solution: (a) w/b ratio of 0.37, (b) w/b ratio of 0.40, and (c) w/b ratio of 0.43

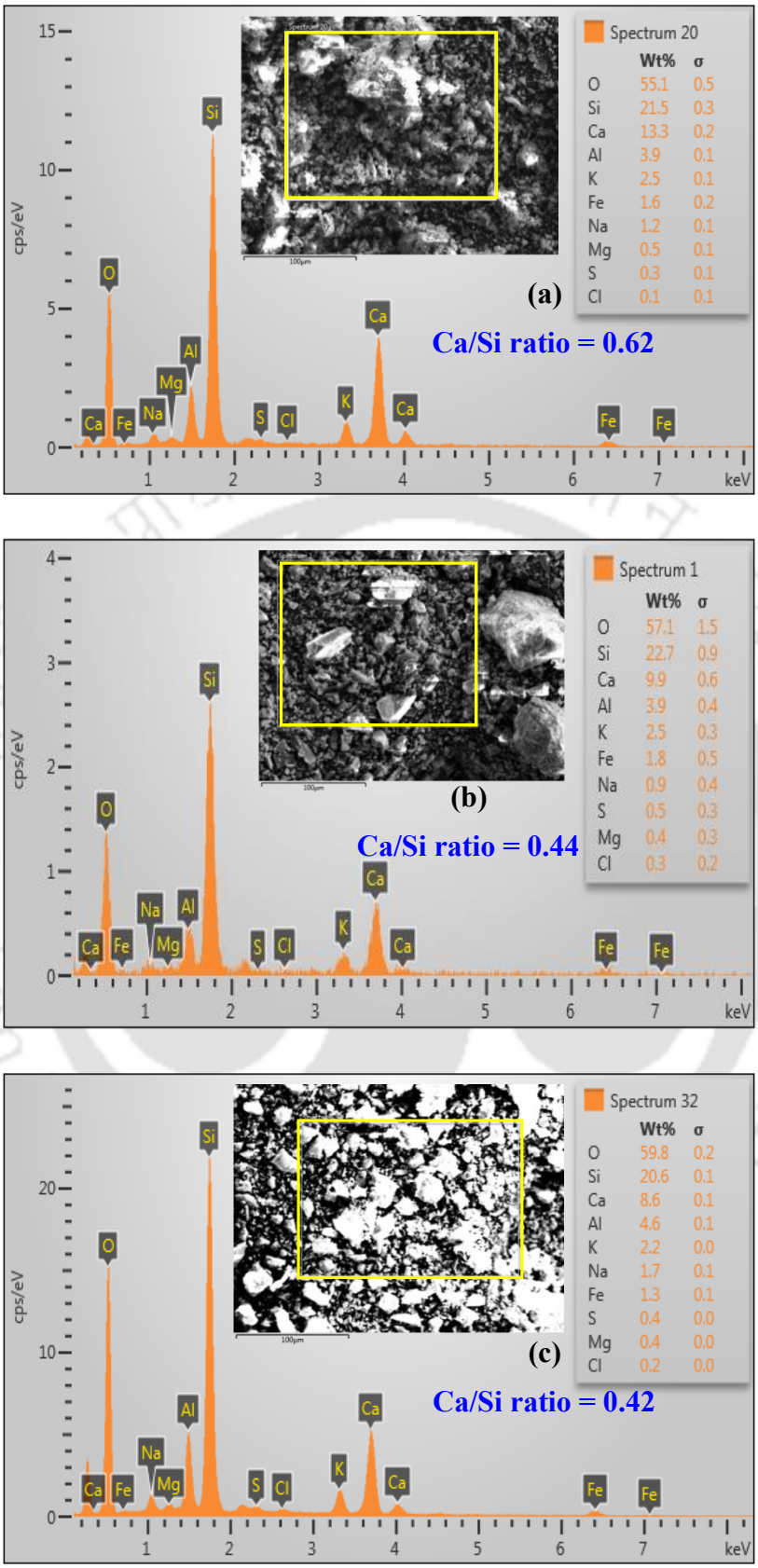

Fig. 7.31 EDX analysis of OPC based SCC mixes at exposure duration of 690 days for 3% NaCl + 3% $MgSO_4$ exposure solution: (a) w/b ratio of 0.37, (b) w/b ratio of 0.40, and (c) w/b ratio of 0.43

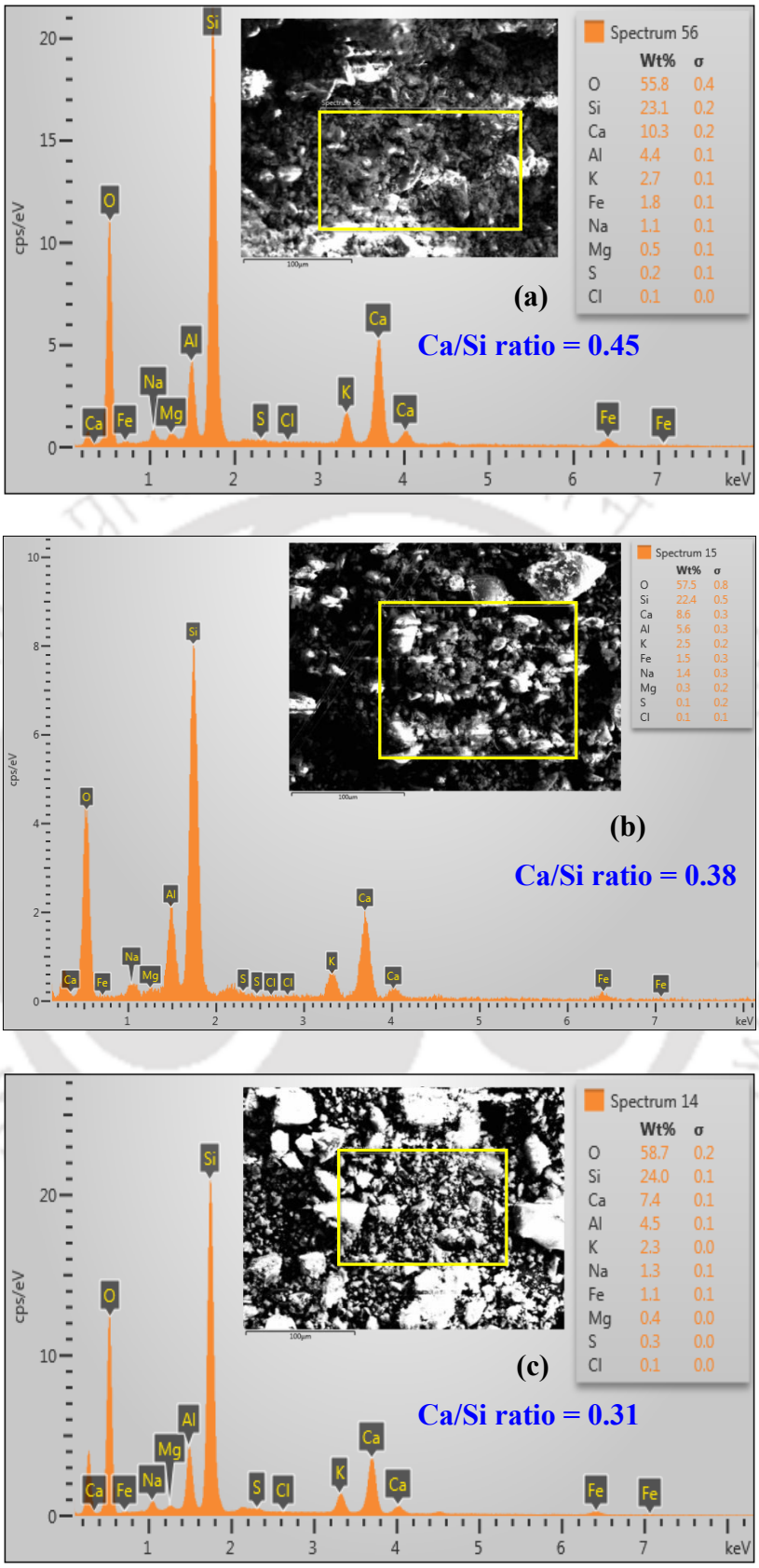

Fig. 7.32 EDX analysis of PPC based SCC mixes at exposure duration of 690 days for 3% NaCl + 3% $MgSO_4$ exposure solution: (a) w/b ratio of 0.37, (b) w/b ratio of 0.40, and (c) w/b ratio of 0.43

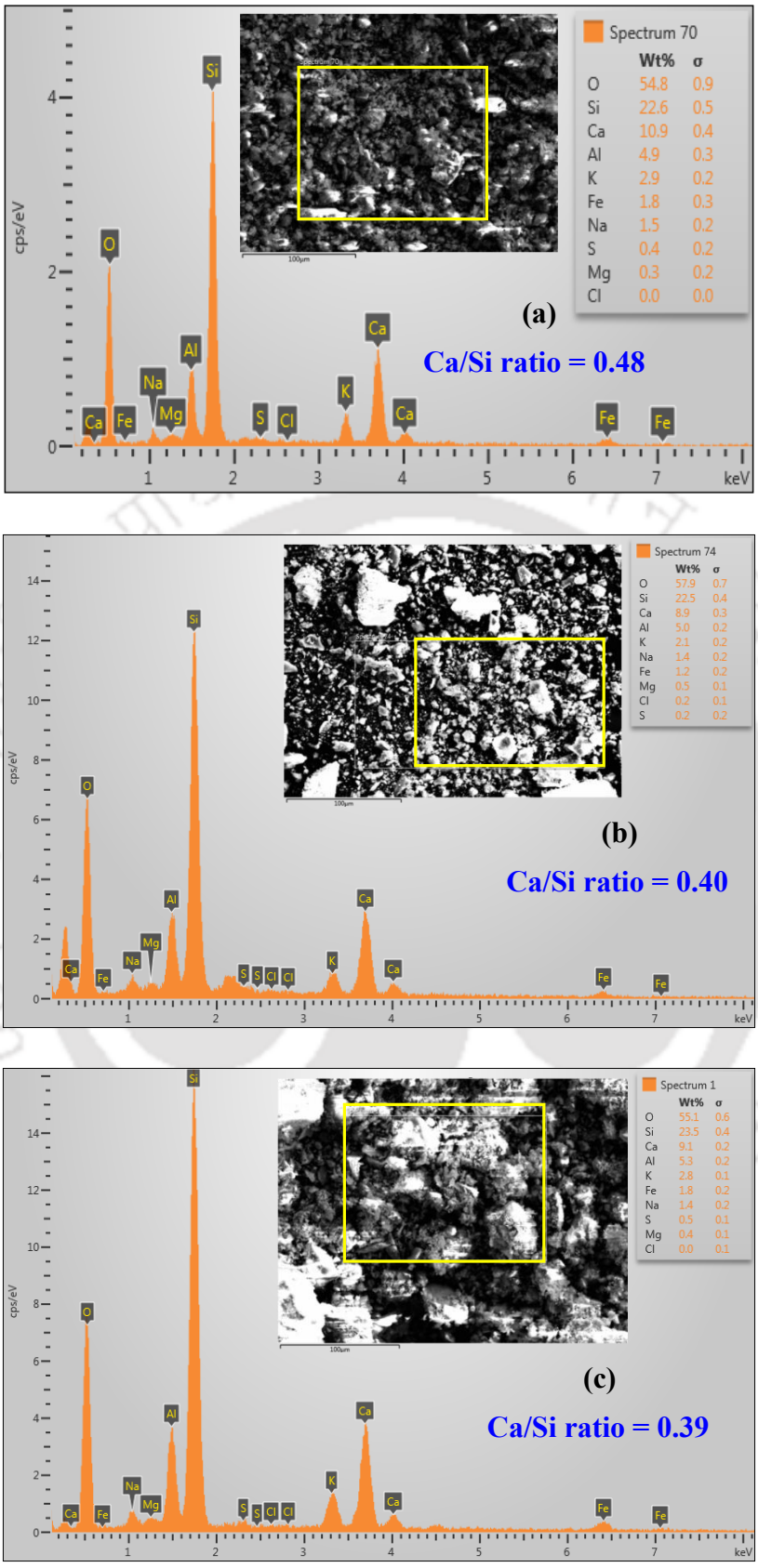

Fig. 7.33 EDX analysis of OPC+20% FA based SCC mixes at exposure duration of 690 days for 3% NaCl + 3% $MgSO_4$ exposure solution: (a) w/b ratio of 0.37, (b) w/b ratio of 0.40, and (c) w/b ratio of 0.43

While evaluating the effect of w/b ratio, it is observed that the corrosion current density was lower in the specimens made with lower w/b ratio as compared to those made with higher w/b ratio for OPC and OPC+20% FA based SCC mixes and for both NaCl + Na_2SO_4 solutions and NaCl + $MgSO_4$ solutions as observed from Fig. 7.20 to Fig. 7.22 and from Fig. 7.23 to Fig. 7.25, respectively. This may be attributed to the formation of denser microstructure at lower w/b ratio that increased the resistivity of concrete. In the case of PPC based SCC specimens, there was no systematic variation in corrosion current density with w/b ratio for both types of combined chloride-sulfate exposure solutions as observed from Fig. 7.20 to Fig. 7.25. From the typical XRD patterns (shown in Fig. 7.26 for 3% NaCl + 3% Na_2SO_4 and Fig. 7.27 for 3% NaCl + 3% $MgSO_4$ exposure solutions) and weight percentage (wt. %) estimated by RIR method (Table 7.4 for or 3% NaCl + 3% Na_2SO_4, and Table 7.5 for 3% NaCl + 3% $MgSO_4$), it is observed that there is no systematic variation in calcium hydroxide (CH) content with w/b ratio in some cases, however in the remaining cases the calcium hydroxide content increased with decrease in w/b ratio in the SCC mixes for both types of combined chloride-sulfate exposure solutions. This may be ascribed to the variations in the extent of reactions of sodium sulfate and magnesium sulfate with calcium hydroxide in the SCC mixes at different w/b ratios, when exposed to the respective combined chloride-sulfate solution. Further from EDX analysis, it is observed that the Ca/Si ratio of C-S-H increased with decrease in w/b ratio for all binders as observed from Fig. 7.28 to Fig. 7.30 for 3% NaCl + 3% Na_2SO_4 exposure solution and from Fig. 7.31 to Fig. 7.33 for 3% NaCl + 3% $MgSO_4$ exposure solution.

While comparing the effect of Na_2SO_4 and $MgSO_4$ on corrosion current density, it is inferred that the corrosion current density of steel reinforcement was lower in the SCC mixes exposed to combined NaCl + $MgSO_4$ solutions as compared to those exposed to combined NaCl + Na_2SO_4 solutions for all binders, w/b ratios and concentration of the solutions over the exposure period as observed from Fig. 7.20 to Fig. 7.25. The lower corrosion current density in SCC specimens exposed to combined NaCl + $MgSO_4$ exposure solutions may be attributed to the formation of magnesium hydroxide (brucite) and comparatively higher amount of ettringite that might have filled the pores in the concrete and decreased the penetration of chloride ions near the rebar level as compared to the SCC mixes exposed to NaCl + Na_2SO_4 solutions. At the end of the exposure period, the corrosion current density of steel reinforcement in the SCC specimens exposed to combined NaCl + Na_2SO exposure solutions were 1.46, 1.15 and 1.24 times higher than those exposed to

combined NaCl + $MgSO_4$ exposure solutions for OPC, PPC and OPC+20% FA base SCC mixes, respectively, irrespective of w/b ratio and concentration of the exposure solution. It may be noted that magnesium hydroxide (MH) in concrete is formed due to the reaction of magnesium sulfate with the calcium hydroxide. The formation of magnesium hydroxide and higher amount of ettringite in the SCC mixes exposed to NaCl + $MgSO_4$ solutions as compared to those exposed to NaCl + Na_2SO_4 solutions is evident from the typical XRD patterns shown in Fig. 7.27 and wt. % of the compounds, estimated using RIR method and presented in Table 7.4 and Table 7.5, for the concrete powder sample collected from the rebar level in the prismatic specimens at the end of exposure period i.e. 690 days. In the XRD patterns shown in Fig. 7.26 and Fig. 7.27, the peaks of magnesium hydroxide (MH) were found at 37.9° 2θ (Fig. 7.27) and those of ettringite (E) were found at 8.8° 2θ, 25.6° 2θ, and 27.5° 2θ (Fig. 7.26 and Fig. 7.27). The formation of higher amount of ettringite in the SCC mixes exposed to NaCl + $MgSO_4$ solutions as compared to those exposed to NaCl + Na_2SO_4 solutions for all binders may be attributed to the reaction of gypsum (released from the reaction of magnesium sulfate with calcium hydroxide) with hydrated calcium aluminates to a greater extent. Further, the typical XRD patterns shown in Fig. 7.27 and wt. % of the compounds shown in Table 7.4 and Table 7.5 indicate lower amount of gypsum (G) in the SCC mixes exposed to NaCl + $MgSO_4$ solutions as compared to those exposed to NaCl + Na_2SO_4 solutions, which is attributed to the consumption of higher amount of gypsum in the reaction with hydrated calcium aluminates to form amount of ettringite in the SCC mixes exposed to NaCl + $MgSO_4$ solutions. The lower amount of calcium hydroxide (CH) in the SCC mixes exposed to NaCl + $MgSO_4$ solutions than that exposed to NaCl + Na_2SO_4 solutions as indicated by the XRD patterns (shown in Fig. 7.26 and Fig. 7.27) and wt. % of the compounds shown in Table 7.4 and Table 7.5, may be attributed to the dominant effect of the reaction of magnesium sulfate with calcium hydroxide to a greater extent in the SCC mixes exposed to NaCl + $MgSO_4$ solutions.

From the XRD results (Fig. 7.27 and Table 7.5), it is observed that the peak intensity and wt. % of magnesium hydroxide (MH) were lower in PPC and OPC+20% FA based SCC mixes as compared to that in OPC based SCC mixes for exposure to 3% NaCl + 3% $MgSO_4$ solution. The lower amount of magnesium hydroxide in PPC and OPC+20% FA based SCC mixes is ascribed to the availability of lower amount of calcium hydroxide that resulted in the formation of lower amount of magnesium hydroxide in the presence of magnesium sulfate. Further, it is inferred that the peak intensity and wt. % of ettringite (E) were mostly

lower in OPC based SCC mixes as compared to that in PPC and OPC+20% FA based SCC mixes in the case of exposure to NaCl + Na_2SO_4 solution as observed from Fig. 7.26 and Table 7.4. The formation of ettringite (E) in the SCC mixes is evident from the typical FESEM images shown in Fig. 7.34 for OPC, PPC and OPC+20% FA based SCC mixes exposed to 3% NaCl + 3% Na_2SO_4 solution wherein the ettringite was appeared in the form of needle-like crystals. The lower amount of ettringite in OPC based SCC mixes may be attributed to the dominant effect of its solubility in the presence of chloride ions to a greater extent as compared to that in PPC and OPC+20% FA based SCC mixes. It may be noted that for exposure to 3% NaCl + 3% Na_2SO_4 solution, the chloride ion concentration in the OPC based SCC mixes was higher as compared to those in PPC and OPC+20% FA based SCC mixes as observed from Table 7.3.

In case of exposure to 3% NaCl + 3% $MgSO_4$ solution, the peak intensity and wt. % of ettringite (E) were higher in OPC based SCC mixes as compared to that in PPC and OPC+20% FA based SCC mixes as observed from Fig. 7.27 and Table 7.5. This may be due to the formation of higher amount of ettringite as a result of reaction of gypsum (G) with hydrated calcium aluminates to a greater extent in OPC based SCC mixes as compared to that in PPC and OPC+20% FA based SCC mixes. Further from Figs. 7.26 - 7.27 and Tables 7.4 - 7.5, it is inferred that the peak intensity and wt. % of ettringite (E) increased with decrease in w/b ratio for both types of combined chloride-sulfate exposure solutions and for all binders. The formation of higher amount of ettringite at lower w/b ratio as compared to that at higher w/b ratio may be attributed to the greater extent of reaction of gypsum with hydrated calcium aluminates in the concrete mixes. The variations in the peak intensity and wt. % of gypsum (G) obtained from the XRD results were not systematic with the w/b ratio for both types of combined chloride-sulfate exposure solutions as observed from Figs. 7.26 - 7.27 and Tables 7.4 - 7.5. Similarly, the variations in the peak intensity and wt. % of gypsum (G) with binder type were not mostly systematic in the SCC mixes exposed to 3% NaCl + 3% $MgSO_4$ solution, however, the peak intensity and wt. % of gypsum (G) were lower in PPC based SCC mixes as compared to those in OPC and OPC+20% FA based SCC mixes in the case of exposure to 3% NaCl + 3% Na_2SO_4 solution as observed from Figs. 7.26 - 7.27 and Tables 7.4 - 7.5. These variations in amount of gypsum in the SCC mixes may be attributed to the variations in the extent of the reaction of sodium sulfate and magnesium sulfate with calcium hydroxide in the SCC mixes

exposed to 3% NaCl + 3% Na_2SO_4 and 3% NaCl + 3% $MgSO_4$ solutions, respectively for different binders and w/b ratios.

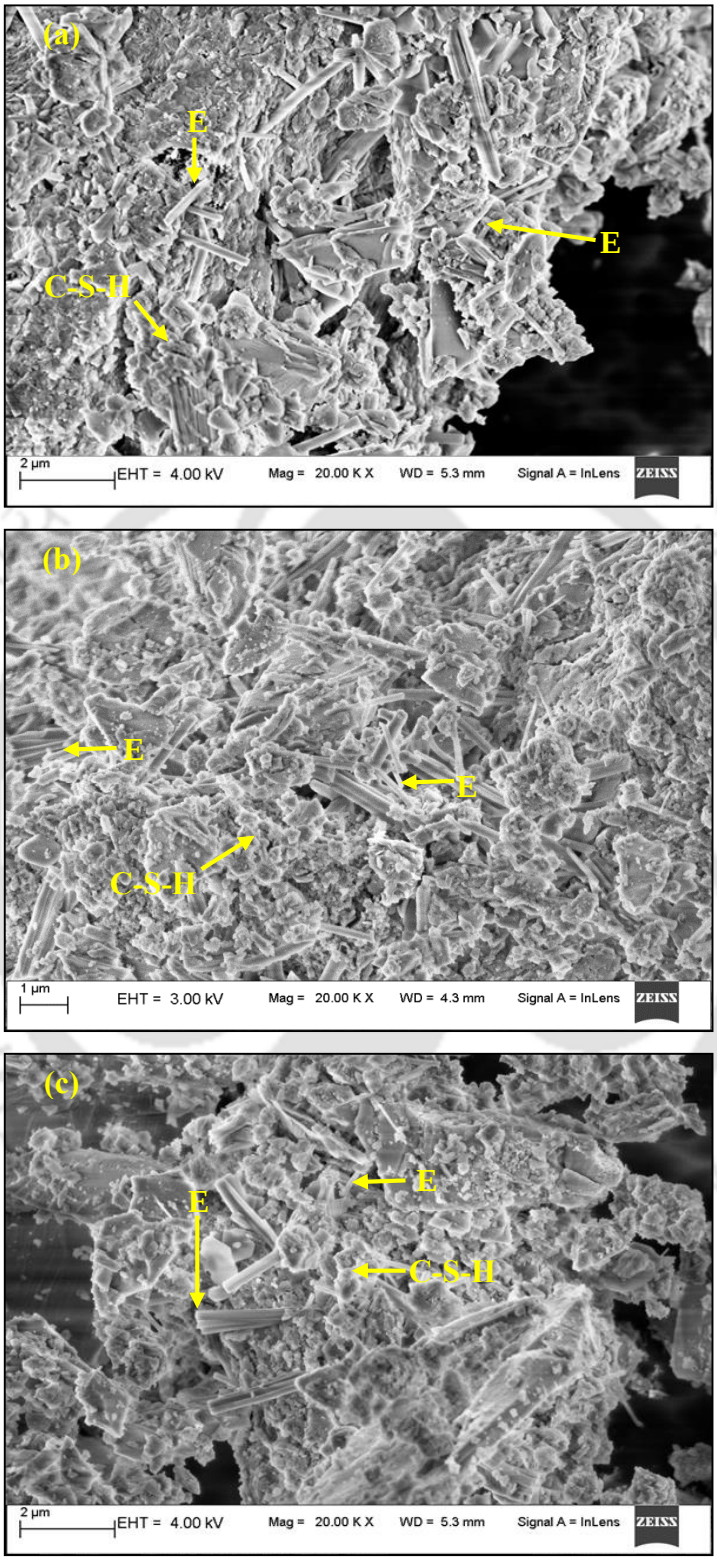

Fig. 7.34 FESEM images of SCC mixes at exposure duration of 690 days for 3% NaCl + 3% Na_2SO_4 exposure solution at w/b ratio of 0.43: (a) OPC, (b) PPC and (c) OPC+20% FA

7.3.3 Comparison between the effects of chloride and combined chloride-sulfate exposure solutions on corrosion current density of steel reinforcement in SCC

From the corrosion current density values shown in Fig. 7.10 to Fig. 7.12 and Fig. 7.20 to Fig. 7.25, it is inferred that the corrosion current density of steel reinforcement in the SCC specimens exposed to only NaCl exposure solution was higher than that exposed to both types of combined chloride-sulfate solutions (NaCl + Na_2SO_4 and NaCl + $MgSO_4$) irrespective of binder type, w/b ratio and concentration of exposure solution. This may be attributed to the effect of the relative diffusion of chloride and sulfate ions into the concrete when exposed to combined chloride-sulfate solutions. The chloride ions diffuse much faster into the concrete than the sulfate ions. As reported in the literature [121,140] the diffusion rate of chloride ions in concrete is generally 10 – 100 times faster than that of sulfate ions. Although, the diffusion of chloride ions is faster as compared to that of sulfate ions, the simultaneous diffusion of sulfate ions along with chloride ions to certain extent might have reduced the ingress of chloride ions into the SCC mixes exposed to combined chloride-sulfate solutions as compared to that exposed to only chloride solutions. The reduced penetration of chloride ions into the SCC mixes exposed to combined chloride-sulfate solutions might have decreased the conductivity thereby resulting in lower corrosion current density in the SCC mixes exposed to combined chloride-sulfate solutions (NaCl + Na_2SO_4 and NaCl + $MgSO_4$) as compared to that exposed to only chloride solutions (NaCl). The penetration of lower amount of chloride ions into the SCC mixes exposed to combined chloride-sulfate solutions (NaCl + Na_2SO_4 and NaCl + $MgSO_4$) is evident from the lower concentrations of total and free chlorides of concrete at the rebar level (Table 7.1 and Table 7.3) in the SCC mixes exposed to combined chloride-sulfate solutions as compared to that exposed to only NaCl solution for all binders and w/b ratios.

At the end of exposure duration (i.e. 690 days), the corrosion current density of steel reinforcement in the SCC specimens made with OPC and exposed to only NaCl solution was 1.46 times and 3.04 times higher than that exposed to combined NaCl + Na_2SO_4 and NaCl + $MgSO_4$ solutions, respectively, irrespective of w/b ratio and concentration of the exposure solution. Similarly for PPC, in the SCC specimens exposed to only NaCl solutions, the corrosion current density was 1.31 and 1.50 times higher than those exposed to combined NaCl + Na_2SO_4 and NaCl + $MgSO_4$ exposure solutions, respectively, irrespective of w/b ratio and concentration of the exposure solution. Further, at the end of exposure period, the corrosion current density of steel reinforcement in the specimens

exposed to only NaCl solution was 1.49 and 1.21 times higher than that exposed to combined NaCl + Na_2SO_4 and NaCl + $MgSO_4$ solutions, respectively for OPC+20% FA based SCC mixes.

7.4 Summary

The results obtained from corrosion potential measurement indicated lower probability of occurrence of steel reinforcement corrosion in SCC mixes exposed to combined chloride - sulfate exposure solutions (NaCl + Na_2SO_4 and NaCl + $MgSO_4$) as compared to that exposed to only chloride solutions (NaCl). Further, it is also inferred that the probability of occurrence of steel reinforcement corrosion increased with an increase in NaCl concentration for both types of exposure solution i.e. only chloride and combined chloride-sulfate exposure solutions in all SCC mixes. The specimens made with OPC based SCC mixes showed more negative corrosion potential values as compared to those made with OPC+20% FA followed by PPC based SCC mixes in both chloride and combined chloride-sulfate solutions, thereby, indicating higher probability of occurrence of corrosion in OPC based SCC mixes. Further, the potential values were mostly more negative at higher w/b ratio as compared to that at lower w/b ratio for all binders and exposure solutions. While evaluating the effect of cation type associated with sulfate ions i.e. Na^+ and Mg^{++} ions, it is observed that the corrosion potential values of steel reinforcement were more negative in the SCC mixes exposed to NaCl + Na_2SO_4 solutions as compared to those exposed to NaCl + $MgSO_4$ solutions for all binders and w/b ratios, which indicates that the cation type associated with sulfate ions affects the initiation of corrosion activity of steel reinforcement, when exposed to combined chloride-sulfate environment.

The results obtained from LPR measurement conducted on SCC specimens indicated that the corrosion current density was lower in OPC based SCC than that in PPC and OPC+20% FA based SCC during the early exposure period, however the opposite variation was observed during the later exposure period for both chloride and combined chloride-sulfate exposure solutions. The lower corrosion current density in PPC and OPC+20% FA based SCC mixes during the later exposure period may be attributed to the formation of denser microstructure as a result of the production of additional C-S-H gel from the pozzolanic reaction that reduced the penetration of chloride ions into the concrete. The consumption of calcium hydroxide in the pozzolanic reaction in PPC and OPC+20% FA based SCC mixes is corroborated with the XRD results wherein the peak intensity calcium hydroxide

(CH) and its wt. % estimated using RIR were lower in PPC and OPC+20% FA based SCC mixes as compared those in OPC based SCC mixes. Further, the variations in peaks intensity (in XRD patterns) and wt. % (estimated from RIR method) of calcium hydroxide (CH) are consistent with the variations in the Ca/Si ratio of C-S-H calculated from EDX analysis on the SCC mixes at the end of the exposure period. The higher corrosion current density in OPC based SCC mixes during the later exposure period may be attributed to penetration of higher concentration of chloride ions into concrete, which is corroborated with the measured free and total chloride concentrations of concrete powder collected from the rebar level at the end of exposure period. The corrosion current density of steel reinforcement increased with increase in NaCl concentration in chloride and combined chloride-sulfate exposure solutions for all the SCC mixes. Further, the corrosion current density values of steel reinforcement in SCC mixes were lower at lower w/b ratio as compared to that at higher w/b ratio for all binders and exposure solutions. While comparing the effect of Na_2SO_4 and $MgSO_4$, it is observed that that the corrosion current density was lower in SCC specimens exposed to combined NaCl+$MgSO_4$ solutions as compared to those exposed to combined NaCl + Na_2SO_4 solutions for all binders, w/b ratios, and solution concentrations over the exposure period. While comparing the effects of chloride and combined chloride-sulfate exposure solutions, it is observed that the corrosion current density in the SCC specimens exposed to only NaCl exposure solution was higher than that exposed to both types of combined chloride-sulfate solutions (NaCl + Na_2SO_4 and NaCl + $MgSO_4$), which may be attributed to the effect of the relative diffusion of chloride and sulfate ions into the concrete when exposed to combined chloride-sulfate solutions. The reduced penetration of chloride ions into the SCC mixes exposed to combined chloride-sulfate solutions might have decreased the corrosion current density in the SCC mixes exposed to combined chloride-sulfate solutions as compared to that exposed to only chloride solutions. The penetration of lower amount of chloride ions into the SCC mixes exposed to combined chloride-sulfate solutions (NaCl + Na_2SO_4 and NaCl + $MgSO_4$) is corroborated with the lower concentrations of total and free chlorides at the rebar level in the SCC mixes exposed to combined chloride-sulfate solutions as compared to that exposed to only chloride solution.

The results of the XRD analysis conducted on the concrete powder samples collected from the steel bar level in the OPC, PPC and OPC+20% FA based SCC mixes exposed to chloride (NaCl) and combined chloride chloride-sulfate (3% NaCl+3% Na_2SO_4 and

3%NaCl + 3% $MgSO_4$) solutions indicated the variations in the formation of compounds such as calcium hydroxide (CH), magnesium hydroxide (MH), calcium chloroaluminate (CCA), ettringite (E) and gypsum (G) as indicated by their respective peak intensities and the variations in wt. % estimated by RIR method. Further, the FESEM images indicated the formation of C-S-H, calcium chloroaluminate and ettringite in the SCC mixes.

CHAPTER 8

CONCLUSIONS AND SUGGESTIONS FOR FURTHER WORK

8.1 General

In this chapter, the conclusions obtained for fresh properties of self-compacting concrete (SCC) mixes made with different types of binder, w/b ratio and admixed with different concentrations of sodium chloride are presented. Further, the conclusions on the effects of binder type, w/b ratio, admixed NaCl concentration and curing age on variations in compressive strength of SCC mixes are presented. Subsequently, conclusions on the changes in the microstructure of SCC mixes and on the variations in chloride binding as well as pH of SCC mixes are presented. Further, the conclusions drawn from corrosion monitoring of steel reinforcement in NaCl admixed SCC mixes through the measurement of corrosion potential and corrosion current density are presented. In addition, the conclusions on the corrosion performance of steel reinforcement in SCC mixes exposed to external chloride and combined chloride-sulfate solutions as well as the variations in free chloride and total chloride concentrations in the vicinity of steel reinforcement in SCC mixes are enumerated. Further, the conclusions on the changes in the microstructure of concrete near the rebar level in the SCC mixes exposed to external chloride and combined chloride-sulfate solutions are presented.

8.2 Conclusions on fresh properties of SCC mixes

- From the viewpoint of fresh properties, the SCC mixes made with PPC showed better performance as compared to other binders as it exhibited higher slump flow spread, T_{50cm} and V-funnel flow times, and passing ratio, but lower segregation index as compared to OPC+20% FA (fly ash) followed by OPC based SCC mixes.
- While evaluating the effect of w/b ratio, the slump flow spread and passing ratio increased, whereas segregation index decreased with the decrease in w/b ratio of SCC mixes. However, there was no systematic variation in T_{50cm} and V-funnel flow times with the w/b ratio of SCC mixes at different concentrations of admixed NaCl.
- With admixed NaCl concentration, the variations in slump flow spread, T_{50cm} flow time, V-funnel flow time, passing ratio, and segregation index of SCC mixes were not systematic at lower w/b ratio. However, at higher w/b ratio, the variations in these parameters with admixed NaCl concentration were systematic, although the

difference in the values of these parameters among different concentrations of admixed NaCl were very less.

- From the analysis of variance (ANOVA), it is concluded that the binder type has significant effect on the fresh properties of SCC followed by w/b ratio. However, admixed NaCl concentration has very less effect on the fresh properties of SCC.

8.3 Conclusions on compressive strength of SCC mixes

- The results of compressive strength showed that at 0% admixed NaCl concentration, the SCC mixes made with OPC exhibited higher compressive strength as compared to those made with OPC+20% FA and PPC at all w/b ratios and curing ages. However, in the case of SCC mixes admixed with NaCl, PPC based SCC mixes showed higher compressive strength as compared to OPC and OPC+20% FA based SCC mixes at all curing ages and w/b ratios.
- There was no systematic variation in the compressive strength of SCC mixes with the concentration of admixed NaCl for all binders, w/b ratios and curing ages. However, at the longer curing age (i.e. 360 days), the SCC mix admixed with higher NaCl concentration (5%) showed lower compressive strength as compared to that admixed with lower concentration of NaCl (1% and 3%).
- The PPC and OPC+20% FA based SCC mixes showed higher rate of increase in compressive strength with curing age as compared to those made with OPC for all w/b ratios and admixed NaCl concentrations.
- From the results of analysis of variance, it is concluded that the curing age has more significant effect on the compressive strength of SCC mixes followed by w/b ratio and binder type. Further, admixed NaCl concentration has comparatively less effect on the compressive strength of SCC mixes as compared to other parameters.
- In OPC based SCC mixes, the Ca/Si ratio of C-S-H obtained from EDX analysis increased whereas it decreased with curing age in PPC and OPC+20% FA based SCC mixes, which is consistent with the compressive strength development with curing age in OPC, PPC, and OPC+20% FA based SCC mixes.

8.4 Conclusions from microstructure characterization of SCC mixes

- The peak intensity and wt. % (estimated using RIR method) of calcium chloroaluminate (CCA), calcium hydroxide (CH), ettringite (E) and gypsum (G) obtained from the XRD patterns indicated the variations in their formations in the

SCC mixes with respect to type of binder, w/b ratio and concentration of admixed NaCl at different cuing ages.

- The XRD results indicated the formation of higher amount of calcium chloroaluminate (CCA) in SCC mixes made with OPC+20% FA as compared to those made with OPC and PPC for all concentrations of admixed NaCl, w/b ratios and curing ages. Further, the SCC mixes admixed with higher concentration of NaCl showed the formation of more amount of CCA as compared to that admixed with lower concentration of NaCl. In addition, the formation of CCA increased with increase in w/b ratio in SCC mixes.
- In the case of control SCC mixes (0% NaCl), the formation of ettringite was higher in OPC+20% FA and PPC based SCC mixes as indicated by their more intense peaks in the XRD patterns as compared to that in OPC based SCC mixes at all w/b ratios and curing ages. However, in the case of NaCl admixed SCC mixes, there was no systematic variation in the formation of ettringite with binder type, w/b ratio and curing age.
- The calcium hydroxide (CH) content was lower in PPC and OPC+20% FA based SCC mixes as compared to that in OPC based SCC mixes as indicated by the XRD results.
- The XRD analysis showed that the calcium hydroxide content (wt. %) was higher in the control (0% NaCl) SCC mixes made with lower w/b ratio as compared to the control (0% NaCl) SCC mixes made with higher w/b ratio, whereas there was no systematic variation in wt. % of CH with w/b ratio in the SCC mixes admixed with different concentrations of NaCl.
- The XRD results indicated higher CH content in the SCC mixes made with 0% NaCl as compared to that in NaCl admixed SCC mixes. This may be ascribed to the effect of chloride ions affecting the hydration and pozzolanic reactions and also due to the variations in the leaching of calcium hydroxide at different w/b ratios in the presence of chloride ions.
- The peak intensity of calcium hydroxide in the XRD patterns increased with curing age in the SCC mixes made with OPC, whereas it deceased with curing age in the SCC mixes made with PPC and OPC+20% FA.
- The variations in the formation of calcium hydroxide (CH) with type of binder, curing age, admixed NaCl concentration and w/b ratio as indicated by the XRD

results are well explained by the CH content calculated from the mass loss in TGA as a result of its dehydration.

- From the results of TGA, it is observed that the mass loss due to the departure of combined water (temperature of 105°C to 480°C) constitutes a significant portion of total mass loss in OPC, PPC and OPC+20% FA based SCC mixes for all w/b ratios, admixed NaCl concentrations and curing ages. Further, the mass loss due to the departure of combined water was lower in PPC based SCC mixes as compared that in OPC+20% FA and OPC based SCC mixes at all w/b ratios and curing ages for different concentrations of admixed NaCl.
- The total mass loss was higher in NaCl admixed SCC mixes as compared to that in control mix (0% NaCl) for all binders, w/b ratios and curing ages. In addition, the total mass loss increased with curing age in OPC based SCC mixes, whereas it decreased with curing age in PPC and OPC+20% FA based SCC mixes.
- The formation of calcium silicate hydrate, calcium chloroaluminate, calcium hydroxide and ettringite in the SCC mixes was indicated by the FESEM images, which further confirms the results of XRD analysis. The obtained FTIR spectra of SCC mixes indicated the functional groups such as –OH, CO_3^{2-}, Si-O and Al-O, which are associated with various compounds formed in SCC mixes.

8.5 Conclusions from chloride analysis and pH of SCC mixes

- The chloride binding as indicated by bound chloride concentration was higher in OPC based SCC mixes as compared to that in OPC+20% FA and PPC based SCC mixes.
- The bound chloride concentration increased with the increase in concentration of admixed NaCl, which corroborates the variations in peak intensity and wt. % of calcium chloroaluminate (from XRD analysis) with the concentration of admixed NaCl in SCC mixes.
- The free chloride concentration decreased whereas the bound chloride concentration increased with the increase in curing age and with the decrease in w/b ratio of the SCC mixes.
- There exists a strong linear relationship between free chloride and total chloride concentrations in the SCC mixes. The rate of increase in free chloride concentration with total chloride concentration as indicated by the slope of linear relationship was

lower in OPC as compared to that in OPC+20% FA followed by PPC based SCC mixes. The lower rate of increase in free chloride concentration with total chloride concentration in OPC based SCC mixes indicates higher chloride binding as compared to that in OPC+20% FA followed by PPC based SCC mixes.

- The rate of increase in free chloride concentration with total chloride concentration decreased with decrease in w/b ratio and with the increase in the curing age of SCC mixes.
- The pH value of OPC based SCC mixes was higher as compared that of PPC and OPC+20% FA based SCC mixes irrespective of w/b ratio, admixed NaCl concentration and curing age.
- The SCC mixes admixed with NaCl showed lower pH value as compared to the control mix (0% NaCl). Further, the pH value of SCC mixes increased with decrease in w/b ratio and with increase in curing age.

8.6 Conclusions from corrosion performance of steel reinforcement in SCC against internal chloride

- The probability of occurrence of steel reinforcement corrosion was lower in all the SCC mixes admixed with NaCl concentrations of 1%, 3% and 5% as the corrosion potential values were less negative than -270 mV (SCE) for both air curing condition (laboratory drying) and exposure to normal water.
- At higher concentrations of admixed NaCl i.e. 7.5% and 12.5%, the corrosion potential was more negative than -270 mV (SCE) thereby indicating greater probability of occurrence of steel reinforcement corrosion in air curing condition.
- The corrosion potential became more negative with increase in exposure period after exposure to 5% NaCl solution in all the SCC mixes. Further, the corrosion potential was more negative in OPC based SCC mixes as compared to that in OPC+20% FA followed by PPC based SCC mixes after exposure to 5% NaCl solution.
- There was no systematic variation in corrosion potential of steel reinforcement in SCC mixes between the two exposure conditions i.e. air curing condition, and normal water curing with alternate wetting-drying cycles.

- The corrosion current density of steel reinforcement was higher in OPC+20% FA based SCC specimens as compared to that in PPC and OPC based SCC mixes exposed to air curing condition.
- For air curing condition, the variation in corrosion current density with exposure period was very less. For exposure to normal water curing with alternate wetting-drying cycles, there was no systematic variation in corrosion current density with exposure period in the case of OPC based SCC mixes, however the corrosion current density mostly decreased with exposure period in the cases of PPC and OPC+20% FA based SCC mixes.
- The corrosion current density of steel reinforcement was lower in OPC based SCC specimens as compared to those in OPC+20% FA and PPC based specimens when exposed to normal water; however, the corrosion density increased significantly in OPC based SCC mixes as compared to OPC+20% FA and PPC based SCC mixes when exposed to 5% NaCl solution with alternate wetting-drying cycles.
- While comparing the effect of exposure condition, the SCC specimens exposed to normal water curing with alternate wetting-drying cycles exhibited lower corrosion current density as compared to those exposed to air curing condition.
- Overall, it is observed that OPC based SCC mixes showed better corrosion performance as compared to PPC and OPC+20% FA based SCC mixes during the early exposure period in the presence of internal chloride however, the opposite variation was observed during the later ages after exposure to 5% NaCl solution.

8.7 Conclusions from corrosion performance of steel reinforcement in SCC exposed to external chloride and combined chloride-sulfate solutions

- The obtained corrosion potential values indicated lower probability of occurrence of steel reinforcement corrosion in SCC mixes exposed to combined chloride-sulfate exposure solutions (NaCl + Na_2SO_4 and NaCl + $MgSO_4$) as compared to that exposed to only chloride solution (NaCl).
- The SCC specimens made with OPC showed higher probability of occurrence of steel reinforcement corrosion as compared to those made with OPC+20% FA followed by PPC in both chloride and combined chloride-sulfate exposure solutions.

- While evaluating the effect of cation type associated with sulfate ions i.e. Na^{+} and Mg^{++} ions, the corrosion potential values of steel reinforcement in the SCC mixes exposed to NaCl + Na_2SO_4 solutions were more negative as compared to those exposed to NaCl + $MgSO_4$ solutions.
- The OPC based SCC mixes showed lower corrosion current density as compared to PPC and OPC+20% FA based SCC mixes during the early exposure period; however, the opposite variation was observed during the later exposure period for both chloride (NaCl) and combined chloride-sulfate exposure solutions (NaCl + Na_2SO_4 and NaCl + $MgSO_4$).
- The higher corrosion current density in OPC based SCC mixes during later exposure period may be attributed to the penetration of chloride ions higher concentration into concrete, which is corroborated with the measured free and total chloride concentrations of concrete powder collected at the rebar level at the end of exposure period.
- The SCC mixes made with lower w/b ratio exhibited less negative corrosion potential and lower corrosion current density as compared to that made with higher w/b ratio.
- The corrosion current density was lower in SCC specimens exposed to combined NaCl + $MgSO_4$ solutions as compared to those exposed to combined NaCl + Na_2SO_4 solutions for all binders, w/b ratios and concentration of the solutions over the exposure period.
- While comparing the effects of chloride and combined chloride-sulfate exposure solutions, the corrosion current density in the SCC specimens exposed to only NaCl solution was higher than that exposed to both types of combined chloride-sulfate solutions (NaCl + Na_2SO_4 and NaCl + $MgSO_4$). This may be attributed to the reduced penetration of chloride ions into the SCC mixes exposed to combined chloride-sulfate solutions.
- The penetration of lower amount of chloride ions into the SCC mixes exposed to combined chloride-sulfate solutions is corroborated with the lower concentration of measured total and free chlorides at the rebar level in the SCC mixes exposed to combined chloride-sulfate solutions as compared to that exposed to only chloride solution.

- The variations in the formation of calcium hydroxide, magnesium hydroxide, calcium chloroaluminate, ettringite and gypsum in the SCC mixes were indicated by their peak intensities and wt. % obtained from the XRD analysis conducted on the concrete powder samples collected from the rebar level in OPC, PPC and OPC+20% FA based SCC mixes exposed to chloride and combined chloride chloride-sulfate solutions.
- The variations in peaks intensity (in XRD patterns) and wt. % (estimated from RIR method) of calcium hydroxide are consistent with the variations in Ca/Si ratio of C-S-H estimated from EDX analysis on the SCC mixes at the end of the exposure period.
- Overall, the SCC mixes made with PPC and OPC+20% FA showed better corrosion performance as compared to that made with OPC based SCC mixes against external chloride (NaCl) and combined chloride-sulfate (NaCl + Na_2SO_4 and NaCl + $MgSO_4$) exposure solutions.
- While comparing the exposure solution, the corrosion performance of steel reinforcement in SCC mixes decreased in the order of: NaCl + $MgSO_4$ > NaCl + Na_2SO_4 > NaCl.

8.8 Practical significance of research findings

The research work on self-compacting concrete presented in the thesis was based on the objectives formulated with respect to the research needs identified from the review of literature presented in Chapter 2. The outcome of the present research work depicting the behaviour of SCC through fresh properties, compressive strength, microstructure, chloride binding, thermal analysis and corrosion of steel reinforcement can be useful for evaluating the suitability of SCC for various practical applications and exposure conditions. Further, on the basis of the research findings, it is recommended that fly ash based blended cement (or ordinary Portland cement added with fly ash) can be considered as the most suitable binder for the production of self-compacting concrete for exposure to aggressive environments such chloride and combined chloride-sulfate exposure conditions.

In the present research work, the ACI and EFNARC guidelines were followed to arrive at the final mix proportioning of SCC mixes that satisfied the accepted criteria for fresh properties. In this context, on the basis of the research outcome obtained from the present study, the guidelines for mix proportioning of SCC for practicing engineers must include

the range of w/b ratio, binder content and its composition, proportion of fine and coarse aggregate contents, and dosage of superplasticizer depending on the level of requirement of filling ability, passing ability and segregation resistance in accordance with the required practical applications.

8.9 Suggestions for further work

Following are the suggestions for further research work:

- The present study can be extended to determine the effect of cation type associated with chloride ions on chloride binding and chloride induced corrosion of steel reinforcement in SCC mixes.
- Further, study can also be carried out to evaluate the effect of combined presence of chloride and sulfate ions on fresh, hardened and durability properties of SCC mixes admixed with different concentration of chloride and sulfate ions.
- Additional research can also be carried out to evaluate the effect of different corrosion inhibitors on chloride induced corrosion performance of steel reinforcement in the SCC mixes made with different types of binder and w/b ratios.

REFERENCES

[1] Zhu W., Gibbs J.C. and Bartos P.J., "Uniformity of in situ properties of self-compacting concrete in full-scale structural elements," Cem. Concr. Compos., vol. 23(1), pp. 57-64, 2001.

[2] Okamura H. and Ouchi M., "Self-compacting concrete," J Adv Concr Technol, vol. 1(1), pp. 5-15, 2003.

[3] Schutter G.D., Bartos P.J.M., Domne P. and Gibbs J., Self-compacting concrete, Whittles publishing, 2008.

[4] EFNARC, "European Guidelines for Self Compacting Concrete, Joint Project Group," Brussels, Belgium, 2005.

[5] Fernandez-Gomez J. and Agranati G., "Evaluation of shrinkage prediction models for self-consolidating concrete," ACI Mater. J., vol. 104(5), pp. 464-473, 2007.

[6] Hemalatha T., Ramaswamy A. and Chandra Kishen J.C., "Simplified mixture design for production of self-consolidating concrete," ACI Mater. J., vol. 112(2), pp. 277-286, 2015.

[7] Khaleel O.R. and Razak H.A., "Mix design method for self -compacting metakaolin concrete with different properties of coarse aggregate.," Mater. Des., vol. 53, pp. 691-700, 2014.

[8] Kanadasan J. and Razak H.A., "Mix design for self-compacting palm oil clinker concrete based on particle packing," Mater. Des., vol. 56, pp. 9-19, 2014.

[9] Ferrara L., Park Y. and Shah S.P., "A method for mix-design of fiber-reinforced self-compacting concrete," Cem. Concr. Res., vol. 37(6), pp. 957-971, 2007.

[10] Okamura H. and Ozawa K., “Mix-design for self-compacting concrete,” Concr. Libr. JSCE, vol. 25, pp. 107-120, 1995.

[11] Edamatsu Y., Nishida N. and Ouchi M., "A rational mix-design method for self-compacting concrete considering interaction between coarse aggregate and mortar particles.," In: Proceedings of the first international RILEM symposium on self-compacting concrete, Stockholm, Sweden, 1999.

[12] Petersson O., Billberg P. and Van B.K., "A model for self-compacting concrete," In: Proceedings of Production Methods and Workability of Concrete, Paisley, Scotland, 1996.

[13] Van B.K. and Montgomery D., "Mixture proportioning method for self-compacting high performance concrete with minimum paste volume," In: Proceedings of the First International RILEM Symposium on Self-Compacting Concrete, Stockholm, Sweden, 1999.

[14] Sedran T. and De Larrard F., "Optimization of self-compacting concrete thanks to packing model," In: Proceedings 1st SCC Symp, RILEM PRO7, Sweden, 1999.

[15] Khayat K.H., Ghezal A. and Hadriche M.S., "Factorial design model for proportioning self-consolidating concrete," Mater. Struct., vol. 32(9), p. 679-686, 1999.

[16] Sonebi M., "Medium strength self-compacting concrete containing fly ash: Modelling using factorial experimental plans," Cem. Concr. Res., vol. 34(7), p. 1199-1208, 2004.

[17] Saak A.W., Jennings H.M. and Shah S.P., "New methodology for designing self-compacting concrete," ACI Mater. J., vol. 98(6), pp. 429-439, 2001.

[18] Bui V.K., Akkaya Y. and Shah S.P., "Rheological model for self-consolidating concrete," ACI Mater. J., vol. 99(6), pp. 549-559, 2002.

[19] Dinakar P., Babu K.G. and Santhanam M., "Durability properties of high volume fly ash self-compacting concretes," Cem. Concr. Compos., vol. 30(10), pp. 880-886, 2008.

[20] Liu M., "Self-compacting concrete with different levels of pulverized fuel ash," Constr. Build. Mater., vol. 24(7), pp. 1245-1252, 2010.

[21] Sonebi M. and Bartos P.J.M., "Filling ability and plastic settlement of self-compacting concrete," Mater. Struct., vol. 35(8), pp. 462-469, 2002.

[22] Shen L., Jovein H.B., Sun Z., Wang Q. and Li W., "Testing dynamic segregation of self-consolidating concrete," Constr. Build. Mater., vol. 75, pp. 465-471., 2015.

[23] Skarendahl Å. and Petersson Ö.,"Report 23: Self-Compacting Concrete–State-of-the-Art Report of Rilem Technical Committee 174-SCC.," RILEM publications SARL, 2000.

[24] Franke L. and Sisomphon K., "A new chemical method for analyzing free calcium hydroxide content in cementing material," Cem. Concr. Res., vol. 34(7), pp. 1161-1165, 2004.

[25] Midgley H.G., "The determination of calcium hydroxide in set Portland cements," Cem. Concr. Res., vol. 9(1), pp. 77-82, 1979.

[26] Bhatty J.I., Dollimore D., Gamlen G.A., Mangabhai R.J. and Olmez H., "Estimation of calcium hydroxide in OPC, OPC/PFA and OPC/PFA/polymer modified systems," Thermochi. Acta, vol. 106, pp. 115-123, 1986.

[27] Saeki T. and Sasaki K., "A model to predict the Ca/Si ratio of C-S-H in concrete containing mineral admixtures," In: 33rd Conference on our world in concrete & structures, Singapore, 2008.

[28] Jawahar J.G., Sashidhar C., Reddy I.R. and Peter J.A., "Micro and macrolevel properties of fly ash blended self -compacting concrete," Mater. Des., vol. 46, pp. 696-705, 2013.

[29] Kavitha O.R., Shanthi V.M., Arulraj G.P. and Sivakumar P., "Fresh, micro-and macrolevel studies of metakaolin blended self-compacting concrete," Appl. Clay Sci., vol. 114, pp. 370-374, 2015.

[30] Mehta P K and Monteriao P J M, Concrete: microstructure, properties, and materials, McGraw-Hill Publishing, 2006.

[31] Dehwah H.A.F., Maslehuddin M. and Austin S.A., " Effect of sulfate ions and associated cation type on the pore solution chemistry in chloride-contaminated plain and blended cements," Cem. Concr. Compos., vol. 25(4-5), pp. 513-525, 2003.

[32] Al-Amoudi O.S.B. and Maslehuddin M., "The effect of chloride and sulfate ions on reinforcement corrosion," Cem. Concr. Res., vol. 23(1), pp. 139-146, 1993.

[33] Neville A.M. and Brooks, J.J., Concrete technology, Pearson Education, 2013.

[34] Zhu J., Zhang Y. and Zhao D., In ICTE 2015, "Durability assessment of an RC railway bridge pier under a chloride-induced corrosion environment," in Fifth International Conference on Transportation Engineering, 2015.

[35] Pradhan B., "Corrosion behavior of steel reinforcement in concrete exposed to composite chloride-sulfate environment," Constr. Build. Mater., vol. 72, pp. 398-410, 2014.

[36] Arya C., Buenfeld N.R. and Newman J.B., "Factors influencing chloride-binding in concrete," Cem. Concr. Res., vol. 20(2), pp. 291-300, 1990.

[37] Luping T. and Nilsson L.O., "Chloride binding capacity and binding isotherms of OPC pastes and mortars," Cem. Concr. Res., vol. 23(2), pp. 247-253, 1993.

[38] Song Z., Jiang L., Zhang Z. and Xiong C., "Distance-associated chloride binding capacity of cement paste subjected to natural diffusion," Constr. Build. Mater., vol. 112(1), pp. 925-932, 2016.

[39] Yuan Q., Shi C., De Schutter G., Audenaert K. and Deng D., " Chloride binding of cement-based materials subjected to external chloride environment–a review," Constr. Build. Mater., vol. 23(1), pp. 1-13, 2009.

[40] Ramachandran V.S., "Possible states of chloride in the hydration of tricalcium silicate in the presence of calcium chloride," Mater. Struct., vol. 4(1), pp. 3-12, 1971.

[41] Al-Amoudi O.S.B., Rasheeduzzafar, Maslehuddin M. and Abduljauwad S.N., " Influence of chloride ions on sulphate deterioration in plain and blended cements," Mag. Concr. Res., vol. 46(167), pp. 113-123, 1994.

[42] Santhanam M., Cohen M. and Olek J., "Differentiating seawater and groundwater sulfate attack in Portland cement mortars," Cem. Concr. Res., vol. 36(12), pp. 2132-2137, 2006.

[43] Kim J.K., Han S.H., Park Y.D. and Noh J.H., "Material properties of self-flowing concrete," ASCE J. Mater. Civ. Eng., vol. 10 (4), pp. 244-249, 1998.

[44] Bouzoubaa N. and Lachemi M., "Self-compacting concrete incorporating high volumes of class F fly ash: Preliminary results," Cem. Concr. Res., vol. 31(3), pp. 413-420, 2001.

[45] Felekoğlu B., Türkel S. and Baradan B., "Effect of water/cement ratio on the fresh and hardened properties of self-compacting concrete," Build. Environ., vol. 42(4), pp.1795-1802, 2007.

[46] Khatib J.M., "Performance of self-compacting concrete containing fly ash," Constr. Build. Mater., vol. 22(9), pp. 1963-1971, 2008.

[47] Sukumar B., Nagamani K. and Raghavan R.S., "Evaluation of strength at early ages of self-compacting concrete with high volume fly ash," Constr. Build. Mater., vol. 22(7), pp. 1394-1401, 2008.

[48] Türkel S. and Kandemir A., "Fresh and hardened properties of SCC made with different aggregate and mineral admixtures," ASCE J. Mater. Civ. Eng., vol. 22(10), pp. 1025-1032, 2010.

[49] Wang H.Y. and Huang W.L., "A study on the properties of fresh self-consolidating glass concrete (SCGC)," Constr. Build. Mater., vol. 24(4), pp. 619-624, 2010.

[50] Girish S., Ranganath R.V. and Vengala J., "Influence of powder and paste on flow properties of SCC," Constr. Build. Mater., vol. 24(12), pp. 2481-2488, 2010.

[51] Safiuddin M., West J.S. and Soudki K.A., "Hardened properties of self-consolidating high performance concrete including rice husk ash," Cem. Concr. Compos., vol. 32(9), pp. 708-717, 2010.

[52] Melo K.A. and Carneiro A.M., "Effect of Metakaolin's finesses and content in self-consolidating concrete," Constr. Build. Mater., vol. 24(8), pp. 1529-1535, 2010.

[53] Uysal M. and Yilmaz K., "Effect of mineral admixtures on properties of self-compacting concrete," Cem. Concr. Compos., vol. 33(7), pp. 771-776, 2011.

[54] Madandoust R. and Mousavi S.Y., "Fresh and hardened properties of self-compacting concrete containing metakaolin," Constr. Build. Mater., vol. 35, pp. 752-760, 2012.

[55] Dehwah H.A.F., "Mechanical properties of self-compacting concrete incorporating quarry dust powder, silica fume or fly ash," Constr. Build. Mater., vol. 26(1), pp. 547-551, 2012.

[56] Naik T.R., Kumar R., Ramme B.W. and Canpolat F., "Development of high-strength, economical self-consolidating concrete," Constr. Build. Mater., vol. 30, pp. 463-469, 2012.

[57] Siddique R., Aggarwal P. and Aggarwal Y., "Influence of water/powder ratio on strength properties of self-compacting concrete containing coal fly ash and bottom ash," Constr. Build. Mater., vol. 29, pp. 73-81, 2012.

[58] Belaidi A.S.E., Azzouz L., Kadri E. and Kenai S., "Effect of natural pozzolana and marble powder on the properties of self-compacting concrete," Constr. Build. Mater., vol. 31, pp. 251-257, 2012.

[59] Uysal M., "The influence of coarse aggregate type on mechanical properties of fly ash additive self-compacting concrete," Constr. Build. Mater., vol. 37, pp. 533-540, 2012.

[60] Jawahar J.G., Sashidhar C., Reddy I.R. and Peter J.A., "Effect of coarse aggregate blending on short-term mechanical properties of self-compacting concrete," Mater. Des., vol. 43, pp. 185-194, 2013.

[61] Ashtiani M.S., Scott A.N. and Dhakal R.P., "Mechanical and fresh properties of high-strength self-compacting concrete containing class C fly ash," Constr. Build. Mater., vol. 47, pp. 1217-1224, 2013.

[62] Ranjbar M.M., Madandoust R., Mousavi S.Y. and Yosefi S., "Effects of natural zeolite on the fresh and hardened properties of self-compacted concrete," Constr. Build. Mater., vol. 47, pp. 806-813, 2013.

[63] Safiuddin M., Salam M.A. and Jumaat M.Z., "Key fresh properties of self-consolidating high-strength POFA concrete," ASCE J. Mater. Civ. Eng., vol. 26(1), pp. 134-142, 2013.

[64] Sfikas I.P., Badogiannis E.G. and Trezos K.G., "Rheology and mechanical characteristics of self-compacting concrete mixtures containing metakaolin," Constr. Build. Mater., vol. 64, pp. 121-129, 2014.

[65] Persson B., "Sulphate resistance of self-compacting concrete," Cem. Concr. Res., vol. 33(12), pp. 1933-1938, 2003.

[66] Nehdi M., Pardhan M. and Koshowski S., "Durability of self-consolidating concrete incorporating high-volume replacement composite cements," Cem. Concr. Res., vol. 34(11), pp. 2103-2112, 2004.

[67] Assie S., Escadeillas G. and Waller V., "Estimates of self-compacting concrete 'potential' durability," Constr. Build. Mater., vol. 21(10), pp. 1909-1917, 2007.

[68] Yazıcı H., "The effect of silica fume and high-volume Class C fly ash on mechanical properties, chloride penetration and freeze–thaw resistance of self-compacting concrete," Constr. Build. Mater., vol. 22(4), pp. 456-462, 2008.

[69] Gesoğlu M., Güneyisi E. and Özbay E., "Properties of self-compacting concretes made with binary, ternary, and quaternary cementitious blends of fly ash, blast furnace slag, and silica fume," Constr. Build. Mater., vol. 23(5), pp. 1847-1854, 2009.

[70] Şahmaran M., Yaman İ.Ö. and Tokyay M., "Transport and mechanical properties of self-consolidating concrete with high volume fly ash," Cem. Concr. Compos., vol. 31(2), pp. 99-106, 2009.

[71] Hossain K.M.A. and Lachemi M., "Fresh, mechanical, and durability characteristics of self-consolidating concrete incorporating volcanic ash," ASCE J. Mater. Civ. Eng., vol. 22(7), pp. 651-657, 2010.

[72] Leemann A., Loser R. and Münch B., "Influence of cement type on ITZ porosity and chloride resistance of self-compacting concrete," Cem. Concr. Compos., vol. 32(2), pp. 116-120, 2010.

[73] Wang H.Y. and Huang W.L., "Durability of self-consolidating concrete using waste LCD glass," Constr. Build. Mater., vol. 24(6), pp. 1008-1013, 2010.

[74] Siddique R., "Properties of self-compacting concrete containing class F fly ash," Mater. Des., vol. 32(3), pp. 1501-1507, 2011.

[75] Hassan A.A., Lachemi M. and Hossain K.M., "Effect of metakaolin and silica fume on the durability of self-consolidating concrete," Cem. Concr. Compos., vol. 34(6), pp. 801-807, 2012.

[76] Kanellopoulos A., Petrou M.F. and Ioannou I., "Durability performance of self-compacting concrete," Constr. Build. Mater., vol. 37, pp. 320-325, 2012.

[77] Pathak N. and Siddique R., "Properties of self-compacting-concrete containing fly ash subjected to elevated temperatures," Constr. Build. Mater., vol. 30, pp. 274-280, 2012.

[78] Uysal M., Yilmaz K. and Ipek M., "The effect of mineral admixtures on mechanical properties, chloride ion permeability and impermeability of self-compacting concrete," Constr. Build. Mater., vol. 27(1), pp. 263-270, 2012.

[79] Ramezanianpour A.A., Kazemian A., Sarvari M. and Ahmadi B., "Use of natural zeolite to produce self-consolidating concrete with low Portland cement content and high durability," ASCE J. Mater. Civ. Eng., vol. 25(5), pp. 589-596, 2013.

[80] El-Chabib H. and Syed A., "Properties of self-consolidating concrete made with high volumes of supplementary cementitious materials," ASCE J. Mater. Civ. Eng., vol. 25(11), pp. 1579-1586, 2013.

[81] Sabet F.A., Libre N.A. and Shekarchi M., "Mechanical and durability properties of self-consolidating high performance concrete incorporating natural zeolite, silica fume and fly ash," Constr. Build. Mater., vol. 44, pp. 175-184, 2013.

[82] Sideris K.K. and Anagnostopoulos N.S., "Durability of normal strength self-compacting concretes and their impact on service life of reinforced concrete structures," Constr. Build. Mater., vol. 41, pp. 491-497, 2013.

[83] Dinakar P., Reddy M.K. and Sharma M., "Behaviour of self- compacting concrete using Portland pozzolana cement with different levels of fly ash," Mater. Des., vol. 46, pp. 609-616, 2013.

[84] Wang H.Y. and Lin C.C., "A study of fresh and engineering properties of self-compacting high slag concrete (SCHSC)," Constr. Build. Mater., vol. 42, pp. 132-136, 2013.

[85] Nikbin I.M., Beygi M.H.A., Kazemi M.T., Amiri J.V., Rabbanifar S., Rahmani E. and Rahimi S., "A comprehensive investigation into the effect of water to cement ratio and powder content on mechanical properties of self-compacting concrete," Constr. Build. Mater., vol. 57, pp. 69-80, 2014.

[86] Celik K., Meral C., Mancio M., Mehta P.K. and Monteiro P.J.M., " A comparative study of self-consolidating concretes incorporating high-volume natural pozzolan or high-volume fly ash," Constr. Build. Mater., vol. 67, pp. 14-19, 2014.

[87] Ryan P.C. and O'Connor A., "Comparing the durability of self-compacting concretes and conventionally vibrated concretes in chloride rich environments," Constr. Build. Mater., vol. 120, pp. 504-513, 2016.

[88] Vivek S.S. and Dhinakaran, G., "Durability characteristics of binary blend high strength SCC," Constr. Build. Mater., vol. 146, pp. 1-8, 2017.

[89] Benli A., Karataş M. and Gurses E., "Effect of sea water and $MgSO_4$ solution on the mechanical properties and durability of self-compacting mortars with fly ash/silica fume," Constr. Build. Mater., vol. 146, pp. 464-474, 2017.

[90] Hassan A.A.A., Hossain K.M.A. and Lachemi M., "Corrosion resistance of self-consolidating concrete in full-scale reinforced beams," Cem. Concr. Compos., vol. 31(1), pp. 29-38, 2009.

[91] Dinakar P., Babu K.G. and Santhanam, M., "Corrosion resistance performance of high-volume fly-ash self-compacting concretes," Mag. Concr. Res., vol. 61(2), pp. 77-85, 2009.

[92] Dehwah H.A.F., "Corrosion resistance of self-compacting concrete incorporating quarry dust powder, silica fume and fly ash," Constr. Build. Mater., vol. 37, pp. 277-282, 2012.

[93] Ahmad S., Adekunle S.K., Maslehuddin M. and Azad A.K., "Properties of self-consolidating concrete made utilizing alternative mineral fillers," Constr. Build. Mater., vol. 68, pp. 268-276, 2014.

[94] Adekunle S., Ahmad S., Maslehuddin M. and Al-Gahtani H.J., "Properties of SCC prepared using natural pozzolana and industrial wastes as mineral fillers," Cem. Concr. Compos., vol. 62, pp. 125-133, 2015.

[95] Ghanooni-Bagha M., Shayanfar M.A., Shirzadi-Javid A.A. and Ziaadiny H., "Corrosion-induced reduction in compressive strength of self-compacting concretes containing mineral admixtures," Constr. Build. Mater., vol. 113, pp. 221-228, 2016.

[96] Ye G., Liu X., De Schutter G., Poppe A.M. and Taerwe L., "Influence of limestone powder used as filler in SCC on hydration and microstructure of cement pastes," Cem. Concr. Compos., vol. 29(2), pp. 94-102, 2007.

[97] Fares H., Remond S., Noumowe A. and Cousture A., "High temperature behaviour of self-consolidating concrete: microstructure and physicochemical properties," Cem. Concr. Res., vol. 40(3), pp. 488-496, 2010.

[98] Mohammed M.K., Dawson A.R. and Thom N.H., "Production, microstructure and hydration of sustainable self-compacting concrete with different types of filler," Constr. Build. Mater., vol. 49, pp. 84-92, 2013.

[99] Siad H., Kamali-Bernard S., Mesbah H.A., Escadeillas G., Mouli M. and Khelafi H., "Characterization of the degradation of self-compacting concretes in sodium sulfate environment: Influence of different mineral admixtures," Constr. Build. Mater., vol. 47, pp. 1188-1200, 2013.

[100] Kannan V. and Ganesan K., "Chloride and chemical resistance of self-compacting concrete containing rice husk ash and metakaolin," Constr. Build. Mater., vol. 51, pp. 225-234, 2014.

[101] Jalal M., Pouladkhan A., Harandi O.F. and Jafari D., "Comparative study on effects of Class F fly ash, nano silica and silica fume on properties of high performance self-compacting concrete," Constr. Build. Mater., vol. 94, pp. 90-104, 2015.

[102] Siad H., Lachemi M., Bernard S.K., Sahmaran M. and Hossain A., "Assessment of the long-term performance of SCC incorporating different mineral admixtures in a magnesium sulphate environment," Constr. Build. Mater., vol. 80, pp. 141-154, 2015.

[103] Kavitha O.R., Shanthi V.M., Arulraj G.P. and Sivakumar V.R., "Microstructural studies on eco-friendly and durable self-compacting concrete blended with metakaolin," Appl. Clay Sci., vol. 124, pp. 143-149, 2016.

[104] Ghoddousi P. and Saadabadi L.A., "Study on hydration products by electrical resistivity for self-compacting concrete with silica fume and metakaolin, " Constr. Build. Mater., vol. 154, pp. 219-228, 2017.

[105] IS 8112: 2013, “Ordinary Portland cement, 43 Grade – Specification,” Bureau of Indian Standards, New Delhi, 2013.

[106] ASTM C150/C150M-12, “Standard Specification for Portland Cement,” ASTM International, West Conshohocken, PA, 2012.

[107] IS: 1489-1991, “Portland-pozzolana cement – Specification, Part 1: Fly Ash Based,” Bureau of Indian Standards, New Delhi, Reaffirmed 2005.

[108] ASTM C595/C595M-12, “Standard Specification for Blended Hydraulic Cements,” ASTM International, West Conshohocken, PA, 2012.

[109] ASTM C618, “Standard specification for coal fly ash and raw or calcined natural pozzolan for use in concrete,” ASTM International, West Conshohocken, PA, 2012.

[110] IS: 4031-1988, “Methods of physical tests for hydraulic cement, Part 11: Determination of density,” Bureau of Indian standard, New Delhi, Reaffirmed 2005.

[111] IS: 2386 -1963 (part -III), “Indian standard methods of test for aggregates for concrete specific gravity, density, voids, absorption and bulking”, Bureau of Indian Standards, 1963, New Delhi, Reaffirmed 2002.

[112] IS: 2386 -1963 (part-I), “Indian standard methods of test for aggregates for concrete, partical size and shape”, Bureau of Indian Standards, 1963, New Delhi, Reaffirmed 2002.

[113] IS: 383 -1970, "Indian Standard specification for coarse and fine aggregates from natural sources for concrete", Bureau of Indian Standards, 1970, New Delhi, Reaffirmed 2002.

[114] Wegian F.M., "Effect of seawater for mixing and curing on structural concrete," The IES Journal Part A: Civil and Structural Engineering, vol. 3(4), pp. 235-243, 2010.

[115] Le H.T., Müller M, Siewert K. and Ludwig H.M., "The mix design for self-compacting high performance concrete containing various mineral admixtures," Mater. Des., vol. 72, pp. 51-62, 2015.

[116] ACI 237R-07, "Self- consolidating concrete," American Concrete Institute, 2007.

[117] Pradhan B. and Bhattacharjee B., "Role of steel and cement type on chloride-induced corrosion in concrete," ACI Mater. J., vol. 104(6), pp. 612-619, 2009.

[118] Güneyisi E., Gesoglu M., Karabog F. and Mermerdas K., "Corrosion behavior of reinforcing steel embedded in chloride contaminated concretes with and without metakaolin," Composites: Part B: Engineering, vol. 45(1), pp. 1288-1295, 2013.

[119] AI-Tayyib A.J., Khan M.S., Allam I.M. and AI-Mana A.I., "Corrosion behavior of pre-rusted rebars after placement in concrete," Cem. Concr. Res., vol. 20(6), pp. 955-960, 1990.

[120] Shaheen F. and Pradhan B., "Influence of sulfate ion and associated cation type on steel reinforcement corrosion in concrete powder aqueous solution in the presence of chloride ions," Cem. Concr. Res., vol. 91, pp. 73-86, 2017.

[121] Dehwah HAF, Maslehuddin M and Austin SA, "Long-term effect of sulfate ions and associated cation type on chloride-induced reinforcement corrosion in Portland concrete," Cem. Concr. Compos., vol. 24, pp. 17-25, 2002.

[122] Zuquan J., Wei S., Yunsheng Z., Jinyang J. and Jianzhong L., "Interaction between sulfate and chloride solution attack of concretes with and without fly ash," Cem. Concr. Res., vol. 37(8), pp. 1223-1232, 2007.

[123] Chung F.H., "Quantitative interpretation of X-ray diffraction patterns, I. Matrix-flushing method of quantitative multicomponent analysis," J. Appl. Cryst., vol. 7, pp. 519-525, 1974a.

[124] Chung F.H., "Quantitative interpretation of X-ray diffraction patterns, II. Adiabatic principle of X-ray diffraction analysis of mixtures," J. Appl. Cryst., vol. 7, pp. 526-531, 1974b.

[125] Chung F.H., "Quantitative interpretation of X-ray diffraction patterns, III. Simultaneous determination of a set of reference intensities," J. Appl. Cryst., vol. 8, pp. 17-19, 1975.

[126] Geng J., Easterbrook D., Li L.Y. and Mo L.W., "The stability of bound chlorides in cement paste with sulfate attack," Cem. Concr. Res., vol. 68, pp. 211-22, 2015.

[127] Taylor H.F.W., Cement chemistry, Second ed., Thomas Telford, 1997.

[128] Pradhan B. and Bhattacharjee B., "Corrosion zones of rebar in chloride contaminated concrete through potentiostatic study in concrete powder solution extracts," Corros. Sci., vol. 49(10), pp. 3935-3952, 2007.

[129] Shaheen F. and Pradhan B., "Effect of chloride and conjoint chloride-sulfate ions on corrosion of reinforcing steel in electrolytic concrete powder solution (ECPS)," Constr. Build. Mater., vol. 101, pp. 99-112, 2015.

[130] Hicks C.R., Fundamental concepts in the design of experiments, 3rd ed., New York: Holt: Rinehart and Winston, 1982.

[131] Saraswathy V. and Song H.W., "Evaluation of corrosion resistance of Portland pozzolana cement and fly ash blended cements in pre-cracked reinforced concrete slabs under accelerated testing conditions," Mater. Chem. Phy., vol. 104(2-3), pp. 356-361, 2007.

[132] Delagrave A., Marchand J., Ollivier J.P., Julien S. and Hazrati K., "Chloride binding capacity of various hydrated cement paste systems," Adv. Cem. based Mater., vol. 6(1), pp. 28-35, 1997.

[133] Rostami V., Shao Y., Boyd A.J. and He Z., "Microstructure of cement paste subject to early carbonation curing," Cem. Concr. Res., vol. 42, no. 1, pp. 186-193, 2015.

[134] Shaikh F.U.A. and Supit S.W.M., "Chloride induced corrosion durability of high volume fly ash concretes containing nano particles," Constr. Build. Mater., vol. 99, pp. 208-225, 2015.

[135] Ramachandran V.S. and Beaudoin J.J., Handbook of Analytical Techniques in Concrete Science and Technology, William Andrew/Noyes Publications, 2001.

[136] Silva D.A.D., Roman H.R. and Gleize P.J.P., "Evidences of chemical interaction between EVA and hydrating Portland cement," Cem. Concr. Res., vol. 32, pp. 1383-1390, 2002.

[137] Mollah M.Y.A., Lu F. and Cocke D.L., "An X-ray diffraction (XRD) and Fourier transform infrared spectroscopic (FT-IR) characterization of the speciation of arsenic (V) in Portland cement type-V," Sci. Total Environ., vol. 224, pp. 57-68, 1998.

[138] Hughes T.L., Methven C.M., Jones T.G., Pelham S.E., Fletcher P. and Hall, C., "Determining cement composition by Fourier transform infrared spectroscopy," Adv. Cem. based Mater., vol. 2, pp. 91-104, 1995.

[139] ASTM C876-15, Standard Test Method for Corrosion Potentials of Uncoated Reinforcing Steel in Concrete, ASTM International, West Conshohocken, PA, 2015.

[140] Liu P.C., "Damage to concrete structures in a marine environment," Mater. Struct., vol. 24(4), pp. 302-307., 1991.

APPENDIX A

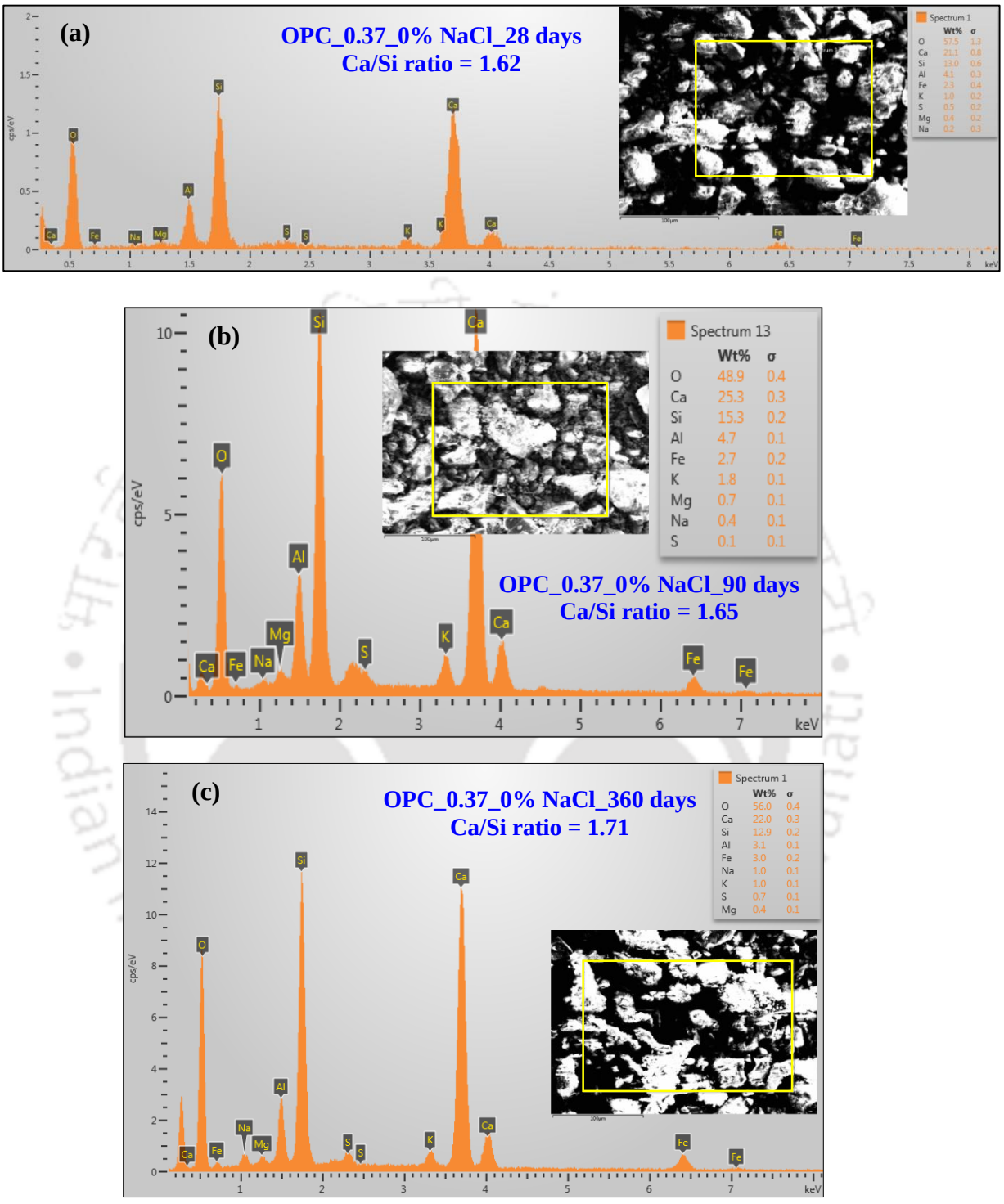

Fig. A1 EDX analysis of OPC based SCC mixes admixed with 0% NaCl, at w/b ratio of 0.37: (a) 28 days, (b) 90 days, and (c) 360 days

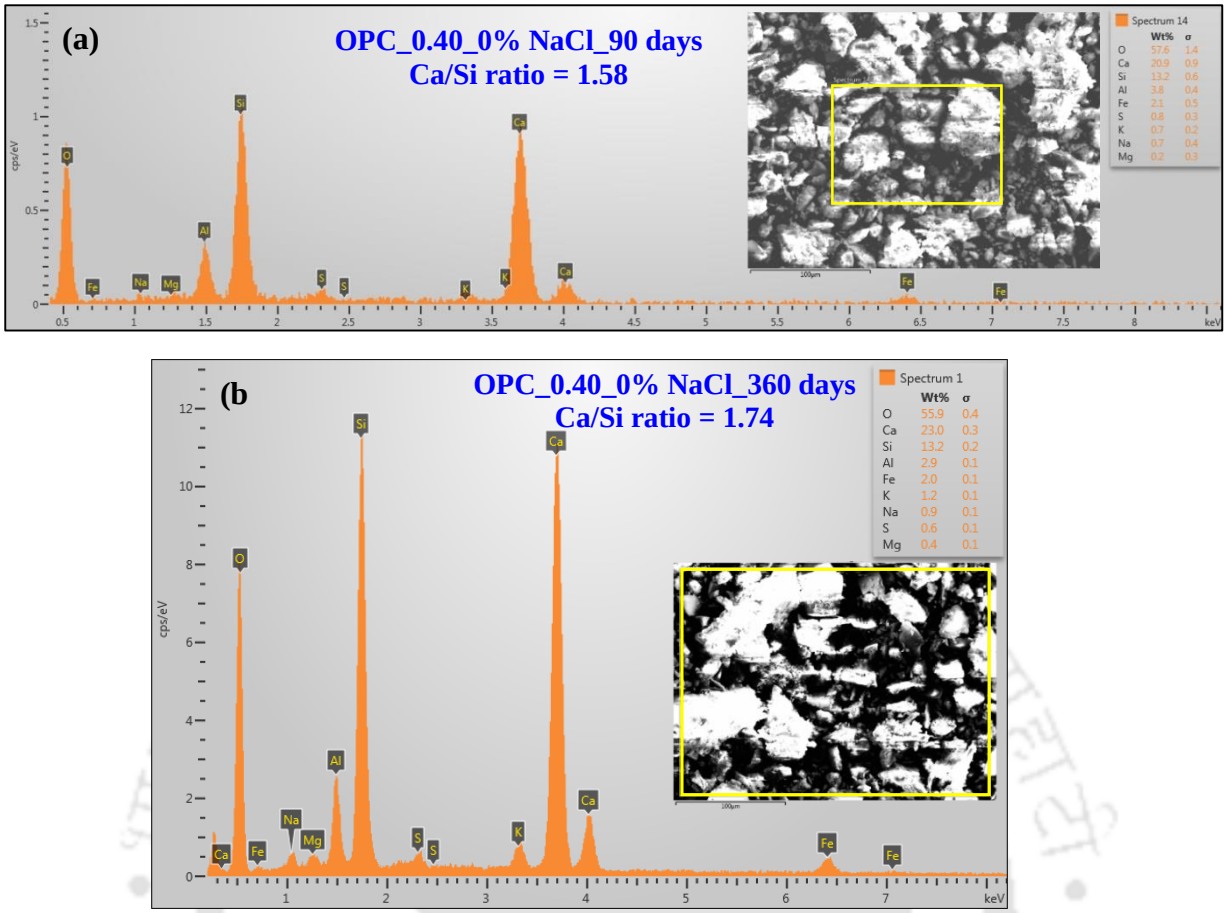

Fig. A2 EDX analysis of OPC based SCC mixes admixed with 0% NaCl, at w/b ratio of 0.40: (a) 90 days, and (b) 360 days

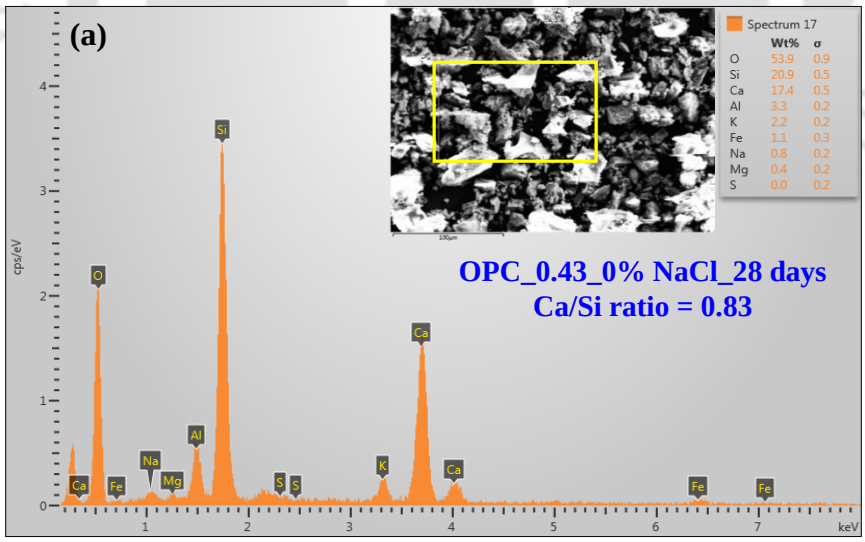

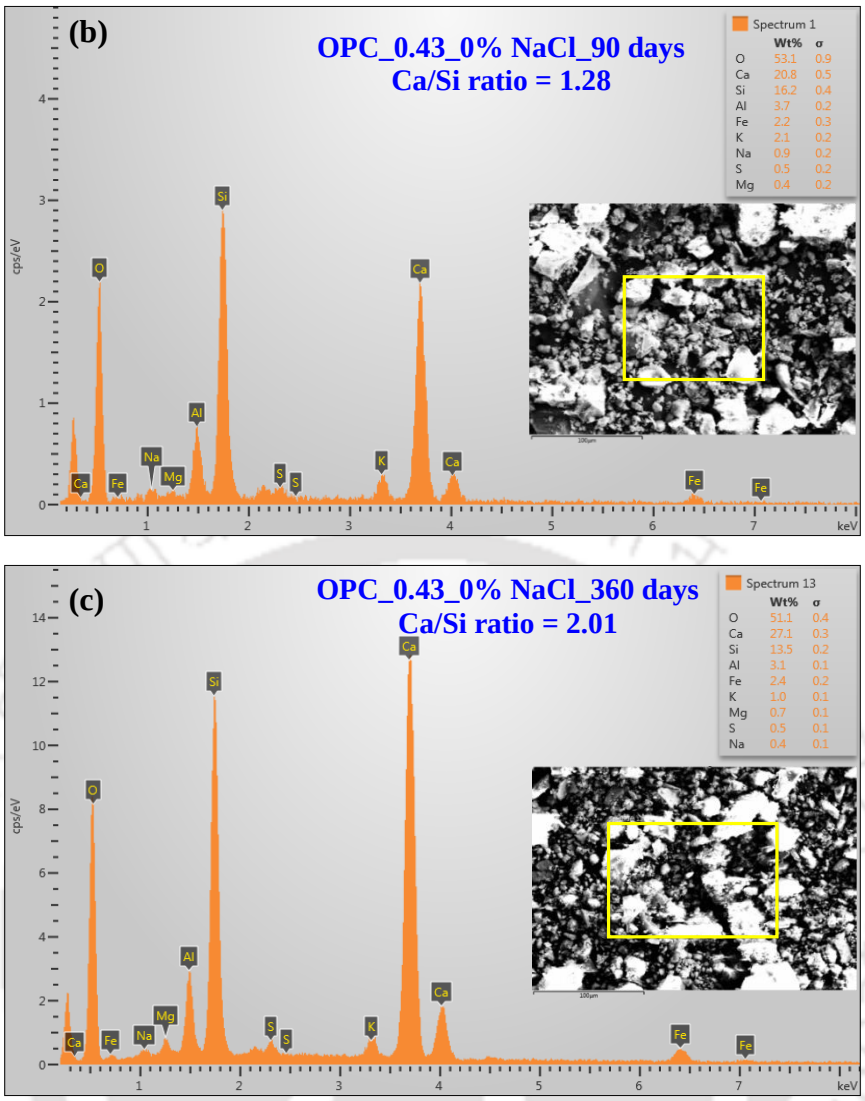

Fig. A3 EDX analysis of OPC based SCC mixes admixed with 0% NaCl, at w/b ratio of 0.43: (a) 28 days, (b) 90 days, and (c) 360 days

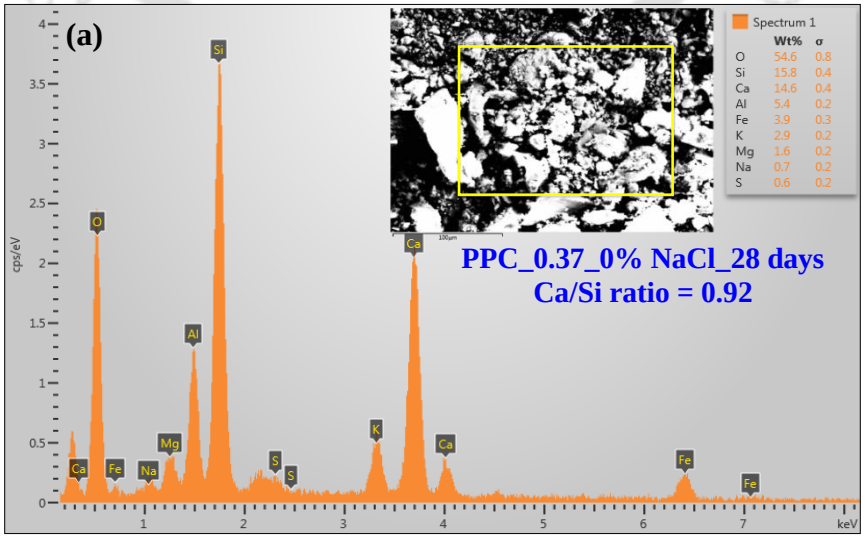

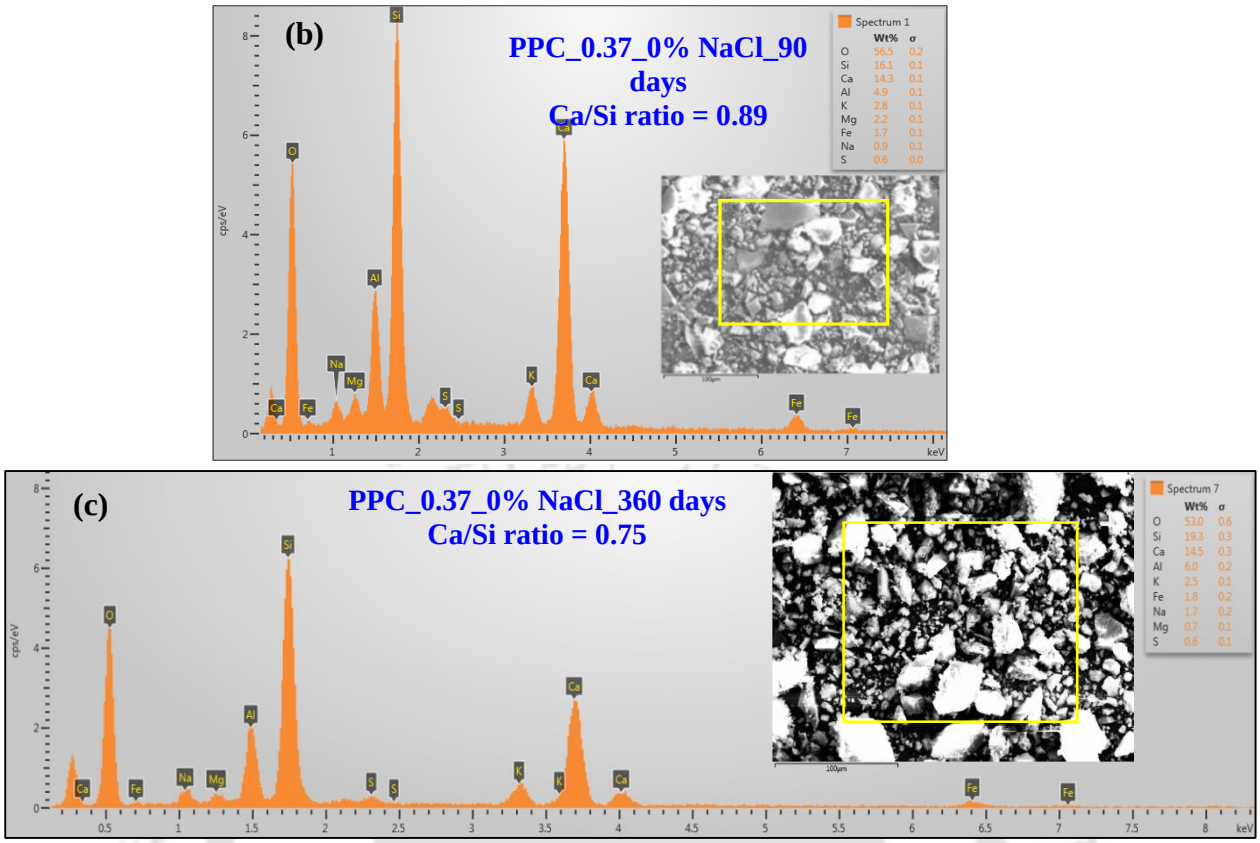

Fig. A4 EDX analysis of PPC based SCC mixes admixed with 0% NaCl, at w/b ratio of 0.37: (a) 28 days, (b) 90 days, and (c) 360 days

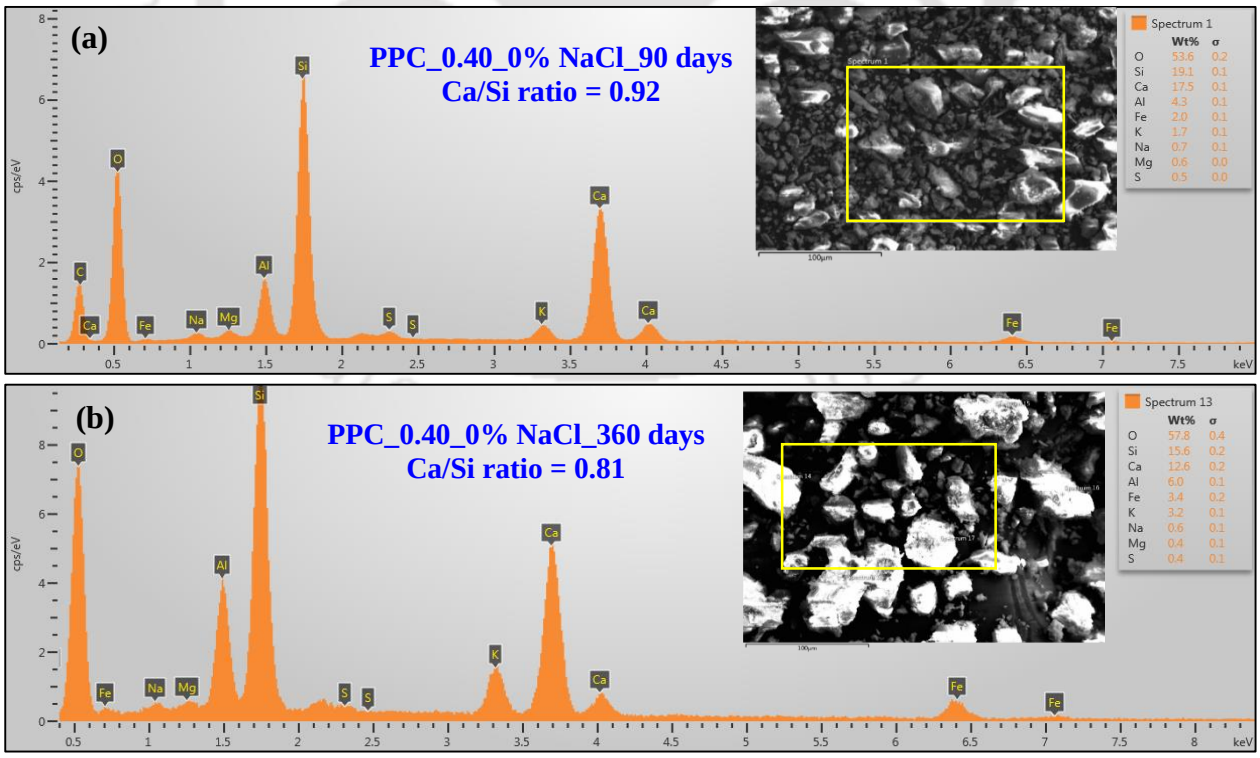

Fig. A5 EDX analysis of PPC based SCC mixes admixed with 0% NaCl, at w/b ratio of 0.40: (a) 90 days, and (b) 360 days

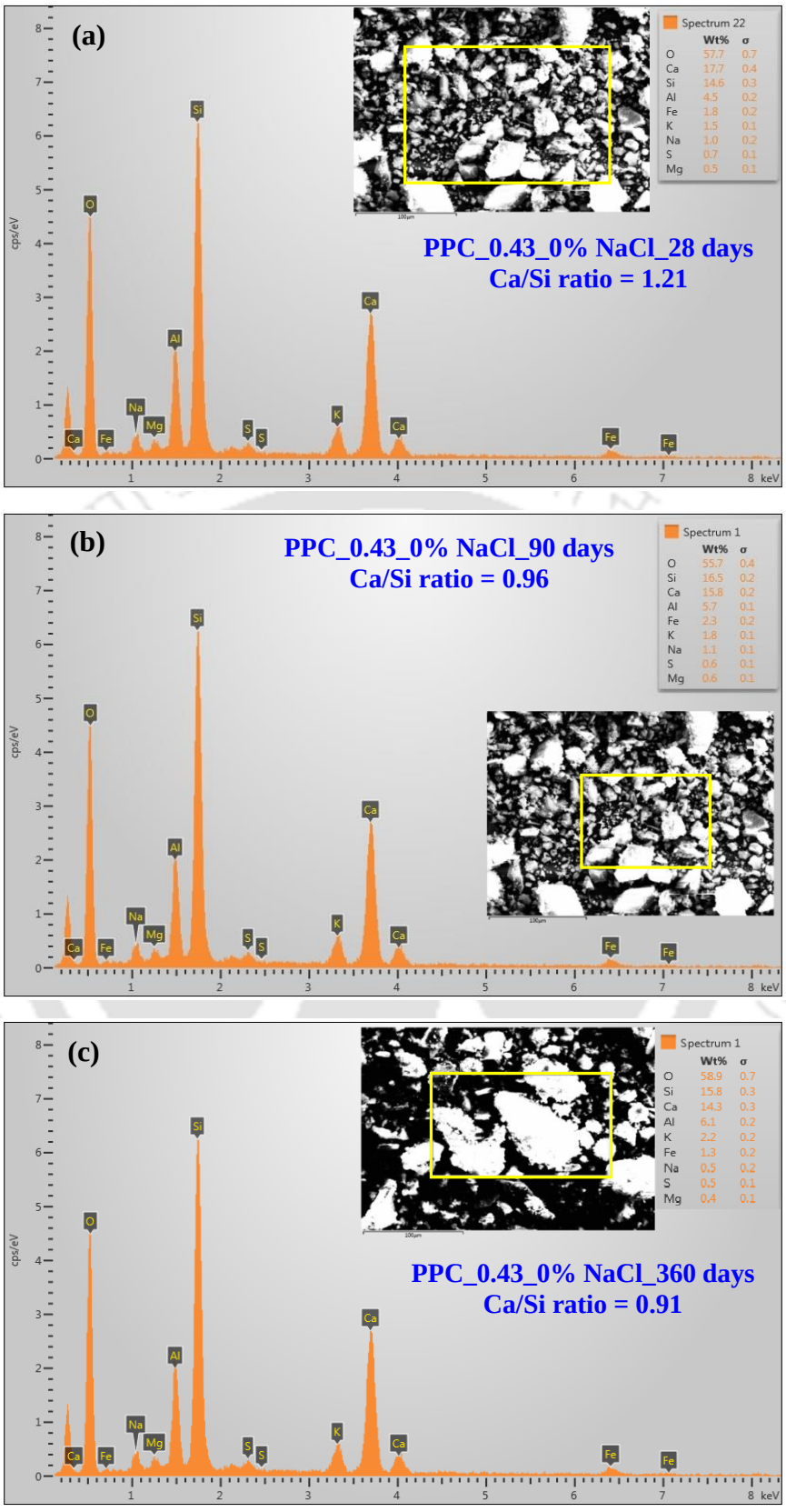

Fig. A6 EDX analysis of PPC based SCC mixes admixed with 0% NaCl, at w/b ratio of 0.43: (a) 28 days, (b) 90 days, and (c) 360 days

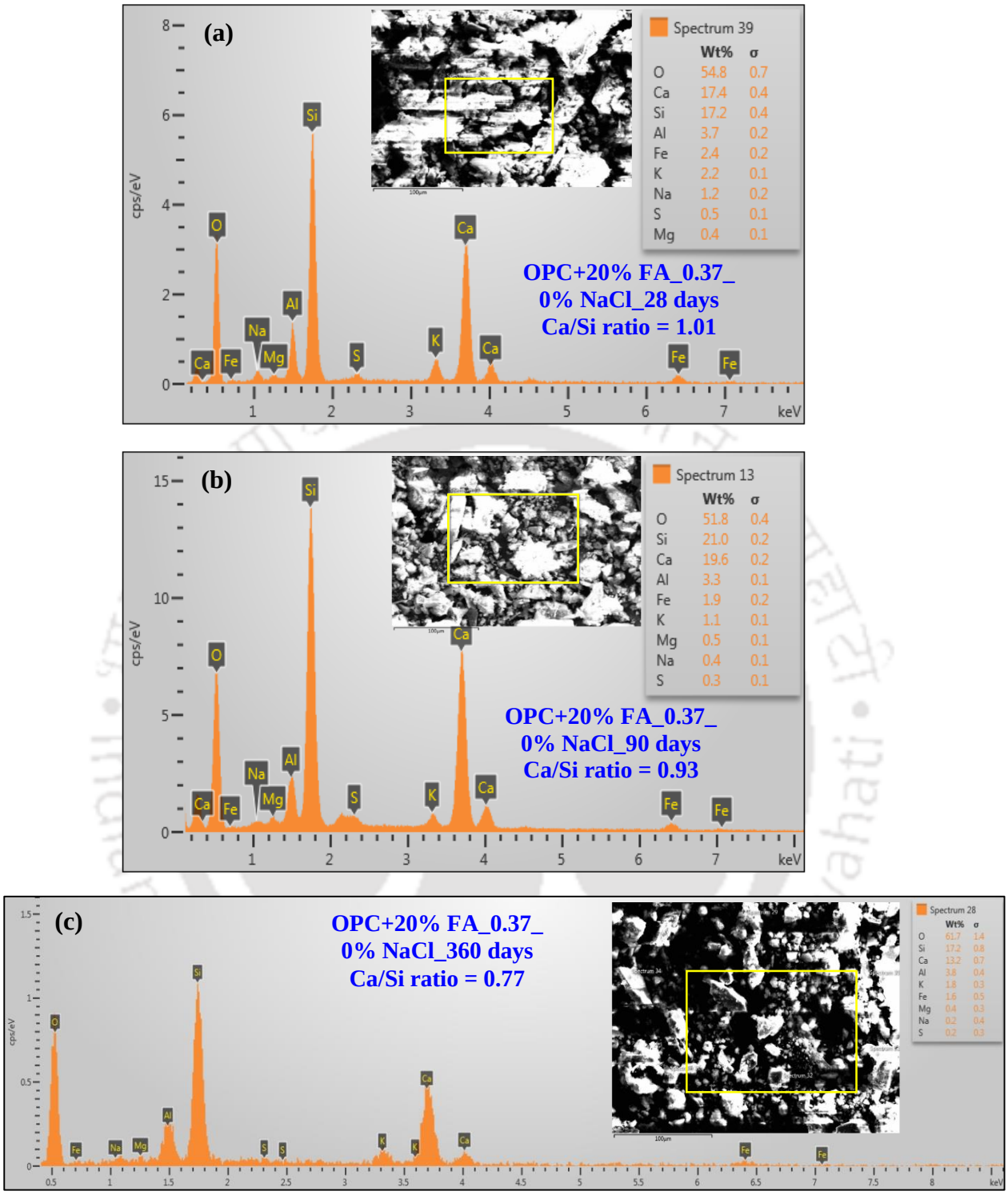

Fig. A7 EDX analysis of OPC+20% FA based SCC mixes admixed with 0% NaCl, at w/b ratio of 0.37: (a) 28 days, (b) 90 days, and (c) 360 days

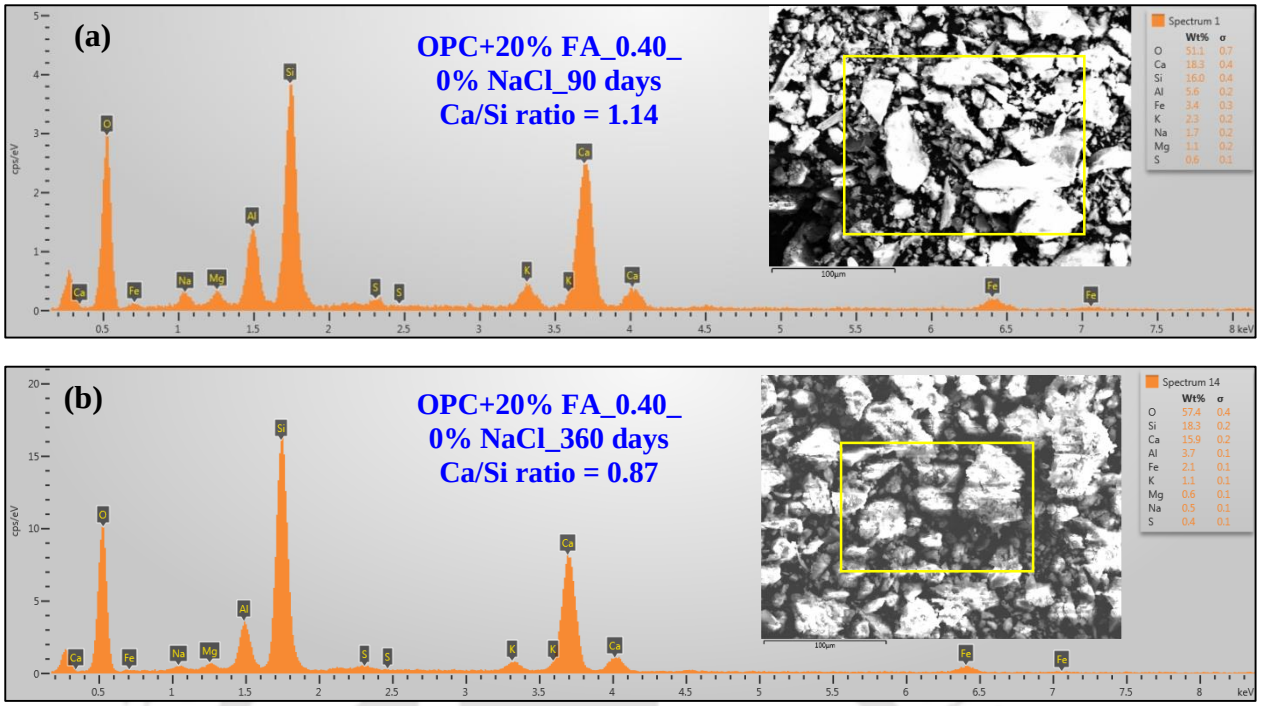

Fig.A8 EDX analysis of OPC+20% FA based SCC mixes admixed with 0% NaCl, at w/b ratio of 0.40: (a) 90 days, and (b) 360 days

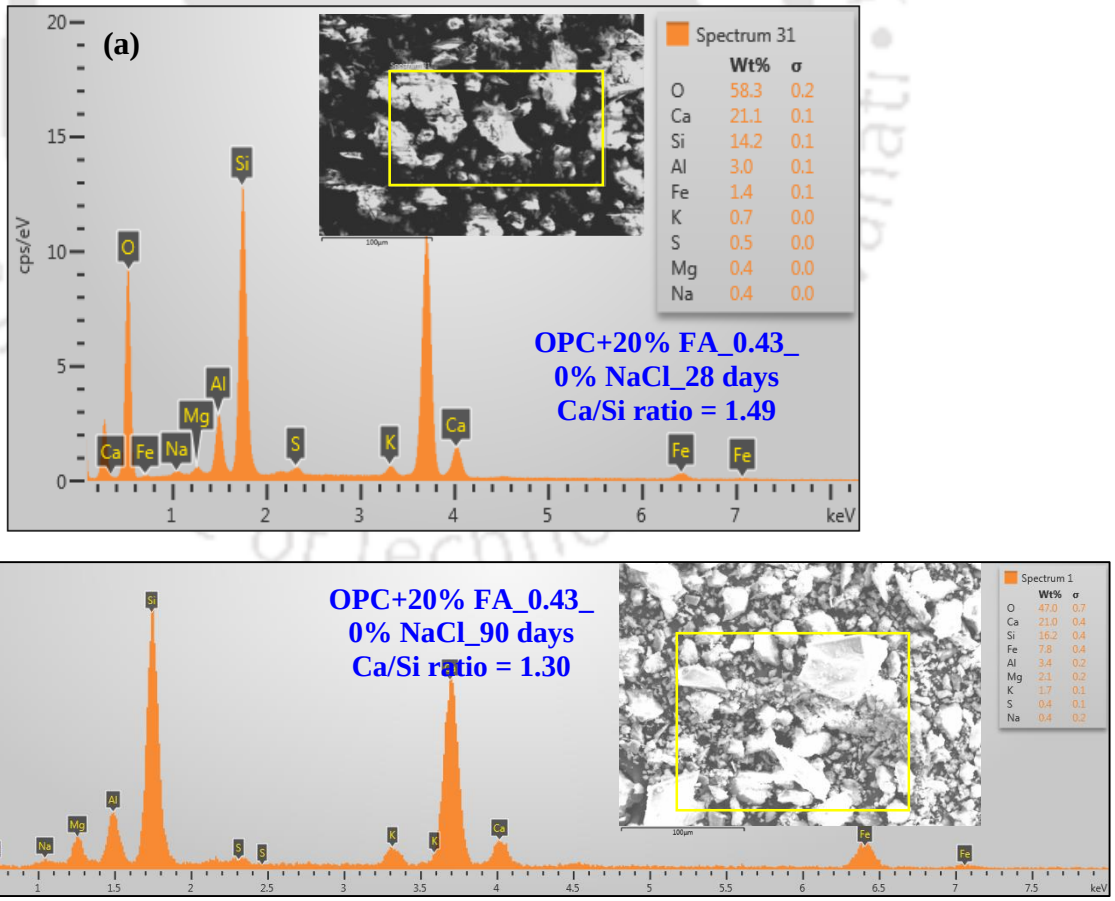

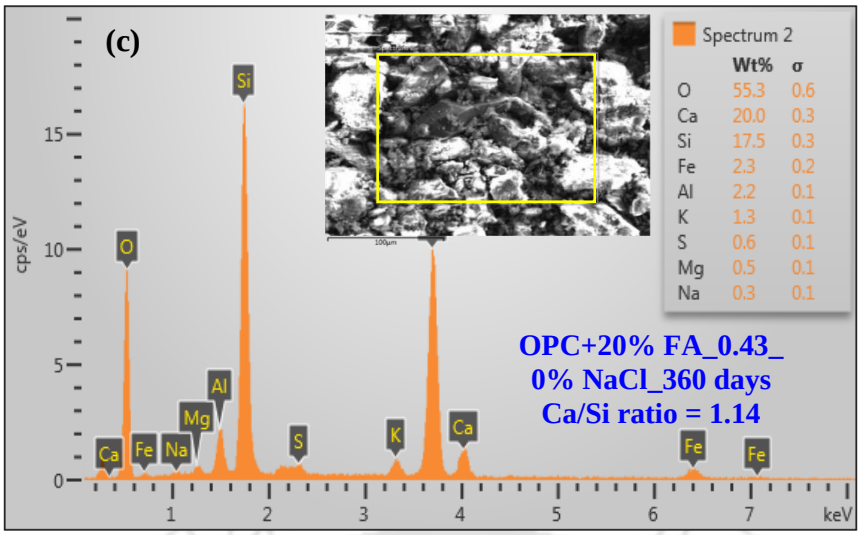

Fig. A9 EDX analysis of OPC+20% FA based SCC mixes admixed with 0% NaCl, at w/b ratio of 0.43: (a) 28 days, (b) 90 days, and (c) 360 days

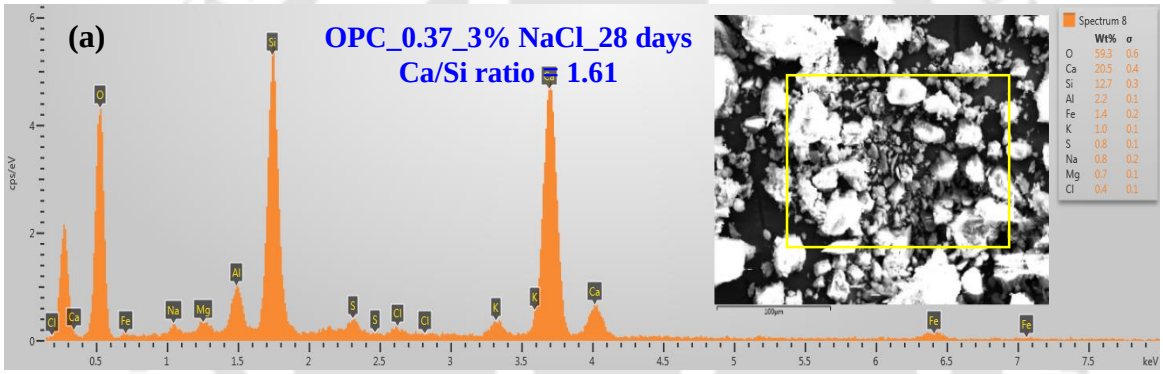

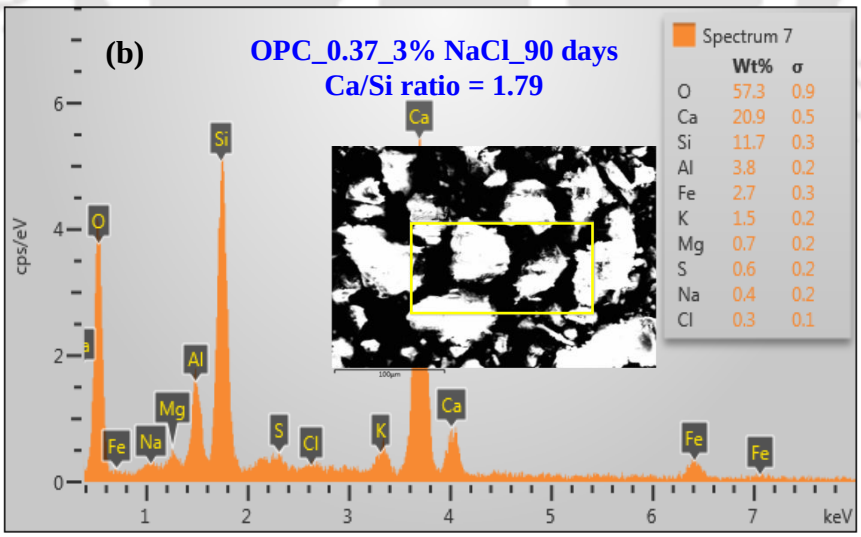

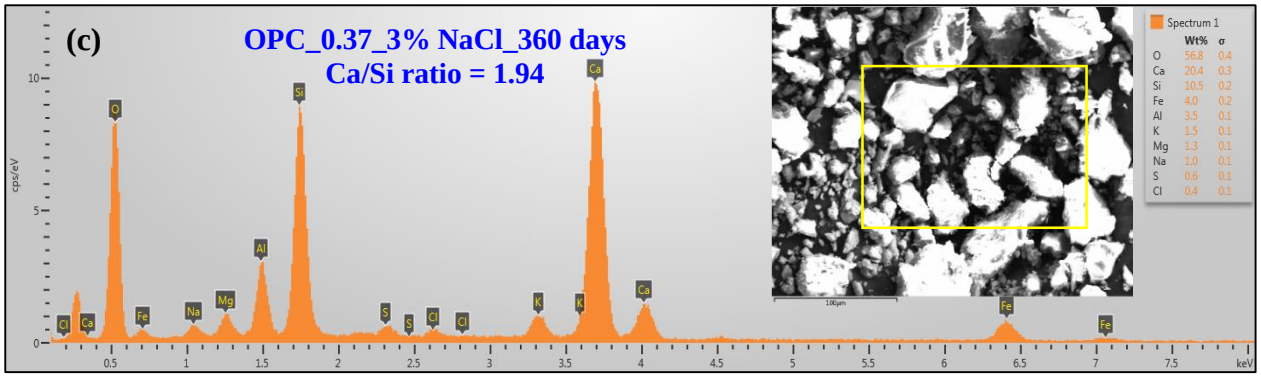

Fig. A10 EDX analysis of OPC based SCC mixes admixed with 3% NaCl, at w/b ratio of 0.37: (a) 28 days, (b) 90 days, and (c) 360 days

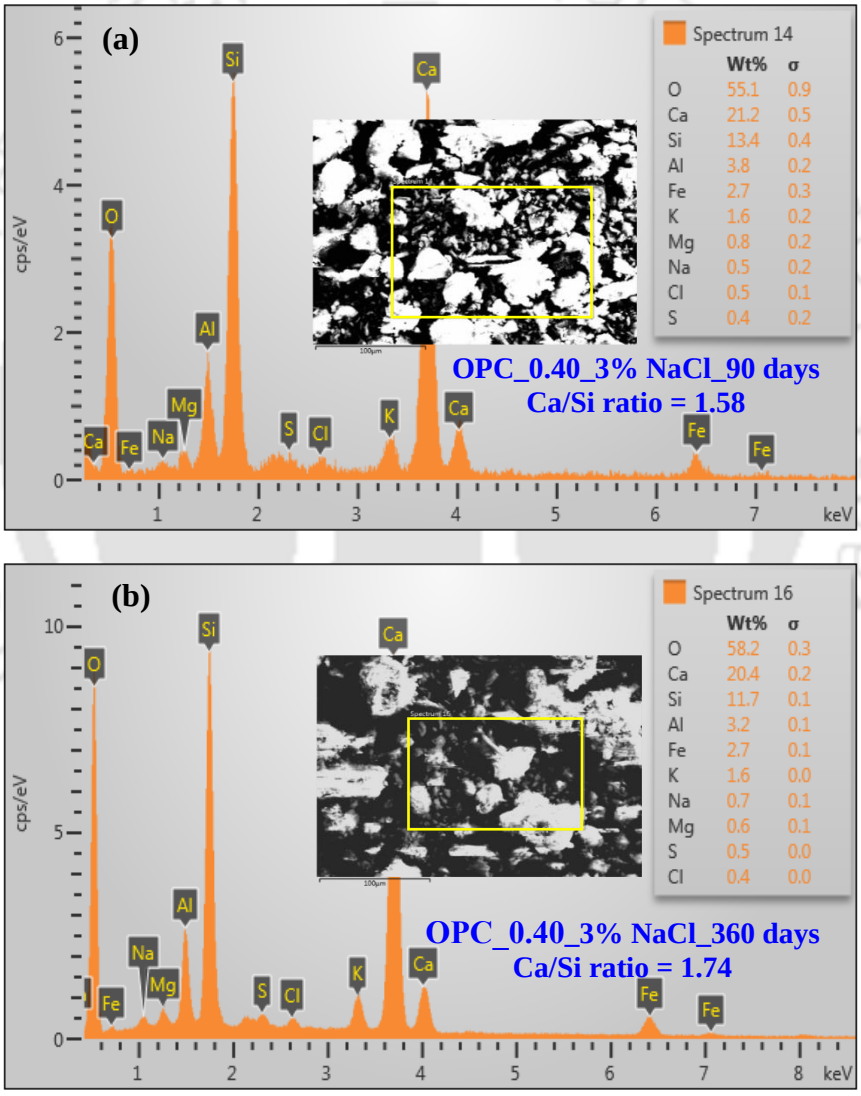

Fig. A11 EDX analysis of OPC based SCC mixes admixed with 3% NaCl, at w/b ratio of 0.40: (a) 90 days, and (b) 360 days

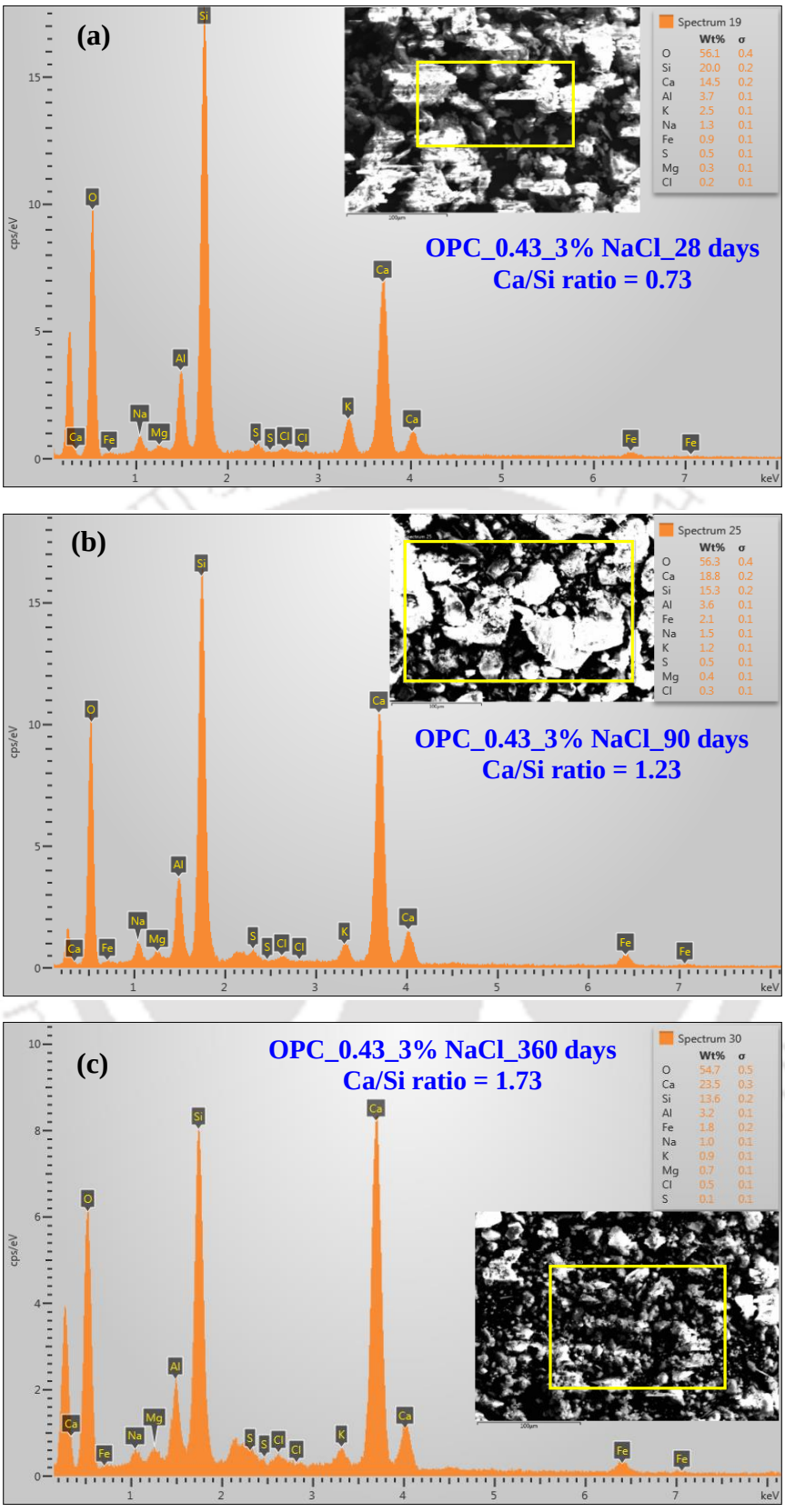

Fig. A12 EDX analysis of OPC based SCC mixes admixed with 3% NaCl, at w/b ratio of 0.43: (a) 28 days, (b) 90 days, and (c) 360 days

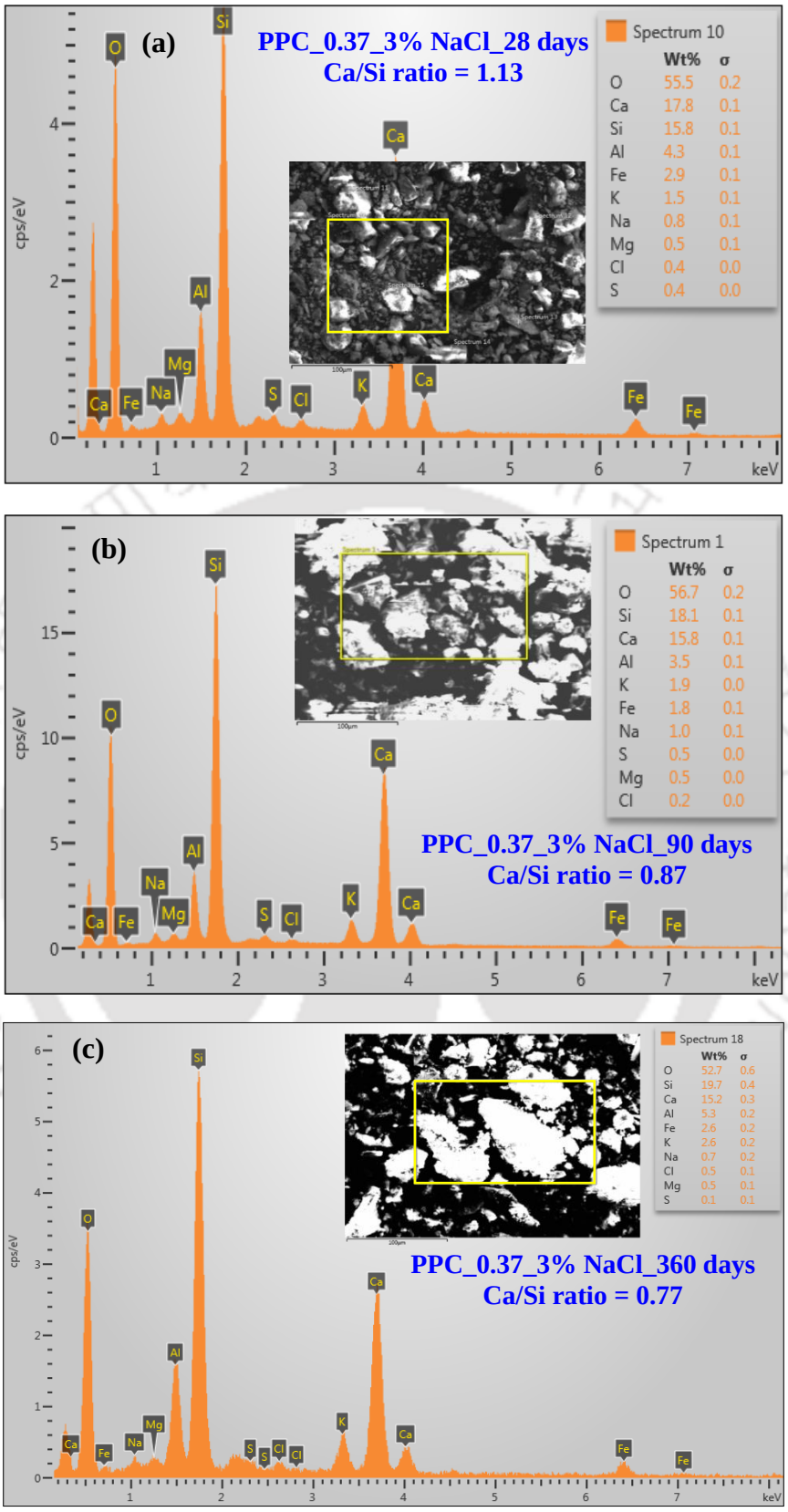

Fig. A13 EDX analysis of PPC based SCC mixes admixed with 3% NaCl, at w/b ratio of 0.37: (a) 28 days, (b) 90 days, and (c) 360 days

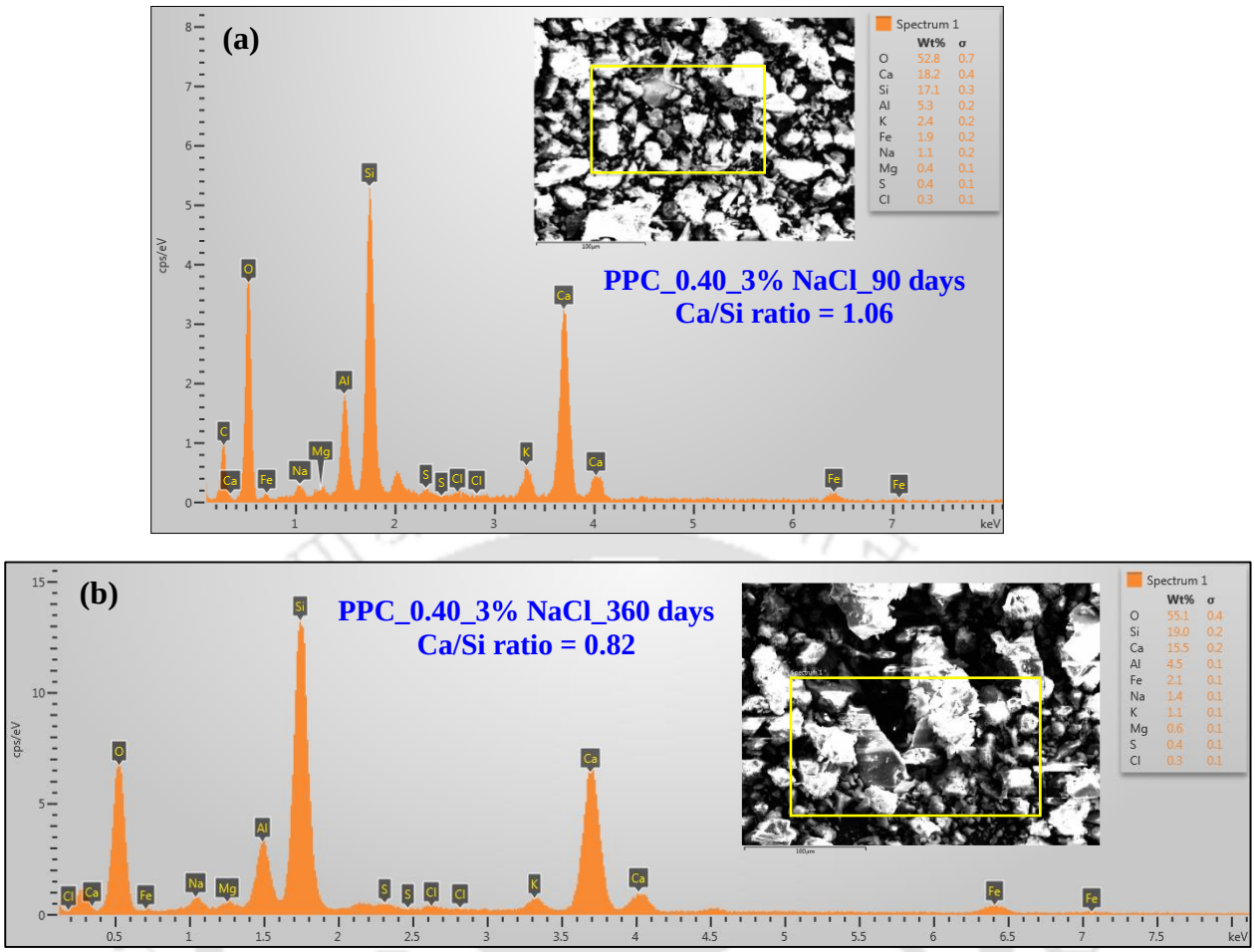

Fig. A14 EDX analysis of PPC based SCC mixes admixed with 3% NaCl, at w/b ratio of 0.40: (a) 90 days, and (c) 360 days

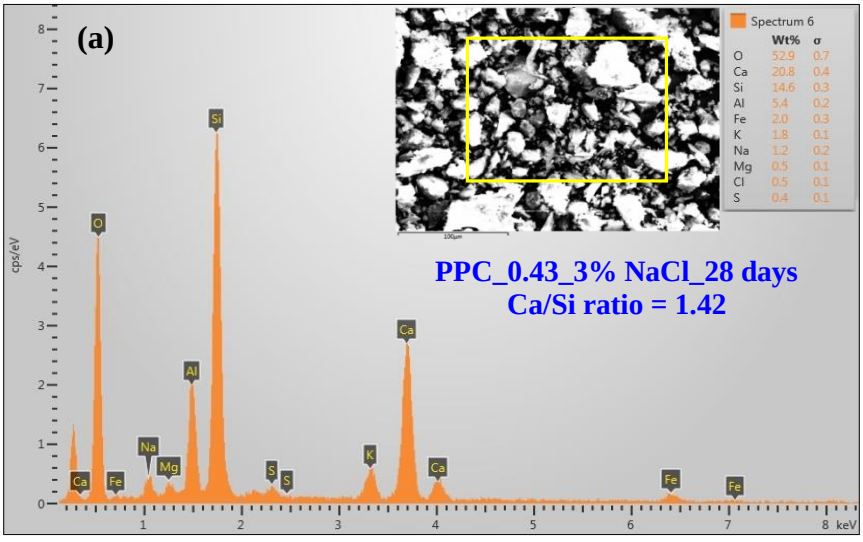

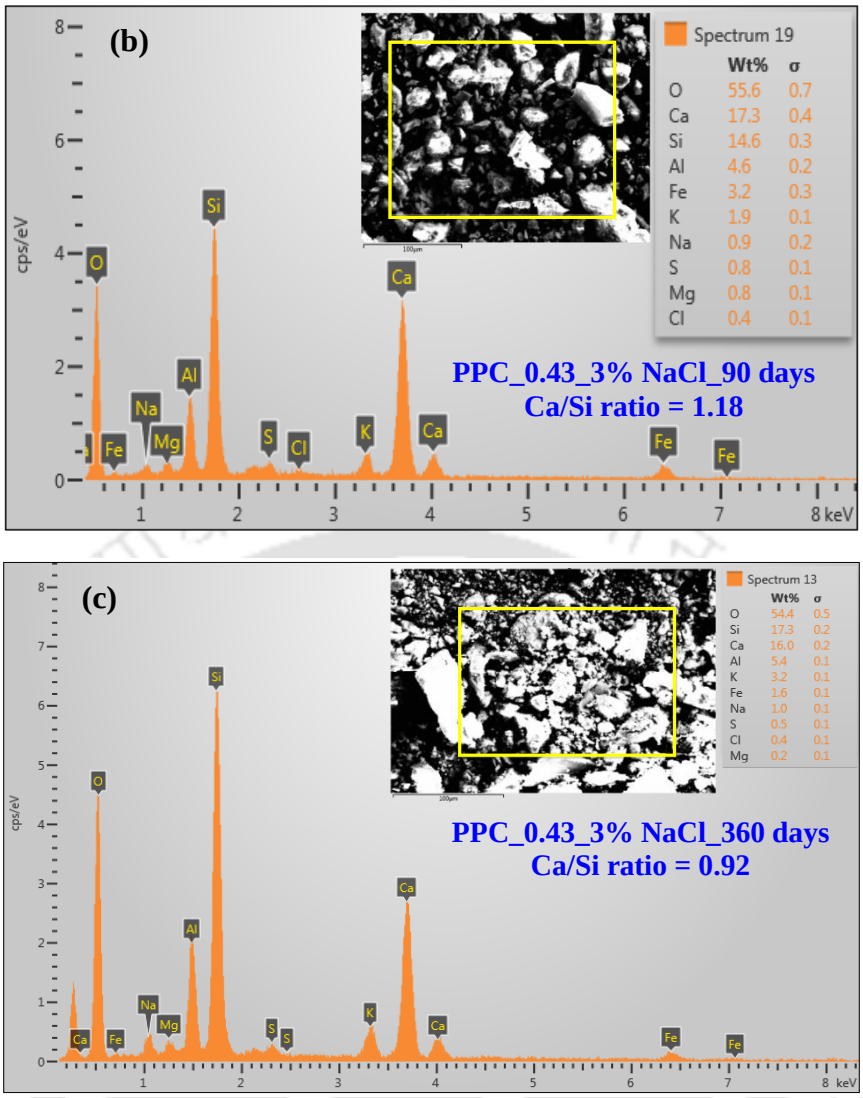

Fig. A15 EDX analysis of PPC based SCC mixes admixed with 3% NaCl, at w/b ratio of 0.43: (a) 28 days, (b) 90 days, and (c) 360 days

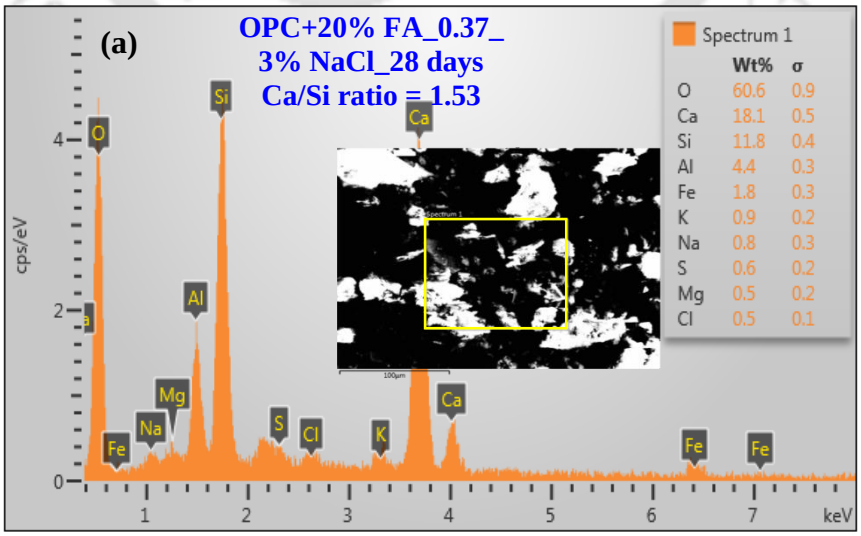

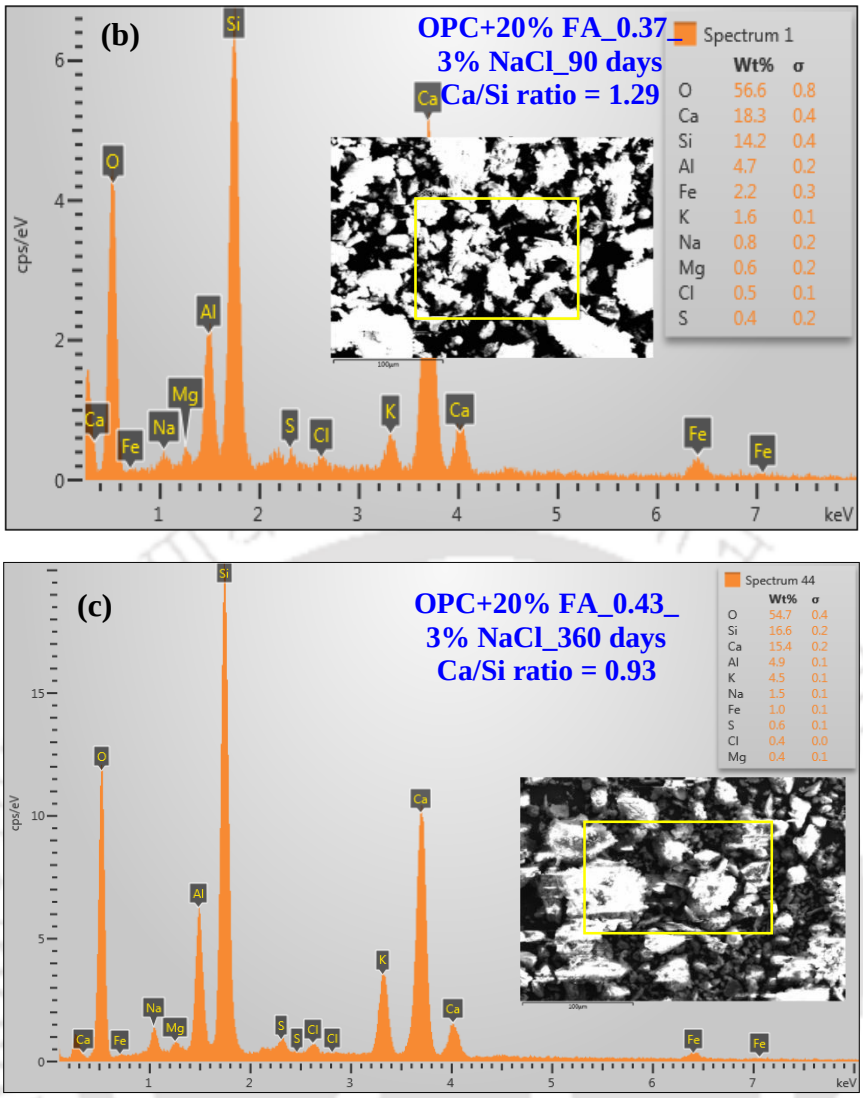

Fig. A16 EDX analysis of OPC+20% FA based SCC mixes admixed with 3% NaCl, at w/b ratio of 0.37: (a) 28 days, (b) 90 days, and (c) 360 days

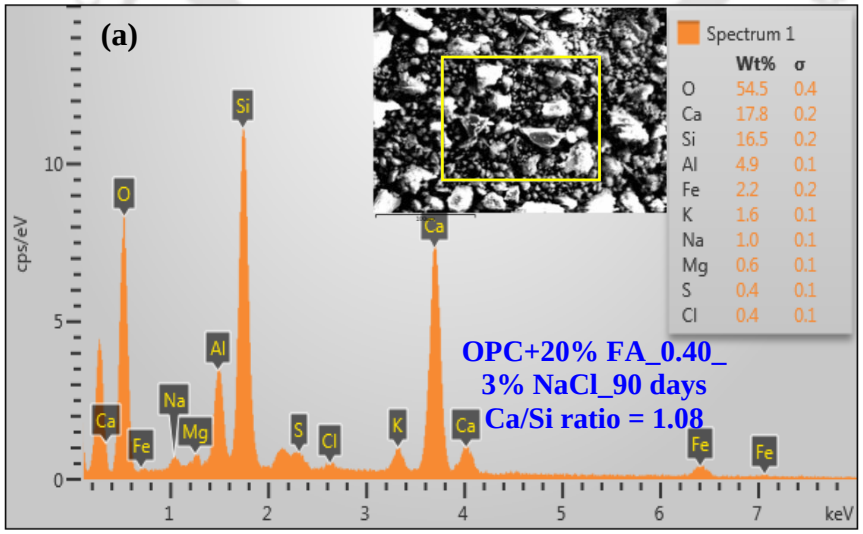

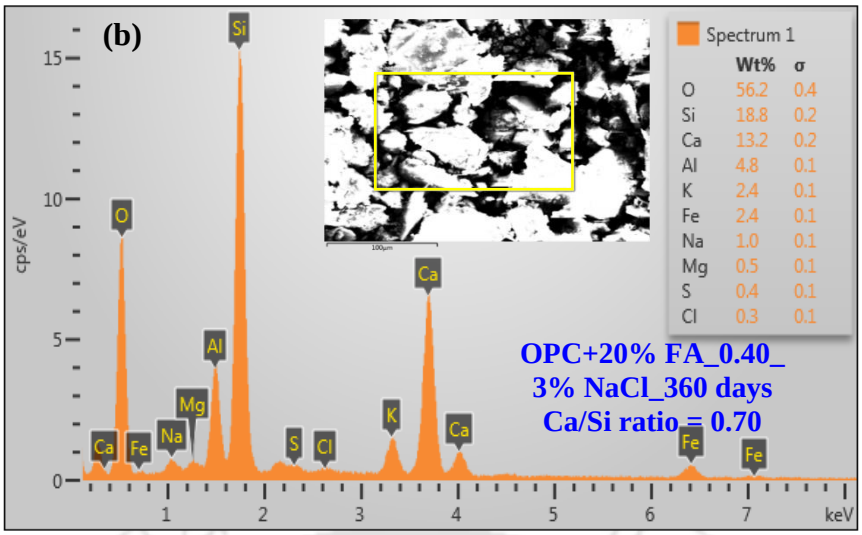

Fig. A17 EDX analysis of OPC+20% FA based SCC mixes admixed with 3% NaCl, at w/b ratio of 0.40: (a) 90 days, and (c) 360 days

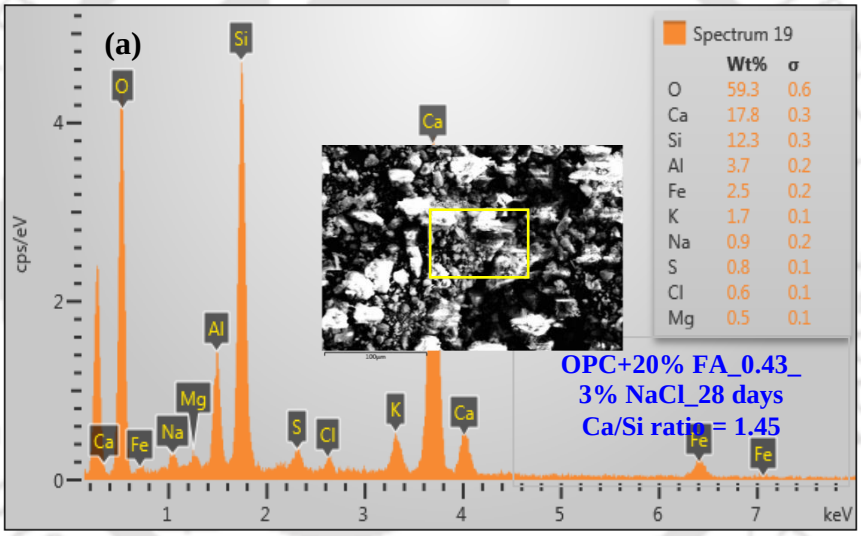

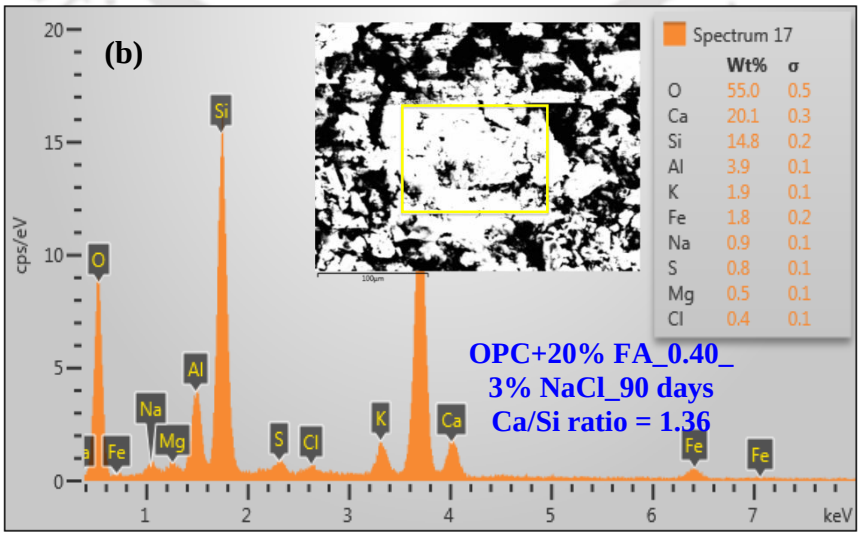

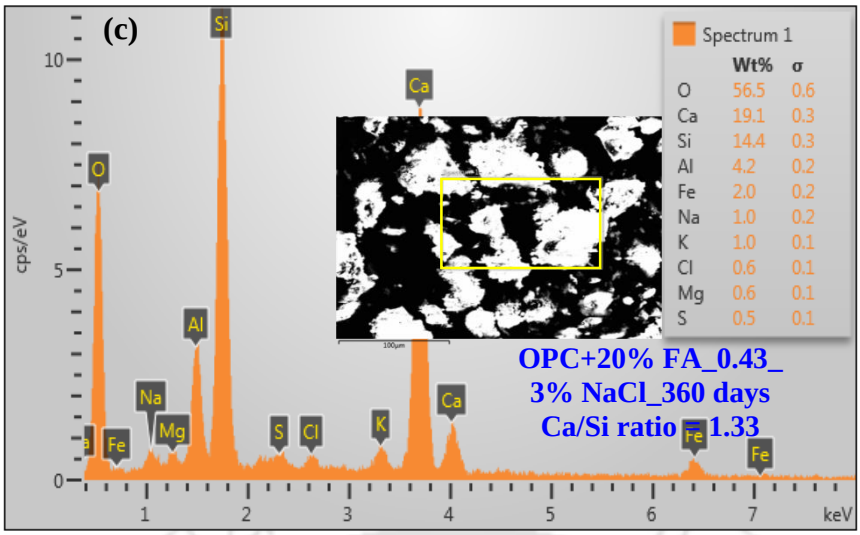

Fig. A18 EDX analysis of OPC+20% FA based SCC mixes admixed with 3% NaCl, at w/b ratio of 0.43: (a) 28 days, (b) 90 days, and (c) 360 days

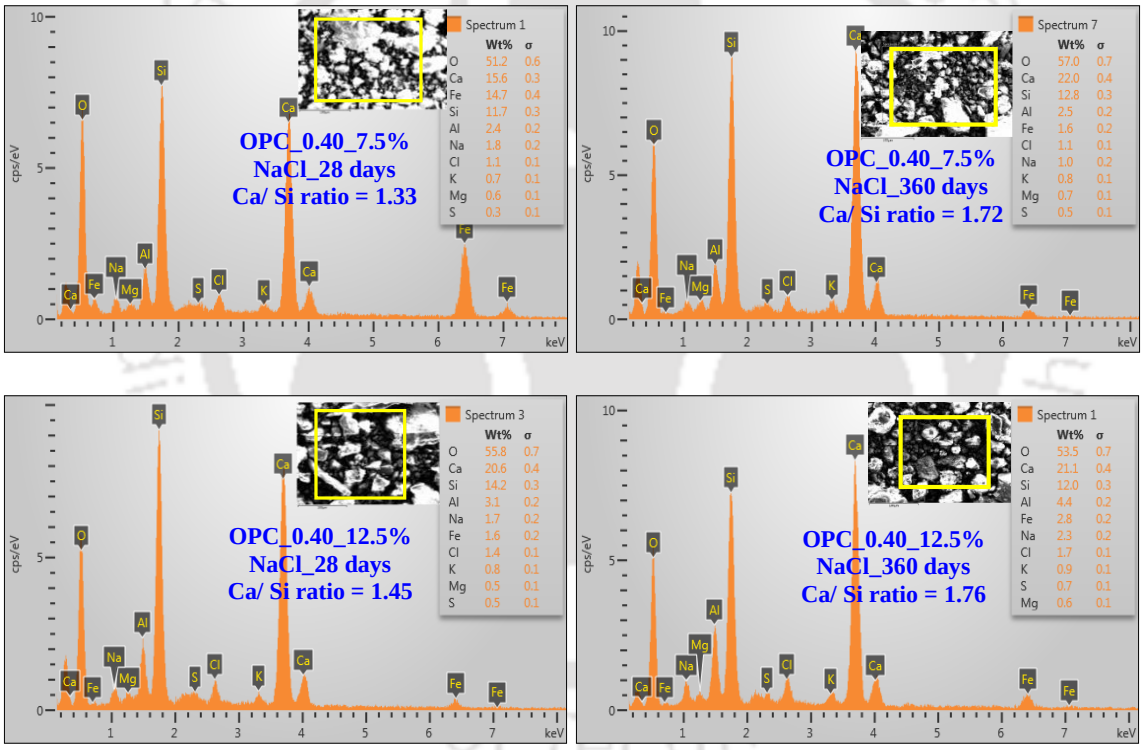

Fig. A19 EDX analysis of OPC based SCC mixes admixed with different NaCl concentrations at w/b ratio of 0.40, for curing ages of 28 days and 360 days

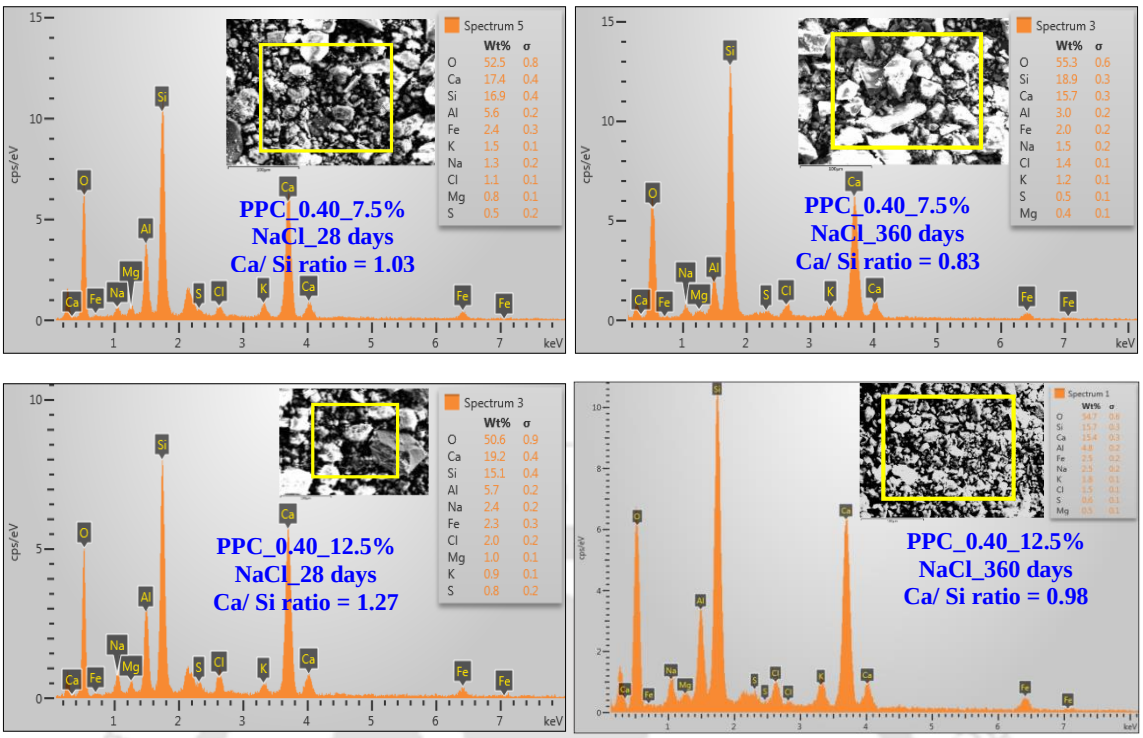

Fig. A20 EDX analysis of PPC based SCC mixes admixed with different NaCl concentrations at w/b ratio of 0.40, for curing ages of 28 days and 360 days

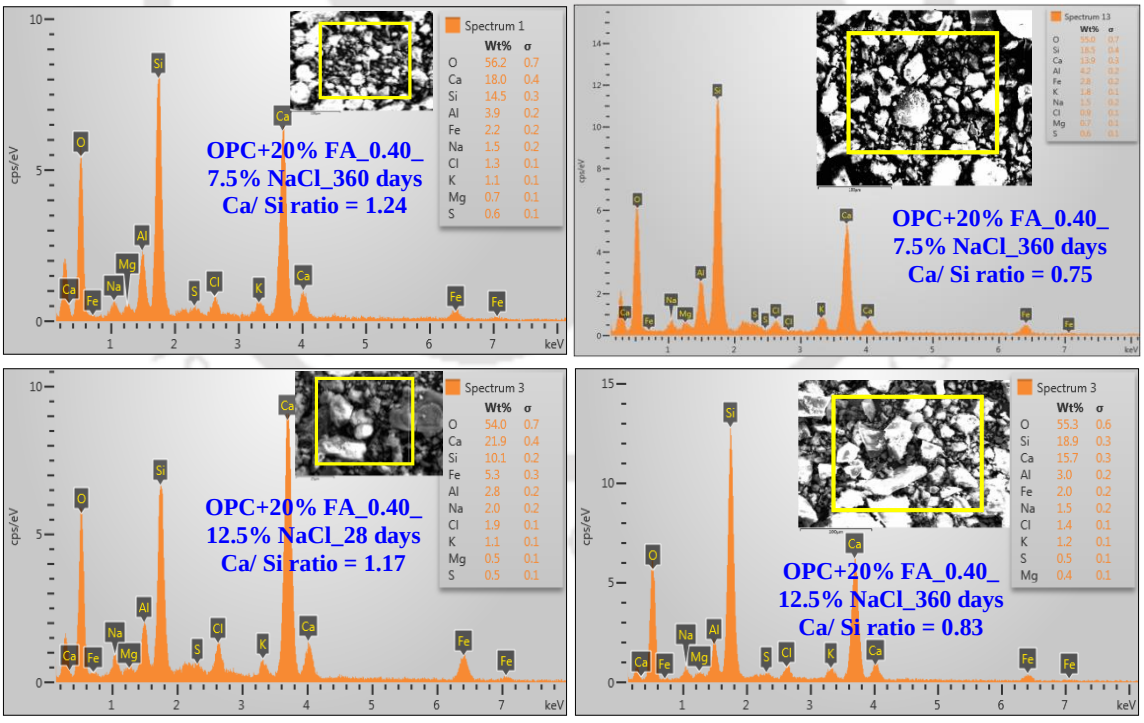

Fig. A21 EDX analysis of OPC+20% FA based SCC mixes admixed with different NaCl concentrations at w/b ratio of 0.40, for curing ages of 28 days and 360 days

APPENDIX B

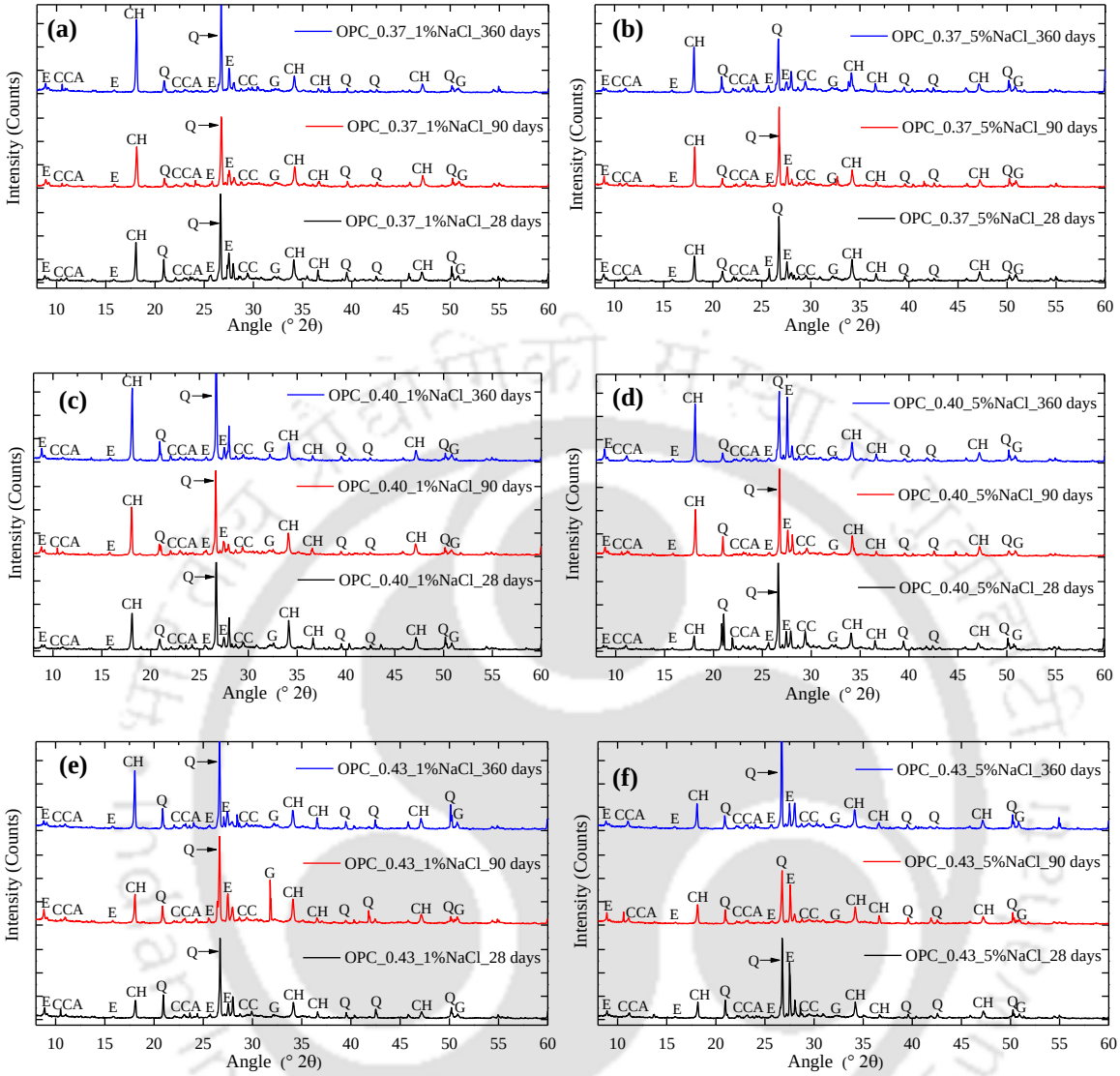

Fig. B1 XRD patterns of OPC based SCC mixes admixed with 1% and 5% NaCl for curing ages of 28, 90 and 360 days at w/b ratios of 0.37, 0.40, and 0.43

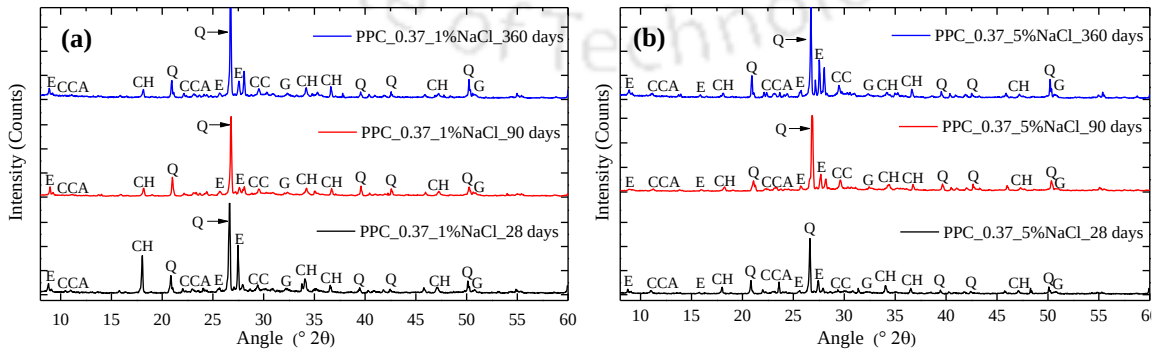

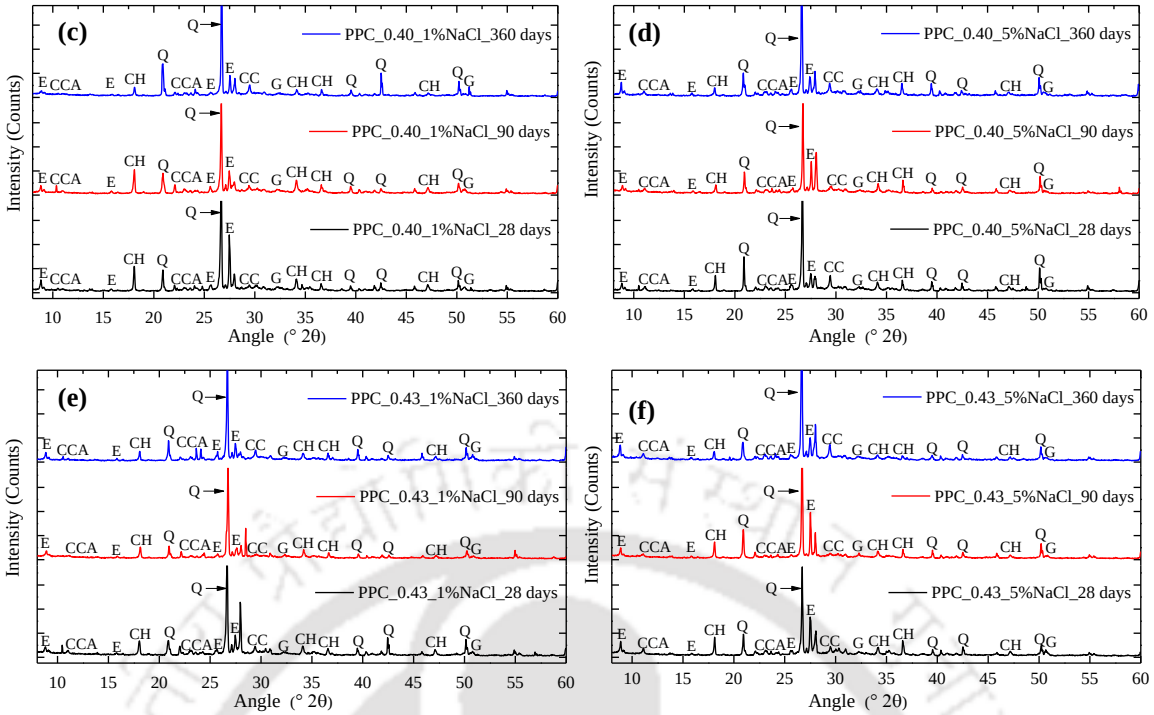

Fig. B2 XRD patterns of PPC based SCC mixes admixed with 1% and 5% NaCl for curing ages of 28, 90 and 360 days at w/b ratios of 0.37, 0.40, and 0.43

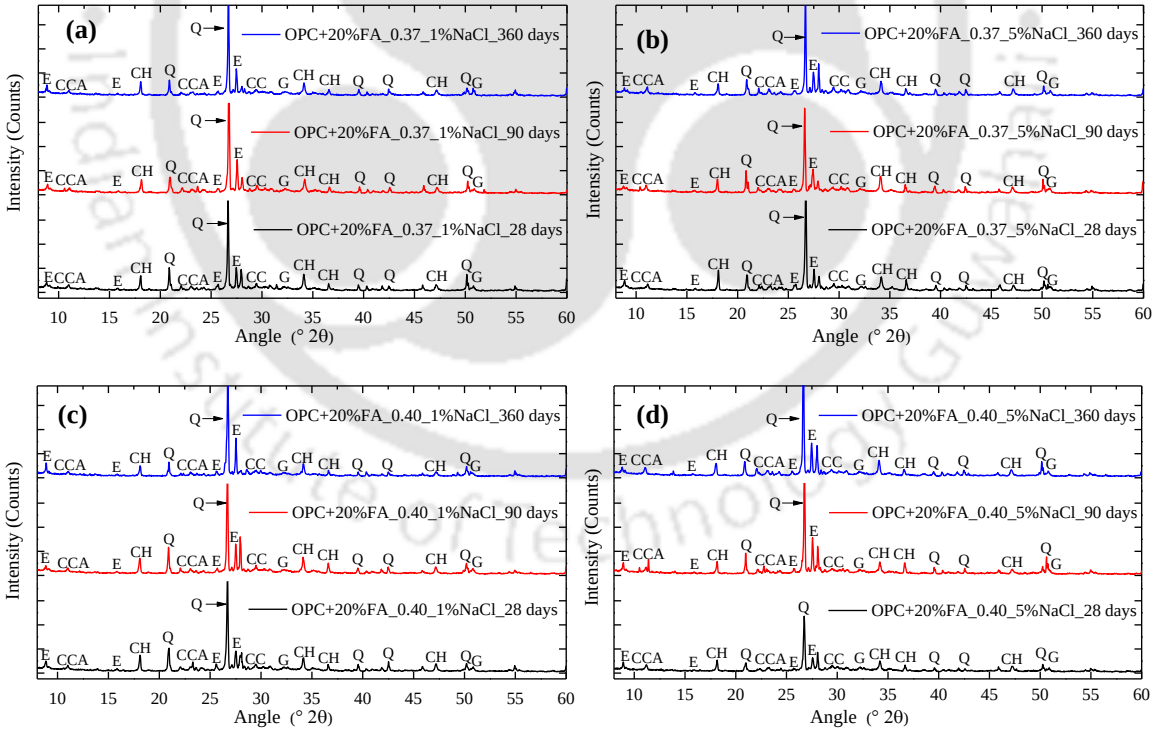

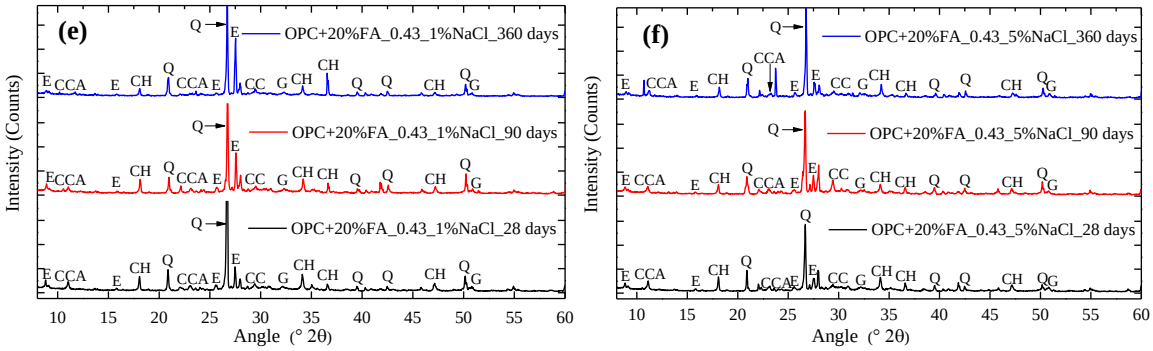

Fig. B3 XRD patterns of OPC+20% FA based SCC mixes admixed with 1% and 5% NaCl for curing ages of 28, 90 and 360 days at w/b ratios of 0.37, 0.40, and 0.43

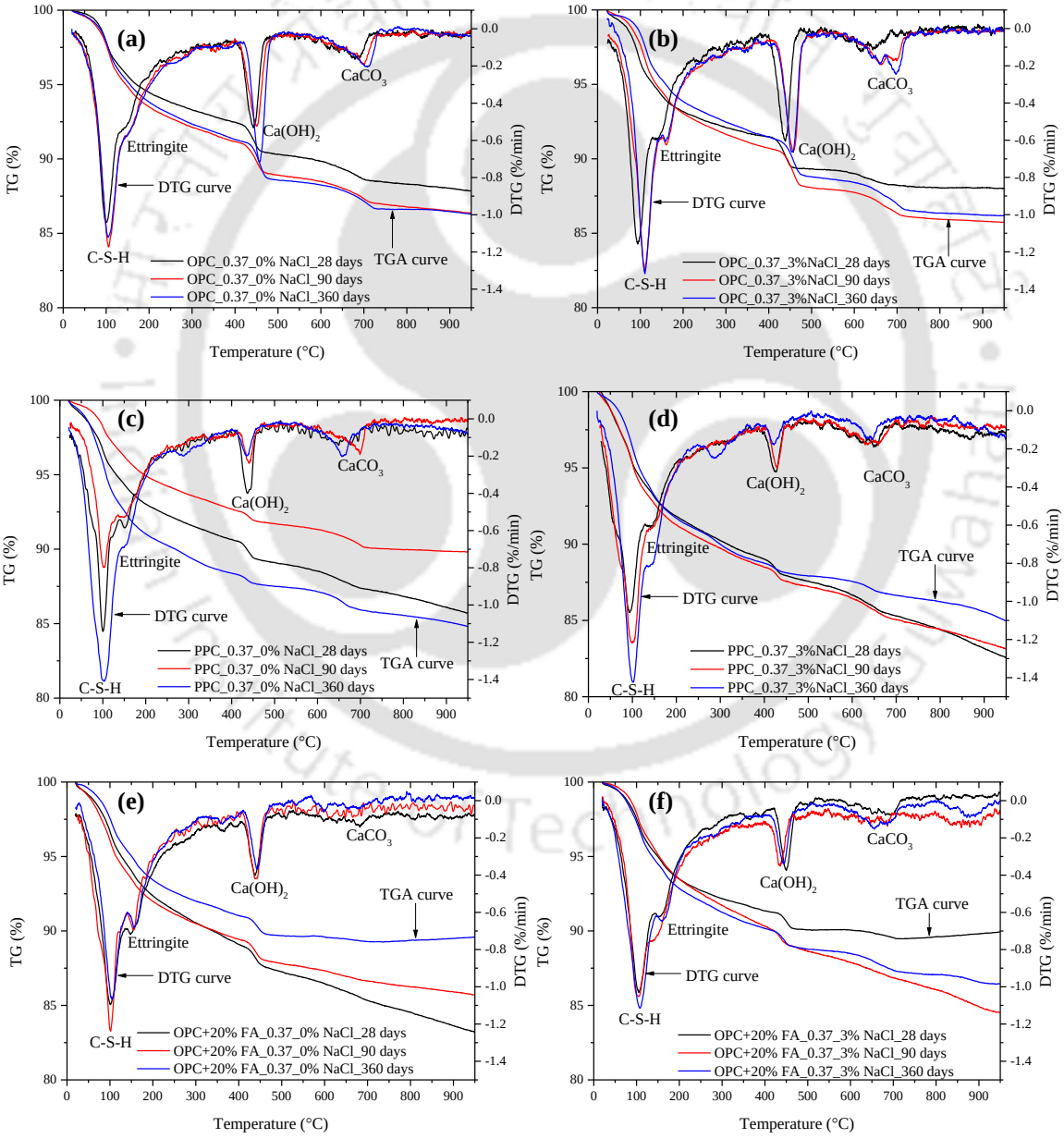

Fig. B4 TGA-DTG curves of OPC based SCC mixes admixed with 0% and 3% NaCl for curing ages of 28, 90 and 360 days at w/b ratio of 0.37

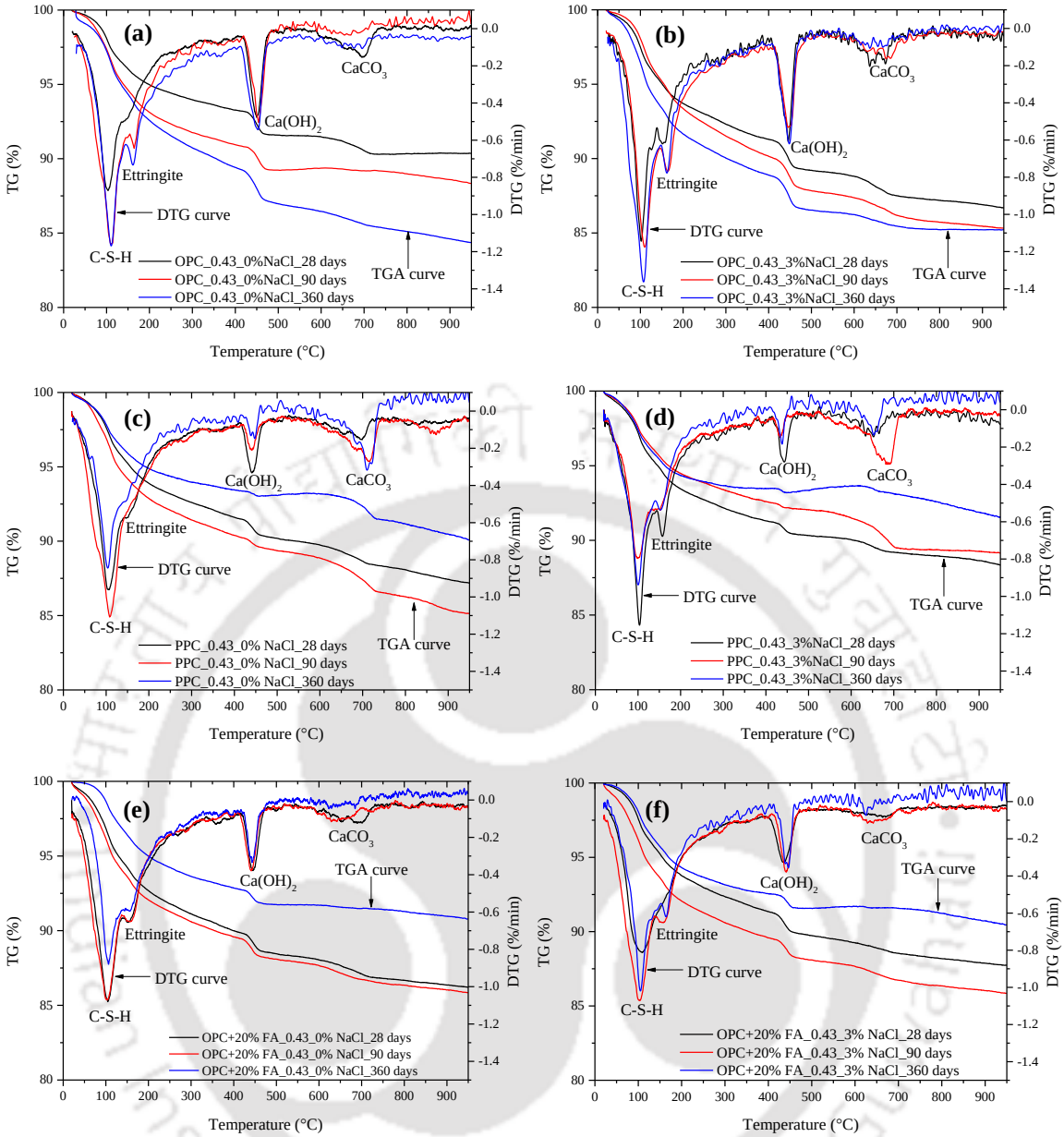

Fig. B5 TGA-DTG curves of OPC based SCC mixes admixed with 0% and 3% NaCl for curing ages of 28, 90 and 360 days at w/b ratio of 0.43

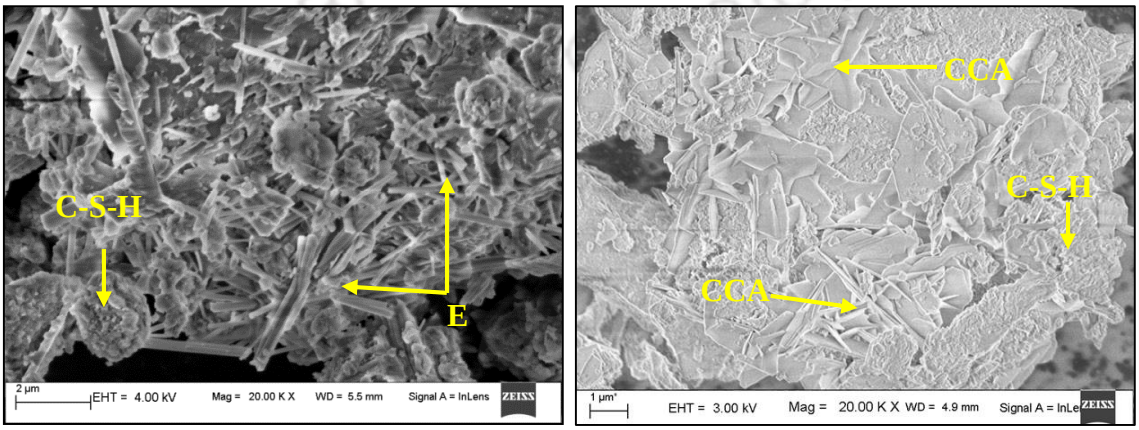

(a) OPC_0.37_ 0% NaCl (28 days) (b) OPC_0.37_3% NaCl (28 days)

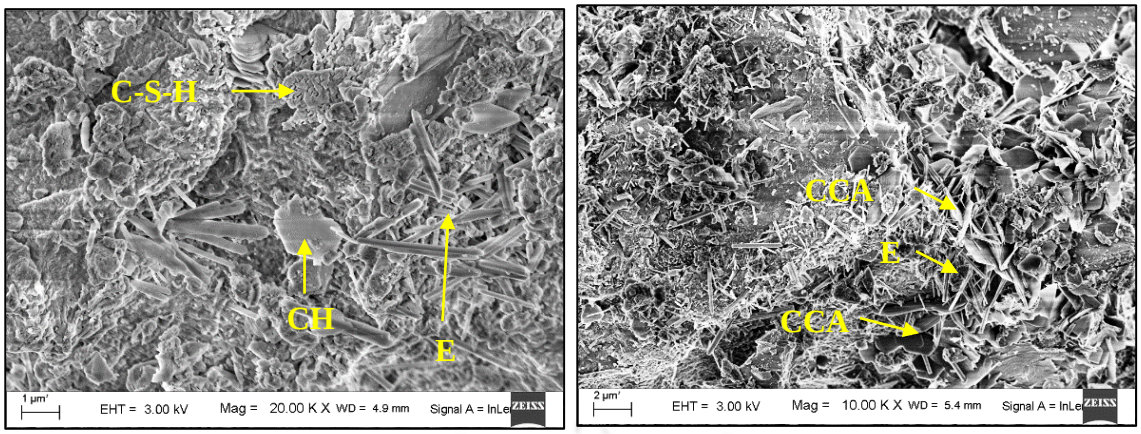

(c) OPC_0.43_ 0% NaCl (28 days) (d) OPC_0.43_3% NaCl (28 days)

Fig. B6 FESEM images of OPC based SCC mixes at w/b ratios of 0.37, 0.40 and 0.43, for 0% and 3% admixed NaCl concentrations, at curing age of 28 days

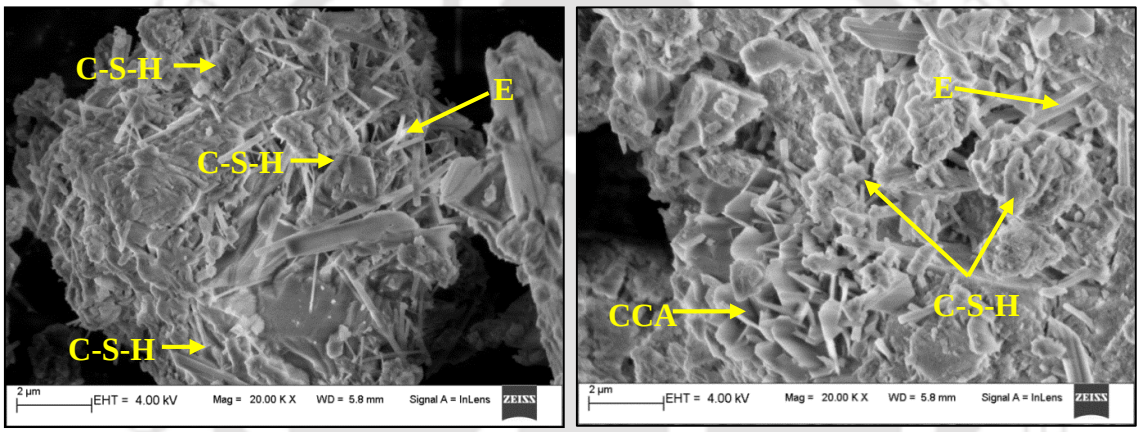

(a) OPC_0.37_ 0% NaCl (90 days) (b) OPC_0.37_3% NaCl (90 days)

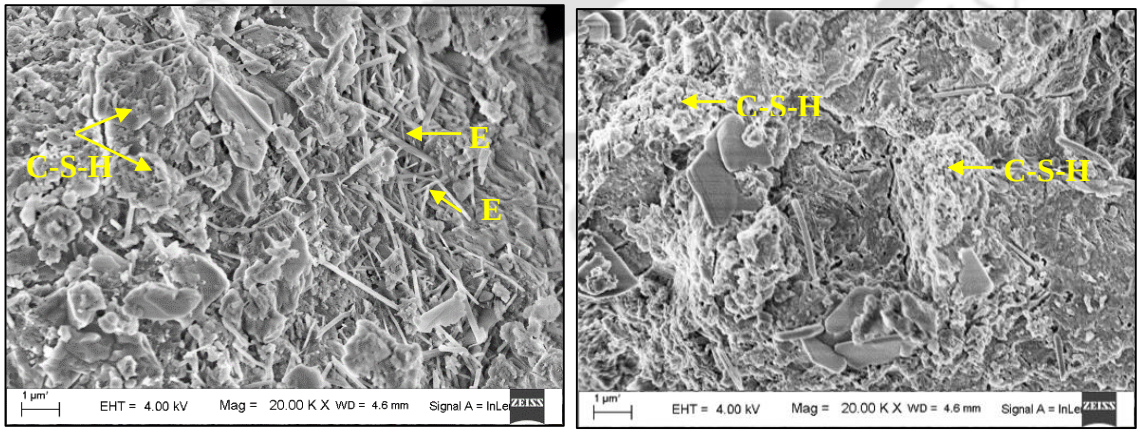

(c) OPC_0.40_ 0% NaCl (90 days) (d) OPC_0.40_3% NaCl (90 days)

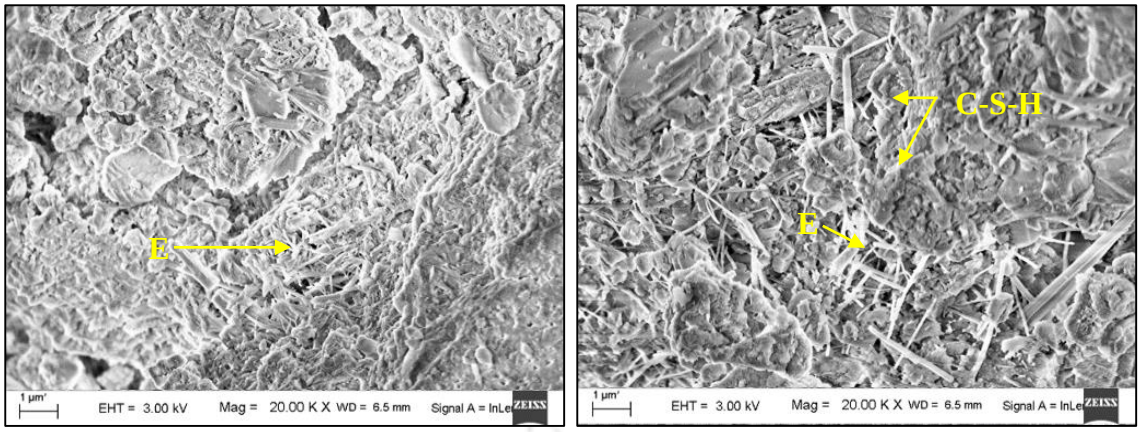

(e) OPC_0.43_ 0% NaCl (90 days) (f) OPC_0.43_3% NaCl (90 days)

Fig. B7 FESEM images of OPC based SCC mixes at w/b ratios of 0.37, 0.40 and 0.43, for 0% and 3% admixed NaCl concentrations, at curing age of 90 days

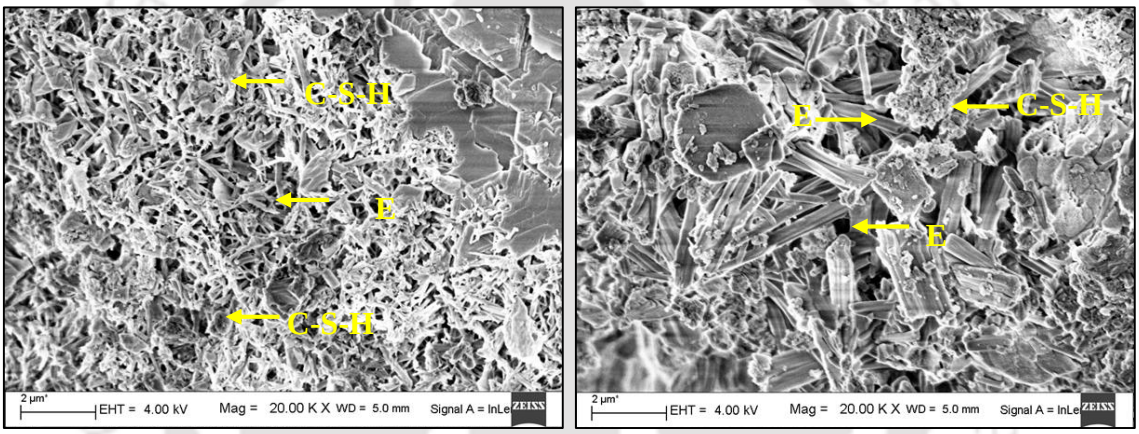

(a) OPC_0.37_ 0% NaCl (360 days) (b) OPC_0.37_3% NaCl (360 days)

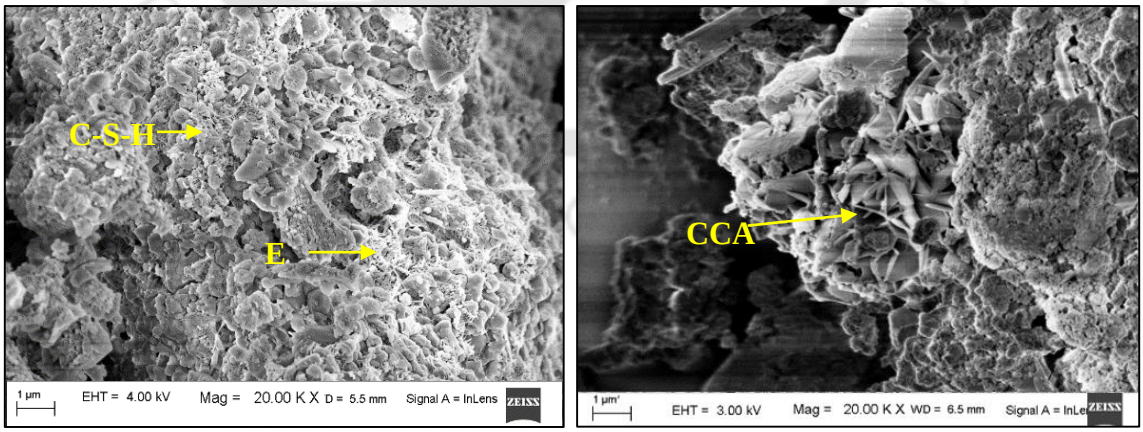

(c) OPC_0.43_ 0% NaCl (360 days) (d) OPC_0.43_3% NaCl (360 days)

Fig. B8 FESEM images of OPC based SCC mixes at w/b ratios of 0.37, 0.40 and 0.43, for 0% and 3% admixed NaCl concentrations, at curing age of 360 days

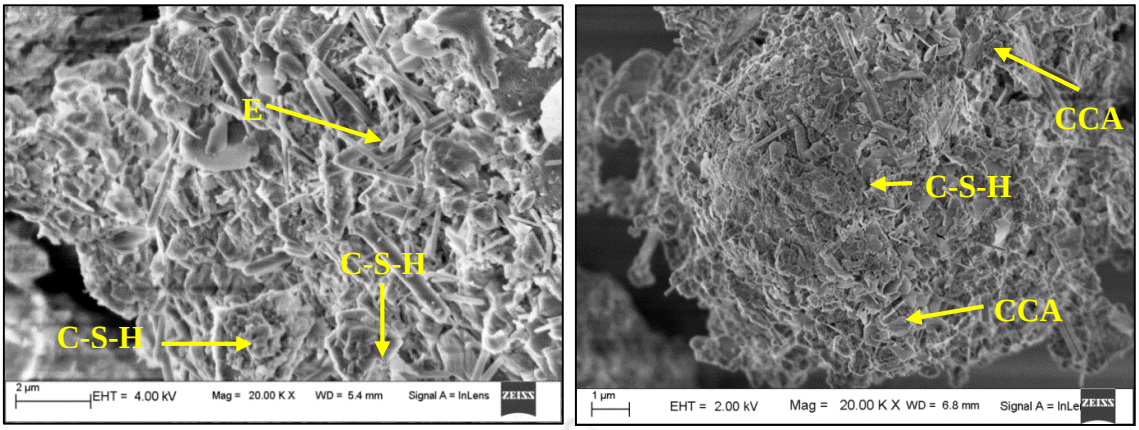

(a) PPC_0.37_ 0% NaCl (28 days) (b) PPC_0.37_3% NaCl (28 days)

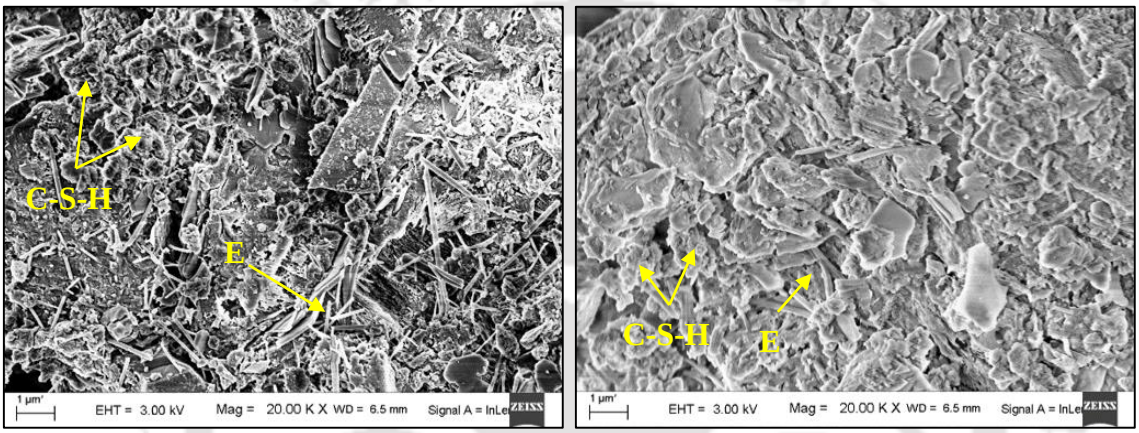

(c) PPC_0.43_ 0% NaCl (28 days)(d) PPC_0.43_3% NaCl (28 days)

Fig. B9 FESEM images of PPC based SCC mixes at w/b ratios of 0.37, 0.40 and 0.43, for 0% and 3% admixed NaCl concentrations, at curing age of 28 days

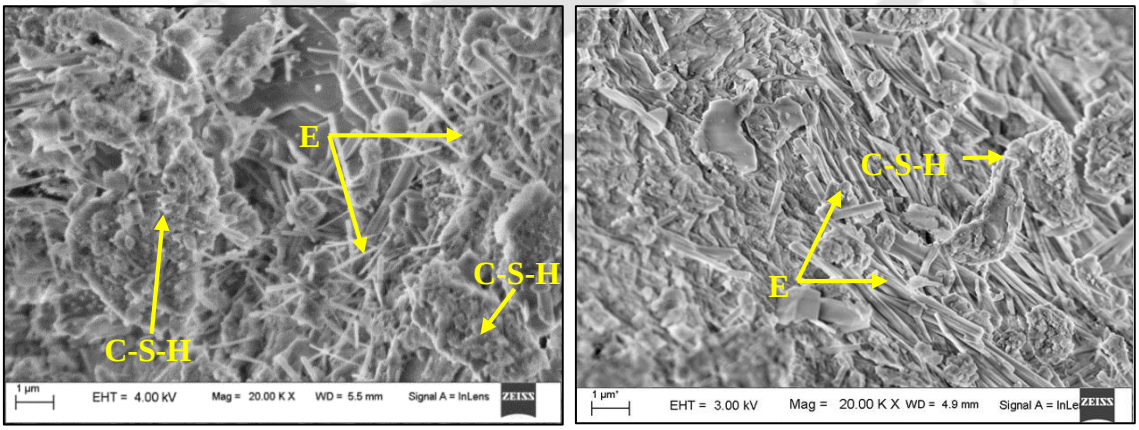

(a) PPC_0.37_ 0% NaCl (90 days) (b) PPC_0.37_3% NaCl (90 days)

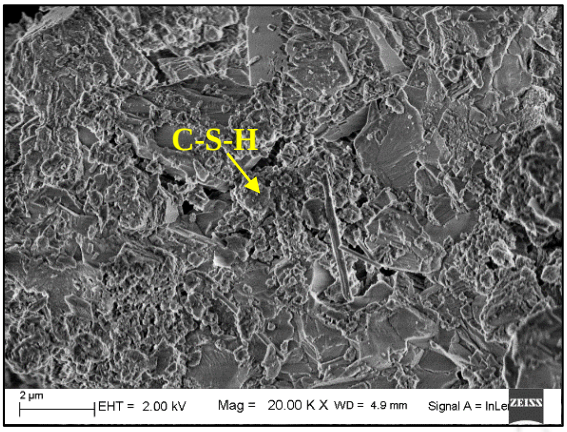

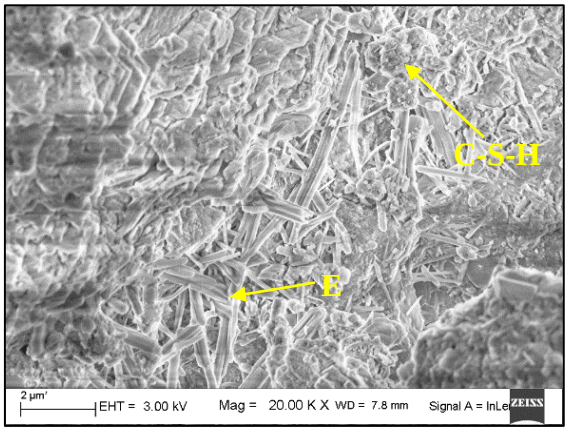

(c) PPC_0.40_ 0% NaCl (90 days) (d) PPC_0.40_3% NaCl (90 days)

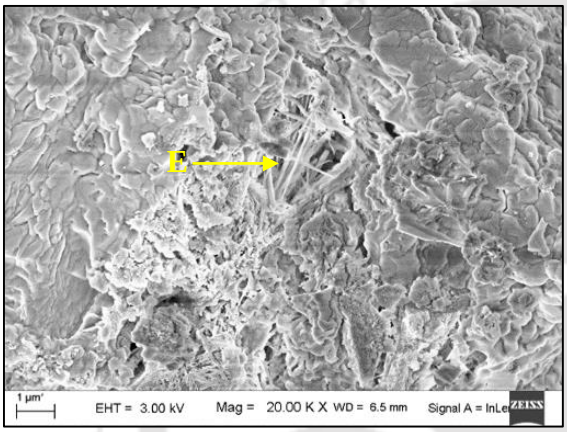

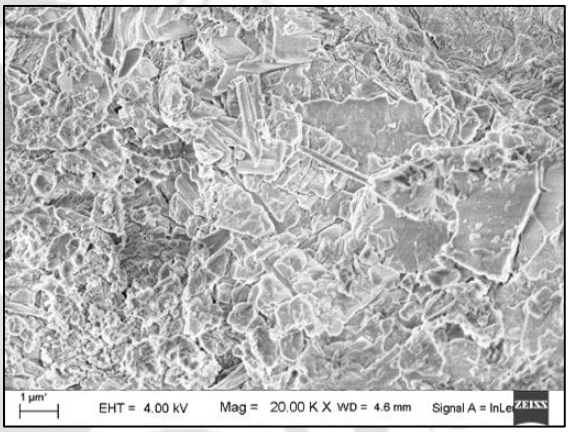

(e) PPC_0.43_ 0% NaCl (90 days) (b) PPC_0.43_3% NaCl (90 days)

Fig. B10 FESEM images of PPC based SCC mixes at w/b ratios of 0.37, 0.40 and 0.43, for 0% and 3% admixed NaCl concentrations, at curing age of 28 days

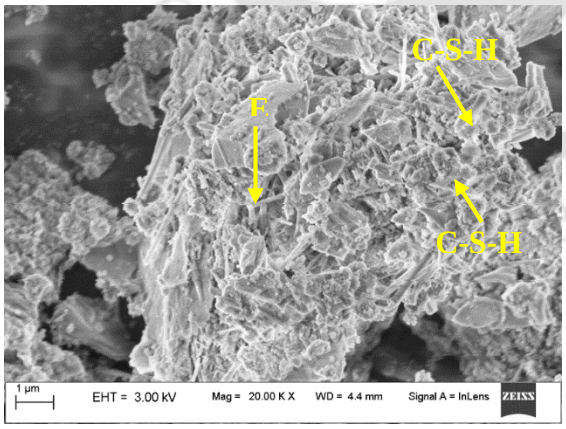

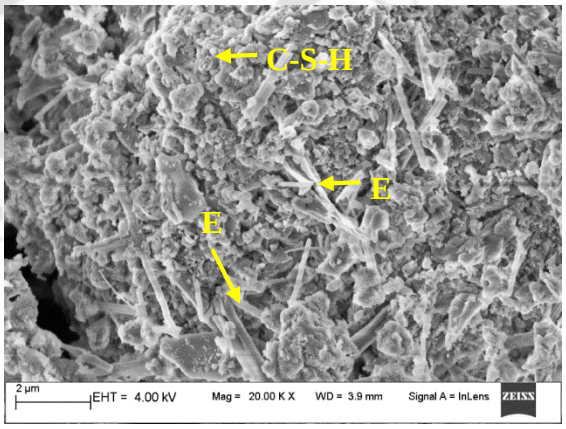

(a) PPC_0.37_ 0% NaCl (360 days) (b) PPC_0.37_3% NaCl (360 days)

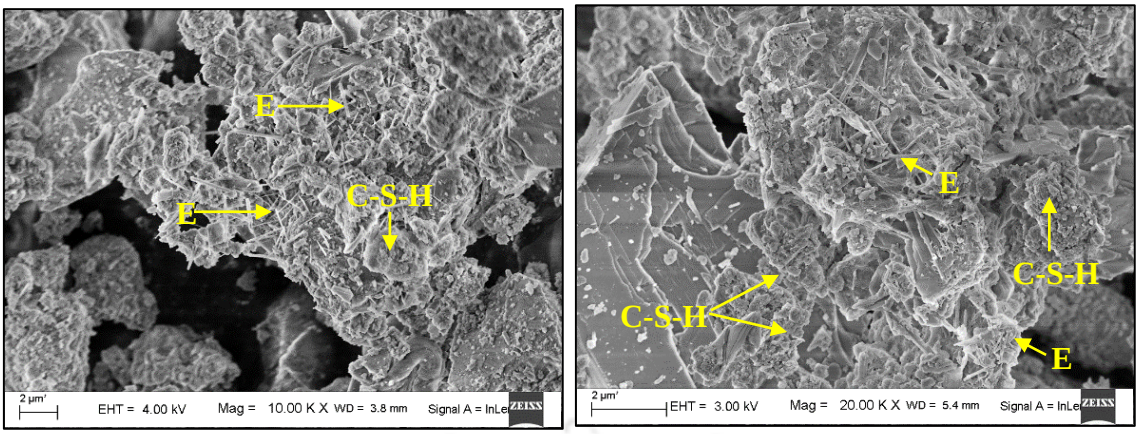

(c) PPC_0.43_ 0% NaCl (360 days) (d) PPC_0.43_3% NaCl (360 days)

Fig. B11 FESEM images of PPC based SCC mixes at w/b ratios of 0.37, 0.40 and 0.43, for 0% and 3% admixed NaCl concentrations, at curing age of 360 days

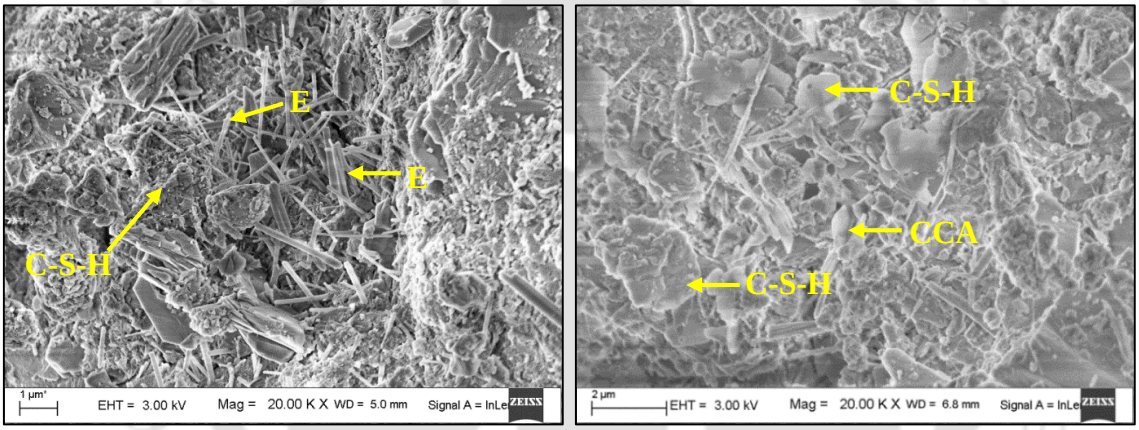

(a) OPC+20% FA_0.37_ 0% NaCl (28 days) (b) OPC+20% FA_0.37_3% NaCl (28 days)

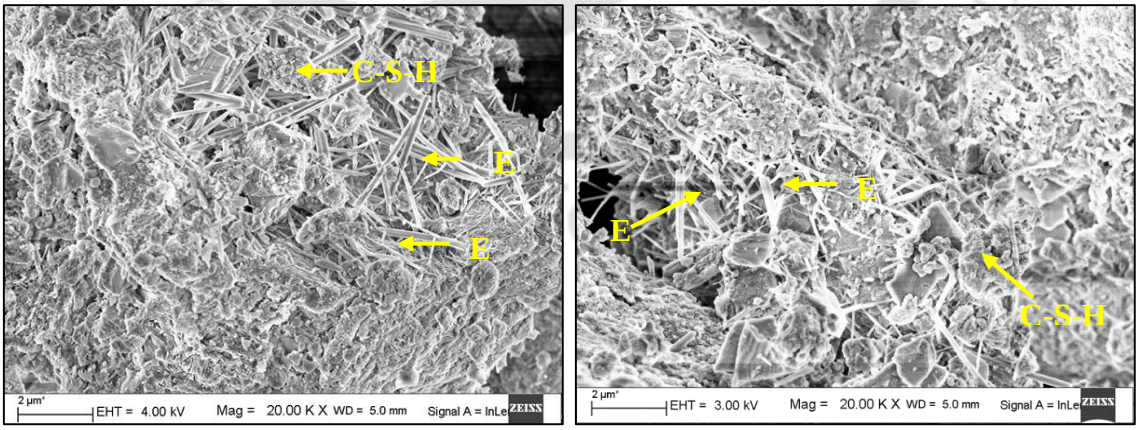

(c) OPC+20% FA_0.43_ 0% NaCl (28 days) (d) OPC+20% FA_0.43_3% NaCl (28 days)

Fig. B12 FESEM images of OPC+20% FA based SCC mixes at w/b ratios of 0.37, 0.40 and 0.43, for 0% and 3% admixed NaCl concentrations, at curing age of 28 days

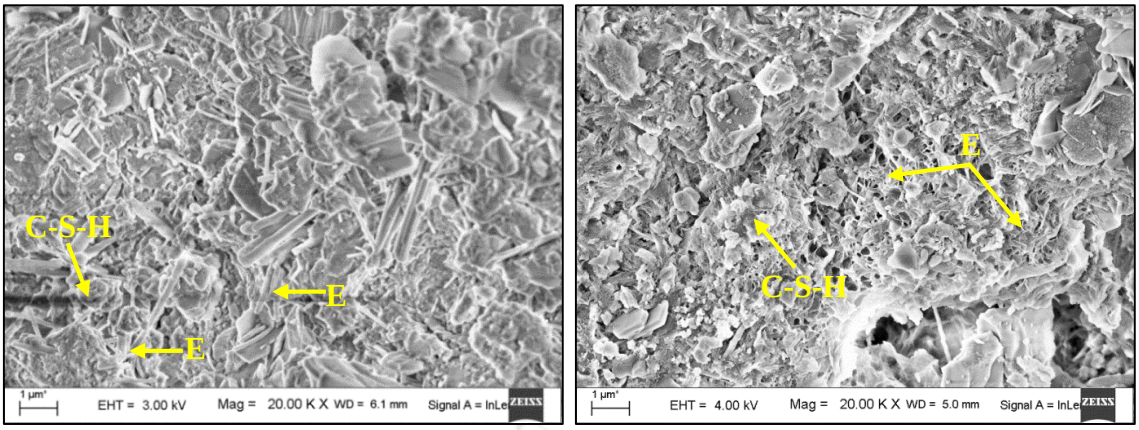

(a) OPC+20% FA_0.37_ 0% NaCl (90 days) (b) OPC+20% FA_0.37_3% NaCl (90 days)

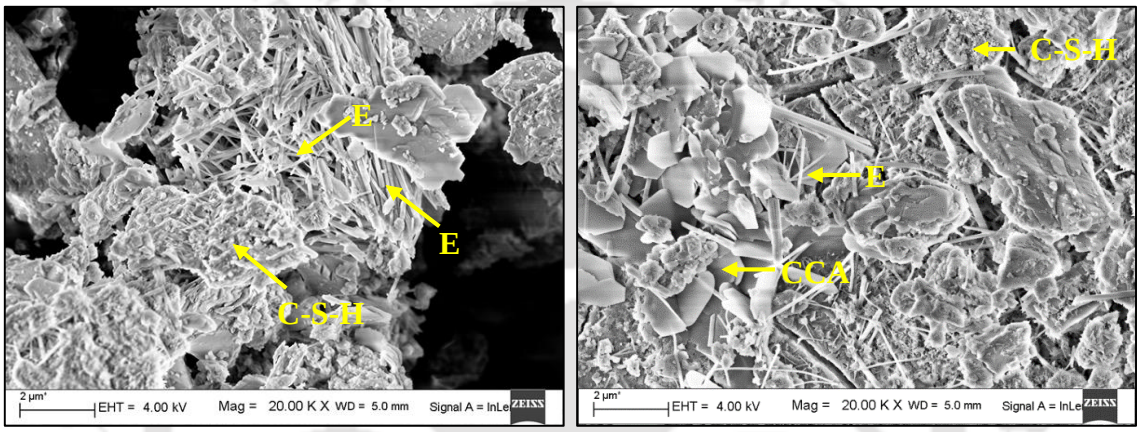

(c) OPC+20% FA_0.40_ 0% NaCl (90 days) (d) OPC+20% FA_0.40_3% NaCl (90 days)

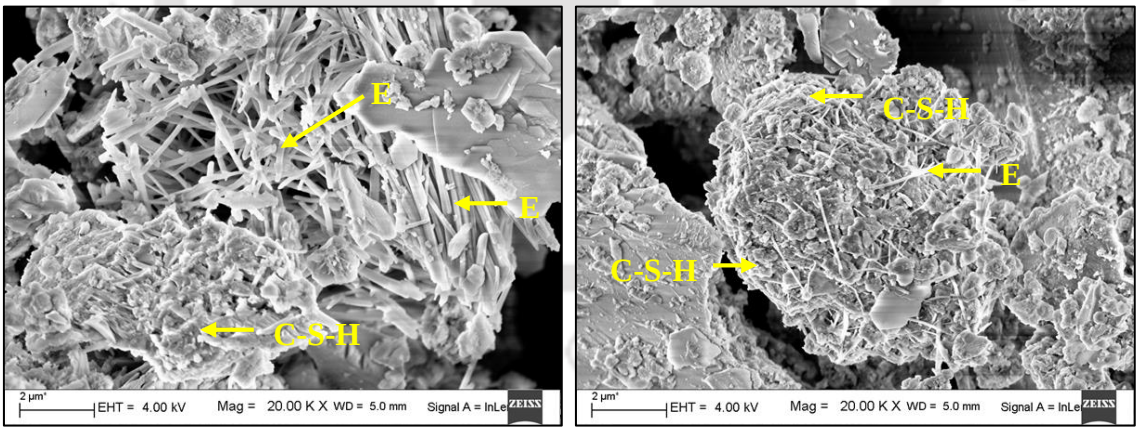

(e) OPC+20% FA_0.43_ 0% NaCl (90 days) (f) OPC+20% FA_0.43_3% NaCl (90 days)

Fig. B13 FESEM images of OPC+20% FA based SCC mixes at w/b ratios of 0.37, 0.40 and 0.43, for 0% and 3% admixed NaCl concentrations, at curing age of 90 days

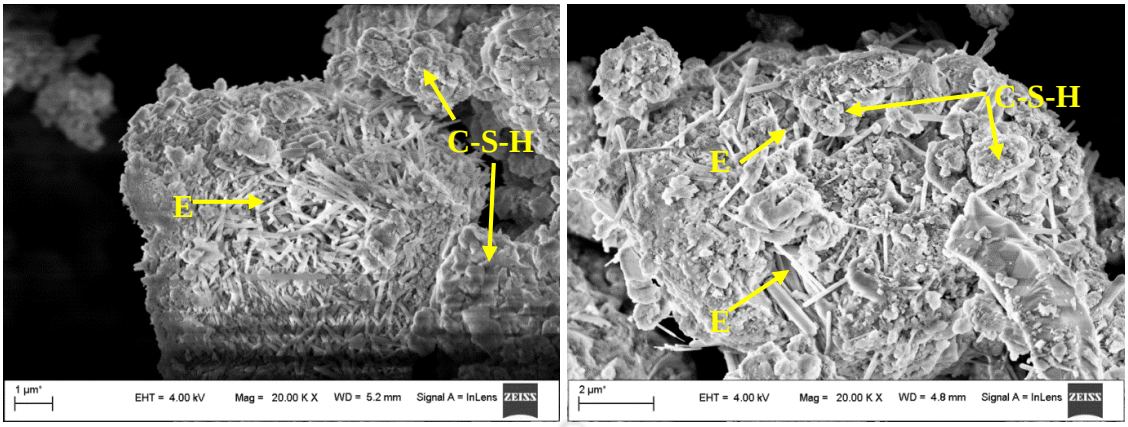

(a) OPC+20% FA_0.37_ 0% NaCl (360days) (b) OPC+20% FA_0.37_3% NaCl (360 days)

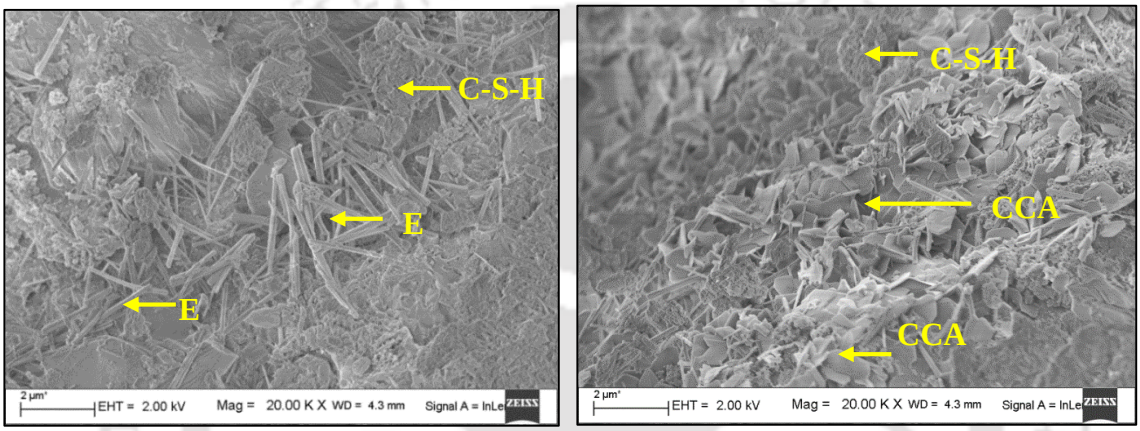

(e) OPC+20% FA_0.43_ 0% NaCl (360days) (f) OPC+20% FA_0.43_3% NaCl (360 days)

Fig. B14 FESEM images of OPC+20% FA based SCC mixes at w/b ratios of 0.37, 0.40 and 0.43, for 0% and 3% admixed NaCl concentrations, at curing age of 360 days

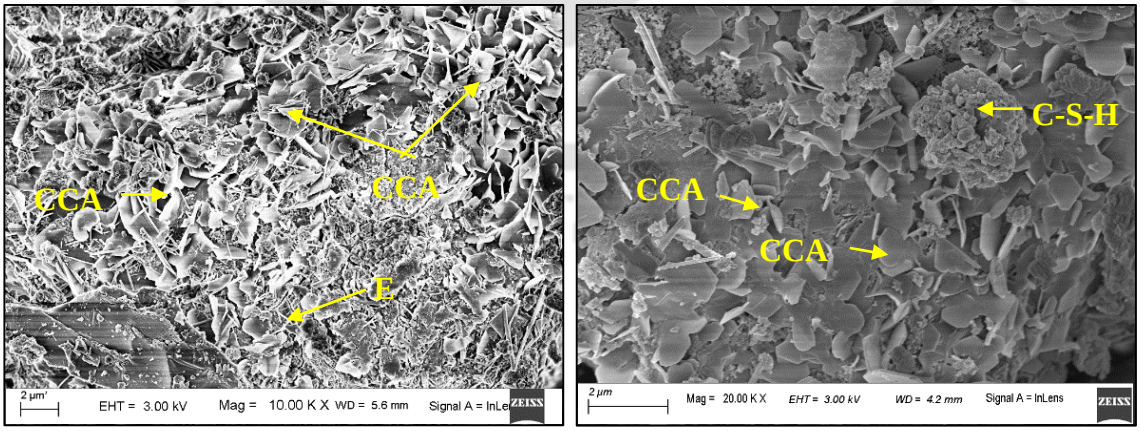

(a) OPC_0.40_3% NaCl (28 days) (b) OPC_0.40_3% NaCl (360 days)

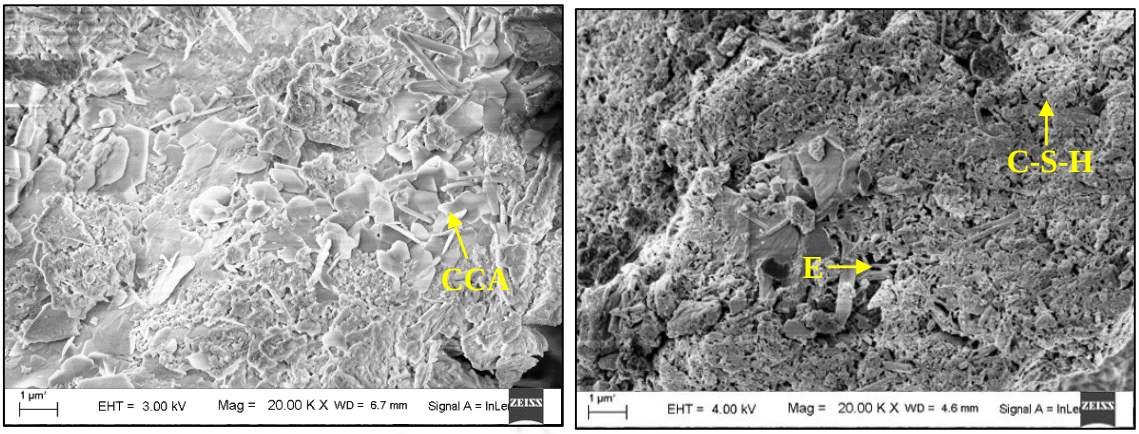

(c) PPC_0.40_3% NaCl (28 days) (d) PPC_0.40_3% NaCl (360 day

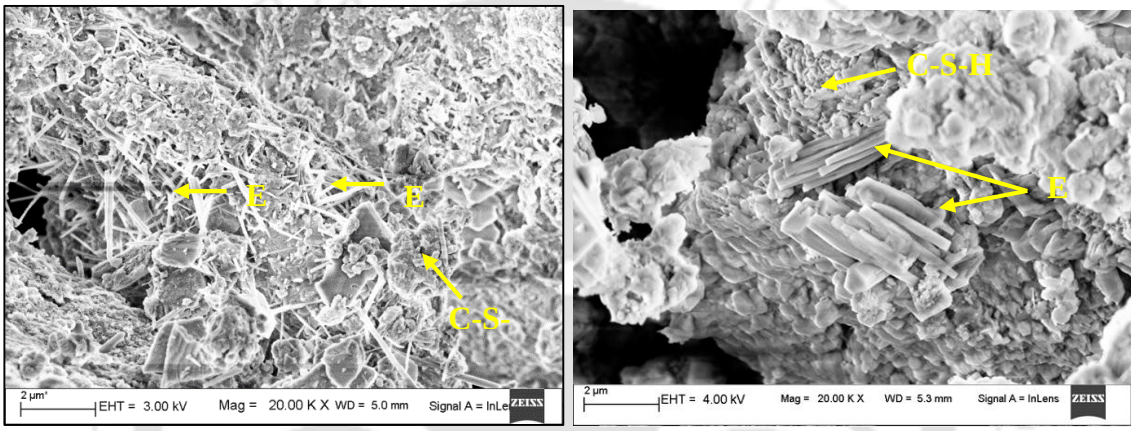

(e) OPC+20% FA_0.40_3% NaCl (28 days) (f) OPC+20% FA_0.40_3% NaCl (360 days)

Fig. B15 FESEM images of SCC mixes admixed with 3% NaCl concentrations for curing ages of 28 and 360 days at w/b ratio of 0.40

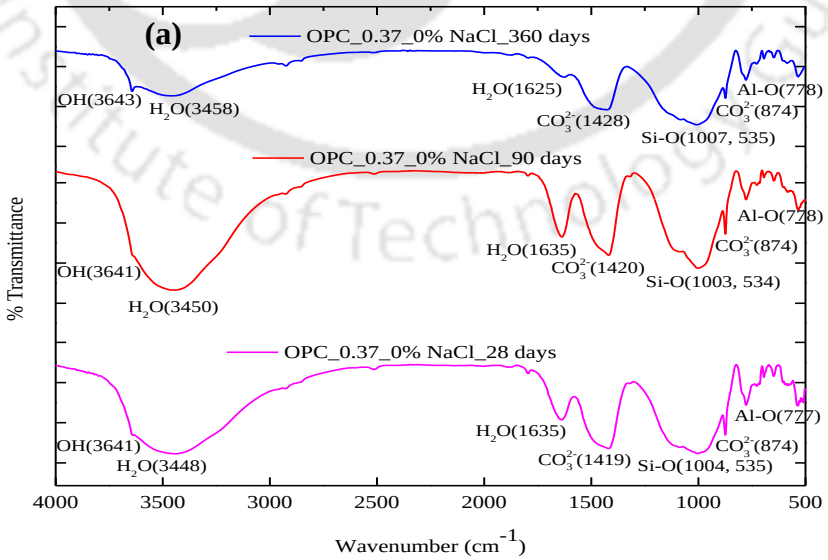

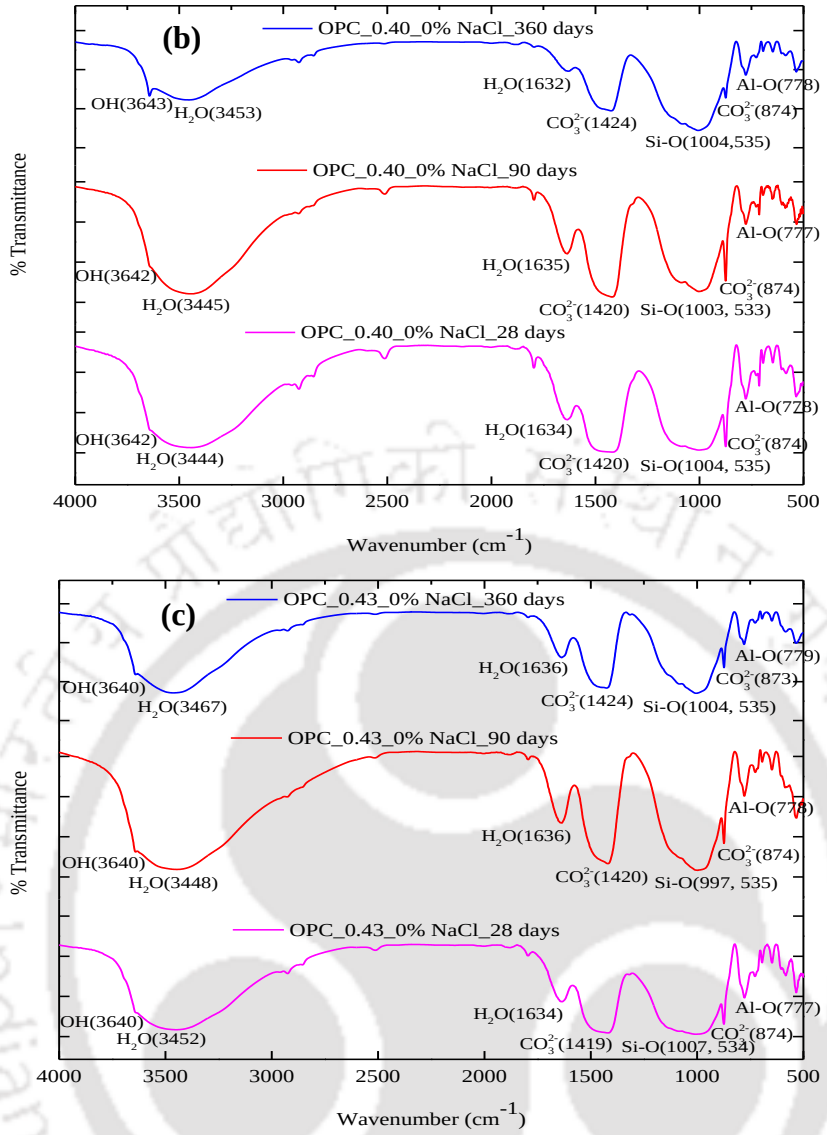

Fig. B16 FTIR spectra of OPC based SCC mixes admixed with 0% NaCl for curing ages of 28, 90 and 360 days: (a) w/b ratio = 0.37, (b) w/b ratio = 0.40, and (c) w/b ratio = 0.43

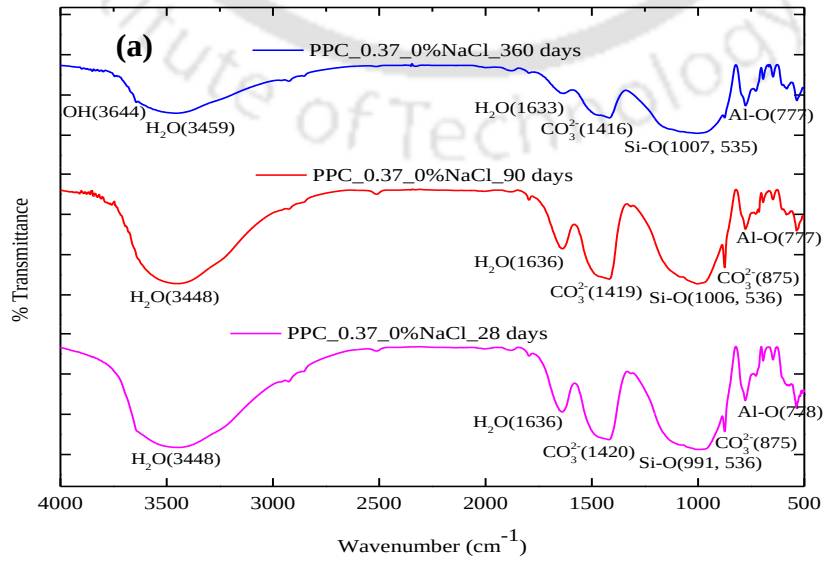

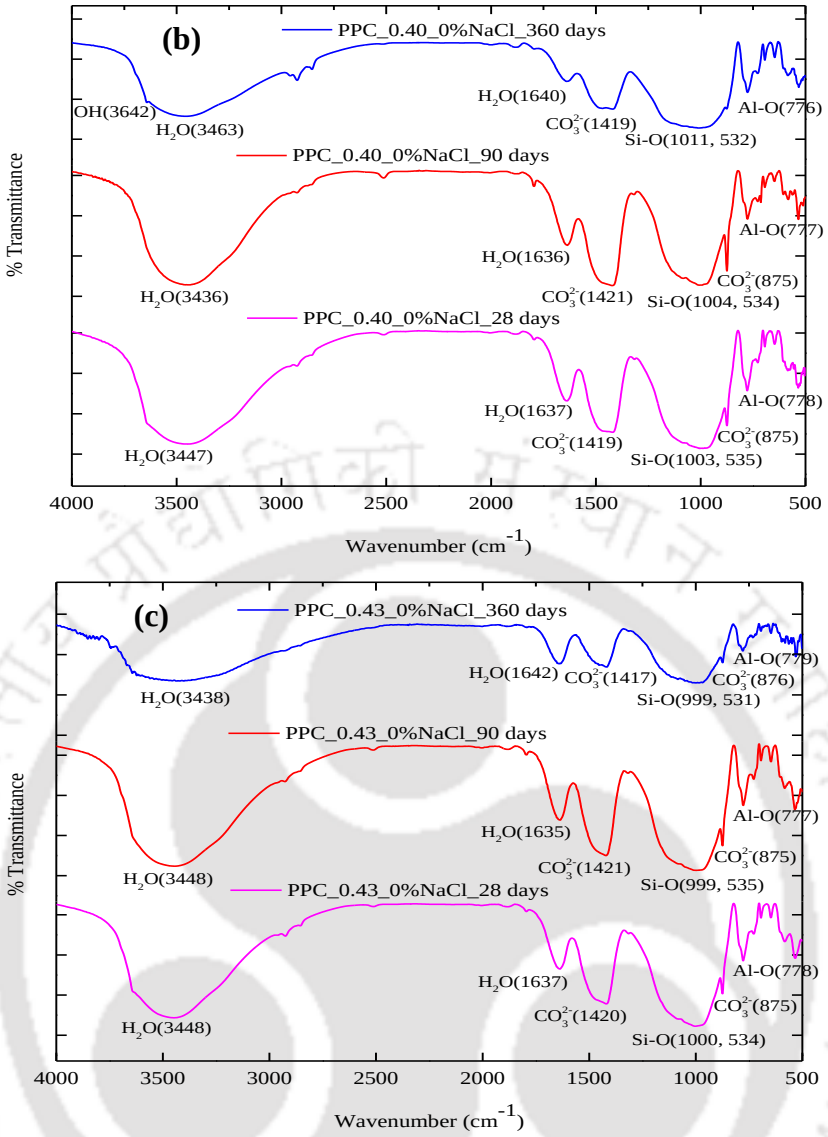

Fig. B17 FTIR spectra of PPC based SCC mixes admixed with 0% NaCl for curing ages of 28, 90 and 360 days: (a) w/b ratio = 0.37, (b) w/b ratio = 0.40, and (c) w/b ratio = 0.43

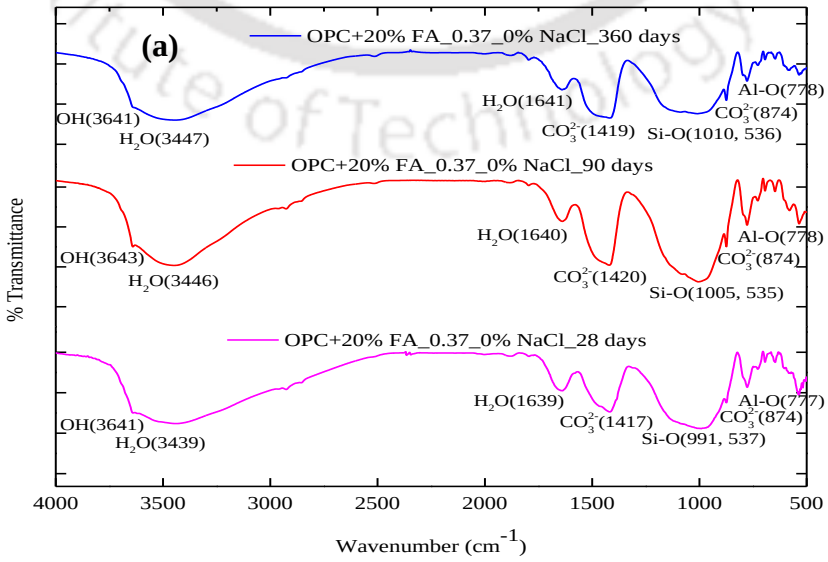

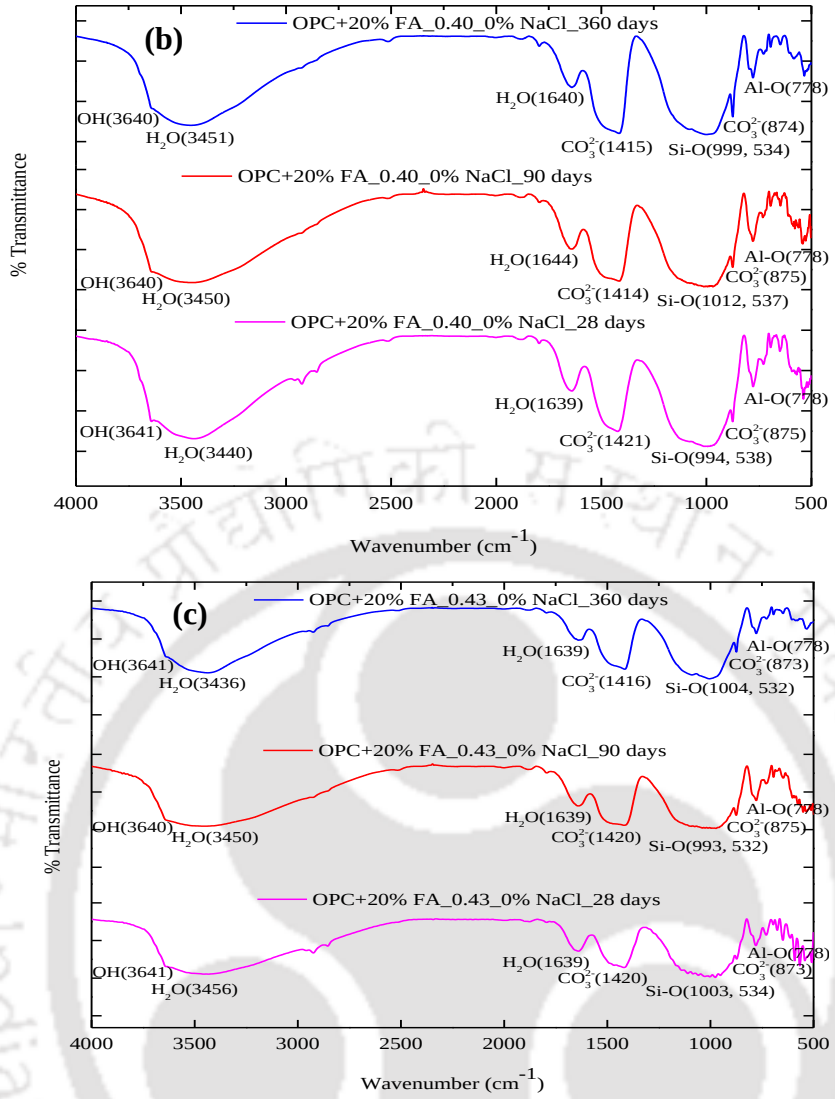

Fig. B18 FTIR spectra of OPC+20% FA based SCC mixes admixed with 0% NaCl for curing ages of 28, 90 and 360 days: (a) w/b ratio = 0.37, (b) w/b ratio = 0.40, and (c) w/b ratio = 0.43

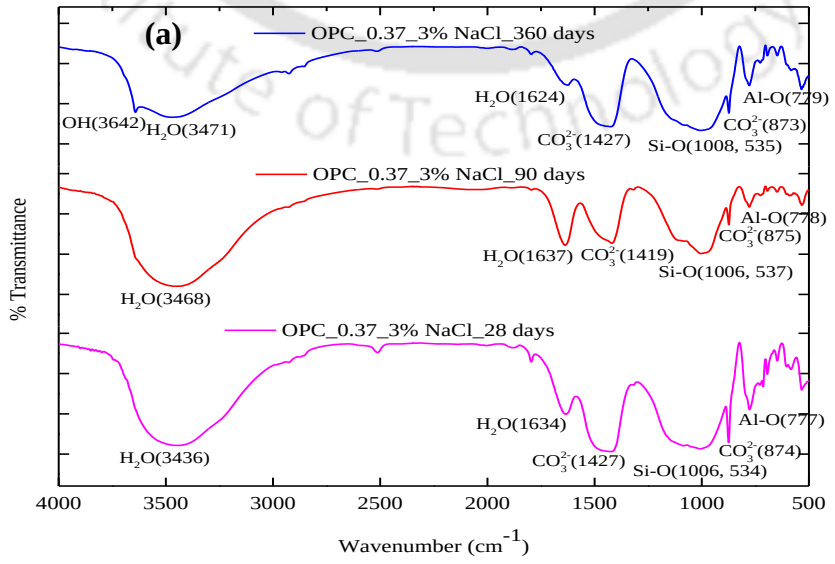

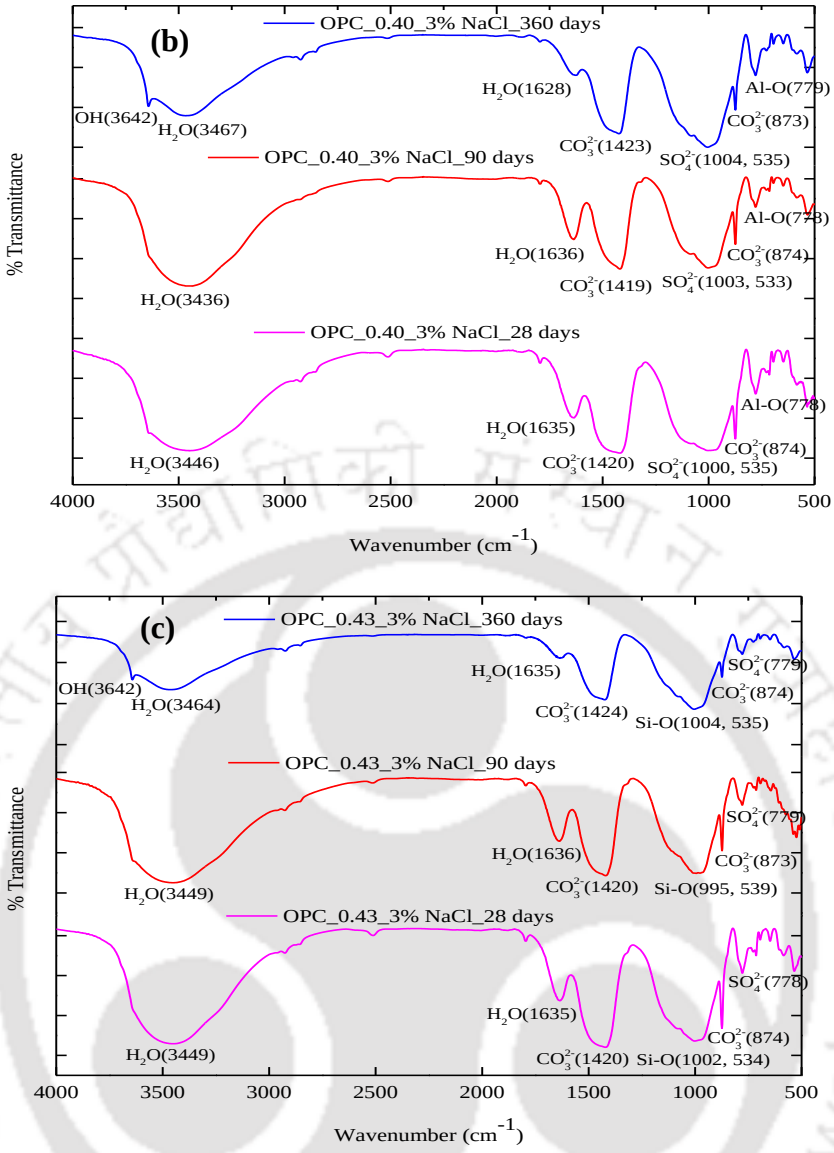

Fig. B19 FTIR spectra of OPC based SCC mixes admixed with 3% NaCl for curing ages of 28, 90 and 360 days: (a) w/b ratio = 0.37, (b) w/b ratio = 0.40, and (c) w/b ratio = 0.43

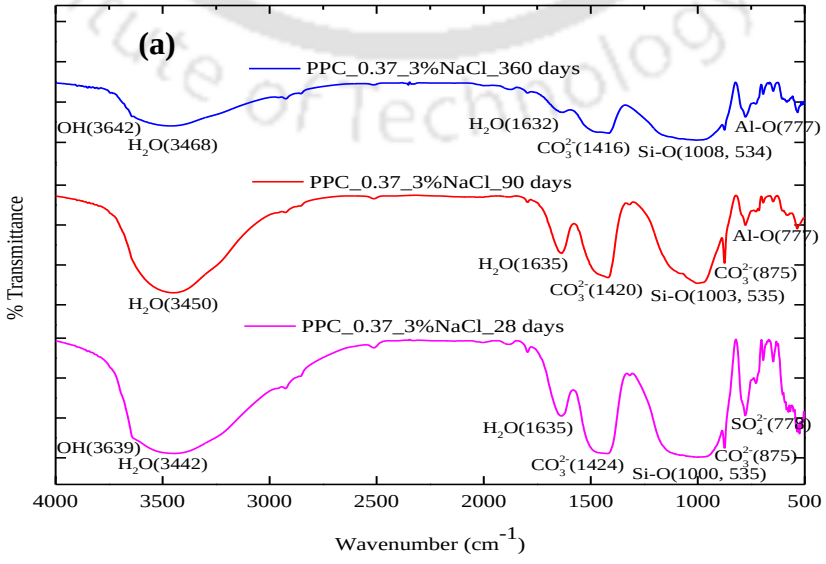

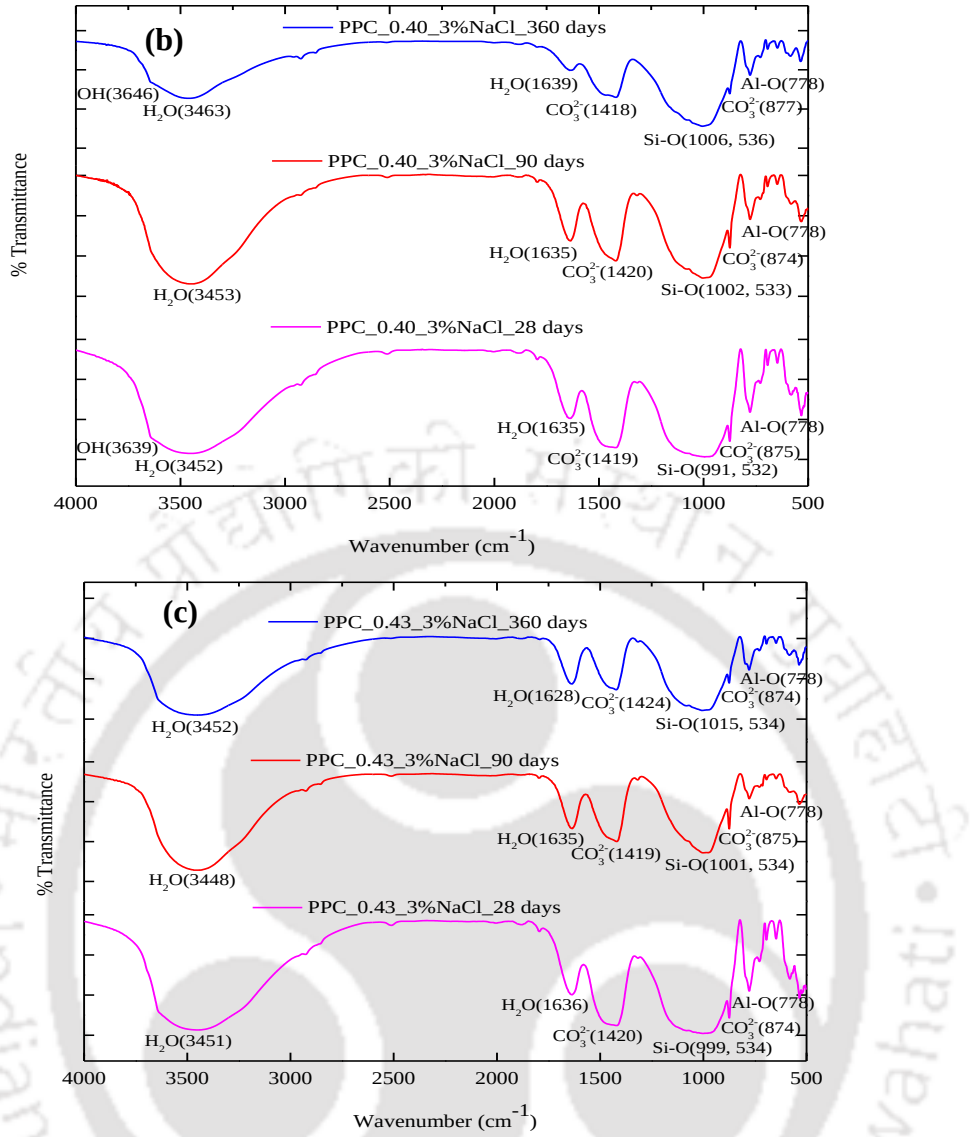

Fig. B20 FTIR spectra of PPC based SCC mixes admixed with 3% NaCl for curing ages of 28, 90 and 360 days: (a) w/b ratio = 0.37, (b) w/b ratio = 0.40, and (c) w/b ratio = 0.43

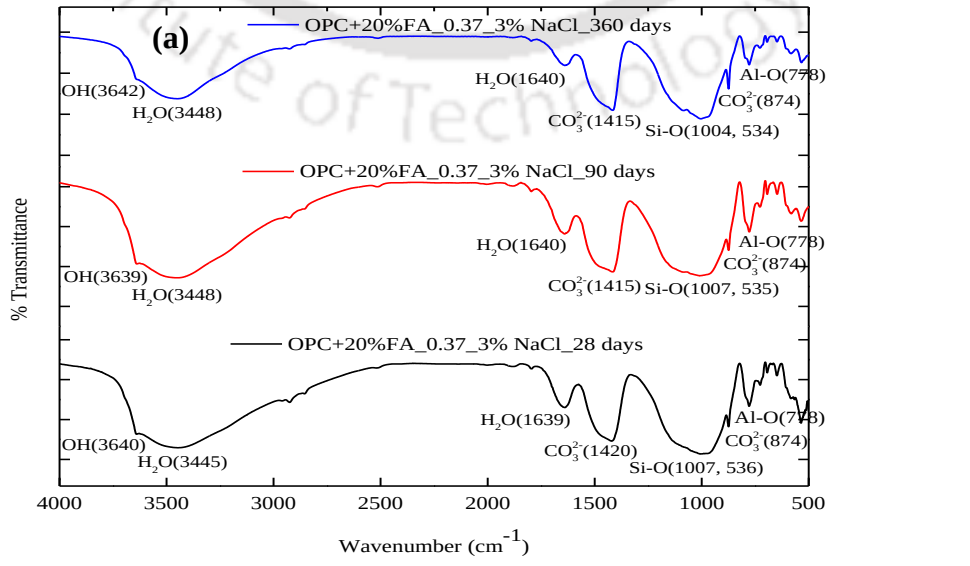

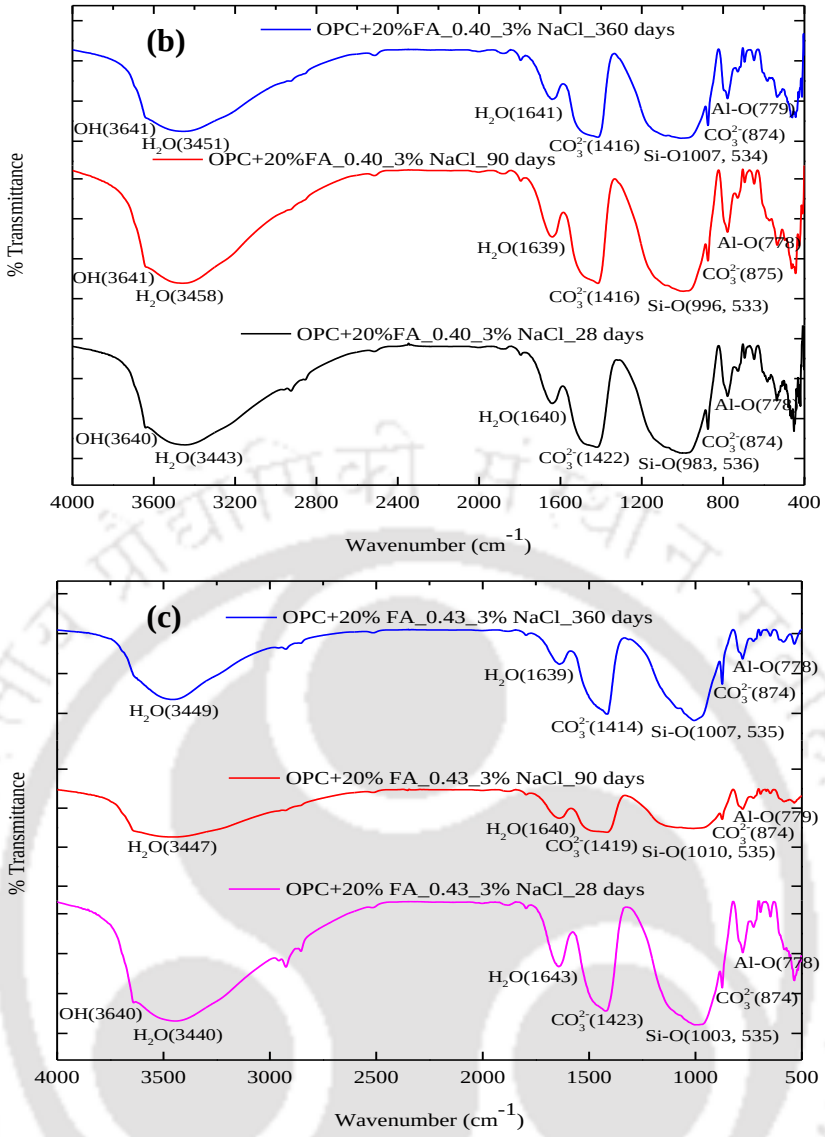

Fig. B21 FTIR spectra of OPC+20% FA based SCC mixes admixed with 3% NaCl for curing ages of 28, 90 and 360 days: (a) w/b ratio = 0.37, (b) w/b ratio = 0.40, and (c) w/b ratio = 0.43

LIST OF PUBLICATIONS

International Journals

1. **Smrati Jain** and Bulu Pradhan, Effect of cement type on hydration, microstructure and thermo-gravimetric behaviour of chloride admixed self-compacting concrete, *Construction and Building Materials*, Volume. 212, (pp. 304-316), 2019. (DOI: 10.1016/j.conbuildmat.2019.04.001)
2. **Smrati Jain** and Bulu Pradhan, Influence of admixed chloride on fresh, mechanical and corrosion behaviour of self-compacting, *Construction and Building Materials*, 2019 *(Under Review).*

Book Chapters

1. **Smrati Jain** and Bulu Pradhan, Corrosion performance of steel in self-compacting concrete exposed to chloride environment. In *Recent Advances in Structural Engineering, Volume 2* (pp. 549-558). Springer, Singapore, 2019. (DOI: 10.1007/978-981-13-0365-4_47)

Conference and Poster Presentation

1. **Smrati Jain**, Arya Anuj Jee and B. Pradhan, Application of modern techniques to evaluate microstructure of concrete, *International Conference on Sophisticated Instruments in Modern Research, ICSIMR-2017*, IIT Guwahati, June 30 - July 1, 2017.
2. Lalrosiama Zote, **Smrati Jain** and Bulu Pradhan, Effect of cement type on fresh and hardened properties of self-compacting concrete, *UKIERI Concrete Congress*, Jalandhar, *November 2-5, 2015*.